Impacts of chemical dispersants on oil-degrading microorganisms

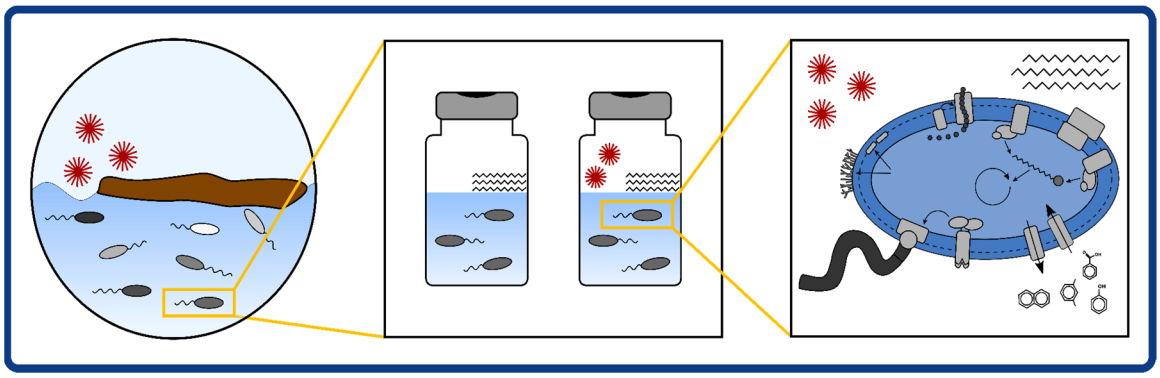

Saskia Rughöft

Impacts of chemical dispersants on oil-degrading microorganisms

Dissertation
der Mathematisch-Naturwissenschaftlichen Fakultät
der Eberhard Karls Universität Tübingen
zur Erlangung des Grades eines
Doktors der Naturwissenschaften
(Dr. rer. nat.)

vorgelegt von
Saskia Rughöft (M.Sc.)
aus Berlin

Tübingen
2020

Gedruckt mit Genehmigung der Mathematisch-Naturwissenschaftlichen Fakultät der Eberhard Karls Universität Tübingen.

Tag der mündlichen Qualifikation:	12.01.2021
Stellvertretender Dekan:	Prof. Dr. József Fortágh
1. Berichterstatter:	Jun.-Prof. Dr. Sara Kleindienst
2. Berichterstatter:	Prof. Dr. Christiane Zarfl

When we try to pick out anything by itself,
we find it hitched to everything else in the universe.

John Muir (1911)

Table of contents

Summary

Accidental crude oil or fuel spills can cause substantial environmental damage in marine ecosystems. During the emergency spill response and remediation efforts after marine oil spills, chemical dispersants (= solvent-surfactant mixtures) are often applied with the aim of reducing ecological and economic damage due to floating and beached oil. However, due to their inherent toxicity potential and a number of uncertainties regarding their ecological effects, the use of chemical dispersants remains controversial. Particularly large knowledge gaps were identified regarding the influence of chemical dispersants on affected seawater microbial communities and specifically oil/hydrocarbon-degrading microorganisms, even though they play a crucial role in determining the fate of spilled oil in the marine environment. The scientific literature on this topic is characterized by largely unexplained contradictory findings and a remarkable lack of data on the underlying causes and mechanisms of the observed dispersant effects on oil-degrading bacteria and their cellular processes. Therefore, the goal of this thesis was to determine and elucidate the impacts of chemical dispersants on oil-degrading microorganisms by examining their effects on different ecological levels.

The first aim of this project was to determine the response of environmental seawater microbial communities from the Arctic Ocean (**Chapter 2**) and the North Sea (**Chapter 3**) to chemical dispersant exposure. This was achieved by performing laboratory microcosm experiments that simulated the water column conditions during a crude oil spill with and without chemical dispersant (Corexit EC9500A) addition, and monitoring oil biodegradation potential, as well as microbial community dynamics. While biodegradation of *n*-alkanes or small aromatic hydrocarbons was not substantially affected by chemical dispersant addition, lower cell numbers and the enrichment of a distinct community of hydrocarbon- and/or dispersant-degrading bacterial taxa were observed. Additionally, persistent organic compounds (likely dispersant-derived solvents) were detected in dispersant-amended microcosms in both experiments, with particularly high levels persisting in the Arctic Ocean seawater microcosms after 32 days. Remarkably, the observed impacts of chemical dispersants were largely consistent across both experiments (i.e. Arctic Ocean and North Sea seawater) and all investigated incubation temperatures (i.e. 1°C, 5°C, 15°C), indicating that they are relatively robust and environmentally relevant. An additional aim of the experiment with Arctic seawater was to determine the effects of biostimulation (i.e. addition of nitrate, ammonium, phosphate) during a simulated oil spill scenario, since this approach has only rarely been systematically compared with chemical dispersant addition. Interestingly, biostimulation led to enhanced microbial growth and biodegradation but did not alter the microbial community of enriched hydrocarbon degraders, in contrast to dispersant addition. Therefore, biostimulation was identified as a promising alternative approach to dispersant application when considering potential future Arctic Ocean oil spills.

The second aim of this thesis was to identify the effects of chemical dispersant exposure on the growth and alkane biodegradation activity of the hydrocarbon-degrading model organism *Marinobacter* sp. TT1 under different culture conditions (**Chapter 4**). Therefore, pure culture experiments with *Marinobacter* sp. TT1 cultures that were pre-adapted to either low or high

n-hexadecane concentrations (i.e. starved and well-fed cultures) were performed by supplying *n*-hexadecane ± Corexit EC9500A to both cultures. The growth of previously starved cells was significantly inhibited when exposed to the dispersant and *n*-hexadecane biodegradation efficiency was lowered by 30%. In addition, fluorescence microscopy suggested that starved cells altered their growing behaviour and modified their production of extracellular polymeric substances when exposed to Corexit. Well-fed cultures did not exhibit dispersant-induced inhibition of growth or *n*-hexadecane degradation. These results showed, for the first time, that substrate limitation, resembling oligotrophic open ocean conditions, can impact the response and hydrocarbon-degrading activities of oil-degrading organisms when exposed to Corexit, highlighting that the environmental relevance of laboratory experimental conditions and how they might affect experimental outcomes should be carefully considered.

The third aim was to zoom in even further and identify the underlying mechanisms of observed chemical dispersant effects on hydrocarbon-degrading bacteria on a cellular level (**Chapter 5**). To this end, additional pure culture experiments with *Marinobacter* sp. TT1 using different carbon sources ± chemical dispersant (Corexit EC9500A) were conducted and a comparative analysis of protein expression profiles associated with the different growth conditions was performed. For the first time, the proteins associated with a proposed microbial metabolism of Corexit components as carbon substrates were identified, revealing that *Marinobacter* sp. TT1 likely metabolized surfactants, cycloalkanes, (heteroatomic) aromatic HCs and linear alkanes (chain length < C_{16}) from the Corexit mixture. At the same time, Corexit-induced changes in the proteome linked to hydrocarbon metabolism, chemotactic motility, biofilm formation, and solvent tolerance mechanisms were discovered. This included increased abundances of proteins required for chemotactic motility, likely related to a variety of bioavailable carbon sources ('attractants') and potentially membrane-damaging levels of surfactants and solvents ('repellents'). In addition, increased abundances of efflux pump proteins known to confer solvent tolerance were detected. The first evidence of alginate biosynthesis associated with the metabolism of *n*-hexadecane in a member of the *Marinobacter* genus was also documented and distinct aggregate morphologies were observed across the growth conditions ± Corexit. Thus, the chemical dispersant Corexit was shown to affect aggregate/biofilm formation and induce solvent-stress response mechanisms in *Marinobacter* sp. TT1.

Taken together, the presented findings significantly deepen our understanding of how and why chemical dispersants impact oil-degrading microorganisms. Dispersant addition will likely impact most marine microbial communities, altering their composition by enriching certain hydrocarbon- or dispersant-degrading taxa and inhibiting others. The underlying mechanisms of these observed impacts involve the chemical dispersant affecting the cellular hydrocarbon metabolism, chemotactic motility, biofilm formation, and inducing solvent-tolerance mechanisms. In addition, chemical dispersants do not appear to typically enhance microbial oil biodegradation processes in the marine environment. Furthermore, several potential explanations for the inconsistent literature regarding dispersant effects on oil biodegradation were uncovered. These novel insights into dispersant impacts on oil-degrading microorganisms could have a wide range of potential environmental implications in the marine environment and should be taken into consideration during future oil spill response planning.

Zusammenfassung

Die ökologischen Folgen von Erdöleinträgen in die Weltmeere durch Öltankerhavarien oder Unfälle auf Ölplattformen sind oft verheerend für das marine Ökosystem. Bei größeren Ölunfällen gehört zu den möglichen Bekämpfungsmaßnahmen auch der Einsatz von chemischen Dispersionsmitteln (Mischungen aus Tensiden und Lösungsmitteln), die ökologische und finanzielle Schäden begrenzen sollen, indem sie Ölteppiche und Ölansammlungen an den Küsten reduzieren. Allerdings ist ihr Einsatz umstritten, da diese Mittel selbst toxisch sein können und ihre ökologischen Effekte noch nicht komplett erforscht sind. Besonders große Wissenslücken existieren bezüglich ihrer Effekte auf die mikrobiellen Gemeinschaften im Meerwasser und die Öl abbauenden Bakterien. Obwohl diese Bakterien die Kohlenwasserstoffe aus dem Öl verstoffwechseln können und somit eine wichtige Rolle bei der Beseitigung von bei Unfällen eingetragenem Öl im Meer spielen. Die wissenschaftliche Literatur zu diesem Thema beinhaltet viele (größtenteils unerklärte) widersprüchliche Ergebnisse und kaum Daten dazu, welche zellulären Mechanismen den beobachteten Effekten von chemischen Dispersionsmitteln auf Kohlenwasserstoff abbauende Bakterien zu Grunde liegen. Deshalb war das Ziel dieser Doktorarbeit, die Auswirkungen von chemischen Dispersionsmitteln auf Öl abbauende Mikroorganismen zu ermitteln und aufzuklären, wofür ihre Effekte auf verschiedenen ökologischen Ebenen untersucht wurden.

Zunächst wurde die Reaktion von mikrobiellen Meerwassergemeinschaften aus dem Arktischen Ozean (**Kapitel 2**) und der Nordsee (**Kapitel 3**) auf den Kontakt mit einem chemischen Dispersionsmittel (Corexit EC9500A) während eines simulierten Ölunfalls bestimmt. Hierfür wurden im Labor Mikrokosmenexperimente durchgeführt, die die Bedingungen im Meerwasser unter einem Ölteppich mit bzw. ohne Anwendung von chemischen Dispersionsmitteln simulierten, um anschließend den Ölabbau und die Entwicklung der mikrobiellen Gemeinschaften zu beobachten. Während der Abbau von Alkanen und kleinen aromatischen Kohlenwasserstoffen nicht wirklich von den chemischen Dispersionsmitteln beeinträchtigt wurde, wurden dennoch niedrigere Zellzahlen und die Entstehung einer anderen mikrobiellen Gemeinschaft aus Kohlenwasserstoff und/oder Dispersionsmittel abbauenden Bakterien beobachtet. Zudem wurden persistente organische Stoffe (vermutlich Lösungsmittel aus dem Dispersionsmitel) in Mikrokosmen mit zugegebenem Dispersionsmittel detektiert, welche in besonders großen Mengen nach 32 Tagen in den Mikrokosmen mit arktischem Meerwasser zurück blieben. Bemerkenswerterweise stimmten die beobachteten Auswirkungen des chemischen Dispersionsmittels in den beiden Experimenten (d.h. mit arktischem und Nordseewasser) und unter allen untersuchten Temperaturbedingungen (d.h. 1°C, 5°C, 15°C) weitgehend überein, was darauf hinweist, dass diese Auswirkungen robust und ökologisch relevant sind. Ein weiteres Ziel des Experiments mit arktischem Meerwasser war es, die Effekte einer Biostimulation (d.h. Zugabe von Nitrat, Ammonium, Phosphat) während des simulierten Ölunfalls zu ermitteln, da diese Maßnahme bisher kaum systematisch mit der Anwendung von chemischen Dispersionsmitteln verglichen worden war. Interessanterweise führte die Biostimulation zu höherem mikrobiellen Wachstum und mehr Abbautätigkeit, wobei die Zusammensetzung der mikrobiellen Gemeinschaft aus Öl abbauenden Bakterien im Gegensatz zur Zugabe des chemischen Dispersionsmittels nicht

verändert wurde. Somit wurde Biostimulation als ein vielversprechender alternativer Ansatz zur Anwendung von chemischen Dispersionsmitteln im Kontext von potentiellen zukünftigen Ölunfällen im Arktischen Ozean identifiziert.

Anschließend wurden die Effekte eines Kontakts mit chemischen Dispersionsmitteln auf das Wachstum und den Alkanabbau des Kohlenwasserstoff abbauenden Modellorganismus *Marinobacter* sp. TT1 unter verschiedenen Kulturbedingungen bestimmt (**Kapitel 4**). Dafür wurden Experimente mit Bakterienkulturen dieses Stammes durchgeführt, welche entweder an niedrige Hexadekanverfügbarkeit (hungernde Kultur) oder hohe Hexadekankonzentrationen (gut ernährte Kultur) angepasst waren und anschließend mit Hexadekan ± Corexit versetzt wurden. Bei Zugabe von Corexit war das Wachstum der vorher hungernden Kultur signifikant gehemmt und es wurde 30% weniger Hexadekan durch die Kultur abgebaut. Zusätzlich deuteten Untersuchungen mittels Fluoreszenzmikroskopie darauf hin, dass die Aggregatbildung und die Produktion von extrazellulären polymeren Substanzen der vorher hungernden Kultur nach Zugabe von Corexit beeinträchtigt waren. Die vorher gut ernährte Kultur zeigte bei Kontakt mit Corexit hingegen keine Hemmung in Wachstum oder Hexadekanabbau. Diese Ergebnisse demonstrierten zum ersten Mal, dass Substratlimitierung, welche die Bedingungen im oligotrophen offenen Ozean widerspiegelt, die Reaktion von Kohlenwasserstoff abbauenden Bakterien auf Corexit beeinflussen kann. Dies unterstreicht auch, wie wichtig es ist, ökologisch relevante Experimentalbedingungen im Labor anzustreben und zu bedenken, wie diese Bedingungen den Ausgang von Experimenten beeinflussen können.

Um aufzuklären, welche Mechanismen den beobachteten Effekten von chemischen Dispersionsmitteln auf Kohlenwasserstoff abbauende Bakterien auf zellulärer Ebene zu Grunde liegen (**Kapitel 5**), wurde schließlich noch weiter ins Detail gegangen und eine vergleichende Proteomanalyse durchgeführt. Hierfür wurden weitere Experimente mit dem Modellorganismus *Marinobacter* sp. TT1 durchgeführt, in denen die Kulturen verschiedene Kohlenstoffsubstrate ± chemisches Dispersionsmittel (Corexit EC9500A) bekamen. Anschließend wurden die mit den verschiedenen Kulturbedingungen assoziierten Proteinexpressionsprofile vergleichend analysiert. Auf diese Weise konnten zum ersten Mal Proteine identifiziert werden, welche mit einem vermuteten mikrobiellen Abbau von Corexitbestandteilen zusammenhängen. Es zeigte sich, dass *Marinobacter* sp. TT1 vermutlich Tenside, Cycloalkane, aromatische Kohlenwasserstoffe und lineare Alkane (Kettenlänge < C_{16}) aus der Corexit Mischung nutzen konnte. Gleichzeitig wurden durch Corexit verursachte Änderungen im Proteom entdeckt, die vor allem mit dem Metabolismus von Kohlenwasserstoffen, chemotaktischer Motilität, Biofilmbildung und Toleranzmechanismen gegenüber Lösungsmitteln in Verbindung standen. Diese Änderungen beinhalteten eine erhöhte Abundanz von Proteinen für chemotaktische Motilität, welche vermutlich durch die hohe Vielfalt an bioverfügbaren Kohlenstoffquellen (sog. Attractants) und möglicherweise membranschädigenden Konzentrationen von Tensiden und Lösungsmitteln (sog. Repellents) ausgelöst worden waren. Außerdem wurden erhöhte Abundanzen von Effluxpumpenproteinen detektiert, welche die Empfindlichkeit gegenüber Lösungsmitteln verringern können. Es konnten zudem die ersten Hinweise auf Alginatbiosynthese in einem *Marinobacter* spp. im Zusammenhang des Hexadekanabbaus dokumentiert werden und es wurde eine unterschiedlich

ausgeprägte Aggregatbildung zwischen den verschiedenen Wachstumsbedingungen beobachtet. Folglich konnte gezeigt werden, dass das chemische Dispersionsmittel Corexit einen Einfluss auf die Aggregat-/Biofilmbildung von *Marinobacter* sp. TT1 hatte und verschiedene Mechanismen der Lösungsmittel-spezifischen Stressabwehr auslöste.

Zusammen betrachtet vertiefen die präsentierten Erkenntnisse unser Verständnis davon wie und warum chemische Dispersionsmittel Auswirkungen auf Öl abbauende Mikroorganismen haben. Die Anwendung von Dispersionsmitteln im Meer hat vermutlich in den meisten Fällen ausgeprägte Effekte auf marine Mikrobengemeinschaften und verändert deren Zusammensetzung, indem bestimmte Kohlenwasserstoff oder Dispersionsmittel abbauende mikrobielle Gruppen bevorzugt angereichert und andere Gruppen gehemmt werden. Diesen Effekten liegen Mechanismen zu Grunde, die beinhalten, dass Dispersionsmittel den zellulären Metabolismus von Kohlenwasserstoffen, chemotaktische Motilität und Biofilmbildung verändern und Toleranzmechanismen gegenüber Lösungsmitteln auslösen. Außerdem scheinen Dispersionsmittel den mikrobiellen Ölabbau im Meer nicht zu stimulieren. Darüber hinaus wurden im Rahmen dieser Doktorarbeit mehrere mögliche Erklärungen für die inkonsistente Literaturlage zur Frage der Auswirkungen von chemischen Dispersionsmitteln auf Öl abbauende Mikroorganismen gefunden. Die in dieser Doktorarbeit erzielten neuen Einblicke könnten weitreichende ökologische Konsequenzen haben und sollten während zukünftiger Planung von Ölunfall-Bekämpfungsmaßnahmen berücksichtigt werden.

List of figures

List of tables

List of abbreviations

API	American Petroleum Institute
CEWAF	Chemically enhanced water-accommodated fraction
CFA	Continuous flow analysis
Cxt	Corexit
DAPI	4′,6-Diamidino-2-phenylindole
DCM	Dichloromethane
DGBE	Dipropylene glycol butyl ether
DNA	Deoxyribonucleic acid
DOC	Dissolved organic carbon
DOSS	Dioctyl sulfosuccinate
DUC	Danish Underground Consortium
DWH	Deepwater Horizon (drilling platform, Gulf of Mexico)
EOE	Estimated oil equivalents
EPS	Extracellular polymeric substances
FC	Log_2 fold change
GC-MC	Gas chromatography coupled to mass spectrometry
HC	Hydrocarbons
HPLC	High-performance liquid chromatography
Hxdc	*n*-Hexadecane
LC-MS/MS	Liquid chromatography–mass spectrometry/mass spectrometry
NMDS	Non-metric multidimensional scaling
PAH	Polycyclic aromatic hydrocarbons
qPCR	Quantitative polymerase chain reaction
SW	Seawater
TPH	Total petroleum hydrocarbons
UCM	Unresolved complex mixture
WAF	Water-accommodated fraction
WAF+N	Water-accommodated fraction with nutrients (nitrate, ammonium, phosphate)

1 Introduction

1.1 Crude oil in the marine environment

Crude oil has been used by human civilizations for construction and military purposes for thousands of years (Simanzhenkov and Idem, 2003) and during the last century, crude oil and its derived fuels became one of the major energy sources fuelling industrialized societies around the globe. The origin of crude oil, typically extracted from reservoirs in the Earth's crust, lies in the geological transformation of organic matter under conditions of high temperatures and pressures and over long time scales (Schobert, 2013). At the elemental level, the resulting crude oils, often also referred to as petroleum, are all fairly similar and only consist of carbon (82–87%) and hydrogen (11–15%), as well as low levels of sulphur, nitrogen and oxygen (typically each < 2%; Schobert, 2013). When considering the molecular composition, however, crude oils are a highly complex mixture of > 10,000 distinct compounds and no two crude oil reservoirs will produce the same chemical composition. Nevertheless, they contain only three major compound classes, i.e. aliphatic (= saturated) hydrocarbons (HCs), aromatic HCs and high molecular weight heteroatomic compounds referred to as asphalts and resins (Figure 1.1). The latter category represents the most complicated fraction of crude oils and only makes up 14% by weight on average (Tissot and Welte, 1978). Aliphatic HCs in crude oil can be further subdivided into alkanes (linear *n*-alkanes and branched-chain alkanes), and cycloalkanes (typically cyclopentanes and cyclohexanes), which are also referred to as paraffins and naphthenes, respectively, in petrochemistry. Together, these aliphatic HCs make up the largest part of the HC fraction in crude oils with an average 33% and 32% by weight, respectively, followed by aromatic HCs (i.e. unsaturated HCs with one or more ring structures), which represent the remaining 35% of the HC fraction (Tissot and Welte, 1978). Due to their widely differing, complex chemical composition, crude oils from different extraction locations are typically compared via a few physicochemical properties, such as the so-called API (= American Petroleum Institute) gravity, which is a measure of how light or heavy (i.e. dense) a liquid is compared to water, with an API gravity > 10 signifying that the oil would float on water. This parameter is often used to categorize crude oils into light (API gravity > 31.1), medium (22.3 – 31.1) and heavy (< 22.3) crude oils. Three different crude oils from the Gulf of Mexico (Macondo MC252 oil) and North Sea oil fields (Grane oil and Danish Underground Consortium = DUC oil) with an API gravity range of 28.4 – 40 were used for the research presented in this thesis (Table 1.1).

Table 1.1: Comparison of composition and properties of the three crude oils used in this thesis. Macondo MC252 crude oil from the Gulf of Mexico was used for experiments in Chapter 2. Grane and DUC crude oils from the North Sea were used for experiments in Chapter 3 and 5, respectively. n.a. = data not available.

	Macondo MC252[1]	Grane[2]	DUC[3]
API gravity and classification	40 light crude oil	28.4 medium crude oil	34.3 light crude oil
Carbon [weight %]	86.6	86.3	n.a.
Sulfur [weight %]	0.39	0.62	0.26
Saturated HCs [volume %]	74	24.6	n.a.
Aromatics [volume %]	16	38.1	n.a.

[1] Reddy *et al.* (2012); [2] ExxonMobil (2018); [3] Personal communication, Constantin App

Crude oil can enter the marine environment via two distinct routes, i.e. geophysical processes at natural seeps on the seafloor or through anthropogenic processes. Both routes are estimated to contribute about half of the total yearly crude oil input into the marine environment (1,300,000 t) on average (US NRC, 2003). Natural HC seeps have been discovered throughout the world's oceans and generate continuous fluxes of oil and/or gas (typically methane) into the marine environment, fueling unique ecosystems (e.g. reviewed by Joye and Kleindienst, 2017). Anthropogenic inputs of crude oil are related to the consumption, transportation and extraction of petroleum, making up 38%, 16% and 3%, respectively, of the total estimated yearly input (US NRC, 2003). Petroleum consumption as the largest fraction mainly introduces crude oil into the sea through land-based inputs via rivers and runoff and the often overlooked operational discharges related to worldwide shipping activities, which consist of countless small discharges of bilge oil, fuel oil residues or oily ballast waters, amounting to 20% of estimated yearly petroleum releases worldwide (US NRC, 2003). Another large fraction which can vary considerably from year to year are accidental transportation-related inputs, i.e. pipeline and tanker spills, which will be the focus of this thesis.

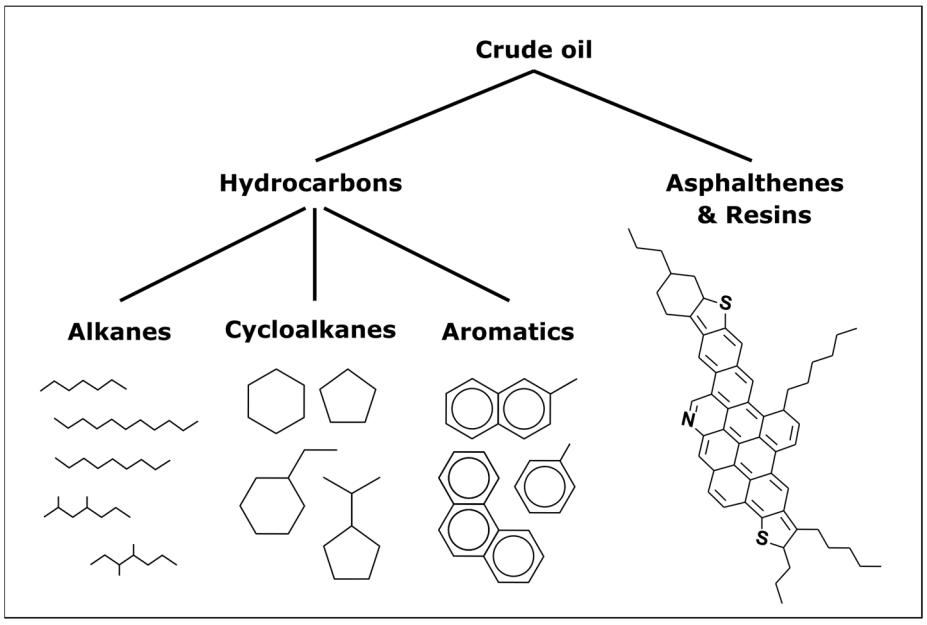

Figure 1.1: Crude oil composition including representative molecular structures of typical hydrocarbon (alkanes, cycloalkanes, aromatics) and non-hydrocarbon (asphaltenes, resins) components.

Once in the marine environment, the fate of crude oil is determined by a myriad of factors related to its own physicochemical properties (e.g. density and viscosity), local weather and oceanographic conditions (e.g. wave activity, UV radiation, wind, currents) and biological processes (US NRC, 2003; Joye *et al.*, 2016b; ITOPF, 2020). Typically, an oil slick would form on the sea surface, which can subsequently spread out, partially dissolve and emulsify with the seawater below and undergo different weathering processes, such as evaporation of low molecular weight HCs, photo-oxidation and microbial biodegradation (Figure 1.2).

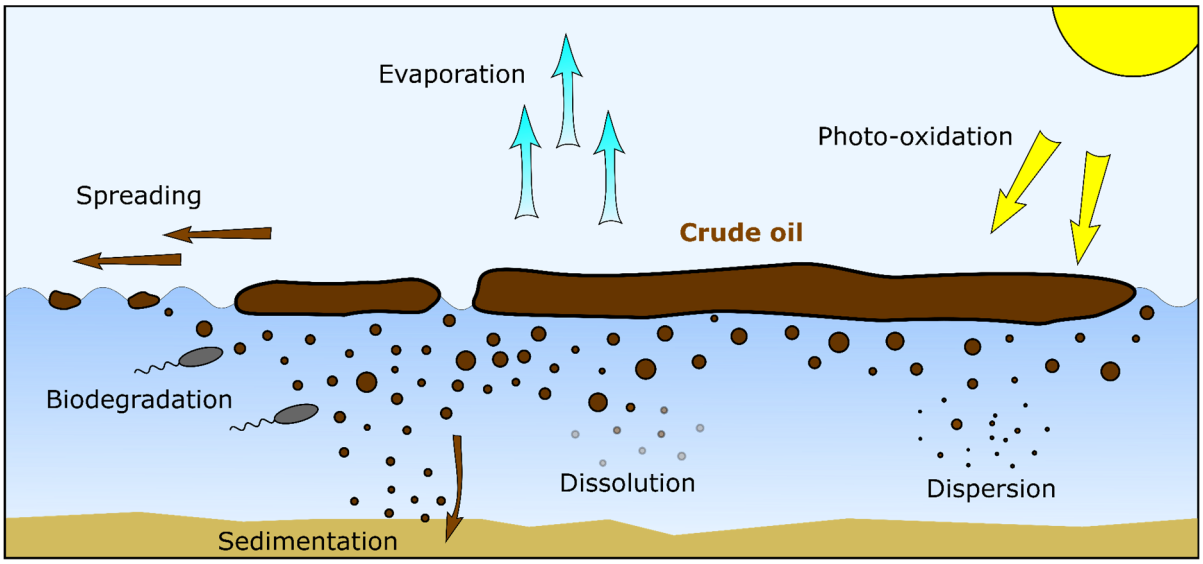

Figure 1.2: Schematic overview of physicochemical and biological processes determining the fate of crude oil in the sea.

1.2 Microbial oil biodegradation

All components of crude oil are biodegradable to a certain extent, even though asphaltenes and resins, for example, are less readily degraded than the HC fraction (Liao *et al.*, 2009; Tavassoli *et al.*, 2012; Hernández-López *et al.*, 2015) and will therefore not be the focus of this thesis. Petroleum HCs, on the other hand, are considered particularly energy rich compounds because their oxidation with oxygen can release large amounts of energy (Widdel and Musat, 2019). This is the reason for their widespread use as fuels for our vehicles, ships and planes and it is also the reason that they represent an attractive energy source for microorganisms. In fact, a wide variety of oil-degrading microorganisms has evolved that can use linear, cyclic, and aromatic HCs as energy and carbon sources for their metabolism (Ollivier and Magot, 2005; Head *et al.*, 2006; Hazen *et al.*, 2016). Numerous HC-degrading archaeal, fungal and algal taxa have been described (Ollivier and Magot, 2005; Spang *et al.*, 2017; Oren, 2019; Prince, 2019) and a recent review identified over 300 bacterial genera with known HC-degrading capabilities (Prince *et al.*, 2019), illustrating that large parts of the microbial world are able to utilize HCs. HC-degrading bacteria have been described from the phyla Actinobacteria (e.g. *Rhodococcus, Mycobacterium*), Bacteroidetes (e.g. *Olleya, Flavobacterium*), Cyanobacteria (e.g. *Anabena, Oscillatoria*), Firmicutes (e.g. *Bacillus, Sarcina*), Verrucomicrobia, Deinococcus-Thermus and even some that fall into the newly described Candidate Phyla Radiation, however, the vast majority of well-characterized HC degraders belong to the gram-negative phylum Proteobacteria (Prince *et* al., 2019). This includes most methanotrophic bacteria, many

anaerobic HC degraders (e.g. several sulfate-reducers belonging to Deltaproteobacteria) and many aerobic marine HC degraders (e.g. *Alteromonas, Colwellia, Glaciecola, Halomonas, Marinobacter, Neptuniibacter, Profundimonas, Pseudomonas, Vibrio*), among them the group termed obligate HC degraders (Yakimov *et al.*, 2007). Currently 11 genera have been reported to contain obligate HC degraders (i.e. *Alcanivorax, Oleiphilus, Oleispira, Oleibacter, Thalassolituus, Marinobacter, Cycloclasticus, Neptunomonas, Algiphilus, Polycyclovorans, Porticoccus*) and many of them have been detected ubiquitously throughout the world's ocean at low abundances that can rapidly increase after petroleum HCs reach the ecosystem (Head *et al.*, 2006; Yakimov *et al.*, 2007; Gutierrez, 2019). Obligate HC-degrading bacteria are characterized by almost exclusively utilizing HCs as their energy and carbon sources, i.e. they might be able to alternatively use a few organic acids (e.g. pyruvate or acetate) when grown in pure culture but do not metabolize amino acids or sugars, prompting questions about their survival in marine environments without obvious oil contamination (Gutierrez, 2019). Interestingly, both biogenic and abiogenic alternative HC sources potentially sustaining these organisms in the ocean have been identified (Lea-Smith *et al.*, 2015; Gutierrez, 2019), such as atmospheric HC deposition from fossil fuel consumption or volcanic eruptions, biomass-derived HCs (e.g. chlorophyll, cell membrane components, lipids) or HC-containing exudates from phytoplankton and algae, which could also explain the large diversity of HC-degrading microorganisms. The genus *Marinobacter*, on the other hand, represents a different common type of marine HC degraders, as its members are versatile heterotrophs who readily utilize a variety of organic carbon sources and opportunistically respond to the most available compounds, including HC inputs in the form of oil pollution (Duran, 2010; Mounier *et al.*, 2014; Kleindienst *et al.*, 2015b; Tremblay *et al.*, 2017). The type strain *Marinobacter hydrocarbonoclasticus* SP.17 (Gauthier *et al.*, 1992), for example, is an efficient alkane degrader and recently, the novel alkane-degrading member *Marinobacter* sp. TT1, selected as model organism for this thesis, was isolated from oil-affected seawater collected during the Deepwater Horizon oil spill in the Gulf of Mexico (Gutierrez *et al.*, 2013b).

The metabolic pathways of aliphatic and aromatic HC degradation are relatively well explored for model organisms like *Alcanivorax borkumensis* and *Pseudomonas putida* (e.g. reviewed by Wang and Shao, 2013; Abbasian *et al.*, 2016) and have recently also been described in other isolates (Park *et al.*, 2017; Gregson *et al.*, 2018, 2020). Due to their lack of functional groups, HCs are relatively unreactive at room temperature, which means that the first step and main hurdle to their biological oxidation is always an activation reaction that introduces a functional group (Widdel and Musat, 2019). The aerobic biodegradation of *n*-alkanes, for example, is initiated by monooxygenases with specific substrate ranges, such as heme-iron monooxygenases (also referred to as soluble cytochrome P450), non-heme-iron monooxygenases (AlkB-type) or, in the case of long-chain alkanes ($C_{18–40}$ chain lengths), different flavin-dependent monooxygenases like AlmA and LadA (Wentzel *et al.*, 2007; Park *et al.*, 2017). The resulting primary alcohols are further oxidized by alcohol and aldehyde dehydrogenases to produce fatty acids which are channelled into the cytosolic fatty acid metabolism via ß-oxidation (Wang and Shao, 2013; Abbasian *et al.*, 2016), leading to biomass production (assimilatory metabolism) and/or release of CO_2 as the final oxidation product (dissimilatory metabolism). Aromatic HC molecules are activated by different ring-hydroxylating mono- or dioxygenases and through further transformations also reach the

cellular tricarboxylic acid (TCA) cycle (Pérez-Pantoja *et al.*, 2010; Abbasian *et al.*, 2016). The anaerobic biodegradation of HCs, e.g. in anoxic marine sediments, typically proceeds much slower and is characterized by more diversity in initial oxidation steps that can involve oxygen-independent hydroxylation and carboxylation or the addition of fumarate (e.g. reviewed by Widdel and Rabus, 2001; Davidova *et al.*, 2019).

This thesis will focus on aerobic microbial oil biodegradation in the marine environment, which is controlled by a number of factors. For example, oxygen and nutrient (i.e. nitrogen, phosphorous, iron) availability (Atlas and Bartha, 1972; Widdel and Musat, 2019), temperature conditions (Venosa and Holder, 2007; Lofthus *et al.*, 2018; Sun and Kostka, 2019) and the site-specific microbial community can all affect the success and rate of marine oil biodegradation. The latter point is particularly important because it will determine what kind of microbial consortia develop in response to oil exposure and since most bacteria only degrade a narrow range of HCs, the cooperation and succession of microbial consortia are typically required for efficient oil removal (Head *et al.*, 2006; McGenity *et al.*, 2012; Wang *et al.*, 2020). Furthermore, due to their different bioavailability, low molecular weight HCs are often degraded faster than high molecular weight compounds and alkanes are often degraded before aromatic HCs by environmental seawater communities during these succession processes (Wang *et al.*, 1998; Head *et al.*, 2006). The bioavailability of lipophilic HCs can, however, also be improved by different HC-degrading microorganisms that were shown to produce extracellular enzymes and/or amphiphilic extracellular polymeric substances (EPS), including biosurfactants, when encountering HCs (Head *et al.*, 2006; McGenity *et al.*, 2012; Gutierrez *et al.*, 2013a).

1.3 Marine crude oil spill scenarios

As described above, the widespread use of crude oil and its derived fuel types inevitably results in oil discharges into the environment. Compared to the more diffuse petroleum inputs of either natural seeps or shipping activity and fuel consumption (also termed chronic pollution), accidental marine crude or fuel oil spills are often characterized by the release of large volumes of petroleum components at one location and over a relatively short time frame. From an ecological perspective, this explains their often catastrophic immediate and long-term consequences on the marine ecosystem (Peterson *et al.*, 2003; Short, 2017). Crude oil slicks present a deadly hazard to mammals and birds that frequent the sea surface layer or affected coastal zones and the most toxic components of crude oil (i.e. the aromatic HCs) also typically dissolve best in the water column below the slick, endangering fish, plankton populations, and benthic organisms like corals, all of which are key players in the marine food web (Peterson *et al.*, 2003; US NRC, 2003; Neuparth *et al.*, 2012; Short, 2017). Additionally, numerous authors have argued that sublethal contamination impacts and long-term effects remain understudied (e.g. Peterson *et al.*, 2003; Kirby and Law, 2010; Neuparth *et al.*, 2012; Barron *et al.*, 2020; Mayer-Pinto *et al.*, 2020). Due to the dramatic and often highly publicized effects of marine oil spills, large public and scientific interests in them, as well as different (inter)national regulations, have developed during the last decades which were often motivated by the most recent large spill disasters (Table 1.2). It is important to note that although the amount of spilled oil is an important parameter to consider when assessing oil spills, it is only one of many factors that determine the extent of environmental and economic damage caused by a spill, with e.g.

smaller nearshore spills often considered particularly harmful and cost intensive (Etkin, 2000; Short, 2017).

One of the first large accidents that was accompanied by a lot of media attention took place in 1967 when the large tanker *Torrey Canyon* ran aground close to the UK Scilly Isles. Within days, 119,000 t of crude oil spilled into the English Channel and towards the French coast, revealing substantial shortcomings in (international) legislation, efficient response technology and the scientific knowledge on potential environmental impacts (Burrows *et al.*, 1974). Documented ecological effects of the spill included at least 10,000 killed birds and significant damage to coastal fauna and flora and these observations were partially responsible for subsequently increasing efforts to improve spill preparedness by different stakeholders (Burrows *et al.*, 1974; Burgherr, 2007). A tanker accident with similar levels of public interest and concern took place when the tanker *Exxon Valdez* grounded on a reef in March 1989, releasing at least 37,000 t of its crude oil cargo into the Prince William Sound in Alaska, USA (US NRC, 2003). The environmental damage to the vulnerable ecosystem was unprecedented and yielded new insights into ecological oil spill impacts, such as the embryotoxicity of crude oil to fish, the indirect effects of oil exposure through ecological food webs, the long-term damages associated with oil persistence on beaches and sometimes decade-spanning recovery of several animal populations (Peterson *et al.*, 2003; US NRC, 2003; Short, 2017; Barron *et al.*, 2020). Much larger spill volumes of crude oil are typically recorded during accidents associated with drilling platforms, of which a few have occurred in the Gulf of Mexico due to widespread oil exploration activities in this area. The first notable one occurred in 1979 when the Ixtoc I exploratory oil well blew out, resulting in the release of an estimated 475,000 t into the Gulf until the well was finally capped 290 days later (Jernelöv and Lindén, 1981). This accident held the title of the world's largest oil spill for a long time and severely affected local fish, shrimp and mollusc populations among others (Jernelöv and Lindén, 1981). In 2010, however, another large well blowout occurred at the Deepwater Horizon (DWH) drilling platform that killed 11 workers on the platform and led to the largest oil spill disaster that was ever recorded (DWH NRDA Trustees, 2016; Short, 2017). An estimated 656,000 t of crude oil (Macondo MC252) was released into the Gulf ecosystem over 84 days until the open well head could be capped (McNutt *et al.*, 2012), where it caused substantial environmental damage, that has been well-characterized compared to other oil spills by a giant interdisciplinary research effort (Beyer *et al.*, 2016; DWH NRDA Trustees, 2016; Murphy *et al.*, 2016; Kujawinski *et al.*, 2020). Among others, salt marshes, seabird populations, marine mammals and fish, phytoplankton populations and seafloor corals were severely affected, with the total damage described as an 'ecosystem-level injury' (Beyer *et al.*, 2016; DWH NRDA Trustees, 2016; Joye *et al.*, 2016a).

Table 1.2: Selected oil spills in the marine environment between 1967 and 2020.

Year	Location	Spill source	Spilled oil	Spill volume	References
1967	Scilly Isles, UK	*Torrey Canyon* (tanker)	Crude oil	119,000 t	ITOPF (2020)
1978	Off Brittany, France	*Amoco Cadiz* (tanker)	Crude oil	223,000 t	ITOPF (2020)
1979	Gulf of Mexico	Ixtoc I (platform)	Crude oil (and gas)	475,000 t	Jernelöv and Lindén (1981)
1989	Prince William Sound, Alaska, USA	*Exxon Valdez* (tanker)	Crude oil	37,000 t	ITOPF (2020)
1991	Genoa, Italy	*Haven* (tanker)	Crude oil	144,000 t	ITOPF (2020)
1991	Persian Gulf, Iraq	Gulf war (intentional release)	Crude oil	1,770,000 t	US NRC (2003)
1992	La Coruna, Spain	*Aegean Sea* (tanker)	Crude oil	74,000 t	ITOPF (2020)
1993	Shetland Islands, UK	*Braer* (tanker)	Crude oil	85,000 t	ITOPF (2020)
1996	Off Wales, UK	*Sea Empress* (tanker)	Crude oil (+ fuel oil)	72,000 t (+ 480 t)	Neuparth *et al.* (2012)
1999	Brittany, France	*Erika* (tanker)	Heavy fuel oil	19,000 t	Neuparth *et al.* (2012)
2002	Off Galicia, Spain	*Prestige* (tanker)	Heavy fuel oil	63,000 t	Neuparth *et al.* (2012)
2004 (may be ongoing)	Gulf of Mexico	Taylor Energy 23051 (platform)	Crude oil	estimates unclear	Mason *et al.* (2019)
2007	South Korea	*Hebei Spirit* (tanker)	Crude oil	11,000 t	ITOPF (2020)
2010	Gulf of Mexico	Deepwater Horizon (platform)	Crude oil (and gas)	at least 656,000 t (+ 250,000 t)	McNutt *et al.* (2012); Joye (2015)
2019	Brittany, France	*Grande America* (container ship)	Heavy fuel oil	2,200 t	BBC News (2019)
2020	Mauritius	*Wakashio* (bulk carrier)	Heavy fuel oil	at least 1,000 t	Khadka (2020)

Generally, the emergency spill response strategies employed after marine oil spills aim to recover a large fraction of the spilled oil and/or reduce the expected ecological harm that it can cause (Figure 1.3). Typical response technologies include mechanical containment of the oil at the sea surface via floating booms around spreading oil slicks and subsequent removal of the oil via specialized skimming equipment, sorbents and/or *in situ* burning of the oil slicks (ExxonMobil, 2014). Additionally, the chemical dispersion of oil slicks into the water column can be achieved by applying so-called chemical dispersant mixtures (ExxonMobil, 2014). The success of all these techniques depends on how fast after the spill they can be applied, on the composition of spilled petroleum substances, and on the weather conditions. Rough seas can complicate or prevent all ship-based operations and boom use, as is frequently the case, such as during the *Torrey Canyon* spill (Burrows *et al.*, 1974), the Ixtoc I spill (Jernelöv and Lindén, 1981), or the *Grande America* spill (Loeffler, 2019).

A complementary approach that can be pursued during or after these physicochemical response strategies puts the microbial oil spill remediation (i.e. bioremediation) potential into focus and aims to enhance naturally occurring oil biodegradation by increasing its speed and efficiency (Swannell *et al.*, 1996; Nikolopoulou and Kalogerakis, 2010; Dave and Ghaly, 2011). Bioremediation-based strategies of oil spill response are often considered less invasive and thus more environmentally friendly than physical or chemical techniques and can also represent the most cost effective response option (Etkin, 2000; Dave and Ghaly, 2011). The attempts to enhance naturally occurring oil biodegradation processes typically encompass supplying additional oil-degrading microorganisms (referred to as bioaugmentation), oxygen (e.g. in the case of sediments or developing anoxic water zones), or nutrients, which is termed biostimulation (Nikolopoulou and Kalogerakis, 2010; Adams *et al.*, 2015). Results of bioaugmentation studies in marine locations or samples have been mixed, largely because the native environmental community already contains seed populations of HC-degrading bacteria that are adapted to the *in situ* conditions in contrast to laboratory strains (Atlas, 1995; Swannell *et al.*, 1996). Biostimulation can be more promising since environmental oil biodegradation is often nutrient-limited in seawater (Atlas and Bartha, 1972; Head *et al.*, 2006). The *Exxon Valdez* spill in Alaska represents a prominent example of biostimulation as a successful oil spill response strategy. Approximately 50 t of nitrogen and 5 t of phosphorous were applied to oiled intertidal shorelines and reportedly enhanced oil biodegradation in these areas (Curl *et al.*, 1992; Bragg *et al.*, 1994). Even though biostimulation is more commonly described for contaminated soil or sediment systems (Adams *et al.*, 2015), it was also shown to improve seawater remediation under laboratory conditions (Coulon *et al.*, 2007; Crisafi *et al.*, 2016; Ortmann *et al.*, 2019; Sun and Kostka, 2019). Ecological concerns mainly relate to applied concentrations since excessive nutrients might also enrich non-targeted microorganisms or cause eutrophic conditions, although open ocean conditions might rather present rapid dilution challenges (Nikolopoulou and Kalogerakis, 2010). It has therefore been recommended to adjust nutrient concentrations and ratios to site-specific requirements (Bragg *et al.*, 1994; Nikolopoulou and Kalogerakis, 2010; Gutierrez *et al.*, 2018) and different commercial fertilizer mixtures (i.e. oleophilic or slow-release products) have been developed, although some of their components themselves were revealed to be hazardous and/or biodegraded before oil HCs in some studies (Swannell *et al.*, 1996; Nikolopoulou and Kalogerakis, 2010).

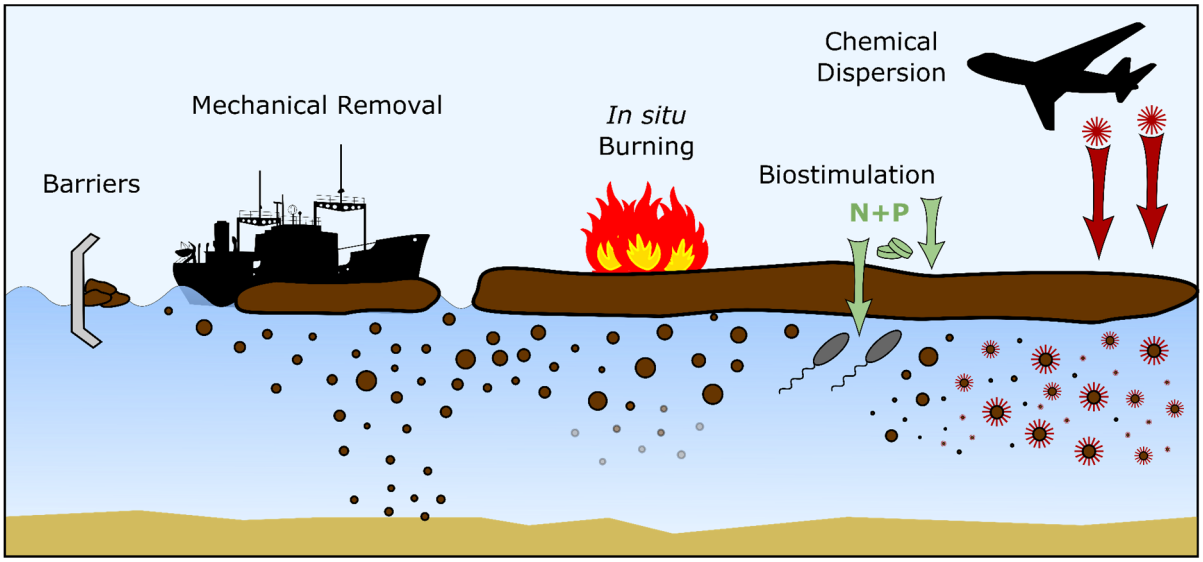

Figure 1.3: Schematic overview of selected emergency response strategies employed during marine crude oil spill scenarios.

According to recent data from the International Tanker Owners Pollution Federation, global tanker spill accidents have decreased significantly over the last 50 years, demonstrating that improved spill prevention and operational safety measures (e.g. double-hulled tankers, increased liability, improved safety management, automatic ship identification systems) have taken effect (Burgherr, 2007; ITOPF, 2020). However, 80% of tanker spills occur within 10 nautical miles of coastlines (ITOPF, 2020) and therefore represent the largest ecological and economic risks (Etkin, 2000; Short, 2017). Additionally, noteworthy oil spills putting vulnerable marine ecosystems at risk are still occurring on a regular basis. This is evidenced by the recent examples of an accidental fuel oil spill in French waters in March 2019 (BBC News, 2019; Loeffler, 2019), the accidental release of over 20,000 t of Diesel oil in Siberia (Norilsk, Russia) that likely reached the Arctic Ocean (May 2020; BBC News, 2020; Skarbo, 2020) or the currently (August 2020) unfolding tanker accident near two environmentally protected marine areas in Mauritius (Khadka, 2020). It is also likely that potential future spills will lead to increasingly complex and difficult spill response conditions, due to oil exploration activities currently moving into deeper waters and previously less impacted regions like the Arctic (Harsem *et al.*, 2015; Gutierrez, 2018; Murawski *et al.*, 2020). At the same time, a lack of ecological baseline data regarding pre-spill conditions in marine ecosystems remains one of the main challenges in assessing immediate and long-term ecological impacts after accidental marine spills (Neuparth *et al.*, 2012; Joye, 2015; Gutierrez, 2018). Therefore, since marine oil spills can still not be avoided completely, improving our understanding of these scenarios in different marine habitats and how best to respond to them remains crucial.

1.4 Chemical dispersant application after marine oil spills

The chemical dispersants applied during oil spill response efforts are solvent-surfactant mixtures meant to improve the dissolution of oil in water by forming dispersant-stabilized small oil droplets (Figure 1.4). Dispersant application is therefore supposed to reduce surface slicks and oil delivery to shoreline ecosystems, as well as increase the oil's bioavailability for biodegradation processes due to an increased oil surface area in the water column (John *et al.*,

2016; US NASEM, 2020). The first documented application of chemical dispersants took place after the *Torrey Canyon* spill in 1967, when a total of 11,500 t of so-called detergent mixtures were applied at sea and on the shorelines to disperse or remove the spilled oil (Burrows *et al.*, 1974). These detergents were highly toxic and major damage was reportedly caused to intertidal marine life (e.g. crustaceans, fish, worms, algae, sea anemones) by the coastal detergent use (O'Sullivan and Richardson, 1967; Burrows *et al.*, 1974). Oil spill response efforts in subsequent years attempted to avoid the application on oiled coastlines or close to vulnerable coastal ecosystems if possible and dispersant formulations were further developed with the aim of reaching lower toxicities (Bellier and Massart, 1979; Bocard *et al.*, 1979; Gilfillan *et al.*, 1985; Prince, 2015). Nevertheless, chemical dispersants have been used in many spill scenarios since then, especially when rough seas prevented other mechanical remediation strategies, although comprehensive documentation is not always publicly available. In total, over 200 instances of dispersant use have reportedly occurred between 1968 and 2007 (Steen and Findlay, 2008). Some known instances of significant dispersant application during marine oil spill remediation efforts include the Ixtoc I spill, the *Amoco Cadiz* spill and the *Sea Empress* spill (Table 1.3). Additionally, several field experiments with near- or offshore oil spill simulations and dispersant applications off the US coast (e.g. 1981 in Maine) or in the North Sea (1991-1996) were performed with second or third generation dispersant mixtures, which provided additional knowledge on their effectiveness and some limited ecological data (Gilfillan *et al.*, 1985; Lewis *et al.*, 1998). Generally, the effectiveness of chemical dispersant application (i.e. the amount of oil additionally dispersed into the water column) depends on the composition and weathering status of spilled crude oil, the water temperature, wave action (or mechanical means of agitation) and the availability of technical equipment for quick and targeted application procedures (Trudel, 1998; Holder *et al.*, 2015; Sørheim *et al.*, 2020).

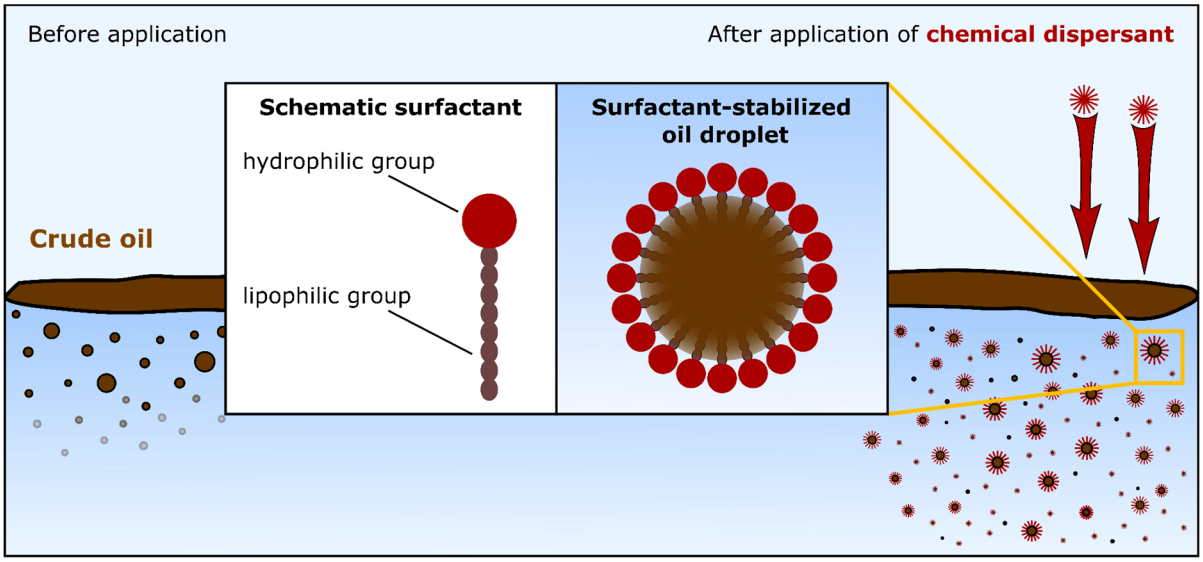

Figure 1.4: Schematic representation of chemical dispersant application and the mechanism of crude oil dispersion from an oil slick. Based on Kleindienst *et al.* (2015a).

In 2010, unprecedented amounts of chemical dispersants were applied in response to the DWH oil spill in the Gulf of Mexico, when at least seven million litres of Corexit EC9500A and EC9527A were used to disperse the estimated 800 million litres of crude oil released into the Gulf ecosystem (US Nat. Comm. DWH, 2011; McNutt *et al.*, 2012). The dispersants were sprayed onto the sea surface from planes or ships and targeted the floating oil slick with the goal of protecting the shorelines of the Gulf (US Nat. Comm. DWH, 2011). In addition to the large amounts of oil released, remediation efforts were further complicated by the fact that the spill was occurring via an open wellhead at 1,500 m depth, i.e. in the deep sea, revealing a general unpreparedness in efficiently responding to such spill conditions. An additional application of chemical dispersants was initiated by injecting Corexit dispersants directly above the leaking wellhead, with the purpose of preventing the released oil from reaching the surface and minimizing the contact of response workers to hazardous chemical dispersants during application (Kujawinski *et al.*, 2011; US Nat. Comm. DWH, 2011; Joye, 2015). This marked the first use of chemical dispersants in the deep ocean and led to the unforeseen formation of a HC- and surfactant-enriched deep sea plume at 1,000–1,200 m depth (Kujawinski *et al.*, 2011; Reddy *et al.*, 2012), which was over 35 km long and up to 200 m high (Camilli *et al.*, 2010). Large concern was expressed by scientists and local citizens over the application of Corexit dispersants in these unprecedented volumes and ways, citing the largely proprietary formulation of these synthetic mixtures and the large knowledge gaps that existed in the scientific literature regarding potential ecological impacts (US Nat. Comm. DWH, 2011; Kleindienst *et al.*, 2015a). Although the fate of spilled oil, gas and applied chemical dispersants has been the subject of numerous studies, available estimates carry considerable uncertainty (Kujawinski *et al.*, 2011; Reddy *et al.*, 2012; Joye, 2015). Generally, it is assumed that a large fraction of released HCs were either deposited on the seafloor by sedimentation as part of oil-containing organic matter (termed marine oil snow) or degraded by seawater microorganisms (Joye, 2015), highlighting the important role of microbiological processes in determining the fate of spilled oil. Ever since the DWH oil spill, numerous scientific studies have been conducted to assess the environmental impacts of the released oil (e.g. reviewed in Beyer *et al.*, 2016; DWH NRDA Trustees, 2016; Joye *et al.*, 2016a) and scientific interest in the impacts of chemical dispersant use in the marine environment was amplified (Kleindienst *et al.*, 2015a; Murphy *et al.*, 2016; Gutierrez, 2017).

1.5 Ecological impacts of chemical dispersant use

Although currently used chemical dispersants are generally considered less toxic than those first used in 1967 during the *Torrey Canyon* disaster and they are assumed to reduce immediate death tolls among birds from floating oil (Prince, 2015), their use remains controversial. This is mainly related to the following factors: Their often proprietary formulation complicates comprehensive toxicity assessments, their components themselves (i.e. solvents and surfactants) can be toxic to biological organisms, their application by design increases the concentration of toxic oil components in the water column, dispersed oil could then be more toxic than both components - crude oil and dispersant - alone (i.e. synergistic toxicity), their long-term ecological effects are mostly unknown and their impact on naturally occurring oil biodegradation processes remains debated (Kleindienst *et al.*, 2015a; Prince, 2015; Gutierrez, 2017; US NASEM, 2020).

Table 1.3: Selected instances of marine chemical dispersant application.

Year	Location	Spill source	Dispersants	Notes	References
1967	Scilly Isles, UK	*Torrey Canyon* (tanker)	BP1002, Dasic	11,500 t; first documented application	Burrows *et al.* (1974)
1978	Off Brittany, France	*Amoco Cadiz* (tanker)	BP 1100 X/WD, Finasol OSR 2/5	at least 13,000 t	Bocard *et al.* (1979)
1979	Gulf of Mexico	Ixtoc I (platform)	mainly Corexit	at least 9,000 t	Jernelöv and Lindén (1981)
1981	Long Cove coast, Maine, USA	Field experiment, simulation of small oil spill	unknown	Part of US field trial series	Gilfillan *et al.* (1985)
1989	Prince William Sound, Alaska, USA	*Exxon Valdez* (tanker)	Corexit EC9527A	Limited test applications documented	(Trudel, 1998); Hunt (2016)
1991 — 1995	North Sea, off eastern UK coast	Field experiments, simulation of small oil spills	Slickgone, BP 1100 X, Corexit, Finasol	Dispersant effectiveness tests at sea	Lewis *et al.* (1998)
1993	Shetland Islands, UK	*Braer* (tanker)	unknown	120 t were applied	Goodland (1998)
1996	Off Wales, UK	*Sea Empress* (tanker)	Slickgone NS/LTSW, Finasol OSR51/52	442 t used to disperse estimated 50% of oil	P.O.S.T. (1996); Lunel (1998)
2007	South Korea	*Hebei Spirit* (tanker)	unknown	unknown	Hunt (2016)
2010	Gulf of Mexico	Deepwater Horizon (platform)	Corexit EC9527A & EC9500A	at least 7,000 t; 1st deep sea application	US Nat. Comm. DWH (2011)

Studies conducted after the DWH spill revealed that dispersant application likely reduced the amount of floating oil, while increasing the area covered by oil slicks (MacDonald *et al.*, 2015), which, together with the subsurface plume formation, likely led to a much larger marine area affected by crude oil components. Additionally, a number of negative environmental effects related to chemical dispersant use and/or dispersed oil were reported, even though in some cases it was impossible to tease apart the toxic effects of crude oil from those of chemical dispersants. Nevertheless, the health of deep water corals and fish stocks, as well as the microbial community responding to the oil spill, appeared to have been impacted by the exposure to

dispersed oil (Joye *et al.*, 2016a). Additional laboratory studies aiming to simulate DWH spill conditions have reported high toxicity of Corexit EC9500A and/or Corexit-dispersed crude oil for several marine organisms (Wise and Wise, 2011; Finch *et al.*, 2017; Brown *et al.*, 2019; Luter *et al.*, 2019; Ugbomeh *et al.*, 2019) and synergistic toxicity of dispersed oil to marine plankton populations and microorganisms (Hook and Osborn, 2012; Radniecki *et al.*, 2013; Rico-Martínez *et al.*, 2013; Almeda *et al.*, 2014; Ozhan *et al.*, 2014). Besides these environmental effects, a number of studies have also suggested negative effects on the health of spill response personnel, volunteers and inhabitants of the Gulf shoreline area due to the large-scale chemical dispersant application and the known hazard classification of several reported Corexit components (Gräbsch, 2016; McGowan *et al.*, 2017).

The impact of chemical dispersant application on native microbial oil-degrading populations as key players determining the fate of oil in the sea, however, had rarely been studied before the large-scale application in 2010, even though stimulation of oil biodegradation due to increased oil bioavailability had long been assumed (Kleindienst *et al.*, 2015a). Today, the impacts of chemical dispersants on microorganisms, specifically HC degraders, are still relatively uncertain and inconsistent reports have led to disputes over best practices (US NASEM, 2020). While dispersant exposure has typically been shown to alter marine microbial community dynamics and enrich a distinct community (Kleindienst *et al.*, 2015b; Suja *et al.*, 2017; Techtmann *et al.*, 2017; Doyle *et al.*, 2018; Sun and Kostka, 2019; Tremblay *et al.*, 2019), studies have produced conflicting results on how dispersants affect the HC biodegradation potential of these communities. Findings range from enhanced (Bælum *et al.*, 2012; Prince *et al.*, 2016) or mostly unaffected HC biodegradation (McFarlin *et al.*, 2014; Tremblay *et al.*, 2019) to toxic or inhibitive effects on microbial HC degradation (Hamdan and Fulmer, 2011; Kleindienst *et al.*, 2015b; Rahsepar *et al.*, 2016; Hackbusch *et al.*, 2020). A number of different explanations for these contradictory findings have been proposed, ranging from methodological issues (e.g. dispersant concentrations, types and weathering status of crude oil or HCs used) to microbiological and ecological considerations (e.g. species-specific dispersant responses and the relevance of the native microbial community composition) (Overholt *et al.*, 2016; Prince *et al.*, 2016; Rahsepar *et al.*, 2016; Techtmann *et al.*, 2017; Doyle *et al.*, 2018). However, many open questions regarding those inconsistent findings remain.

Moreover, several studies have demonstrated that chemical dispersants like Corexit EC9500A can inhibit certain HC-degrading bacteria in their growth and activity, observed in both pure cultures (Hamdan and Fulmer, 2011; Overholt *et al.*, 2016; Hackbusch *et al.*, 2020) and seawater microcosm experiments (Techtmann *et al.*, 2017; Doyle *et al.*, 2018). Members of the aforementioned alkane-degrading genus *Marinobacter*, in particular, can become negatively affected by chemical dispersant exposure. This has been described in several studies but does not seem to apply to all *Marinobacter* spp. (Hamdan and Fulmer, 2011; Kleindienst *et al.*, 2015b; Techtmann *et al.*, 2017; Tremblay *et al.*, 2017; Doyle *et al.*, 2018; Tremblay *et al.*, 2019), further illustrating the inconsistent state of the scientific literature on this topic.

Remarkably, there are also still substantial knowledge gaps regarding the underlying causes and mechanisms of the observed dispersant effects on HC-degrading bacteria. It remains largely unknown how chemical dispersants, such as Corexit, might affect the metabolism and cellular processes of HC degraders and, in turn, how exposure leads to the different observed microbial responses. This knowledge could be crucial to untangling the contradictory findings in the

literature. Corexit EC9500A was reported to contain a petroleum distillate fraction, propylene glycols, and different anionic and nonionic surfactants in mostly unknown proportions (Place *et al.*, 2016; Choyke and Ferguson, 2019). Thus, these components themselves could cause detrimental effects to microbial cells (e.g. described by Partearroyo *et al.*, 1990; Sikkema *et al.*, 1995; Ramos *et al.*, 2002; Krell *et al.*, 2012; Inacio *et al.*, 2016), and/or synergistic toxicity effects of dispersed oil exposure could be at play (e.g. described by Radniecki *et al.*, 2013; Rico-Martínez *et al.*, 2013; Ozhan *et al.*, 2014). Remarkably, a few HC-degrading bacteria belonging to the genera *Colwellia*, *Alcanivorax* and *Acinetobacter* were shown to degrade and grow on components of Corexit EC9500A as well (Chakraborty *et al.*, 2012; Overholt *et al.*, 2016), which opens up even more potential routes of chemical dispersant exposure affecting environmental microbial communities during marine oil spill scenarios.

Even though many open questions remain, most recent studies of chemical dispersant impacts on oil-degrading microorganisms were conducted with the DWH spill in mind. As a result, the Gulf of Mexico ecosystem is now relatively well characterized in this regard compared to many other ecosystems of interest (Murphy *et al.*, 2016). One of these ecosystems assessed in this thesis is the relatively pristine and vulnerable environment of the Arctic Ocean. In comparison, this ocean remains relatively unexplored in this regard, even though crude oil and fuel spill risks associated with shipping traffic and/or oil exploration activities are increasing due to the decline in Arctic sea ice coverage (Meier *et al.*, 2014; Harsem *et al.*, 2015; US NPC, 2015; Harriss, 2016). Spill impacts are assumed to be potentially disastrous in the vulnerable Arctic ecosystem, however, predictions are hindered by a lack of ecological baseline knowledge for this region (Lee *et al.*, 2015; US NPC, 2015; Aune *et al.*, 2018; Nevalainen *et al.*, 2018). So far, dispersant application in the Arctic is rare and has only occurred to a small extent during field trials (Curl *et al.*, 1992; Ernest, 1993; Trudel, 1998). However, almost all member countries of the Arctic Council currently consider dispersant application as a spill response option (Arctic Council, 2013; US NASEM, 2020), highlighting the need for additional research in this unique ecosystem. The second marine ecosystem explored in this thesis is the North Sea, an area that has experienced much more ship traffic, oil exploration and oil pollution than the Arctic Ocean. In fact, it was highlighted as one of six areas worldwide with a high spill volume (Burgherr, 2007). And although oil pollution in the North Sea has been decreasing, the ongoing oil extraction activities, increasing shipping traffic, new offshore wind platforms, and the ageing nature of several oil production platforms in the area were all identified as current oil spill risks (Carpenter, 2019). While the North Sea has been more thoroughly characterized microbiologically than the Arctic Ocean (Brakstad and Lødeng, 2005; Wiltshire *et al.*, 2010; Gertler *et al.*, 2012; Teeling *et al.*, 2012; Chronopoulou *et al.*, 2015), the impacts of chemical dispersants on seawater microbial communities in areas like the German Bight are not well characterized (Grote *et al.*, 2018; de Almeida Couto *et al.*, 2019).

Consequently, many open research questions regarding the impacts of chemical dispersants on microbial HC biodegradation remain (also discussed e.g. in Kleindienst *et al.*, 2015a; Joye *et al.*, 2016b; Kleindienst and Joye, 2017) and this thesis will present a number of findings with the aim to further elucidate these complex scenarios.

1.6 Research questions and thesis structure

The application of chemical dispersants during marine oil spill response efforts routinely takes place to supplement more weather-dependent physical response strategies and reduce harmful impacts of crude oil pollution to birds and shorelines. However, their ecological effects remain controversial. Particularly large knowledge gaps remain regarding the impacts of chemical dispersants on affected seawater microbial communities and native oil-degrading bacteria in particular, with the current literature characterized by largely unexplained contradictory findings. Moreover, several marine ecosystems remain underexplored in this regard and the effects of chemical dispersant exposure on cellular processes of HC-degrading bacteria are unknown to date. Therefore, in order to improve our knowledge and understanding of chemical dispersant impacts on oil-degrading microorganisms, the main research questions and respective experimental approaches covered in this thesis are as follows (see also Figure 1.5).

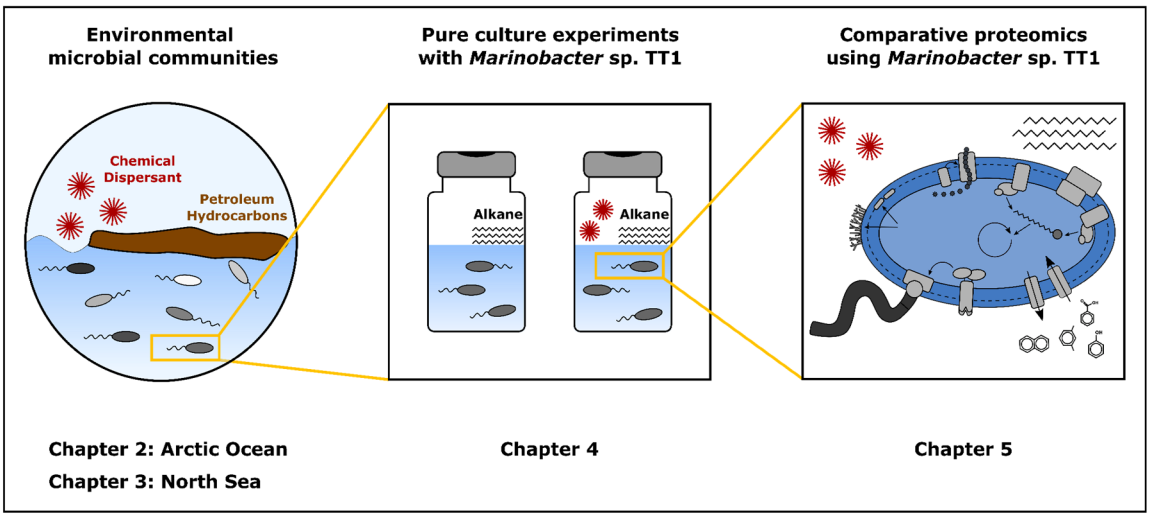

Figure 1.5: Schematic overview of the structure of this thesis and the experiments presented hereafter, which were performed to further elucidate impacts of chemical dispersants on oil-degrading microorganisms.

I) How do chemical dispersants impact environmental seawater microbial communities and their oil biodegradation potential in different marine habitats?

The first aim was to characterize the response of environmental seawater microbial communities from the Arctic Ocean (**Chapter 2**) and the North Sea (**Chapter 3**) to chemical dispersant exposure during a simulated crude oil spill scenario. This was achieved by performing large laboratory microcosm experiments that simulated the water column conditions during a crude oil spill with and without chemical dispersant (Corexit EC9500A) addition. Using samples from these microcosms, microbial cell numbers were quantified via fluorescence microscopy and quantitative PCR (qPCR), microbial productivity was quantified via incorporation rates of ^{3}H-leucine and microbial community composition and dynamics were identified via 16S rRNA gene amplicon sequencing. Additionally, remaining *n*-alkane, naphthalene and phenanthrene concentrations were quantified via gas chromatography coupled with mass spectrometry (GC-MS), dissolved organic carbon (DOC) levels were measured and ^{14}C-labelled HC oxidation activity was quantified in order to characterize HC biodegradation

progress in microcosms. Moreover, the effects of a biostimulation treatment on microbial community dynamics and oil biodegradation potential were compared to chemical dispersant addition in Arctic Ocean microcosms, in order to assess the potential for alternative or additional bioremediation approaches in this ecosystem (**Chapter 2**).

II) What is the effect of chemical dispersants on growth and biodegradation activity of the HC degrader *Marinobacter* sp. TT1 isolated during the DWH spill?

The second aim covered in this thesis was to identify the effects of chemical dispersant exposure on the growth and alkane biodegradation activity of the DWH isolate *Marinobacter* sp. TT1 (**Chapter 4**). This was achieved by performing pure culture experiments using the representative petroleum HC *n*-hexadecane ± Corexit EC9500A and subsequently quantifying microbial cell numbers via fluorescence microscopy and remaining *n*-hexadecane concentrations via GC-MS. Additionally, the effects of environmentally relevant versus typical laboratory substrate availability were investigated in these experiments as one potential factor that could explain the contradictory dispersant effects on HC degraders reported in the literature by performing the described experiment with previously carbon-starved or well-fed *Marinobacter* sp. TT1 cultures.

III) How do dispersants affect the HC metabolism and other cellular processes of the model organism *Marinobacter* sp. TT1?

The third aim was to identify the underlying mechanisms of observed chemical dispersant effects on HC-degrading bacteria on a cellular level (**Chapter 5**). To this end, additional pure culture experiments with the selected model organism *Marinobacter* sp. TT1 using different carbon sources ± chemical dispersant (Corexit EC9500A) were performed and a comparative analysis of protein expression profiles associated with the different growth conditions was achieved. This included the characterization of proteins associated with HC metabolism in strain TT1 and the identification of different metabolic and cellular processes that were affected by chemical dispersant exposure. Additionally, microbial cell numbers (via fluorescence microscopy) and remaining *n*-hexadecane concentrations (via GC-MS) were quantified.

1.7 References

Abbasian, F., Lockington, R., Megharaj, M., and Naidu, R. (2016) A review on the genetics of aliphatic and aromatic hydrocarbon degradation. *Appl Biochem Biotechnol* **178**(2): 224-250.

Adams, G.O., Fufeyin, P.T., Okoro, S.E., and Ehinomen, I. (2015) Bioremediation, biostimulation and bioaugmention: A review. *Int J Environ Bioremediat Biodegrad* **3**(1): 28-39.

Almeda, R., Hyatt, C., and Buskey, E.J. (2014) Toxicity of dispersant Corexit 9500A and crude oil to marine microzooplankton. *Ecotoxicol Environ Saf* **106**: 76-85.

Altschul, S.F., Gish, W., Miller, W., Myers, E.W., and Lipman, D.J. (1990) Basic local alignment search tool. *J Mol Biol* **215**(3): 403-410.

Arctic Council (2013). Agreement on cooperation on marine oil pollution preparedness and response in the Arctic. Kiruna, Sweden. Available from: https://oaarchive.arctic-council.org/handle/11374/529 [Accessed July 20, 2020].

Atlas, R.M., and Bartha, R. (1972) Degradation and mineralization of petroleum in sea water: Limitation by nitrogen and phosphorous. *Biotechnol Bioeng* **14**(3): 309-318.

Atlas, R.M. (1995) Petroleum biodegradation and oil spill bioremediation. *Mar Pollut Bull* **31**(4-12): 178-182.

Aune, M., Aniceto, A.S., Biuw, M., Daase, M., Falk-Petersen, S., Leu, E. *et al.* (2018) Seasonal ecology in ice-covered Arctic seas: Considerations for spill response decision making. *Mar Environ Res* **141**: 275-288.

Bælum, J., Borglin, S., Chakraborty, R., Fortney, J.L., Lamendella, R., Mason, O.U. *et al.* (2012) Deep-sea bacteria enriched by oil and dispersant from the Deepwater Horizon spill. *Environ Microbiol* **14**(9): 2405-2416.

Barron, M.G., Vivian, D.N., Heintz, R.A., and Yim, U.H. (2020) Long-term ecological impacts from oil spills: Comparison of *Exxon Valdez*, *Hebei Spirit*, and Deepwater Horizon. *Environ Sci Technol*.

BBC News (2019) *Grande America*: France braces for oil spill damage after ship blaze. In *BBC News*. Published on: March 14, 2019. Available from: https://www.bbc.com/news/world-europe-47574143 [Accessed August 28, 2020].

BBC News (2020) Russian Arctic oil spill pollutes big lake near Norilsk. In *BBC News*. Published on: June 9, 2020. Available from: https://www.bbc.com/news/world-europe-52977740 [Accessed August 28, 2020].

Bellier, P., and Massart, G. (1979) The *Amoco Cadiz* oil spill cleanup operations – an overview of the organization, control, and evaluation of the cleanup techniques employed. *International Oil Spill Conference*: American Petroleum Institute, pp. 141-146.

Berenshtein, I., Paris, C.B., Perlin, N., Alloy, M.M., Joye, S.B., and Murawski, S. (2020) Invisible oil beyond the Deepwater Horizon satellite footprint. *Science Advances* **6**(7): eaaw8863.

Beyer, J., Trannum, H.C., Bakke, T., Hodson, P.V., and Collier, T.K. (2016) Environmental effects of the Deepwater Horizon oil spill: A review. *Mar Pollut Bull* **110**(1): 28-51.

Bocard, C., Renault, P., and Croquette, J. (1979) Cleaning products used in operations after the *Amoco Cadiz* disaster. *International Oil Spill Conference*: American Petroleum Institute, pp. 163-167.

Bolyen, E., Rideout, J.R., Dillon, M.R., Bokulich, N.A., Abnet, C.C., Al-Ghalith, G.A. *et al.* (2019) Reproducible, interactive, scalable and extensible microbiome data science using QIIME 2. *Nature biotechnology* **37**(8): 852-857.

Bowman, J.P., Gosink, J.J., McCAMMON, S.A., Lewis, T.E., Nichols, D.S., Nichols, P.D. *et al.* (1998) *Colwellia demingiae* sp. nov., *Colwellia hornerae* sp. nov., *Colwellia rossensis* sp. nov. and *Colwellia psychrotropica* sp. nov.: Psychrophilic Antarctic species with the ability to synthesize docosahexaenoic acid (22:Ω63). *Int J Syst Evol Microbiol* **48**(4): 1171-1180.

Bragg, J.R., Prince, R.C., Harner, E.J., and Atlas, R.M. (1994) Effectiveness of bioremediation for the *Exxon Valdez* oil spill. *Nature* **368**(6470): 413-418.

Brakstad, O., and Lødeng, A. (2005) Microbial diversity during biodegradation of crude oil in seawater from the North Sea. *Microb Ecol* **49**(1): 94-103.

Brakstad, O.G., Lofthus, S., Ribicic, D., and Netzer, R. (2017) Biodegradation of petroleum oil in cold marine environments. In *Psychrophiles: From biodiversity to biotechnology*: Springer, pp. 613-644.

Brakstad, O.G., Davies, E.J., Ribicic, D., Winkler, A., Brönner, U., and Netzer, R. (2018) Biodegradation of dispersed oil in natural seawaters from Western Greenland and a Norwegian fjord. *Polar Biology* **41**(12): 2435-2450.

Brown, C., Williamson, K., and Galvez, F. (2019) The influence of salinity on the toxicity of Corexit at multiple life stages of Gulf killifish. *Comparative Biochemistry and Physiology Part C: Toxicology & Pharmacology* **221**: 38-48.

Burgherr, P. (2007) In-depth analysis of accidental oil spills from tankers in the context of global spill trends from all sources. *J Hazard Mat* **140**: 245-256.

Burrows, P., Rowley, C., and Owen, D. (1974) *Torrey Canyon*: A case study in accidental pollution. *Scottish Journal of Political Economy* **21**(3): 237-258.

Callahan, B.J., McMurdie, P.J., Rosen, M.J., Han, A.W., Johnson, A.J.A., and Holmes, S.P. (2016) DADA2: High-resolution sample inference from Illumina amplicon data. *Nat Methods* **13**(7): 581-583.

Camilli, R., Reddy, C.M., Yoerger, D.R., Van Mooy, B.A., Jakuba, M.V., Kinsey, J.C. *et al.* (2010) Tracking hydrocarbon plume transport and biodegradation at Deepwater Horizon. *Science* **330**(6001): 201-204.

Campeão, M.E., Swings, J., Silva, B.S., Otsuki, K., Thompson, F.L., and Thompson, C.C. (2019) ″*Candidatus* Colwellia aromaticivorans″ sp. nov.,″*Candidatus* Halocyntiibacter alkanivorans″ sp. nov., and ″*Candidatus* Ulvibacter alkanivorans″ sp. nov. genome sequences. *Microbiology Resource Announcements* **8**(15).

Campo, P., Venosa, A.D., and Suidan, M.T. (2013) Biodegradability of Corexit 9500 and dispersed South Louisiana crude oil at 5 and 25°C. *Environ Sci Technol* **47**(4): 1960-1967.

Canul-Chan, M., Sanchez-Gonzalez, M., González-Burgos, A., Zepeda, A., and Rojas-Herrera, R. (2018) Population structures shift during the biodegradation of crude and fuel oil by an indigenous consortium. *International journal of environmental science and technology* **15**(1): 1-16.

Caporaso, J.G., Kuczynski, J., Stombaugh, J., Bittinger, K., Bushman, F.D., Costello, E.K. *et al.* (2010) QIIME allows analysis of high-throughput community sequencing data. *Nat Methods* **7**(5): 335-336.

Carpenter, A. (2019) Oil pollution in the North Sea: The impact of governance measures on oil pollution over several decades. *Hydrobiologia* **845**(1): 109-127.

Chakraborty, R., Borglin, S.E., Dubinsky, E.A., Andersen, G.L., and Hazen, T.C. (2012) Microbial response to the MC-252 oil and Corexit 9500 in the Gulf of Mexico. *Front Microbiol* **3**: 357.

Chen, C., Liu, Q., Liu, C., and Yu, J. (2017) Effect of different enrichment strategies on microbial community structure in petroleum-contaminated marine sediment in Dalian, China. *Mar Pollut Bull* **117**(1-2): 274-282.

Choyke, S., and Ferguson, P.L. (2019) Molecular characterization of nonionic surfactant components of the Corexit 9500® oil spill dispersant by high-resolution mass spectrometry. *Rapid Commun Mass Spectrom* **33**(22): 1683-1694.

Chrastansky, A., and Callies, U. (2009) Model-based long-term reconstruction of weather-driven variations in chronic oil pollution along the German North Sea coast. *Mar Pollut Bull* **58**(7): 967-975.

Chronopoulou, P.M., Sanni, G.O., Silas-Olu, D.I., van der Meer, J.R., Timmis, K.N., Brussaard, C.P., and McGenity, T.J. (2015) Generalist hydrocarbon-degrading bacterial communities in the oil-polluted water column of the North Sea. *Microb Biotechnol* **8**(3): 434-447.

Coulon, F., McKew, B.A., Osborn, A.M., McGenity, T.J., and Timmis, K.N. (2007) Effects of temperature and biostimulation on oil-degrading microbial communities in temperate estuarine waters. *Environ Microbiol* **9**(1): 177-186.

Crisafi, F., Genovese, M., Smedile, F., Russo, D., Catalfamo, M., Yakimov, M. *et al.* (2016) Bioremediation technologies for polluted seawater sampled after an oil-spill in Taranto Gulf (Italy): A comparison of biostimulation, bioaugmentation and use of a washing agent in microcosm studies. *Mar Pollut Bull* **106**(1-2): 119-126.

Curl, H.C., Barton, K., and Harris, L. (1992). Oil spill case histories, 1967-1991: Summaries of significant U.S. and international spills. Seattle, Washington, USA: NOAA Hazardous Materials Response and Assessment Division. Report No.: Report No. HMRAD 92-11. Available from: https://repository.library.noaa.gov/view/noaa/1671 [Accessed July 20, 2020].

Dave, D., and Ghaly, A.E. (2011) Remediation technologies for marine oil spills: A critical review and comparative analysis. *American Journal of Environmental Sciences* **7**(5): 423.

Davidova, I.A., Marks, C.R., and Suflita, J.M. (2019) Anaerobic hydrocarbon-degrading Deltaproteobacteria. In *Taxonomy, genomics and ecophysiology of hydrocarbon-degrading microbes*. McGenity, T.J. (ed), pp. 207-243.

de Almeida Couto, C.R., de Assis Leite, D.C., Jurelevicius, D., van Elsas, J.D., and Seldin, L. (2019) Chemical and biological dispersants differently affect the bacterial communities of uncontaminated and oil-contaminated marine water. *Brazilian Journal of Microbiology* **51**(2): 691-700.

Diéguez, A., and Romalde, J. (2017) Draft genome sequences of *Neptuniibacter* sp. strains LFT 1.8 and ATR 1.1. *Genome Announcements* **5**(5).

Dombrowski, N., Donaho, J.A., Gutierrez, T., Seitz, K.W., Teske, A.P., and Baker, B.J. (2016) Reconstructing metabolic pathways of hydrocarbon-degrading bacteria from the Deepwater Horizon oil spill. *Nat Microbiol* **1**(7): 1-7.

Doyle, S.M., Whitaker, E.A., De Pascuale, V., Wade, T.L., Knap, A.H., Santschi, P.H. *et al.* (2018) Rapid formation of microbe-oil aggregates and changes in community composition in coastal surface water following exposure to oil and the dispersant Corexit. *Front Microbiol* **9**: 689.

Duran, R. (2010) *Marinobacter*. *Handbook of Hydrocarbon and Lipid Microbiology*. Timmis, K.N. (ed). Heidelberg, Germany: Springer, pp. 1725-1735. 10.1007/978-3-540-77587-4_122.

DWH NRDA Trustees (2016). Deepwater Horizon oil spill: Final programmatic damage assessment and restoration plan and final programmatic environmental impact statement. Available from: http://www.gulfspillrestoration.noaa.gov/restoration-planning/gulf-plan [Accessed June 16, 2020].

Dyksterhouse, S.E., Gray, J.P., Herwig, R.P., Lara, J.C., and Staley, J.T. (1995) *Cycloclasticus pugetii* gen. nov., sp. nov., an aromatic hydrocarbon-degrading bacterium from marine sediments. *Int J Syst Bacteriol* **45**(1): 116-123.

Ernest, P. (1993). The *Exxon Valdez* oil spill: Final report, state of Alaska response. Anchorage, AK, USA: Alaska Department of Environmental Conservation. Available from: http://www.evostc.state.ak.us/static/PDFs/deccleanuptechniques.pdf [Accessed July 19, 2020].

Etkin, D.S. (2000) Worldwide analysis of marine oil spill cleanup cost factors. *Arctic and marine oilspill program technical seminar*: Environment Canada, pp. 161-174.

Ewels, P.A., Peltzer, A., Fillinger, S., Patel, H., Alneberg, J., Wilm, A. *et al.* (2020) The nf-core framework for community-curated bioinformatics pipelines. *Nature Biotechnology* **38**(3): 276-278.

ExxonMobil (2014). Oil spill response field manual. USA: ExxonMobil Research and Engineering Company. Available from: https://corporate.exxonmobil.com/-/media/Global/Files/risk-management-and-safety/Oil-Spill-Response-Field-Manual_2014.pdf [Accessed July 19, 2020].

ExxonMobil (2018). Grane crude oil assay. Spring, Texas, USA. Available from: https://corporate.exxonmobil.com/Crude-oils/Crude-trading/Grane [Accessed August 20, 2020].

Fasca, H., de Castilho, L.V., de Castilho, J.F.M., Pasqualino, I.P., Alvarez, V.M., de Azevedo Jurelevicius, D., and Seldin, L. (2018) Response of marine bacteria to oil contamination and to high pressure and low temperature deep sea conditions. *MicrobiologyOpen* **7**(2): e00550.

Finch, B.E., Marzooghi, S., Di Toro, D.M., and Stubblefield, W.A. (2017) Phototoxic potential of undispersed and dispersed fresh and weathered Macondo crude oils to Gulf of Mexico marine organisms. *Environ Toxicol Chem* **36**(10): 2640-2650.

Gauthier, M.J., Lafay, B., Christen, R., Fernandez, L., Acquaviva, M., Bonin, P., and Bertrand, J.-C. (1992) *Marinobacter hydrocarbonoclasticus* gen. nov., sp. nov., a new, extremely halotolerant, hydrocarbon-degrading marine bacterium. *Int J Syst Evol Microbiol* **42**(4): 568-576.

Gerdes, B., Brinkmeyer, R., Dieckmann, G., and Helmke, E. (2005) Influence of crude oil on changes of bacterial communities in Arctic sea-ice. *FEMS Microbiol Ecol* **53**(1): 129-139.

Gertler, C., Näther, D.J., Cappello, S., Gerdts, G., Quilliam, R.S., Yakimov, M.M., and Golyshin, P.N. (2012) Composition and dynamics of biostimulated indigenous oil-degrading microbial consortia from the Irish, North and Mediterranean seas: A mesocosm study. *FEMS Microbiol Ecol* **81**(3): 520-536.

Gilfillan, E.S., Page, D.S., Hanson, S.A., Foster, J.C., Hotham, J., Vallas, D. *et al.* (1985) Tidal area dispersant experiment, Searsport Maine: An overview. *International Oil Spill Conference*: American Petroleum Institute, pp. 553-559.

Goodland, J. (1998) The *Braer* oil spill in Shetland, 1993 to 1997. *Dispersant Use in Alaska: A Technical Update*. Trudel, B.K. (ed). Anchorage, Alaska, USA: Prince William Sound Oil Spill Recovery Institute.

Gräbsch, C. (2016) Health effects of mineral oil, dispersants and oil-dispersant-mixtures. In *The use of dispersants to combat oil spills in Germany at sea*. Grote, M., Nagel, A., Nies, H., Rauterberg, J., and Wahrendorf, D.-S. (eds). Berlin, Germany: Federal Institute for Risk Assessment, pp. 37-47.

Gregson, B.H., Metodieva, G., Metodiev, M.V., Golyshin, P.N., and McKew, B.A. (2018) Differential protein expression during growth on medium versus long-chain alkanes in the obligate marine hydrocarbon-degrading bacterium *Thalassolituus oleivorans* MIL-1. *Front Microbiol* **9**: 3130.

Gregson, B.H., Metodieva, G., Metodiev, M.V., Golyshin, P.N., and McKew, B.A. (2020) Protein expression in the obligate hydrocarbon-degrading psychrophile *Oleispira antarctica* RB-8 during alkane degradation and cold tolerance. *Environ Microbiol* **22**(5): 1870-1883.

Grote, M., van Bernem, C., Böhme, B., Callies, U., Calvez, I., Christie, B. *et al.* (2018) The potential for dispersant use as a maritime oil spill response measure in German waters. *Mar Pollut Bull* **129**(2): 623-632.

Gutierrez, T., Nichols, P.D., Whitman, W.B., and Aitken, M.D. (2012) *Porticoccus hydrocarbonoclasticus* sp. nov., an aromatic hydrocarbon-degrading bacterium identified in laboratory cultures of marine phytoplankton. *Appl Environ Microbiol* **78**(3): 628-637.

Gutierrez, T., Berry, D., Yang, T., Mishamandani, S., McKay, L., Teske, A., and Aitken, M.D. (2013a) Role of bacterial exopolysaccharides (EPS) in the fate of the oil released during the Deepwater Horizon oil spill. *PloS one* **8**(6): e67717.

Gutierrez, T., Singleton, D.R., Berry, D., Yang, T., Aitken, M.D., and Teske, A. (2013b) Hydrocarbon-degrading bacteria enriched by the Deepwater Horizon oil spill identified by cultivation and DNA-SIP. *ISME J* **7**(11): 2091-2104.

Gutierrez, T., Rhodes, G., Mishamandani, S., Berry, D., Whitman, W.B., Nichols, P.D. *et al.* (2014) Polycyclic aromatic hydrocarbon degradation of phytoplankton-associated *Arenibacter* spp. and description of

Arenibacter algicola sp. nov., an aromatic hydrocarbon-degrading bacterium. *Appl Environ Microbiol* **80**(2): 618-628.
Gutierrez, T. (2017) Dispersants: The good, the bad and the rise of a new bio-based generation. *Arch Pet Environ Biotechnol* **10**: 2574-7614.
Gutierrez, T. (2018) Preparing for the next big oil spill at sea: A microbiological perspective. *Journal of Marine Microbiology* **2**(1): 13-14.
Gutierrez, T., Morris, G., Ellis, D., Bowler, B., Jones, M., Salek, K. *et al.* (2018) Hydrocarbon-degradation and MOS-formation capabilities of the dominant bacteria enriched in sea surface oil slicks during the Deepwater Horizon oil spill. *Mar Pollut Bull* **135**: 205-215.
Gutierrez, T. (2019) Occurrence and roles of the obligate hydrocarbonoclastic bacteria in the ocean when there is no obvious hydrocarbon contamination. In *Taxonomy, genomics and ecophysiology of hydrocarbon-degrading microbes*. McGenity, T.J. (ed), pp. 337-352.
Hackbusch, S., Noirungsee, N., Viamonte, J., Sun, X., Bubenheim, P., Kostka, J.E. *et al.* (2020) Influence of pressure and dispersant on oil biodegradation by a newly isolated *Rhodococcus* strain from deep-sea sediments of the Gulf of Mexico. *Mar Pollut Bull* **150**: 110683.
Hamdan, L.J., and Fulmer, P.A. (2011) Effects of Corexit EC9500A on bacteria from a beach oiled by the Deepwater Horizon spill. *Aquat Microb Ecol* **63**(2): 101-109.
Harriss, R. (2016) Arctic offshore oil: Great risks in an evolving ocean. *Environment: Science and Policy for Sustainable Development* **58**(3): 18-29.
Harsem, Ø., Heen, K., Rodrigues, J., and Vassdal, T. (2015) Oil exploration and sea ice projections in the Arctic. *The Polar Record* **51**(1): 91.
Harwati, T.U., Kasai, Y., Kodama, Y., Susilaningsih, D., and Watanabe, K. (2007) Characterization of diverse hydrocarbon-degrading bacteria isolated from Indonesian seawater. *Microbes and Environments* **22**(4): 412-415.
Harwati, T.U., Kasai, Y., Kodama, Y., Susilaningsih, D., and Watanabe, K. (2009) *Tropicibacter naphthalenivorans* gen. nov., sp. nov., a polycyclic aromatic hydrocarbon-degrading bacterium isolated from Semarang Port in Indonesia. *Int J Syst Evol Microbiol* **59**(2): 392-396.
Hazen, T.C., Dubinsky, E.A., DeSantis, T.Z., Andersen, G.L., Piceno, Y.M., Singh, N. *et al.* (2010) Deep-sea oil plume enriches indigenous oil-degrading bacteria. *Science* **330**(6001): 204-208.
Hazen, T.C., Prince, R.C., and Mahmoudi, N. (2016) Marine oil biodegradation. *Environ Sci Technol* **50**(5): 2121-2129.
Head, I.M., Jones, D.M., and Röling, W.F. (2006) Marine microorganisms make a meal of oil. *Nat Rev Microbiol* **4**(3): 173-182.
Hedlund, B.P., Geiselbrecht, A.D., Bair, T.J., and Staley, J.T. (1999) Polycyclic aromatic hydrocarbon degradation by a new marine bacterium, *Neptunomonas naphthovorans* gen. nov., sp. nov. *Appl Environ Microbiol* **65**(1): 251-259.
Hernández-López, E., Ayala, M., and Vazquez-Duhalt, R. (2015) Microbial and enzymatic biotransformations of asphaltenes. *Petroleum Science and Technology* **33**(9): 1017-1029.
Hoefs, M.J., Van Heemst, J.D., Gelin, F., Koopmans, M.P., Van Kaam-Peters, H.M., Schouten, S. *et al.* (1995) Alternative biological sources for 1,2,3,4-tetramethylbenzene in flash pyrolysates of kerogen. *Organic Geochemistry* **23**(10): 975-979.
Holder, E.L., Conmy, R.N., and Venosa, A.D. (2015) Comparative laboratory-scale testing of dispersant effectiveness of 23 crude oils using four different testing protocols. *J Environ Prot* **6**(06): 628.
Hook, S.E., and Osborn, H.L. (2012) Comparison of toxicity and transcriptomic profiles in a diatom exposed to oil, dispersants, dispersed oil. *Aquatic Toxicology* **124**: 139-151.
Hunt, A. (2016) Operational experience worldwide. In *The use of dispersants to combat oil spills in Germany at sea*. Grote, M., Nagel, A., Nies, H., Rauterberg, J., and Wahrendorf, D.-S. (eds). Berlin, Germany: Federal Institute for Risk Assessment, pp. 69-81.
Inacio, A.S., Domingues, N.S., Nunes, A., Martins, P.T., Moreno, M.J., Estronca, L.M. *et al.* (2016) Quaternary ammonium surfactant structure determines selective toxicity towards bacteria: Mechanisms of action and clinical implications in antibacterial prophylaxis. *J Antimicrob Chemother* **71**(3): 641-654.
ITOPF (2020). Oil tanker spill statistics 2019. London, UK: International Tanker Owners Pollution Federation. Available from: http://www.itopf.org/fileadmin/data/Documents/Company_Lit/Oil_Spill_Stats_brochure_2020_for_web.pdf [Accessed May 27, 2020].
Jernelöv, A., and Lindén, O. (1981) Ixtoc I: A case study of the world's largest oil spill. *Ambio*: 299-306.
John, V., Arnosti, C., Field, J., Kujawinski, E., and McCormick, A. (2016) The role of dispersants in oil spill remediation: Fundamental concepts, rationale for use, fate, and transport issues. *Oceanography* **29**(3): 108-117.
Joye, S.B. (2015) Deepwater Horizon, 5 years on. *Science* **349**(6248): 592-593.

Joye, S.B., Bracco, A., Özgökmen, T.M., Chanton, J.P., Grosell, M., MacDonald, I.R. *et al.* (2016a) The Gulf of Mexico ecosystem, six years after the Macondo oil well blowout. *Deep Sea Res Part II Top Stud Oceanogr* **129**: 4-19.

Joye, S.B., Kleindienst, S., Gilbert, J.A., Handley, K.M., Weisenhorn, P., Overholt, W.A., and Kostka, J.E. (2016b) Responses of microbial communities to hydrocarbon exposures. *Oceanography* **29**(3): 136-149.

Joye, S.B., and Kleindienst, S. (2017) Hydrocarbon seep ecosystems. In *Life at vents and seeps*. Kallmeyer, J. (ed), pp. 33-52.

Kasai, Y., Kishira, H., and Harayama, S. (2002) Bacteria belonging to the genus *Cycloclasticus* play a primary role in the degradation of aromatic hydrocarbons released in a marine environment. *Appl Environ Microbiol* **68**(11): 5625-5633.

Khadka, N.S. (2020) Why the Mauritius oil spill is so serious. In *BBC News*. Published on: August 12, 2020. Available from: https://www.bbc.com/news/world-africa-53754751 [Accessed August 28, 2020].

Kirby, M.F., and Law, R.J. (2010) Accidental spills at sea: Risk, impact, mitigation and the need for co-ordinated post-incident monitoring. *Mar Pollut Bull* **60**(6): 797-803.

Kirchman, D. (2001) Measuring bacterial biomass production and growth rates from leucine incorporation in natural aquatic environments. *Methods Microbiol* **30**: 227–237.

Kleindienst, S., Paul, J.H., and Joye, S.B. (2015a) Using dispersants after oil spills: Impacts on the composition and activity of microbial communities. *Nat Rev Microbiol* **13**(6): 388-396.

Kleindienst, S., Seidel, M., Ziervogel, K., Grim, S., Loftis, K., Harrison, S. *et al.* (2015b) Chemical dispersants can suppress the activity of natural oil-degrading microorganisms. *Proc Natl Acad Sci USA* **112**(48): 14900-14905.

Kleindienst, S., Grim, S., Sogin, M., Bracco, A., Crespo-Medina, M., and Joye, S.B. (2016) Diverse, rare microbial taxa responded to the Deepwater Horizon deep-sea hydrocarbon plume. *ISME J* **10**(2): 400-415.

Kleindienst, S., and Joye, S.B. (2017) Global aerobic degradation of hydrocarbons in aquatic systems. *Aerobic Utilization of Hydrocarbons, Oils and Lipids*: 1-18.

Knapik, K., Bagi, A., Krolicka, A., and Baussant, T. (2019) Discovery of functional gene markers of bacteria for monitoring hydrocarbon pollution in the marine environment: A metatranscriptomics approach. *bioRxiv*: 857391.

Knapik, K., Bagi, A., Krolicka, A., and Baussant, T. (2020) Metatranscriptomic analysis of oil-exposed seawater bacterial communities archived by an environmental sample processor (ESP). *Microorganisms* **8**(5): 744.

Kover, S.C., Rosario-Ortiz, F.L., and Linden, K.G. (2014) Photochemical fate of solvent constituents of Corexit oil dispersants. *Water Res* **52**: 101-111.

Krell, T., Lacal, J., Guazzaroni, M.E., Busch, A., Silva-Jimenez, H., Fillet, S. *et al.* (2012) Responses of *Pseudomonas putida* to toxic aromatic carbon sources. *J Biotechnol* **160**(1-2): 25-32.

Kujawinski, E.B., Kido Soule, M.C., Valentine, D.L., Boysen, A.K., Longnecker, K., and Redmond, M.C. (2011) Fate of dispersants associated with the Deepwater Horizon oil spill. *Environ Sci Technol* **45**(4): 1298-1306.

Kujawinski, E.B., Reddy, C.M., Rodgers, R.P., Thrash, J.C., Valentine, D.L., and White, H.K. (2020) The first decade of scientific insights from the Deepwater Horizon oil release. *Nature Reviews Earth & Environment* **1**: 237–250.

Lea-Smith, D.J., Biller, S.J., Davey, M.P., Cotton, C.A., Sepulveda, B.M.P., Turchyn, A.V. *et al.* (2015) Contribution of cyanobacterial alkane production to the ocean hydrocarbon cycle. *Proc Natl Acad Sci USA* **112**(44): 13591-13596.

Lee, K., Boufadel, M., Chen, B., Foght, J., Hodson, P., Swanson, S., and Venosa, A. (2015). Expert panel report on the behaviour and environmental impacts of crude oil released into aqueous environments. Ottawa, ON, Canada: Royal Society of Canada.

Lewis, A., Crosbie, A., Davies, L., and Lunel, T. (1998) The AEA ′97 North Sea field trials on oil weathering and aerial application of dispersants. *Dispersant Use in Alaska: A Technical Update*. Trudel, B.K. (ed). Anchorage, Alaska, USA: Prince William Sound Oil Spill Recovery Insitute.

Lewis, A., and Prince, R.C. (2018) Integrating dispersants in oil spill response in Arctic and other icy environments. *Environ Sci Technol* **52**(11): 6098-6112.

Liao, Y., Geng, A., and Huang, H. (2009) The influence of biodegradation on resins and asphaltenes in the Liaohe Basin. *Organic Geochemistry* **40**(3): 312-320.

Liu, C., Wang, W., Wu, Y., Zhou, Z., Lai, Q., and Shao, Z. (2011) Multiple alkane hydroxylase systems in a marine alkane degrader *Alcanivorax dieselolei* B-5. *Environ Microbiol* **13**(5): 1168-1178.

Liu, J., Bacosa, H.P., and Liu, Z. (2017) Potential environmental factors affecting oil-degrading bacterial populations in deep and surface waters of the northern Gulf of Mexico. *Front Microbiol* **7**: 2131.

Loeffler, J. (2019) France tries to contain oil spill as 2000 cars, freighter sink off coast. In *Interesting Engineering*. Published on: March 23, 2019. Available from: https://interestingengineering.com/france-tries-to-contain-oil-spill-as-2000-cars-freighter-sink-off-coast [Accessed August 28, 2020].

Lofthus, S., Netzer, R., Lewin, A.S., Heggeset, T.M.B., Haugen, T., and Brakstad, O.G. (2018) Biodegradation of *n*-alkanes on oil-seawater interfaces at different temperatures and microbial communities associated with the degradation. *Biodegradation* **29**(2): 141-157.

Lunel, T. (1998) *Sea Empress* spill: Dispersant operations, effectiveness and effectiveness monitoring. *Dispersant Use in Alaska: A Technical Update*. Trudel, B.K. (ed). Anchorage, Alaska, USA: Prince William Sound Oil Spill Recovery Institute.

Luter, H.M., Whalan, S., Andreakis, N., Wahab, M.A., Botté, E.S., Negri, A.P., and Webster, N.S. (2019) The effects of crude oil and dispersant on the larval sponge holobiont. *mSystems* **4**: e00743-00719.

MacDonald, I.R., Garcia-Pineda, O., Beet, A., Daneshgar Asl, S., Feng, L., Graettinger, G. *et al.* (2015) Natural and unnatural oil slicks in the Gulf of Mexico. *Journal of Geophysical Research: Oceans* **120**(12): 8364-8380.

Martin, M. (2011) Cutadapt removes adapter sequences from high-throughput sequencing reads. *EMBnet journal* **17**(1): 10-12.

Mas-Lladó, M., Piña-Villalonga, J.M., Brunet-Galmés, I., Nogales, B., and Bosch, R. (2014) Draft genome sequences of two isolates of the Roseobacter group, *Sulfitobacter* sp. strains 3SOLIMAR09 and 1FIGIMAR09, from harbors of Mallorca Island (Mediterranean sea). *Genome Announcements* **2**(3).

Mason, A.L., Taylor, J.C., and MacDonald, I.R. (2019). An integrated assessment of oil and gas release into the marine environment at the former Taylor Energy MC20 site. Silver Spring, MD, USA: NOAA National Ocean Service, N.C.f.C.O.S. Available from: https://repository.library.noaa.gov/view/noaa/20612 [Accessed August 30, 2020].

Mason, O.U., Hazen, T.C., Borglin, S., Chain, P.S., Dubinsky, E.A., Fortney, J.L. *et al.* (2012) Metagenome, metatranscriptome and single-cell sequencing reveal microbial response to Deepwater Horizon oil spill. *ISME J* **6**(9): 1715-1727.

Mason, O.U., Han, J., Woyke, T., and Jansson, J.K. (2014) Single-cell genomics reveals features of a *Colwellia* species that was dominant during the Deepwater Horizon oil spill. *Front Microbiol* **5**: 332.

Mayer-Pinto, M., Ledet, J., Crowe, T.P., and Johnston, E.L. (2020) Sublethal effects of contaminants on marine habitat-forming species: A review and meta-analysis. *Biological Reviews*(10.1111/brv.12630).

McFarlin, K.M., Prince, R.C., Perkins, R., and Leigh, M.B. (2014) Biodegradation of dispersed oil in arctic seawater at -1°C. *PloS One* **9**(1): e84297.

McFarlin, K.M. (2017) The biodegradation of oil and the dispersant Corexit 9500 in Arctic seawater. *Thesis*, PhD in Biological Sciences. University of Alaska Fairbanks, Department of Biology and Wildlife; Fairbanks, Alaska, USA.

McFarlin, K.M., Questel, J.M., Hopcroft, R.R., and Leigh, M.B. (2017) Bacterial community structure and functional potential in the northeastern Chukchi Sea. *Cont Shelf Res* **136**: 20-28.

McFarlin, K.M., Perkins, M.J., Field, J.A., and Leigh, M.B. (2018) Biodegradation of crude oil and Corexit 9500 in Arctic seawater. *Front Microbiol* **9**: 1788.

McGenity, T.J., Folwell, B.D., McKew, B.A., and Sanni, G.O. (2012) Marine crude-oil biodegradation: A central role for interspecies interactions. *Aquatic Biosystems* **8**(1): 10.

McGowan, C.J., Kwok, R.K., Engel, L.S., Stenzel, M.R., Stewart, P.A., and Sandler, D.P. (2017) Respiratory, dermal, and eye irritation symptoms associated with Corexit EC9527A/EC9500A following the Deepwater Horizon oil spill: Findings from the GuLF STUDY. *Environ Health Perspect* **125**(9): 097015.

McMurdie, P.J., and Holmes, S. (2013) Phyloseq: An R package for reproducible interactive analysis and graphics of microbiome census data. *PloS one* **8**(4): e61217.

McNutt, M.K., Camilli, R., Crone, T.J., Guthrie, G.D., Hsieh, P.A., Ryerson, T.B. *et al.* (2012) Review of flow rate estimates of the Deepwater Horizon oil spill. *Proc Natl Acad Sci USA* **109**(50): 20260-20267.

Meier, W.N., Hovelsrud, G.K., Van Oort, B.E., Key, J.R., Kovacs, K.M., Michel, C. *et al.* (2014) Arctic sea ice in transformation: A review of recent observed changes and impacts on biology and human activity. *Rev Geophys* **52**(3): 185-217.

Meng, L., Liu, H., Bao, M., and Sun, P. (2016) Microbial community structure shifts are associated with temperature, dispersants and nutrients in crude oil-contaminated seawaters. *Mar Pollut Bull* **111**(1-2): 203-212.

Methé, B.A., Nelson, K.E., Deming, J.W., Momen, B., Melamud, E., Zhang, X. *et al.* (2005) The psychrophilic lifestyle as revealed by the genome sequence of *Colwellia psychrerythraea* 34h through genomic and proteomic analyses. *Proc Natl Acad Sci USA* **102**(31): 10913-10918.

Militon, C., Jezequel, R., Gilbert, F., Corsellis, Y., Sylvi, L., Cravo-Laureau, C. *et al.* (2015) Dynamics of bacterial assemblages and removal of polycyclic aromatic hydrocarbons in oil-contaminated coastal marine sediments subjected to contrasted oxygen regimes. *Environ Sci Pollut Res* **22**(20): 15260-15272.

Mounier, J., Camus, A., Mitteau, I., Vaysse, P.J., Goulas, P., Grimaud, R., and Sivadon, P. (2014) The marine bacterium *Marinobacter hydrocarbonoclasticus* SP17 degrades a wide range of lipids and hydrocarbons through the formation of oleolytic biofilms with distinct gene expression profiles. *FEMS Microbiolgy Ecology* **90**(3): 816-831.

Murawski, S.A., Hollander, D.J., Gilbert, S., and Gracia, A. (2020) Deepwater oil and gas production in the Gulf of Mexico and related global trends. In *Scenarios and responses to future deep oil spills*: Springer, pp. 16-32.

Murphy, D., Gemmell, B., Vaccari, L., Li, C., Bacosa, H., Evans, M. *et al.* (2016) An in-depth survey of the oil spill literature since 1968: Long term trends and changes since Deepwater Horizon. *Mar Pollut Bull* **113**(1-2): 371-379.

Muyzer, G., De Waal, E.C., and Uitterlinden, A.G. (1993) Profiling of complex microbial populations by denaturing gradient gel electrophoresis analysis of polymerase chain reaction amplified genes coding for 16s rRNA. *Appl Environ Microbiol* **59**(3): 695-700.

Nadkarni, M.A., Martin, F.E., Jacques, N.A., and Hunter, N. (2002) Determination of bacterial load by real-time pcr using a broad-range (universal) probe and primers set. *Microbiology* **148**(1): 257-266.

Nagashima, H., Zulkharnain, A.B., Maeda, R., Fuse, H., Iwata, K., and Omori, T. (2010) Cloning and nucleotide sequences of carbazole degradation genes from marine bacterium *Neptuniibacter* sp. strain CAR-SF. *Curr Microbiol* **61**(1): 50-56.

Naysim, L., Kang, H.J., and Jeon, C.O. (2014) *Zhongshania aliphaticivorans* sp. nov., an aliphatic hydrocarbon-degrading bacterium isolated from marine sediment, and transfer of *Spongiibacter borealis* Jang *et al.* 2011 to the genus *Zhongshania* as *Zhongshania borealis* comb. nov. *Int J Syst Evol Microbiol* **64**(11): 3768-3774.

Nedashkovskaya, O.I., Kukhlevskiy, A.D., Zhukova, N.V., and Kim, S.B. (2016) *Amylibacter ulvae* sp. nov., a new alphaproteobacterium isolated from the pacific green alga *Ulva fenestrata*. *Arch Microbiol* **198**(3): 251-256.

Neuparth, T., Moreira, S., Santos, M., and Reis-Henriques, M. (2012) Review of oil and HNS accidental spills in Europe: Identifying major environmental monitoring gaps and drawing priorities. *Mar Pollut Bull* **64**(6): 1085-1095.

Nevalainen, M., Helle, I., and Vanhatalo, J. (2018) Estimating the acute impacts of Arctic marine oil spills using expert elicitation. *Mar Pollut Bull* **131**: 782-792.

Nie, Y., Chi, C.-Q., Fang, H., Liang, J.-L., Lu, S.-L., Lai, G.-L. *et al.* (2014) Diverse alkane hydroxylase genes in microorganisms and environments. *Sci Rep* **4**: 4968.

Nikolopoulou, M., and Kalogerakis, N. (2010) Biostimulation strategies for enhanced bioremediation of marine oil spills including chronic pollution. In *Handbook of hydrocarbon and lipid microbiology*, pp. 2521-2529.

O'Sullivan, A., and Richardson, A.J. (1967) The *Torrey Canyon* disaster and intertidal marine life. *Nature* **214**(5087): 448-448.

Oh, J.-S., and Roh, D.-H. (2018) Draft genome sequence of *Zhongshania marina* DSW25-10 T isolated from seawater. *The Microbiological Society of Korea* **54**(4): 480-482.

Ollivier, B., and Magot, M. (2005) *Petroleum microbiology*. Washington, DC, USA: ASM Press, .

Oren, A. (2019) Aerobic hydrocarbon-degrading archaea. In *Taxonomy, genomics and ecophysiology of hydrocarbon-degrading microbes*. McGenity, T.J. (ed), pp. 41-51.

Ortmann, A.C., Cobanli, S.E., Wohlgeschaffen, G., Thamer, P., McIntyre, C., Mason, J., and King, T.L. (2019) Inorganic nutrients have a significant, but minimal, impact on a coastal microbial community's response to fresh diluted bitumen. *Mar Pollut Bull* **139**: 381-389.

OSAT (2010). Summary report for sub-sea and sub-surface oil and dispersant detection: Sampling and monitoring. New Orleans, USA. Available from: https://www.restorethegulf.gov/sites/default/files/documents/pdf/OSAT_Report_FINAL_17DEC.pdf [Accessed August 20, 2020].

Otte, J.M., Blackwell, N., Soos, V., Rughöft, S., Maisch, M., Kappler, A. *et al.* (2018) Sterilization impacts on marine sediment - are we able to inactivate microorganisms in environmental samples? *FEMS Microbiol Ecol* **94**(12).

Overholt, W.A., Marks, K.P., Romero, I.C., Hollander, D.J., Snell, T.W., and Kostka, J.E. (2016) Hydrocarbon-degrading bacteria exhibit a species-specific response to dispersed oil while moderating ecotoxicity. *Appl Environ Microbiol* **82**(2): 518-527.

Ozhan, K., Parsons, M.L., and Bargu, S. (2014) How were phytoplankton affected by the Deepwater Horizon oil spill? *BioScience* **64**(9): 829-836.

P.O.S.T., U. (1996). The *Sea Empress* oil spill (p.O.S.T. Note 75). Parliamentary office of Science and Technology (UK). Available from: http://www.parliament.uk/documents/post/pn075.pdf [Accessed August 29, 2020].

Park, C., Shin, B., Jung, J., Lee, Y., and Park, W. (2017) Metabolic and stress responses of *Acinetobacter oleivorans* DR1 during long-chain alkane degradation. *Microb Biotechnol* **10**(6): 1809-1823.
Parker, A.M., Ferrer, I., Thurman, E.M., Rosario-Ortiz, F.L., and Linden, K.G. (2014) Determination of corexit components used in the Deepwater Horizon cleanup by liquid chromatography-ion trap mass spectrometry. *Anal Methods* **6**(15): 5498-5502.
Partearroyo, M.A., Ostolaza, H., Goñi, F.M., and Barberá-Guillem, E. (1990) Surfactant-induced cell toxicity and cell lysis: A study using B16 melanoma cells. *Biochem Pharmacol* **40**(6): 1323-1328.
Passow, U. (2016) Formation of rapidly-sinking, oil-associated marine snow. *Deep Sea Res Part II Top Stud Oceanogr* **129**: 232-240.
Passow, U., and Ziervogel, K. (2016) Marine snow sedimented oil released during the Deepwater Horizon spill. *Oceanography* **29**(3): 118-125.
Pérez-Pantoja, D., González, B., and Pieper, D. (2010) Aerobic degradation of aromatic hydrocarbons. In *Handbook of hydrocarbon and lipid microbiology*. K.N., T. (ed). Berlin, Heidelberg, Germany: Springer.
Personna, Y.R., King, T., Boufadel, M.C., Zhang, S., and Axe, L. (2016) Dual effects of a dispersant and nutrient supplementation on weathered Endicott oil biodegradation in seawater. *AIMS Environmental Science* **3**(4): 739.
Peterson, C.H., Rice, S.D., Short, J.W., Esler, D., Bodkin, J.L., Ballachey, B.E., and Irons, D.B. (2003) Long-term ecosystem response to the *Exxon Valdez* oil spill. *Science* **302**(5653): 2082-2086.
Place, B.J., Perkins, M.J., Sinclair, E., Barsamian, A.L., Blakemore, P.R., and Field, J.A. (2016) Trace analysis of surfactants in Corexit oil dispersant formulations and seawater. *Deep Sea Res Part II Top Stud Oceanogr* **129**: 273-281.
Pluskal, T., Castillo, S., Villar-Briones, A., and Orešič, M. (2010) MZmine 2: Modular framework for processing, visualizing, and analyzing mass spectrometry-based molecular profile data. *BMC Bioinformatics* **11**(1): 395.
Prince, R., Kelley, B., and Butler, J. (2016) Three widely-available dispersants substantially increase the biodegradation of otherwise undispersed oil. *J Marine Sci Res Dev* **6**(183).
Prince, R.C. (2015) Oil spill dispersants: Boon or bane? *Environ Sci Technol* **49**(11): 6376-6384.
Prince, R.C. (2019) Eukaryotic hydrocarbon degraders. In *Taxonomy, genomics and ecophysiology of hydrocarbon-degrading microbes*. McGenity, T.J. (ed), pp. 1-20.
Prince, R.C., Amande, T.J., and McGenity, T.J. (2019) Prokaryotic hydrocarbon degraders. In *Taxonomy, genomics and ecophysiology of hydrocarbon-degrading microbes*. McGenity, T.J. (ed), pp. 1-39.
Pruesse, E., Quast, C., Knittel, K., Fuchs, B.M., Ludwig, W., Peplies, J., and Glöckner, F.O. (2007) SILVA: A comprehensive online resource for quality checked and aligned ribosomal rna sequence data compatible with ARB. *Nucleic Acids Res* **35**(21): 7188-7196.
R Core Team (2019). R: A language and environment for statistical computing. Vienna, Austria.
Radniecki, T.S., Schneider, M.C., and Semprini, L. (2013) The influence of Corexit 9500A and weathering on Alaska North Slope crude oil toxicity to the ammonia oxidizing bacterium *Nitrosomonas europaea*. *Mar Pollut Bull* **68**(1-2): 64-70.
Rahsepar, S., Smit, M.P., Murk, A.J., Rijnaarts, H.H., and Langenhoff, A.A. (2016) Chemical dispersants: Oil biodegradation friend or foe? *Mar Pollut Bull* **108**(1): 113-119.
Ramos, J.L., Duque, E., Gallegos, M.T., Godoy, P., Ramos-Gonzalez, M.I., Rojas, A. *et al.* (2002) Mechanisms of solvent tolerance in gram-negative bacteria. *Annu Rev Microbiol* **56**: 743-768.
Reddy, C.M., Arey, J.S., Seewald, J.S., Sylva, S.P., Lemkau, K.L., Nelson, R.K. *et al.* (2012) Composition and fate of gas and oil released to the water column during the Deepwater Horizon oil spill. *Proc Natl Acad Sci USA* **109**(50): 20229-20234.
Redmond, M.C., and Valentine, D.L. (2012) Natural gas and temperature structured a microbial community response to the Deepwater Horizon oil spill. *Proc Natl Acad Sci USA* **109**(50): 20292-20297.
Ribicic, D., Netzer, R., Hazen, T.C., Techtmann, S.M., Drabløs, F., and Brakstad, O.G. (2018) Microbial community and metagenome dynamics during biodegradation of dispersed oil reveals potential key-players in cold Norwegian seawater. *Mar Pollut Bull* **129**(1): 370-378.
Rico-Martínez, R., Snell, T.W., and Shearer, T.L. (2013) Synergistic toxicity of Macondo crude oil and dispersant Corexit 9500A® to the *Brachionus plicatilis* species complex (Rotifera). *Environ Pollut* **173**: 5-10.
Rivers, A.R., Sharma, S., Tringe, S.G., Martin, J., Joye, S.B., and Moran, M.A. (2013) Transcriptional response of bathypelagic marine bacterioplankton to the Deepwater Horizon oil spill. *ISME J* **7**(12): 2315-2329.
Rodrigues, E.M., Morais, D.K., Pylro, V.S., Redmile-Gordon, M., de Oliveira, J.A., Roesch, L.F.W. *et al.* (2018) Aliphatic hydrocarbon enhances phenanthrene degradation by autochthonous prokaryotic communities from a pristine seawater. *Microb Ecol* **75**(3): 688-700.
Rubin-Blum, M., Antony, C.P., Borowski, C., Sayavedra, L., Pape, T., Sahling, H. *et al.* (2017) Short-chain alkanes fuel mussel and sponge *Cycloclasticus* symbionts from deep-sea gas and oil seeps. *Nat Microbiol* **2**(8): 17093.

Salerno, J.L., Little, B., Lee, J., and Hamdan, L.J. (2018) Exposure to crude oil and chemical dispersant may impact marine microbial biofilm composition and steel corrosion. *Front Mar Sci* **5**: 196.
Sanni, G.O., Coulon, F., and McGenity, T.J. (2015) Dynamics and distribution of bacterial and archaeal communities in oil-contaminated temperate coastal mudflat mesocosms. *Environ Sci Pollut Res* **22**(20): 15230-15247.
Schobert, H. (2013) *Chemistry of fossil fuels and biofuels*. New York, USA: Cambridge University Press.
Severin, T., Bacosa, H., Sato, A., and Erdner, D. (2016) Dynamics of *Heterocapsa* sp. and the associated attached and free-living bacteria under the influence of dispersed and undispersed crude oil. *Letters in applied microbiology* **63**(6): 419-425.
Short, J.W. (2017) Advances in understanding the fate and effects of oil from accidental spills in the United States beginning with the *Exxon Valdez*. *Arch Environ Contam Toxicol* **73**(1): 5-11.
Sieradzki, E.T., Morando, M., and Fuhrman, J.A. (2019) Metagenomics and stable isotope probing offer insights into metabolism of polycyclic aromatic hydrocarbons degraders in chronically polluted seawater. *bioRxiv*: 777730.
Sikkema, J., de Bont, J.A., and Poolman, B. (1995) Mechanisms of membrane toxicity of hydrocarbons. *Microbiol Rev* **59**(2): 201-222.
Simanzhenkov, V., and Idem, R. (2003) *Crude oil chemistry*. New York, USA: Marcel Dekker, Inc.
Skarbo, S. (2020) Poisonous fuel from major Norilsk diesel leak may already be in the Arctic ocean. In *The Siberian Times*. Published on: June 24, 2020. Available from: http://siberiantimes.com/other/others/news/poisonous-fuel-from-major-norilsk-diesel-leak-may-already-be-in-the-arctic-ocean/ [Accessed August 28, 2020].
Sørheim, K.R., Daling, P.S., Cooper, D., Buist, I., Faksness, L.-G., Altin, D. *et al.* (2020). Characterization of low sulfur fuel oils (LSFO): A new generation of marine fuel oils. Trondheim, Norway: SINTEF Ocean AS. Report No.: OC2020 A-050. Available from: http://www.itopf.org/fileadmin/data/Documents/RDaward/Final_report_LSFO_Multipartner__3.1_.pdf [Accessed July 16, 2020].
Spang, A., Caceres, E.F., and Ettema, T.J. (2017) Genomic exploration of the diversity, ecology, and evolution of the archaeal domain of life. *Science* **357**(6351).
Steen, A., and Findlay, A. (2008) Frequency of dispersant use worldwide. *International Oil Spill Conference*: American Petroleum Institute, pp. 645-649.
Steinle, L., Schmidt, M., Bryant, L., Haeckel, M., Linke, P., Sommer, S. *et al.* (2016) Linked sediment and water-column methanotrophy at a man-made gas blowout in the North Sea: Implications for methane budgeting in seasonally stratified shallow seas. *Limnol Oceanogr* **61**(S1): S367-S386.
Straub, D., Blackwell, N., Fuentes, A.L., Peltzer, A., Nahnsen, S., and Kleindienst, S. (2019) Interpretations of microbial community studies are biased by the selected 16s rRNA gene amplicon sequencing pipeline. *bioRxiv*: 2019.2012.2017.880468.
Suja, L.D., Summers, S., and Gutierrez, T. (2017) Role of EPS, dispersant and nutrients on the microbial response and MOS formation in the subarctic northeast atlantic. *Front Microbiol* **8**: 676.
Sun, H., Gao, W., Fan, H., Wang, H., and Wei, D. (2015) Cloning, purification and evaluation of the enzymatic properties of a novel arylacetonitrilase from *Luminiphilus syltensis* NOR5-1B: A potential biocatalyst for the synthesis of mandelic acid and its derivatives. *Biotechnology Letters* **37**(8): 1655-1661.
Sun, X., and Kostka, J.E. (2019) Hydrocarbon-degrading microbial communities are site specific, and their activity is limited by synergies in temperature and nutrient availability in surface ocean waters. *Appl Environ Microbiol* **85**(15): e00443-00419.
Suzuki, T., Yazawa, T., Morishita, N., Maruyama, A., and Fuse, H. (2019) Genetic and physiological characteristics of a novel marine propylene-assimilating *Halieaceae* bacterium isolated from seawater and the diversity of its alkene and epoxide metabolism genes. *Microbes and Environments*: ME18053.
Swannell, R.P., Lee, K., and McDonagh, M. (1996) Field evaluations of marine oil spill bioremediation. *Microbiol Rev* **60**(2): 342-365.
Tavassoli, T., Mousavi, S., Shojaosadati, S., and Salehizadeh, H. (2012) Asphaltene biodegradation using microorganisms isolated from oil samples. *Fuel* **93**: 142-148.
Techtmann, S.M., Zhuang, M., Campo, P., Holder, E., Elk, M., Hazen, T.C. *et al.* (2017) Corexit 9500 enhances oil biodegradation and changes active bacterial community structure of oil-enriched microcosms. *Appl Environ Microbiol* **83**(10): e03462-03416.
Teeling, H., Fuchs, B.M., Becher, D., Klockow, C., Gardebrecht, A., Bennke, C.M. *et al.* (2012) Substrate-controlled succession of marine bacterioplankton populations induced by a phytoplankton bloom. *Science* **336**(6081): 608-611.
Tissot, B.P., and Welte, D.H. (1978) *Petroleum formation and occurrence: A new approach to oil and gas exploration*. Berlin, Germany: Springer-Verlag.

Tremblay, J., Yergeau, E., Fortin, N., Cobanli, S., Elias, M., King, T.L. *et al.* (2017) Chemical dispersants enhance the activity of oil- and gas condensate-degrading marine bacteria. *ISME J* **11**(12): 2793-2808.
Tremblay, J., Fortin, N., Elias, M., Wasserscheid, J., King, T.L., Lee, K., and Greer, C.W. (2019) Metagenomic and metatranscriptomic responses of natural oil degrading bacteria in the presence of dispersants. *Environ Microbiol* **21**(7): 2307-2319.
Trudel, B.K. (1998) Dispersant application in Alaska: A technical update. *Dispersant Use in Alaska: A Technical Update*. Trudel, B.K. (ed). Anchorage, Alaska, USA: Prince William Sound Oil Spill Recovery Institute.
Ugbomeh, A., Bob-manuel, K., Green, A., and Taylorharry, O. (2019) Biochemical toxicity of Corexit 9500 dispersant on the gills, liver and kidney of juvenile *Clarias gariepinus*. *Fisheries and Aquatic Sciences* **22**(1): 15.
US NASEM (2020). The use of dispersants in marine oil spill response. Washington, DC: The National Academies Press (US).
US Nat. Comm. DWH (2011). The use of surface and subsea dispersants during the BP Deepwater Horizon oil spill. Working Paper. Washington, DC, USA: National Commission on the BP Deepwater Horizon Oil Spill and Offshore Drilling. Available from: http://purl.fdlp.gov/GPO/gpo184 [Accessed April 20, 2019].
US NPC (2015). Arctic potential: Realizing the promise of U.S. Arctic oil and gas resources. Washington, DC, USA: National Petroleum Council. Available from: https://www.npcarcticreport.org/ [Accessed July 19, 2020].
US NRC (2003). Oil in the sea III: Inputs, fates, and effects. Washington, DC, USA: The National Academies Press (US). Report No.: 0309084385. Available from: https://www.nap.edu/catalog/10388/oil-in-the-sea-iii-inputs-fates-and-effects
US NRC (2014). Responding to oil spills in the U.S. Arctic marine environment. Washington, DC, USA: The National Academies Press. Report No.: 978-0-309-29886-5
Valencia-Agami, S.S., Cerqueda-García, D., Putzeys, S., Uribe-Flores, M.M., García-Cruz, N.U., Pech, D. *et al.* (2019) Changes in the bacterioplankton community structure from southern Gulf of Mexico during a simulated crude oil spill at mesocosm scale. *Microorganisms* **7**(10): 441.
Van Beilen, J.B., Marín, M.M., Smits, T.H., Röthlisberger, M., Franchini, A.G., Witholt, B., and Rojo, F. (2004) Characterization of two alkane hydroxylase genes from the marine hydrocarbonoclastic bacterium *Alcanivorax borkumensis*. *Environ Microbiol* **6**(3): 264-273.
Venosa, A.D., and Holder, E.L. (2007) Biodegradability of dispersed crude oil at two different temperatures. *Mar Pollut Bull* **54**(5): 545-553.
Vergeynst, L., Kjeldsen, K.U., Lassen, P., and Rysgaard, S. (2018a) Bacterial community succession and degradation patterns of hydrocarbons in seawater at low temperature. *J Hazard Mat* **353**: 127-134.
Vergeynst, L., Wegeberg, S., Aamand, J., Lassen, P., Gosewinkel, U., Fritt-Rasmussen, J. *et al.* (2018b) Biodegradation of marine oil spills in the Arctic with a Greenland perspective. *Sci Total Environ* **626**: 1243-1258.
Wang, C., Huang, Y., Zhang, Z., Hao, H., and Wang, H. (2020) Absence of the nahG-like gene caused the syntrophic interaction between *Marinobacter* and other microbes in PAH-degrading process. *J Hazard Mat* **384**: 121387.
Wang, W., and Shao, Z. (2013) Enzymes and genes involved in aerobic alkane degradation. *Front Microbiol* **4**: 116.
Wang, W., Zhong, R., Shan, D., and Shao, Z. (2014) Indigenous oil-degrading bacteria in crude oil-contaminated seawater of the Yellow Sea, China. *Appl Microbiol Biotechnol* **98**(16): 7253-7269.
Wang, Z., Fingas, M., Blenkinsopp, S., Sergy, G., Landriault, M., Sigouin, L. *et al.* (1998) Comparison of oil composition changes due to biodegradation and physical weathering in different oils. *Journal of Chromatography A* **809**(1-2): 89-107.
Wentzel, A., Ellingsen, T.E., Kotlar, H.-K., Zotchev, S.B., and Throne-Holst, M. (2007) Bacterial metabolism of long-chain *n*-alkanes. *Appl Microbiol Biotechnol* **76**(6): 1209-1221.
White, H.K., Lyons, S.L., Harrison, S.J., Findley, D.M., Liu, Y., and Kujawinski, E.B. (2014) Long-term persistence of dispersants following the Deepwater Horizon oil spill. *Environmental Science & Technology Letters* **1**(7): 295-299.
Wickham, H. (2016) Ggplot2: Elegant graphics for data analysis. New York, USA: Springer.
Widdel, F., and Rabus, R. (2001) Anaerobic biodegradation of saturated and aromatic hydrocarbons. *Curr Opin Biotechnol* **12**(3): 259-276.
Widdel, F., and Musat, F. (2019) Energetic and other quantitative aspects of microbial hydrocarbon utilization: An introduction. In *Aerobic utilization of hydrocarbons, oils and lipids*, pp. 1-41.
Wilkinson, J., Beegle-Krause, C.J., Evers, K.-U., Hughes, N., Lewis, A., Reed, M., and Wadhams, P. (2017) Oil spill response capabilities and technologies for ice-covered Arctic marine waters: A review of recent developments and established practices. *Ambio* **46**(3): 423-441.

Wiltshire, K.H., Kraberg, A., Bartsch, I., Boersma, M., Franke, H.-D., Freund, J. *et al.* (2010) Helgoland Roads, North Sea: 45 years of change. *Estuaries and Coasts* **33**(2): 295-310.
Wise, J., and Wise, J.P. (2011) A review of the toxicity of chemical dispersants. *Rev Environ Health* **26**(4): 281-300.
Word, J.Q., Clark, J.R., and Word, L.S. (2014) Comparison of the acute toxicity of Corexit 9500 and household cleaning products. *Hum Ecol Risk Assess* **21**(3): 707-725.
Yakimov, M.M., Giuliano, L., Gentile, G., Crisafi, E., Chernikova, T.N., Abraham, W.-R. *et al.* (2003) *Oleispira antarctica* gen. nov., sp. nov., a novel hydrocarbonoclastic marine bacterium isolated from Antarctic coastal sea water. *Int J Syst Evol Microbiol* **53**(3): 779-785.
Yakimov, M.M., Timmis, K.N., and Golyshin, P.N. (2007) Obligate oil-degrading marine bacteria. *Curr Opin Biotechnol* **18**(3): 257-266.
Yang, T., Nigro, L.M., Gutierrez, T., Joye, S.B., Highsmith, R., and Teske, A. (2016) Pulsed blooms and persistent oil-degrading bacterial populations in the water column during and after the Deepwater Horizon blowout. *Deep Sea Res Part II Top Stud Oceanogr* **129**: 282-291.
Zakharenko, A.S., Galachyants, Y.P., Morozov, I.V., Shubenkova, O.V., Morozov, A.A., Ivanov, V.G. *et al.* (2019) Bacterial communities in areas of oil and methane seeps in pelagic of Lake Baikal. *Microb Ecol* **78**(2): 269-285.

Chapter 2 – Personal contribution

The microcosm experiment was designed by myself and Jun.-Prof. Sara Kleindienst. Preparation of water-accommodated fractions, establishment of microcosms, daily rotations of microcosms, sampling of microcosms, radiotracer assays, DNA extraction and amplification for amplicon sequencing or qPCR, hydrocarbon extraction, data visualization and statistical data analysis were performed by myself. Bioinformatic analysis of sequencing data was performed by Dr. Daniel Straub and results were interpreted by myself together with Dr. Daniel Straub and Jun.-Prof. Sara Kleindienst. GC-MS measurements of hydrocarbon extracts were performed by Dr. Rafael Tarozo and Dr. Christian Hallmann, the resulting chromatograms were analysed by myself with their input and the results were interpreted by myself together with Dr. Rafael Tarozo, Dr. Christian Hallmann and Jun.-Prof. Sara Kleindienst. The results from all other analyses were interpreted by myself together with Jun.-Prof. Sara Kleindienst and input from Prof. Andreas Kappler. The manuscript was written by myself and revised by all co-authors. Dr. Daniel Straub, Dr. Rafael Tarozo and Dr. Christian Hallmann wrote the method descriptions for bioinformatics analyses and GC-MS measurements, respectively.

2 Distinct impacts of nutrient and dispersant application on oil-degrading microbial communities in Arctic Ocean oil spill scenarios

Saskia Rughöft[1], Daniel Straub[1,2], Rafael Tarozo[3], Christian Hallmann[3,4], Andreas Kappler[5] and Sara Kleindienst[1]

[1] Microbial Ecology, Center for Applied Geosciences, University of Tübingen, Germany
[2] Quantitative Biology Center, University of Tübingen, Germany
[3] Organic Paleobiogeochemistry, Max Planck Institute for Biogeochemistry, Jena, Germany
[4] MARUM, University of Bremen, Bremen, Germany
[5] Geomicrobiology, Center for Applied Geosciences, University of Tübingen, Germany

Unpublished manuscript

2.1 Abstract

Chemical dispersant application is a widely used response strategy during marine oil spills. However, alternative approaches may be of interest to limit potential negative ecosystem effects. Our goal was to compare the impacts of chemical dispersant or nutrient addition, i.e. biostimulation, during oil spill scenarios on native microbial communities from the increasingly pollutant-exposed Arctic Ocean. Therefore, seawater laboratory microcosms amended with crude oil components as water-accommodated fractions (WAF) ± nutrients, oil-dispersant mixtures as chemically enhanced WAFs (CEWAF), or dispersant alone were monitored over 32 days. Compared to oil-only treatments, biostimulation led to enhanced microbial growth and marine oil snow formation, faster oil-derived dissolved organic carbon (DOC) biodegradation and higher ^{14}C-hexadecane oxidation rates, while dispersant addition resulted in lower cell numbers and the persistence of high CEWAF-derived DOC levels in microcosms after 32 days. Hydrocarbon biodegradation was detected in all treatments. Microbial community dynamics, including known hydrocarbon-degrading taxa such as *Oleispira*, *Colwellia* and *Neptunomonas*, were markedly affected by dispersant addition but not by biostimulation. Our study shows that biostimulation could be a promising alternative approach to dispersant application when considering potential future Arctic Ocean oil spills.

2.2 Introduction

Accidental marine crude oil or fuel spills cause substantial environmental damage in marine ecosystems (Peterson *et al.*, 2003; Short, 2017). Even though the frequency of marine oil spills has been decreasing (ITOPF, 2020), potential future spills might lead to increasingly complex and difficult spill response conditions, due to oil exploration activities moving into deeper waters and previously less impacted regions like the Arctic (Harsem *et al.*, 2015; Gutierrez, 2018; Murawski *et al.*, 2020). The fate of oil in marine environments is determined by a number of physicochemical and biological processes. Among these, biodegradation of petroleum hydrocarbons (HCs) is a key factor, carried out by a wide variety of ubiquitous microorganisms that play a crucial role in oil spill remediation (Head *et al.*, 2006; Joye *et al.*, 2016b). In addition, a number of technological emergency spill response strategies are typically employed after marine oil spills, including mechanical containment and removal, *in situ* burning, or chemical dispersion of released oil (ExxonMobil, 2014).

Chemical dispersants are solvent-surfactant mixtures applied to disperse oil into the water column and, thus, reduce surface slicks and coastal oiling. Following the *Deepwater Horizon* (DWH) oil spill in the Gulf of Mexico in 2010, for example, seven million litres of dispersants (Corexit EC9500A and EC9527A) were applied in response to the discharge of an estimated 800 million liters of crude oil into the Gulf ecosystem (US Nat. Comm. DWH, 2011; McNutt *et al.*, 2012). While the impacts of the oil spill on the Gulf's ecosystem are relatively well documented (DWH NRDA Trustees, 2016; McGowan *et al.*, 2017), the ecological impact of chemical dispersant application, especially on native microbial oil-degrading populations, is still under debate and conflicting reports have led to disputes over best practices (US NASEM, 2020).

Biostimulation represents an alternative approach to oil spill remediation since its main goal is to enhance naturally occurring oil biodegradation processes, typically by supplying limiting nutrients (Nikolopoulou and Kalogerakis, 2010). Large oil inputs cause a drastic shift in the bioavailable *in situ* C:N:P ratio and therefore, microbial HC degradation is often limited by nutrient concentrations in seawater (Atlas and Bartha, 1972). After the large Exxon Valdez tanker spill in Alaska in 1989, for example, approximately 50 tons of nitrogen and 5 tons of phosphorous were applied and accelerated oil biodegradation at an estimated 2,000 km of oiled intertidal shorelines (Curl *et al.*, 1992; Bragg *et al.*, 1994). Even though biostimulation is more commonly described for contaminated soil or sediment systems (Adams *et al.*, 2015), it was also shown to improve seawater remediation under laboratory conditions (Coulon *et al.*, 2007; Crisafi *et al.*, 2016; Ortmann *et al.*, 2019; Sun and Kostka, 2019). The impacts of chemical dispersant application and biostimulation treatments on seawater microbial communities during an oil spill scenario, however, have only rarely been compared systematically (Meng *et al.*, 2016; Personna *et al.*, 2016).

Particularly relatively pristine and vulnerable environments like the Arctic Ocean remain largely unexplored in this regard, even though crude oil and fuel spill risks are increasing: The continuing decline in Arctic sea ice coverage has caused rising interests in Arctic oil exploration and shipping routes by different stakeholders (Meier *et al.*, 2014; Harsem *et al.*, 2015; US NPC, 2015; Harriss, 2016). Spill impacts are assumed to be potentially disastrous in the vulnerable Arctic ecosystem, however, predictions are hindered by a lack of ecological baseline knowledge

for this region (Lee *et al.*, 2015; US NPC, 2015; Aune *et al.*, 2018; Nevalainen *et al.*, 2018). The application of chemical dispersants in the Arctic remains controversial, due to these knowledge gaps and additional unknowns, e.g. regarding its effectiveness at low temperatures, particularly for heavy fuel oils (Holder *et al.*, 2015; Sørheim *et al.*, 2020). Only limited marine dispersant applications in the Arctic have occurred up to now according to publicly available information, i.e. in the form of small test applications off the coast of Alaska, USA (Curl *et al.*, 1992; Ernest, 1993; Trudel, 1998). However, almost all member countries of the Arctic Council currently consider dispersant application as a spill response option (Arctic Council, 2013; US NASEM, 2020). Since Arctic environmental conditions (e.g. darkness, low temperatures, sea ice, remoteness) will present unprecedented technological challenges for oil spill remediation (US NRC, 2014; Wilkinson *et al.*, 2017), dispersant application by aircraft has previously been recommended for these conditions (Lewis and Prince, 2018). For the same reasons, biostimulation treatments enhancing the *in situ* oil biodegradation potential that is already present (McFarlin *et al.*, 2017; Vergeynst *et al.*, 2018b and references therein), might likewise be of interest in future Arctic oil spill scenarios.

Therefore, the main objectives of this study were i.) to characterize the response of microbial communities from the central Arctic Ocean to a simulated large oil spill scenario and ii.) to compare the effects of nutrient or dispersant addition on these microbial communities and their oil biodegradation potential. Thus, Arctic Ocean seawater laboratory microcosms were amended with crude oil components as water-accommodated fractions (WAF) ± nutrients (N; i.e. nitrate, ammonium, phosphate), oil-dispersant mixtures as chemically enhanced WAFs (CEWAF), or dispersant alone, and monitored over an incubation period of 32 days at 1°C or 15°C (Fig. 2.1).

2.3 Experimental procedures

2.3.1 Seawater samples

During research cruise PS101 on *RV Polarstern*, 160 liters of seawater were collected in October 2016 from a depth of 150 m in the central Arctic Ocean (086° 51.45' N, 061° 28.95' E; *in situ* temperature -1.7°C; Fig. S2.1). The seawater was stored at 0°C aboard the ship, transported to the laboratory in Tübingen while cooled consistently, sampled for microbiological analyses (referred to as *in situ*-like samples herein), used immediately for the preparation of water-accommodated fractions (WAFs), and stored at 4°C until the start of the experiment (7 days). Nutrient concentrations in the seawater samples were determined on board *RV Polarstern* as 8.91 µM nitrate, 0.02 µM nitrite, 0.56 µM phosphate and 3.63 µM silicate (personal communication, Gunter Wegener).

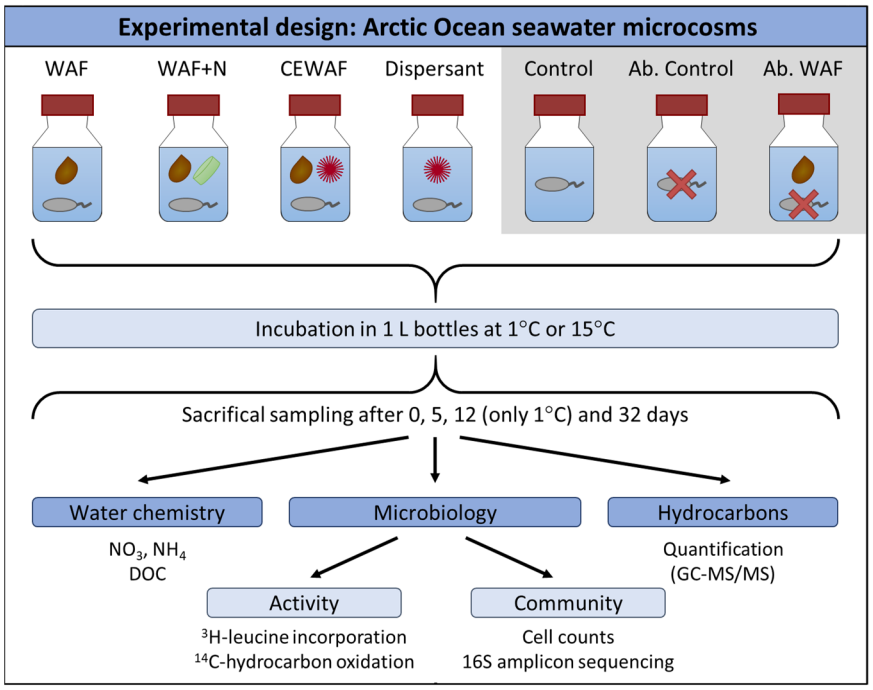

Figure 2.1: Experimental design of this study. Seawater microcosms simulating water column conditions during a large Arctic Ocean oil spill scenario were established in triplicate, incubated at 1°C or 15°C, and sampled sacrificially after 0, 5, 12 (only 1°C), and 32 days. Treatments received the following amendments (adjusted for similar final DOC content) at the start of the experiment: crude oil-derived water accommodated fraction (WAF, ab. WAF), WAF and nutrients (WAF+N), chemically enhanced WAF (CEWAF, contains Corexit dispersant), or dispersant alone. Additional control treatments received no amendments (Control, Ab. Control) and/or contained only sterilized (= abiotic) seawater (Ab. Control, Ab. WAF).

2.3.2 Water-accommodated fractions, and establishment and sampling of microcosms

All WAF solutions were prepared with Macondo MC252 surrogate crude oil (provided by BP) according to Kleindienst *et al.* (2015b) with minor modifications (see SI). Seawater (SW) microcosms were established using 850 ml of seawater (gently mixed in a separate, pre-cleaned 25 L HDPE-container beforehand) in 1 L glass bottles with teflon-lined caps. Five different treatments were prepared by adding (1) 50 ml of sterilized SW (Control), (2) 50 ml of WAF solution (WAF-derived DOC = 276 µM), (3) 50 ml WAF solution and 200 µl of nutrient solution (WAF+N), (4) 2 ml CEWAF solution (CEWAF-derived DOC = 280 µM) and 48 ml sterilized SW, or (5) 1 ml Dispersant solution (Dispersant-derived DOC = 256 µM) and 49 ml sterilized SW. The respective volumes of added WAF solutions were chosen to simulate a large oil spill scenario (Kleindienst *et al.*, 2016a) and adjusted with the goal of obtaining comparable levels of dissolved organic carbon (DOC) across all hydrocarbon-amended microcosms at the start of the experiment. WAF+N treatments were amended with 100 µM ammonium chloride, 100 µM potassium nitrate, and 10 µM potassium phosphate (final concentrations, respectively). Abiotic controls containing either (6) 900 ml sterilized SW (Ab. Control) or (7) 850 ml sterilized SW and 50 ml WAF (Ab. WAF) were also prepared.

Microcosms were established in triplicates, except for abiotic WAF controls where only duplicates were established due to limited WAF solution volumes. Subsequently, microcosms were separated into two groups which were incubated in the dark at either 1°C or 15°C. All microcosm bottles were gently turned at least once every 24 hours. All biotic treatments were

sampled sacrificially at four time points (1°C microcosms; after 0, 5, 12, 32 days) or three time points (15°C microcosms; after 0, 5, 32 days). For the abiotic SW controls, the same biological triplicate bottles were sub-sampled at all time points, while the abiotic WAF controls were sampled sacrificially only after 0 and 32 days. Sampling of the microcosms was performed after inverting bottles gently a few times by removing aliquots for each respective analysis in the following order: water chemistry (oxygen, pH, salinity, nutrients, DOC), ^{14}C-hydrocarbon oxidation assay, ^{3}H-leucine incorporation, total cell counts, DNA, hydrocarbons.

2.3.3 Geochemical, molecular and microbiological analyses

Nutrients (nitrate, phosphate, and ammonium), DOC, and HC concentrations were monitored during the course of the experiment (see SI). HC extraction from water samples was performed using dichloromethane (twice) and *n*-hexane (once) and concentrated extracts were measured via gas chromatography coupled to mass spectrometry (GC-MS) (see SI). Microbial community composition and cell numbers were investigated for each sample using 16S rRNA amplicon Illumina sequencing, quantitative PCR (qPCR) and total cell counts (see SI). Sequencing data was analysed with nf-core/ampliseq v1.1.0, which performed all following analysis steps and includes required software (Ewels *et al.*, 2020; see also SI; Straub *et al.*, 2020). Microbial activity was measured using ^{3}H-leucine incorporation analysis and ^{14}C-hexadecane and ^{14}C-naphthalene oxidation assays (see SI).

2.3.4 Data analysis

To test whether observed differences in microbial productivity, cell numbers, ^{14}C-hexadecane oxidation rates, as well as nutrient, DOC and HC concentrations between the different treatments (at one time point) or between time points (for one treatment type) were statistically significant, ANOVA followed by Tukey post-hoc test ($p < 0.05$) for multiple comparisons was used. Beforehand, the data sets of interest were tested for normally distributed residuals (tested with Shapiro-Wilks test, $p > 0.05$) and homogeneous variances (tested with Levene test, $p > 0.05$). qPCR data was log-transformed before testing. The R programming language (R Core Team, 2019) was used to perform all described tests and all presented data was plotted using ggplot2 v3.3.2 (Wickham, 2016) in R.

2.4 Results

2.4.1 Microbial growth and activity

In microcosms incubated at 1°C (i.e. close to *in situ* temperature conditions), the bacterial productivity (Fig. 2.2B) determined via ^{3}H-leucine incorporation rates increased in all biotic treatments after the start of incubation, with peak rates recorded after 12 days in all treatments (421.18–483.17 nM carbon d^{-1} in HC-amended samples). After 32 days, the productivity in dispersant-containing treatments (i.e. CEWAF and dispersant-only) had decreased to levels similar to control treatments, while the activity in both WAF treatments was significantly ($p < 0.0001$) higher, with the nutrient-amended WAF treatment showing the highest sustained activity (218.56 nM carbon d^{-1}). Cell numbers determined via cell counts (Fig. 2.2A) showed that the observed increase in bacterial productivity was followed by increasing cell numbers in all HC-amended treatments, with nutrient-amended treatments reaching the highest average cell

numbers (1.6 x 10^6 cells ml^{-1} after 32 days) and with cell numbers in dispersant-containing treatments decreasing again after 32 days. Cell numbers estimated via 16S rRNA gene qPCR showed the same trend, i.e. significantly ($p < 0.0001$) higher estimated cell numbers in WAF and WAF+N treatments compared to dispersant-containing treatments at the end of the incubation period (Fig. S2.2). The formation of white macroscopic aggregates was first observed in both WAF treatments after 10 days and long flocs had formed after 32 days in all WAF-containing bottles, with nutrient-amended treatments showing a higher aggregate density and larger aggregate sizes (maximum length = 2–4 cm in WAF+N vs. 0.5–2 cm in WAF; Fig. S2.3). Fluorescence microscopy using dead-live staining revealed that WAF aggregates contained large numbers of living cells (Fig. S2.3). Only very few aggregates were observed in CEWAF treatments after 32 days (maximum length = 1-3 mm) and no macroscopic aggregates were observed in dispersant or control treatments. The detected nutrient dynamics associated with the observed microbial growth and activity revealed that nitrate concentrations were depleted in WAF treatments after 32 days and significantly ($p < 0.05$) lower than in all other treatments (Fig. S2.4). Incubations at 15°C generally showed similar trends regarding microbial growth and activity, aggregate formation, and nitrate depletion (Fig. S2.2 and S2.4).

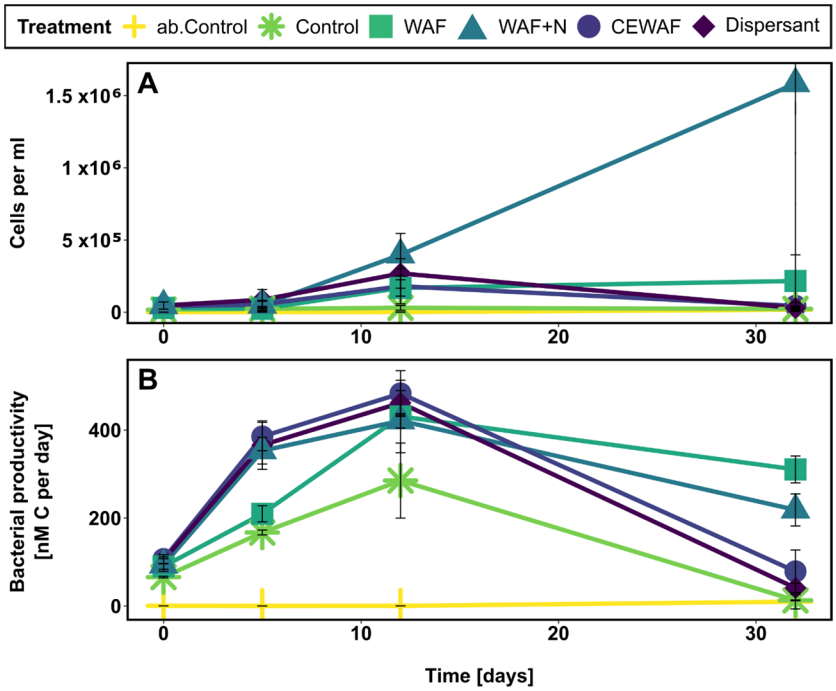

Figure 2.2: Microbial cell numbers and activity in 1°C seawater microcosms simulating water column conditions during an Arctic Ocean oil spill scenario. Treatments received crude oil-derived water accommodated fraction (WAF), WAF and nutrients (WAF+N), chemically enhanced WAF (CEWAF, contains Corexit dispersant), or dispersant alone. Control treatments received no amendments and/or contained only sterilized seawater (Control, abiotic Control). Results shown are averages of sacrificial, triplicate microcosms (standard deviations are based on triplicates). **A**) Cell numbers [cells ml^{-1}] as determined by DAPI total cell counts. **B**) Rates of microbial productivity measured via ^{3}H-leucine incorporation assays.

2.4.2 Microbial community dynamics

The β-diversity of 16S rRNA gene-based microbial community composition differed across treatments and time points in 1°C microcosms (Fig. 3.2A), highlighting distinct microbial community dynamics across treatments. At the start of the experiment, all communities were

comparable and also similar to samples taken directly after the seawater reached our laboratory (termed '*In situ*-like'). Additionally, biotic control treatments with and without nutrient addition remained quite similar to each other during the incubation period. The HC-amended communities, however, evolved differently over time with a clear separation observed between the WAF±N treatments and the dispersant-containing treatments. These different microbial community dynamics were characterized by distinct enriched genera, either detected in WAF±N or in CEWAF and dispersant-only treatments (Fig. 3.2B). Even though *Oleispira* and unclassified *Saccharospirillaceae* (with 95.60% 16S rRNA gene sequence identity to *Oceaniserpentilla haliotis*) were initially enriched in all HC-amended treatments, albeit to a different relative 16S rRNA gene sequence abundance (14-53% and 15-33%, respectively), dispersant-containing treatments contained at least one notable, additional enriched taxon already after 5 days (i.e. *Sinobacterium*; up to 16%) and were mostly dominated by *Colwellia* for the rest of the incubation period (up to 82%). In contrast, *Polaribacter* and unclassified *Flavobacteriaceae* (notably with 100% 16S rRNA gene sequence identity to *Polaribacter dokdonensis*) dominated both WAF treatments at these later time points (up to 83% together). Additionally, unclassified *Cryomorphaceae* (with 90.12% 16S rRNA gene sequence identity to *Owenweeksia* sp. strain SC180) became enriched in both dispersant-containing treatments after 32 days (up to 12%), whereas *Neptunomonas* was enriched in both WAF treatments at the end of the incubation period (up to 20%), with a few distinct additional taxa only enriched in either WAF (*Loktanella*; 4%) or WAF+N (*Profundimonas, Psychroserpens, Pacificibacter*; 10-22%) treatments. Dispersant treatments furthermore revealed a number of enriched archaeal taxa linked to ammonia oxidation (e.g. *Cand*. Nitrosopumilus and *Cand*. Nitrosopelagicus) at the end of the incubation period. Thus, dispersant addition led to more drastic changes in microbial community dynamics than nutrient addition, compared to WAF treatments. This trend was also observed in microcosms incubated at 15°C, even though distinct microbial community compositions were detected (Fig. S2.5). Both WAF treatments were, for example, mainly dominated by *Neptunomonas*, while CEWAF treatments were dominated by *Neptunomonas* or *Colwellia* and the enriched taxa in dispersant-only microcosms were mainly *Colwellia*, *Oleispira* and *Ulvibacter*.

2.4.3 Microbial oil biodegradation potential

Different analytical approaches indicated that some HC biodegradation took place in all HC-amended treatments during the incubation period, even though a precise quantification of the added oil HC components was challenging due to the chemical heterogeneity within (i.e. multi-phase system including oil droplets and differing amounts of microbial exudates and aggregates) and across microcosms (i.e. chemically or mechanically dispersed oil components, heightened effects of natural biological variation due to sacrificial sampling). Analysis of DOC concentrations in microcosms incubated at 1°C revealed that, at the start of the experiment, similarly elevated DOC levels that were significantly higher ($p < 0.00001$) than background seawater concentrations were achieved across all HC-amended treatments (343.40–428.33 µM; Fig. 2.4A). Data from abiotic WAF control treatments after 32 days indicated that no significant abiotic loss of DOC or other quantified hydrocarbons had occurred during the microcosm incubations. The DOC concentrations in both WAF treatments, however, decreased significantly ($p < 0.0001$) within the incubation period, suggesting that the native microbial

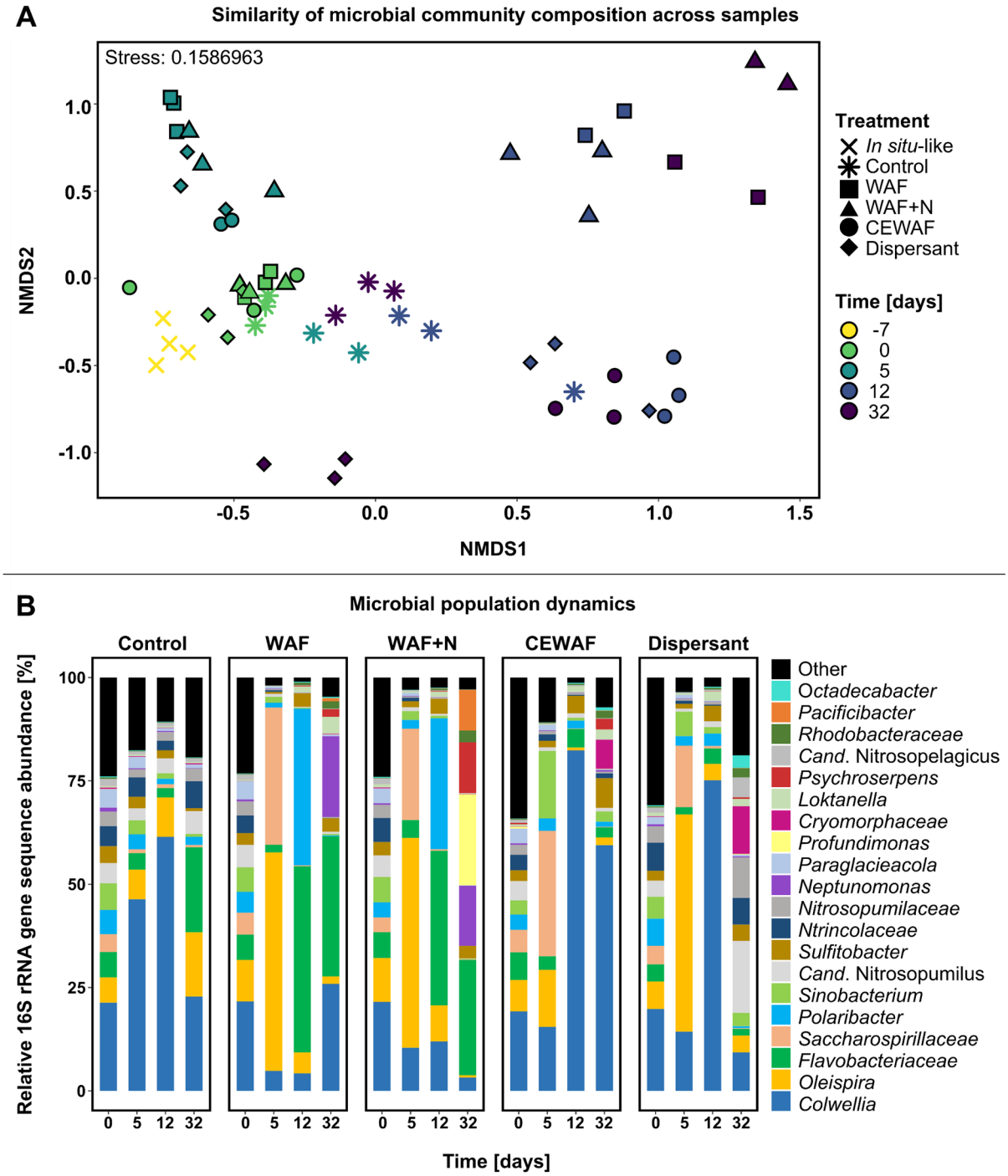

Figure 2.3: Changes in microbial community composition in 1°C seawater microcosms simulating water column conditions during an Arctic Ocean oil spill scenario as determined by 16S rRNA gene amplicon sequencing. Treatments received crude oil-derived water accommodated fraction (WAF), WAF and nutrients (WAF+N), chemically enhanced WAF (CEWAF, contains Corexit dispersant), or dispersant alone. Control treatments received no amendments. **A**) Non-metric multidimensional scaling (NMDS) plot based on Bray Curtis diversity showing the similarity of microbial community compositions across samples. The stress achieved is indicated in the top left of the plot. *In situ*-like samples were taken directly after seawater samples reached the laboratory (1 week before start of experiment). **B**) Microbial population dynamics (averages of sacrificial triplicate microcosms) of most abundant taxa in microcosms at genus level (sorted by average abundance across samples and labelled with the highest descriptive taxonomic level).

community degraded most WAF-derived DOC until reaching background DOC levels (191.67–198.91 µM on average) within 32 days, with a significantly ($p < 0.01$) faster DOC decrease in nutrient treatments. In contrast, the DOC content of both dispersant-containing treatments remained significantly ($p < 0.0001$) higher through the end of the experiment (332.41–378.38 µM). The same trends were observed in microcosms incubated at 15°C, except for a faster DOC decrease in both WAF treatments (Fig. S2.6A).

Using ^{14}C-labelled HC substrate, naphthalene oxidation activity was mainly detected in WAF treatments (0.24–1.11 ng L^{-1} d^{-1}), with a late increase in activity in CEWAF treatments that was only detected in 15°C incubations (1.28 ng L^{-1} d^{-1}; Fig S2.7). Even though ^{14}C-hexadecane oxidation activity was detected in all HC-amended treatments, the rates observed in WAF+N treatments (1.28 ng L^{-1} d^{-1}) after 5 days were significantly ($p < 0.01$) higher than in WAF or CEWAF treatments (Fig. S2.7; data only available for 15°C incubations due to technical issues). HC quantification via GC-MS indicated that *n*-alkanes of intermediate chain lengths ($C_{12–18}$), i.e. alkanes within the substrate range of most well-characterized microbial alkane hydroxylases (Van Beilen *et al.*, 2004; Liu *et al.*, 2011), decreased significantly ($p < 0.05$) in all treatments, with CEWAF treatments reaching the lowest remaining levels (11% of T_0 concentrations) after 32 days (Fig. 2.4C). A decrease of longer alkanes ($C_{19–36}$) and phenanthrenes was detected in CEWAF treatments, whereas a similar potential biodegradation pattern might have been masked by fluctuations in the data of WAF and WAF+N treatments (data not shown). Additionally, a comparison between treatments was complicated by different HC compositions of the initial HC amendments, for example in the case of naphthalenes which were only detected in WAF treatments (Fig. 2.4D). However, a few other clear trends could be observed: A decrease in naphthalenes appeared to be enhanced in WAF+N treatments compared to WAF treatments, while all detected *n*-alkanes, naphthalenes and phenanthrenes decreased more in 15°C incubations compared to 1°C incubations (Fig. S2.6). Moreover, a bulk parameter encompassing all detected compounds in the obtained GC-MS chromatograms (termed ‘total petroleum hydrocarbons (TPH) equivalents’) revealed very similar dynamics compared to the DOC data, i.e. significantly ($p < 0.05$) higher persisting levels of added organic compounds in dispersant-containing treatments compared to both WAF treatments after 32 days (Fig. 2.4B).

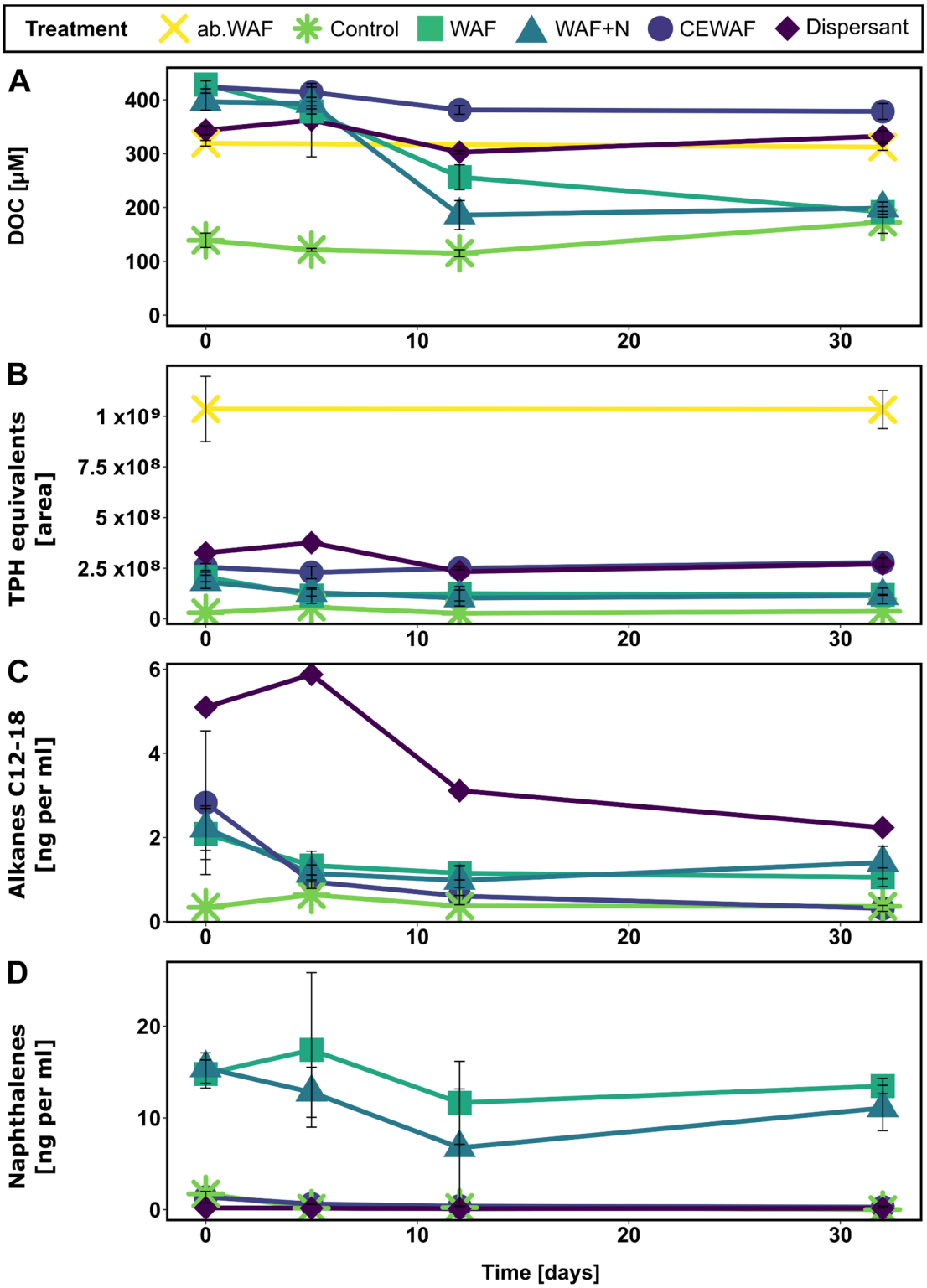

Figure 2.4: Hydrocarbon and DOC concentrations in 1°C seawater microcosms simulating water column conditions during an Arctic Ocean oil spill scenario. Treatments received crude oil-derived water accommodated fraction (WAF), WAF and nutrients (WAF+N), chemically enhanced WAF (CEWAF, contains Corexit dispersant), or dispersant alone. Control treatments received no amendments (Control) and/or contained only sterilized seawater and WAF (abiotic WAF; only included for bulk parameters). Results shown are averages of sacrificial, triplicate microcosms (standard deviations are based on triplicates). **A**) Dissolved organic carbon (DOC) concentrations [µM] show that amendments were adjusted to similar DOC levels at the start of the experiment. **B-D**) Total petroleum hydrocarbon (TPH) equivalents, *n*-alkanes (C_{12}-C_{18}) and naphthalenes are shown as determined by via GC-MS quantification [ng ml^{-1}].

2.5 Discussion

2.5.1 Response of Arctic seawater community to simulated oil spill scenario

The investigated native microbial community from the central Arctic Ocean responded to the input of crude oil-derived HCs with increased growth, activity and aggregate formation (Fig. 2.5). The observed microbial aggregates were likely marine (oil) snow (i.e. consisting of microorganisms, their exudates and oil), which was previously also reported in similar microcosm studies (Kleindienst *et al.*, 2015b; Passow, 2016; Suja *et al.*, 2017; Doyle *et al.*, 2018) and played an important role after the DWH oil spill in the Gulf of Mexico (Passow and Ziervogel, 2016). Two of the dominant taxa also contain well-characterized HC-degrading species, such as the psychrophilic alkane degrader *Oleispira antarctica* (Yakimov *et al.*, 2003) or the aromatic HC degrader *Neptunomonas naphthovorans* (Hedlund *et al.*, 1999), while the dominant *Saccharospirillaceae* ASV was closely related to the unclassified *Oceanospirillales* member that became enriched during the DWH spill in the Gulf of Mexico (98.40% 16S rRNA gene sequence identity to clone HM587889 from Hazen *et al.*, 2010) which has been linked to alkane degradation (Mason *et al.*, 2012; Redmond and Valentine, 2012). Additionally, several other enriched taxa were previously detected in association with oil pollution and/or have been linked to HC biodegradation, such as *Polaribacter* (Redmond and Valentine, 2012; Wang *et al.*, 2014), *Sulfitobacter* (Gerdes *et al.*, 2005; Mas-Lladó *et al.*, 2014; Fasca *et al.*, 2018) and *Loktanella* (Harwati *et al.*, 2007; Sanni *et al.*, 2015). This suggests that they played a role as primary and/or secondary HC degraders in the WAF treatments. Our results demonstrate that seed populations of HC degrading bacteria are ubiquitous, even in the central Arctic Ocean, which agrees with earlier studies that investigated other Arctic Ocean areas (McFarlin *et al.*, 2017; Vergeynst *et al.*, 2018a; Vergeynst *et al.*, 2018b). These findings are further supported by the detected biodegradation of $C_{12\text{-}18}$ *n*-alkanes, bulk DOC and TPH equivalents, and the observed ^{14}C-naphthalene and ^{14}C-hexadecane oxidation activity in WAF treatments, pointing towards high HC biodegradation potential at our field site. Previous studies have reported similar microbial biodegradation patterns of petroleum HCs in microcosm incubations using Arctic or subarctic seawater from different locations, including less biodegradation of aromatic HCs in some cases (reviewed e.g. by Vergeynst *et al.*, 2018b). Thus, the native microbial community from the central Arctic Ocean displayed a considerable oil biodegradation potential in response to the input of crude oil-derived HCs, demonstrating a promising basis for Arctic oil spill bioremediation approaches. Furthermore, the observed effects of a higher incubation temperature (15°C) on the seawater microbial community (i.e. different enriched taxa and HC degraders, increased biodegradation activity) were in agreement with previous microcosm studies as well (Coulon *et al.*, 2007; Liu *et al.*, 2017a; Lofthus *et al.*, 2018; Sun and Kostka, 2019).

2.5.2 Impacts of biostimulation on microbial community dynamics and oil biodegradation potential

Biostimulation (i.e. nutrient addition along with WAF addition) led to increased marine (oil) snow formation, higher cell numbers (Fig. 2.5) and sustained elevated microbial productivity at the end of the incubation period, while nitrate was depleted in WAF treatments without nutrient addition during the incubation period. Furthermore, biostimulation resulted in

enhanced biodegradation of oil-derived DOC, naphthalenes and higher detected ^{14}C-HC oxidation rates. This suggests that the Arctic Ocean microbial community was nitrogen-limited in their response to the simulated oil spill under *in situ* nutrient conditions, which is in agreement with previous reports using Arctic (Personna *et al.*, 2016; Ortmann *et al.*, 2019; Sun and Kostka, 2019) or temperate seawater (Coulon *et al.*, 2007; Crisafi *et al.*, 2016). Remarkably, the same microbial key players were enriched in WAF+N and WAF setups, with the biostimulation treatments only differing slightly after 32 days; a trend that was consistently observed at both incubation temperatures. This shows that even though the microbial community was nutrient-limited, nutrient addition did not alter the dominating microbial community dynamics induced by WAF addition, while enabling the same known/suspected HC degraders to enhance their growth and activity. Although this is in agreement with a previous study on microbial responses to diluted bitumen and nutrient addition in coastal Canadian seawater (Ortmann *et al.*, 2019), several other studies have described nutrient addition as affecting microbial community composition in oil-polluted seawater (Crisafi *et al.*, 2016; Meng *et al.*, 2016; Sun and Kostka, 2019). Thus, the effects of nutrient addition on oil-enriched microbial taxa might depend on the initial community composition, nutrient availability or additional unknown factors. Overall, our findings suggest that biostimulation treatments could help to accelerate bioremediation by stimulating indigenous microbial key players that are responsible for oil biodegradation in the context of future marine oil spills in the Arctic Ocean.

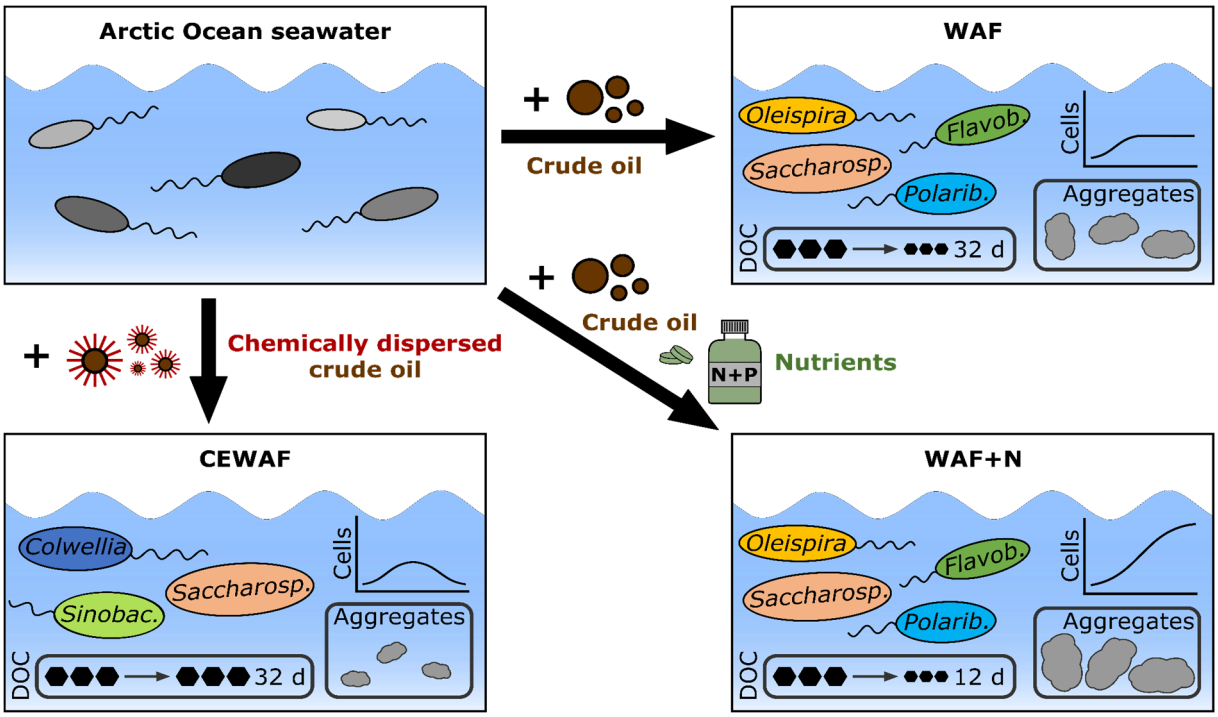

Figure 2.5: Schematic overview of major findings obtained in this study on microbial community dynamics and pollutant biodegradation potential in microcosms simulating water column conditions during an Arctic Ocean oil spill scenario. Dominant bacterial genera (key players), dissolved organic carbon concentrations (DOC), microbial aggregate/oil snow formation (MOSS) and microbial growth (cells) are indicated.

2.5.3 Impacts of dispersant addition on the microbial community and oil biodegradation potential

Compared to WAF treatments, dispersant addition led to lower detected cell numbers and microbial productivity at the end of the incubation period and considerably less microbial aggregate formation (Fig. 2.5). Interestingly, previous studies have reported both enhanced (Suja *et al.*, 2017; Doyle *et al.*, 2018) and impeded (Kleindienst *et al.*, 2015b; Passow, 2016) microbial aggregate formation after dispersant/CEWAF addition. Thus, these dynamics still remain to be further investigated and likely differ between locations and/or seawater sampling depth. Another notable effect of dispersant addition were the distinct microbial community compositions that developed during the incubation period, with both CEWAF and dispersant-only treatments mainly dominated by *Colwellia* and a few additional taxa found in both CEWAF and dispersant microcosms (e.g. unclassified *Cryomorphaceae*). The genus *Colwellia* mostly contains psychrophilic marine bacteria, with some members also described as degraders of alkanes and aromatic HCs (Bælum *et al.*, 2012; Redmond and Valentine, 2012; Sieradzki *et al.*, 2019). *Colwellia* also became enriched during the DWH oil spill (Redmond and Valentine, 2012; Mason *et al.*, 2014; Kleindienst *et al.*, 2016a) and in a few subsequent studies after Corexit application (Bælum *et al.*, 2012; Kleindienst *et al.*, 2015b; Techtmann *et al.*, 2017; McFarlin *et al.*, 2018), resulting in speculation regarding their possible preference for utilizing Corexit components, which is further supported by our results. The detected *Cryomorphaceae* were not closely related to any isolated organism, complicating the assessment of their role in Corexit-containing microcosms. However, previous studies have reported enriched unclassified members of *Cryomorphaceae* in seawater contaminated with oil and dispersant (Severin *et al.*, 2016; Salerno *et al.*, 2018), oil-contaminated marine sediments (Militon *et al.*, 2015) or hexadecane and pyrene-amended seawater (Rodrigues *et al.*, 2018), pointing to a potential role of yet-to-be isolated members of this family in HC and/or dispersant degradation. Our findings therefore suggest that Corexit components, added via CEWAF or Dispersant addition, enriched potential dispersant-degrading taxa instead of the typical oil-degrading key players and confirm numerous previous reports of dispersant addition substantially altering marine microbial dynamics (Kleindienst *et al.*, 2015b; Suja *et al.*, 2017; Techtmann *et al.*, 2017; Doyle *et al.*, 2018; Sun and Kostka, 2019). These observations might partially be explained by bioavailable HC components of Corexit itself or potential toxic/inhibitory effects of Corexit components on the metabolism and biofilm formation of HC degrading bacteria, as further discussed in **Chapter 4 and 5** of this thesis.

In contrast to WAF microcosms, the DOC/TPH equivalent levels in dispersant-containing microcosms did not decrease as much over the course of the incubation, indicating that a majority of the added oil/Corexit-derived organic compounds was not biodegraded by the microbial community within 32 days. Thus, even though alkane and phenenthrene biodegradation was detected in these microcosms, a large amount of CEWAF- and Dispersant-derived organic compounds appeared to show a high persistence in this study, raising a potential ecological concern, particularly for vulnerable environments like the Arctic Ocean. Obtained GC-MS chromatograms suggested that these persistent substances in dispersant-amended microcosms were mainly small, polar organic compounds, which might have been related to the propylene glycols and dipropylene glycol butyl ethers reportedly contained in Corexit (Kover *et al.*, 2014; Parker *et al.*, 2014). Persistent levels of these compounds were also detected

in water and sediment samples 4 months after the DWH spill (OSAT, 2010) and a long-term persistence of the Corexit surfactant dioctyl sulfosuccinate (DOSS) was reported for affected deep waters and sediments after the DWH spill (Kujawinski *et al.*, 2011; White *et al.*, 2014). Other authors have also described that either no or only slow biodegradation of the Corexit surfactant dioctyl sulfosuccinate (DOSS) was detected at cold temperatures (Campo *et al.*, 2013; Techtmann *et al.*, 2017). The persistence of less biodegradable Corexit-derived compounds could also explain the decreased microbial cell numbers and activity at the end of the experiment, which were only observed in dispersant-containing treatments. After easily degradable oil- and dispersant-derived HCs like alkanes had been metabolized, the remaining organic compounds might have been less bioavailable or even harmful to a certain extent, thereby potentially hindering the enrichment of secondary degraders as well, which had likely taken place in the WAF microcosms.

2.5.4 Conclusions

Our results reveal a considerable *in situ* oil biodegradation potential in pelagic seawater of the central Arctic Ocean and suggest that biostimulation could be a promising strategy to enhance this biodegradation potential in the case of future marine Arctic oil spills. The use of chemical dispersants such as Corexit, however, should be considered carefully in these waters because of its effects on microbial population dynamics and the risk of leaving persisting dispersant- or dispersant/oil- derived components in this relatively pristine environment.

Acknowledgements

This study was funded by the Baden-Württemberg Foundation's Elite Program for Postdocs and by the Deutsche Forschungsgemeinschaft (DFG, German Research Foundation - fellowship grant #326028733). We would also like to thank Gunter Wegener for providing seawater samples, BP for providing Macondo crude oil, Stephane Le Floch for providing Corexit EC9500A, Ellen Röhm for CFA measurements, Bernice Nisch for DOC measurements, Thomas Haug for providing facilities to perform radiotracer assays, Wolfgang Gerber for macroscopic aggregate photographs, Juliane Riedel for help with cell counting, as well as Lu Lu and Anjela Vogel for sampling assistance.

2.6 Supplemental information

2.6.1 Supplemental experimental procedures

Water-accommodated fractions. All WAF solutions were prepared with Macondo crude oil (provided by BP) according to Kleindienst et al. (2015b) with minor modifications. Briefly, for the WAF solutions, 850 ml of sterilized seawater (0.2 µm-filtered, 3x pasteurized at 65°C for 2 hours) were amended with 150 ml crude oil, mixed by magnetic stirring for 60 hours (500 rpm, RT, dark) and subsequently allowed to settle for 90 min before the aqueous phase was sub-sampled, avoiding inclusion of organic phases. CEWAFs were prepared using an additional 15 ml of Corexit EC9500A dispersant (dispersant-to-oil ratio = 1:10, v/v), and dispersant-only solutions were prepared with only 850 ml of sterile seawater and 15 ml of Corexit EC9500A. Both dispersant-containing solutions were allowed a longer settling time (4 h) in order to improve our ability to separate aqueous and organic phases. WAF, CEWAF and dispersant solutions were prepared 4 days before initiation of the experiment and stored at 4°C until usage, while subsamples were examined for potential cell contamination via DAPI staining and measured to obtain dissolved organic carbon (DOC) concentrations (see below). In order to ensure contaminant-free containers for WAF solutions and the experimental microcosms, all glassware was HCl- and Milli-Q-rinsed and subsequently baked (300°C, 8 hours) and all bottle caps were teflon-lined, HCl- and Milli-Q-rinsed and pre-baked (150°C, 8 hours) as well.

DOC and nutrient analysis. DOC was quantified in two technical replicates of 21 ml (0.45 µm-filtered before analysis) per sampled microcosm with a carbon analyzer (highTOC; Elementar, Germany). Nitrite, nitrate, and ammonium concentrations were quantified in subsamples from each microcosm using a continuous-flow analyzer (Seal Analytical, Germany). For continuous flow analysis, nitrate is reduced to nitrite with hydrazine sulfate and quantified photometrically with N-1-naphthyl ethylenediamine at 520 nm.

Hydrocarbon quantification using GC-MS. Samples for HC quantification were stored at -20°C until the extraction process was initiated. Aliquots of 450 ml from each microcosm were extracted twice by liquid/liquid extraction using dichloromethane (DCM; 100 ml) and once with *n*-hexane (100 ml). Mixtures were vigorously shaken for 3 min with the respective solvent in a glass separatory funnel (1 L), allowing the phases to settle for 10 min before removing the organic phase as a crude extract. The empty microcosm bottles were also extracted once with DCM after removing the sample aliquot in order to include hydrocarbons that might have attached to the glass surface. Only pre-baked (300°C, 8 h) glassware was used for handling of extracts and care was taken to never use the same glassware for samples of different treatment types (i.e. WAF, CEWAF, dispersant). The crude extracts were combined and reduced to a volume of 10–20 mL in a rotary evaporator (Rotavapor R-300, Buchi; Flawil, Switzerland), by evaporating DCM (40°C, 750 mbar) and *n*-hexane (45°C, 450 mbar). Potentially co-extracted water was removed by passing extracts through salt columns ($NaSO_4$ in a glass-wool plugged Pasteur pipette) and the extract volumes were subsequently further reduced to a volume of appr. 1 ml under the fume hood. Deuterated *n*-triacontane was added as internal standard (1 µg ml^{-1}) and the extracts were used to quantify individual alkane and aromatic HC concentrations by

coupled gas chromatography and mass spectrometry (Trace GC and TSQ Quantum XLS Ultra; Thermo Scientific). Volumes of 1 µL out of 1 mL were introduced using a PTV injector (ramped from 45°C to 320°C at 12°C/sec) in splitless mode (2.5 min) and separated on a VF1-MS capillary column (40 m length, 0.1 mm inner diameter and 0.1 µm film thickness) using 0.8 mL/min constant flow of helium 5.0 (Westphalen AG) as the carrier gas. The GC oven temperature was held isothermal at 50°C for 2.5 min, then ramped to 150°C at 15°C/min and subsequently to 320°C at 10°C/min and held for 15 min. Ionization of the organic compounds was achieved by electron impact at 70 eV and emission current of 50 µA. The ion source was kept at 250°C and the mass spectrometer was operated in full scan mode (m/z 50–550 with cycle time of 0.5 sec). Analytes were quantified using integrated peak areas in relation to the internal standard without correcting for individual response factors.
Due to a systematic contamination issue in hydrocarbon extracts, the range of retention times affected by a significant hump of UCM (23.39–26.17) was ignored from the perspective of peak identification and quantification in all samples. The obtained chromatograms were analysed using MZmine v2.42 (Pluskal *et al.*, 2010) via targeted peak detection and RANSAC peak alignment for *n*-alkanes ($C_{12–36}$ chain length), naphthalenes and phenanthrenes. Detected peak areas were normalized using the peak area of the internal standard to achieve semi-quantitative data of remaining alkane and aromatic HC concentrations (ng ml^{-1}) in microcosms. Bulk TPH equivalents were determined via toggle peak detection (baseline window: 500) in Xcalibur v4.2 (Thermo Fisher Scientific) and thus represent all compounds from the crude HC extracts detected via GC-MS analysis. This likely excluded larger and/or highly polar compounds due to fractionation in the used injector.

DNA extraction. Aliquots of 300 ml were sampled from the microcosms, filtered through Sterivex filter membranes (0.2 µm pore size; SVGP01050, Merck Millipore; Darmstadt, Germany) and stored at -20°C until further analysis. Upon starting the DNA extraction, filter membranes were cut into small pieces under sterile conditions and the FastDNA SPIN Kit for Soil (MP Biomedical; Eschwege, Germany) was used to extract DNA according to the manufacturer's instructions with minor modifications: Homogenization was performed on a vortex adapter (10 min at full speed; Vortex-genie 2, Scientific Industries; Bohemia, USA), 1 min centrifugation steps were extended to 2 min and spin filters were incubated in a water bath (5 min, 55°C) before DNA elution, to increase yields. Genomic DNA was eluted in 100 µl buffer and stored at -20°C.

Quantitative PCR (qPCR). To estimate the abundances of bacterial 16S rRNA genes, quantitative PCR was performed on an iQ5 real-time PCR detection system (Bio-Rad Laboratories GmbH, Munich, Germany) using SsoAdvanced Universal SYBR Green Supermix (Bio-Rad Laboratories GmbH). 16S rRNA genes were amplified in DNA extracts using the primers 341F (5`-CCTACGGGAGGCAGCAG-3`) (Muyzer *et al.*, 1993) and 797R (5`-GGACTACCAGGGTATCTAATCCTGTT-3`) (Nadkarni *et al.*, 2002) and the following cycling conditions: 2 min at 98°C, 40 cycles of 5 s at 98°C and 12 s at 60°C. Standard curves were generated using serial dilutions plasmid vectors (pCR2.1, Invitrogen, Darmstadt, Germany), containing a cloned 16S rRNA gene fragment from *Thiomonas* sp. BF04. Triplicate qPCR assays of each sample were performed. Data analysis was done using the iQ5 optical

system software, version 2.0 (Bio-Rad Laboratories GmbH). Cell numbers per ml SW were calculated from the qPCR-derived gene copy numbers, using 5.0 as correction factors to account for the possibility of multiple gene copies per genome (https://rrndb.umms.med.umich.edu/).

Illumina MiSeq amplicon sequencing and sequence analysis. 16S rRNA genes were amplified for amplicon sequencing using a two-step PCR, optimized for low DNA concentrations detected in several samples. First, a booster PCR using KAPA HiFi HotStart Readymix (Kapa Biosystems, Inc., Wilmington, MA, USA) was run using the universal primer pair 515f/806r (Caporaso *et al.*, 2010) and the following cycling conditions: 95°C for 3 min, 20 cycles of 95°C for 30 sec, 55°C for 30 sec, 72°C for 30 sec, and finally, 72°C for 5 min. For the second PCR, the same cycling conditions applied but the primer pair 515f/806r with fused Illumina adapters was used. Subsequent library preparation steps and sequencing were performed by Microsynth AG (Balgach, Switzerland). Sequencing was performed on an Illumina MiSeq sequencing system (Illumina, San Diego, CA, USA) using the 2×250 bp MiSeq Reagent Kit v2 and between 25,132 and 199,265 read pairs were obtained for each sample.
Sequencing data was analysed with nf-core/ampliseq v1.1.0, which performed all following analysis steps and includes required software (Ewels *et al.*, 2020; Straub *et al.*, 2020). Primers were trimmed, and untrimmed sequences were discarded (<2%) with Cutadapt v1.16 (Martin, 2011). Adapter and primer-free sequences were imported into QIIME2 v2018.06 (Bolyen *et al.*, 2019), quality checked with demux (https://github.com/qiime2/q2-demux), and processed with DADA2 v 1.6.0 (Callahan *et al.*, 2016) to remove PhiX contamination, trim reads (before median quality drops below 35, that is forward 181, reverse 175), correct errors, merge read pairs and remove PCR chimeras and finally amplicon sequencing variants (ASVs) were obtained. Alpha rarefaction curves were produced with the QIIME2 diversity alpha-rarefaction plugin which indicated that the richness of the samples has been fully observed. A Naive Bayes classifier was fitted with 16S rRNA gene sequences extracted from SILVA v132 QIIME compatible database 99% identity clustered sequences (Pruesse *et al.*, 2007) using the PCR primer sequences. ASVs were classified by taxon using the fitted classifier (https://github.com/qiime2/q2-feature-classifier). A genus abundance table was produced and correspondence analysis was performed using Phyloseq v1.22.3 (McMurdie and Holmes, 2013) in R v3.4.4 (R Core Team, 2019), and the five or three samples with highest distance to their replicates were removed from analysis of 1°C or 15°C data, respectively. After removing outliers, the analysis was repeated. 18 ASVs with <5% relative abundance per sample classified as chloroplast or mitochondria were removed. The remaining 2320 ASVs had their abundances extracted by q2-feature-table (https://github.com/qiime2/q2-feature-table). Non-metric multidimensional scaling (NMDS) ordinations were generated based on Bray-Curtis dissimilarity between samples using Phyloseq v1.30.0 (McMurdie and Holmes, 2013) in R v3.6.0 (R Core Team, 2019). Dominant ASVs of interest were further characterized using the blastn suite (Altschul *et al.*, 1990).

DAPI cell counts. For total cell counts, samples were fixed with 1% paraformaldehyde and stored at 4°C until further processing. Microbial cell numbers were monitored using cell counts via 4′,6-diamidino-2-phenylindole (DAPI) staining in combination with fluorescence

microscopy after dissolving microbial aggregates as described in **Chapter 4** of this thesis. For each filter, a minimum of 600 cells or 80 grids were randomly selected and manually counted.

^{3}H-leucine incorporation assay. By quantifying the rate of ^{3}H-leucine incorporation into microbial biomass, the rate of total microbial biomass production in the sample can be estimated (Kirchman, 2001). Aliquots were stored at 4°C overnight between sampling and analysis. For each microcosm sample, two technical replicates and one acid-killed control replicate were analysed. ^{3}H-leucine incorporation assays were performed as described by Otte *et al.* (2018). Here, replicates were incubated with a final concentration of 3.6-4.4 nmol l^{-1} ^{3}H-leucine (specific activity of 103 Ci $mmol^{-1}$) for 3-4.5 h (day 0: 3 h, day 5/12/32: 4.5 h) at 1°C or 15°C, respectively.

^{14}C-hydrocarbon oxidation assays. Rates of ^{14}C-hydrocarbon oxidation were determined in separate assays using ^{14}C-labeled *n*-hexadecane and naphthalene as substrates. Aliquots were stored at 4°C overnight between sampling and analysis. The assays were performed for all microcosm samples and for each sample triplicate, one killed control replicate (mixed sample of triplicates) was analysed additionally. Incubations were set up as described in Kleindienst *et al.* (2015b) with the following minor modifications: Killed controls were amended with 2 M NaOH solution (final concentration of 0.4 M NaOH) right after tracer addition and activity was halted the same way in all samples after incubation. Samples were incubated for 24 h at 1.5°C or 15°C, respectively. To remove tracer ^{14}C-hydrocarbons, samples were shaken overnight (16 hours) with 1 g of activated carbon (granular, 20-60 mesh; VWR) and 0.2 g of silica (reverse-bonded C_{18} silica gel; Sigma Aldrich) were additionally added in the case of the hexadecane assay. After sample distillation, 4 ml of scintillation cocktail (Permafluor E+; Perkin Elmer) was added to the scintillation vials and radioactivity was quantified immediately using a liquid scintillation counter (5 min count time; Packard TRI-CARB 2500TR, PerkinElmer). Due to methodological issues, samples from the 1°C incubations were lost during ^{14}C-hexadecane assay analysis.

2.6.2 Supplemental figures

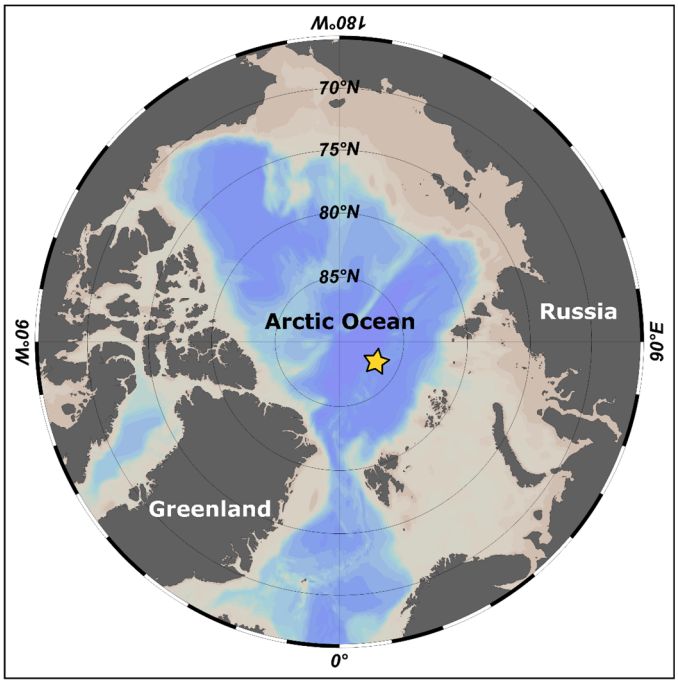

Figure S 2.1: Location of seawater sampling site in the central Arctic Ocean (086° 51.45' N, 061° 28.95' E; *in situ* temperature -1.7°C). Samples were taken from a depth of 150 m in October 2016 during research cruise PS101 on *RV Polarstern.*

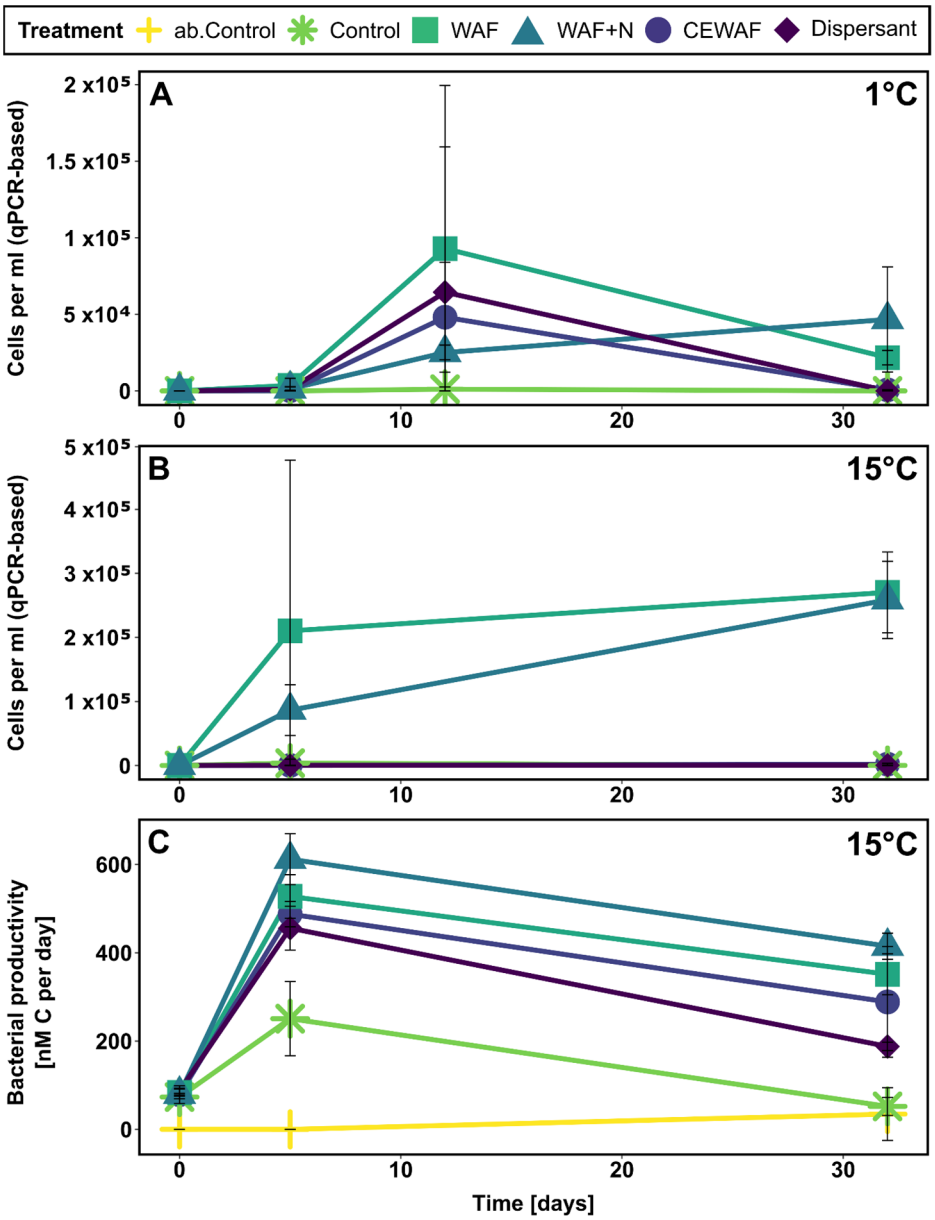

Figure S 2.2: qPCR-based microbial cell numbers and radiotracer-based activity in 1°C and 15°C seawater microcosms simulating water column conditions during an Arctic Ocean oil spill scenario. Results shown are averages of sacrificial, triplicate microcosms (standard deviations are based on triplicates). **A/B**) Cell numbers in 1°C (A) and 15°C (B) incubations as determined by qPCR-amplification of 16S rRNA gene copy numbers. **C**) Rates of microbial productivity in 15°C incubations as measured via ^{3}H-leucine incorporation assays.

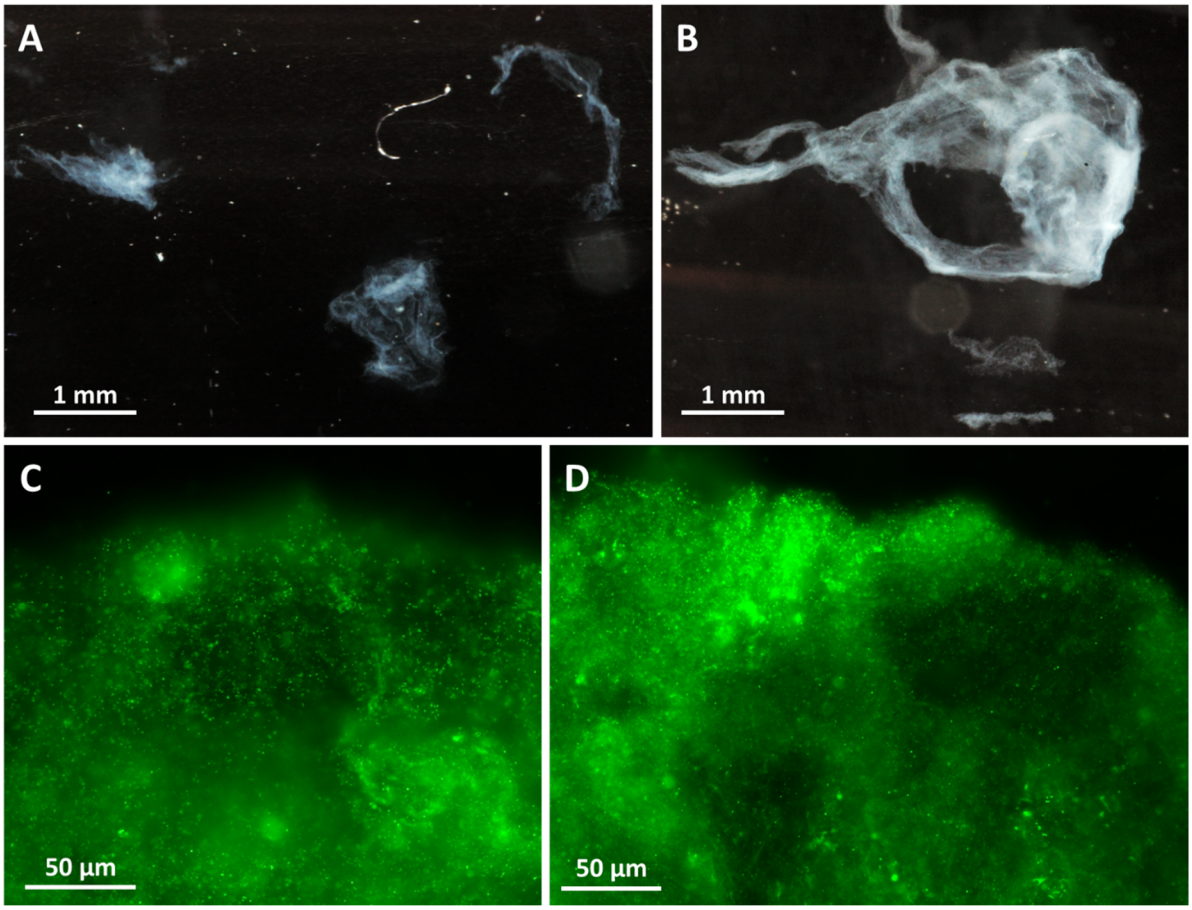

Figure S 2.3: Microbial aggregates observed in 1°C seawater microcosms simulating water column conditions during an Arctic Ocean oil spill scenario after nutrient addition (WAF+N treatments). **A/B**) Photographs of aggregates fixed with paraformaldehyde (1% v/v) after 32 days of incubation. **C/D**) Fluorescence microscopy images of aggregates obtained after 12 days of incubation. Living cells are stained with SYTO 9 stain (green).

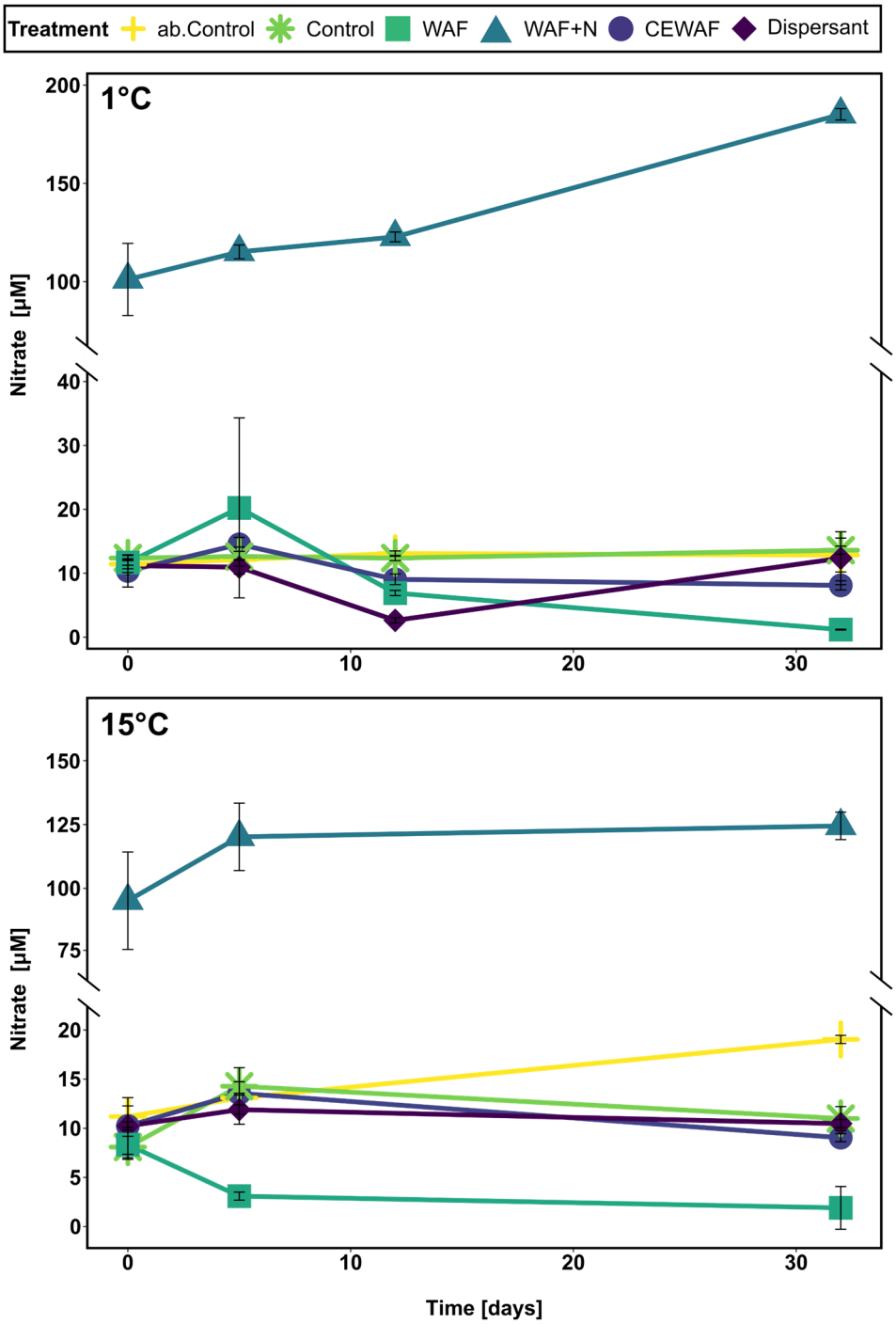

Figure S 2.4: Nitrate concentrations in 1°C (top) and 15°C (bottom) seawater microcosms simulating water column conditions during an Arctic Ocean oil spill scenario. Concentrations were determined by continuous flow analysis and results are shown as averages of sacrificial, triplicate microcosms (standard deviations are based on triplicates). Data are presented using a divided y-axis in order to better visualize the nitrate content in treatments with (WAF+N) and without nutrient addition (all other treatments).

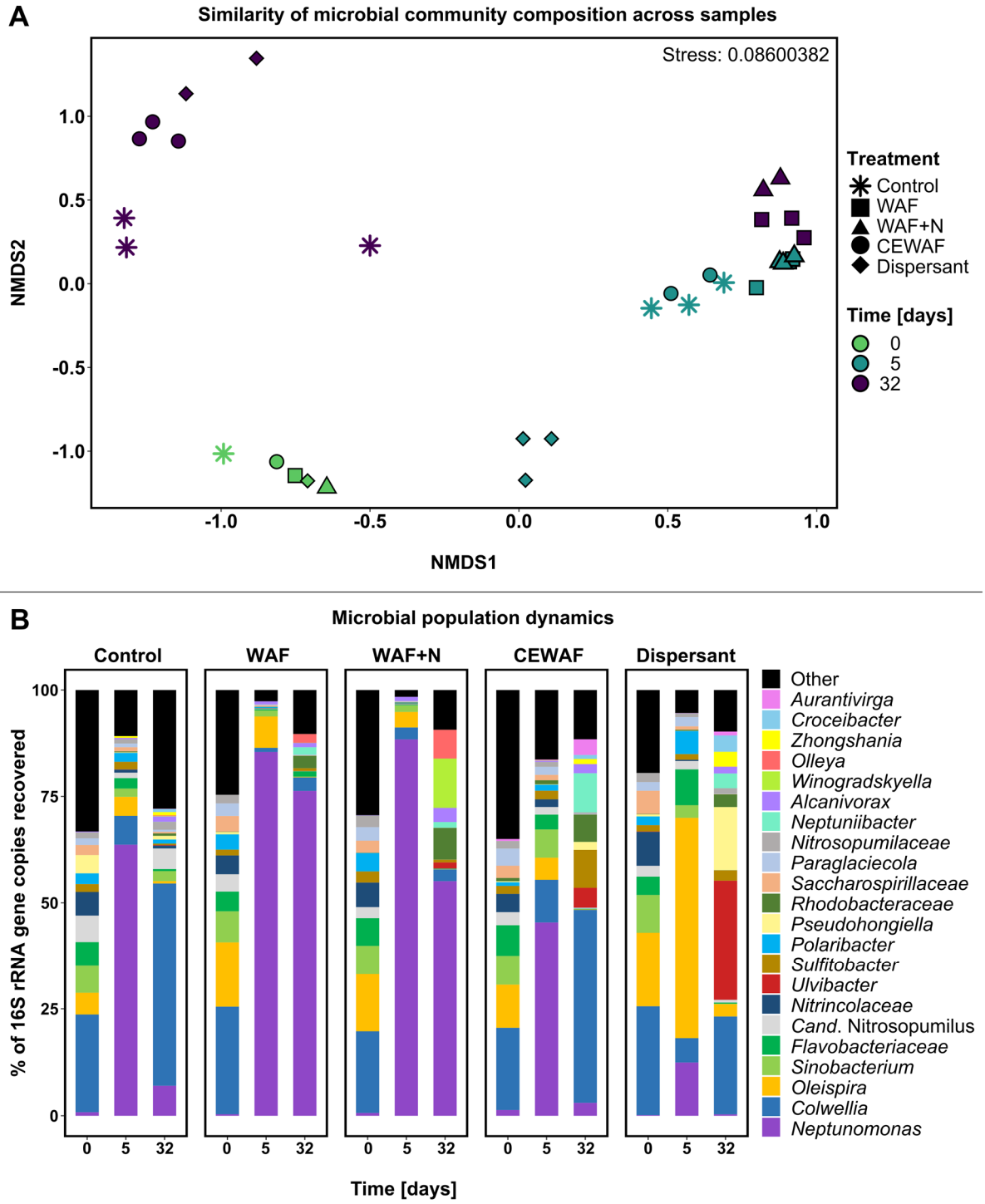

Figure S 2.5: Changes in microbial community composition in 15°C seawater microcosms simulating water column conditions during an Arctic Ocean oil spill scenario as determined by 16S rRNA gene amplicon sequencing. Treatments received the following amendments crude oil-derived water accommodated fraction (WAF), WAF and nutrients (WAF+N), chemically enhanced WAF (CEWAF, contains Corexit dispersant), or dispersant alone. Control treatments received no amendments (Control). **A**) Non-metric multidimensional scaling (NMDS) plot based on Bray-Curtis diversity showing the similarity of microbial community compositions across samples. The stress achieved is indicated in the top right of the plot. **B**) Microbial population dynamics (averages of sacrificial triplicate microcosms) of most abundant taxa in microcosms at genus level (sorted by average abundance across samples and labelled with the highest descriptive taxonomic level).

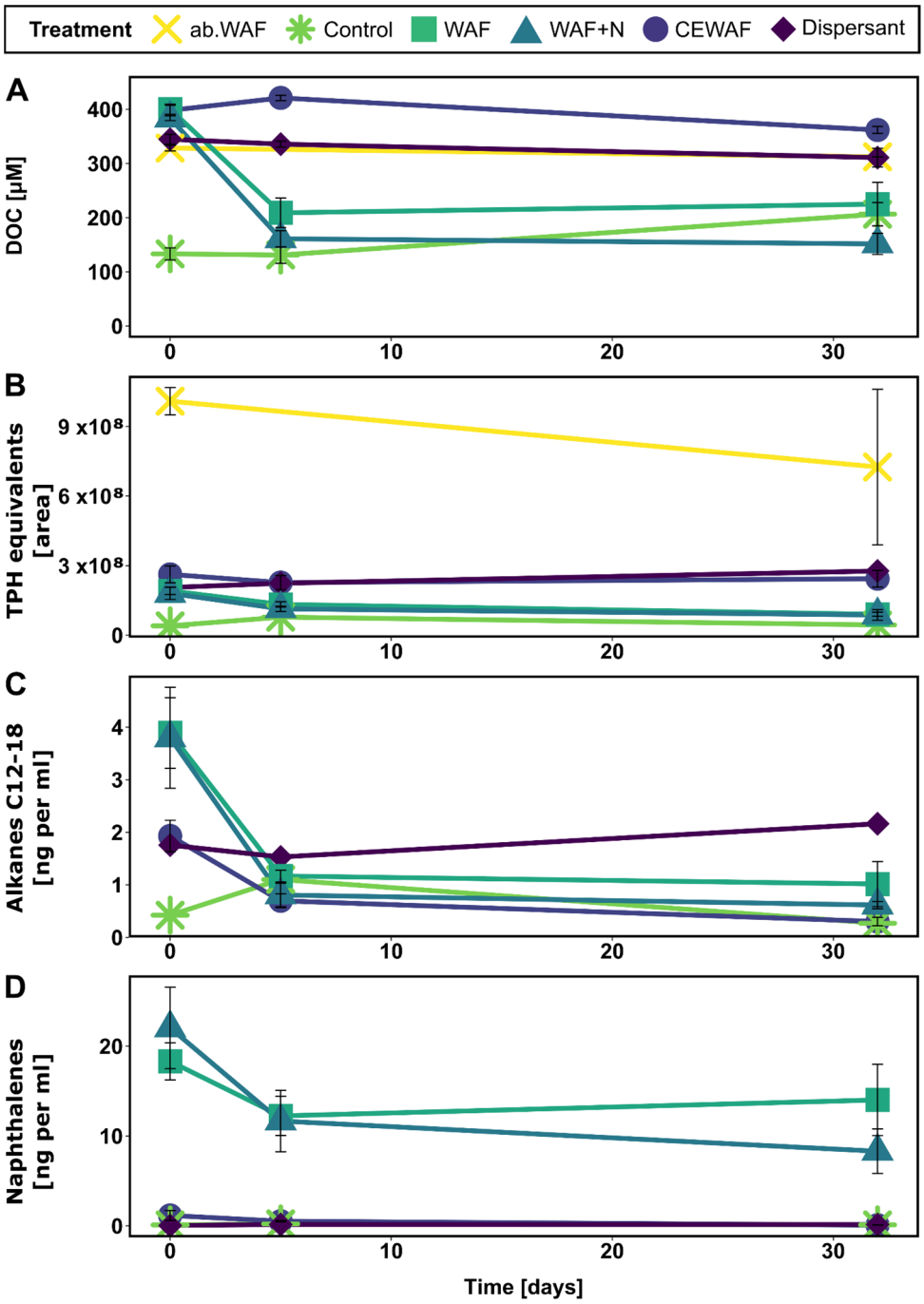

Figure S 2.6: Hydrocarbon and DOC concentrations in 15°C seawater microcosms simulating water column conditions during an Arctic Ocean oil spill scenario. Treatments received the following amendments at the start of the experiment: crude oil-derived water accommodated fraction (WAF), WAF and nutrients (WAF+N), chemically enhanced WAF (CEWAF, contains Corexit dispersant) or dispersant alone. Additional control treatments received no amendments (Control) and/or contained only sterilized seawater and WAF (abiotic WAF; only included for bulk parameters). Results shown are averages of sacrificial, triplicate microcosms (standard deviations are based on triplicates). **A**) Dissolved organic carbon (DOC) concentrations show that amendments were adjusted to similar DOC levels at the start of the experiment. **B-D**) Total petroleum hydrocarbon (TPH) equivalents, *n*-alkanes (C_{12-18}) and naphthalenes are shown as determined by via GC-MS quantification.

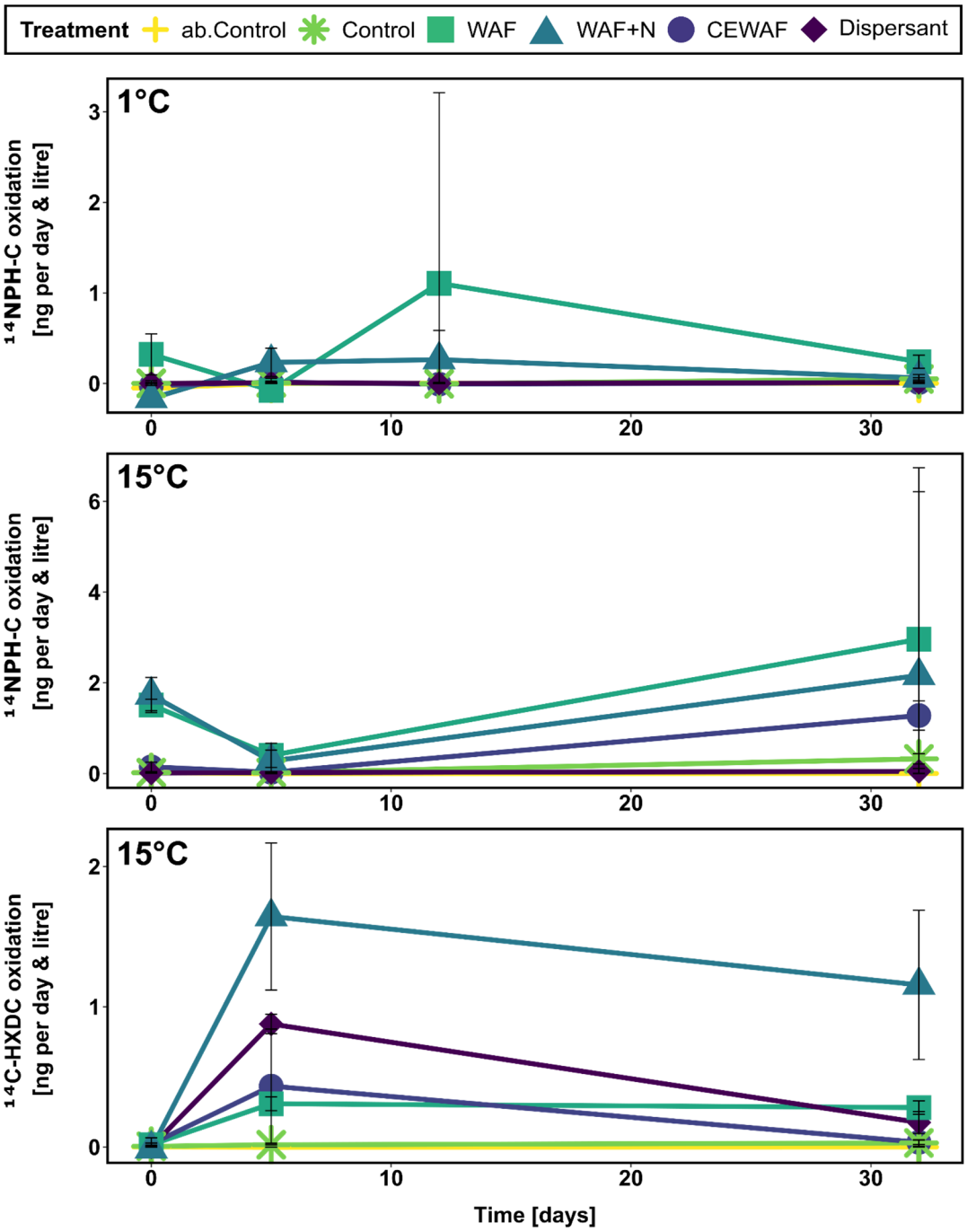

Figure S 2.7: ^{14}C-hydrocarbon oxidation rates detected in seawater microcosms simulating water column conditions during an Arctic Ocean oil spill scenario. Results shown are averages of sacrificial, triplicate microcosms (standard deviations are based on triplicates). **A/B**) ^{14}C-naphthalene (NPH) oxidation rates at 1°C and 15°C. **C**) ^{14}C-hexadecane (HXD) oxidation rates at 15°C. Data on ^{14}C-hexadecane (HXD) oxidation rates in 1°C incubations was lost due to technical issues.

2.7 References

Adams, G.O., Fufeyin, P.T., Okoro, S.E., and Ehinomen, I. (2015) Bioremediation, biostimulation and bioaugmention: A review. *Int J Environ Bioremediat Biodegrad* **3**(1): 28-39.

Altschul, S.F., Gish, W., Miller, W., Myers, E.W., and Lipman, D.J. (1990) Basic local alignment search tool. *J Mol Biol* **215**(3): 403-410.

Arctic Council (2013). Agreement on cooperation on marine oil pollution preparedness and response in the Arctic. Kiruna, Sweden. Available from: https://oaarchive.arctic-council.org/handle/11374/529 [Accessed July 20, 2020].

Atlas, R.M., and Bartha, R. (1972) Degradation and mineralization of petroleum in sea water: Limitation by nitrogen and phosphorous. *Biotechnol Bioeng* **14**(3): 309-318.

Aune, M., Aniceto, A.S., Biuw, M., Daase, M., Falk-Petersen, S., Leu, E. *et al.* (2018) Seasonal ecology in ice-covered Arctic seas: Considerations for spill response decision making. *Mar Environ Res* **141**: 275-288.

Bælum, J., Borglin, S., Chakraborty, R., Fortney, J.L., Lamendella, R., Mason, O.U. *et al.* (2012) Deep-sea bacteria enriched by oil and dispersant from the Deepwater Horizon spill. *Environ Microbiol* **14**(9): 2405-2416.

Bolyen, E., Rideout, J.R., Dillon, M.R., Bokulich, N.A., Abnet, C.C., Al-Ghalith, G.A. *et al.* (2019) Reproducible, interactive, scalable and extensible microbiome data science using QIIME 2. *Nature biotechnology* **37**(8): 852-857.

Bragg, J.R., Prince, R.C., Harner, E.J., and Atlas, R.M. (1994) Effectiveness of bioremediation for the *Exxon Valdez* oil spill. *Nature* **368**(6470): 413-418.

Callahan, B.J., McMurdie, P.J., Rosen, M.J., Han, A.W., Johnson, A.J.A., and Holmes, S.P. (2016) DADA2: High-resolution sample inference from Illumina amplicon data. *Nat Methods* **13**(7): 581-583.

Campo, P., Venosa, A.D., and Suidan, M.T. (2013) Biodegradability of Corexit 9500 and dispersed South Louisiana crude oil at 5 and 25°C. *Environ Sci Technol* **47**(4): 1960-1967.

Caporaso, J.G., Kuczynski, J., Stombaugh, J., Bittinger, K., Bushman, F.D., Costello, E.K. *et al.* (2010) QIIME allows analysis of high-throughput community sequencing data. *Nat Methods* **7**(5): 335-336.

Coulon, F., McKew, B.A., Osborn, A.M., McGenity, T.J., and Timmis, K.N. (2007) Effects of temperature and biostimulation on oil-degrading microbial communities in temperate estuarine waters. *Environ Microbiol* **9**(1): 177-186.

Crisafi, F., Genovese, M., Smedile, F., Russo, D., Catalfamo, M., Yakimov, M. *et al.* (2016) Bioremediation technologies for polluted seawater sampled after an oil-spill in Taranto Gulf (Italy): A comparison of biostimulation, bioaugmentation and use of a washing agent in microcosm studies. *Mar Pollut Bull* **106**(1-2): 119-126.

Curl, H.C., Barton, K., and Harris, L. (1992). Oil spill case histories, 1967-1991: Summaries of significant U.S. and international spills. Seattle, Washington, USA: NOAA Hazardous Materials Response and Assessment Division. Report No.: Report No. HMRAD 92-11. Available from: https://repository.library.noaa.gov/view/noaa/1671 [Accessed July 20, 2020].

Doyle, S.M., Whitaker, E.A., De Pascuale, V., Wade, T.L., Knap, A.H., Santschi, P.H. *et al.* (2018) Rapid formation of microbe-oil aggregates and changes in community composition in coastal surface water following exposure to oil and the dispersant Corexit. *Front Microbiol* **9**: 689.

DWH NRDA Trustees (2016). Deepwater Horizon oil spill: Final programmatic damage assessment and restoration plan and final programmatic environmental impact statement. Available from: http://www.gulfspillrestoration.noaa.gov/restoration-planning/gulf-plan [Accessed June 16, 2020].

Ernest, P. (1993). The *Exxon Valdez* oil spill: Final report, state of Alaska response. Anchorage, AK, USA: Alaska Department of Environmental Conservation. Available from: http://www.evostc.state.ak.us/static/PDFs/deccleanuptechniques.pdf [Accessed July 19, 2020].

Ewels, P.A., Peltzer, A., Fillinger, S., Patel, H., Alneberg, J., Wilm, A. *et al.* (2020) The nf-core framework for community-curated bioinformatics pipelines. *Nature Biotechnology* **38**(3): 276-278.

ExxonMobil (2014). Oil spill response field manual. USA: ExxonMobil Research and Engineering Company. Available from: https://corporate.exxonmobil.com/-/media/Global/Files/risk-management-and-safety/Oil-Spill-Response-Field-Manual_2014.pdf [Accessed July 19, 2020].

Fasca, H., de Castilho, L.V., de Castilho, J.F.M., Pasqualino, I.P., Alvarez, V.M., de Azevedo Jurelevicius, D., and Seldin, L. (2018) Response of marine bacteria to oil contamination and to high pressure and low temperature deep sea conditions. *MicrobiologyOpen* **7**(2): e00550.

Gerdes, B., Brinkmeyer, R., Dieckmann, G., and Helmke, E. (2005) Influence of crude oil on changes of bacterial communities in Arctic sea-ice. *FEMS Microbiol Ecol* **53**(1): 129-139.

Gutierrez, T. (2018) Preparing for the next big oil spill at sea: A microbiological perspective. *Journal of Marine Microbiology* **2**(1): 13-14.

Harriss, R. (2016) Arctic offshore oil: Great risks in an evolving ocean. *Environment: Science and Policy for Sustainable Development* **58**(3): 18-29.

Harsem, Ø., Heen, K., Rodrigues, J., and Vassdal, T. (2015) Oil exploration and sea ice projections in the Arctic. *The Polar Record* **51**(1): 91.
Harwati, T.U., Kasai, Y., Kodama, Y., Susilaningsih, D., and Watanabe, K. (2007) Characterization of diverse hydrocarbon-degrading bacteria isolated from Indonesian seawater. *Microbes and Environments* **22**(4): 412-415.
Hazen, T.C., Dubinsky, E.A., DeSantis, T.Z., Andersen, G.L., Piceno, Y.M., Singh, N. *et al.* (2010) Deep-sea oil plume enriches indigenous oil-degrading bacteria. *Science* **330**(6001): 204-208.
Head, I.M., Jones, D.M., and Röling, W.F. (2006) Marine microorganisms make a meal of oil. *Nat Rev Microbiol* **4**(3): 173-182.
Hedlund, B.P., Geiselbrecht, A.D., Bair, T.J., and Staley, J.T. (1999) Polycyclic aromatic hydrocarbon degradation by a new marine bacterium, *Neptunomonas naphthovorans* gen. nov., sp. nov. *Appl Environ Microbiol* **65**(1): 251-259.
Holder, E.L., Conmy, R.N., and Venosa, A.D. (2015) Comparative laboratory-scale testing of dispersant effectiveness of 23 crude oils using four different testing protocols. *J Environ Prot* **6**(06): 628.
ITOPF (2020). Oil tanker spill statistics 2019. London, UK: International Tanker Owners Pollution Federation. Available from: http://www.itopf.org/fileadmin/data/Documents/Company_Lit/Oil_Spill_Stats_brochure_2020_for_web.pdf [Accessed May 27, 2020].
Joye, S.B., Kleindienst, S., Gilbert, J.A., Handley, K.M., Weisenhorn, P., Overholt, W.A., and Kostka, J.E. (2016) Responses of microbial communities to hydrocarbon exposures. *Oceanography* **29**(3): 136-149.
Kirchman, D. (2001) Measuring bacterial biomass production and growth rates from leucine incorporation in natural aquatic environments. *Methods Microbiol* **30**: 227–237.
Kleindienst, S., Seidel, M., Ziervogel, K., Grim, S., Loftis, K., Harrison, S. *et al.* (2015) Chemical dispersants can suppress the activity of natural oil-degrading microorganisms. *Proc Natl Acad Sci USA* **112**(48): 14900-14905.
Kleindienst, S., Grim, S., Sogin, M., Bracco, A., Crespo-Medina, M., and Joye, S.B. (2016) Diverse, rare microbial taxa responded to the Deepwater Horizon deep-sea hydrocarbon plume. *ISME J* **10**(2): 400-415.
Kover, S.C., Rosario-Ortiz, F.L., and Linden, K.G. (2014) Photochemical fate of solvent constituents of Corexit oil dispersants. *Water Res* **52**: 101-111.
Kujawinski, E.B., Kido Soule, M.C., Valentine, D.L., Boysen, A.K., Longnecker, K., and Redmond, M.C. (2011) Fate of dispersants associated with the Deepwater Horizon oil spill. *Environ Sci Technol* **45**(4): 1298-1306.
Lee, K., Boufadel, M., Chen, B., Foght, J., Hodson, P., Swanson, S., and Venosa, A. (2015). Expert panel report on the behaviour and environmental impacts of crude oil released into aqueous environments. Ottawa, ON, Canada: Royal Society of Canada.
Lewis, A., and Prince, R.C. (2018) Integrating dispersants in oil spill response in Arctic and other icy environments. *Environ Sci Technol* **52**(11): 6098-6112.
Liu, C., Wang, W., Wu, Y., Zhou, Z., Lai, Q., and Shao, Z. (2011) Multiple alkane hydroxylase systems in a marine alkane degrader *Alcanivorax dieselolei* B-5. *Environ Microbiol* **13**(5): 1168-1178.
Liu, J., Bacosa, H.P., and Liu, Z. (2017) Potential environmental factors affecting oil-degrading bacterial populations in deep and surface waters of the northern Gulf of Mexico. *Front Microbiol* **7**: 2131.
Lofthus, S., Netzer, R., Lewin, A.S., Heggeset, T.M.B., Haugen, T., and Brakstad, O.G. (2018) Biodegradation of *n*-alkanes on oil-seawater interfaces at different temperatures and microbial communities associated with the degradation. *Biodegradation* **29**(2): 141-157.
Martin, M. (2011) Cutadapt removes adapter sequences from high-throughput sequencing reads. *EMBnet journal* **17**(1): 10-12.
Mas-Lladó, M., Piña-Villalonga, J.M., Brunet-Galmés, I., Nogales, B., and Bosch, R. (2014) Draft genome sequences of two isolates of the Roseobacter group, *Sulfitobacter* sp. strains 3SOLIMAR09 and 1FIGIMAR09, from harbors of Mallorca Island (Mediterranean sea). *Genome Announcements* **2**(3).
Mason, O.U., Hazen, T.C., Borglin, S., Chain, P.S., Dubinsky, E.A., Fortney, J.L. *et al.* (2012) Metagenome, metatranscriptome and single-cell sequencing reveal microbial response to Deepwater Horizon oil spill. *ISME J* **6**(9): 1715-1727.
Mason, O.U., Han, J., Woyke, T., and Jansson, J.K. (2014) Single-cell genomics reveals features of a *Colwellia* species that was dominant during the Deepwater Horizon oil spill. *Front Microbiol* **5**: 332.
McFarlin, K.M., Questel, J.M., Hopcroft, R.R., and Leigh, M.B. (2017) Bacterial community structure and functional potential in the northeastern Chukchi Sea. *Cont Shelf Res* **136**: 20-28.
McFarlin, K.M., Perkins, M.J., Field, J.A., and Leigh, M.B. (2018) Biodegradation of crude oil and Corexit 9500 in Arctic seawater. *Front Microbiol* **9**: 1788.

McGowan, C.J., Kwok, R.K., Engel, L.S., Stenzel, M.R., Stewart, P.A., and Sandler, D.P. (2017) Respiratory, dermal, and eye irritation symptoms associated with Corexit EC9527A/EC9500A following the Deepwater Horizon oil spill: Findings from the GuLF STUDY. *Environ Health Perspect* **125**(9): 097015.

McMurdie, P.J., and Holmes, S. (2013) Phyloseq: An R package for reproducible interactive analysis and graphics of microbiome census data. *PloS one* **8**(4): e61217.

McNutt, M.K., Camilli, R., Crone, T.J., Guthrie, G.D., Hsieh, P.A., Ryerson, T.B. *et al.* (2012) Review of flow rate estimates of the Deepwater Horizon oil spill. *Proc Natl Acad Sci USA* **109**(50): 20260-20267.

Meier, W.N., Hovelsrud, G.K., Van Oort, B.E., Key, J.R., Kovacs, K.M., Michel, C. *et al.* (2014) Arctic sea ice in transformation: A review of recent observed changes and impacts on biology and human activity. *Rev Geophys* **52**(3): 185-217.

Meng, L., Liu, H., Bao, M., and Sun, P. (2016) Microbial community structure shifts are associated with temperature, dispersants and nutrients in crude oil-contaminated seawaters. *Mar Pollut Bull* **111**(1-2): 203-212.

Militon, C., Jezequel, R., Gilbert, F., Corsellis, Y., Sylvi, L., Cravo-Laureau, C. *et al.* (2015) Dynamics of bacterial assemblages and removal of polycyclic aromatic hydrocarbons in oil-contaminated coastal marine sediments subjected to contrasted oxygen regimes. *Environ Sci Pollut Res* **22**(20): 15260-15272.

Murawski, S.A., Hollander, D.J., Gilbert, S., and Gracia, A. (2020) Deepwater oil and gas production in the Gulf of Mexico and related global trends. In *Scenarios and responses to future deep oil spills*: Springer, pp. 16-32.

Muyzer, G., De Waal, E.C., and Uitterlinden, A.G. (1993) Profiling of complex microbial populations by denaturing gradient gel electrophoresis analysis of polymerase chain reaction amplified genes coding for 16s rRNA. *Appl Environ Microbiol* **59**(3): 695-700.

Nadkarni, M.A., Martin, F.E., Jacques, N.A., and Hunter, N. (2002) Determination of bacterial load by real-time pcr using a broad-range (universal) probe and primers set. *Microbiology* **148**(1): 257-266.

Nevalainen, M., Helle, I., and Vanhatalo, J. (2018) Estimating the acute impacts of Arctic marine oil spills using expert elicitation. *Mar Pollut Bull* **131**: 782-792.

Nikolopoulou, M., and Kalogerakis, N. (2010) Biostimulation strategies for enhanced bioremediation of marine oil spills including chronic pollution. In *Handbook of hydrocarbon and lipid microbiology*, pp. 2521-2529.

Ortmann, A.C., Cobanli, S.E., Wohlgeschaffen, G., Thamer, P., McIntyre, C., Mason, J., and King, T.L. (2019) Inorganic nutrients have a significant, but minimal, impact on a coastal microbial community's response to fresh diluted bitumen. *Mar Pollut Bull* **139**: 381-389.

OSAT (2010). Summary report for sub-sea and sub-surface oil and dispersant detection: Sampling and monitoring. New Orleans, USA. Available from: https://www.restorethegulf.gov/sites/default/files/documents/pdf/OSAT_Report_FINAL_17DEC.pdf [Accessed August 20, 2020].

Otte, J.M., Blackwell, N., Soos, V., Rughöft, S., Maisch, M., Kappler, A. *et al.* (2018) Sterilization impacts on marine sediment - are we able to inactivate microorganisms in environmental samples? *FEMS Microbiol Ecol* **94**(12).

Parker, A.M., Ferrer, I., Thurman, E.M., Rosario-Ortiz, F.L., and Linden, K.G. (2014) Determination of corexit components used in the Deepwater Horizon cleanup by liquid chromatography-ion trap mass spectrometry. *Anal Methods* **6**(15): 5498-5502.

Passow, U. (2016) Formation of rapidly-sinking, oil-associated marine snow. *Deep Sea Res Part II Top Stud Oceanogr* **129**: 232-240.

Passow, U., and Ziervogel, K. (2016) Marine snow sedimented oil released during the Deepwater Horizon spill. *Oceanography* **29**(3): 118-125.

Personna, Y.R., King, T., Boufadel, M.C., Zhang, S., and Axe, L. (2016) Dual effects of a dispersant and nutrient supplementation on weathered Endicott oil biodegradation in seawater. *AIMS Environmental Science* **3**(4): 739.

Peterson, C.H., Rice, S.D., Short, J.W., Esler, D., Bodkin, J.L., Ballachey, B.E., and Irons, D.B. (2003) Long-term ecosystem response to the *Exxon Valdez* oil spill. *Science* **302**(5653): 2082-2086.

Pluskal, T., Castillo, S., Villar-Briones, A., and Orešič, M. (2010) MZmine 2: Modular framework for processing, visualizing, and analyzing mass spectrometry-based molecular profile data. *BMC Bioinformatics* **11**(1): 395.

Pruesse, E., Quast, C., Knittel, K., Fuchs, B.M., Ludwig, W., Peplies, J., and Glöckner, F.O. (2007) SILVA: A comprehensive online resource for quality checked and aligned ribosomal rna sequence data compatible with ARB. *Nucleic Acids Res* **35**(21): 7188-7196.

R Core Team (2019). R: A language and environment for statistical computing. Vienna, Austria.

Redmond, M.C., and Valentine, D.L. (2012) Natural gas and temperature structured a microbial community response to the Deepwater Horizon oil spill. *Proc Natl Acad Sci USA* **109**(50): 20292-20297.

Rodrigues, E.M., Morais, D.K., Pylro, V.S., Redmile-Gordon, M., de Oliveira, J.A., Roesch, L.F.W. *et al.* (2018) Aliphatic hydrocarbon enhances phenanthrene degradation by autochthonous prokaryotic communities from a pristine seawater. *Microb Ecol* **75**(3): 688-700.

Salerno, J.L., Little, B., Lee, J., and Hamdan, L.J. (2018) Exposure to crude oil and chemical dispersant may impact marine microbial biofilm composition and steel corrosion. *Front Mar Sci* **5**: 196.

Sanni, G.O., Coulon, F., and McGenity, T.J. (2015) Dynamics and distribution of bacterial and archaeal communities in oil-contaminated temperate coastal mudflat mesocosms. *Environ Sci Pollut Res* **22**(20): 15230-15247.

Severin, T., Bacosa, H., Sato, A., and Erdner, D. (2016) Dynamics of *Heterocapsa* sp. and the associated attached and free-living bacteria under the influence of dispersed and undispersed crude oil. *Letters in applied microbiology* **63**(6): 419-425.

Short, J.W. (2017) Advances in understanding the fate and effects of oil from accidental spills in the United States beginning with the *Exxon Valdez*. *Arch Environ Contam Toxicol* **73**(1): 5-11.

Sieradzki, E.T., Morando, M., and Fuhrman, J.A. (2019) Metagenomics and stable isotope probing offer insights into metabolism of polycyclic aromatic hydrocarbons degraders in chronically polluted seawater. *bioRxiv*: 777730.

Sørheim, K.R., Daling, P.S., Cooper, D., Buist, I., Faksness, L.-G., Altin, D. *et al.* (2020). Characterization of low sulfur fuel oils (LSFO): A new generation of marine fuel oils. Trondheim, Norway: SINTEF Ocean AS. Report No.: OC2020 A-050. Available from: http://www.itopf.org/fileadmin/data/Documents/RDaward/Final_report_LSFO_Multipartner__3.1_.pdf [Accessed July 16, 2020].

Straub, D., Blackwell, N., Fuentes, A.L., Peltzer, A., Nahnsen, S., and Kleindienst, S. (2019) Interpretations of microbial community studies are biased by the selected 16s rRNA gene amplicon sequencing pipeline. *bioRxiv*: 2019.2012.2017.880468.

Suja, L.D., Summers, S., and Gutierrez, T. (2017) Role of EPS, dispersant and nutrients on the microbial response and MOS formation in the subarctic northeast atlantic. *Front Microbiol* **8**: 676.

Sun, X., and Kostka, J.E. (2019) Hydrocarbon-degrading microbial communities are site specific, and their activity is limited by synergies in temperature and nutrient availability in surface ocean waters. *Appl Environ Microbiol* **85**(15): e00443-00419.

Techtmann, S.M., Zhuang, M., Campo, P., Holder, E., Elk, M., Hazen, T.C. *et al.* (2017) Corexit 9500 enhances oil biodegradation and changes active bacterial community structure of oil-enriched microcosms. *Appl Environ Microbiol* **83**(10): e03462-03416.

Trudel, B.K. (1998) Dispersant application in Alaska: A technical update. *Dispersant Use in Alaska: A Technical Update*. Trudel, B.K. (ed). Anchorage, Alaska, USA: Prince William Sound Oil Spill Recovery Institute.

US NASEM (2020). The use of dispersants in marine oil spill response. Washington, DC: The National Academies Press (US).

US Nat. Comm. DWH (2011). The use of surface and subsea dispersants during the BP Deepwater Horizon oil spill. Working Paper. Washington, DC, USA: National Commission on the BP Deepwater Horizon Oil Spill and Offshore Drilling. Available from: http://purl.fdlp.gov/GPO/gpo184 [Accessed April 20, 2019].

US NPC (2015). Arctic potential: Realizing the promise of U.S. Arctic oil and gas resources. Washington, DC, USA: National Petroleum Council. Available from: https://www.npcarcticreport.org/ [Accessed July 19, 2020].

US NRC (2014). Responding to oil spills in the U.S. Arctic marine environment. Washington, DC, USA: The National Academies Press. Report No.: 978-0-309-29886-5

Van Beilen, J.B., Marín, M.M., Smits, T.H., Röthlisberger, M., Franchini, A.G., Witholt, B., and Rojo, F. (2004) Characterization of two alkane hydroxylase genes from the marine hydrocarbonoclastic bacterium *Alcanivorax borkumensis*. *Environ Microbiol* **6**(3): 264-273.

Vergeynst, L., Kjeldsen, K.U., Lassen, P., and Rysgaard, S. (2018a) Bacterial community succession and degradation patterns of hydrocarbons in seawater at low temperature. *J Hazard Mat* **353**: 127-134.

Vergeynst, L., Wegeberg, S., Aamand, J., Lassen, P., Gosewinkel, U., Fritt-Rasmussen, J. *et al.* (2018b) Biodegradation of marine oil spills in the Arctic with a Greenland perspective. *Sci Total Environ* **626**: 1243-1258.

Wang, W., Zhong, R., Shan, D., and Shao, Z. (2014) Indigenous oil-degrading bacteria in crude oil-contaminated seawater of the Yellow Sea, China. *Appl Microbiol Biotechnol* **98**(16): 7253-7269.

White, H.K., Lyons, S.L., Harrison, S.J., Findley, D.M., Liu, Y., and Kujawinski, E.B. (2014) Long-term persistence of dispersants following the Deepwater Horizon oil spill. *Environmental Science & Technology Letters* **1**(7): 295-299.

Wickham, H. (2016) Ggplot2: Elegant graphics for data analysis. New York, USA: Springer.

Wilkinson, J., Beegle-Krause, C.J., Evers, K.-U., Hughes, N., Lewis, A., Reed, M., and Wadhams, P. (2017) Oil spill response capabilities and technologies for ice-covered Arctic marine waters: A review of recent developments and established practices. *Ambio* **46**(3): 423-441.

Yakimov, M.M., Giuliano, L., Gentile, G., Crisafi, E., Chernikova, T.N., Abraham, W.-R. *et al.* (2003) *Oleispira antarctica* gen. nov., sp. nov., a novel hydrocarbonoclastic marine bacterium isolated from Antarctic coastal sea water. *Int J Syst Evol Microbiol* **53**(3): 779-785.

Chapter 3 – Personal contribution

The microcosm experiment was designed by myself and Jun.-Prof. Sara Kleindienst. Preparation of water-accommodated fractions, establishment of microcosms, daily rotations of microcosms, sampling of microcosms, radiotracer assays, DNA extraction and amplification for amplicon sequencing, hydrocarbon extraction, data visualization, data interpretation and statistical data analysis were performed by myself. Bioinformatic analysis of sequencing data was performed by Dr. Daniel Straub. GC-MS measurements of hydrocarbon extracts were performed by Dr. Rafael Tarozo and Dr. Christian Hallmann and the resulting chromatograms were analysed by myself with their input. The manuscript was written by myself.

3 Chemical dispersant addition affects the composition and growth of North Sea microbial communities under simulated oil spill conditions

Saskia Rughöft[1], Daniel Straub[1,2], Rafael Tarozo[3], Christian Hallmann[3,4], Sara Kleindienst[1]

[1] Microbial Ecology, Center for Applied Geosciences, University of Tübingen, Germany
[2] Quantitative Biology Center, University of Tübingen, Germany
[3] Organic Paleobiogeochemistry, Max Planck Institute for Biogeochemistry, Jena, Germany
[4] MARUM, University of Bremen, Bremen, Germany

Unpublished manuscript

3.1 Abstract

Although chemical dispersant application is a widely used response strategy during large marine oil spills, knowledge gaps regarding the ecological impacts on different marine ecosystems, especially on microbial oil-degrading populations, remain. Our goal was to identify the impacts of chemical dispersant addition during a simulated oil spill scenario on native microbial communities from a well-characterized North Sea field site. Seawater laboratory microcosms amended with crude oil components as water-accommodated fractions (WAF), oil-dispersant mixtures as chemically enhanced WAFs (CEWAF), or dispersant alone were incubated at typical summer (15°C) and winter (5°C) temperatures and monitored over 35 days. Compared to oil-only treatments, dispersant addition resulted in significantly lower cell numbers and markedly altered microbial community dynamics, revealing a number of mainly dispersant-enriched microbial taxa. Nevertheless, an enrichment of known hydrocarbon-degrading taxa (e.g. *Zhongshania*, *Pseudohongiella*, *Colwellia*, *Neptuniibacter* or *Cycloclasticus*) was detected in all hydrocarbon-amended microcosms. Biodegradation of aliphatic and aromatic hydrocarbons was identified in all treatments and unaffected by dispersant addition. The analysis of dissolved organic carbon (DOC) concentrations, however, revealed the persistence of significant CEWAF/dispersant-derived DOC levels in respective microcosms after 35 days. Our findings demonstrate a large *in situ* oil biodegradation potential in the investigated seawater and provide novel insights into dispersant impacts on North Sea microbial communities, which will enable ecologically-informed decision making in future oil spill scenarios.

3.2 Introduction

Accidental marine crude or fuel oil spills can cause abrupt and quickly spreading environmental damage on the marine ecosystem (Peterson *et al.*, 2003; Short, 2017). Even though oil pollution in the North Sea has been decreasing, several remaining oil pollution and spill risks have been identified recently, such as ongoing oil extraction processes, increasing shipping traffic, new offshore wind platforms, and the ageing nature of several oil production platforms in the area (Carpenter, 2019). The fate of oil in marine environments is controlled by a number of physicochemical processes and microbial biodegradation of petroleum hydrocarbons (HCs). Thus, marine HC-degrading microorganisms play a crucial role in spill remediation (Head *et al.*, 2006; Joye *et al.*, 2016b). Additionally, a number of technological emergency spill response and clean-up strategies are available after marine oil spills, including mechanical containment and removal, *in situ* burning or chemical dispersion of released oil (ExxonMobil, 2014).
Chemical dispersants are solvent-surfactant mixtures applied to reduce surface slicks and coastal oiling by dispersing oil into the water column. During the Deepwater Horizon oil spill in the Gulf of Mexico in 2010, an unprecedented amount of dispersants (seven million liters; Corexit EC9500A and EC9527A) were applied in response to the discharge of an estimated 800 million liters of crude oil into the Gulf ecosystem (US Nat. Comm. DWH, 2011; McNutt *et al.*, 2012). Since then, several medical and ecological concerns related to chemical dispersant use have been raised (e.g. Kleindienst *et al.*, 2015b; McGowan *et al.*, 2017). The impact of chemical dispersant application on native microbial oil-degrading populations in particular is still under debate. While dispersant exposure has been shown to alter marine microbial community dynamics (Kleindienst *et al.*, 2015b; Suja *et al.*, 2017; Techtmann *et al.*, 2017; Doyle *et al.*, 2018; Sun and Kostka, 2019; Tremblay *et al.*, 2019), conflicting results have been reported on how dispersants affect the HC biodegradation potential of these microbial communities, with findings ranging from enhanced (Bælum *et al.*, 2012; Prince *et al.*, 2016) or unaffected HC biodegradation (McFarlin *et al.*, 2014; Tremblay *et al.*, 2019) to toxic or inhibitive effects on microbial HC degradation (Hamdan and Fulmer, 2011; Kleindienst *et al.*, 2015b; Rahsepar *et al.*, 2016; Hackbusch *et al.*, 2020). Several studies have additionally demonstrated inhibition effects of dispersants on certain species/strains of HC-degrading bacteria, observed in both pure cultures (Hamdan and Fulmer, 2011; Overholt *et al.*, 2016; Hackbusch *et al.*, 2020) and seawater microcosm experiments (Techtmann *et al.*, 2017; Doyle *et al.*, 2018).
When considering oil spill frequency and chronic pollution indicators, oil pollution in the North Sea has consistently decreased over the last decades, however, areas impacted by major shipping routes and/or offshore industry remain at risk (Carpenter, 2019). The oil biodegradation potential of North Sea microbial communities was analysed previously (Brakstad and Lødeng, 2005; Gertler *et al.*, 2012; Chronopoulou *et al.*, 2015) and especially the seawater surrounding the German offshore island Helgoland has been the subject of several detailed studies with a focus on phytoplankton and nutrient dynamics (Wiltshire *et al.*, 2010; Teeling *et al.*, 2012). However, the impacts of chemical dispersants on seawater microbial communities in areas like the German Bight are not well explored (de Almeida Couto *et al.*, 2019). To our knowledge, chemical dispersant application has not yet occurred in this area but dispersant use is being considered as a secondary spill response option for German North Sea waters (Grote *et al.*, 2018).

Therefore, the main objectives of this study were to characterize the response of microbial communities from the North Sea to a simulated oil spill scenario under summer and winter temperature conditions and to determine the effects of dispersant addition on these microbial communities and their HC biodegradation potential. North Sea seawater laboratory microcosms were amended with WAF, CEWAF, or dispersant, incubated (35 days at 15°C or 5°C) and monitored by quantifying microbial growth, community dynamics, and HC biodegradation activity/potential across treatment types (Fig. 3.1).

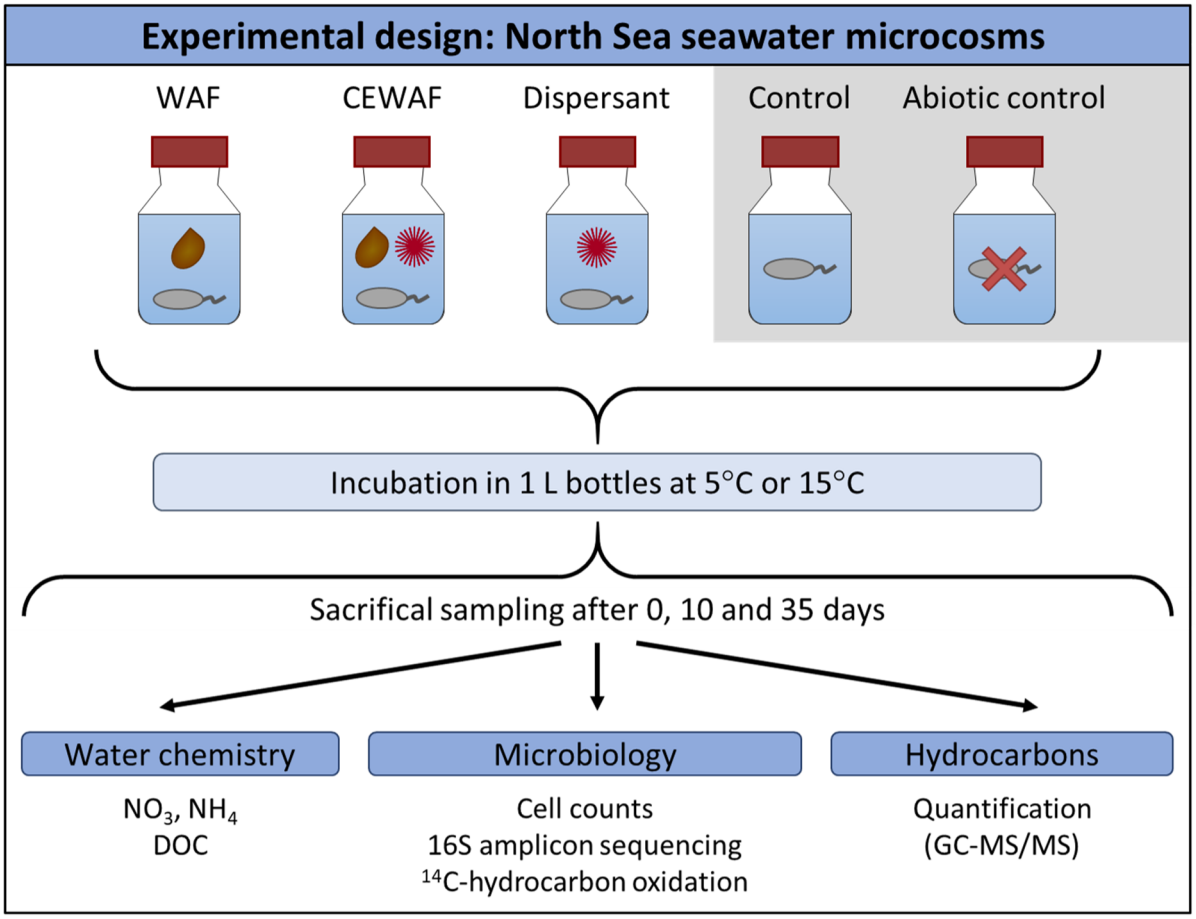

Figure 3.1: Experimental design of this study. Seawater microcosms simulating water column conditions during a North Sea oil spill scenario were established in triplicate, incubated at 15°C or 5°C and sampled sacrificially (15°C: after 0, 10, and 35 days; 5°C: after 0 and 35 days). Treatments received the following amendments (adjusted for similar final DOC content): crude oil-derived water accommodated fraction (WAF), chemically enhanced WAF (CEWAF, contains Corexit dispersant) or dispersant-only solutions. Additional control treatments received no amendments, i.e. control and abiotic control, of which the latter only contained sterilized seawater.

3.3 Experimental procedures

3.3.1 Seawater sampling

Surface seawater was collected in August 2016 off the coast of Helgoland in the North Sea (54.1867 N, 7.8983 E; 1.2 m depth; *in situ* temperature 16°C) and provided by the Biological Institute Helgoland (BAH) of the Alfred Wegener Institute. The sampling site is well-characterized regarding spring phytoplankton bloom dynamics and long-term phytoplankton and biogeochemical data sets are available (Wiltshire *et al.*, 2010; Teeling *et al.*, 2012). The seawater was stored at 4°C, transported to the laboratory in Tübingen while cooled consistently and used immediately for the preparation of water-accommodated fractions (WAFs), and stored at 4°C until the start of the experiment (12 days).

3.3.2 Water-accommodated fractions

All WAF solutions were prepared with Grane crude oil (kindly provided by Stephane Le Floch) according to Kleindienst *et al.* (2015b) with minor modifications, as described in **Chapter 2** of this thesis. Briefly, for the WAF solutions, 850 ml of sterilized seawater (0.2 µm-filtered, 2x pasteurized at 65°C for 2 hours) were amended with 150 ml crude oil, mixed by magnetic stirring for 55 hours (500 rpm, RT, dark) and subsequently allowed to settle for 60-90 min before the aqueous phase was sub-sampled, avoiding inclusion of organic phases. CEWAFs were prepared using an additional 15 ml of Corexit EC9500A dispersant (dispersant-to-oil ratio = 1:10, v/v), and dispersant-only solutions were prepared with only 850 ml of sterile seawater and 15 ml of Corexit EC 9500A. WAF, CEWAF and dispersant solutions were prepared 3 days before initiation of the experiment and stored at 4°C, while subsamples were examined for potential cell contamination via DAPI staining and measured to obtain dissolved organic carbon (DOC) concentrations (see below). To ensure contaminant-free containers for WAF solutions and the experimental microcosms, all glassware was HCl- and Milli-Q-rinsed and subsequently baked (300°C, 8 hours) and all bottle caps were teflon-lined, HCl- and Milli-Q-rinsed and pre-baked (150°C, 8 hours).

3.3.3 Setup and sampling of microcosm

Seawater (SW) microcosms were established using a total of 900 ml of seawater (gently mixed in a separate, pre-cleaned 25 L HDPE-container beforehand) in 1 L glass bottles with teflon-lined caps. Four different treatments were prepared using (1) only 900 ml SW (Control), (2) 887.7 ml SW and 12.3 ml of WAF solution (WAF-derived DOC = 135 µM), (3) 899 ml SW and 1 ml CEWAF solution (CEWAF-derived DOC = 136 µM), or (4) 899.5 ml SW and 0.5 ml dispersant solution (dispersant-derived DOC = 138 µM). The respective volumes of added WAF solutions were chosen to simulate a medium to large oil spill scenario (Kleindienst *et al.*, 2016a) and adjusted with the goal of obtaining comparable DOC levels across all hydrocarbon-amended microcosms at the start of the experiment. Abiotic controls containing (5) 900 ml sterilized SW were prepared contemporaneously.

Microcosms were established in triplicates, except for T_0 microcosms at 5°C. Subsequently, microcosms were separated into two groups, which were incubated in the dark at either 15°C (summer *in situ* temperature) or 5°C (winter *in situ* temperature). All microcosm bottles were gently turned at least once every 24 hours. All summer treatments were sampled sacrificially at

three time points (15°C microcosms; after 0, 10, 35 days) and all winter treatments at two time points (5°C microcosms; after 0 and 35 days). Due to the duration of microcosm establishment, the first sampling (T_0) was performed about 8-10 hours after microcosm setup. Sampling of the microcosms was performed after inverting bottles gently a few times by removing aliquots for each analysis described below in the following order: water chemistry (oxygen, pH, salinity, nutrients, DOC), ^{14}C-hydrocarbon oxidation assays, total cell counts, DNA, hydrocarbon quantification.

3.3.4 Geochemical analyses

DOC, nutrient (i.e. nitrate, ammonium) and HC concentrations in microcosms were monitored during the course of the experiment as described in **Chapter 2**. HC extraction from one (dispersant-only, Control) or two (WAF, CEWAF) sampled microcosms per triplicate was performed using dichloromethane (twice) and *n*-hexane (once) and concentrated extracts were measured via GC-MS (see **Chapter 2**).

3.3.5 Microbiological and molecular analyses

Microbial cell numbers of free cells (i.e. not in large aggregates) were determined for two (WAF) or one (all other treatments) sampled 15°C microcosm per triplicate via total cell counts (see **Chapter 2**). Additionally, microbial cell numbers were estimated using 16S rRNA gene-based quantitative PCR (qPCR) for all sampled microcosms (see **Chapter 2**). Microbial biodegradation activity was measured using ^{14}C-hexadecane and ^{14}C-naphthalene oxidation assays for two samples (technical replicates) from one microcosm for each set of biological triplicate microcosms and one killed control replicate (mixed sample of triplicates) was analysed additionally as described in (Kleindienst *et al.*, 2015b) and in **Chapter 2** of this thesis. Microbial community composition was investigated for all sampled microcosms (except for T_0 at 15°C: duplicates were selected) using 16S rRNA gene amplicon Illumina sequencing (see **Chapter 2**). Sequencing data was analysed with nf-core/ampliseq v1.1.0, which performed all following analysis steps and includes required software (Ewels *et al.*, 2020; see also Chapter 2; Straub *et al.*, 2020).

3.3.6 Data analysis

To test whether observed differences in qPCR-based cell numbers between the different treatments (at one time point) were statistically significant, data were log-transformed before ANOVA followed by Tukey *post-hoc* test ($p < 0.05$) for multiple comparisons was used. Beforehand, the data set had been tested for normally distributed residuals (tested with Shapiro-Wilks test, $p > 0.05$) and homogeneous variances (tested with Levene test, $p > 0.05$). To test whether observed differences in DOC concentrations between the different treatments (at one time point) or between time points (for one treatment type) were statistically significant, Kruskal-Wallis rank sum tests followed by Nemenyi's *post-hoc* test of multiple comparisons ($p < 0.05$) were performed because normal distribution of the data could not be assumed. The R programming language was used to perform all described tests and all presented data was plotted using ggplot2 v3.3.2 (Wickham, 2016) in R v3.6.0 (R Core Team, 2019).

3.4 Results

3.4.1 Microbial growth

In microcosms incubated at 15°C (i.e. close to *in situ* summer temperature conditions), a substantial increase in cell count numbers was only observed in WAF treatments after 10 days (reaching 7.88 x 10^5 free cells ml^{-1}), while cell count numbers after 35 days were lower and similar to values at the start of the experiment in all treatments (i.e. 1.15–1.43 x 10^5 free cells ml^{-1}; Figure 3.2A). Cell numbers estimated via 16S rRNA gene-targeted qPCR showed the same trend with only cell numbers in WAF treatments after 10 days being significantly ($p < 0.05$) higher than in control microcosms (Figure 3.2B). While qPCR-based cell numbers for 5°C microcosms after 35 days were one or two orders of magnitude below 15°C incubations (Figure 3.2C), significantly ($p < 0.05$) increased cell numbers were also only detected in WAF treatments, suggesting that microbial growth occurred later or was sustained for longer in WAF treatments at the lower incubation temperature. During fluorescence microscopy, several aggregates containing large numbers of microbial cells (Figure S3.1) were observed, predominantly in WAF-amended microcosm samples. Since aggregated cells were impossible to count accurately, cell count results only cover free non-aggregated cells and are therefore likely somewhat underestimated, especially for WAF samples.

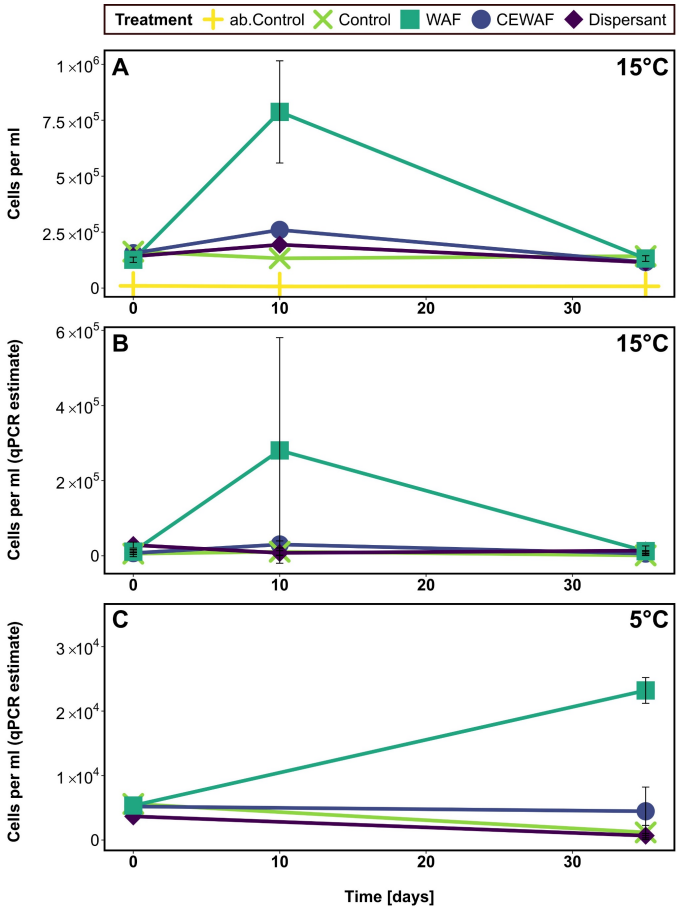

Figure 3.2: Microbial cell numbers in seawater microcosms simulating water column conditions during a North Sea oil spill scenario. Results shown are averages of sacrificial, duplicate (A) or triplicate (B/C) microcosms (error bars show standard deviations). **A)** Cell numbers (cells ml^{-1}) as determined by DAPI total cell counts. ab. Control represents abiotic control microcosms. **B/C)** Cell numbers (cells ml^{-1}) as estimated by 16S rRNA gene-targeted qPCR in 15°C (B) and 5°C microcosms (C).

3.4.2 Microbial community dynamics

According to non-metric multidimensional scaling (NMDS) ordination analysis, the β-diversity of 16S rRNA gene-based microbial community composition differed across treatments, time points and incubation temperatures (Fig. 3.3). While all microcosm microbial communities were similar to each other at the start of the experiment, they evolved differently over time with a clear separation observed between the WAF treatments and the dispersant-containing (i.e. CEWAF and dispersant-only) treatments after 10 and 35 days. Although the microbial communities also evolved differently across the different incubation temperatures, this trend was observed in both 5°C and 15°C microcosms.

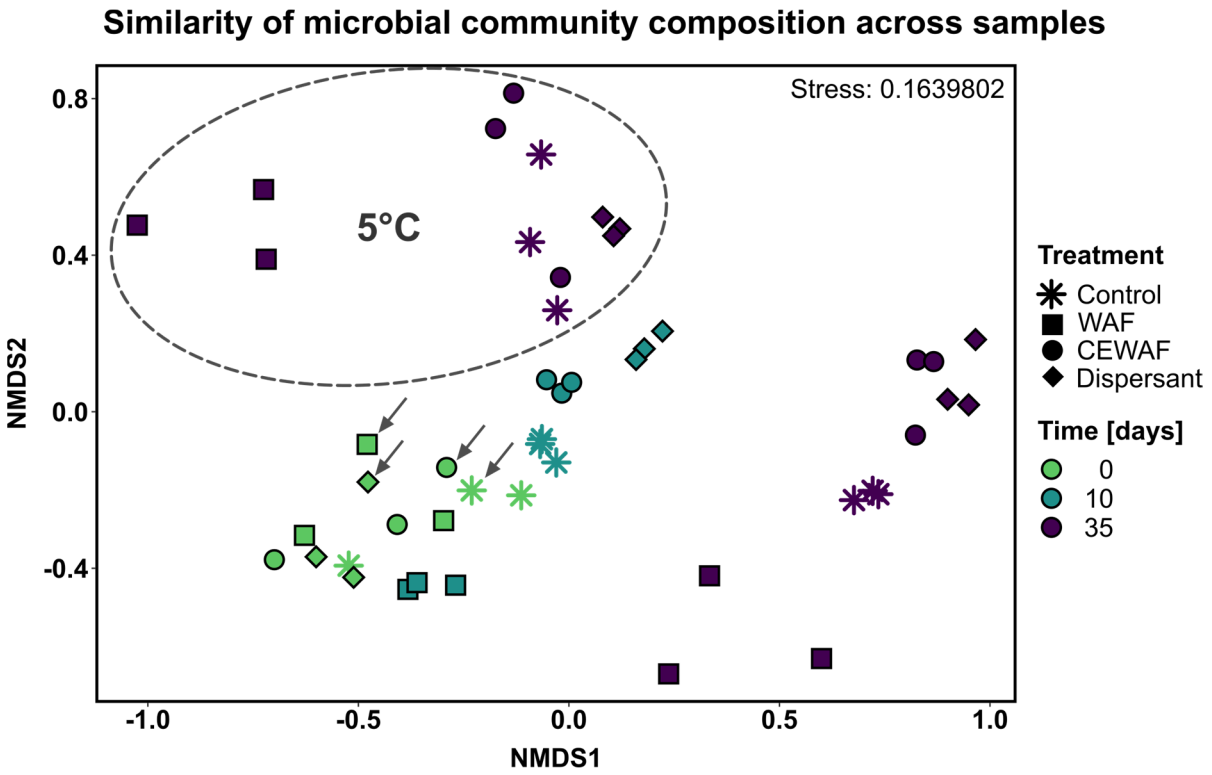

Figure 3.3: Similarity of microbial community composition in seawater microcosms at 15°C and 5°C simulating water column conditions during a North Sea oil spill scenario as determined by 16S rRNA gene amplicon sequencing. Non-metric multidimensional scaling (NMDS) plot based on Bray Curtis diversity showing the similarity of microbial community compositions across samples. The stress achieved is indicated in the top right of the plot. 5°C microcosm samples are indicated by arrows (T_0) and an ellipsis (35 days).

These microbial community dynamics were quite diverse but nevertheless characterized by distinct dominant genera, with many of them either detected in WAF or in CEWAF and dispersant-only treatments (Fig. 3.4). Even though *Zhongshania*, for example, was a dominant taxon in all microcosms at the start of the experiment with 38-49% relative 16S rRNA gene sequence abundance at 15°C and 10–21% at 5°C, their relative abundance decreased in dispersant-containing microcosms at both temperatures during the incubation period, while remaining a dominant group in WAF treatments (14–34% in 15°C and 5°C microcosms at later time points). *Pseudohongiella*, on the other hand, was detected in all microcosms at the beginning (at ≥ 2%) and increased in relative abundance during the experiment in all HC-amended treatments (up to 15%), except for WAF microcosms at 5°C. *Gimesia* (99.2% 16S

rRNA gene sequence identity to *Gimesia maris*, formerly *Planctomyces maris*) likewise increased in relative abundance in all 15°C HC-amended treatments after 35 days (from < 0.1% up to 6%). Several notable taxa only became dominant in dispersant-containing microcosms (i.e. CEWAF and dispersant-only) at 15°C or 5°C, illustrating the distinct microbial community dynamics described above. This included the genera *Colwellia* (up to 9%), *Neptuniibacter* (up to 11%), *Ulvibacter* (up to 2%), *Marivita* (up to 6%), and the family *Porticoccaceae* (up to 7%; with 93.68% 16S rRNA gene sequence identity to *Oleiphilus messinensis*) in 15°C incubations and additionally taxa such as *Luteolibacter* (up to 7%) and *Sulfitobacter* (up to 2%) in 5°C incubations. Remarkably, although all microbial communities were still highly similar at the first sampling time point (T_0), *Oleispira* was found to be abudant in dispersant-only microcosms across both incubation temperatures at this time (up to 9% relative abundance). Another notable taxon in dispersant-only microcosms was classified as *Halieaceae* (up to 18%) and showed a 96.8% 16S rRNA gene sequence identity to *Luminiphilus syltensis*. A distinct group of taxa were abundant in WAF treatments, e.g. *Amylibacter* (up to 7% at 15°C), *Cycloclasticus* (up to 4% at 5°C), and several taxa that were only taxonomically annotated until family level, such as unclassified *Rhodobacteraceae* (up to 7%) with 100% 16S rRNA gene sequence identity to *Tropicibacter litoreus*, unclassified *Saprospiraceae* (up to 8%) with 92.9% 16S rRNA gene sequence identity to *Lewinella nigricans* and unclassified *Cryomorphaceae* (up to 3%) with 90.8% 16S rRNA gene sequence identity to *Candidatus* Fluviicola riflensis. In addition, two taxa that were associated with dispersant-containing samples in 15°C incubations appeared to also increase in relative abundance in WAF treatments at 5°C (i.e. *Colwellia*, *Neptuniibacter*).

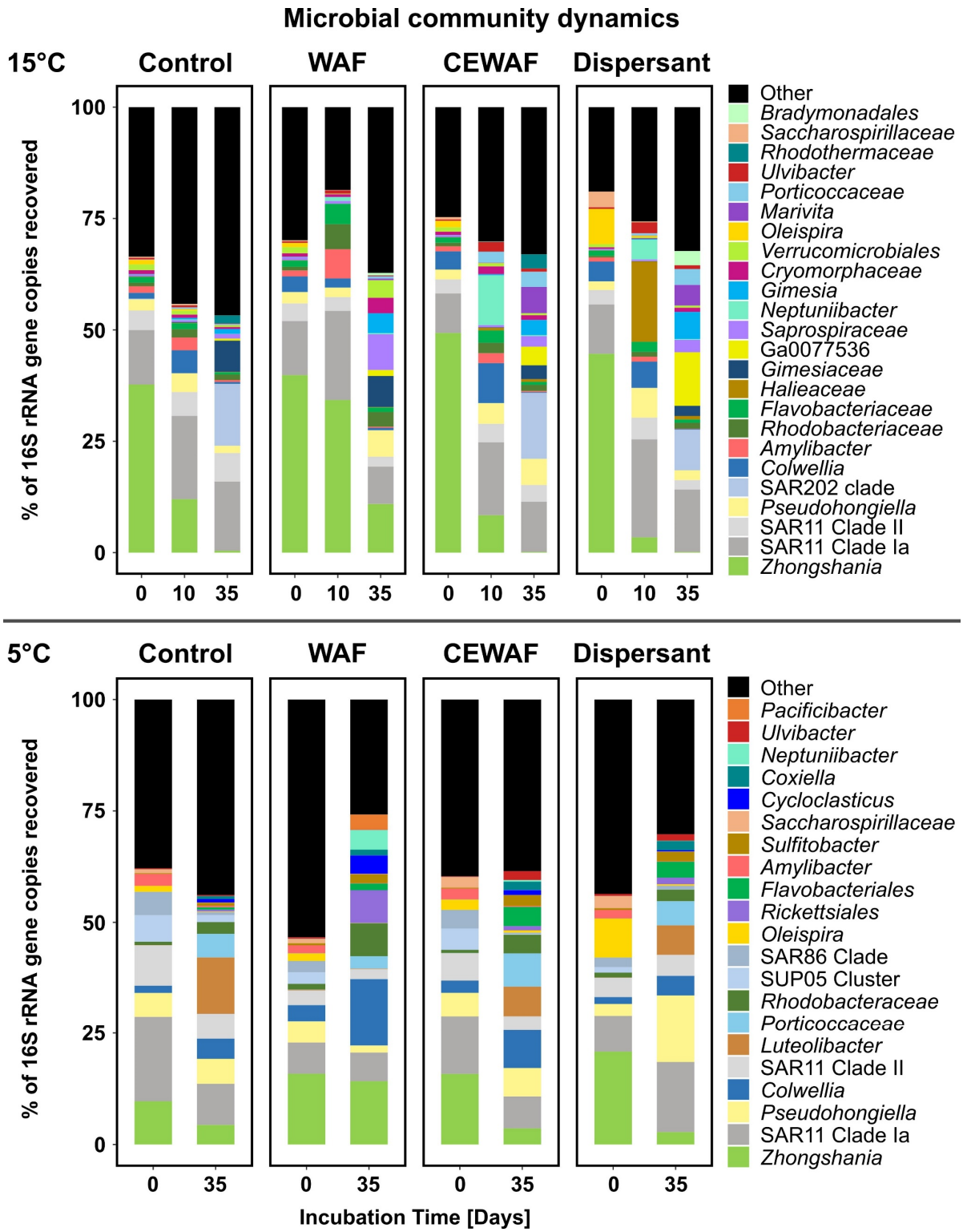

Figure 3.4: Changes in microbial community composition in 15°C and 5°C seawater microcosms simulating water column conditions during a North Sea oil spill scenario as determined by 16S rRNA gene amplicon sequencing. Microbial population dynamics (averages of sacrificial triplicate microcosms) are shown as most abundant taxa in microcosms at genus level (sorted by average abundance across samples and labelled with the highest descriptive taxonomic level).

3.4.3 Microbial oil biodegradation potential

Even though a precise quantification of the added oil HC components was challenging due to the chemical heterogeneity within and across microcosms (see also **Chapter 2**), different analytical approaches indicated that biodegradation of aliphatic and aromatic HCs took place in all HC-amended treatments during the incubation period. First, DOC analysis revealed a significant ($p < 0.05$) DOC decrease in WAF treatments within the incubation period at 15°C (Figure 3.5), suggesting that the native microbial community degraded most WAF-derived DOC before reaching DOC levels similar to the control treatment (final concentration: 174.57 µM on average) within 35 days. However, while the DOC content of both dispersant-containing treatments was initially similar compared to WAF microcosms, it did not decrease significantly ($p > 0.15$) until the end of the experiment (250.05–295.85 µM remained). In 5°C incubations, the remaining DOC concentrations were also significantly ($p < 0.05$) lower in WAF setups compared to dispersant-containing treatments after 35 days (196.91 µM and 300.70–321.38 µM, respectively). Second, the performed radiotracer assays revealed high ^{14}C-naphthalene and ^{14}C-hexadecane oxidation rates in WAF treatments (up to 23.14 and 5.69 ng L^{-1} d^{-1}, respectively) and slightly lower oxidation rates in CEWAF treatments (up to 17.65 and 2.16 ng L^{-1} d^{-1}, respectively), with ^{14}C-hexadecane oxidation rates appearing to decrease in all treatments over the incubation period (Figure S3.2). Detected ^{14}C-labelled HC oxidation rates in 5°C microcosms were consistently lower than in 15°C incubations at the analysed time points (after 0 and 35 days). Third, HC quantification via GC-MS showed that *n*-alkanes ($C_{12–36}$) decreased notably in all treatments, reaching 18–48% of initial concentrations after 35 days (Figure 3.6). Additionally, even though initial concentrations differed between treatments, naphthalenes and phenanthrenes decreased in all treatments before reaching 1-7% of initial concentrations in WAF and CEWAF microcosms at the end of the experiment. The initial concentrations of naphthalenes and phenanthrenes in dispersant-only microcosms were very low (≤ 0.15 ng ml^{-1}), which is why they were excluded from biodegradation analysis. Finally, a bulk parameter encompassing all detected compounds in the obtained GC-MS chromatograms (termed 'total petroleum hydrocarbons (TPH) equivalents') also revealed a decrease in detected compounds across all microcosms, even though final TPH equivalent levels after 35 days appeared slightly higher in dispersant-containing treatments compared to WAF treatments.

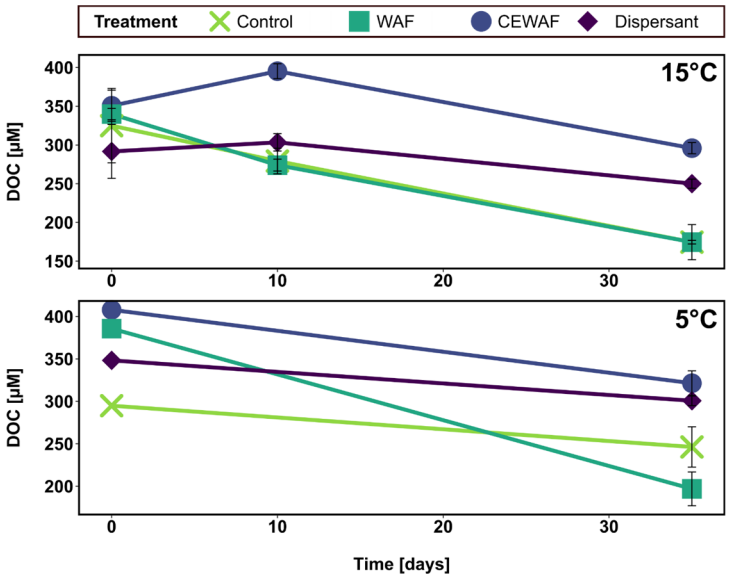

Figure 3.5: Dissolved organic carbon (DOC) concentrations in 15°C and 5°C seawater microcosms simulating water column conditions during a North Sea oil spill scenario. Results shown are averages of sacrificial, triplicate microcosms except for the T_0 samples at 5°C (error bars show standard deviations).

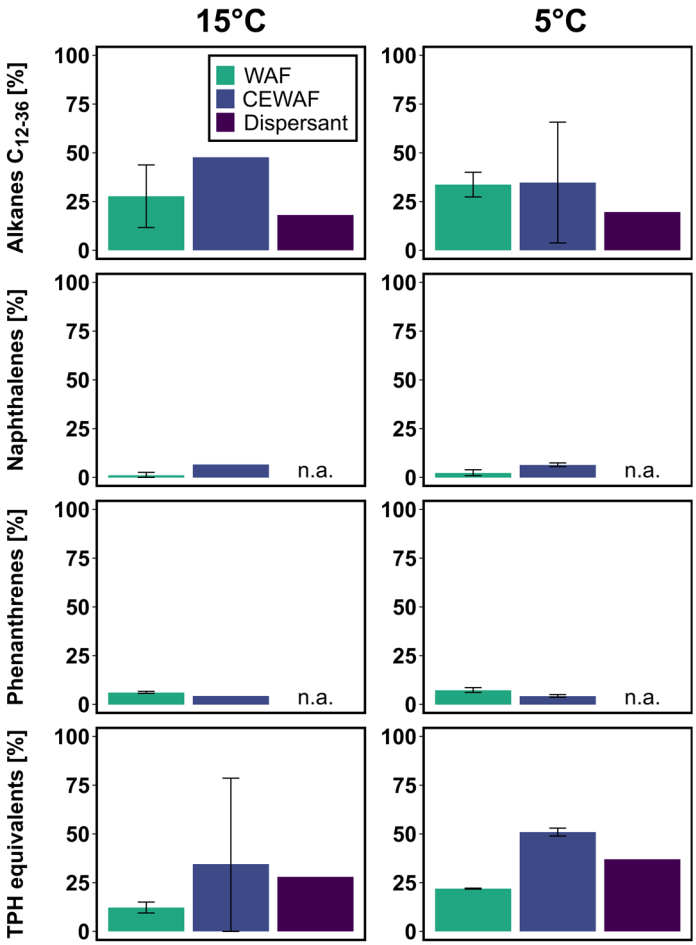

Figure 3.6: Hydrocarbon concentrations after 35 days in 15°C and 5°C seawater microcosms simulating water column conditions during a simulated North Sea oil spill scenario. Total alkanes ($C_{12\text{-}36}$), naphthalenes, phenanthrenes and bulk TPH equivalents are shown as remaining percentages of initial concentrations at T_0 as determined by via GC-MS quantification. Results shown are averages of sacrificial replicate microcosms for WAF and CEWAF treatments (error bars show standard deviations).

3.5 Discussion

3.5.1 Response of North Sea seawater community to a simulated oil spill scenario

The observed microbial dynamics in WAF-amended microcosms revealed that the investigated North Sea seawater microbial community responded to the input of crude oil components with significant growth, aggregate formation and a distinct shift in microbial community composition. According to previous studies under similar conditions (Kleindienst *et al.*, 2015b; Passow, 2016; Suja *et al.*, 2017; Doyle *et al.*, 2018; see also Chapter 2 in this thesis), the observed microbial aggregates could have been marine (oil) snow (i.e. consisting of microorganisms, their exudates and oil), which played an important role after the DWH oil spill in the Gulf of Mexico (Passow and Ziervogel, 2016). Several of the enriched microbial genera detected in WAF microcosms also contain species with reported alkane and/or aromatic HC biodegradation capabilities, either described in isolated representatives or reported based on genome/transcriptome analysis. This includes *Zhongshania* (Naysim *et al.*, 2014; Oh and Roh, 2018), *Pseudohongiella* (Sieradzki *et al.*, 2019), *Gimesia* (Nie *et al.*, 2014; Canul-Chan *et al.*, 2018), *Cycloclasticus* (Dyksterhouse *et al.*, 1995; Kasai *et al.*, 2002; Rubin-Blum *et al.*, 2017), *Neptuniibacter* (Nagashima *et al.*, 2010; Diéguez and Romalde, 2017), *Colwellia* (Bælum *et al.*, 2012; Redmond and Valentine, 2012; Campeão *et al.*, 2019; Sieradzki *et al.*, 2019) and *Tropicibacter* (Harwati *et al.*, 2009). Additionally, unclassified *Cryomorphaceae* and *Saprospiraceae* were also detected in association with oil pollution in previous studies (Militon *et al.*, 2015; Severin *et al.*, 2016; McFarlin, 2017; Doyle *et al.*, 2018; Salerno *et al.*, 2018), pointing to a potential role of yet-to-be isolated members of these families in oil biodegradation. Until now, no HC biodegradation capabilities have been described for *Amylibacter*, but members from this group have been isolated from algae (Nedashkovskaya *et al.*, 2016) known as a biological HC source (Hoefs *et al.*, 1995) as is often the case for other HC-degrading bacteria (Gutierrez *et al.*, 2014). *Amylibacter* was additionally detected in association with a gas blowout in the North Sea (Steinle *et al.*, 2016), thus, this genus could have played a role as primary or secondary HC degrader. Interestingly, no enrichment of the common HC degraders *Alkanivorax, Halomonas* or *Pseudoalteromonas* was detected in this study, which is in contrast to a few previous studies of North Sea oil-degrading microbial communities (Gertler *et al.*, 2012; Chronopoulou *et al.*, 2015). However, several of the other enriched taxa in this study were previously also reported in comparable studies using North Sea seawater (Brakstad and Lødeng, 2005; Gertler *et al.*, 2012; Teeling *et al.*, 2012; Knapik *et al.*, 2020). Thus, WAF addition appears to have enriched a diverse community of different primary and/or secondary HC degraders at 15°C and 5°C, which were only present as rare seed populations beforehand in some cases (as previously discussed by e.g. Head *et al.*, 2006; Yang *et al.*, 2016). In other cases, such as *Zhongshania, Pseudohongiella*, and *Colwellia,* however, they were already present at ≥ 1% relative 16S rRNA gene sequence abundance in control treatments at the start of the experiment which either suggests that they are versatile heterotrophs only opportunistically utilizing HCs and/or that the sampled North Sea surface waters contained other sources of bioavailable HCs, which might have prepared or primed the native microbial community for an efficient oil spill response. These sources could, for example, be HC-containing exudates from phytoplankton and/or macroalgaea (Gutierrez, 2019) or associated with the (relatively limited) boat traffic surrounding Helgoland or chronic oil pollution levels

in the German Bight (Chrastansky and Callies, 2009; Gertler *et al.*, 2012). The detection of taxa commonly associated with obligatory HC degraders (i.e. *Cycloclasticus* and *Oleispira*; Yakimov *et al.*, 2007) in control treatments at the start of the experiments also supports the availability of HCs even before the performed oil spill simulation in the sampled seawater.
The development of a HC-degrading microbial community is further illustrated by the high detected oil biodegradation potential in WAF microcosms at both incubation temperatures. Our results suggest that, within 35 days, all added oil-derived DOC including *n*-alkanes, naphthalenes and phenanthrenes was degraded by the microbial community at both incubation temperatures, even though detected cell numbers and ^{14}C-HC oxidation rates were lower at 5°C. Additionally, the trends detected in GC-MS HC quantification data, in ^{14}C-hydrocarbon oxidation rates and suspected enriched HC degraders (i.e. decreasing *Zhongshania* and increasing *Pseudohongiella* or *Cycloclasticus* sequence abundances) all point to aliphatic HCs being degraded before aromatic HCs in the established microcosms. Similar biodegradation patterns and comparable or slower rates of biodegradation were previously reported e.g. for oil-derived alkanes in winter North Sea seawater (Brakstad and Lødeng, 2005), crude oil in Thames estuary water (Coulon *et al.*, 2007) and chemically dispersed oil in seawater from a Norwegian fjord (Ribicic *et al.*, 2018).

3.5.2 Impacts of dispersant addition on microbial community dynamics and oil biodegradation

In comparison to WAF microcosms, chemical dispersant (i.e. Corexit) addition in the form of CEWAF or dispersant-only solution led to less microbial growth even though the same amount of DOC was added at the beginning of the experiment. While an undetected rapid increase and subsequent decrease in cell numbers in these Corexit-containing treatments cannot be excluded due to the long time intervals between the sampling points, the observed cell numbers at both incubation temperatures suggest that either less of the added organic carbon was bioavailable as microbial substrate or that other Corexit-associated growth-inhibiting mechanisms might have played a role (as discussed in **Chapter 2 and 5** in this thesis).
Chemical dispersant addition also affected the microbial community composition, with CEWAF treatments containing a microbial β-diversity more similar to dispersant-only than WAF treatments and a number of microbial taxa mainly enriched in dispersant-containing microcosms, which confirms previous reports of dispersant exposure altering marine microbial community dynamics (Kleindienst *et al.*, 2015b; Suja *et al.*, 2017; Techtmann *et al.*, 2017; Doyle *et al.*, 2018; de Almeida Couto *et al.*, 2019; Sun and Kostka, 2019; Tremblay *et al.*, 2019). However, these microcosms also contained several HC-metabolizing microbial groups, similar to WAF treatments. Besides *Neptuniibacter*, *Colwellia* and *Gimesia* (see above), this included the following taxa: *Ulvibacter* (Brakstad *et al.*, 2017; Campeão *et al.*, 2019), *Porticoccaceae* (Gutierrez *et al.*, 2012; Ribicic *et al.*, 2018; Knapik *et al.*, 2020) and *Sulfitobacter* (Mas-Lladó *et al.*, 2014; Fasca *et al.*, 2018). Additionally, *Marivita* and *Luteolibacter* were also detected in association with oil pollution in previous studies (Severin *et al.*, 2016; Chen *et al.*, 2017a; Valencia-Agami *et al.*, 2019; Zakharenko *et al.*, 2019), which could indicate a potential role for them in HC biodegradation. The specific enrichment of all these taxa in dispersant-containing microcosms was likely caused by the biodegradable HC fraction of the utilized dispersant Corexit or their increased tolerance for dispersant exposure

enabling them to outcompete other taxa (see also **Chapter 5**). *Colwellia* and *Neptuniibacter* were, for example, enriched in the DWH plume and likely played a role in the oil biodegradation during the DWH spill in the Gulf of Mexico (Redmond and Valentine, 2012; Rivers *et al.*, 2013; Mason *et al.*, 2014; Dombrowski *et al.*, 2016; Kleindienst *et al.*, 2016a). The isolate *Colwellia* sp. RC25 was also shown to degrade different Corexit components (Chakraborty *et al.*, 2012) and *Neptuniibacter* sp. CAR-SF can degrade the aromatic heterocyclic (i.e. N-containing) compound carbazole (Nagashima *et al.*, 2010), which could mean that other aromatic heterocyclic compounds derived from oil and/or Corexit (see also **Chapter 5**) might also be degradable by members of *Neptuniibacter*. Furthermore, the genus *Colwellia*, *Ulvibacter*, and *Sulfitobacter* and the family *Porticoccaceae* previously also became enriched by chemically dispersed oil in similar experiments using Norwegian fjord sweater (Brakstad *et al.*, 2018; Ribicic *et al.*, 2018). The *Colwellia* members additionally detected in relatively high sequence abundances in 5°C WAF microcosms might have been enriched due to the psychrophilic nature of *Colwellia* isolates (Bowman *et al.*, 1998; Methé *et al.*, 2005) and they might have been different ecotypes with a preference for oil HCs (as discussed e.g. by Kleindienst *et al.*, 2015b; Joye *et al.*, 2016b; McFarlin *et al.*, 2018). Dispersant-only microcosms developed a very similar community to CEWAF microcosms, with the exception of enriched *Oleispira* and *Halieaceae* at the beginning and end of the experiment, respectively. Since the genus *Oleispira* contains the obligate alkane degrader *Oleispira antarctica* (Yakimov *et al.*, 2003), it was likely enriched due to the high amount of Corexit-derived bioavailable alkanes added to these microcosms (Word *et al.*, 2014; McFarlin *et al.*, 2018; Choyke and Ferguson, 2019) and appeared to be the most rapidly responding taxon across treatments. It can also not be excluded that a subsequent, slower enrichment of *Oleispira* occurred in the other treatments as well between day 0 and 10. Interestingly, *Halieceae* members were recently shown to possess the ability to degrade (short) alkanes and alkenes (Knapik *et al.*, 2019; Suzuki *et al.*, 2019), while *Luminiphilus syltensis*, specifically, can utilize an arylacetonitrilase to hydrolyse another type of N-containing aromatic HC (Sun *et al.*, 2015). In conclusion, dispersant addition likely led to the development of a diverse dispersant- and HC-degrading microbial community with several different key players than the WAF-enriched community.

Interestingly, the high persisting DOC concentrations in dispersant-containing microcosms point to dispersant- or CEWAF-derived DOC containing less biodegradable compounds than the WAF-derived DOC, which aligns with the lower detected microbial growth rates. The rapid observed *n*-alkane, naphthalene and phenanthrene biodegradation patterns and enriched HC-degrading microbial taxa, however, are in stark contrast to those results as they suggest that HC biodegradation was unaffected by dispersant addition, similar to previous studies using Alaskan or Canadian seawater (McFarlin *et al.*, 2014; Tremblay *et al.*, 2019). Nevertheless, our findings suggest that while dispersant addition did not impede biodegradation of the quantified aliphatic and aromatic HCs by the North Sea microbial community, microbial growth and community dynamics were markedly affected and persistent dispersant-derived compounds in the water column potentially remained present after 35 days.

3.5.3 Conclusions

The presented data demonstrates a large *in situ* oil biodegradation potential in North Sea seawater from Helgoland and suggests that the native microbial community is primed for an efficient bioremediation response to future accidental or shipping-related oil inputs. The application of the chemical dispersant Corexit did not substantially affect the biodegradation of aliphatic or aromatic hydrocarbons but had considerable impacts on microbial growth and population dynamics with unknown long-term effects. Additionally, the risks of potentially persistent dispersant-derived components should be considered carefully in future oil spill response decision making. While incubation at lower winter-like temperatures likely slowed down and/or lowered microbial growth and biodegradation activity, similar impacts of chemical dispersants on the microbial community were observed and the same oil biodegradation was achieved within 35 days. More research is needed regarding the response of North Sea microbial communities to oil spill scenarios further away from the coast and the effects of alternative bioremediation-focused spill response techniques such as biostimulation on North Sea microbial communities and their oil biodegradation potential.

Acknowledgements

This study was funded by the Baden-Württemberg Foundation's Elite Program for Postdocs and by the Deutsche Forschungsgemeinschaft (DFG, German Research Foundation - fellowship grant #326028733). We would also like to thank Ute Kieb for providing seawater samples, Maximilian Schmidt for seawater transport assistance, Stephane Le Floch for providing Grane crude oil and Corexit EC9500A, Ellen Röhm for CFA measurements, Bernice Nisch for DOC measurements, Thomas Haug for providing facilities to perform radiotracer assays and Juliane Riedel for help with DAPI cell counts.

3.6 Supplemental information

3.6.1 Supplemental figures

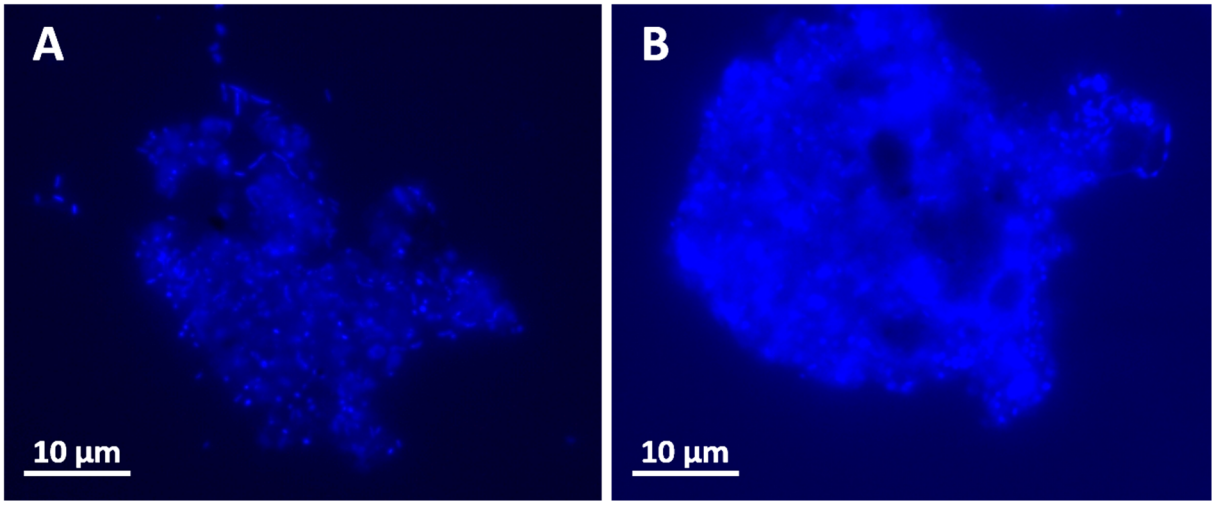

Figure S 3.1: Microbial aggregates observed in seawater microcosms simulating water column conditions during a North Sea oil spill scenario after addition of crude oil-derived water accommodated fraction (WAF). Fluorescence microscopy images of aggregates obtained after 10 (**A**) and 35 (**B**) days of incubation. Cells are stained with 4′,6 diamidino-2 phenylindole (DAPI; appears blue).

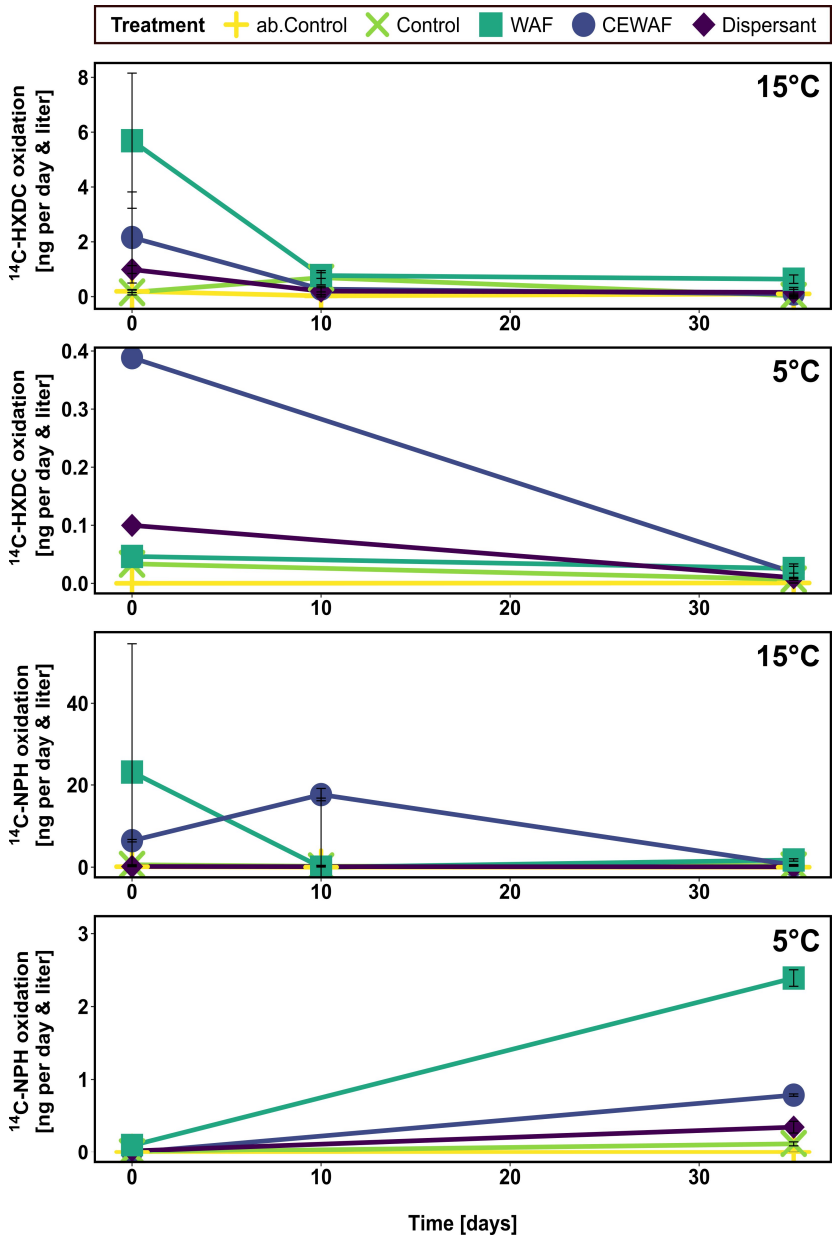

Figure S 3.2: ^{14}C-hydrocarbon oxidation rates detected in seawater microcosms simulating water column conditions during a North Sea oil spill scenario. Results shown are averages of duplicate microcosms (error bars shown are standard deviations). From top to bottom: ^{14}C-hexadecane (HXD) oxidation rates at 15°C and 5°C. ^{14}C-naphthalene (NPH) oxidation rates at 15°C and 5°C.

3.7 References

Bælum, J., Borglin, S., Chakraborty, R., Fortney, J.L., Lamendella, R., Mason, O.U. *et al.* (2012) Deep-sea bacteria enriched by oil and dispersant from the Deepwater Horizon spill. *Environ Microbiol* **14**(9): 2405-2416.

Bowman, J.P., Gosink, J.J., McCAMMON, S.A., Lewis, T.E., Nichols, D.S., Nichols, P.D. *et al.* (1998) *Colwellia demingiae* sp. nov., *Colwellia hornerae* sp. nov., *Colwellia rossensis* sp. nov. and *Colwellia psychrotropica* sp. nov.: Psychrophilic Antarctic species with the ability to synthesize docosahexaenoic acid (22:Ω63). *Int J Syst Evol Microbiol* **48**(4): 1171-1180.

Brakstad, O., and Lødeng, A. (2005) Microbial diversity during biodegradation of crude oil in seawater from the North Sea. *Microb Ecol* **49**(1): 94-103.

Brakstad, O.G., Lofthus, S., Ribicic, D., and Netzer, R. (2017) Biodegradation of petroleum oil in cold marine environments. In *Psychrophiles: From biodiversity to biotechnology*: Springer, pp. 613-644.

Brakstad, O.G., Davies, E.J., Ribicic, D., Winkler, A., Brönner, U., and Netzer, R. (2018) Biodegradation of dispersed oil in natural seawaters from Western Greenland and a Norwegian fjord. *Polar Biology* **41**(12): 2435-2450.

Campeão, M.E., Swings, J., Silva, B.S., Otsuki, K., Thompson, F.L., and Thompson, C.C. (2019) "*Candidatus* Colwellia aromaticivorans" sp. nov.,"*Candidatus* Halocyntiibacter alkanivorans" sp. nov., and "*Candidatus* Ulvibacter alkanivorans" sp. nov. genome sequences. *Microbiology Resource Announcements* **8**(15).

Canul-Chan, M., Sanchez-Gonzalez, M., González-Burgos, A., Zepeda, A., and Rojas-Herrera, R. (2018) Population structures shift during the biodegradation of crude and fuel oil by an indigenous consortium. *International journal of environmental science and technology* **15**(1): 1-16.

Carpenter, A. (2019) Oil pollution in the North Sea: The impact of governance measures on oil pollution over several decades. *Hydrobiologia* **845**(1): 109-127.

Chakraborty, R., Borglin, S.E., Dubinsky, E.A., Andersen, G.L., and Hazen, T.C. (2012) Microbial response to the MC-252 oil and Corexit 9500 in the Gulf of Mexico. *Front Microbiol* **3**: 357.

Chen, C., Liu, Q., Liu, C., and Yu, J. (2017) Effect of different enrichment strategies on microbial community structure in petroleum-contaminated marine sediment in Dalian, China. *Mar Pollut Bull* **117**(1-2): 274-282.

Choyke, S., and Ferguson, P.L. (2019) Molecular characterization of nonionic surfactant components of the Corexit 9500® oil spill dispersant by high-resolution mass spectrometry. *Rapid Commun Mass Spectrom* **33**(22): 1683-1694.

Chrastansky, A., and Callies, U. (2009) Model-based long-term reconstruction of weather-driven variations in chronic oil pollution along the German North Sea coast. *Mar Pollut Bull* **58**(7): 967-975.

Chronopoulou, P.M., Sanni, G.O., Silas-Olu, D.I., van der Meer, J.R., Timmis, K.N., Brussaard, C.P., and McGenity, T.J. (2015) Generalist hydrocarbon-degrading bacterial communities in the oil-polluted water column of the North Sea. *Microb Biotechnol* **8**(3): 434-447.

Coulon, F., McKew, B.A., Osborn, A.M., McGenity, T.J., and Timmis, K.N. (2007) Effects of temperature and biostimulation on oil-degrading microbial communities in temperate estuarine waters. *Environ Microbiol* **9**(1): 177-186.

de Almeida Couto, C.R., de Assis Leite, D.C., Jurelevicius, D., van Elsas, J.D., and Seldin, L. (2019) Chemical and biological dispersants differently affect the bacterial communities of uncontaminated and oil-contaminated marine water. *Brazilian Journal of Microbiology* **51**(2): 691-700.

Diéguez, A., and Romalde, J. (2017) Draft genome sequences of *Neptuniibacter* sp. strains LFT 1.8 and ATR 1.1. *Genome Announcements* **5**(5).

Dombrowski, N., Donaho, J.A., Gutierrez, T., Seitz, K.W., Teske, A.P., and Baker, B.J. (2016) Reconstructing metabolic pathways of hydrocarbon-degrading bacteria from the Deepwater Horizon oil spill. *Nat Microbiol* **1**(7): 1-7.

Doyle, S.M., Whitaker, E.A., De Pascuale, V., Wade, T.L., Knap, A.H., Santschi, P.H. *et al.* (2018) Rapid formation of microbe-oil aggregates and changes in community composition in coastal surface water following exposure to oil and the dispersant Corexit. *Front Microbiol* **9**: 689.

Dyksterhouse, S.E., Gray, J.P., Herwig, R.P., Lara, J.C., and Staley, J.T. (1995) *Cycloclasticus pugetii* gen. nov., sp. nov., an aromatic hydrocarbon-degrading bacterium from marine sediments. *Int J Syst Bacteriol* **45**(1): 116-123.

Ewels, P.A., Peltzer, A., Fillinger, S., Patel, H., Alneberg, J., Wilm, A. *et al.* (2020) The nf-core framework for community-curated bioinformatics pipelines. *Nature Biotechnology* **38**(3): 276-278.

ExxonMobil (2014). Oil spill response field manual. USA: ExxonMobil Research and Engineering Company. Available from: https://corporate.exxonmobil.com/-/media/Global/Files/risk-management-and-safety/Oil-Spill-Response-Field-Manual_2014.pdf [Accessed July 19, 2020].

Fasca, H., de Castilho, L.V., de Castilho, J.F.M., Pasqualino, I.P., Alvarez, V.M., de Azevedo Jurelevicius, D., and Seldin, L. (2018) Response of marine bacteria to oil contamination and to high pressure and low temperature deep sea conditions. *MicrobiologyOpen* **7**(2): e00550.

Gertler, C., Näther, D.J., Cappello, S., Gerdts, G., Quilliam, R.S., Yakimov, M.M., and Golyshin, P.N. (2012) Composition and dynamics of biostimulated indigenous oil-degrading microbial consortia from the Irish, North and Mediterranean seas: A mesocosm study. *FEMS Microbiol Ecol* **81**(3): 520-536.

Grote, M., van Bernem, C., Böhme, B., Callies, U., Calvez, I., Christie, B. *et al.* (2018) The potential for dispersant use as a maritime oil spill response measure in German waters. *Mar Pollut Bull* **129**(2): 623-632.

Gutierrez, T., Nichols, P.D., Whitman, W.B., and Aitken, M.D. (2012) *Porticoccus hydrocarbonoclasticus* sp. nov., an aromatic hydrocarbon-degrading bacterium identified in laboratory cultures of marine phytoplankton. *Appl Environ Microbiol* **78**(3): 628-637.

Gutierrez, T., Rhodes, G., Mishamandani, S., Berry, D., Whitman, W.B., Nichols, P.D. *et al.* (2014) Polycyclic aromatic hydrocarbon degradation of phytoplankton-associated *Arenibacter* spp. and description of *Arenibacter algicola* sp. nov., an aromatic hydrocarbon-degrading bacterium. *Appl Environ Microbiol* **80**(2): 618-628.

Gutierrez, T. (2019) Occurrence and roles of the obligate hydrocarbonoclastic bacteria in the ocean when there is no obvious hydrocarbon contamination. In *Taxonomy, genomics and ecophysiology of hydrocarbon-degrading microbes*. McGenity, T.J. (ed), pp. 337-352.

Hackbusch, S., Noirungsee, N., Viamonte, J., Sun, X., Bubenheim, P., Kostka, J.E. *et al.* (2020) Influence of pressure and dispersant on oil biodegradation by a newly isolated *Rhodococcus* strain from deep-sea sediments of the Gulf of Mexico. *Mar Pollut Bull* **150**: 110683.

Hamdan, L.J., and Fulmer, P.A. (2011) Effects of Corexit EC9500A on bacteria from a beach oiled by the Deepwater Horizon spill. *Aquat Microb Ecol* **63**(2): 101-109.

Harwati, T.U., Kasai, Y., Kodama, Y., Susilaningsih, D., and Watanabe, K. (2009) *Tropicibacter naphthalenivorans* gen. nov., sp. nov., a polycyclic aromatic hydrocarbon-degrading bacterium isolated from Semarang Port in Indonesia. *Int J Syst Evol Microbiol* **59**(2): 392-396.

Head, I.M., Jones, D.M., and Röling, W.F. (2006) Marine microorganisms make a meal of oil. *Nat Rev Microbiol* **4**(3): 173-182.

Hoefs, M.J., Van Heemst, J.D., Gelin, F., Koopmans, M.P., Van Kaam-Peters, H.M., Schouten, S. *et al.* (1995) Alternative biological sources for 1,2,3,4-tetramethylbenzene in flash pyrolysates of kerogen. *Organic Geochemistry* **23**(10): 975-979.

Joye, S.B., Kleindienst, S., Gilbert, J.A., Handley, K.M., Weisenhorn, P., Overholt, W.A., and Kostka, J.E. (2016) Responses of microbial communities to hydrocarbon exposures. *Oceanography* **29**(3): 136-149.

Kasai, Y., Kishira, H., and Harayama, S. (2002) Bacteria belonging to the genus *Cycloclasticus* play a primary role in the degradation of aromatic hydrocarbons released in a marine environment. *Appl Environ Microbiol* **68**(11): 5625-5633.

Kleindienst, S., Seidel, M., Ziervogel, K., Grim, S., Loftis, K., Harrison, S. *et al.* (2015) Chemical dispersants can suppress the activity of natural oil-degrading microorganisms. *Proc Natl Acad Sci USA* **112**(48): 14900-14905.

Kleindienst, S., Grim, S., Sogin, M., Bracco, A., Crespo-Medina, M., and Joye, S.B. (2016) Diverse, rare microbial taxa responded to the Deepwater Horizon deep-sea hydrocarbon plume. *ISME J* **10**(2): 400-415.

Knapik, K., Bagi, A., Krolicka, A., and Baussant, T. (2019) Discovery of functional gene markers of bacteria for monitoring hydrocarbon pollution in the marine environment: A metatranscriptomics approach. *bioRxiv*: 857391.

Knapik, K., Bagi, A., Krolicka, A., and Baussant, T. (2020) Metatranscriptomic analysis of oil-exposed seawater bacterial communities archived by an environmental sample processor (ESP). *Microorganisms* **8**(5): 744.

Mas-Lladó, M., Piña-Villalonga, J.M., Brunet-Galmés, I., Nogales, B., and Bosch, R. (2014) Draft genome sequences of two isolates of the Roseobacter group, *Sulfitobacter* sp. strains 3SOLIMAR09 and 1FIGIMAR09, from harbors of Mallorca Island (Mediterranean sea). *Genome Announcements* **2**(3).

Mason, O.U., Han, J., Woyke, T., and Jansson, J.K. (2014) Single-cell genomics reveals features of a *Colwellia* species that was dominant during the Deepwater Horizon oil spill. *Front Microbiol* **5**: 332.

McFarlin, K.M., Prince, R.C., Perkins, R., and Leigh, M.B. (2014) Biodegradation of dispersed oil in arctic seawater at -1°C. *PloS One* **9**(1): e84297.

McFarlin, K.M. (2017) The biodegradation of oil and the dispersant Corexit 9500 in Arctic seawater. *Thesis*, PhD in Biological Sciences. University of Alaska Fairbanks, Department of Biology and Wildlife; Fairbanks, Alaska, USA.

McFarlin, K.M., Perkins, M.J., Field, J.A., and Leigh, M.B. (2018) Biodegradation of crude oil and Corexit 9500 in Arctic seawater. *Front Microbiol* **9**: 1788.

McGowan, C.J., Kwok, R.K., Engel, L.S., Stenzel, M.R., Stewart, P.A., and Sandler, D.P. (2017) Respiratory, dermal, and eye irritation symptoms associated with Corexit EC9527A/EC9500A following the Deepwater Horizon oil spill: Findings from the GuLF STUDY. *Environ Health Perspect* **125**(9): 097015.

McNutt, M.K., Camilli, R., Crone, T.J., Guthrie, G.D., Hsieh, P.A., Ryerson, T.B. *et al.* (2012) Review of flow rate estimates of the Deepwater Horizon oil spill. *Proc Natl Acad Sci USA* **109**(50): 20260-20267.

Methé, B.A., Nelson, K.E., Deming, J.W., Momen, B., Melamud, E., Zhang, X. *et al.* (2005) The psychrophilic lifestyle as revealed by the genome sequence of *Colwellia psychrerythraea* 34h through genomic and proteomic analyses. *Proc Natl Acad Sci USA* **102**(31): 10913-10918.

Militon, C., Jezequel, R., Gilbert, F., Corsellis, Y., Sylvi, L., Cravo-Laureau, C. *et al.* (2015) Dynamics of bacterial assemblages and removal of polycyclic aromatic hydrocarbons in oil-contaminated coastal marine sediments subjected to contrasted oxygen regimes. *Environ Sci Pollut Res* **22**(20): 15260-15272.

Nagashima, H., Zulkharnain, A.B., Maeda, R., Fuse, H., Iwata, K., and Omori, T. (2010) Cloning and nucleotide sequences of carbazole degradation genes from marine bacterium *Neptuniibacter* sp. strain CAR-SF. *Curr Microbiol* **61**(1): 50-56.

Naysim, L., Kang, H.J., and Jeon, C.O. (2014) *Zhongshania aliphaticivorans* sp. nov., an aliphatic hydrocarbon-degrading bacterium isolated from marine sediment, and transfer of *Spongiibacter borealis* Jang *et al.* 2011 to the genus *Zhongshania* as *Zhongshania borealis* comb. nov. *Int J Syst Evol Microbiol* **64**(11): 3768-3774.

Nedashkovskaya, O.I., Kukhlevskiy, A.D., Zhukova, N.V., and Kim, S.B. (2016) *Amylibacter ulvae* sp. nov., a new alphaproteobacterium isolated from the pacific green alga *Ulva fenestrata*. *Arch Microbiol* **198**(3): 251-256.

Nie, Y., Chi, C.-Q., Fang, H., Liang, J.-L., Lu, S.-L., Lai, G.-L. *et al.* (2014) Diverse alkane hydroxylase genes in microorganisms and environments. *Sci Rep* **4**: 4968.

Oh, J.-S., and Roh, D.-H. (2018) Draft genome sequence of *Zhongshania marina* DSW25-10 T isolated from seawater. *The Microbiological Society of Korea* **54**(4): 480-482.

Overholt, W.A., Marks, K.P., Romero, I.C., Hollander, D.J., Snell, T.W., and Kostka, J.E. (2016) Hydrocarbon-degrading bacteria exhibit a species-specific response to dispersed oil while moderating ecotoxicity. *Appl Environ Microbiol* **82**(2): 518-527.

Passow, U. (2016) Formation of rapidly-sinking, oil-associated marine snow. *Deep Sea Res Part II Top Stud Oceanogr* **129**: 232-240.

Passow, U., and Ziervogel, K. (2016) Marine snow sedimented oil released during the Deepwater Horizon spill. *Oceanography* **29**(3): 118-125.

Peterson, C.H., Rice, S.D., Short, J.W., Esler, D., Bodkin, J.L., Ballachey, B.E., and Irons, D.B. (2003) Long-term ecosystem response to the *Exxon Valdez* oil spill. *Science* **302**(5653): 2082-2086.

Prince, R., Kelley, B., and Butler, J. (2016) Three widely-available dispersants substantially increase the biodegradation of otherwise undispersed oil. *J Marine Sci Res Dev* **6**(183).

R Core Team (2019). R: A language and environment for statistical computing. Vienna, Austria.

Rahsepar, S., Smit, M.P., Murk, A.J., Rijnaarts, H.H., and Langenhoff, A.A. (2016) Chemical dispersants: Oil biodegradation friend or foe? *Mar Pollut Bull* **108**(1): 113-119.

Redmond, M.C., and Valentine, D.L. (2012) Natural gas and temperature structured a microbial community response to the Deepwater Horizon oil spill. *Proc Natl Acad Sci USA* **109**(50): 20292-20297.

Ribicic, D., Netzer, R., Hazen, T.C., Techtmann, S.M., Drabløs, F., and Brakstad, O.G. (2018) Microbial community and metagenome dynamics during biodegradation of dispersed oil reveals potential key-players in cold Norwegian seawater. *Mar Pollut Bull* **129**(1): 370-378.

Rivers, A.R., Sharma, S., Tringe, S.G., Martin, J., Joye, S.B., and Moran, M.A. (2013) Transcriptional response of bathypelagic marine bacterioplankton to the Deepwater Horizon oil spill. *ISME J* **7**(12): 2315-2329.

Rubin-Blum, M., Antony, C.P., Borowski, C., Sayavedra, L., Pape, T., Sahling, H. *et al.* (2017) Short-chain alkanes fuel mussel and sponge *Cycloclasticus* symbionts from deep-sea gas and oil seeps. *Nat Microbiol* **2**(8): 17093.

Salerno, J.L., Little, B., Lee, J., and Hamdan, L.J. (2018) Exposure to crude oil and chemical dispersant may impact marine microbial biofilm composition and steel corrosion. *Front Mar Sci* **5**: 196.

Severin, T., Bacosa, H., Sato, A., and Erdner, D. (2016) Dynamics of *Heterocapsa* sp. and the associated attached and free-living bacteria under the influence of dispersed and undispersed crude oil. *Letters in applied microbiology* **63**(6): 419-425.

Short, J.W. (2017) Advances in understanding the fate and effects of oil from accidental spills in the United States beginning with the *Exxon Valdez*. *Arch Environ Contam Toxicol* **73**(1): 5-11.

Sieradzki, E.T., Morando, M., and Fuhrman, J.A. (2019) Metagenomics and stable isotope probing offer insights into metabolism of polycyclic aromatic hydrocarbons degraders in chronically polluted seawater. *bioRxiv*: 777730.

Steinle, L., Schmidt, M., Bryant, L., Haeckel, M., Linke, P., Sommer, S. *et al.* (2016) Linked sediment and water-column methanotrophy at a man-made gas blowout in the North Sea: Implications for methane budgeting in seasonally stratified shallow seas. *Limnol Oceanogr* **61**(S1): S367-S386.

Straub, D., Blackwell, N., Fuentes, A.L., Peltzer, A., Nahnsen, S., and Kleindienst, S. (2019) Interpretations of microbial community studies are biased by the selected 16s rRNA gene amplicon sequencing pipeline. *bioRxiv*: 2019.2012.2017.880468.

Suja, L.D., Summers, S., and Gutierrez, T. (2017) Role of EPS, dispersant and nutrients on the microbial response and MOS formation in the subarctic northeast atlantic. *Front Microbiol* **8**: 676.

Sun, H., Gao, W., Fan, H., Wang, H., and Wei, D. (2015) Cloning, purification and evaluation of the enzymatic properties of a novel arylacetonitrilase from *Luminiphilus syltensis* NOR5-1B: A potential biocatalyst for the synthesis of mandelic acid and its derivatives. *Biotechnology Letters* **37**(8): 1655-1661.

Sun, X., and Kostka, J.E. (2019) Hydrocarbon-degrading microbial communities are site specific, and their activity is limited by synergies in temperature and nutrient availability in surface ocean waters. *Appl Environ Microbiol* **85**(15): e00443-00419.

Suzuki, T., Yazawa, T., Morishita, N., Maruyama, A., and Fuse, H. (2019) Genetic and physiological characteristics of a novel marine propylene-assimilating *Halieaceae* bacterium isolated from seawater and the diversity of its alkene and epoxide metabolism genes. *Microbes and Environments*: ME18053.

Techtmann, S.M., Zhuang, M., Campo, P., Holder, E., Elk, M., Hazen, T.C. *et al.* (2017) Corexit 9500 enhances oil biodegradation and changes active bacterial community structure of oil-enriched microcosms. *Appl Environ Microbiol* **83**(10): e03462-03416.

Teeling, H., Fuchs, B.M., Becher, D., Klockow, C., Gardebrecht, A., Bennke, C.M. *et al.* (2012) Substrate-controlled succession of marine bacterioplankton populations induced by a phytoplankton bloom. *Science* **336**(6081): 608-611.

Tremblay, J., Fortin, N., Elias, M., Wasserscheid, J., King, T.L., Lee, K., and Greer, C.W. (2019) Metagenomic and metatranscriptomic responses of natural oil degrading bacteria in the presence of dispersants. *Environ Microbiol* **21**(7): 2307-2319.

US Nat. Comm. DWH (2011). The use of surface and subsea dispersants during the BP Deepwater Horizon oil spill. Working Paper. Washington, DC, USA: National Commission on the BP Deepwater Horizon Oil Spill and Offshore Drilling. Available from: http://purl.fdlp.gov/GPO/gpo184 [Accessed April 20, 2019].

Valencia-Agami, S.S., Cerqueda-García, D., Putzeys, S., Uribe-Flores, M.M., García-Cruz, N.U., Pech, D. *et al.* (2019) Changes in the bacterioplankton community structure from southern Gulf of Mexico during a simulated crude oil spill at mesocosm scale. *Microorganisms* **7**(10): 441.

Wickham, H. (2016) Ggplot2: Elegant graphics for data analysis. New York, USA: Springer.

Wiltshire, K.H., Kraberg, A., Bartsch, I., Boersma, M., Franke, H.-D., Freund, J. *et al.* (2010) Helgoland Roads, North Sea: 45 years of change. *Estuaries and Coasts* **33**(2): 295-310.

Word, J.Q., Clark, J.R., and Word, L.S. (2014) Comparison of the acute toxicity of Corexit 9500 and household cleaning products. *Hum Ecol Risk Assess* **21**(3): 707-725.

Yakimov, M.M., Giuliano, L., Gentile, G., Crisafi, E., Chernikova, T.N., Abraham, W.-R. *et al.* (2003) *Oleispira antarctica* gen. nov., sp. nov., a novel hydrocarbonoclastic marine bacterium isolated from Antarctic coastal sea water. *Int J Syst Evol Microbiol* **53**(3): 779-785.

Yakimov, M.M., Timmis, K.N., and Golyshin, P.N. (2007) Obligate oil-degrading marine bacteria. *Curr Opin Biotechnol* **18**(3): 257-266.

Yang, T., Nigro, L.M., Gutierrez, T., Joye, S.B., Highsmith, R., and Teske, A. (2016) Pulsed blooms and persistent oil-degrading bacterial populations in the water column during and after the Deepwater Horizon blowout. *Deep Sea Res Part II Top Stud Oceanogr* **129**: 282-291.

Zakharenko, A.S., Galachyants, Y.P., Morozov, I.V., Shubenkova, O.V., Morozov, A.A., Ivanov, V.G. *et al.* (2019) Bacterial communities in areas of oil and methane seeps in pelagic of Lake Baikal. *Microb Ecol* **78**(2): 269-285.

Chapter 4 – Personal contribution

The experiments were conceptualised by myself and Jun.-Prof. Sara Kleindienst. The strain *Marinobacter* sp. TT1 was isolated and provided by Prof. Tony Gutierrez. Starved-culture experiments including cell counts and *n*-hexadecane quantifications were performed by myself and Anjela Vogel. Well-fed culture experiments including cell counts and *n*-hexadecane quantifications were performed by myself. Data visualization and statistical analysis were performed by myself. Data were interpreted and discussed by myself together with Jun.-Prof. Sara Kleindienst, Prof. Tony Gutierrez, and Prof. Samantha B. Joye. The manuscript was written by myself under the supervision of Jun.-Prof. Sara Kleindienst and revised by all co-authors.

4 Starvation-dependent inhibition of the hydrocarbon degrader *Marinobacter* sp. TT1 by a chemical dispersant

Saskia Rughöft[1], Anjela Vogel[1], Samantha B. Joye[2], Tony Gutierrez[3], Sara Kleindienst[1]

[1] Microbial Ecology, Center for Applied Geosciences, University of Tübingen, Germany
[2] Department of Marine Sciences, University of Georgia, Athens GA, USA 30602-3636
[3] Institute of Mechanical, Process and Energy Engineering, School of Engineering and Physical Sciences, Heriot-Watt University, Edinburgh, EH14 4AS, United Kingdom

Slightly modified version published in ***Journal of Marine Science and Engineering***

Rughöft, S., Vogel, A.L., Joye, S.B., Gutierrez, T., Kleindienst, S. (2020) Starvation-Dependent Inhibition of the Hydrocarbon Degrader *Marinobacter* sp. TT1 by a Chemical Dispersant. *J Mar Sci Eng* **8**(11): 925. https://doi.org/10.3390/jmse8110925

4.1 Abstract

During marine oil spills, chemical dispersants are used routinely to disperse surface slicks, transferring the hydrocarbon constituents of oil into the aqueous phase. Still, a comprehensive understanding of how dispersants affect natural populations of hydrocarbon-degrading bacteria, particularly under environmentally relevant conditions, is lacking. We investigated the impacts of the dispersant Corexit EC9500A on the marine hydrocarbon degrader *Marinobacter* sp. TT1 when pre-adapted to either low *n*-hexadecane concentrations (starved culture) or high *n*-hexadecane concentrations (well-fed culture). The growth of previously starved cells was inhibited when exposed to the dispersant, as evidenced by 55% lower cell numbers and 30% lower *n*-hexadecane biodegradation efficiency compared to cells grown on *n*-hexadecane alone. Cultures that were well-fed did not exhibit dispersant-induced inhibition of growth or *n*-hexadecane degradation. In addition, fluorescence microscopy revealed an amorphous cell aggregate structure when the starved culture was exposed to dispersants, suggesting that starved cells altered their growing behaviour and possibly modified their production of extracellular polymeric substances. Our findings indicate that substrate limitation, resembling oligotrophic open ocean conditions, can impact the response and hydrocarbon-degrading activities of oil-degrading organisms when exposed to Corexit, and highlight the need for further work to better understand the implications of environmental stressors on oil biodegradation and microbial community dynamics.

4.2 Introduction

During major marine oil spills, chemical dispersants are applied routinely with the aim of breaking up surface slicks and dispersing the oil into the water column. Following the Deepwater Horizon blowout in the Gulf of Mexico on April 20th of 2010, seven million liters of dispersant (Corexit EC9500A and EC9527A) were applied in response to the discharge of an estimated 800 million liters of crude oil into the Gulf ecosystem (US Nat. Comm. DWH, 2011; McNutt *et al.*, 2012). The impacts of the oil spill on the Gulf's ecosystem and the health of its human inhabitants are well documented (DWH NRDA Trustees, 2016; McGowan *et al.*, 2017). However, the impact of chemical dispersant application on native microbial oil-degrading populations is still unclear and conflicting reports have led to disputes over best practices (US NASEM, 2020).

Some studies have documented enhanced hydrocarbon (HC) degradation in the presence of dispersants (Bælum *et al.*, 2012; Prince *et al.*, 2016; Tremblay *et al.*, 2017), while others have suggested toxic or inhibitive effects on microbial oil degradation (Hamdan and Fulmer, 2011; Kleindienst *et al.*, 2015b; Rahsepar *et al.*, 2016; Hackbusch *et al.*, 2020). A number of different explanations for these contradictory findings have been proposed, ranging from methodological issues (e.g. dispersant concentrations, types and weathering status of crude oil or HCs used) to microbiological and ecological considerations (e.g. species-/strain-specific dispersant responses and the relevance of the native microbial community composition) (Overholt *et al.*, 2016; Prince *et al.*, 2016; Rahsepar *et al.*, 2016; Techtmann *et al.*, 2017; Doyle *et al.*, 2018).

To our knowledge, however, the pre-spill conditions that HC-degrading microorganisms face in oligotrophic (i.e. nutrient-/substrate-limited) ocean waters have not been considered as a factor that can predict their physiological response to oil and chemical dispersant exposure. Most published studies have used either laboratory cultures of HC-degrading bacteria supplemented with high substrate and nutrient concentrations, or natural seawater communities in microcosm experiments generously supplemented with nutrients (Prince *et al.*, 2016; Tremblay *et al.*, 2017). At the same time, substrate and nutrient limitations have been shown to affect hydrophobicity, production of extracellular polymeric substances, and biodegradation potential of HC-degrading isolates (Leung *et al.*, 2005; Khleifat, 2007; Santisi *et al.*, 2015; Putthividhya *et al.*, 2016). Only few studies have previously investigated the impact of dispersant exposure in combination with different nutrient concentrations on oil biodegradation, and these studies produced conflicting results (Foght and Westlake, 1982; Lindstrom and Braddock, 2002; Kleindienst *et al.*, 2015b). The effects of dispersants on substrate-limited HC degraders remain largely unexplored.

In this study, the marine hydrocarbon-degrading strain *Marinobacter* sp. TT1 (isolated during the Deepwater Horizon spill (Gutierrez *et al.*, 2013b)) was grown on *n*-hexadecane under either substrate starvation or typical well-fed laboratory conditions before the experiment, the former resembling *in situ* conditions of the open ocean. The genus *Marinobacter* includes several ubiquitous HC-degrading species that respond positively to marine oil spills (Duran, 2010; Mounier *et al.*, 2014; Kleindienst *et al.*, 2015b; Tremblay *et al.*, 2017). Furthermore, some *Marinobacter* spp. have been reported to be inhibited by chemical dispersant exposure (Hamdan and Fulmer, 2011; Kleindienst *et al.*, 2015b; Techtmann *et al.*, 2017; Tremblay *et al.*, 2017). The aim of this study was to investigate the impact of chemical dispersant exposure on

the growth and *n*-hexadecane biodegradation activity of *Marinobacter* sp. TT1 cultures pre-adapted to low or high HC substrate concentrations.

4.3 Experimental procedures

4.3.1 Bacterial strain and pre-adaptation of cultures

The strain *Marinobacter* sp. TT1 was isolated from a deep-sea plume water sample collected during the active phase of the Deepwater Horizon oil spill using *n*-hexadecane for enrichment (Gutierrez *et al.*, 2013b). In this study, *Marinobacter* sp. TT1 was cultivated in ONR7a minimal medium (Dyksterhouse *et al.*, 1995) supplemented with different carbon substrates and grown (dark, 20°C, 120 rpm on shaker) in half-filled 20 ml glass headspace vials (pre-baked at 300°C for 8 h) with PTFE-lined crimp lids. For inoculation, 200 µl of the respective pre-cultures were transferred.

The well-fed pre-culture was revived from a previously well-fed glycerol stock (*Marinobacter* sp. TT1 in complex medium), transferred into liquid ONR7a minimal medium and subsequently supplied with 100 mg l^{-1} *n*-hexadecane weekly, providing an almost constant substrate supply. The starved pre-culture was revived from a previously starved glycerol stock (substrate-starved *Marinobacter* sp. TT1 in minimal medium), transferred into liquid ONR7a medium and subsequently supplied with 50 mg l^{-1} *n*-hexadecane once every three weeks. Thus, the starved pre-culture was adapted to survive periods with no substrate availability, mimicking the conditions of oligotrophic open ocean waters. Both pre-cultures were then transferred with 100 mg l^{-1} *n*-hexadecane once (three days before the start of the experiment), mimicking a large hydrocarbon pulse similar to an oil spill scenario. All pre-cultures were originally stemming from the same original culture and before the start of the experiment, both *Marinobacter* sp. TT1 pre-cultures were confirmed to be the same strain by sequencing of the 16S rRNA gene fragment (100% identity) that was amplified using primer pairs 341f/907r (Muyzer *et al.*, 1993).

4.3.2 Experimental setup

All experimental pre-cultures were grown on *n*-hexadecane without prior exposure to Corexit EC9500A (see above). At the start of the respective experiments, the following five culture conditions were set up for both the starved and the well-fed pre-culture: i.) no added carbon substrate (Control), ii.) 100 mg l^{-1} *n*-hexadecane, iii.) 100 mg l^{-1} *n*-hexadecane and 10 mg l^{-1} Corexit, or iv.) 100 mg l^{-1} Corexit. All treatments were run in triplicate and sampled sacrificially after 0, 2 and 5 days, except for setups (i) and (iv) which were only sampled at the start and end of the experiment. Due to concerns about gas phase losses during sampling, separate triplicates were used for setups (ii) and (iii) to obtain samples for cell counts and hydrocarbon quantification analysis. Additionally, abiotic control setups for hydrocarbon quantification were prepared, containing no inoculum and either v.) 100 mg l^{-1} *n*-hexadecane or vi.) 100 mg l^{-1} *n*-hexadecane and 10 mg l^{-1} Corexit.

4.3.3 Cell counts

For cell counts, samples were fixed with 1% paraformaldehyde and stored at 4°C until further processing. To reduce cell aggregate formation that would preclude accurate cell count measurements, 1% (w/v) EDTA was added to the samples before sonication (20% intensity,

30 seconds; Sonoplus ultrasonic homogeniser, Bandelin electronic GmbH & Co. KG, Berlin, Germany), a procedure that was optimized for this culture. Samples were then filtered onto Isopore polycarbonate membrane filters (GTTP, 0.2 µm; Millipore) and stained with 4′,6-diamidino-2-phenylindole (DAPI; 1 µg ml^{-1}) for 10 min, washed with ddH_2O for 5 min, rinsed in ethanol (80%), and then air dried in the dark at room temperature. Membrane filters were embedded using a 1:4 mixture of Vectashield mounting medium (Vector Laboratories, Burlingame, California) and Citifluor AF2 glycerol solution (EMS Acquisition Corp., Hatfield, Pennsylvania) before the slides were analyzed using fluorescence microscopy (Leica DM 5500 B; Leica Microsystems, Wetzlar, Germany). Images were taken at a magnification of 1000x with a Leica DFC 360 FX camera using the Leica Application Suite Advanced Fluorescence software (2.6.0.766). Cell counts of the images were performed using the 'Find Maxima' function (noise tolerance = 7) of the Fiji distribution of ImageJ (Schindelin *et al.*, 2012), counting a minimum of 20 images and 600 cells per sample.

4.3.4 Hydrocarbon quantification

For *n*-hexadecane quantification, deuterated *n*-hexadecane (D34, Sigma-Aldrich, St. Louis, USA) was added to the samples as internal standard (20 mg l^{-1}) before extracting the entire vial using 9 ml cyclohexane (purity 99.9 %, Carl ROTH, Karlsruhe, Germany). Vials were shaken at 300 rpm for half an hour, the phases were allowed to separate overnight (20°C) and then subsamples of the cyclohexane were used to quantify the residual *n*-hexadecane via gas chromatography (Agilent 6890N GC; Agilent Technologies, Santa Clara, California) coupled with mass spectrometry (Agilent 5973 MS). For separation, a J+W Scientific DB-5MS (30 m length, 0.25 mm ID, 0.25 µm film thickness) capillary column was used. The device was operated in a pulsed splitless mode with a Helium flow of 0.8 ml/min. Oven temperature was initiated at 65°C (4 min), then ramped at 10°C/min to 220°C, further ramped at 20°C/min to 310°C and held at this temperature for 5 min.

4.3.5 Data analysis

To test whether differences in cell numbers or *n*-hexadecane concentrations between the cultures grown with and without Corexit at the same time points were statistically significant, ANOVA followed by Tukey *post-hoc* test ($p < 0.05$) for multiple comparisons was used. Beforehand, it had been tested if residuals were normally distributed (tested with Shapiro-Wilks test, $p > 0.05$) and variances were homogenous (tested with Levene test, $p > 0.05$). The R programming language (R Core Team, 2019) was used to perform all described tests and produce all presented figures.

4.4 Results and Discussion

4.4.1 Rapid response by starved *Marinobacter* sp. TT1 to a high hydrocarbon pulse

Starved *Marinobacter* sp. TT1 achieved 58% higher cell numbers compared to the well-fed culture (4.95×10^8 vs. 2.85×10^8 cells ml^{-1}, respectively; Fig. 4.1) and degraded about 30% more of the *n*-hexadecane after five days (0.89 vs. 33.87 mg *n*-hexadecane l^{-1} remained, respectively). This more robust response of starved cells to a hydrocarbon pulse aligns with previous observations of rapid feast responses in starved bacteria. Starved aquatic bacteria are known to react immediately by expressing very high uptake rates after receiving a 'shock' substrate pulse (Straškrabová, 1983). Further, a bathypelagic *Marinobacter*, maintained under starvation for 1.6 years, grew rapidly after being pulsed with fresh organic matter (Sebastian *et al.*, 2019). The high relevance of this opportunistic lifestyle for HC-degrading marine bacteria, including *Marinobacter* sp. as a known opportunitroph (Singer *et al.*, 2011), has been discussed previously (Kleindienst *et al.*, 2016b; Sun and Kostka, 2019). Similar substrate-pulse responses have been described for aromatic HC-degrading bacterial strains as well (Leung *et al.*, 2005; Khleifat, 2007).

4.4.2 Only starved *Marinobacter* sp. TT1 was consistently inhibited after Corexit exposure

The growth of starved cultures of *Marinobacter* sp. TT1 was inhibited in the treatment containing both *n*-hexadecane and Corexit compared to the *n*-hexadecane only treatment. With added Corexit, growth of these cells was 55% lower (2.22×10^8 vs. 4.95×10^8 cells ml^{-1}; $p = 0.0103$; Fig. 4.1) and 30% less *n*-hexadecane was biodegraded (33.94 vs. 0.89 mg *n*-hexadecane l^{-1} remained, $p = 0.0224$) after five days. In addition, larger cell aggregates were observed in starved cultures with added Corexit (appr. 0.5-1.5 cm long versus < 1 mm in *n*-hexadecane only treatments; Fig. S4.1) and fluorescence microscopy revealed a changed, amorphous structure of these aggregates lacking defined, visible cell morphologies (Fig. 4.2). Well-fed cultures, in contrast, showed no significant difference in growth or microscopic aggregate structure between *n*-hexadecane treatments with and without Corexit, and a smaller difference between aggregate sizes (ranging between 1-5 mm size; Fig. S4.1). However, significantly less *n*-hexadecane was degraded in the treatment with both *n*-hexadecane and Corexit compared to the *n*-hexadecane treatment after two days (79.56 vs. 40.93 mg *n*-hexadecane l^{-1} remained, $p = 0.0193$); similar residual *n*-hexadecane was noted in both treatments after five days. Interestingly, in the Corexit-only treatments (i.e. in the absence of *n*-hexadecane), growth was observed for both starved and well-fed cultures after five days (from 2.4×10^6 to 3.3×10^7 or 1.5×10^8 cells ml^{-1}, respectively), indicating that *Marinobacter* sp. TT1 can use Corexit components as a growth substrate. No macroscopic cell aggregates were observed. Notably, the well-fed culture reached higher cell numbers under these conditions. This could be explained by a more pronounced inhibition of the starved culture caused by Corexit exposure or by a longer lag phase in the starved culture when adapting to a new substrate. Growth on Corexit compounds has previously been reported for other HC degraders, such as *Colwellia* sp., *Alcanivorax* sp. and *Acinetobacter* sp. (Chakraborty *et al.*, 2012; Overholt *et al.*, 2016).

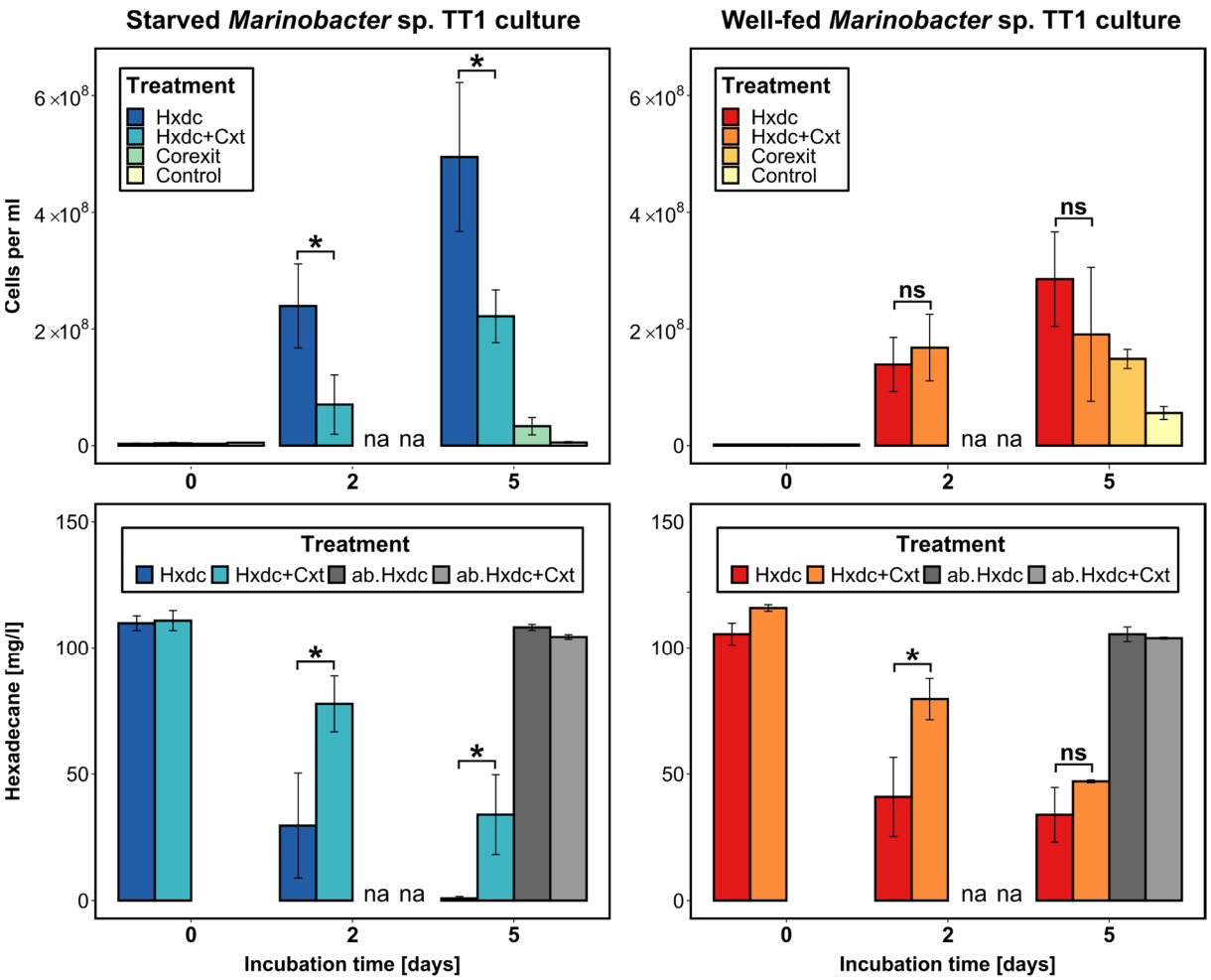

Figure 4.1: Cell numbers [cells ml^{-1}] and residual *n*-hexadecane concentrations [mg l^{-1}] in cultures inoculated with either starved (left) or well-fed (right) *Marinobacter* sp. TT1 during the incubation period of 5 days (means ± SD; n = 3). *n*-Hexadecane was supplied at 100 mg l^{-1} with or without 10 mg l^{-1} of Corexit. Corexit alone was supplied at 100 mg l^{-1}. Abiotic controls were supplied with the same respective concentrations but without inoculum. No carbon source was added to the control treatment. Significance levels are only shown for comparisons of treatments with *n*-hexadecane alone against those with both *n*-hexadecane and Corexit (* $p < 0.05$, ns = not significant). Hxdc = *n*-hexadecane; Cxt = Corexit; ab. = abiotic control; na = not analysed.

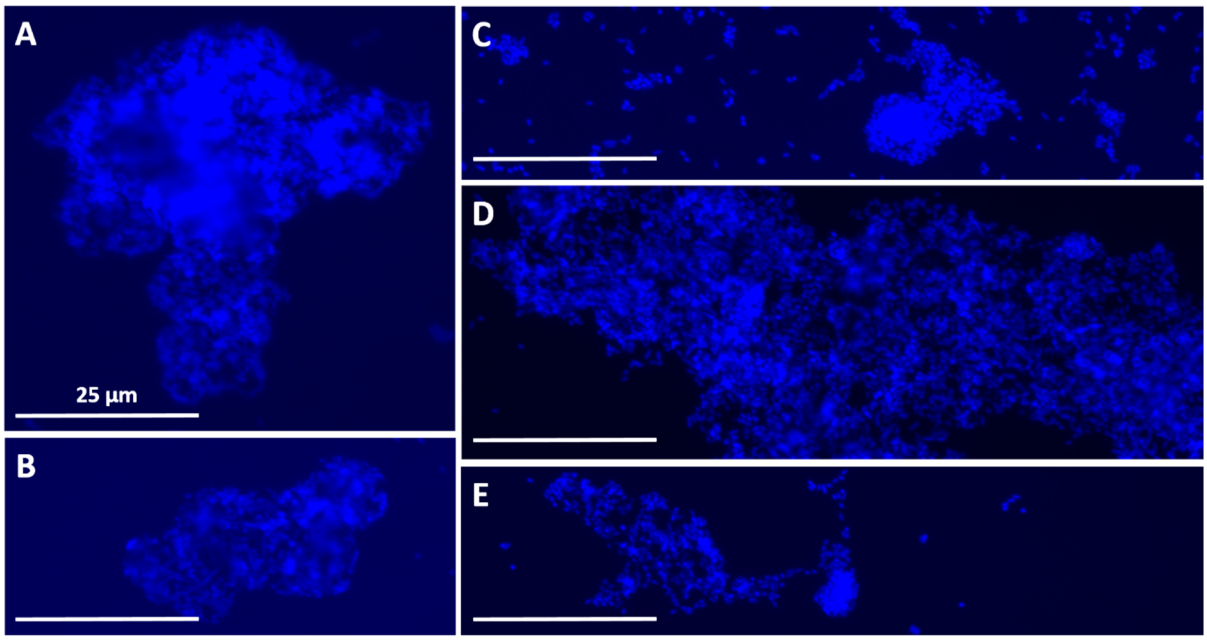

Figure 4.2: Fluorescence microscopy images of aggregates in *Marinobacter* sp. TT1 cultures after five days of incubation. Cells are stained with 4′,6 diamidino-2 phenylindole (DAPI; appears blue). **A/B)** Amorphous aggregates from starved cultures that received 100 mg l^{-1} *n*-hexadecane and 10 mg l^{-1} Corexit. **C)** Aggregates from starved cultures that received only 100 mg l^{-1} *n*-hexadecane. **D/E)** Aggregates from well-fed cultures that received 100 mg l^{-1} *n*-hexadecane (D) or 100 mg l^{-1} *n*-hexadecane and 10 mg l^{-1} Corexit (E).

4.4.3 Potential mechanisms underlying the observed inhibition effects in starved *Marinobacter* sp. TT1

The underlying mechanism(s) of the pronounced response of starved *Marinobacter* sp. TT1 to dispersant exposure still remain to be elucidated. However, a number of recognized starvation effects could trigger the observed inhibition effects. First, changes in cell surface hydrophobicity, cell motility, and production of extracellular polymeric substances occur in response to starvation in marine bacteria (Kjelleberg and Hermansson, 1984; Yam and Tang, 2007; Santisi *et al.*, 2015; Putthividhya *et al.*, 2016) – these cell properties are important for a successful HC-degrading lifestyle (Joye *et al.*, 2018). Based on our observations, a modified production of extracellular polymeric substances induced by dispersant exposure in starved cells might have led to the amorphous cell aggregate structure on the microscopic level. Second, carbon starvation responses can induce membrane modifications, such as the degradation of membrane phospholipids (Fida *et al.*, 2013; Kaberdin *et al.*, 2015; Bergkessel *et al.*, 2016) which could lead to higher membrane sensitivity to dispersant components (e.g. surfactants and solvents) and, in turn, compromise cell physiologies. Membrane modifications could also be another reason for the observed amorphous cell shapes. Additionally, key proteins in alkane metabolism (i.e. AlkB, AupA/B) are associated with the cell membrane (Rojo, 2009; Mounier *et al.*, 2018) and could thus be detrimentally affected in starved cells exposed to chemical dispersants.

The ecological theory of multiple stressors can also explain these results. Organisms are often exposed to multiple stressors at once under *in situ* conditions and the cumulative biological effects of these stressors can be synergistic, i.e. distinct from the additive effects of individual stressors (Folt *et al.*, 1999; Crain *et al.*, 2008). Synergistic effects of dispersants and other

stressors have been described in a few studies. For example, Corexit 9257 inhibited oil biodegradation the most under nutrient limited conditions (Foght and Westlake, 1982). Similarly, phytoplankton was more sensitive to dispersants under nutrient-limited conditions (Ozhan and Bargu, 2014) and the HC degrader *Rhodococcus* sp. PC20 was more inhibited by dispersant exposure under high pressure conditions (Hackbusch *et al.*, 2020). Therefore, (previous) environmental stress – in this case substrate limitation – can lead to different microbial responses to dispersant or dispersant-hydrocarbon exposure, potentially explaining the observed more severe response of starved hydrocarbon degraders to chemical dispersants.

4.4.4 Environmental implications

While some previous studies reported clear inhibition responses of *Marinobacter* when exposed to chemical dispersants (Hamdan and Fulmer, 2011; Kleindienst *et al.*, 2015b), other experiments reported both inhibited and stimulated members of the genus *Marinobacter* (Techtmann *et al.*, 2017; Tremblay *et al.*, 2017; Doyle *et al.*, 2018). Ecotype-specific dispersant responses might explain some of these previous observations (as discussed in e.g. Techtmann *et al.*, 2017), but this study is the first to identify substrate-level adaptation as a factor that affects how marine HC-degrading microorganisms could respond during an oil spill at sea when chemical dispersants are used. Due to the inherent spatial and temporal heterogeneity of substrate and nutrient availability in the marine environment, the observations reported here could have wide reaching environmental implications. Contrary to obligate HC-degrading bacteria, members of *Marinobacter* are known as versatile heterotrophs that can use a wide range of substrates (Duran, 2010; Mounier *et al.*, 2014). Yet, their ubiquity in the marine environment is largely confined to oligotrophic (i.e. nutrient-/substrate-limited) waters which make up at least 18% (estimated oligotrophic gyre area; Polovina *et al.*, 2008; Signorini *et al.*, 2015) of the global ocean. The substrate history of marine HC degraders depends on their lifestyle (e.g. free-living or particle-attached), their niches (e.g. surface or deep waters, polar or tropical latitudes), the dynamics of their environment (e.g. local seasonality, bloom regimes) and the levels of natural and anthropogenic substrate emissions (e.g. chronic or dynamic HC inputs via natural oil seeps, ship traffic or accidental oil releases). Based on the presented findings, all of these factors could play a role in determining the impacts of chemical dispersants on marine HC biodegradation *in situ* and need to be taken into account during the decision-making process of potential dispersant applications.

4.4.5 Conclusions

To our knowledge, this is the first study demonstrating that the pre-adapted state (i.e. substrate history) of marine hydrocarbon-degrading bacteria can have a significant effect on how these organisms will respond in the event of an oil spill where chemical dispersants are used. These observations help to explain previously inconsistent findings about dispersant impacts in the literature and highlight the need for considering *in situ* environmental conditions (e.g. oligotrophic versus copiotrophic substrate/nutrient adaptation) when conducting laboratory experiments where a single change in parameters could propagate and lead to different findings. To better inform future decisions on dispersant use in marine oil spill situations, there is a critical need for additional baseline knowledge of environmental microbial communities, including their nutritional status, and for systematic screenings of cultured representatives

regarding their response to dispersants under environmentally relevant conditions and more insights into how and why dispersants might affect their physiology.

Acknowledgements

This study was funded by the Baden-Württemberg Foundation's Elite Program for Postdocs and by the Deutsche Forschungsgemeinschaft (DFG, German Research Foundation - fellowship grant #326028733). We would also like to thank the U.S. National Oceanic and Atmospheric Administration for providing Corexit EC9500A, Renate Seelig and Peter Grathwohl for GC-MS measurements and Anja Pohl for help with culture maintenance.

4.5 Supplemental information

4.5.1 Supplemental figures

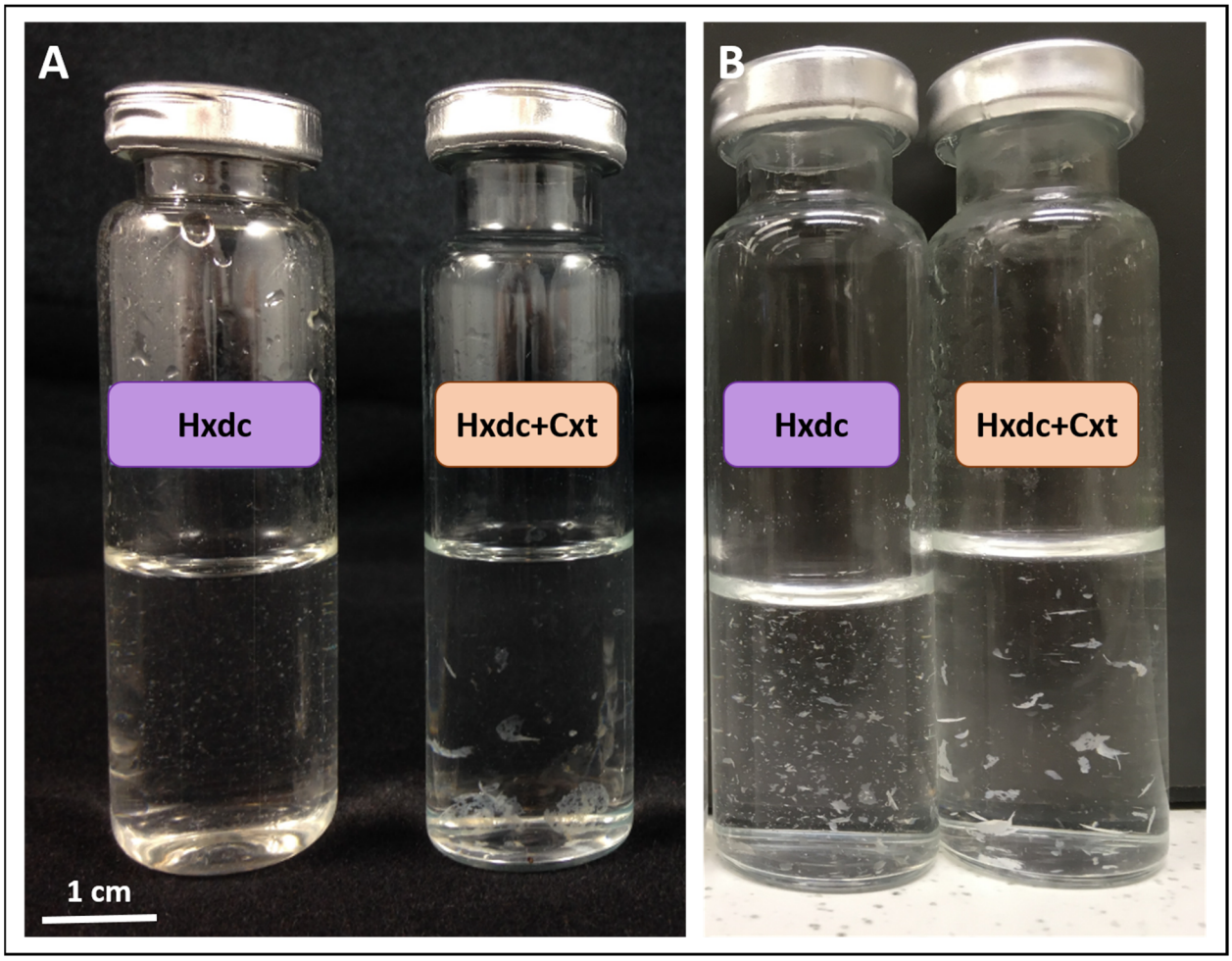

Figure S 4.1: Aggregate morphology in *Marinobacter* sp. TT1 cultures after five days of incubation. Treatments contained the following carbon sources: 100 mg l^{-1} *n*-hexadecane (Hxdc) or 100 mg l^{-1} *n*-hexadecane and 10 mg l^{-1} Corexit (Hxdc+Cxt). **A**) Starved cultures. **B**) Well-fed cultures.

4.6 References

Bælum, J., Borglin, S., Chakraborty, R., Fortney, J.L., Lamendella, R., Mason, O.U. *et al.* (2012) Deep-sea bacteria enriched by oil and dispersant from the Deepwater Horizon spill. *Environ Microbiol* **14**(9): 2405-2416.

Bergkessel, M., Basta, D.W., and Newman, D.K. (2016) The physiology of growth arrest: Uniting molecular and environmental microbiology. *Nat Rev Microbiol* **14**(9): 549-562.

Chakraborty, R., Borglin, S.E., Dubinsky, E.A., Andersen, G.L., and Hazen, T.C. (2012) Microbial response to the MC-252 oil and Corexit 9500 in the Gulf of Mexico. *Front Microbiol* **3**: 357.

Crain, C.M., Kroeker, K., and Halpern, B.S. (2008) Interactive and cumulative effects of multiple human stressors in marine systems. *Ecol Lett* **11**(12): 1304-1315.

Doyle, S.M., Whitaker, E.A., De Pascuale, V., Wade, T.L., Knap, A.H., Santschi, P.H. *et al.* (2018) Rapid formation of microbe-oil aggregates and changes in community composition in coastal surface water following exposure to oil and the dispersant Corexit. *Front Microbiol* **9**: 689.

Duran, R. (2010) *Marinobacter*. *Handbook of Hydrocarbon and Lipid Microbiology*. Timmis, K.N. (ed). Heidelberg, Germany: Springer, pp. 1725-1735. 10.1007/978-3-540-77587-4_122.

DWH NRDA Trustees (2016). Deepwater Horizon oil spill: Final programmatic damage assessment and restoration plan and final programmatic environmental impact statement. Available from: http://www.gulfspillrestoration.noaa.gov/restoration-planning/gulf-plan [Accessed June 16, 2020].

Dyksterhouse, S.E., Gray, J.P., Herwig, R.P., Lara, J.C., and Staley, J.T. (1995) *Cycloclasticus pugetii* gen. nov., sp. nov., an aromatic hydrocarbon-degrading bacterium from marine sediments. *Int J Syst Bacteriol* **45**(1): 116-123.

Fida, T.T., Moreno-Forero, S.K., Heipieper, H.J., and Springael, D. (2013) Physiology and transcriptome of the polycyclic aromatic hydrocarbon-degrading *Sphingomonas* sp. LH128 after long-term starvation. *Microbiology* **159**(Pt 9): 1807-1817.

Foght, J., and Westlake, D. (1982) Effect of the dispersant Corexit 9527 on the microbial degradation of Prudhoe Bay oil. *Can J Microbiol* **28**(1): 117-122.

Folt, C.L., Chen, C.Y., Moore, M.V., and Burnaford, J. (1999) Synergism and antagonism among multiple stressors. *Limnol Oceanogr* **44**: 864-877.

Gutierrez, T., Singleton, D.R., Berry, D., Yang, T., Aitken, M.D., and Teske, A. (2013) Hydrocarbon-degrading bacteria enriched by the Deepwater Horizon oil spill identified by cultivation and DNA-SIP. *ISME J* **7**(11): 2091-2104.

Hackbusch, S., Noirungsee, N., Viamonte, J., Sun, X., Bubenheim, P., Kostka, J.E. *et al.* (2020) Influence of pressure and dispersant on oil biodegradation by a newly isolated *Rhodococcus* strain from deep-sea sediments of the Gulf of Mexico. *Mar Pollut Bull* **150**: 110683.

Hamdan, L.J., and Fulmer, P.A. (2011) Effects of Corexit EC9500A on bacteria from a beach oiled by the Deepwater Horizon spill. *Aquat Microb Ecol* **63**(2): 101-109.

Joye, S., Kleindienst, S., and Pena-Montenegro, T.D. (2018) Snapshot: Microbial hydrocarbon bioremediation. *Cell* **172**(6): 1336-1336 e1331.

Kaberdin, V.R., Montanchez, I., Parada, C., Orruno, M., Arana, I., and Barcina, I. (2015) Unveiling the metabolic pathways associated with the adaptive reduction of cell size during *Vibrio harveyi* persistence in seawater microcosms. *Microb Ecol* **70**(3): 689-700.

Khleifat, K.M. (2007) Effect of substrate adaptation, carbon starvation and cell density on the biodegradation of phenol by *Actinobacillus* sp. *Fresenius Environ Bull* **16**(7): 726-730.

Kjelleberg, S., and Hermansson, M. (1984) Starvation-induced effects on bacterial surface characteristics. *Appl Environ Microbiol* **48**(3): 497-503.

Kleindienst, S., Seidel, M., Ziervogel, K., Grim, S., Loftis, K., Harrison, S. *et al.* (2015) Chemical dispersants can suppress the activity of natural oil-degrading microorganisms. *Proc Natl Acad Sci USA* **112**(48): 14900-14905.

Kleindienst, S., Grim, S., Sogin, M., Bracco, A., Crespo-Medina, M., and Joye, S.B. (2016) Diverse, rare microbial taxa responded to the Deepwater Horizon deep-sea hydrocarbon plume. *ISME J* **10**(2): 400-415.

Leung, K.T., Moore, M., Lee, H., and Trevors, J.T. (2005) Effect of carbon starvation on *p*-nitrophenol degradation by a *Moraxella* strain in buffer and river water. *FEMS Microbiol Ecol* **51**(2): 237-245.

Lindstrom, J.E., and Braddock, J.F. (2002) Biodegradation of petroleum hydrocarbons at low temperature in the presence of the dispersant Corexit 9500. *Mar Pollut Bull* **44**: 739-747.

McGowan, C.J., Kwok, R.K., Engel, L.S., Stenzel, M.R., Stewart, P.A., and Sandler, D.P. (2017) Respiratory, dermal, and eye irritation symptoms associated with Corexit EC9527A/EC9500A following the Deepwater Horizon oil spill: Findings from the GuLF STUDY. *Environ Health Perspect* **125**(9): 097015.

McNutt, M.K., Camilli, R., Crone, T.J., Guthrie, G.D., Hsieh, P.A., Ryerson, T.B. *et al.* (2012) Review of flow rate estimates of the Deepwater Horizon oil spill. *Proc Natl Acad Sci USA* **109**(50): 20260-20267.

Mounier, J., Camus, A., Mitteau, I., Vaysse, P.J., Goulas, P., Grimaud, R., and Sivadon, P. (2014) The marine bacterium *Marinobacter hydrocarbonoclasticus* SP17 degrades a wide range of lipids and hydrocarbons through the formation of oleolytic biofilms with distinct gene expression profiles. *FEMS Microbiolgy Ecology* **90**(3): 816-831.

Mounier, J., Hakil, F., Branchu, P., Naïtali, M., Goulas, P., Sivadon, P., and Grimaud, R. (2018) AupA and AupB are outer and inner membrane proteins involved in alkane uptake in *Marinobacter hydrocarbonoclasticus* SP17. *mBio* **9**(3): e00520-00518.

Muyzer, G., De Waal, E.C., and Uitterlinden, A.G. (1993) Profiling of complex microbial populations by denaturing gradient gel electrophoresis analysis of polymerase chain reaction amplified genes coding for 16s rRNA. *Appl Environ Microbiol* **59**(3): 695-700.

Overholt, W.A., Marks, K.P., Romero, I.C., Hollander, D.J., Snell, T.W., and Kostka, J.E. (2016) Hydrocarbon-degrading bacteria exhibit a species-specific response to dispersed oil while moderating ecotoxicity. *Appl Environ Microbiol* **82**(2): 518-527.

Ozhan, K., and Bargu, S. (2014) Distinct responses of Gulf of Mexico phytoplankton communities to crude oil and the dispersant Corexit EC9500A under different nutrient regimes. *Ecotoxicology* **23**(3): 370-384.

Polovina, J.J., Howell, E.A., and Abecassis, M. (2008) Ocean's least productive waters are expanding. *Geophys Res Lett* **35**(3): L03618.

Prince, R., Kelley, B., and Butler, J. (2016) Three widely-available dispersants substantially increase the biodegradation of otherwise undispersed oil. *J Marine Sci Res Dev* **6**(183).

Putthividhya, A., Kukor, J.J., and Abriola, L.M. (2016) The effects of substrate exposure history and carbon starvation-induced stress on the EPS synthesis of TCE degrading toluene oxidizing soil bacteria. *Environ Earth Sci* **75**(9).

R Core Team (2019). R: A language and environment for statistical computing. Vienna, Austria.

Rahsepar, S., Smit, M.P., Murk, A.J., Rijnaarts, H.H., and Langenhoff, A.A. (2016) Chemical dispersants: Oil biodegradation friend or foe? *Mar Pollut Bull* **108**(1): 113-119.

Rojo, F. (2009) Degradation of alkanes by bacteria. *Environ Microbiol* **11**(10): 2477-2490.

Santisi, S., Genovese, M., Crisafi, F., Gentile, G., Volta, A., Bonsignore, M., and Cappello, S. (2015) Effects of growth conditions on hydrophobicity in marine obligate hydrocarbonoclastic bacteria. *Intern J Microbiol Appl* **2**(2): 50-55.

Schindelin, J., Arganda-Carreras, I., Frise, E., Kaynig, V., Longair, M., Pietzsch, T. *et al.* (2012) Fiji: An open-source platform for biological image analysis. *Nat Methods* **9**(7): 676–682.

Sebastian, M., Estrany, M., Ruiz-Gonzalez, C., Forn, I., Sala, M.M., Gasol, J.M., and Marrase, C. (2019) High growth potential of long-term starved deep ocean opportunistic heterotrophic bacteria. *Front Microbiol* **10**: 760.

Signorini, S.R., Franz, B.A., and McClain, C.R. (2015) Chlorophyll variability in the oligotrophic gyres: Mechanisms, seasonality and trends. *Front Mar Sci* **2**: 1-11.

Singer, E., Webb, E.A., Nelson, W.C., Heidelberg, J.F., Ivanova, N., Pati, A., and Edwards, K.J. (2011) Genomic potential of *Marinobacter aquaeolei*, a biogeochemical "opportunitroph". *Appl Environ Microbiol* **77**(8): 2763-2771.

Straškrabová, V. (1983) The effect of substrate shock on populations of starving aquatic bacteria. *J Appl Bacteriol* **54**: 217-224.

Sun, X., and Kostka, J.E. (2019) Hydrocarbon-degrading microbial communities are site specific, and their activity is limited by synergies in temperature and nutrient availability in surface ocean waters. *Appl Environ Microbiol* **85**(15): e00443-00419.

Techtmann, S.M., Zhuang, M., Campo, P., Holder, E., Elk, M., Hazen, T.C. *et al.* (2017) Corexit 9500 enhances oil biodegradation and changes active bacterial community structure of oil-enriched microcosms. *Appl Environ Microbiol* **83**(10): e03462-03416.

Tremblay, J., Yergeau, E., Fortin, N., Cobanli, S., Elias, M., King, T.L. *et al.* (2017) Chemical dispersants enhance the activity of oil- and gas condensate-degrading marine bacteria. *ISME J* **11**(12): 2793-2808.

US NASEM (2020). The use of dispersants in marine oil spill response. Washington, DC: The National Academies Press (US).

US Nat. Comm. DWH (2011). The use of surface and subsea dispersants during the BP Deepwater Horizon oil spill. Working Paper. Washington, DC, USA: National Commission on the BP Deepwater Horizon Oil Spill and Offshore Drilling. Available from: http://purl.fdlp.gov/GPO/gpo184 [Accessed April 20, 2019].

Yam, E.M., and Tang, K.W. (2007) Effects of starvation on aggregate colonization and motility of marine bacteria. *Aquat Microb Ecol* **48**(3): 207-215.

Chapter 5 – Personal contribution

The microcosm experiment was designed by myself and Jun.-Prof. Sara Kleindienst with input from Dr. Nico Jehmlich. The strain *Marinobacter* sp. TT1 was isolated and provided by Prof. Tony Gutierrez. I performed the experiment and subsequent cell counts and *n*-hexadecane quantifications. Protein extraction, LC-MS/MS analysis and mass spectra analysis were performed by Dr. Nico Jehmlich. Subsequent analysis of quantification data including data visualization and statistical analysis was performed by myself with input from Dr. Nico Jehmlich. Results were interpreted and discussed by myself together with Jun.-Prof. Sara Kleindienst and Dr. Nico Jehmlich. The manuscript was written by myself under the supervision of Jun.-Prof. Sara Kleindienst and revised by all co-authors.

5 Comparative proteomics of *Marinobacter* sp. TT1 reveals Corexit impacts on hydrocarbon metabolism, chemotactic motility and biofilm formation

Saskia Rughöft[1], Nico Jehmlich[2], Tony Gutierrez[3] and Sara Kleindienst[1]

[1] Microbial Ecology, Center for Applied Geosciences, University of Tübingen, Germany
[2] Department of Molecular Systems Biology, Helmholtz Centre for Environmental Research – UFZ GmbH, Leipzig, Germany
[3] Institute of Mechanical, Process & Energy Engineering, Heriot-Watt University, Edinburgh, UK

Published in ***Microorganisms***

Rughöft, S., Jehmlich, N., Gutierrez, T., Kleindienst, S. (2021) Comparative Proteomics of *Marinobacter* sp. TT1 Reveals Corexit Impacts on Hydrocarbon Metabolism, Chemotactic Motility, and Biofilm Formation. *Microorganisms* **9**(1): 3. https://doi.org/10.3390/microorganisms9010003

5.1 Abstract

The application of chemical dispersants during marine oil spills can affect the community composition and activity of marine microorganisms. Several studies have indicated that certain marine hydrocarbon-degrading bacteria, such as *Marinobacter* spp., can be inhibited by chemical dispersants, resulting in lower abundances and/or reduced biodegradation rates. However, a major knowledge gap exists regarding the mechanisms underlying these physiological effects. Here, we performed comparative proteomics of the Deepwater Horizon isolate *Marinobacter* sp. TT1 grown under different conditions. Strain TT1 received different carbon sources (pyruvate vs. *n*-hexadecane) with and without added dispersant (Corexit EC9500A). Additional treatments contained crude oil in the form of a water-accommodated fraction (WAF) or chemically-enhanced WAF (CEWAF; with Corexit). For the first time, we identified the proteins associated with alkane metabolism and alginate biosynthesis in strain TT1, report on its potential for aromatic hydrocarbon biodegradation and present a protein-based proposed metabolism of Corexit components as carbon substrates. Our findings revealed that Corexit exposure affects hydrocarbon metabolism, chemotactic motility, biofilm formation, and induces solvent tolerance mechanisms like efflux pumps in strain TT1. This study provides novel insights into dispersant impacts on microbial hydrocarbon degraders that should be taken into consideration for future oil spill response actions.

Originality-Significance Statement:

This is the first proteomics study elucidating the impacts of the chemical dispersant Corexit on the cellular processes of a marine hydrocarbon degrader - *Marinobacter* sp. TT1, isolated from the Deepwater Horizon oil spill. The proteins associated with a proposed microbial metabolism of Corexit components as carbon substrates and Corexit-induced changes in the proteome linked to hydrocarbon metabolism, chemotactic motility, biofilm formation, and solvent tolerance are highlighted for the first time. In addition, the first evidence of alginate biosynthesis in a member of the *Marinobacter* genus is provided.

5.2 Introduction

Chemical dispersants are routinely applied during major marine oil spills to break up surface slicks and disperse oil in the water column. Following the Deepwater Horizon (DWH) oil spill in the Gulf of Mexico in 2010, for instance, seven million litres of dispersants (Corexit EC9500A and EC9527A) were applied in response to the release of an estimated 800 million litres of crude oil into the Gulf ecosystem (US Nat. Comm. DWH, 2011; McNutt *et al.*, 2012). Dispersant exposure has consistently been shown to alter marine microbial community dynamics and to select for specific taxa responding to inputs of petroleum hydrocarbons (HCs) (Kleindienst *et al.*, 2015b; Suja *et al.*, 2017; Techtmann *et al.*, 2017; Doyle *et al.*, 2018; Sun and Kostka, 2019; Tremblay *et al.*, 2019). However, studies have produced conflicting results on how dispersants might affect the HC biodegradation potential of microbial communities, with findings ranging from enhanced (Bælum *et al.*, 2012; Prince *et al.*, 2016) to unaffected (McFarlin *et al.*, 2014; Tremblay *et al.*, 2019) or decreased HC degradation activities (Kleindienst *et al.*, 2015b), and the underlying mechanisms remaining unresolved.

Dispersant impacts have also been highlighted by several studies that demonstrated inhibition effects of dispersants on certain species/strains of HC-degrading bacteria, observed in both pure cultures (Hamdan and Fulmer, 2011; Overholt *et al.*, 2016; Hackbusch *et al.*, 2020) and seawater microcosm experiments (Techtmann *et al.*, 2017; Doyle *et al.*, 2018). Members of the genus *Marinobacter*, in particular, have been shown to become negatively affected by chemical dispersant exposure (Hamdan and Fulmer, 2011; Kleindienst *et al.*, 2015b; Techtmann *et al.*, 2017; Tremblay *et al.*, 2017; Doyle *et al.*, 2018). This genus includes several ubiquitous marine HC degraders that often represent alkane-degrading key players responding to oil spillage in the marine environment (Duran, 2010; Kleindienst *et al.*, 2015b; Tremblay *et al.*, 2019). Recent work in our group with *Marinobacter* sp. strain TT1 has furthermore demonstrated that this strain is able to grow on Corexit EC9500A as sole carbon and energy source (see **Chapter 4** in this thesis), similar to other marine HC-degrading isolates belonging to the genera *Colwellia*, *Alcanivorax* or *Acinetobacter* that were shown to utilize components of the dispersant mixture (Chakraborty *et al.*, 2012; Overholt *et al.*, 2016).

The metabolic pathways of HC biodegradation are relatively well characterized in several HC-degrading isolates (reviewed e.g. in Wang and Shao, 2013; Abbasian *et al.*, 2016). Aerobic alkane biodegradation, for example, is typically performed via a sequential oxidation process by a few key enzymes (i.e. alkane monooxygenases or cytochrome P450 oxidases, alcohol dehydrogenases and aldehyde dehydrogenases) and connects to the cytosolic fatty acid metabolism. However, it remains largely unknown how chemical dispersants, such as Corexit, might affect the metabolism and cellular processes of HC degraders and, in turn, how exposure leads to the different observed microbial responses. While the exact composition of chemical dispersants remains proprietary, Corexit EC9500A was reported to contain a petroleum distillate fraction, propylene glycols, and different anionic and nonionic surfactants (Place *et al.*, 2016; Choyke and Ferguson, 2019). These components may themselves cause detrimental effects to microbial cells even in the absence of crude oil, since surfactants are known to induce several potentially cytotoxic effects by partitioning within cell membranes, potentially impairing permeability processes and the functioning of membrane proteins (Partearroyo *et al.*,

1990; Van der Werf *et al.*, 1995; Inacio *et al.*, 2016). Solvent stress caused by high concentrations of (individual or a mixture of) HCs is known to trigger specific adaptations or avoidance responses in HC-degrading bacteria, such as efflux pump expression or negative chemotactic behavior (Young and Mitchell, 1973; Ramos *et al.*, 2002; Shitashiro *et al.*, 2005; Krell *et al.*, 2012), as well as changes in membrane lipid composition (Sikkema *et al.*, 1995). Furthermore, chemically dispersed oil can exhibit synergistic toxicity to marine microorganisms, i.e. higher toxicity than oil alone (Radniecki *et al.*, 2013; Rico-Martínez *et al.*, 2013; Ozhan *et al.*, 2014).

The alkane degrader *Marinobacter* sp. TT1 was isolated during the DWH oil spill (Gutierrez *et al.*, 2013b) and recent work in our group has shown that its growth and biodegradation of *n*-hexadecane can be detrimentally impacted by Corexit exposure (see **Chapter 4** in this thesis), which may explain why this strain did not become enriched during the DWH spill (Gutierrez *et al.*, 2013b). Since the genomic potential of strain TT1 and the mechanisms underlying how Corexit affects its physiology and metabolism remain unknown, we conducted a comparative proteomics study in order to, for the first time, i) characterize the HC-degrading metabolism of *Marinobacter* sp. TT1 based on proteomics, ii) identify which of the previously reported components of Corexit might be metabolized by this strain, and iii) elucidate potential effects of Corexit exposure on the strain's cellular processes. For this, the protein profiles of *Marinobacter* sp. TT1 were analyzed when grown in the presence or absence of Corexit EC9500A (Cxt), on pyruvate or *n*-hexadecane (Hxdc), or using a crude oil water-accommodated fraction (WAF) or chemically enhanced WAF (CEWAF; containing Corexit EC9500A) that simulate crude oil and/or Corexit exposure in the marine water column in the event of an oil spill at sea (Fig. S5.1).

5.3 Experimental procedures

5.3.1 Experimental design

At the start of the experiment, the following treatments for *Marinobacter* sp. TT1 were established in half-filled 20 ml glass headspace vials (Fig. S5.1) using four different pre-cultures, adapted to different carbon substrates (see SI). The *n*-hexadecane-adapted pre-culture was used to inoculate (1) cultures with no added carbon substrate (Control), (2) cultures with 100 mg l^{-1} *n*-hexadecane (Hxdc), and (3) cultures with 100 mg l^{-1} *n*-hexadecane and 10 mg l^{-1} Corexit (Hxdc+Cxt). The Corexit-adapted pre-culture was used to establish treatments with (4) 100 mg l^{-1} Corexit (Corexit), whereas the WAF-adapted pre-culture was used to inoculate treatments with either (5) 1 ml of WAF solution (6 mg l^{-1} WAF-derived dissolved organic carbon) or (6) 200 µl of CEWAF solution (6 mg l^{-1} CEWAF-derived dissolved organic carbon). The pyruvate-adapted pre-culture was used to inoculate cultures containing (7) 3 mM (264 mg l^{-1}) pyruvate. All treatments were run in triplicate and sampled sacrificially after 0 and 4 days, except for the pyruvate-containing treatments which were sampled after 1 day due to a faster growth with this substrate, as determined in pre-experiments. Due to concerns about gas-phase losses during sampling, separate triplicate cultures were prepared for treatments (2) and (3), in order to separately obtain samples for cell counts and HC quantification analysis. Separate replicate cultures were prepared for protein analysis from all seven treatments and each sampled after 1 day (pyruvate treatments) or 4 days (all other treatments). Additionally,

abiotic controls were prepared for HC or pyruvate quantification, containing no inoculum and either (8) 100 mg l^{-1} *n*-hexadecane (ab. Hxdc), (9) 100 mg l^{-1} *n*-hexadecane and 10 mg l^{-1} Corexit (ab. Hxdc+Cxt), or (10) 3 mM of pyruvate.

5.3.2 Cell counts and quantification of pyruvate and hydrocarbon concentrations

Cell counts for *Marinobacter* sp. strain TT1 were measured using the DNA-specific stain 4′,6-diamidino-2-phenylindole (DAPI) with the aid of an epifluorescence microscope in order to monitor growth of the strain in all treatment conditions (see SI). Concentrations of pyruvate or *n*-hexadecane were quantified using, respectively, high-performance liquid chromatography (HPLC) or gas chromatography coupled with mass spectrometry (GC-MS) (see SI).

5.3.3 Protein extraction and proteome analysis

For protein analysis, 100 ml of culture replicates were pooled per sample triplicate, filtered onto Sterivex filters (Merck Millipore, Thermo Fisher Scientific, Waltham, MA, USA) and immediately frozen. The filters were cut into small pieces and dissolved in 1 ml lysis buffer (8 M Urea, 2 M Thiourea, 1 mM PMSF). Cells on the filters were disrupted by bead beating (FastPrep-24, MP Biomedicals, Sanra Ana, CA, USA; 5.5 ms, 1 min, 3 cycles) followed by ultra-sonication (UP50H, Hielscher, Teltow, Germany; cycle 0.5, amplitude 60%) and centrifugation (10,000 x g, 10 min). The protein lysate was loaded on SDS-gel and run for 10 min. The gel piece was cut, washed and incubated with 25 mM 1,4-dithiothreitol (in 20 mM ammonium bicarbonate) for 1 h and 100 mM iodoacetamide (in 20 mM ammonium bicarbonate) for 30 min, and destained, dehydrated and proteolytically cleaved overnight at 37 °C with trypsin (Promega). The digested peptides were extracted and desalted using ZipTip-µC18 tips (Merck Millipore, Darmstadt, Germany). The peptide lysates were re-suspended in 0.1% formic acid and analysed by nanoliquid chromatography mass spectrometry (LC-MS/MS; UltiMate 3000 RSLCnano, Dionex, Thermo Fisher Scientific). Mass spectrometric analyses of eluted peptide lysates were performed on a Q Exactive HF mass spectrometer (Thermo Fisher Scientific) coupled with a TriVersa NanoMate (Advion, Ltd., Harlow, UK). LC gradient, ionization mode and mass spectrometry mode were used as described in (Haange *et al.*, 2019). The mass spectrometry proteomics data have been deposited to the ProteomeXchange Consortium via the PRIDE (Perez-Riverol *et al.*, 2019) partner repository with the dataset identifier PXD021108.

5.3.4 Data analysis

Data resulting from LC-MS/MS measurements were analysed with the Proteome Discoverer (v.2.4, Thermo Fischer Scientific) using SEQUEST HT. The protein-coding sequences of the reference UniProt proteome of *Marinobacter* sp. DSM 26291 (= strain TT1; protein-coding sequence entries 4,109, TaxID: 1761792) were used as database. Search settings were set to trypsin (Full), max. missed cleavage: 2, precursor mass tolerance: 10 ppm, fragment mass tolerance: 0.02 Da. The obtained label-free quantification intensities were further analysed using Perseus v1.6.1.5 (Tyanova *et al.*, 2016). For statistical tests, abundance data were log2 transformed, normalized (median-centered) and filtered. Only proteins with at least five peptide spectrum matches (PSM) and identified in at least two biological triplicates of at least one growth condition were considered for statistical analysis. A permutation-based FDR approach

was used to identify proteins with significantly different abundances between growth conditions, while correcting for multiple testing (parameters: S0 = 0, FDR 0.05, 1,000 randomizations). First, a multiple sample test (ANOVA) was performed on all 17 samples (one outlier had to be removed) grouped by treatment to gain an overview of the data. Hierarchical clustering was performed using the Spearman correlation–based distance (300 clusters, 10 iterations). Subsequently, two-sample tests (Student's *t*-test) were run for specific pairwise sample comparisons of interest for this study's objectives, followed by Tukey's honestly significant difference post hoc tests ($q < 0.05$). Proteins of interest were further characterized using the blastp suite (Altschul *et al.*, 1990), the UniParc clustering feature of UniProt (UniProt Consortium, 2019), KEGG's KOALA (KEGG Orthohology And Links Annotation; Kanehisa *et al.*, 2016) and pathway mapper (Kanehisa and Sato, 2020) tools. The genetic organization of gene clusters of interest was assessed using the genome of *Marinobacter* sp. DSM 26291 (= strain TT1; IMG genome ID: 2619618959) and the JGI IMG/M database (Chen *et al.*, 2019). The R programming language (R Core Team, 2019) was used to produce all presented data plots.

5.4 Results

5.4.1 Growth and substrate utilization of *Marinobacter* sp. TT1

Growth of *Marinobacter* sp. TT1 was observed on all substrates, reaching similar orders of magnitude for almost all growth conditions and displaying different macroscopic growth patterns (Fig. 5.1A and S5.2, see also supplemental results). Biodegradation of pyruvate (61% after one day; Fig. 5.1B) or *n*-hexadecane (respectively 46% or 67% degraded after four days in treatments with or without Corexit; Fig. 5.1B) was confirmed via GC-MS or HPLC measurements for the respective treatments.

5.4.2 Overview of proteomic analysis

The proteomic analysis resulted in a total of 3,008 proteins (ranging from 1 to 4,289 peptide-spectrum matches per protein), representing a recovery of 73% of *Marinobacter* sp. TT1's proteome (4,109 proteins; UniProtKB proteome UP000199211). Distinct protein profiles were detected for all treatments, while similar proteome patterns were observed in biological replicate samples (Fig. S5.3). Across the different treatments (i.e. Pyruvate, Hxdc, Hxdc+Cxt, Corexit, WAF, and CEWAF), 2,154 proteins were significantly differentially abundant according to a multiple sample test (ANOVA; permutation-based FDR < 0.05). However, due to the much lower biomass available in WAF and CEWAF samples, and the higher inter-replicate variability, proteome data from WAF and CEWAF treatments was mainly compared to each other and interpreted with caution. When considering specific pairwise sample comparisons (Student's *t*-test, permutation-based FDR < 0.05), a total of 1,140 proteins were detected in significantly different abundances during growth on *n*-hexadecane compared to the non-HC control (pyruvate) with 50% of them in higher abundance on *n*-hexadecane (Tab. S1). When considering the effects of Corexit exposure, 36 proteins were significantly differentially abundant during growth on *n*-hexadecane with Corexit compared to the *n*-hexadecane treatments (with 55% of them more abundant with Corexit; Tab. S2). Additionally, 1,286 proteins were significantly differentially abundant during growth on Corexit compared to

growth on *n*-hexadecane with 43% more abundant on Corexit (Tab. S3). Only two proteins were detected as significantly differentially abundant between the WAF and CEWAF treatments (Tab. S4).

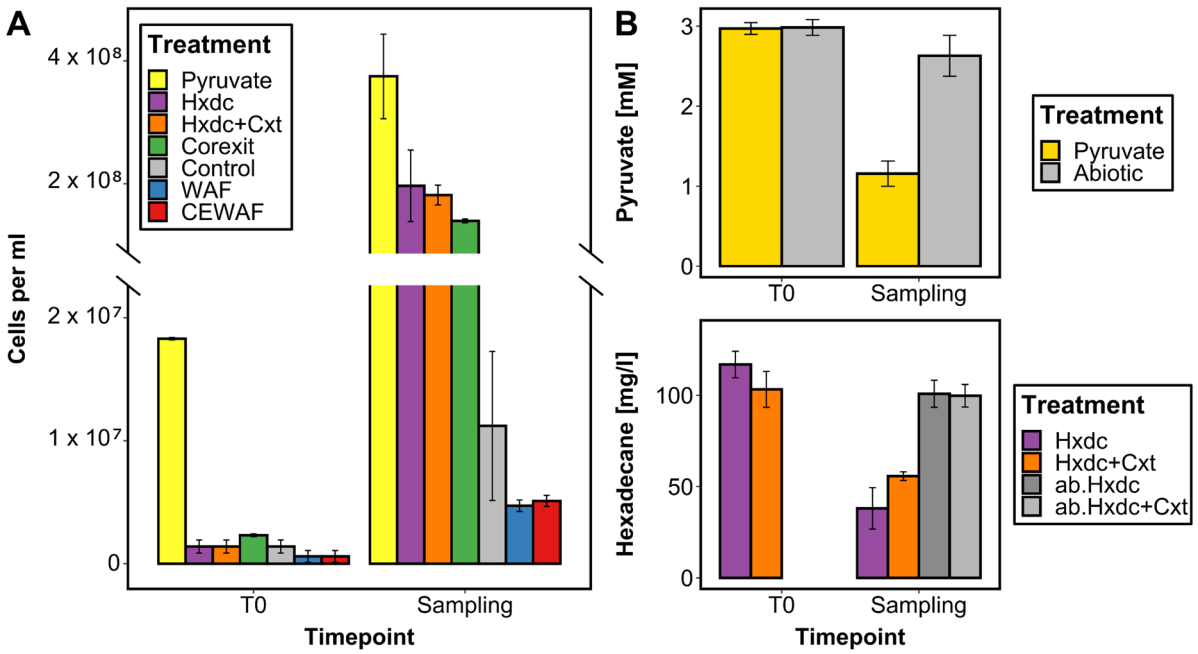

Figure 5.1: Growth and biodegradation of carbon sources supplied to Marinobacter sp. TT1 cultures, sampled for proteomic analysis after 1 day (pyruvate treatments) or 4 days (all other treatments) of incubation. Treatments contained the following carbon sources: 3 mM pyruvate (Pyruvate), 100 mg l^{-1} *n*-hexadecane (Hxdc), 100 mg l^{-1} *n*-hexadecane and 10 mg l^{-1} Corexit (Hxdc+Cxt), 100 mg l^{-1} Corexit (Corexit), no carbon source (Control), 6 mg l^{-1} WAF-derived DOC (WAF) or 6 mg l^{-1} CEWAF-derived DOC (CEWAF). Results shown are averages of sacrificial, triplicate cultures (standard deviations are based on triplicates). ab. = abiotic controls without inoculum. **A**) Cell numbers determined by fluorescence microscopy are presented using a divided y-axis in order to better visualize the lower cell numbers in WAF and CEWAF treatments. **B**) Pyruvate and n hexadecane concentrations were determined via HPLC or GC-MS measurements, respectively.

5.4.3 Proteome of *Marinobacter* sp. TT1 grown on *n*-hexadecane

The protein profile of *Marinobacter* sp. TT1 grown on *n*-hexadecane indicated upregulated metabolisms for alkane degradation and alginate biosynthesis, with additional upregulated processes including peptidoglycan and lipopolysaccharide (LPS) synthesis, as well as oxidative stress responses (Fig. 5.2). Only one of the alkane 1-monooxygenases encoded in the genome of *Marinobacter* sp. TT1 (UniProt ID: A0A1I4KVH1) was more abundant during growth on *n*-hexadecane than in the non-HC control treatment (log_2 fold change [FC] = 3). This alkane 1-monooxygenase was found to have 83% amino-acid sequence identity to the AlkB2 enzyme (A0A455W7K7) of *Marinobacter hydrocarbonoclasticus* YB03 and might also be homologous to AlkB2 (Q0VTH3) of *Alcanivorax borkumensis* SK2 (59.03% amino-acid sequence identity). Additionally, a putative P450 cytochrome alkane hydroxylase (A0A1I4KEY9) was detected in significantly higher abundance compared to the non-HC control (FC = 4.5). Two proteins putatively involved in the transport of alkanes into the cell were also significantly more abundant during growth of strain TT1 on *n*-hexadecane: a long-chain fatty acid transport protein (FC = 4.9; A0A1I4JKC5) and an Ig-like domain containing protein (FC = 4.6; A0A1I4JKB4).

These were identified as putative homologues of the alkane uptake proteins AupA (H8WEC1; 83% amino-acid sequence identity) and AupB (H8WEC0; 56% amino-acid sequence identity), respectively, which were previously described in *Marinobacter hydrocarbonoclasticus* SP17 (Mounier *et al.*, 2018). The electron transfer proteins rubredoxin-NAD+ reductase (A0A1I4K5F9), ferredoxin (A0A1I4MH37), and a ferredoxin-NADP reductase (A0A1I4KTN3) were likewise significantly more abundant during growth on *n*-hexadecane (FC ≥ 1.2) and thus likely involved in the first terminal *n*-hexadecane oxidation step. Finally, four alcohol dehydrogenases (A0A1I4J3P7, A0A1I4ISL3, A0A1I4MI03, A0A1I4H5P2) and one aldehyde dehydrogenase (A0A1I4K5K4) probably involved in the subsequent oxidation steps of *n*-hexadecane metabolism, were also significantly more abundant (FC = 0.7 to 5.0). Interestingly, a large number of proteins associated with the extracellular polysaccharide (EPS) alginate involved in biofilm formation were significantly more abundant during growth on *n*-hexadecane compared to pyruvate (FC = 2.1 to 5.8). This included (homologues of) the following proteins involved in the biosynthesis and export of the polysaccharide alginate: AlgD (A0A1I4LFN3), Alg44 (A0A1I4LF83), AlgE (A0A1I4LF78), AlgF (A0A1I4LFF1), AlgA (A0A1I4JXV5, A0A1I4LGW8), AlgC (A0A1I4LG98), and the regulatory proteins MucB (A0A1I4IUP7), AlgR (A0A1I4JGY9), and AlgZ (A0A1I4JH21). These proteins were found to be encoded by three different alginate-related gene clusters in the genome of *Marinobacter* sp. TT1 (*algD844KEGIJFXLAC* [SAMN04487868_11444-56], *algU-mucABC* [SAMN04487868_104201-04] and *algRZ* [SAMN04487868_10662-63]) with the first gene cluster showing a notably similar organization (Fig. S5.4) to the alginate operons described in *Pseudomonas aeruginosa* (Gacesa, 1998) and *Alcanivorax borkumensis* (Schneiker *et al.*, 2006). All abundant proteins from this first putative operon (AlgD, Alg44, AlgE, AlgF, AlgA, AlgC) were also detected in significantly higher abundances during growth on *n*-hexadecane when compared to the Corexit only treatment (FC = 1.9 to 6.3). Furthermore, a number of proteins required for peptidoglycan or lipopolysaccharide (LPS) biosynthesis, five different phospholipases and several enzymes possibly involved in mitigating oxidative stress, were found to be significantly more abundant in the *n*-hexadecane treatment compared to the pyruvate treatment (FC = 0.4 to 3.7; Tab. S1, Fig. S5.5).

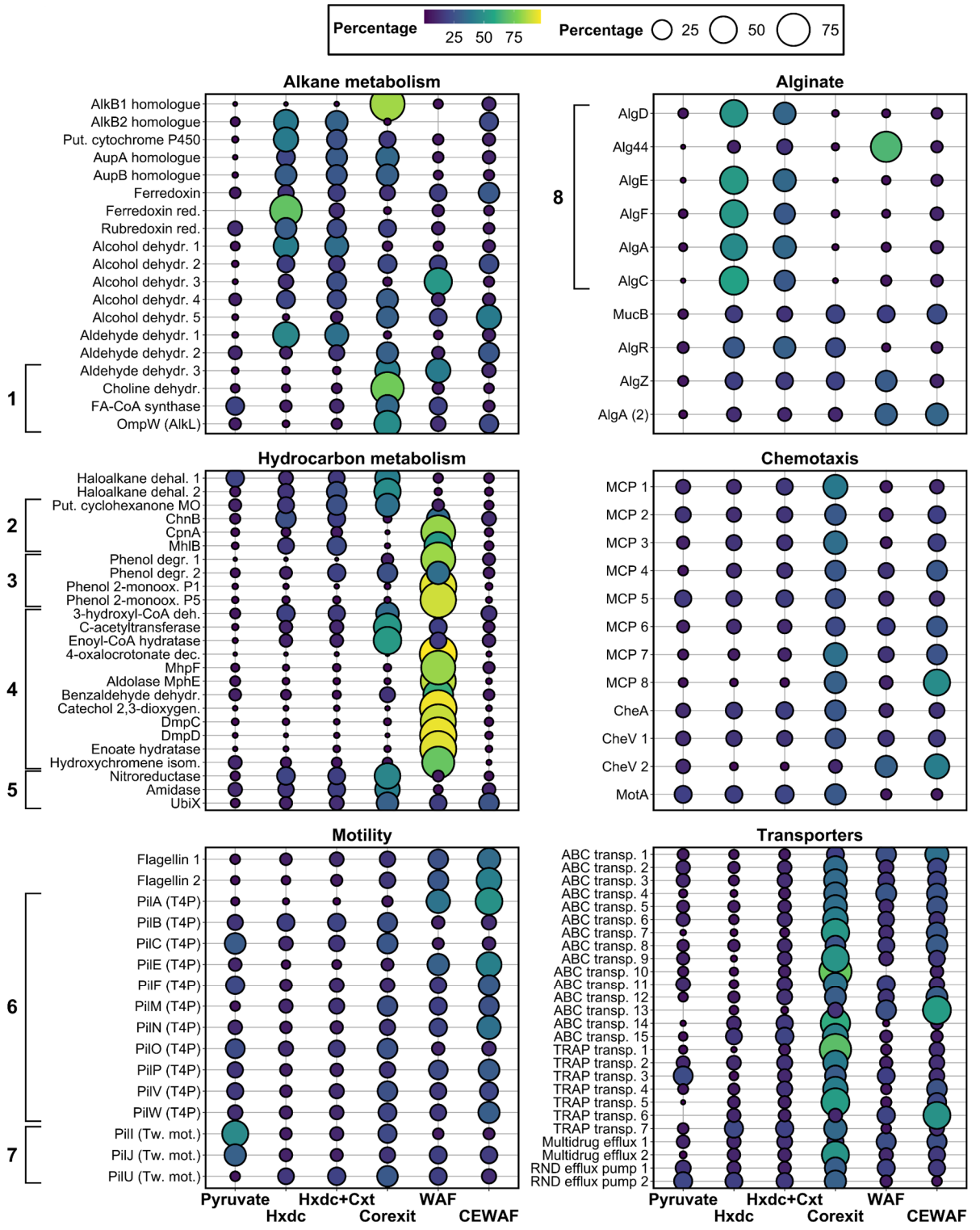

Figure 5.2: Normalized, relative mean abundances (symbolized by circle size and colour; sum per protein = 100%) of a selection of significantly (q-value < 0.05) differentially abundant proteins associated with alkane metabolism, alginate synthesis, non-alkane HC metabolism, chemotaxis, motility and transmembrane transport systems during growth of Marinobacter sp. TT1 cultures on different carbon sources. Treatments received either pyruvate, *n*-hexadecane (Hxdc), *n*-hexadecane and Corexit (Hex+Cxt), only Corexit (Corexit), crude oil WAF, or chemically enhanced WAF (CEWAF). 1 = proteins belonging to the proposed *alk* operon (plus AlkB1 homologue); 2 = Cycloaliphatic HC metabolism; 3 = Phenol metabolism; 4 = Aromatic HC metabolism; 5 = Aminobenzoate metabolism; 6 = Type IV pilus assembly; 7 = Twitching motility; 8 = Proteins belonging to the proposed *alg* operon. See Tab. S8 for protein names.

5.4.4 Protein profiles of *Marinobacter* sp. TT1 during Corexit exposure

The protein profile of *Marinobacter* sp. TT1 when influenced by dispersant exposure pointed towards upregulated alkane and non-linear HC metabolism, different transporter systems (i.e. ABC/TRAP-type, efflux pumps), as well as pronounced chemotaxis and motility processes (Fig. 5.2).

Corexit versus *n*-Hexadecane. The alkane 1-monooxygenase (A0A1I4KVH1) and putative P450 cytochrome alkane hydroxylase (A0A1I4KEY9) that were abundant during growth on *n*-hexadecane were significantly less abundant in cultures grown on Corexit (FC = 4.3 and 1.2, respectively). However, the second alkane 1-monooxygenase (A0A1I4KFD0) was significantly more abundant in the Corexit-only treatment (FC = 8). This enzyme has only low amino-acid sequence identity (36.07%) to the other alkane 1-monooxygenase of *Marinobacter* sp. TT1 (A0A1I4KVH1) but is 99.75% identical (amino-acid sequence identity) to the AlkB1 enzyme of *Marinobacter* hydrocarbonoclasticus VT8 (A1TXS2), and is a homologue of AlkB1 (Q0VKZ3) from Alcanivorax borkumensis SK2 (87.16% amino-acid sequence identity). A number of proteins encoded by the genes located downstream from the AlkB1 homologue in the genome of strain TT1 were significantly more abundant in Corexit treatments as well: an aldehyde dehydrogenase (FC = 4.6; A0A1I4KFQ9), a choline dehydrogenase (FC = 4.7; A0A1I4KF71), a fatty-acyl-CoA synthase (FC = 2.2; A0A1I4KER1), and an outer membrane protein with putative homology to AlkL (FC = 4.5; A0A1I4KF83). While two alcohol dehydrogenases (FC = 4.1, A0A1I4KKP8; FC = 0.5, A0A1I4H5P2) and another aldehyde dehydrogenase (FC = 1.8; A0A1I4KKB9) were also significantly more abundant, most of the proteins likely involved in *n*-hexadecane metabolism (i.e. detected in high abundances in the *n*-hexadecane-amended treatments) were less abundant in Corexit treatments. However, several enzymes potentially involved in the biodegradation and metabolism of aromatic and other HCs were significantly more abundant in Corexit treatments (average FC = 1.9), including enzymes assigned to the metabolism of haloalkanes, cycloaliphatic HCs, phenols, benzoates and aminobenzoates (Tab. S5). Interestingly, a few proteins involved in sulphur metabolism were also significantly more abundant in Corexit treatments (average FC = 1.8), i.e. a sulfotransferase (A0A1I4KTW4), the sulphur carrier protein FdhD (A0A1I4NAC8), and a thioester reductase (A0A1I4JTH2).

According to KEGG's ortholog annotation tool (KOALA), the largest fractions of annotated proteins significantly more abundant in Corexit compared to *n*-hexadecane treatments belonged to the KEGG orthology (KO) categories of 'signaling and cellular processes' (24%) and 'environmental information processing' (22%; Fig. S5.6A). Within these categories, a large group of proteins with significantly higher abundances compared to *n*-hexadecane treatments (FC = 0.4 to 5.9) were assigned to transport systems, including 13 TRAP-type mannitol/chloroaromatic transporter proteins, 5 efflux pump proteins and 27 amino acid ABC transporter proteins (13 of these specifically for branched-chain amino acids). The second largest group (FC = 0.2 to 5.3) was assigned to cellular processes of chemotaxis and motility (i.e. 11 methyl-accepting chemotaxis proteins [MCPs], 12 type IV pilus proteins, 3 twitching motility proteins and 5 flagellar proteins), with several of these proteins also significantly more abundant when compared to the pyruvate treatments.

***n*-Hexadecane/Corexit vs. *n*-hexadecane.** The annotated proteins detected in significantly higher abundances in the *n*-hexadecane with Corexit treatment compared to the *n*-hexadecane treatment belonged mainly to the KO categories of 'signalling and cellular processes' (27%) and 'environmental information processing' (27%; Fig. S5.6B). This included five transporter-affiliated proteins (FC = 0.5 to 2.6; A0A1I4MNH9, A0A1I4KD04, A0A1I4IF13, A0A1I4I3J1, A0A1I4H9T9) and one MCP (FC = 0.5; A0A1I4MSJ0). Interestingly, the putative P450 cytochrome alkane hydroxylase (FC = 0.7; A0A1I4KEY9) and the ferredoxin-NADP reductase (FC = 2.5; A0A1I4KTN3), abundant in *n*-hexadecane treatments, were significantly less abundant in the cultures with added Corexit.

CEWAF versus WAF. Even though only two proteins with significantly different abundances were detected between the more environmentally relevant treatments WAF and CEWAF, probably due to the high detected inter-replicate variance, some systematic notable differences could still be observed. Among those proteins found in higher abundance in the WAF treatment, according to a *p*-value-truncated *t*-test (62 proteins; $p < 0.05$; Tab. S6), the largest annotated fractions belonged to the KO categories of 'xenobiotics biodegradation and metabolism' (20%) and 'carbohydrate metabolism' (18%; Fig. S5.6D). This included several enzymes with predicted functions in the metabolism of non-linear HCs (Tab. S7) – i.e. the biodegradation of cycloaliphatics, phenols, naphthalenes, benzoates, and xylenes (average FC = 4.3). On the other hand, the proteins detected in higher abundance in CEWAF cultures (85 proteins; $p < 0.05$; Tab. S6) mainly belonged to the KO categories 'environmental information processing' (20%) and 'signalling and cellular processes' (16%; Fig. S5.S6C). Notable proteins from these categories included, for instance, three MCPs (FC = 0.5 to 2.1; A0A1I4LXM2, A0A1I4HAX6, A0A1I4MFB0), three flagellar proteins (FC = 0.8 to 1.4; FliG, FliK, FlgL; A0A1I4HL94, A0A1I4HME7, A0A1I4J7M9), the pilus assembly protein FimV (FC = 0.8; A0A1I4M1I2), and five proteins associated with ABC or TRAP-type transporter systems (FC = 0.9 to 2.2; A0A1I4MSA8, A0A1I4L200, A0A1I4HXQ3, A0A1I4KD04, A0A1I4IE06). Generally, many of the detected proteins associated with chemotaxis and motility were most abundant in the Corexit and CEWAF treatments when comparing all hydrocarbon-amended treatments (Fig. 5.2). Most of the previously described proteins involved in the metabolism of *n*-alkanes were also detected in both WAF and CEWAF cultures with only one notable difference between these treatments. While both alkane 1-monooxygenases were detected in the CEWAF treatment, only the AlkB1 homologue (A0A1I4KFD0) was also detected in the WAF treatment.

5.5 Discussion

The obtained protein profiles of *Marinobacter* sp. TT1 illustrated the strain's ability to metabolize a wide range of HC compounds, produce alginate, utilize Corexit components as substrates, and elucidated additional physiological adaptation processes to Corexit exposure (see Fig. 5.3).

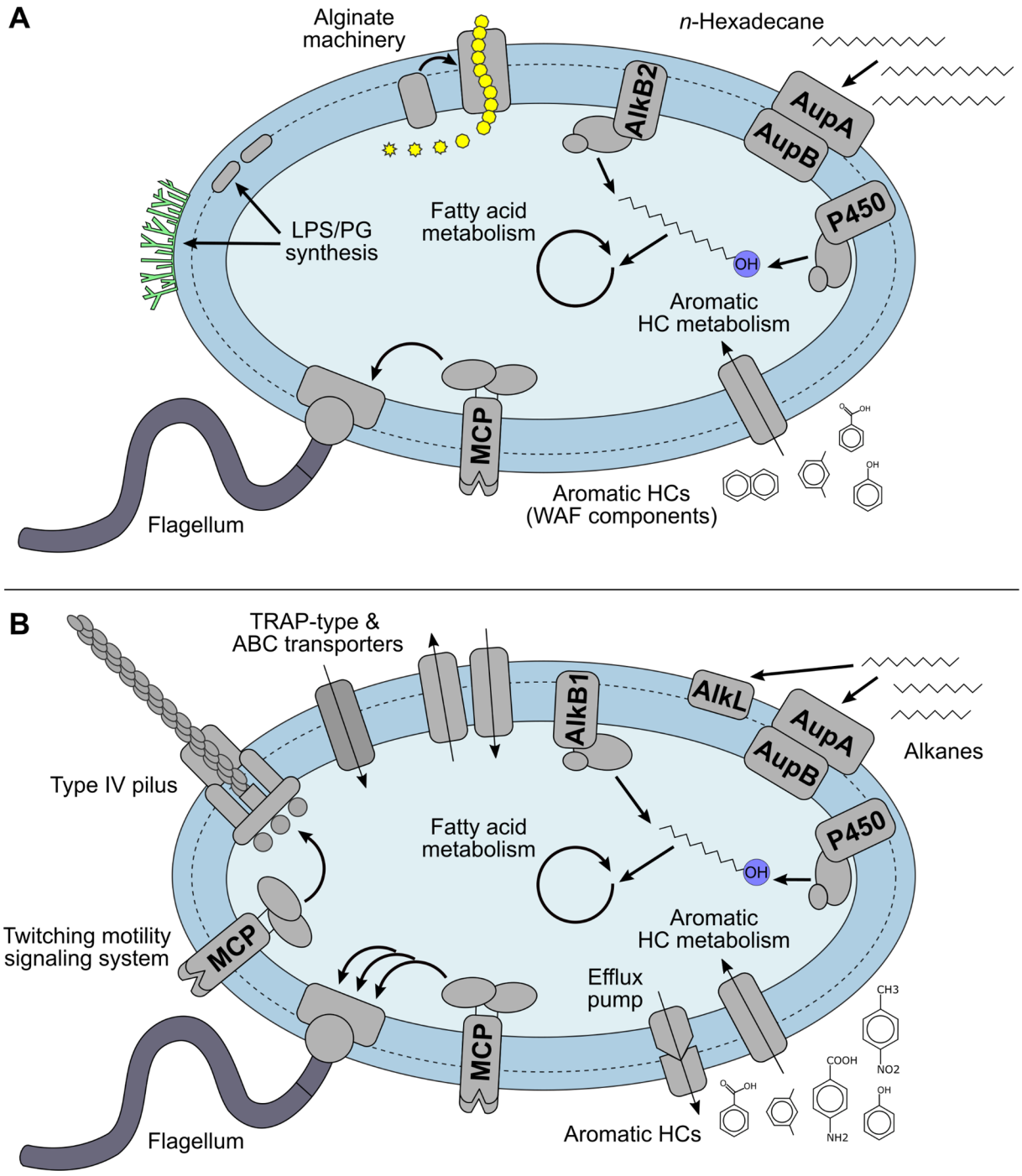

Figure 5.3: Schematic overview of the metabolism of *Marinobacter* sp. TT1 when **A**) utilizing hydrocarbons (*n*-hexadecane or WAF), or **B**) growing on components of Corexit and/or with Corexit exposure. Abbreviations: LPS = lipopolysaccharide, PG = peptidoglycan, HC = hydrocarbon, WAF = water-accommodated fraction, MCP = methyl-accepting chemotaxis protein, TRAP = tripartite ATP-independent periplasmic, ABC = ATP-binding cassette. See Tab. S8 for protein names.

5.5.1 Hydrocarbon metabolism of *Marinobacter* sp. TT1

The *n*-hexadecane metabolism of *Marinobacter* sp. TT1 appears relatively analogous to the alkane metabolism of other marine alkane degraders (Mounier *et al.*, 2014; Gregson *et al.*, 2019; Gregson *et al.*, 2020), with our results suggesting important roles for the AupAB, AlkB2 and cytochrome P450 homologues and a number of involved dehydrogenases (see also supplemental discussion). Several proteins implicated in cell envelope modification, oxidative stress response and a number of chaperones were also significantly abundant during growth on *n*-hexadecane, pointing towards an involvement of these proteins in the alkane-degrading lifestyle and associated biofilm formation in bacteria like strain TT1, as previously discussed (Kato *et al.*, 2009; Jung *et al.*, 2011; Vaysse *et al.*, 2011; Barbato *et al.*, 2016; Ennouri *et al.*, 2017).

WAFs are often used to simulate the subsurface state of crude oil in the water column in the event of an oil spill at sea. They typically contain alkanes and mostly low-molecular weight aromatic HCs, such as BTEX (benzene, toluene, ethylbenzene, xylene) or PAH compounds (Faksness *et al.*, 2008; Bera *et al.*, 2020). The proteins we detected from strain TT1 corroborate this, since enzymes assigned to the metabolism of benzoates, xylenes, naphthalene, phenols, and cycloaliphatic HCs were found in highest abundances in the WAF treatments. Only the AlkB1 homologue was detected which likely degrades shorter alkanes (e.g. C_5-C_{12}) like the AlkB1 of *A. borkumensis* SK2 (Van Beilen *et al.*, 2004). This makes sense since longer-chain alkanes are less likely to be found in WAFs due to their poor solubilities. We therefore posit that alkane metabolism by strain TT1 played a minor role in WAF treatments compared to the degradation of aromatics. Our findings reveal that the HC-degrading metabolic spectrum of strain TT1 is much wider than previously reported (Gutierrez *et al.*, 2013b) and add to the growing body of evidence that members of the genus *Marinobacter* are, in addition to degrading alkanes, also capable of utilizing aromatic HCs as a sole source of carbon and energy (Duran, 2010; Bonin *et al.*, 2015; Dombrowski *et al.*, 2016).

5.5.2 Alginate biosynthesis of *Marinobacter* sp. TT1

Growth of *Marinobacter* sp. TT1 on *n*-hexadecane was apparently associated with an upregulation in alginate metabolism. Alginate is a polysaccharide composed of multiple monomer subunits which are synthesized from fructose-6-phosphate, polymerized and exported across the outer membrane by proteins of the alginate machinery of which several homologues were detected in this study (Fig. S7; reviewed e.g. in Urtuvia *et al.*, 2017). Alginate is commercially extracted from seaweed for industrial applications and, thus, of biotechnological interest (Hay *et al.*, 2013), however, there are currently only two well-characterized bacterial producers of alginate (*Pseudomonas aeruginosa* and *Azotobacter vinelandii*). To our knowledge, this is the first evidence of an alginate operon in *Marinobacter* as well as the induction of alginate proteins by alkane biodegradation. Evidence for a potential link between HC biodegradation and alginate gene transcription was previously very sparse (Sabirova *et al.*, 2011; Gunasekera *et al.*, 2013). However, alginate plays a well-documented role in the formation of resistant mucoid biofilms by pathogenic *P. aeruginosa* (Ghafoor *et al.*, 2011; Moradali and Rehm, 2019), and *alg*-gene mutants of *A. borkumensis* were reported to have a reduced capacity for binding to lipophilic stains (Manilla-Pérez *et al.*, 2010). Growth of *M. hydrocarbonoclasticus* SP17 on *n*-hexadecane was also shown to depend on biofilm

formation for accessing non-dissolved *n*-hexadecane (Vaysse *et al.*, 2011; Mounier *et al.*, 2014). Thus, alginate likely plays an important role in the *n*-hexadecane-degrading lifestyle of *Marinobacter* sp. TT1 and probably constitutes a large part of the aggregates and biofilms observed in this study when grown on *n*-hexadecane.

5.5.3 Biodegradation of Corexit components by *Marinobacter* sp. TT1

Proteins potentially involved in the metabolism of alkanes, aromatic HCs, and surfactants were detected in the Corexit treatments, suggesting that these proteins might be involved in the utilization of dispersant components as carbon sources by *Marinobacter* sp. TT1 (Fig. 5.3B).

Alkane metabolism. A number of proteins associated with the utilization of *n*-alkanes as carbon and energy sources (e.g. AlkB1 homologue, AupA/B homologues, putative P450 hydroxylase) were detected in high abundances when strain TT1 was supplied with the chemical dispersant Corexit as sole carbon substrate. This suggests that alkanes are a biodegradable part of the petroleum distillate fraction in Corexit, which was also previously reported (McFarlin *et al.*, 2018; Choyke and Ferguson, 2019). The high abundance of the AlkB1 homologue (compared to the highly abundant AlkB2 homologue in *n*-hexadecane treatments) also suggests that mainly alkanes of shorter chain-length than *n*-hexadecane were available, which is in agreement with previous reports of C_9-C_{16} hydrocarbons making up the petroleum distillate fraction of Corexit (Word *et al.*, 2014).

Five proteins encoded adjacently to the AlkB1 homologue in the genome of strain TT1 had assigned functions in alkane and fatty acid metabolism, and four of them were detected in highest abundances in Corexit treatments. This may suggest that this respective gene cluster forms part of strain TT1's *alk* operon, which would putatively be induced by alkanes shorter than *n*-hexadecane (Fig. S5.8). This operon also included a homologue of *alkL* from P. putida GPo1 which encodes an outer membrane protein known for facilitating the uptake of C_7-C_{16} alkanes (Julsing *et al.*, 2012; Grant *et al.*, 2014). Therefore, both the AupAB and AlkL homologues were likely involved in uptake of alkanes from Corexit across the outer membrane. The alkane metabolism detected in Corexit treatments additionally differed from the observed *n*-hexadecane metabolism of strain TT1 regarding the abundance profiles of detected alcohol and aldehyde dehydrogenases, while two other *n*-hexadecane-metabolizing enzymes were also significantly less abundant in *n*-hexadecane treatments with added Corexit. These observations might again be due to different substrate ranges of these enzymes or it could be related to other Corexit components affecting them in an unknown manner. A similar pattern of differential HC degradation gene expression was reported recently in a metatranscriptomic study, assessing dispersant impacts on marine microbial communities affected by crude oil or diluted bitumen input (Tremblay *et al.*, 2019). Thus, Corexit exposure apparently not only supplies additional alkane substrates for marine HC degraders, but may also influence their active HC metabolism in additional ways.

Metabolism of other Corexit components. A number of proteins putatively assigned to the degradation of other HCs were detected during growth on Corexit, specifically haloalkanes, cyclohexanones, phenols, benzoates/xylenes and N-containing aromatic HCs (i.e. nitrotoluenes, aminobenzoates), which might have been metabolized by strain TT1. It is furthermore possible that the surfactant constituents of Corexit – i.e. dioctyl sulfosuccinate (DOSS), Span 80, Tween 80 and Tween 85 (Place *et al.*, 2016) – were degraded by strain TT1, either completely or

partially, thus serving as additional sources of carbon for the strain. Many HC-degrading bacteria (including *Marinobacter algicola* and *M. salarius*) have been shown to utilize Tween surfactants during routine strain characterization (Green *et al.*, 2006; Ng *et al.*, 2014). Microbial degradation of DOSS has also been reported (Chakraborty *et al.*, 2012; Seidel *et al.*, 2016; Techtmann *et al.*, 2017) and presumably proceeds via ester bond hydrolysis and metabolism of resulting alkyl chains and sulfosuccinates (Hales, 1993; Garcia *et al.*, 2009; Seidel *et al.*, 2016). Thus, the surfactant alkyl and acyl side chains might have been degraded by the detected AlkB1 homologue, cytochrome P450 hydroxylase, or lipases, while the proteins related to sulphur metabolism detected in Corexit treatments might have been involved in DOSS metabolism. Moreover, the solvent fraction of Corexit reportedly contains propylene glycol and dipropylene glycol monobutyl ether (Kover *et al.*, 2014) which could also have been degraded by strain TT1 as shown for other isolates (Chakraborty *et al.*, 2012). In order to establish a better connection of these potential substrates to the observed proteomic response of strain TT1, further experimental studies using only specific surfactants or glycols as carbon substrates are required. In general, these novel insights into the specific catabolism of strain TT1 growing on Corexit as a sole carbon source support previous reports of enriched suspected Corexit-degraders in marine communities exposed to Corexit (Kleindienst *et al.*, 2015b; Techtmann *et al.*, 2017; McFarlin *et al.*, 2018).

5.5.4 Additional cellular processes affected by Corexit exposure in *Marinobacter* sp. TT1

All protein profiles from treatments with Corexit showed similar trends (see also supplemental discussion), suggesting that dispersant exposure affected the interaction of *Marinobacter* sp. TT1 cells with their environment, evidenced by upregulated efflux pumps, other transmembrane transporter systems, chemotactic motility and changed biofilm formation behaviour (Fig. 5.3B). Some of these trends were also observed in the few transcriptomic studies currently available on Corexit affecting marine microorganisms in microcosm experiments (Peña-Montenegro *et al.*; Tremblay *et al.*, 2019) and *in situ* analysis from the DWH subsurface plume (Rivers *et al.*, 2013), although it remains unclear to what extent the plume metatranscriptomics data were influenced by Corexit and oil exposure.

Transmembrane transporter systems. Efflux pumps play an important role in conferring solvent tolerance to bacteria like *P. putida* (Ramos *et al.*, 2002; Krell *et al.*, 2012) and, thus, they are probably used by *Marinobacter* sp. TT1 to expel harmful solvents or metabolic intermediates from the cell when exposed to higher concentrations of Corexit. The highly abundant TRAP-type transporters in Corexit treatments, on the other hand, likely played a role in the uptake of Corexit components since they are known to typically transport organic acids and sulfonates (Mulligan *et al.*, 2011; Rosa *et al.*, 2018). Some TRAP-type transporters were also shown to import aromatic compounds like 4-chlorobenzoate and lignin-derived monomers (Chae and Zylstra, 2006; Salmon *et al.*, 2013). The majority of highly abundant transporters in Corexit treatments were amino acid/amide ABC (ATP-binding cassette) transporters, with about half of them specifically branched-chain amino acid (BCAA) transporters. A similar enrichment of ABC transporter genes and/or transcripts was previously reported for seawater microcosms amended with Corexit and oil or bitumen (Tremblay *et al.*, 2019), petroleum-contaminated microbial mats (Aubé *et al.*, 2020), dibutyl phthalate-contaminated black soils (Xu *et al.*, 2018) and in *Sphingomonas* sp. GY2B during Tween 80-enhanced phenanthrene

degradation (Liu *et al.*, 2017b). Generally, ABC transporters accept a wide range of substrates (Davidson *et al.*, 2008; Jones and George, 2013). It remains unclear why specifically BCAA transporters showed such high abundances in Corexit treatments, but we offer a few hypothetical scenarios: First, an increased demand for BCAAs could have been caused by increased requirements for branched-chain fatty acids which were recently linked to both the maintenance of membrane fluidity during exposure to stressors like aromatic HCs (Murínová and Dercová, 2014; Nowak and Mrozik, 2016) and a novel quorum sensing system in gram-negative bacteria (Zhou *et al.*, 2015) that can affect EPS and biofilm formation behaviours (Zhou *et al.*, 2017). Alternatively, ABC transporters can also facilitate solute efflux (Hosie *et al.*, 2001) and several microbial ABC transporters, that had initially been annotated differently, have been implicated in the transport of aromatic HCs as demonstrated by experimental evidence (Noda *et al.*, 2003; Giuliani *et al.*, 2011; Michalska *et al.*, 2012). Thus, the detected ABC transporters might have transported branched/aromatic HCs or surfactants, either as substrates into the cell or out of the cytoplasm, reinforcing the activity of efflux pumps.

Chemotactic motility and biofilm formation. Chemotactic behaviour plays an important role in HC biodegradation (reviewed e.g. by Parales and Ditty, 2017), by either increasing bioavailability of HC substrates (i.e. moving towards attractants) or enabling bacteria to avoid toxic HCs or high concentration of HCs (i.e. movement away from repellents). Accordingly, a few chemotaxis proteins and a number of flagellar proteins were significantly more abundant in *n*-hexadecane treatments compared to the non-HC controls. However, Corexit-containing treatments systematically showed significantly higher abundances of chemotactic motility-related proteins compared to other HC-containing treatments (i.e. *n*-hexadecane, WAF). Therefore, chemotaxis and motility were probably involved in the response of strain TT1 to Corexit exposure. One the one hand, strain TT1 was likely chemotactically attracted to Corexit components that it could metabolize. On the other hand, a pronounced negative chemotactic response to other harmful components could explain the higher abundance of different chemotactic sensor and flagellum-regulator proteins (i.e. MCPs and CheA/Y, respectively), which would align with previous observations of Corexit inhibiting some *Marinobacter* spp. (Hamdan and Fulmer, 2011; Kleindienst *et al.*, 2015b; Techtmann *et al.*, 2017; Tremblay *et al.*, 2017; Doyle *et al.*, 2018). The more abundant type IV pilus and twitching motility proteins additionally might enable strain TT1 to regulate its motility in a more sophisticated manner for this purpose, similar to *P. aeruginosa* that can synergistically utilize both flagella- and pili-mediated motility mechanisms and switch between them if needed (Conrad *et al.*, 2011). Finally, chemotaxis and motility also play important roles in biofilm establishment and formation (Sauer *et al.*, 2002; Wang *et al.*, 2013; O'Toole and Wong, 2016).

Several of our findings point towards Corexit exposure inducing changes in cellular processes associated with aggregate/biofilm formation in strain TT1 (i.e. alginate production, chemotactic motility, putative quorum sensing processes), which likely led to the distinct observed aggregate morphologies. Hydrophobic alginate-based biofilms were probably most beneficial for growth on *n*-hexadecane (Jung *et al.*, 2011; Vaysse *et al.*, 2011; Mounier *et al.*, 2014). In treatments with added Corexit, however, chemotactic processes might have resulted in stronger autoaggregation behaviour, providing a higher stress tolerance to cells utilizing *n*-hexadecane during Corexit exposure. When growing only on Corexit, HC substrates were more bioavailable and increased cell motility might have been more advantageous than aggregating when adapting

to the higher Corexit concentration. This would mirror the different biofilm phenotypes observed in *P. aeruginosa*, i.e. alginate-based mucoid biofilms versus type IV pili-mediated biofilms based on other exopolysaccharides (Ghafoor *et al.*, 2011; Wang *et al.*, 2013).

5.5.5 Environmental implications of proteomic findings

The DWH disaster was a significant offshore oil spill in deep waters and represented a unique opportunity to study the response of indigenous bacterial communities to a major influx of crude oil and chemical dispersants. However, many knowledge gaps remained regarding how to link the genetic capability of enriched taxa to their role in the degradation of oil and Corexit and how to explain the observed physiological effects caused by Corexit exposure. Our findings point towards Corexit exposure inducing changes in cellular processes associated with aggregate/biofilm formation in strain TT1, which is in agreement with previous reports showing that Corexit exposure can affect EPS secretion and aggregate formation in seawater microbial communities (Kleindienst *et al.*, 2015b; Passow, 2016; Suja *et al.*, 2017; Doyle *et al.*, 2018) and, thus, might have played an important role in the observed formation of marine oil snow during the DWH oil spill (Passow and Ziervogel, 2016). Moreover, this is the first protein-based evidence of a marine HC degrader utilizing alkanes and potentially aromatic HCs and surfactants from Corexit as carbon substrates, while adapting to Corexit exposure by additionally upregulating chemotactic motility, uptake and efflux transporters. These findings suggest that, even though strain TT1 was able to metabolize certain Corexit components, a number of additional cellular adjustments were necessary, pointing towards Corexit-induced stress experienced by the cells, such as surfactant/solvent-stress potentially affecting cell membrane functioning. Our results support the previously theorized metabolic contributions of *Marinobacter* members during the DWH oil spill (Gutierrez *et al.*, 2013b; Dombrowski *et al.*, 2016) and help explain reports of Corexit inhibiting certain HC degraders, while enriching other suspected Corexit-degrading bacteria during simulated marine oil spill scenarios.

Acknowledgements

This study was funded by the Baden-Württemberg Foundation's Elite Program for Postdocs and by the Deutsche Forschungsgemeinschaft (DFG, German Research Foundation - fellowship grant #326028733). We would also like to thank Grunde Jomaas and Kim Gustavson for providing the DUC crude oil, the U.S. National Oceanic and Atmospheric Administration for providing Corexit EC9500A, Ellen Röhm for HPLC measurements, Renate Seelig and Peter Grathwohl for GC-MS measurements, Constantin App for (CE)WAF preparation and Anja Pohl for help with culture maintenance and sampling.

5.6 Supplemental information

5.6.1 Supplemental results

Growth of *Marinobacter* sp. TT1

Growth of *Marinobacter* sp. TT1 was observed on all substrates, reaching similar orders of magnitude for almost all growth conditions. The treatments supplied with *n*-hexadecane ± Corexit, Corexit only or pyruvate had all reached cell numbers of 10^8 cells ml^{-1} at the proteome sampling timepoints (1.40 – 3.75 x 10^8 cells ml^{-1}; Fig. 1). Different macroscopic growth patterns were observed between these treatments with a classical homogeneous increase in optical density in pyruvate-containing cultures and growth in differently sized aggregates in the other three treatments (Corexit: barely visible aggregates; *n*-hexadecane: thin biofilm at water-HC interface and appr. 1-mm-sized aggregates in medium; *n*-hexadecane + Corexit: large, thin aggregates ranging from 1-1.5 cm size; Fig. S2). Even though cell numbers were lower in WAF and CEWAF treatments, growth was still observed at about one order of magnitude after four days when samples were taken for proteomics (from 6.00 x 10^5 cells ml^{-1} to 4.72 or 5.10 x 10^6 cells ml^{-1}, respectively).

5.6.2 Supplemental discussion

n-Hexadecane metabolism of *Marinobacter* sp. TT1

The pathway for *n*-hexadecane degradation of *Marinobacter* sp. TT1 is relatively analogous to the alkane metabolism of other marine alkane degraders like *M. hydrocarbonoclasticus* SP17 (Mounier *et al.*, 2014), *A. borkumensis* SK2 (Gregson *et al.*, 2019) or *Oleispira antarctica* RB-8 (Gregson *et al.*, 2020). Our results suggest important roles for the AupAB, AlkB2 and cytrochrome P450 homologues and a number of involved dehydrogenases. The AupA homologue likely enables strain TT1 to take up *n*-hexadecane from the outer membrane, with the AupB homologue guiding the alkane to the inner membrane, where the terminal oxidation machinery is located (Mounier *et al.*, 2018). Both the AlkB2 homologue and the putative cytochrome P450 hydroxylase of strain TT1 can likely perform the first oxidation step by utilizing either rubredoxin or ferredoxin (and the respective reductases) as redox partners to yield *n*-hexadecanol. The other alkane monooxygenase (AlkB1 homologue) might not have been detected in higher abundances in *n*-hexadecane treatments because it likely degrades shorter alkanes, similar to *A. borkumensis* SK2, whose AlkB1 metabolizes shorter alkanes (C5-C12), while AlkB2 degrades longer alkanes (C8-C16) (Van Beilen *et al.*, 2004). This pattern of monooxygenase induction by different substrate ranges has also been reported for other alkane degraders with multiple monooxygenases and hydroxylases (Liu *et al.*, 2011; Park *et al.*, 2017; Li *et al.*, 2020). Finally, several different dehydrogenases were detected that can perform the next oxidation steps from alcohol via aldehyde to fatty acid during *n*-hexadecane biodegradation in *Marinobacter* sp. TT1.

Differences in protein profiles of treatments with and without Corexit

The comparison of *n*-hexadecane treatments with Corexit treatments yielded large differences even though alkane metabolism was a central function of both proteomes, thus illustrating the extensive long-term cellular adaptations to both, growth in the presence of Corexit and growth on Corexit compounds. Although the proteomes detected in treatments with *n*-hexadecane and

Corexit were also distinct from *n*-hexadecane only proteomes, less significant differences were detected. This is likely because a lower concentration of Corexit was added and *n*-hexadecane metabolism seemed to be predominating under these conditions. The low number of statistically significant differences between WAF and CEWAF proteomes was likely due to less observed microbial growth and a higher inter-replicate variability caused by the more heterogeneous chemistry of these cultures. Nonetheless, these two treatments represented the most environmentally relevant simulation of water column conditions after oil spill scenarios and highlighted a few key cellular and metabolic processes induced by WAF or CEWAF addition, respectively.

5.6.3 Supplemental experimental procedures

Bacterial strain and culture conditions

The strain *Marinobacter* sp. TT1 (= *Marinobacter* sp. DSM 26291) was isolated from deep-sea plume water samples collected during the Deepwater Horizon oil spill, using *n*-hexadecane as enrichment substrate (Gutierrez *et al.*, 2013b). It is closely related to *M. salarius* R9SW1 and *M. algicola* DG893 with 99.43% and 99.07% 16S rRNA gene sequence identity, respectively. In this study, strain TT1 was cultivated on ONR7a minimal medium (Dyksterhouse *et al.*, 1995), supplemented with different carbon substrates and grown (dark, 20°C, 120 rpm on shaker) in half-filled 20 ml glass headspace vials (baked at 300°C for 8 h) with PTFE-lined crimp lids. For inoculation, 200 µl of the respective pre-cultures were transferred.

For the proteomics experiment, four different pre-cultures (originating from the same glycerol stock) were used. They were adapted to grow on one of the following carbon substrates, respectively: pyruvate, *n*-hexadecane, Corexit EC9500A, or crude oil water-accommodated fraction. At the start of the experiment, all pre-cultures were three days old and had been grown without prior Corexit exposure, with the exception of the Corexit-adapted pre-culture. The WAF solution was prepared together with a CEWAF solution for the experiment using DUC crude oil (Dutch Underground Consortium) according to (Kleindienst *et al.*, 2015b) and used within one week of preparation.

Cell counts

For cell counts, samples were fixed with 1% paraformaldehyde (PFA) and stored at 4°C until further processing. To reduce cell aggregates, 1% (w/v) EDTA was added to the samples before sonication (20% intensity, 30 seconds; Sonoplus ultrasonic homogeniser, Bandelin electronic GmbH & Co. KG), a procedure that was optimized for this culture. Samples were then filtered onto Isopore polycarbonate membrane filters (GTTP, 0.2 µm; Millipore) and stained with 4′,6-diamidino-2-phenylindole (DAPI; 1 µg ml^{-1}) for 10 min, washed with ddH_2O for 5 min, rinsed in ethanol (80%), and air dried in the dark at room temperature. Membrane filters were embedded using a 1:4 mixture of Vectashield mounting medium (Vector Laboratories, Burlingame, USA) and Citifluor AF2 glycerol solution (EMS Acquisition Corp., Hatfield, USA) before the slides were analyzed using fluorescence microscopy (Leica DM 5500 B; Leica Microsystems). Images were taken at a magnification of 1000x with a Leica DFC 360 FX camera using the Leica Application Suite Advanced Fluorescence software (2.6.0.766). Cell counts of the images were performed using the 'Find Maxima' function (noise tolerance = 7)

of the Fiji distribution of ImageJ (Schindelin *et al.*, 2012), counting a minimum of 20 images and 600 cells per sample.

Pyruvate and hydrocarbon quantification

Pyruvate was quantified by high-performance liquid chromatography (HPLC; Shimadzu Prominence, Japan) equipped with an Aminex HPX 87H column (Bio Rad, Austria) and a SPD-M10A VP photo-diode array detector (flow rate 0.6 ml min^{-1}; oven at 40°C, 5 mM H_2SO_4 as eluent).

For *n*-hexadecane quantification, deuterated *n*-hexadecane (D34, Sigma-Aldrich, St. Louis, USA) was added to the samples as internal standard (20 mg l^{-1}) before extracting the entire vial using 9 ml cyclohexane (purity 99.9%, Carl ROTH, Karlsruhe, Germany). Vials were shaken at 300 rpm for half an hour, phases were allowed to separate overnight and subsamples of the cyclohexane were used to quantify the remaining *n*-hexadecane concentrations via gas chromatography (Agilent 6890N GC) coupled with mass spectrometry (Agilent 5973 MS). For separation, a J + W Scientific DB-5MS (30 m length, 0.25 mm ID, 0.25 µm film thickness) capillary column was used. The device was operated in a pulsed splitless mode with a Helium flow of 0.8 ml/min. Oven temperature was initiated at 65°C (4 min), then ramped at 10°C/min to 220°C, further ramped at 20°C/min to 310°C and held at this temperature for 5 min.

5.6.4 Supplemental figures

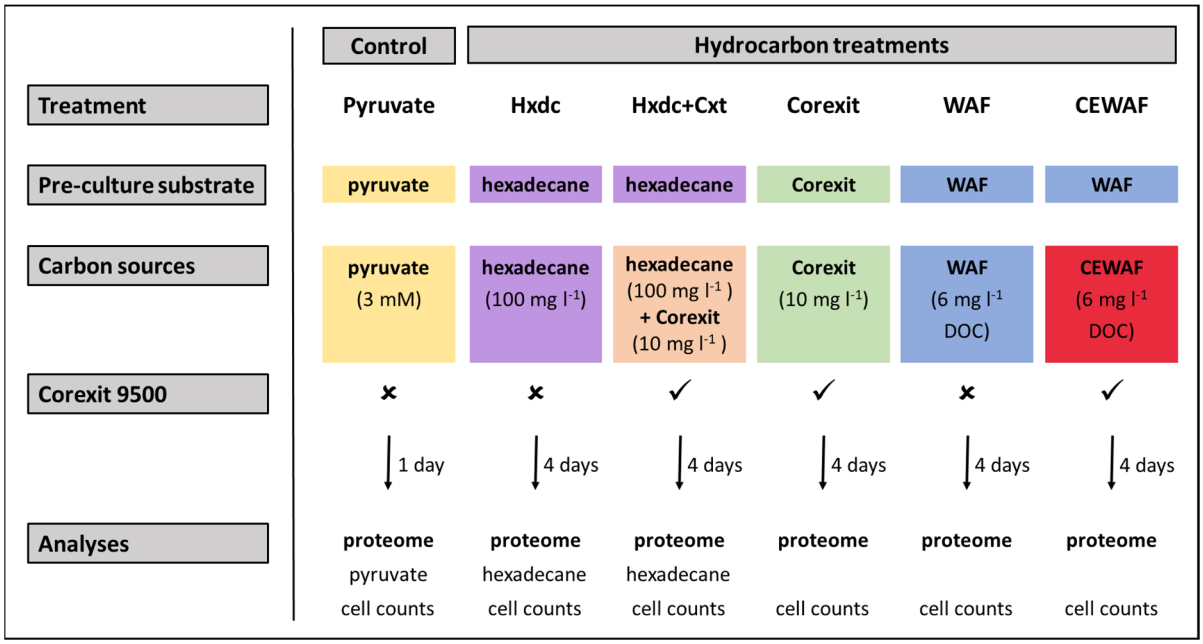

Figure S 5.1: Overview of culture conditions assessed in this proteomics study. Additional non-proteomics treatments included an inoculated control culture with no added substrate and abiotic controls containing either 100 mg l^{-1} *n*-hexadecane or 100 mg l^{-1} *n*-hexadecane and 10 mg l^{-1} Corexit. Abbreviations: Hxdc = *n*-hexadecane, Cxt = Corexit EC9500A, WAF = water-accommodated fraction, CEWAF = chemically enhanced WAF, DOC = dissolved organic carbon.

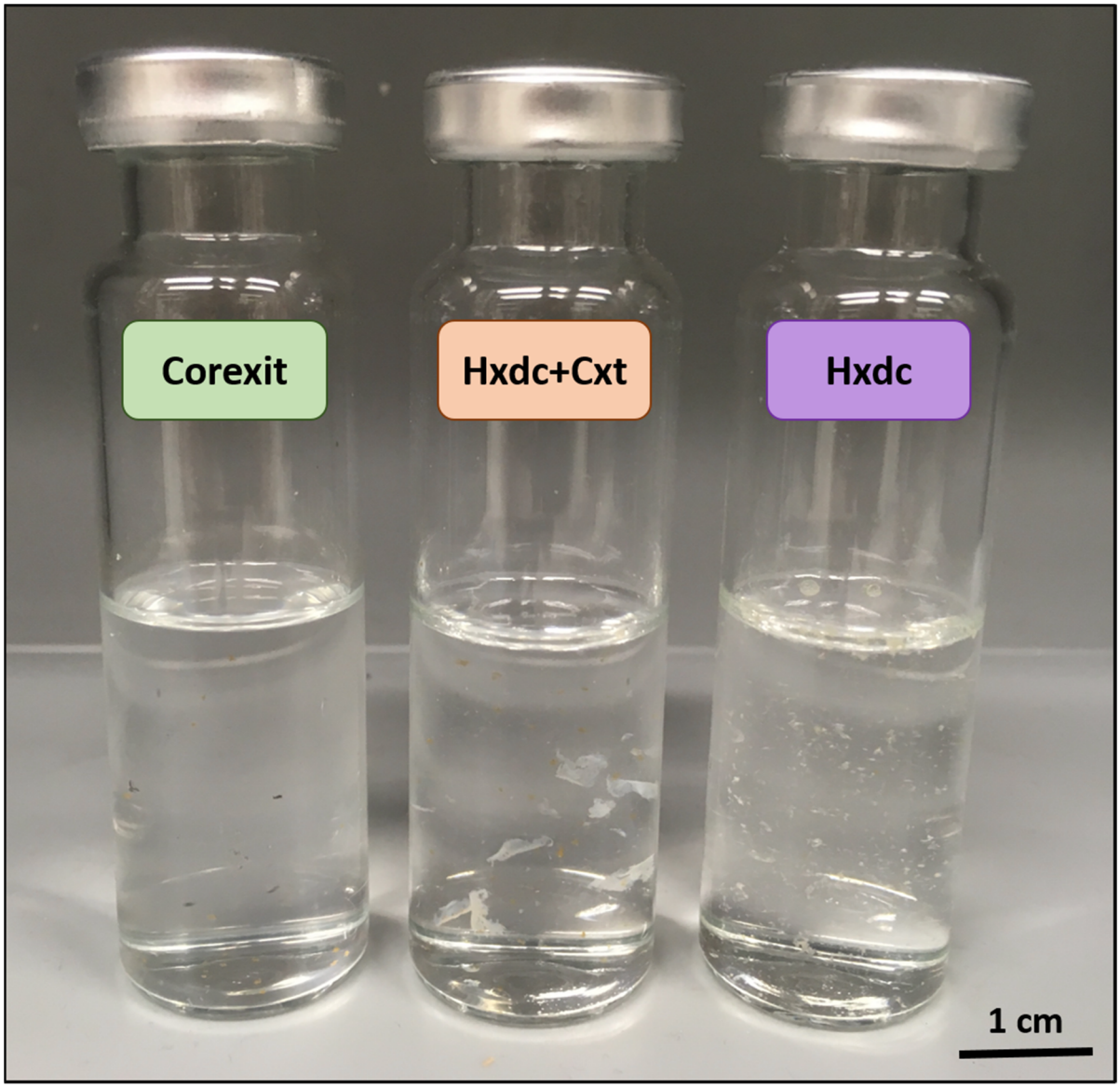

Figure S 5.2: Aggregate morphology in *Marinobacter* sp. TT1 cultures after four days of incubation. Treatments contained the following carbon sources: 100 mg l^{-1} Corexit (Corexit), 100 mg l^{-1} *n*-hexadecane and 10 mg l^{-1} Corexit (Hxdc+Cxt), or 100 mg l^{-1} *n*-hexadecane (Hxdc).

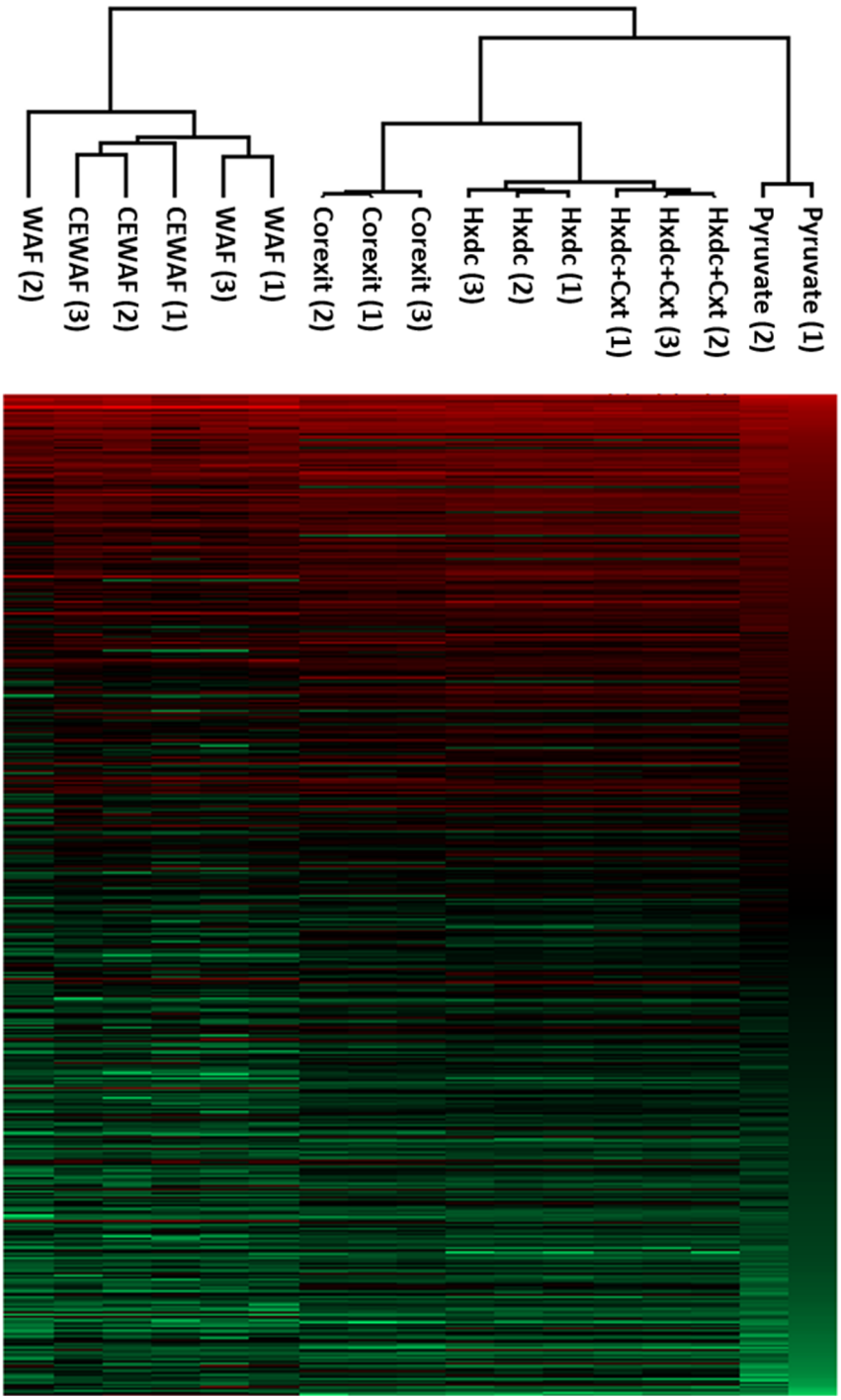

Figure S 5.3: Hierarchical clustering analysis (including heatmap) of protein expression profiles of *Marinobacter* sp. TT1 cultures after 1 day (pyruvate treatments) or 4 days (all other treatments) of incubation. Treatments received the following carbon sources: 3 mM (264 mg l^{-1}) pyruvate (Pyruvate), 100 mg l^{-1} *n*-hexadecane (Hxdc), 100 mg l^{-1} *n*-hexadecane and 10 mg l^{-1} Corexit (Hxdc+Cxt), 100 mg l^{-1} Corexit (Corexit), 6 mg l^{-1} WAF-derived DOC (WAF), or 6 mg l^{-1} chemically enhanced WAF-derived DOC (CEWAF).

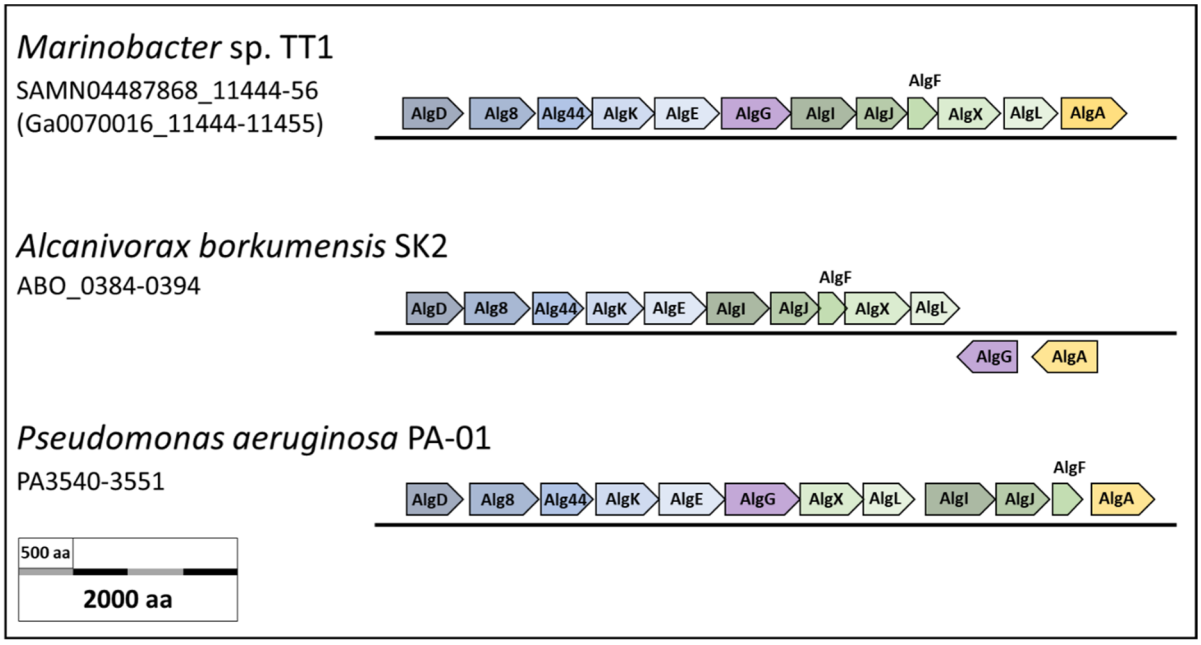

Figure S 5.4: Genetic organization of alginate operons in *Pseudomonas aeruginosa* PAO1 (IMG genome ID: 637000218), *Alcanivorax borkumensis* SK2 (IMG genome ID: 637000004) and the proposed alginate operon in *Marinobacter* sp. TT1 (displayed gene names based on genome annotation and/or homologous *P. aeruginosa* genes; IMG genome ID: 2619618959).

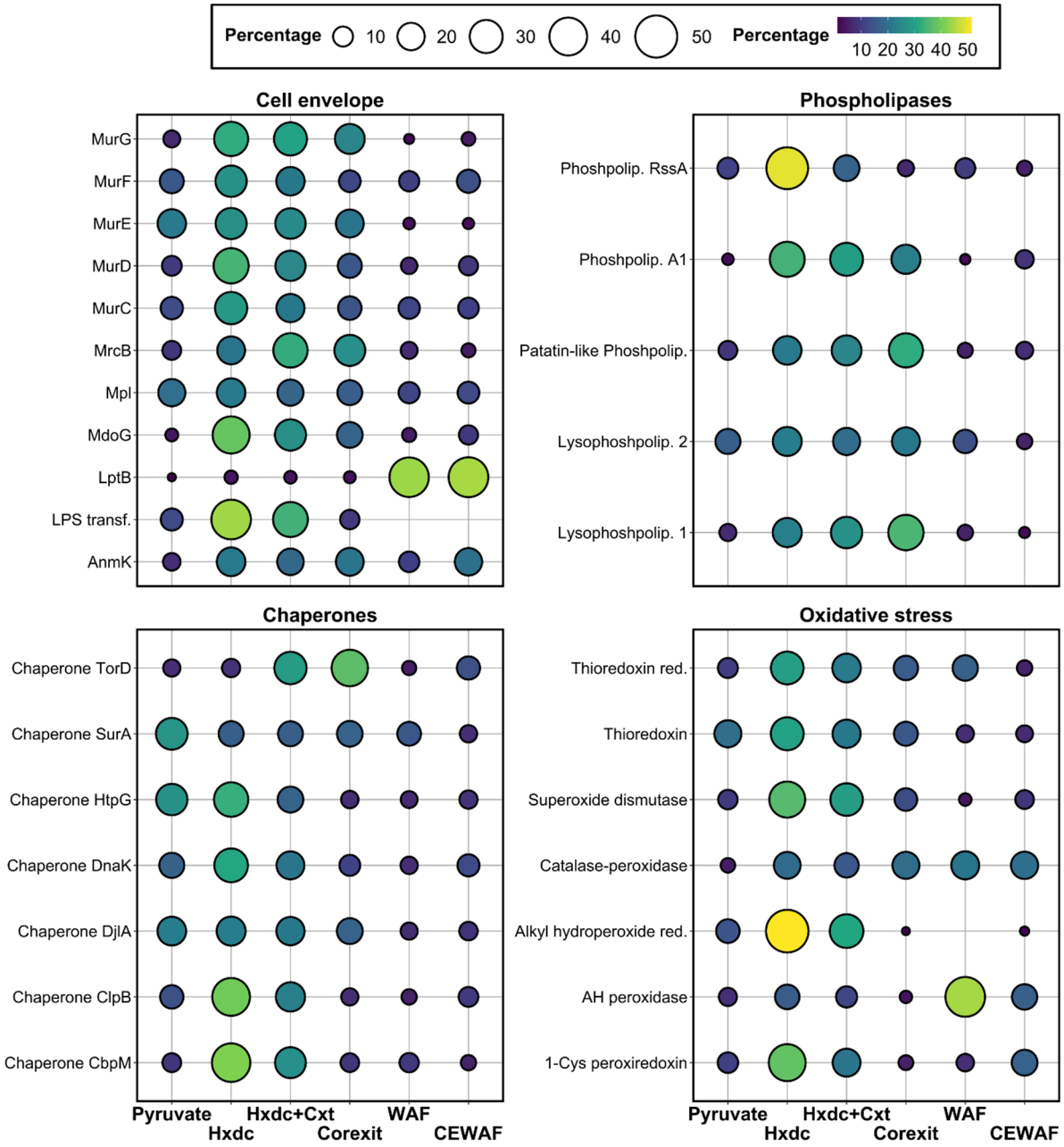

Figure S 5.5: Normalized, relative mean abundances (symbolized by circle size and colour; sum per protein = 100%) of significantly (*q*-value < 0.05) differentially expressed proteins associated with peptidoglycan and LPS synthesis (Cell envelope), phospholipases, chaperones, oxidative stress response enzymes during growth of *Marinobacter* sp. TT1 cultures on different carbon sources. Treatments received either pyruvate, *n*-hexadecane (Hxdc), *n*-hexadecane and Corexit (Hxdc+Cxt), only Corexit (Corexit), crude oil WAF, or chemically enhanced WAF (CEWAF). Protein names/abbreviations given as indicated in Tab. S8.

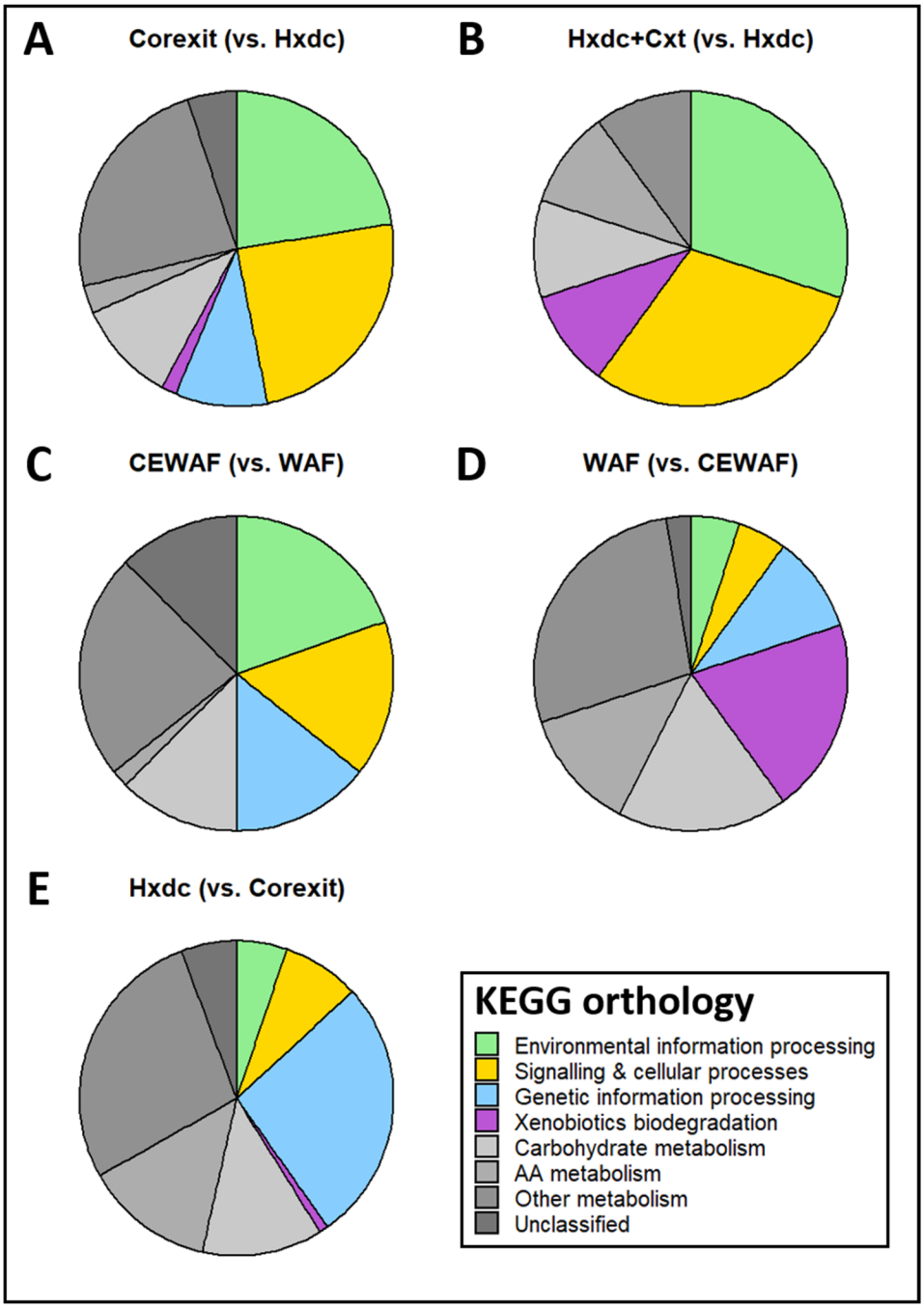

Figure S 5.6: KEGG orthology annotations for significantly (p-value < 0.05; WAF vs. CEWAF: t-test p-value < 0.05) more abundant proteins in pairwise comparisons of *Marinobacter* sp. TT1 proteomes during growth on different carbon sources. Treatments received either pyruvate, *n*-hexadecane (Hxdc), *n*-hexadecane and Corexit (Hxdc+Cxt), only Corexit (Corexit), crude oil WAF, or chemically enhanced WAF (CEWAF). **A)** Significantly upregulated proteins in Corexit compared to Hxdc cultures. **B)** Significantly upregulated proteins in Hxdc+Cxt compared to Hxdc cultures. **C)** Significantly upregulated proteins in CEWAF compared to WAF cultures. **D)** Significantly upregulated proteins in WAF compared to CEWAF cultures. **E)** Significantly upregulated proteins in Hxdc compared to Corexit cultures.

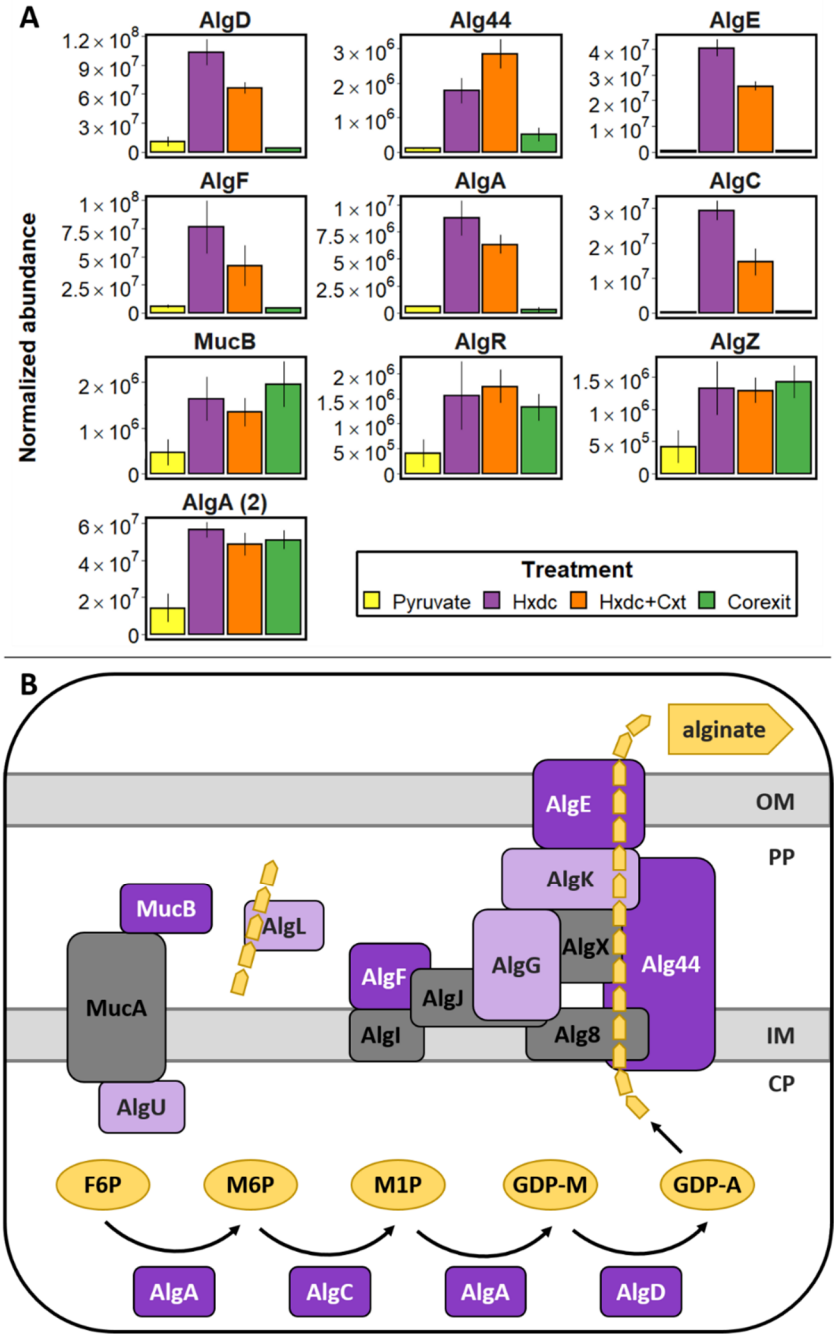

Figure S 5.7: Alginate biosynthesis and export in *Marinobacter* sp. TT1. **A)** Normalized abundances (averages ± SD; n = 3) of significantly (*q*-value < 0.05) differentially abundant alginate protein homologues during growth on different carbon sources. Treatments received 3 mM (264 mg l^{-1}) pyruvate (Pyruvate), 100 mg l^{-1} *n*-hexadecane (Hxdc), 100 mg l^{-1} *n*-hexadecane and 10 mg l^{-1} Corexit (Hxdc+Cxt), or 100 mg l^{-1} Corexit (Corexit). **B)** Schematic overview of the proposed alginate biosynthesis complex in *Marinobacter* sp. TT1 based on the alginate complex in *Pseudomonas aeruginosa* (Hay *et al.*, 2013). Proteins are coloured in dark purple, light purple or grey to illustrate significantly higher abundances in *n*-hexadecane compared to pyruvate treatments, their detection or lack thereof in this study, respectively. Protein names given as indicated in Tab. S8. OM/IM = outer/inner membrane; PP/CP = periplasm/cytoplasm; F6P = Fructose-6-phoshate; M6P/M1P = Mannose-6-phosphate/-1-phosphate; GDP-M/A = Guanosine diphosphate-mannose/mannuronic acid.

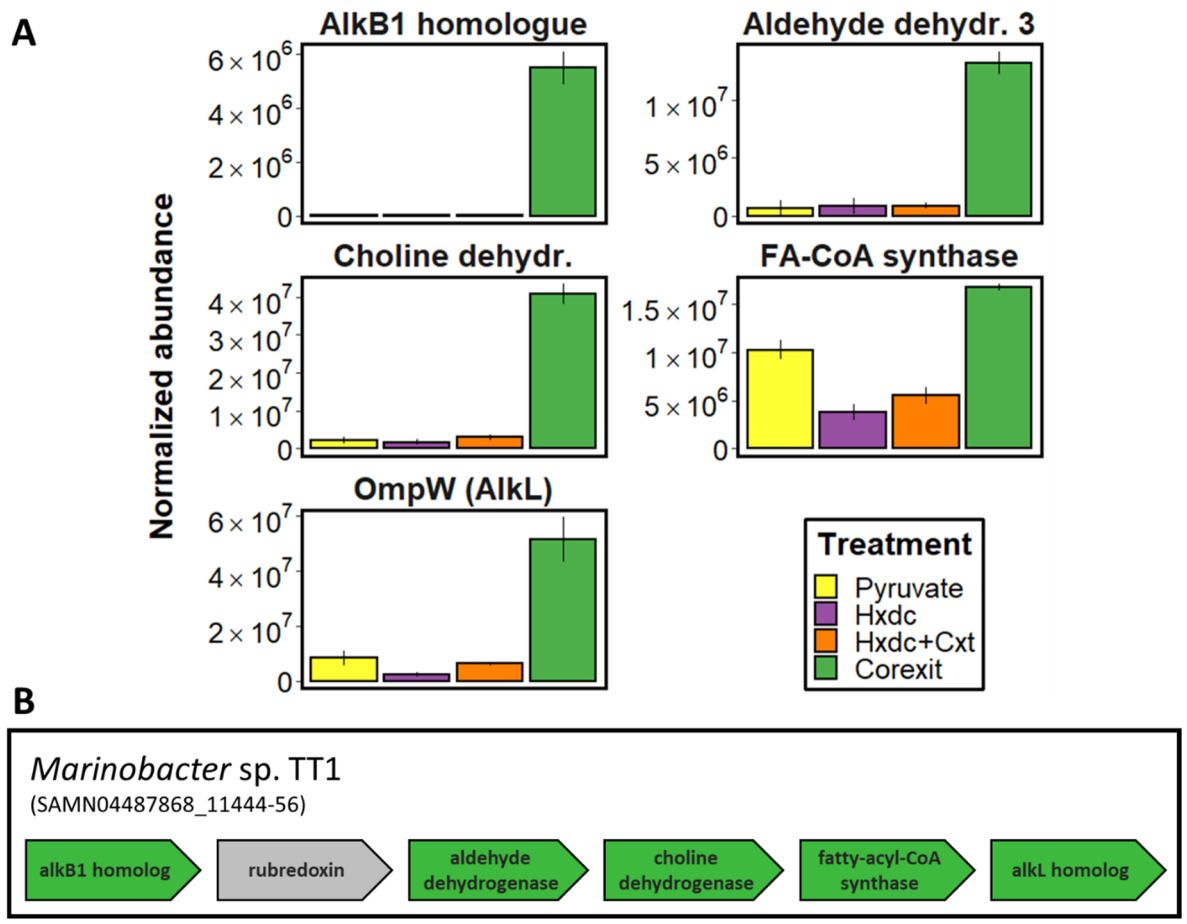

Figure S 5.8: Proposed *alk* operon in *Marinobacter* sp. TT1. **A)** Normalized abundances (averages ± SD; n = 3) of significantly ($q < 0.05$) differentially expressed proteins of the *alkB1* homologue operon during growth on different carbon sources. Treatments received either pyruvate, *n*-hexadecane (Hxdc), *n*-hexadecane and Corexit (Hxdc+Cxt), or only Corexit (Corexit). **B)** Schematic representation of the genes downstream of *alkB1* (proposed *alk* operon; SAMN04487868_109138-42) in the genome of *Marinobacter* sp. TT1. Proteins encoded by green genes were significantly more abundant in Corexit treatments compared to Pyruvate, Hxdc or Hxdc+Cxt treatments. Proteins encoded by grey genes were not detected in this study. Protein names given as indicated in Tab. S8.

5.6.5 Supplemental tables

For supplemental tables, please refer to the appendix of this thesis.

5.7 References

Abbasian, F., Lockington, R., Megharaj, M., and Naidu, R. (2016) A review on the genetics of aliphatic and aromatic hydrocarbon degradation. *Appl Biochem Biotechnol* **178**(2): 224-250.

Altschul, S.F., Gish, W., Miller, W., Myers, E.W., and Lipman, D.J. (1990) Basic local alignment search tool. *J Mol Biol* **215**(3): 403-410.

Aubé, J., Senin, P., Bonin, P., Pringault, O., Jeziorski, C., Bouchez, O. *et al.* (2020) Meta-omics provides insights into the impact of hydrocarbon contamination on microbial mat functioning. *Microb Ecol*: 1-10.

Bælum, J., Borglin, S., Chakraborty, R., Fortney, J.L., Lamendella, R., Mason, O.U. *et al.* (2012) Deep-sea bacteria enriched by oil and dispersant from the Deepwater Horizon spill. *Environ Microbiol* **14**(9): 2405-2416.

Barbato, M., Scoma, A., Mapelli, F., De Smet, R., Banat, I.M., Daffonchio, D. *et al.* (2016) Hydrocarbonoclastic *Alcanivorax* isolates exhibit different physiological and expression responses to *n*-dodecane. *Front Microbiol* **7**: 1-14.

Bera, G., Doyle, S., Passow, U., Kamalanathan, M., Wade, T.L., Sylvan, J.B. *et al.* (2020) Biological response to dissolved versus dispersed oil. *Mar Pollut Bull* **150**: 110713.

Bonin, P., Vieira, C., Grimaud, R., Militon, C., Cuny, P., Lima, O. *et al.* (2015) Substrates specialization in lipid compounds and hydrocarbons of *Marinobacter* genus. *Environ Sci Pollut Res* **22**(20): 15347-15359.

Chae, J.-C., and Zylstra, G.J. (2006) 4-Chlorobenzoate uptake in *Comamonas* sp. strain DJ-12 is mediated by a tripartite ATP-independent periplasmic transporter. *J Bacteriol* **188**(24): 8407-8412.

Chakraborty, R., Borglin, S.E., Dubinsky, E.A., Andersen, G.L., and Hazen, T.C. (2012) Microbial response to the MC-252 oil and Corexit 9500 in the Gulf of Mexico. *Front Microbiol* **3**: 357.

Chen, I.-M.A., Chu, K., Palaniappan, K., Pillay, M., Ratner, A., Huang, J. *et al.* (2019) IMG/M v. 5.0: An integrated data management and comparative analysis system for microbial genomes and microbiomes. *Nucleic Acids Res* **47**(D1): D666-D677.

Choyke, S., and Ferguson, P.L. (2019) Molecular characterization of nonionic surfactant components of the Corexit 9500® oil spill dispersant by high-resolution mass spectrometry. *Rapid Commun Mass Spectrom* **33**(22): 1683-1694.

Conrad, J.C., Gibiansky, M.L., Jin, F., Gordon, V.D., Motto, D.A., Mathewson, M.A. *et al.* (2011) Flagella and pili-mediated near-surface single-cell motility mechanisms in *P. aeruginosa*. *Biophys J* **100**(7): 1608-1616.

Davidson, A.L., Dassa, E., Orelle, C., and Chen, J. (2008) Structure, function, and evolution of bacterial ATP-binding cassette systems. *Microbiol Mol Biol Rev* **72**(2): 317-364.

Dombrowski, N., Donaho, J.A., Gutierrez, T., Seitz, K.W., Teske, A.P., and Baker, B.J. (2016) Reconstructing metabolic pathways of hydrocarbon-degrading bacteria from the Deepwater Horizon oil spill. *Nat Microbiol* **1**(7): 1-7.

Doyle, S.M., Whitaker, E.A., De Pascuale, V., Wade, T.L., Knap, A.H., Santschi, P.H. *et al.* (2018) Rapid formation of microbe-oil aggregates and changes in community composition in coastal surface water following exposure to oil and the dispersant Corexit. *Front Microbiol* **9**: 689.

Duran, R. (2010) *Marinobacter*. *Handbook of Hydrocarbon and Lipid Microbiology*. Timmis, K.N. (ed). Heidelberg, Germany: Springer, pp. 1725-1735. 10.1007/978-3-540-77587-4_122.

Dyksterhouse, S.E., Gray, J.P., Herwig, R.P., Lara, J.C., and Staley, J.T. (1995) *Cycloclasticus pugetii* gen. nov., sp. nov., an aromatic hydrocarbon-degrading bacterium from marine sediments. *Int J Syst Bacteriol* **45**(1): 116-123.

Ennouri, H., d'Abzac, P., Hakil, F., Branchu, P., Naïtali, M., Lomenech, A.M. *et al.* (2017) The extracellular matrix of the oleolytic biofilms of *Marinobacter hydrocarbonoclasticus* comprises cytoplasmic proteins and T2SS effectors that promote growth on hydrocarbons and lipids. *Environ Microbiol* **19**(1): 159-173.

Faksness, L.-G., Brandvik, P.J., and Sydnes, L.K. (2008) Composition of the water accommodated fractions as a function of exposure times and temperatures. *Mar Pollut Bull* **56**(10): 1746-1754.

Gacesa, P. (1998) Bacterial alginate biosynthesis: Recent progress and future prospects. *Microbiology* **144**: 1133-1143.

Garcia, M., Campos, E., Marsal, A., and Ribosa, I. (2009) Biodegradability and toxicity of sulphonate-based surfactants in aerobic and anaerobic aquatic environments. *Water Res* **43**(2): 295-302.

Ghafoor, A., Hay, I.D., and Rehm, B.H. (2011) Role of exopolysaccharides in *Pseudomonas aeruginosa* biofilm formation and architecture. *Appl Environ Microbiol* **77**(15): 5238-5246.

Giuliani, S.E., Frank, A.M., Corgliano, D.M., Seifert, C., Hauser, L., and Collart, F.R. (2011) Environment sensing and response mediated by ABC transporters. *BMC Genomics* **12**(1): 1-14.

Grant, C., Deszcz, D., Wei, Y.-C., Martinez-Torres, R.J., Morris, P., Folliard, T. *et al.* (2014) Identification and use of an alkane transporter plug-in for applications in biocatalysis and whole-cell biosensing of alkanes. *Sci Rep* **4**: 5844.

Green, D.H., Bowman, J.P., Smith, E.A., Gutierrez, T., and Bolch, C.J. (2006) *Marinobacter algicola* sp. nov., isolated from laboratory cultures of paralytic shellfish toxin-producing dinoflagellates. *Int J Syst Evol Microbiol* **56**(3): 523-527.

Gregson, B.H., Metodieva, G., Metodiev, M.V., and McKew, B.A. (2019) Differential protein expression during growth on linear versus branched alkanes in the obligate marine hydrocarbon-degrading bacterium *Alcanivorax borkumensis* SK2(T). *Environ Microbiol* **21**(7): 2347-2359.

Gregson, B.H., Metodieva, G., Metodiev, M.V., Golyshin, P.N., and McKew, B.A. (2020) Protein expression in the obligate hydrocarbon-degrading psychrophile *Oleispira antarctica* RB-8 during alkane degradation and cold tolerance. *Environ Microbiol* **22**(5): 1870-1883.

Gunasekera, T.S., Striebich, R.C., Mueller, S.S., Strobel, E.M., and Ruiz, O.N. (2013) Transcriptional profiling suggests that multiple metabolic adaptations are required for effective proliferation of *Pseudomonas aeruginosa* in jet fuel. *Environ Sci Technol* **47**(23): 13449-13458.

Gutierrez, T., Singleton, D.R., Berry, D., Yang, T., Aitken, M.D., and Teske, A. (2013) Hydrocarbon-degrading bacteria enriched by the Deepwater Horizon oil spill identified by cultivation and DNA-SIP. *ISME J* **7**(11): 2091-2104.

Haange, S.-B., Jehmlich, N., Hoffmann, M., Weber, K., Lehmann, J.r., von Bergen, M., and Slanina, U. (2019) Disease development is accompanied by changes in bacterial protein abundance and functions in a refined model of dextran sulfate sodium (DSS)-induced colitis. *J Proteome Res* **18**(4): 1774-1786.

Hackbusch, S., Noirungsee, N., Viamonte, J., Sun, X., Bubenheim, P., Kostka, J.E. *et al.* (2020) Influence of pressure and dispersant on oil biodegradation by a newly isolated *Rhodococcus* strain from deep-sea sediments of the Gulf of Mexico. *Mar Pollut Bull* **150**: 110683.

Hales, S.G. (1993) Biodegradation of the anionic surfactant dialkyl sulphosuccinate. *Environ Toxicol Chem* **12**(10): 1821-1828.

Hamdan, L.J., and Fulmer, P.A. (2011) Effects of Corexit EC9500A on bacteria from a beach oiled by the Deepwater Horizon spill. *Aquat Microb Ecol* **63**(2): 101-109.

Hay, I.D., Ur Rehman, Z., Moradali, M.F., Wang, Y., and Rehm, B.H. (2013) Microbial alginate production, modification and its applications. *Microb Biotechnol* **6**(6): 637-650.

Hosie, A.H., Allaway, D., Jones, M., Walshaw, D., Johnston, A., and Poole, P.S. (2001) Solute-binding protein-dependent ABC transporters are responsible for solute efflux in addition to solute uptake. *Mol Microbiol* **40**(6): 1449-1459.

Inacio, A.S., Domingues, N.S., Nunes, A., Martins, P.T., Moreno, M.J., Estronca, L.M. *et al.* (2016) Quaternary ammonium surfactant structure determines selective toxicity towards bacteria: Mechanisms of action and clinical implications in antibacterial prophylaxis. *J Antimicrob Chemother* **71**(3): 641-654.

Jones, P.M., and George, A.M. (2013) Mechanism of the ABC transporter ATPase domains: Catalytic models and the biochemical and biophysical record. *Crit Rev Biochem Mol Biol* **48**(1): 39-50.

Julsing, M.K., Schrewe, M., Cornelissen, S., Hermann, I., Schmid, A., and Bühler, B. (2012) Outer membrane protein AlkL boosts biocatalytic oxyfunctionalization of hydrophobic substrates in *Escherichia coli*. *Appl Environ Microbiol* **78**(16): 5724-5733.

Jung, J., Noh, J., and Park, W. (2011) Physiological and metabolic responses for hexadecane degradation in *Acinetobacter oleivorans* DR1. *The Journal of Microbiology* **49**(2): 208-215.

Kanehisa, M., Sato, Y., and Morishima, K. (2016) BlastKOALA and GhostKOALA: KEGG tools for functional characterization of genome and metagenome sequences. *J Mol Biol* **428**(4): 726-731.

Kanehisa, M., and Sato, Y. (2020) KEGG mapper for inferring cellular functions from protein sequences. *Protein Sci* **29**(1): 28-35.

Kato, T., Miyanaga, A., Kanaya, S., and Morikawa, M. (2009) Alkane inducible proteins in *Geobacillus thermoleovorans* B23. *BMC Microbiology* **9**(1): 60.

Kleindienst, S., Seidel, M., Ziervogel, K., Grim, S., Loftis, K., Harrison, S. *et al.* (2015) Chemical dispersants can suppress the activity of natural oil-degrading microorganisms. *Proc Natl Acad Sci USA* **112**(48): 14900-14905.

Kover, S.C., Rosario-Ortiz, F.L., and Linden, K.G. (2014) Photochemical fate of solvent constituents of Corexit oil dispersants. *Water Res* **52**: 101-111.

Krell, T., Lacal, J., Guazzaroni, M.E., Busch, A., Silva-Jimenez, H., Fillet, S. *et al.* (2012) Responses of *Pseudomonas putida* to toxic aromatic carbon sources. *J Biotechnol* **160**(1-2): 25-32.

Li, Y., Pan, J., and Ma, Y. (2020) Elucidation of multiple alkane hydroxylase systems in biodegradation of crude oil *n*-alkane pollution by *Pseudomonas aeruginosa* DN1. *J Appl Microbiol* **128**(1): 151-160.

Liu, C., Wang, W., Wu, Y., Zhou, Z., Lai, Q., and Shao, Z. (2011) Multiple alkane hydroxylase systems in a marine alkane degrader *Alcanivorax dieselolei* B-5. *Environ Microbiol* **13**(5): 1168-1178.

Liu, S., Guo, C., Lin, W., Wu, F., Lu, G., Lu, J., and Dang, Z. (2017) Comparative transcriptomic evidence for Tween80-enhanced biodegradation of phenanthrene by *Sphingomonas* sp. GY2B. *Sci Total Environ* **609**: 1161-1171.

Manilla-Pérez, E., Reers, C., Baumgart, M., Hetzler, S., Reichelt, R., Malkus, U. *et al.* (2010) Analysis of lipid export in hydrocarbonoclastic bacteria of the genus *Alcanivorax*: Identification of lipid export-negative mutants of *Alcanivorax borkumensis* SK2 and *Alcanivorax jadensis* T9. *J Bacteriol* **192**(3): 643-656.
McFarlin, K.M., Prince, R.C., Perkins, R., and Leigh, M.B. (2014) Biodegradation of dispersed oil in arctic seawater at -1°C. *PloS One* **9**(1): e84297.
McFarlin, K.M., Perkins, M.J., Field, J.A., and Leigh, M.B. (2018) Biodegradation of crude oil and Corexit 9500 in Arctic seawater. *Front Microbiol* **9**: 1788.
McNutt, M.K., Camilli, R., Crone, T.J., Guthrie, G.D., Hsieh, P.A., Ryerson, T.B. *et al.* (2012) Review of flow rate estimates of the Deepwater Horizon oil spill. *Proc Natl Acad Sci USA* **109**(50): 20260-20267.
Michalska, K., Chang, C., Mack, J.C., Zerbs, S., Joachimiak, A., and Collart, F.R. (2012) Characterization of transport proteins for aromatic compounds derived from lignin: Benzoate derivative binding proteins. *J Mol Biol* **423**(4): 555-575.
Moradali, M.F., and Rehm, B.H. (2019) The role of alginate in bacterial biofilm formation. *Extracellular Sugar-Based Biopolymers Matrices*. Cohen, E., and Merzendorfer, H. (eds): Springer, pp. 517-537.
Mounier, J., Camus, A., Mitteau, I., Vaysse, P.J., Goulas, P., Grimaud, R., and Sivadon, P. (2014) The marine bacterium *Marinobacter hydrocarbonoclasticus* SP17 degrades a wide range of lipids and hydrocarbons through the formation of oleolytic biofilms with distinct gene expression profiles. *FEMS Microbiolgy Ecology* **90**(3): 816-831.
Mounier, J., Hakil, F., Branchu, P., Naïtali, M., Goulas, P., Sivadon, P., and Grimaud, R. (2018) AupA and AupB are outer and inner membrane proteins involved in alkane uptake in *Marinobacter hydrocarbonoclasticus* SP17. *mBio* **9**(3): e00520-00518.
Mulligan, C., Fischer, M., and Thomas, G.H. (2011) Tripartite ATP-independent periplasmic (TRAP) transporters in bacteria and archaea. *FEMS Microbiol Rev* **35**(1): 68-86.
Murínová, S., and Dercová, K. (2014) Response mechanisms of bacterial degraders to environmental contaminants on the level of cell walls and cytoplasmic membrane. *Int J Microbiol* **2014**: 873081.
Ng, H.J., Lopez-Perez, M., Webb, H.K., Gomez, D., Sawabe, T., Ryan, J. *et al.* (2014) *Marinobacter salarius* sp. nov. and *Marinobacter similis* sp. nov., isolated from sea water. *PLoS One* **9**(9): e106514.
Noda, K.-I., Watanabe, K., and Maruhashi, K. (2003) Isolation of the *Pseudomonas aeruginosa* gene affecting uptake of dibenzothiophene in *n*-tetradecane. *J Biosci Bioeng* **95**(5): 504-511.
Nowak, A., and Mrozik, A. (2016) Facilitation of co-metabolic transformation and degradation of monochlorophenols by *Pseudomonas* sp. CF600 and changes in its fatty acid composition. *Water Air Soil Pollut* **227**(3): 83.
O'Toole, G.A., and Wong, G.C. (2016) Sensational biofilms: Surface sensing in bacteria. *Curr Opin Microbiol* **30**: 139-146.
Overholt, W.A., Marks, K.P., Romero, I.C., Hollander, D.J., Snell, T.W., and Kostka, J.E. (2016) Hydrocarbon-degrading bacteria exhibit a species-specific response to dispersed oil while moderating ecotoxicity. *Appl Environ Microbiol* **82**(2): 518-527.
Ozhan, K., Parsons, M.L., and Bargu, S. (2014) How were phytoplankton affected by the Deepwater Horizon oil spill? *BioScience* **64**(9): 829-836.
Parales, R.E., and Ditty, J.L. (2017) Chemotaxis to hydrocarbons. *Cellular Ecophysiology of Microbe. Handbook of Hydrocarbon and Lipid Microbiology*. Krell, T. (ed): Springer International Publishing, pp. 1-20. 10.1007/978-3-319-20796-4_43-1.
Park, C., Shin, B., Jung, J., Lee, Y., and Park, W. (2017) Metabolic and stress responses of *Acinetobacter oleivorans* DR1 during long-chain alkane degradation. *Microb Biotechnol* **10**(6): 1809-1823.
Partearroyo, M.A., Ostolaza, H., Goñi, F.M., and Barberá-Guillem, E. (1990) Surfactant-induced cell toxicity and cell lysis: A study using B16 melanoma cells. *Biochem Pharmacol* **40**(6): 1323-1328.
Passow, U. (2016) Formation of rapidly-sinking, oil-associated marine snow. *Deep Sea Res Part II Top Stud Oceanogr* **129**: 232-240.
Passow, U., and Ziervogel, K. (2016) Marine snow sedimented oil released during the Deepwater Horizon spill. *Oceanography* **29**(3): 118-125.
Peña-Montenegro, T.D., Kleindienst, S., Allen, A.E., Eren, M.A., Sánchez, J.A., Arnold, J., and Joye, S.B. (unpublished) Metatranscriptomic analysis reveals responses of deepsea microbial communities to oil and dispersant exposure.
Perez-Riverol, Y., Csordas, A., Bai, J., Bernal-Llinares, M., Hewapathirana, S., Kundu, D.J. *et al.* (2019) The PRIDE database and related tools and resources in 2019: Improving support for quantification data. *Nucleic Acids Res* **47**(D1): D442-D450.
Place, B.J., Perkins, M.J., Sinclair, E., Barsamian, A.L., Blakemore, P.R., and Field, J.A. (2016) Trace analysis of surfactants in Corexit oil dispersant formulations and seawater. *Deep Sea Res Part II Top Stud Oceanogr* **129**: 273-281.

Prince, R., Kelley, B., and Butler, J. (2016) Three widely-available dispersants substantially increase the biodegradation of otherwise undispersed oil. *J Marine Sci Res Dev* **6**(183).
R Core Team (2019). R: A language and environment for statistical computing. Vienna, Austria.
Radniecki, T.S., Schneider, M.C., and Semprini, L. (2013) The influence of Corexit 9500A and weathering on Alaska North Slope crude oil toxicity to the ammonia oxidizing bacterium *Nitrosomonas europaea*. *Mar Pollut Bull* **68**(1-2): 64-70.
Ramos, J.L., Duque, E., Gallegos, M.T., Godoy, P., Ramos-Gonzalez, M.I., Rojas, A. *et al.* (2002) Mechanisms of solvent tolerance in gram-negative bacteria. *Annu Rev Microbiol* **56**: 743-768.
Rico-Martínez, R., Snell, T.W., and Shearer, T.L. (2013) Synergistic toxicity of Macondo crude oil and dispersant Corexit 9500A® to the *Brachionus plicatilis* species complex (Rotifera). *Environ Pollut* **173**: 5-10.
Rivers, A.R., Sharma, S., Tringe, S.G., Martin, J., Joye, S.B., and Moran, M.A. (2013) Transcriptional response of bathypelagic marine bacterioplankton to the Deepwater Horizon oil spill. *ISME J* **7**(12): 2315-2329.
Rosa, L.T., Bianconi, M.E., Thomas, G.H., and Kelly, D.J. (2018) Tripartite ATP-independent periplasmic (TRAP) transporters and tripartite tricarboxylate transporters (TTT): From uptake to pathogenicity. *Front Cell Infect Microbiol* **8**: 33.
Sabirova, J.S., Becker, A., Lünsdorf, H., Nicaud, J.-M., Timmis, K.N., and Golyshin, P.N. (2011) Transcriptional profiling of the marine oil-degrading bacterium *Alcanivorax borkumensis* during growth on *n*-alkanes. *FEMS Microbiol Lett* **319**(2): 160-168.
Salmon, R.C., Cliff, M.J., Rafferty, J.B., and Kelly, D.J. (2013) The CouPSTU and TarPQM transporters in *Rhodopseudomonas palustris*: Redundant, promiscuous uptake systems for lignin-derived aromatic substrates. *PloS One* **8**(3): e59844.
Sauer, K., Camper, A.K., Ehrlich, G.D., Costerton, J.W., and Davies, D.G. (2002) *Pseudomonas aeruginosa* displays multiple phenotypes during development as a biofilm. *J Bacteriol* **184**(4): 1140-1154.
Schindelin, J., Arganda-Carreras, I., Frise, E., Kaynig, V., Longair, M., Pietzsch, T. *et al.* (2012) Fiji: An open-source platform for biological image analysis. *Nat Methods* **9**(7): 676–682.
Schneiker, S., Martins dos Santos, V.A., Bartels, D., Bekel, T., Brecht, M., Buhrmester, J. *et al.* (2006) Genome sequence of the ubiquitous hydrocarbon-degrading marine bacterium *Alcanivorax borkumensis*. *Nat Biotechnol* **24**(8): 997-1004.
Seidel, M., Kleindienst, S., Dittmar, T., Joye, S.B., and Medeiros, P.M. (2016) Biodegradation of crude oil and dispersants in deep seawater from the Gulf of Mexico: Insights from ultra-high resolution mass spectrometry. *Deep Sea Res Part II Top Stud Oceanogr* **129**: 108-118.
Shitashiro, M., Tanaka, H., soo Hong, C., Kuroda, A., Takiguchi, N., Ohtake, H., and Kato, J. (2005) Identification of chemosensory proteins for trichloroethylene in *Pseudomonas aeruginosa*. *J Biosci Bioeng* **99**(4): 396-402.
Sikkema, J., de Bont, J.A., and Poolman, B. (1995) Mechanisms of membrane toxicity of hydrocarbons. *Microbiol Rev* **59**(2): 201-222.
Suja, L.D., Summers, S., and Gutierrez, T. (2017) Role of EPS, dispersant and nutrients on the microbial response and MOS formation in the subarctic northeast atlantic. *Front Microbiol* **8**: 676.
Sun, X., and Kostka, J.E. (2019) Hydrocarbon-degrading microbial communities are site specific, and their activity is limited by synergies in temperature and nutrient availability in surface ocean waters. *Appl Environ Microbiol* **85**(15): e00443-00419.
Techtmann, S.M., Zhuang, M., Campo, P., Holder, E., Elk, M., Hazen, T.C. *et al.* (2017) Corexit 9500 enhances oil biodegradation and changes active bacterial community structure of oil-enriched microcosms. *Appl Environ Microbiol* **83**(10): e03462-03416.
Tremblay, J., Yergeau, E., Fortin, N., Cobanli, S., Elias, M., King, T.L. *et al.* (2017) Chemical dispersants enhance the activity of oil- and gas condensate-degrading marine bacteria. *ISME J* **11**(12): 2793-2808.
Tremblay, J., Fortin, N., Elias, M., Wasserscheid, J., King, T.L., Lee, K., and Greer, C.W. (2019) Metagenomic and metatranscriptomic responses of natural oil degrading bacteria in the presence of dispersants. *Environ Microbiol* **21**(7): 2307-2319.
Tyanova, S., Temu, T., Sinitcyn, P., Carlson, A., Hein, M.Y., Geiger, T. *et al.* (2016) The Perseus computational platform for comprehensive analysis of (prote)omics data. *Nat Methods* **13**(9): 731-740.
UniProt Consortium (2019) Uniprot: A worldwide hub of protein knowledge. *Nucleic Acids Res* **47**(D1): D506-D515.
Urtuvia, V., Maturana, N., Acevedo, F., Pena, C., and Diaz-Barrera, A. (2017) Bacterial alginate production: An overview of its biosynthesis and potential industrial production. *World J Microbiol Biotechnol* **33**(11): 198.
US Nat. Comm. DWH (2011). The use of surface and subsea dispersants during the BP Deepwater Horizon oil spill. Working Paper. Washington, DC, USA: National Commission on the BP Deepwater Horizon Oil Spill and Offshore Drilling. Available from: http://purl.fdlp.gov/GPO/gpo184 [Accessed April 20, 2019].

Van Beilen, J.B., Marín, M.M., Smits, T.H., Röthlisberger, M., Franchini, A.G., Witholt, B., and Rojo, F. (2004) Characterization of two alkane hydroxylase genes from the marine hydrocarbonoclastic bacterium *Alcanivorax borkumensis*. *Environ Microbiol* **6**(3): 264-273.

Van der Werf, M., Hartmans, S., and Van den Tweel, W. (1995) Permeabilization and lysis of *Pseudomonas pseudoalcaligenes* cells by Triton X-100 for efficient production of D-malate. *Appl Microbiol Biotechnol* **43**(4): 590-594.

Vaysse, P.J., Sivadon, P., Goulas, P., and Grimaud, R. (2011) Cells dispersed from *Marinobacter hydrocarbonoclasticus* SP17 biofilm exhibit a specific protein profile associated with a higher ability to reinitiate biofilm development at the hexadecane–water interface. *Environ Microbiol* **13**(3): 737-746.

Wang, S., Parsek, M.R., Wozniak, D.J., and Ma, L.Z. (2013) A spider web strategy of type IV pili-mediated migration to build a fibre-like Psl polysaccharide matrix in *Pseudomonas aeruginosa* biofilms. *Environ Microbiol* **15**(8): 2238-2253.

Wang, W., and Shao, Z. (2013) Enzymes and genes involved in aerobic alkane degradation. *Front Microbiol* **4**: 116.

Word, J.Q., Clark, J.R., and Word, L.S. (2014) Comparison of the acute toxicity of Corexit 9500 and household cleaning products. *Hum Ecol Risk Assess* **21**(3): 707-725.

Xu, W., You, Y., Wang, Z., Chen, W., Zeng, J., Zhao, X., and Su, Y. (2018) Dibutyl phthalate alters the metabolic pathways of microbes in black soils. *Sci Rep* **8**(1): 2605.

Young, L., and Mitchell, R. (1973) Negative chemotaxis of marine bacteria to toxic chemicals. *Appl Microbiol* **25**(6): 972-975.

Zhou, L., Yu, Y., Chen, X., Diab, A.A., Ruan, L., He, J. *et al.* (2015) The multiple DSF-family QS signals are synthesized from carbohydrate and branched-chain amino acids via the FAS elongation cycle. *Sci Rep* **5**: 13294.

Zhou, L., Zhang, L.H., Camara, M., and He, Y.W. (2017) The DSF family of quorum sensing signals: Diversity, biosynthesis, and turnover. *Trends Microbiol* **25**(4): 293-303.

6 General discussion and outlook

Chemical dispersants are often applied during the emergency response and remediation efforts after marine oil spills with the aim of reducing ecological and economic damage due to floating and/or beached oil. However, due to their inherent toxicity potential and a number of uncertainties regarding their ecological effects, their use remains controversial. Particularly large knowledge gaps remain regarding the influence of chemical dispersants on affected seawater microbial communities and specifically oil-degrading bacteria, with the current literature characterized by largely unexplained contradictory findings. Therefore, the goal of this thesis was to determine and elucidate the impacts of chemical dispersant on oil-degrading microorganisms by examining this question on different ecological levels. First, environmental seawater microbial communities from two habitats that were previously underexplored in this regard (i.e. Arctic Ocean and North Sea) were investigated and the impacts of chemical dispersants on microbial community dynamics (i.e. growth, composition) and oil biodegradation potential were identified. Subsequently, chemical dispersant effects on the growth and alkane biodegradation activity of the selected model organism *Marinobacter* sp. TT1 were quantified under two different culture conditions with distinct carbon substrate histories. Finally, a comparative proteomic study was conducted to zoom in even further and determine the impacts of chemical dispersants on the HC metabolism and other cellular processes of *Marinobacter* sp. TT1 in order to elucidate the underlying mechanisms of dispersant impacts on HC-degrading microorganisms. The obtained results provided a number of novel insights and several potential explanations for inconsistencies in the existing literature. In the following, the results presented in this thesis are briefly summarized and considered in the context of the scientific literature, before their environmental implications are discussed, and future perspectives for this research field are presented.

6.1 Impacts of chemical dispersants on seawater microbial communities

Although several previous studies have characterized the impact of chemical dispersants on seawater microbial communities, the experiments presented in **Chapter 2 and 3** are among the first to investigate microbial communities from the central Arctic Ocean or the North Sea in this context, respectively, and to look at both microbial community dynamics and HC biodegradation potential using a broad array of analytical approaches. As a result, the obtained findings deepen our knowledge about chemical dispersant impacts on environmental seawater communities (Figure 6.1). In order to discuss their significance, results from both microcosm studies will first be briefly reviewed and compared. Both studies revealed considerable *in situ* oil biodegradation potential, with all oil-derived DOC having been biodegraded at *in situ*-like temperatures after 32 or 35 days in the Arctic Ocean and North Sea microcosms, respectively. Interestingly, this oil biodegradation potential was not substantially affected by chemical dispersant addition when considering *n*-alkanes or small PAHs, while considerable effects on microbial growth and community composition were detected in both habitats. Specifically, lower cell numbers and the enrichment of a distinct community of HC- and/or dispersant-degrading bacterial taxa were observed. Additionally, persistent oil- and/or dispersant-derived

organic compounds were detected in dispersant-amended microcosms in both experiments, with particularly high levels persisting in the Arctic Ocean seawater microcosms after 32 days. Remarkably, the observed impacts of chemical dispersants were largely consistent across both experiments. Neither biogeography (i.e. Arctic Ocean versus North Sea seawater), initial microbial seawater community compositions, different levels of previous petroleum inputs, nor water temperature substantially changed the observed effects of chemical dispersant exposure on environmental microbial communities. This suggests that the underlying mechanisms (see also section 6.2) leading to altered microbial community dynamics (i.e. lower growth and altered composition) are not site- or community-specific but would rather be expected to unfold in a similar manner in most marine ecosystems. Therefore, similar functional effects on the microbial ecology of affected sites could be expected on the basis of the presented findings (see also section 6.3).

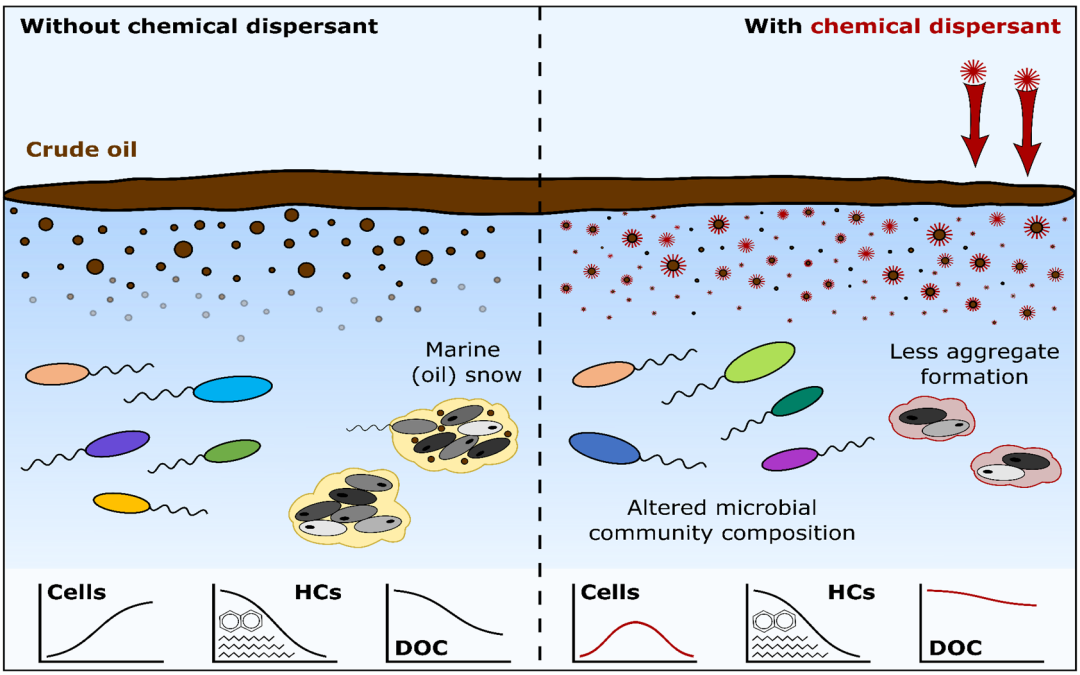

Figure 6.1: Schematic overview of impacts of chemical dispersants on seawater microbial communities, as observed in North Sea and Arctic Ocean seawater microcosms (**Chapter 2 and 3**): altered microbial community composition, reduced aggregate formation and cell numbers, mostly unaffected biodegradation of hydrocarbons (HCs; i.e. *n*-alkanes, naphthalenes) and higher remaining dissolved organic carbon (DOC) levels due to persistent organic compounds.

Clear effects of incubation temperatures on HC biodegradation efficiency and community composition were, on the other hand, observed in both experiments, confirming previous studies that described less/slower HC biodegradation at colder seawater temperatures (e.g. Coulon *et al.*, 2007; Brakstad *et al.*, 2018; Lofthus *et al.*, 2018). The only notable differences between the temperate and the Arctic microbial communities were observed regarding the specific dominant HC- or dispersant-degrading taxa and a much higher microbial α-diversity in North Sea microcosms throughout the incubation period. This could be due to the North Sea community being pre-adapted (or primed) to respond to petroleum HC inputs. Thus, it contained more different microbial groups with HC-degrading capabilities already at the start of the experiment compared to the Arctic Ocean community, where only a small number of

HC-degrading taxa became very abundant in response to the oil spill simulation. The reason for this primed state are likely higher chronic HC pollution levels in the investigated North Sea waters (Chrastansky and Callies, 2009). Since the seawater was sampled in summer, biogenic HCs and other organic matter from decaying phytoplankton bloom-associated biomass could also have played a role in sustaining different opportunistic heterotrophs with HC-degrading capabilities in the microbial community (e.g. discussed in Gutierrez, 2019).

When considering the obtained findings in the context of the scientific literature, they confirm previous reports from different habitats of chemical dispersant addition altering microbial community dynamics and enriching suspected dispersant- as well as oil-degrading taxa (Kleindienst *et al.*, 2015b; Suja *et al.*, 2017; Techtmann *et al.*, 2017; Doyle *et al.*, 2018; Sun and Kostka, 2019; Tremblay *et al.*, 2019). The detection of some of the enriched taxa (e.g. *Colwellia, Polaribacter, Sulfitobacter, Pseudohongiella Amylibacter, Marivita* or *Luteolibacter*) also expands our knowledge on these microbial groups regarding their preferences or potential roles during marine oil spill scenarios. Moreover, the dichotomy in the detected HC concentrations, which indicated largely unaffected biodegradation of typically quantified *n*-alkanes and small aromatic HCs while other dispersant-derived organic compounds appeared less biodegradable, could help to explain the inconsistent findings in the literature regarding chemical dispersant effects on oil biodegradation (e.g. Kleindienst *et al.*, 2015b; Prince *et al.*, 2016). Depending on whether selected groups of HCs or bulk parameters such as total petroleum HCs (TPH) or estimated oil equivalents (EOE) are quantified, different findings regarding biodegradation efficiency might be reported when certain dispersant-derived organic compounds show persistence. The issue of persistent dispersant components was additionally highlighted by a very recently published study, which reports a persistent Corexit-derived compound identified as dipropylene glycol butyl ether (DGBE) in Arctic seawater microcosms after 30 days (Gofstein *et al.*, 2020; published online August 21, 2020). This agrees well with the presented findings in **Chapter 2 and 3** and the persistence of DGBE in marine samples affected by the DWH spill several months after the spill (OSAT, 2010). The industrial solvent DGBE was shown to possess some toxicity to different vertebrates, leading to concerns about its accumulation in wastewater-affected aquatic environments (Bridie *et al.*, 1979; Johnson *et al.*, 2005; Sitarek *et al.*, 2012; Chen *et al.*, 2016). Even though biodegradation of DGBE has been demonstrated (e.g. Chen *et al.*, 2016), it appears to not be biodegradable for Arctic seawater microbial communities. Consequently, additional concerns about Corexit application in the pristine Arctic marine environment and its implications for the marine food web are raised by the findings in this thesis.

Another aim of the experiment with Arctic seawater was to determine the effects of biostimulation (i.e. addition of nitrate, ammonium, phosphate) during a simulated oil spill scenario, since this approach has only rarely been systematically compared with chemical dispersant addition. Interestingly, biostimulation led to enhanced microbial growth and oil-derived DOC biodegradation but did not alter the microbial community of enriched HC degraders much, in contrast to dispersant addition. This showed that even though the oil-degrading microbial seawater community was nutrient-limited, additional nutrients only enabled oil-enriched taxa to increase their activity and did not lead to different copiotrophic taxa overgrowing the oil degraders. Previous Arctic/Antarctic biostimulation experiments have also consistently demonstrated enhanced oil biodegradation rates, although mainly for

sediment/beach conditions (e.g. reviewed by Brakstad *et al.*, 2017). Therefore, biostimulation can be considered a promising approach to enhance the *in situ* biodegradation potential in the Arctic Ocean itself and compensate for the limitations posed by low water temperatures. Moreover, biostimulation approaches should be considered instead of chemical dispersant use in potential future Arctic Ocean oil spill scenarios because the associated effects on microbial dynamics and oil biodegradation would likely be more favourable.

6.2 Impacts of chemical dispersants on the HC degrader *Marinobacter* sp. TT1

The obtained results from experiments with the HC-degrading model organism *Marinobacter* sp. TT1 significantly advance our understanding of how and why chemical dispersants can affect the growth and biodegradation activity of oil-degrading microorganisms (Figure 6.2).

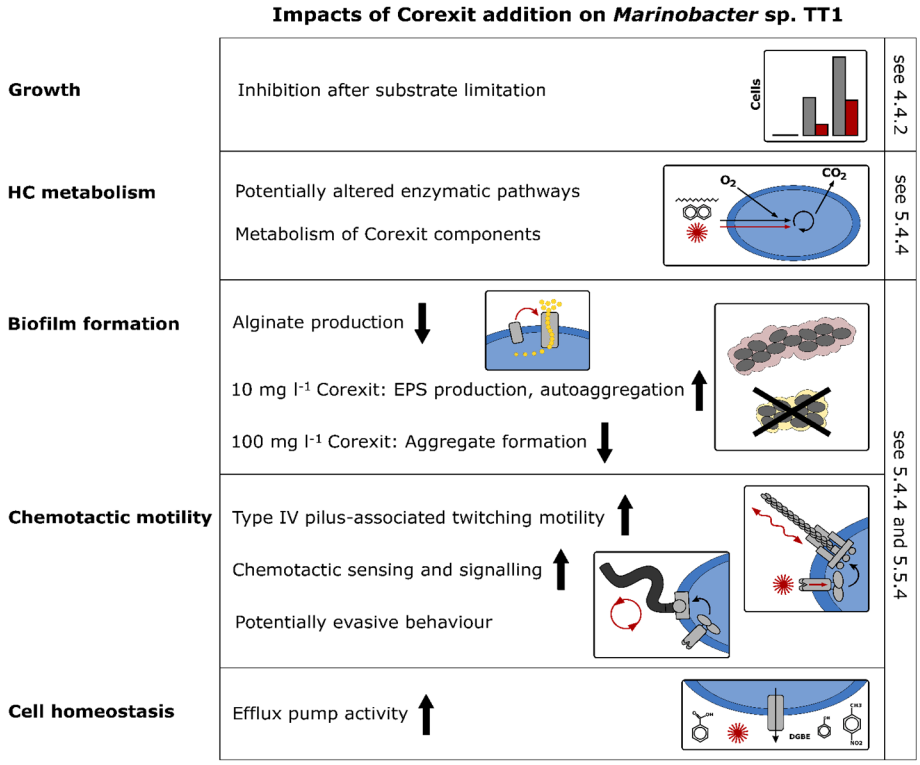

Figure 6.2: Overview of observed and suspected impacts of the chemical dispersant Corexit on the hydrocarbon degrader *Marinobacter* sp. TT1 as presented in Chapter 4 and 5 of this thesis, organized by the five categories growth, hydrocarbon (HC) metabolism, biofilm formation, Chemotactic motility, cell homeostasis. Arrows indicate an increase or decrease with their upward or downward orientation, respectively. EPS = extracellular polymeric substances, DGBE = dipropylene glycol butyl ether.

In **Chapter 4**, it was demonstrated for the first time that previously experienced substrate limitations can have a significant effect on whether or not HC-degrading bacteria are inhibited by chemical dispersant exposure. These findings illustrate the importance of carefully considering the environmental relevance of laboratory experimental conditions and how they might affect experimental outcomes. Similarly, the presented data reinforce the relevance of considering potentially cumulative effects of multiple stressors experienced by organisms in the environment, which are often overlooked in the interest of simplified experimental conditions, leading to scientific findings of questionable environmental relevance. Observations of *Marinobacter* sp. TT1 only being inhibited by chemical dispersant addition under certain

conditions in the presented study might also help to further explain the inconsistent findings in the literature. Most of the published studies have investigated either typical laboratory cultures of HC-degrading bacteria supplemented with high substrate and nutrient concentrations, or natural seawater communities in microcosm experiments generously supplemented with nutrients (e.g. McFarlin *et al.*, 2014; Prince *et al.*, 2016; Tremblay *et al.*, 2017), which could have substantially affected experimental results and led to an underestimation of chemical dispersant impacts on oil-degrading microorganisms. In addition, observations presented in **Chapter 4** also suggested that the inhibition of the starved strain TT1 by chemical dispersant exposure might partially have been related to changes in EPS production and/or aggregate forming behaviour, which was further supported by the results presented in **Chapter 5** (see also section 6.3).

The work presented in **Chapter 5** represents the first proteome-level investigation of the impacts of chemical dispersants (here: Corexit EC9500A) on the cellular processes of a marine hydrocarbon degrader and thus provided many novel insights. For the first time, the proteins associated with a proposed microbial metabolism of Corexit components as carbon substrates were identified, revealing that *Marinobacter* sp. TT1 likely metabolized cycloalkanes, (heteroatomic) aromatic HCs, surfactants and linear alkanes (chain length < C_{16}) from the Corexit mixture, using proteins partially encoded by a putative *alk* operon for the latter group. At the same time, Corexit-induced changes in the proteome linked to HC metabolism, chemotactic motility, biofilm formation, and solvent tolerance mechanisms were discovered. These changes included increased abundances of proteins required for chemotactic motility, likely related to complex motility requirements due to a variety of bioavailable carbon sources ('attractants') and potentially membrane-damaging levels of surfactants and solvents ('repellents'). Another observed response to high Corexit-derived solvent concentrations by strain TT1 was an increase of suspected aromatic HC export proteins and efflux pump proteins, which are known to confer solvent tolerance in other isolates (Ramos *et al.*, 2002; Krell *et al.*, 2012). In addition, the first evidence of alginate biosynthesis in a member of the *Marinobacter* genus was obtained and the associated proteins were more abundant when strain TT1 was utilizing *n*-hexadecane as carbon substrate compared to growth on Corexit, even though *n*-alkane metabolism was a prominent feature in both respective proteomes. Together with the distinct observed aggregate morphologies, those findings strongly suggested that the chemical dispersant Corexit affected aggregate/biofilm formation in *Marinobacter* sp. TT1. This confirmed initial observations from **Chapter 4** and provided new evidence related to dispersant-altered marine (oil) snow formation that reportedly played an important role during the DWH oil spill in the Gulf of Mexico (Passow and Ziervogel, 2016; see also section 6.3).

Based on these novel proteome-based insights, the Corexit-induced inhibition of growth and biodegradation activity in a previously starved *Marinobacter* sp. TT1 culture (**Chapter 4**) was likely caused by solvents and/or surfactants from the Corexit mixture affecting membrane and cell functioning, as well as aggregation behaviour, making evasive motility or upregulation of efflux proteins necessary. These adaptations required cellular resources which might not have been available to the starved culture in the way they were available to the well-fed culture. Furthermore, starvation itself has been shown to induce membrane modifications and changes in motility or EPS production (Kjelleberg and Hermansson, 1984; Yam and Tang, 2007; Fida

et al., 2013; Bergkessel *et al.*, 2016; Putthividhya *et al.*, 2016), which could have led to an increased sensitivity to chemical dispersant exposure in starved cells.

Together, the presented results establish clear patterns of chemical dispersant impacts on the marine HC degrader *Marinobacter* sp. TT1 and help to further illuminate or explain a number of previous scientific findings. First, the previously theorized role of this strain (and other *Marinobacter* members) during the DWH oil spill are mostly supported by the presented experiments. For example, the detection of extensive alkane and aromatic HC degradation, as well as chemotactic capabilities in this isolate align with metagenomic findings on a closely related *Marinobacter* sp. from DWH-affected water samples (Dombrowski *et al.*, 2016). Furthermore, although strain TT1 was isolated from HC- and Corexit-enriched plume water collected during the DWH spill, its *in situ* relative abundance was reportedly below 1% (Gutierrez *et al.*, 2013b), and previous seawater microcosm experiments simulating DWH plume conditions reported decreased abundances of *Marinobacter* spp. after addition of the chemical dispersant Corexit (Kleindienst *et al.*, 2015b). These previous findings are further elucidated by the presented data in this thesis regarding Corexit-induced inhibition effects on *Marinobacter* sp. TT1 under certain culture conditions. It seems likely that the observed inhibition effects in a previously starved culture of strain TT1 might have mirrored the processes shaping the microbial community that was enriched in deep, otherwise relatively oligotrophic plume waters of the Gulf of Mexico during the DWH spill. Thus, the low detected *in situ* abundances of efficient HC-degrading members of *Marinobacter* might have been due to the large-scale application of Corexit in the deep waters of the Gulf.

In addition, the presented protein-based evidence of a marine HC degrader utilizing alkanes, aromatic HCs and potentially surfactants from Corexit as carbon substrates further elucidates and supports the previously speculated development of Corexit-degrading rather than oil-degrading microbial communities after Corexit addition during (simulated) oil spill scenarios (e.g. Kleindienst *et al.*, 2015b). Next, the detected cellular adaptations of *Marinobacter* sp. TT1 illustrate the potential of Corexit to induce a stress response in marine HC degraders and thus support the hypothesis that the generally detected changes in microbial seawater community composition after Corexit addition are not only driven by Corexit components enriching certain taxa but also by Corexit-induced stress inhibiting other taxa. As a result, Corexit addition likely causes complex shifts in intra-community competition between different microbial taxa and thereby alters microbial community dynamics, as documented for an arctic and temperate habitat in this thesis (**Chapter 2 and 3**) and numerous additional habitats in the literature (e.g. Kleindienst *et al.*, 2015b; Suja *et al.*, 2017; Sun and Kostka, 2019; Tremblay *et al.*, 2019).

Finally, the detected metabolism of Corexit-derived, relatively short *n*-alkanes shines a new light on the occasionally reported stimulation of only *n*-alkane biodegradation after chemical dispersant application in previous microcosm studies (e.g. Campo *et al.*, 2013; Tremblay *et al.*, 2017). Since the exact composition of dispersants such as Corexit remains proprietary and the commonly available methods of HC quantification cannot distinguish between oil- and Corexit-derived *n*-alkanes, the reported stimulation effects could mainly be related to the biodegradation of shorter, more bioavailable *n*-alkanes from the added dispersant mixture as opposed to the presumed more efficient biodegradation of oil components. Consequently, whether or not the microbial community enriched by chemical dispersant addition would also generally represent an efficient oil-degrading community remains unclear. Nevertheless, when taking into account

these considerations, the detected inhibition of a previously starved HC-degrading strain, the persistence of dispersant- and possibly oil-derived components in microcosm experiments and the inconsistent results in the literature, the available evidence does not support the assumption of chemical dispersants typically stimulating microbial oil biodegradation processes in the marine environment (e.g. Prince *et al.*, 2016; Brakstad *et al.*, 2017).

6.3 Environmental implications

Together, the novel insights presented in this thesis could have a wide range of potential environmental implications, of which a few selected additional aspects will be discussed in the following section. The implications of how chemical dispersants alter microbial community dynamics, for example, are hard to pin down exactly but could be highly relevant for the marine environment. The data presented in **Chapter 2 and 3** shows drastic shifts in community dynamics and suggests that the inhibiting effects of chemical dispersants on certain microbial taxa could continue for over a month due to persistent dispersant components. Even though microbial seawater communities are typically very diverse and contain functional redundancy, shifts in marine microbial community composition are often associated with shifting functional properties of the community as well (Allison and Martiny, 2008; Fuhrman *et al.*, 2015; Galand *et al.*, 2018). The observed community shifts could therefore cause short- or long-term changes in the microbial carbon cycle of affected waters, which would, in turn, produce ripple effects throughout the marine food web and interconnected nutrient (e.g. nitrogen, phosphate) cycles and would differ from those shifts caused by oil-only inputs. Marine bacteria are the main drivers of marine biogeochemical cycles (Arrigo, 2005; Falkowski *et al.*, 2008) and heterotrophs like the HC degraders represent a crucial part of the so-called microbial loop (Pomeroy *et al.*, 2007; Strom, 2008) at the basis of the marine food web, connecting the primary producers (i.e. phytoplankton) with the rest of the ecosystem. Thus, whatever strongly affects them could indirectly have larger ecosystem-level effects as well by disrupting the marine food web and biogeochemical cycles. These connections should increasingly be considered in ecological research, in addition to direct effects of the documented increase in oil toxicity levels for marine life immediately after chemical dispersant use (Kleindienst *et al.*, 2015a; Prince, 2015). A few studies have attempted to elucidate these microbial ecological connections in the context of oil spill conditions, revealing e.g. that chemically dispersed oil can indirectly cause harmful algal blooms by negatively affecting tintinnid and ciliate populations, which are phytoplankton grazers (Almeda *et al.*, 2018). Furthermore, dispersant exposure was shown to significantly inhibit diatoms and ciliates and thereby disrupt the transfer of carbon from the microbial food web to higher trophic levels, potentially reducing fish stocks (Ortmann *et al.*, 2012). In addition, the importance of considering interconnected microbial carbon and nitrogen cycles during oil spill scenarios was, for example, also illustrated by the beneficial effects of increased nitrate availability for microbial oil biodegradation demonstrated in Arctic Ocean seawater microcosms (**Chapter 2**). Similarly, it was discovered that microbial nitrogen fixation was a key function of microbial communities in beach sediments affected by the DWH spill, enabling efficient oil biodegradation even under otherwise nitrogen-limited conditions (Rodriguez-R *et al.*, 2015; Shin *et al.*, 2019). An enrichment of other genetic functions related to nitrogen, phosphorous, sulphur and iron cycling was also detected in contaminated sediment

and seawater samples from the DWH spill, indicating their importance for microbial responses to (dispersed) oil inputs (Mason *et al.*, 2012; Rodriguez-R *et al.*, 2015).

Interestingly, among the environmental factors that could have modulated microbial responses to chemical dispersant exposure in the presented experiments, only substrate history (i.e. previously experienced carbon starvation) was shown to change how the dispersant Corexit affected microbial growth and biodegradation activity in strain TT1. This finding is very environmentally relevant for opportunistic heterotroph bacteria like *Marinobacter* spp. since they are adapted to surviving long periods of low substrate availability (Singer *et al.*, 2011; Vaysse *et al.*, 2011; Sebastian *et al.*, 2019). In the open ocean environment, substrate availability is characterised by large fluctuations on temporal and spatial scales, illustrated e.g. by the difference between particle-/phytoplankton-associated and free-living microbial lifestyles or seasonal inputs of large carbon quantities associated with phytoplankton bloom regimes (Teeling *et al.*, 2012; Sun and Kostka, 2019). A few studies have also described physiological adaptations to substrate limitations in *Marinobacter hydrocarbonoclasticus* SP17 by comparing sessile cells growing in *n*-hexadecane-associated biofilms and the planktonic cells released from the biofilm which need to survive without a new substrate source for a while in the environment (Klein *et al.*, 2008; Vaysse *et al.*, 2011). These reports provide further evidence for the environmental relevance of previously experienced substrate limitation in marine HC-degrading bacteria and the importance of considering this factor when assessing impacts of stressors like chemical dispersants. According to multiple stressor theory, additional stressors such as nutrient limitation and non-HC pollutant exposure (e.g. heavy metals, pesticides, halogenated compounds) could also play a role in modulating the sensitivity of oil-degrading microorganisms to chemical dispersant exposure in the marine environment.

Remarkably, evidence for impacts of chemical dispersant exposure on microbial aggregate or biofilm formation was observed in all experiments described in this thesis. In seawater microcosm experiments (**Chapter 2 and 3**), crude oil addition resulted in increased formation of microbial aggregates (likely 'marine oil snow') which was noticeably decreased in microcosms with additional chemical dispersant application. Pure culture experiments with the model organism *Marinobacter* sp. TT1 revealed the formation of much larger microbial aggregates when *n*-hexadecane and Corexit were both supplied compared to culture conditions with only *n*-hexadecane, while the smallest aggregates were observed in cultures only supplied with Corexit (**Chapter 4 and 5**). Additionally, an amorphous microscopic structure of aggregates formed by the starved culture negatively impacted by Corexit addition was observed, which differed from the microscopic structure of all other formed aggregates in the experiments of **Chapter 4.** Observations made during the DWH spill suggest that these observed dispersant-induced effects are environmentally relevant (Joye *et al.*, 2016a; Passow and Ziervogel, 2016), with previous laboratory studies reporting both enhanced (Suja *et al.*, 2017; Doyle *et al.*, 2018) and inhibited (Kleindienst *et al.*, 2015b; Passow, 2016) microbial aggregate formation due to chemical dispersant addition. The findings of this thesis suggest that Corexit might affect aggregate formation by altering EPS (e.g. alginate) production, chemotactic motility, quorum sensing processes, the bioavailability of HC substrates and/or by inhibiting microbial growth. Additionally, other studies have reported that Corexit (or the contained surfactants) might inhibit aggregate coagulation by dispersing EPS (Joye *et al.*, 2016a; Passow and Ziervogel, 2016), which could have played an additional role in seawater

microcosms described in **Chapter 2**. However, it is also known that EPS production can represent a bacterial stress response, resulting in the formation of protective biofilms (Flemming *et al.*, 2016) and thus, Corexit-derived solvents and surfactants might induce increased EPS formation (Jones and George, 2013; US NASEM, 2020), which seemed to apply in *Marinobacter* sp. TT1 cultures with *n*-hexadecane and Corexit (**Chapter 5**). The outcome of these opposing processes, meaning either increased or decreased aggregate formation due to dispersant addition, likely depends on the investigated microbial community and their available resources in the environment. Either way, these impacts can substantially affect the fate of spilled oil (Joye *et al.*, 2016a; Passow and Ziervogel, 2016) and the aforementioned microbial loop in the marine environment and therefore represent another route of potentially large-scale ecological dispersant impacts mediated by microorganisms. This is further illustrated by the increasingly recognized ubiquity and importance of microbial biofilms in the environment, including in the global oceans (Flemming and Wuertz, 2019).

Although the focus of this thesis is on the microbiological perspective, potential implications of the presented findings for future oil spill response decision making will also briefly be discussed. From an ecological standpoint, the preferred option would always be to either prevent marine oil spills completely or, alternatively, remove most of the spilled oil immediately by mechanical means. Unfortunately, these options are not always available, leading to complex spill response scenarios and the associated decision making. This thesis generally confirms a number of ecological concerns about chemical dispersant use during marine oil spill scenarios, such as the potential inhibition of oil-degrading bacteria and the persistence of suspected hazardous dispersant components. As a result, the use of chemical dispersants should always be very carefully considered and weighed against all other options including the expected ecological costs and benefits. Typically, these considerations are formalised as a 'net environmental benefit analysis' (or similar analyses) and many countries demand different types of toxicity tests and the use of these formalized decision-making tools before allowing chemical dispersant use in their waters and/or in coastal regions (Baker, 1995; Kirby and Law, 2008; Grote *et al.*, 2018). These analyses can be helpful tools during emergency spill response efforts where quick decisions are often needed. However, not all relevant ecological effects can/will be included in these assessments and many knowledge gaps regarding ecological effects of dispersant use still remain at this time, which means that these analyses more than likely contain a number of blind spots. The microbial sphere, for example, is often overlooked. It should also be noted that the weighing of ecological benefits and costs of chemical dispersant use is a highly complex matter and its results largely depend on previously established priorities among potentially affected species/organisms and habitats. For example, it has been argued that dispersants limit the total ecological damage of oil spills by protecting bird populations and coastlines (Lunel, 1998; Prince, 2015), which implies that the potential negative effects on marine life in the water column or on the seafloor are weighed as less costly (ecologically or economically). However, these kinds of decisions are not always based on a solid evidence-based foundation due to limitations in available (long-term) data and differing interests of the involved stakeholders, such as scientists, elected officials, oil/shipping industry and the tourism industry (see also Trudel, 1998). Consequently, more ecosystem-level studies on short- and long-term effects of chemically dispersed oil versus oil-only

contamination effects are desperately needed in order to enable the emergency oil spill responders to implement improved, evidence-based decision making tools. Everything considered, it is possible that chemical dispersant use provides net environmental benefits under certain spill conditions when well-established, targeted application strategies are applied (e.g. Baker, 1995; Lunel, 1998). Nevertheless, their application represents an additional ecological risk during marine oil spill scenarios and, based on the available data, the unprecedented large-scale application of Corexit dispersants during the DWH spill could have increased negative spill impacts on some ecosystem levels (Joye *et al.*, 2016a; McGowan *et al.*, 2017), e.g. by increasing the area affected by invisible but toxic HC concentrations (MacDonald *et al.*, 2015; Berenshtein *et al.*, 2020). It likely also led to lower oil biodegradation rates, due to much of the dispersed oil being sequestered in a deep water plume at cold temperatures or rapidly transferred to the seafloor (i.e. to low oxygen levels and temperatures), resulting in less oil biodegradation and weathering possibilities and affecting a larger area of the ecosystem for longer time scales (Joye, 2015; Kleindienst *et al.*, 2015a; MacDonald *et al.*, 2015; Joye *et al.*, 2016a; Passow and Ziervogel, 2016). These impacts should serve as a cautionary tale and be carefully considered during future oil spill response planning.

6.4 Research outlook and future perspectives

The results presented in this thesis significantly deepen and advance our understanding of how and why chemical dispersants impact oil-degrading microorganisms. Overall, dispersant addition will likely have drastic effects on most marine microbial communities and, in many cases, *in situ* oil biodegradation might not be enhanced. Additionally, several potential explanations for the inconsistent literature regarding dispersant effects on oil biodegradation were uncovered (i.e. the importance of environmentally relevant experimental/culture conditions, different HC quantification approaches and persistent dispersant components and/or potential preferential biodegradation of other dispersant components), highlighting that environmental implications of laboratory experiments are difficult to determine since only limited parts of the big picture can be revealed by each experiments. As a result, this thesis also has its limitations, which should be acknowledged briefly. For example, an inherent issue of labour-intensive seawater microcosm experiments is the snapshot nature of the results obtained at each sampling time point, which can only be extrapolated to the unsampled fraction of the incubation period to a certain extent. Additionally, bottle effects can never be completely controlled for and the used seawater samples represent only one ecological condition within the large variation occurring across time (e.g. seasonality or diurnal cycles in surface seawater) and/or space in the environment. Many of the employed analytical techniques also have their own inherent limitations (e.g. HC quantification in heterogeneous systems ± proprietary dispersant mixtures) and potential biases (e.g. PCR amplification and primer selection biases), even though care was taken to reduce and acknowledge these issues wherever applicable and a broad range of methods was combined whenever possible. A few other factors possibly limiting the broad applicability of the presented results are that this study mainly focused on one group of oil-degrading microorganisms (i.e. bacteria), only considered one HC-degrading model organism (i.e. *Marinobacter* sp. TT1) and one common type of chemical dispersant (i.e. Corexit EC9500A).

Many open questions and unresolved ecological and microbial concerns remain besides those already mentioned above and a few of those will be presented in the following section. First, the impacts of chemical dispersants on non-bacterial microorganisms remains understudied, even though the available data suggests that phytoplankton, for example, might be much more sensitive than bacteria (e.g. Ortmann *et al.*, 2012) and several HC-degrading archaea (Spang *et al.*, 2017; Oren, 2019; Prince *et al.*, 2019), fungi and algae (Fukuda and Ohta, 2019; Prince, 2019) have been described. All of these groups (plus marine viruses) coexist with bacteria in the marine environment and their often overlooked interactions (see e.g. Strom, 2008; Fuhrman *et al.*, 2015; Coutinho *et al.*, 2017; Grossart *et al.*, 2019) could also affect bacterial oil biodegradation or the response of bacterial taxa to chemical dispersants. Second, the potential persistence of dispersant-derived compounds in different marine ecosystems and the associated ecological effects (i.e. direct/indirect toxicity to different groups of organisms) definitely require additional study. Tackling these questions will likely be complicated by the still largely proprietary composition of commercial dispersant mixtures such as Corexit and by the fact that the quantification of these mixtures or their components remains analytically challenging, although significant advances were made in this regard recently (Place *et al.*, 2016; Perkins, 2017). Nevertheless, resolving these questions before the next large scale application of chemical dispersants seems crucial, especially when considering the increasing oil spill risks in cold seawater habitats like the deep ocean or the Arctic Ocean (Meier *et al.*, 2014; US NPC, 2015; Harriss, 2016). Third, alternative spill remediation strategies that could be pursued either instead of chemical dispersant use or in order to reduce the amount of applied chemical dispersants after marine oil spills and thereby reduce harmful ecological impacts should be further developed and tested. A number of promising techniques (besides biostimulation) have been identified by different researchers in the last years, such as the application of biosurfactants produced by HC-degrading laboratory cultures (Chong and Li, 2017; Perfumo *et al.*, 2018), the so-called electrobioremediation of contaminated marine sediments (Daghio *et al.*, 2017) or the use of natural sorbent materials to remove oil slicks (Ge *et al.*, 2016; Bayık and Altın, 2017; Mojžiš *et al.*, 2019). These strategies should also be tested in combination with each other under different environmental conditions, since e.g. the combined application of nutrients and biosurfactants has been shown to enhance crude oil biodegradation in seawater considerably (Nikolopoulou and Kalogerakis, 2008). Fourth, an increased abundance of plastic debris (micro-/macroplastics) in the global oceans has recently been described (Cózar *et al.*, 2014; Ostle *et al.*, 2019; Everaert *et al.*, 2020) but the effects of these relatively recently added particles on the pelagic microbial community or oil-degrading microorganisms in particular remain largely unknown (Avio *et al.*, 2017; Everaert *et al.*, 2020). It seems likely that plastic particles could represent a new habitat for oil-degrading bacteria because of their hydrophobicity, plastic polymers being derived from crude oil and because HCs might accumulate on plastic particles in aquatic environments (Avio *et al.*, 2017; Burns and Boxall, 2018). In fact, HC degraders have been detected in microbial biofilms on marine plastics and/or have been shown to possess plastic polymer-degrading capabilities as well (Delacuvellerie *et al.*, 2019; Erni-Cassola *et al.*, 2020; Zadjelovic *et al.*, 2020). Therefore, these new hotspots might provide HC-degrading bacteria with new substrate and/or new sites for biofilm formation in the marine water column. In turn, this could affect their distribution, abundances and activity und thus result in different baseline conditions before oil spills and/or affect their sensitivity to

chemical dispersant exposure. Finally, the sea surface microlayer could be of particular interest for future investigations of the activity and distribution of HC-degrading microorganisms. This thin boundary layer between the global oceans and the atmosphere is the most immediately affected by the formation of oil slicks during marine oil spills and/or subsequent applications of chemical dispersants and it reportedly harbours large amounts of (bio-)surfactants, microbial aggregates, and distinct microbial communities, including HC-degrading bacteria (Rambeloarisoa *et al.*, 1984; Wurl *et al.*, 2017; Rahlff *et al.*, 2019).

In order to address these and other open questions, future studies should consider employing a number of additional methods. Systematic studies with the goal of determining the response of different microbial taxa to chemical dispersant mixtures or their components, could for example benefit from emerging microfluidics-based approaches in aquatic ecotoxicology (e.g. reviewed by Campana and Wlodkowic, 2018). These experimental systems provide the opportunity to produce large, robust data sets on the effects of single or multiple environmental stressors and could be combined with single-cell proteomic or transcriptomic approaches in a subsequent step (see e.g. Chen *et al.*, 2017b; Kaster and Sobol, 2020) in order to identify the specific affected cellular processes. On the community level, (meta-)transcriptomic or metaproteomic approaches could similarly be applied to significantly enhance the resolution at which the processes unfolding in seawater microcosms or field experiments and the contribution of certain microbial key players to these processes can be monitored (Tremblay *et al.*, 2019). Alternatively, quantitative PCR (qPCR) assays targeting functional marker gene mRNAs for HC biodegradation steps, EPS production or other stress response-associated processes could be utilized to characterize the microbial activity and dispersant response in seawater microcosm experiments. The marker gene *intI1* represents an intriguing example because its detection in environmental samples is used as an indicator for anthropogenic pollution (Gillings *et al.*, 2015). It could be very useful to develop a similar marker gene qPCR assay associated with different expected responses of the *in situ* microbial community to chemical dispersant exposure in order to provide site-specific guidance for spill response decision making. The increasingly popular technique of stable isotope probing (SIP) represents another promising tool (see e.g. Gutierrez and Kleindienst, 2020) that could be used to identify specific key HC-degrading microorganisms in seawater microcosms with and without chemical dispersant exposure and thus confirm the role of dominant or rare microbial groups detected under both conditions. Furthermore, different techniques could be used to gather more insight into how chemical dispersants affect the cell membranes of HC-degrading microorganisms because these effects are suspected to play a large role in dispersant-induced cellular stress responses but are not easily uncovered by molecular biological methods. For this purpose, the membrane lipid composition, the cell surface hydrophobicity and/or the membrane fluidity (e.g. via the Laurdan assay; Sánchez *et al.*, 2007) could be measured in different isolates before and after chemical dispersant exposure to learn more about these suspected impacts. Scanning electron microscopy (SEM) and particularly novel methods such as cryo-FIB-SEM (see e.g. Hayles and de Winter, 2020), might also be able to provide insights into potential membrane changes associated with chemical dispersant exposure.

In conclusion, several additional research questions need to be resolved before the impacts of chemical dispersants on oil-degrading microorganisms in the environment can be fully understood and thus, more easily predicted. And as long as we still depend on crude oil to fuel the energy demands in our societies and oil spills cannot be prevented completely, more research with the aim of reducing negative ecological impacts of our activities will be needed. Therefore, research on the ecological effects of marine oil spills and applied spill remediation strategies, as well as the collection of baseline (microbial) ecological data in marine ecosystems with significant oil spill risks, remains an urgent matter. The findings presented in this thesis represent one piece of this complex puzzle and will hopefully be followed by others until the picture becomes even clearer.

6.5 References

Abbasian, F., Lockington, R., Megharaj, M., and Naidu, R. (2016) A review on the genetics of aliphatic and aromatic hydrocarbon degradation. *Appl Biochem Biotechnol* **178**(2): 224-250.

Adams, G.O., Fufeyin, P.T., Okoro, S.E., and Ehinomen, I. (2015) Bioremediation, biostimulation and bioaugmention: A review. *Int J Environ Bioremediat Biodegrad* **3**(1): 28-39.

Allison, S.D., and Martiny, J.B. (2008) Resistance, resilience, and redundancy in microbial communities. *Proc Natl Acad Sci USA* **105**: 11512-11519.

Almeda, R., Hyatt, C., and Buskey, E.J. (2014) Toxicity of dispersant Corexit 9500A and crude oil to marine microzooplankton. *Ecotoxicol Environ Saf* **106**: 76-85.

Almeda, R., Cosgrove, S., and Buskey, E.J. (2018) Oil spills and dispersants can cause the initiation of potentially harmful dinoflagellate blooms ("red tides"). *Environ Sci Technol* **52**(10): 5718-5724.

Altschul, S.F., Gish, W., Miller, W., Myers, E.W., and Lipman, D.J. (1990) Basic local alignment search tool. *J Mol Biol* **215**(3): 403-410.

Arctic Council (2013). Agreement on cooperation on marine oil pollution preparedness and response in the Arctic. Kiruna, Sweden. Available from: https://oaarchive.arctic-council.org/handle/11374/529 [Accessed July 20, 2020].

Arrigo, K.R. (2005) Marine microorganisms and global nutrient cycles. *Nature* **437**(7057): 349-355.

Atlas, R.M., and Bartha, R. (1972) Degradation and mineralization of petroleum in sea water: Limitation by nitrogen and phosphorous. *Biotechnol Bioeng* **14**(3): 309-318.

Atlas, R.M. (1995) Petroleum biodegradation and oil spill bioremediation. *Mar Pollut Bull* **31**(4-12): 178-182.

Aubé, J., Senin, P., Bonin, P., Pringault, O., Jeziorski, C., Bouchez, O. *et al.* (2020) Meta-omics provides insights into the impact of hydrocarbon contamination on microbial mat functioning. *Microb Ecol*: 1-10.

Aune, M., Aniceto, A.S., Biuw, M., Daase, M., Falk-Petersen, S., Leu, E. *et al.* (2018) Seasonal ecology in ice-covered Arctic seas: Considerations for spill response decision making. *Mar Environ Res* **141**: 275-288.

Avio, C.G., Gorbi, S., and Regoli, F. (2017) Plastics and microplastics in the oceans: From emerging pollutants to emerged threat. *Mar Environ Res* **128**: 2-11.

Bælum, J., Borglin, S., Chakraborty, R., Fortney, J.L., Lamendella, R., Mason, O.U. *et al.* (2012) Deep-sea bacteria enriched by oil and dispersant from the Deepwater Horizon spill. *Environ Microbiol* **14**(9): 2405-2416.

Baker, J.M. (1995) Net environmental benefit analysis for oil spill response. *International Oil Spill Conference*: American Petroleum Institute, pp. 611-614.

Barbato, M., Scoma, A., Mapelli, F., De Smet, R., Banat, I.M., Daffonchio, D. *et al.* (2016) Hydrocarbonoclastic *Alcanivorax* isolates exhibit different physiological and expression responses to *n*-dodecane. *Front Microbiol* **7**: 1-14.

Barron, M.G., Vivian, D.N., Heintz, R.A., and Yim, U.H. (2020) Long-term ecological impacts from oil spills: Comparison of *Exxon Valdez*, *Hebei Spirit*, and Deepwater Horizon. *Environ Sci Technol*.

Bayık, G.D., and Altın, A. (2017) Production of sorbent from paper industry solid waste for oil spill cleanup. *Mar Pollut Bull* **125**(1-2): 341-349.

BBC News (2019) *Grande America*: France braces for oil spill damage after ship blaze. In *BBC News*. Published on: March 14, 2019. Available from: https://www.bbc.com/news/world-europe-47574143 [Accessed August 28, 2020].

BBC News (2020) Russian Arctic oil spill pollutes big lake near Norilsk. In *BBC News*. Published on: June 9, 2020. Available from: https://www.bbc.com/news/world-europe-52977740 [Accessed August 28, 2020].

Bellier, P., and Massart, G. (1979) The *Amoco Cadiz* oil spill cleanup operations – an overview of the organization, control, and evaluation of the cleanup techniques employed. *International Oil Spill Conference*: American Petroleum Institute, pp. 141-146.

Bera, G., Doyle, S., Passow, U., Kamalanathan, M., Wade, T.L., Sylvan, J.B. *et al.* (2020) Biological response to dissolved versus dispersed oil. *Mar Pollut Bull* **150**: 110713.

Bergkessel, M., Basta, D.W., and Newman, D.K. (2016) The physiology of growth arrest: Uniting molecular and environmental microbiology. *Nat Rev Microbiol* **14**(9): 549-562.

Beyer, J., Trannum, H.C., Bakke, T., Hodson, P.V., and Collier, T.K. (2016) Environmental effects of the Deepwater Horizon oil spill: A review. *Mar Pollut Bull* **110**(1): 28-51.

Bocard, C., Renault, P., and Croquette, J. (1979) Cleaning products used in operations after the *Amoco Cadiz* disaster. *International Oil Spill Conference*: American Petroleum Institute, pp. 163-167.

Bolyen, E., Rideout, J.R., Dillon, M.R., Bokulich, N.A., Abnet, C.C., Al-Ghalith, G.A. *et al.* (2019) Reproducible, interactive, scalable and extensible microbiome data science using QIIME 2. *Nature biotechnology* **37**(8): 852-857.

Bonin, P., Vieira, C., Grimaud, R., Militon, C., Cuny, P., Lima, O. *et al.* (2015) Substrates specialization in lipid compounds and hydrocarbons of *Marinobacter* genus. *Environ Sci Pollut Res* **22**(20): 15347-15359.

Bowman, J.P., Gosink, J.J., McCAMMON, S.A., Lewis, T.E., Nichols, D.S., Nichols, P.D. *et al.* (1998) *Colwellia demingiae* sp. nov., *Colwellia hornerae* sp. nov., *Colwellia rossensis* sp. nov. and *Colwellia psychrotropica* sp. nov.: Psychrophilic Antarctic species with the ability to synthesize docosahexaenoic acid (22:Ω63). *Int J Syst Evol Microbiol* **48**(4): 1171-1180.

Bragg, J.R., Prince, R.C., Harner, E.J., and Atlas, R.M. (1994) Effectiveness of bioremediation for the *Exxon Valdez* oil spill. *Nature* **368**(6470): 413-418.

Brakstad, O., and Lødeng, A. (2005) Microbial diversity during biodegradation of crude oil in seawater from the North Sea. *Microb Ecol* **49**(1): 94-103.

Brakstad, O.G., Lofthus, S., Ribicic, D., and Netzer, R. (2017) Biodegradation of petroleum oil in cold marine environments. In *Psychrophiles: From biodiversity to biotechnology*: Springer, pp. 613-644.

Brakstad, O.G., Davies, E.J., Ribicic, D., Winkler, A., Brönner, U., and Netzer, R. (2018) Biodegradation of dispersed oil in natural seawaters from Western Greenland and a Norwegian fjord. *Polar Biology* **41**(12): 2435-2450.

Bridie, A., Wolff, C., and Winter, M. (1979) The acute toxicity of some petrochemicals to goldfish. *Water Res* **13**(7): 623-626.

Brown, C., Williamson, K., and Galvez, F. (2019) The influence of salinity on the toxicity of Corexit at multiple life stages of Gulf killifish. *Comparative Biochemistry and Physiology Part C: Toxicology & Pharmacology* **221**: 38-48.

Burgherr, P. (2007) In-depth analysis of accidental oil spills from tankers in the context of global spill trends from all sources. *J Hazard Mat* **140**: 245-256.

Burns, E.E., and Boxall, A.B. (2018) Microplastics in the aquatic environment: Evidence for or against adverse impacts and major knowledge gaps. *Environ Toxicol Chem* **37**(11): 2776-2796.

Burrows, P., Rowley, C., and Owen, D. (1974) *Torrey Canyon*: A case study in accidental pollution. *Scottish Journal of Political Economy* **21**(3): 237-258.

Callahan, B.J., McMurdie, P.J., Rosen, M.J., Han, A.W., Johnson, A.J.A., and Holmes, S.P. (2016) DADA2: High-resolution sample inference from Illumina amplicon data. *Nat Methods* **13**(7): 581-583.

Camilli, R., Reddy, C.M., Yoerger, D.R., Van Mooy, B.A., Jakuba, M.V., Kinsey, J.C. *et al.* (2010) Tracking hydrocarbon plume transport and biodegradation at Deepwater Horizon. *Science* **330**(6001): 201-204.

Campana, O., and Wlodkowic, D. (2018) Ecotoxicology goes on a chip: Embracing miniaturized bioanalysis in aquatic risk assessment. *Environ Sci Technol* **52**(3): 932-946.

Campeão, M.E., Swings, J., Silva, B.S., Otsuki, K., Thompson, F.L., and Thompson, C.C. (2019) "*Candidatus* Colwellia aromaticivorans" sp. nov.,"*Candidatus* Halocyntiibacter alkanivorans" sp. nov., and "*Candidatus* Ulvibacter alkanivorans" sp. nov. Genome sequences. *Microbiol Resour Announc* **8**(15).

Campo, P., Venosa, A.D., and Suidan, M.T. (2013) Biodegradability of Corexit 9500 and dispersed South Louisiana crude oil at 5 and 25°C. *Environ Sci Technol* **47**(4): 1960-1967.

Canul-Chan, M., Sanchez-Gonzalez, M., González-Burgos, A., Zepeda, A., and Rojas-Herrera, R. (2018) Population structures shift during the biodegradation of crude and fuel oil by an indigenous consortium. *International journal of environmental science and technology* **15**(1): 1-16.

Caporaso, J.G., Kuczynski, J., Stombaugh, J., Bittinger, K., Bushman, F.D., Costello, E.K. *et al.* (2010) QIIME allows analysis of high-throughput community sequencing data. *Nat Methods* **7**(5): 335-336.

Carpenter, A. (2019) Oil pollution in the North Sea: The impact of governance measures on oil pollution over several decades. *Hydrobiologia* **845**(1): 109-127.

Chae, J.-C., and Zylstra, G.J. (2006) 4-Chlorobenzoate uptake in *Comamonas* sp. strain DJ-12 is mediated by a tripartite ATP-independent periplasmic transporter. *J Bacteriol* **188**(24): 8407-8412.

Chakraborty, R., Borglin, S.E., Dubinsky, E.A., Andersen, G.L., and Hazen, T.C. (2012) Microbial response to the MC-252 oil and Corexit 9500 in the Gulf of Mexico. *Front Microbiol* **3**: 357.

Chen, C., Liu, Q., Liu, C., and Yu, J. (2017a) Effect of different enrichment strategies on microbial community structure in petroleum-contaminated marine sediment in Dalian, China. *Mar Pollut Bull* **117**(1-2): 274-282.

Chen, I.-M.A., Chu, K., Palaniappan, K., Pillay, M., Ratner, A., Huang, J. *et al.* (2019) IMG/M v. 5.0: An integrated data management and comparative analysis system for microbial genomes and microbiomes. *Nucleic Acids Res* **47**(D1): D666-D677.

Chen, M., Fan, R., Zou, W., Zhou, H., Tan, Z., and Li, X. (2016) Bioaugmentation for treatment of full-scale diethylene glycol monobutyl ether (DGBE) wastewater by *Serratia* sp. BDG-2. *J Hazard Mat* **309**: 20-26.

Chen, Z., Chen, L., and Zhang, W. (2017b) Tools for genomic and transcriptomic analysis of microbes at single-cell level. *Front Microbiol* **8**: 1831.

Chong, H., and Li, Q. (2017) Microbial production of rhamnolipids: Opportunities, challenges and strategies. *Microbial cell factories* **16**(1): 137.

Choyke, S., and Ferguson, P.L. (2019) Molecular characterization of nonionic surfactant components of the Corexit 9500® oil spill dispersant by high-resolution mass spectrometry. *Rapid Commun Mass Spectrom* **33**(22): 1683-1694.
Chrastansky, A., and Callies, U. (2009) Model-based long-term reconstruction of weather-driven variations in chronic oil pollution along the German North Sea coast. *Mar Pollut Bull* **58**(7): 967-975.
Chronopoulou, P.M., Sanni, G.O., Silas-Olu, D.I., van der Meer, J.R., Timmis, K.N., Brussaard, C.P., and McGenity, T.J. (2015) Generalist hydrocarbon-degrading bacterial communities in the oil-polluted water column of the North Sea. *Microb Biotechnol* **8**(3): 434-447.
Conrad, J.C., Gibiansky, M.L., Jin, F., Gordon, V.D., Motto, D.A., Mathewson, M.A. *et al.* (2011) Flagella and pili-mediated near-surface single-cell motility mechanisms in *P. aeruginosa*. *Biophys J* **100**(7): 1608-1616.
Coulon, F., McKew, B.A., Osborn, A.M., McGenity, T.J., and Timmis, K.N. (2007) Effects of temperature and biostimulation on oil-degrading microbial communities in temperate estuarine waters. *Environ Microbiol* **9**(1): 177-186.
Coutinho, F.H., Silveira, C.B., Gregoracci, G.B., Thompson, C.C., Edwards, R.A., Brussaard, C.P. *et al.* (2017) Marine viruses discovered via metagenomics shed light on viral strategies throughout the oceans. *Nat Comm* **8**(1): 1-12.
Cózar, A., Echevarría, F., González-Gordillo, J.I., Irigoien, X., Úbeda, B., Hernández-León, S. *et al.* (2014) Plastic debris in the open ocean. *Proc Natl Acad Sci USA* **111**(28): 10239-10244.
Crain, C.M., Kroeker, K., and Halpern, B.S. (2008) Interactive and cumulative effects of multiple human stressors in marine systems. *Ecol Lett* **11**(12): 1304-1315.
Crisafi, F., Genovese, M., Smedile, F., Russo, D., Catalfamo, M., Yakimov, M. *et al.* (2016) Bioremediation technologies for polluted seawater sampled after an oil-spill in Taranto Gulf (Italy): A comparison of biostimulation, bioaugmentation and use of a washing agent in microcosm studies. *Mar Pollut Bull* **106**(1-2): 119-126.
Curl, H.C., Barton, K., and Harris, L. (1992). Oil spill case histories, 1967-1991: Summaries of significant U.S. and international spills. Seattle, Washington, USA: NOAA Hazardous Materials Response and Assessment Division. Report No.: Report No. HMRAD 92-11. Available from: https://repository.library.noaa.gov/view/noaa/1671 [Accessed July 20, 2020].
Daghio, M., Aulenta, F., Vaiopoulou, E., Franzetti, A., Arends, J.B., Sherry, A. *et al.* (2017) Electrobioremediation of oil spills. *Water Res* **114**: 351-370.
Dave, D., and Ghaly, A.E. (2011) Remediation technologies for marine oil spills: A critical review and comparative analysis. *American Journal of Environmental Sciences* **7**(5): 423.
Davidova, I.A., Marks, C.R., and Suflita, J.M. (2019) Anaerobic hydrocarbon-degrading Deltaproteobacteria. In *Taxonomy, genomics and ecophysiology of hydrocarbon-degrading microbes*. McGenity, T.J. (ed), pp. 207-243.
Davidson, A.L., Dassa, E., Orelle, C., and Chen, J. (2008) Structure, function, and evolution of bacterial ATP-binding cassette systems. *Microbiol Mol Biol Rev* **72**(2): 317-364.
de Almeida Couto, C.R., de Assis Leite, D.C., Jurelevicius, D., van Elsas, J.D., and Seldin, L. (2019) Chemical and biological dispersants differently affect the bacterial communities of uncontaminated and oil-contaminated marine water. *Brazilian Journal of Microbiology* **51**(2): 691-700.
Delacuvellerie, A., Cyriaque, V., Gobert, S., Benali, S., and Wattiez, R. (2019) The plastisphere in marine ecosystem hosts potential specific microbial degraders including *Alcanivorax borkumensis* as a key player for the low-density polyethylene degradation. *J Hazard Mat* **380**: 120899.
Diéguez, A., and Romalde, J. (2017) Draft genome sequences of *Neptuniibacter* sp. strains LFT 1.8 and ATR 1.1. *Genome Announcements* **5**(5).
Dombrowski, N., Donaho, J.A., Gutierrez, T., Seitz, K.W., Teske, A.P., and Baker, B.J. (2016) Reconstructing metabolic pathways of hydrocarbon-degrading bacteria from the Deepwater Horizon oil spill. *Nat Microbiol* **1**(7): 1-7.
Doyle, S.M., Whitaker, E.A., De Pascuale, V., Wade, T.L., Knap, A.H., Santschi, P.H. *et al.* (2018) Rapid formation of microbe-oil aggregates and changes in community composition in coastal surface water following exposure to oil and the dispersant Corexit. *Front Microbiol* **9**: 689.
Duran, R. (2010) *Marinobacter*. *Handbook of Hydrocarbon and Lipid Microbiology*. Timmis, K.N. (ed). Heidelberg, Germany: Springer, pp. 1725-1735. 10.1007/978-3-540-77587-4_122.
DWH NRDA Trustees (2016). Deepwater Horizon oil spill: Final programmatic damage assessment and restoration plan and final programmatic environmental impact statement. Available from: http://www.gulfspillrestoration.noaa.gov/restoration-planning/gulf-plan [Accessed June 16, 2020].
Dyksterhouse, S.E., Gray, J.P., Herwig, R.P., Lara, J.C., and Staley, J.T. (1995) *Cycloclasticus pugetii* gen. nov., sp. nov., an aromatic hydrocarbon-degrading bacterium from marine sediments. *Int J Syst Bacteriol* **45**(1): 116-123.

Ennouri, H., d'Abzac, P., Hakil, F., Branchu, P., Naïtali, M., Lomenech, A.M. *et al.* (2017) The extracellular matrix of the oleolytic biofilms of *Marinobacter hydrocarbonoclasticus* comprises cytoplasmic proteins and T2SS effectors that promote growth on hydrocarbons and lipids. *Environ Microbiol* **19**(1): 159-173.
Ernest, P. (1993). The *Exxon Valdez* oil spill: Final report, state of Alaska response. Anchorage, AK, USA: Alaska Department of Environmental Conservation. Available from: http://www.evostc.state.ak.us/static/PDFs/deccleanuptechniques.pdf [Accessed July 19, 2020].
Erni-Cassola, G., Wright, R.J., Gibson, M.I., and Christie-Oleza, J.A. (2020) Early colonization of weathered polyethylene by distinct bacteria in marine coastal seawater. *Microb Ecol* **79**(3): 517-526.
Etkin, D.S. (2000) Worldwide analysis of marine oil spill cleanup cost factors. *Arctic and marine oilspill program technical seminar*: Environment Canada, pp. 161-174.
Everaert, G., De Rijcke, M., Lonneville, B., Janssen, C., Backhaus, T., Mees, J. *et al.* (2020) Risks of floating microplastic in the global ocean. *Environ Pollut*: 115499.
Ewels, P.A., Peltzer, A., Fillinger, S., Patel, H., Alneberg, J., Wilm, A. *et al.* (2020) The nf-core framework for community-curated bioinformatics pipelines. *Nature Biotechnology* **38**(3): 276-278.
ExxonMobil (2014). Oil spill response field manual. USA: ExxonMobil Research and Engineering Company. Available from: https://corporate.exxonmobil.com/-/media/Global/Files/risk-management-and-safety/Oil-Spill-Response-Field-Manual_2014.pdf [Accessed July 19, 2020].
ExxonMobil (2018). Grane crude oil assay. Spring, Texas, USA. Available from: https://corporate.exxonmobil.com/Crude-oils/Crude-trading/Grane [Accessed August 20, 2020].
Faksness, L.-G., Brandvik, P.J., and Sydnes, L.K. (2008) Composition of the water accommodated fractions as a function of exposure times and temperatures. *Mar Pollut Bull* **56**(10): 1746-1754.
Falkowski, P.G., Fenchel, T., and Delong, E.F. (2008) The microbial engines that drive earth's biogeochemical cycles. *science* **320**(5879): 1034-1039.
Fasca, H., de Castilho, L.V., de Castilho, J.F.M., Pasqualino, I.P., Alvarez, V.M., de Azevedo Jurelevicius, D., and Seldin, L. (2018) Response of marine bacteria to oil contamination and to high pressure and low temperature deep sea conditions. *MicrobiologyOpen* **7**(2): e00550.
Fida, T.T., Moreno-Forero, S.K., Heipieper, H.J., and Springael, D. (2013) Physiology and transcriptome of the polycyclic aromatic hydrocarbon-degrading *Sphingomonas* sp. LH128 after long-term starvation. *Microbiology* **159**(Pt 9): 1807-1817.
Finch, B.E., Marzooghi, S., Di Toro, D.M., and Stubblefield, W.A. (2017) Phototoxic potential of undispersed and dispersed fresh and weathered Macondo crude oils to Gulf of Mexico marine organisms. *Environ Toxicol Chem* **36**(10): 2640-2650.
Flemming, H.-C., Wingender, J., Szewzyk, U., Steinberg, P., Rice, S.A., and Kjelleberg, S. (2016) Biofilms: An emergent form of bacterial life. *Nat Rev Microbiol* **14**(9): 563.
Flemming, H.-C., and Wuertz, S. (2019) Bacteria and archaea on earth and their abundance in biofilms. *Nat Rev Microbiol* **17**(4): 247-260.
Foght, J., and Westlake, D. (1982) Effect of the dispersant Corexit 9527 on the microbial degradation of Prudhoe Bay oil. *Can J Microbiol* **28**(1): 117-122.
Folt, C.L., Chen, C.Y., Moore, M.V., and Burnaford, J. (1999) Synergism and antagonism among multiple stressors. *Limnol Oceanogr* **44**: 864-877.
Fuhrman, J.A., Cram, J.A., and Needham, D.M. (2015) Marine microbial community dynamics and their ecological interpretation. *Nat Rev Microbiol* **13**(3): 133-146.
Fukuda, R., and Ohta, A. (2019) Genetic features and regulation of *n*-alkane metabolism in yeasts. In *Aerobic utilization of hydrocarbons, oils and lipids*. Rojo, F. (ed): Springer, pp. 1-13.
Gacesa, P. (1998) Bacterial alginate biosynthesis: Recent progress and future prospects. *Microbiology* **144**: 1133-1143.
Galand, P.E., Pereira, O., Hochart, C., Auguet, J.C., and Debroas, D. (2018) A strong link between marine microbial community composition and function challenges the idea of functional redundancy. *ISME J* **12**(10): 2470-2478.
Garcia, M., Campos, E., Marsal, A., and Ribosa, I. (2009) Biodegradability and toxicity of sulphonate-based surfactants in aerobic and anaerobic aquatic environments. *Water Res* **43**(2): 295-302.
Gauthier, M.J., Lafay, B., Christen, R., Fernandez, L., Acquaviva, M., Bonin, P., and Bertrand, J.-C. (1992) *Marinobacter hydrocarbonoclasticus* gen. nov., sp. nov., a new, extremely halotolerant, hydrocarbon-degrading marine bacterium. *Int J Syst Evol Microbiol* **42**(4): 568-576.
Ge, J., Zhao, H.Y., Zhu, H.W., Huang, J., Shi, L.A., and Yu, S.H. (2016) Advanced sorbents for oil-spill cleanup: Recent advances and future perspectives. *Advanced materials* **28**(47): 10459-10490.
Gerdes, B., Brinkmeyer, R., Dieckmann, G., and Helmke, E. (2005) Influence of crude oil on changes of bacterial communities in Arctic sea-ice. *FEMS Microbiol Ecol* **53**(1): 129-139.

Gertler, C., Näther, D.J., Cappello, S., Gerdts, G., Quilliam, R.S., Yakimov, M.M., and Golyshin, P.N. (2012) Composition and dynamics of biostimulated indigenous oil-degrading microbial consortia from the Irish, North and Mediterranean seas: A mesocosm study. *FEMS Microbiol Ecol* **81**(3): 520-536.
Ghafoor, A., Hay, I.D., and Rehm, B.H. (2011) Role of exopolysaccharides in *Pseudomonas aeruginosa* biofilm formation and architecture. *Appl Environ Microbiol* **77**(15): 5238-5246.
Gilfillan, E.S., Page, D.S., Hanson, S.A., Foster, J.C., Hotham, J., Vallas, D. *et al.* (1985) Tidal area dispersant experiment, Searsport Maine: An overview. *International Oil Spill Conference*: American Petroleum Institute, pp. 553-559.
Gillings, M.R., Gaze, W.H., Pruden, A., Smalla, K., Tiedje, J.M., and Zhu, Y.-G. (2015) Using the class 1 integron-integrase gene as a proxy for anthropogenic pollution. *ISME J* **9**(6): 1269-1279.
Giuliani, S.E., Frank, A.M., Corgliano, D.M., Seifert, C., Hauser, L., and Collart, F.R. (2011) Environment sensing and response mediated by ABC transporters. *BMC Genomics* **12**(1): 1-14.
Gofstein, T.R., Perkins, M., Field, J., and Leigh, M.B. (2020) The interactive effects of crude oil and Corexit 9500 on their biodegradation in Arctic seawater. *Appl Environ Microbiol* **86**(21): e01194-01120.
Goodland, J. (1998) The *Braer* oil spill in Shetland, 1993 to 1997. *Dispersant Use in Alaska: A Technical Update*. Trudel, B.K. (ed). Anchorage, Alaska, USA: Prince William Sound Oil Spill Recovery Institute.
Gräbsch, C. (2016) Health effects of mineral oil, dispersants and oil-dispersant-mixtures. In *The use of dispersants to combat oil spills in Germany at sea*. Grote, M., Nagel, A., Nies, H., Rauterberg, J., and Wahrendorf, D.-S. (eds). Berlin, Germany: Federal Institute for Risk Assessment, pp. 37-47.
Grant, C., Deszcz, D., Wei, Y.-C., Martinez-Torres, R.J., Morris, P., Folliard, T. *et al.* (2014) Identification and use of an alkane transporter plug-in for applications in biocatalysis and whole-cell biosensing of alkanes. *Sci Rep* **4**: 5844.
Green, D.H., Bowman, J.P., Smith, E.A., Gutierrez, T., and Bolch, C.J. (2006) *Marinobacter algicola* sp. nov., isolated from laboratory cultures of paralytic shellfish toxin-producing dinoflagellates. *Int J Syst Evol Microbiol* **56**(3): 523-527.
Gregson, B.H., Metodieva, G., Metodiev, M.V., Golyshin, P.N., and McKew, B.A. (2018) Differential protein expression during growth on medium versus long-chain alkanes in the obligate marine hydrocarbon-degrading bacterium *Thalassolituus oleivorans* MIL-1. *Front Microbiol* **9**: 3130.
Gregson, B.H., Metodieva, G., Metodiev, M.V., and McKew, B.A. (2019) Differential protein expression during growth on linear versus branched alkanes in the obligate marine hydrocarbon-degrading bacterium *Alcanivorax borkumensis* SK2(T). *Environ Microbiol* **21**(7): 2347-2359.
Gregson, B.H., Metodieva, G., Metodiev, M.V., Golyshin, P.N., and McKew, B.A. (2020) Protein expression in the obligate hydrocarbon-degrading psychrophile *Oleispira antarctica* RB-8 during alkane degradation and cold tolerance. *Environ Microbiol* **22**(5): 1870-1883.
Grossart, H.-P., Van den Wyngaert, S., Kagami, M., Wurzbacher, C., Cunliffe, M., and Rojas-Jimenez, K. (2019) Fungi in aquatic ecosystems. *Nat Rev Microbiol* **17**(6): 339-354.
Grote, M., van Bernem, C., Böhme, B., Callies, U., Calvez, I., Christie, B. *et al.* (2018) The potential for dispersant use as a maritime oil spill response measure in German waters. *Mar Pollut Bull* **129**(2): 623-632.
Gunasekera, T.S., Striebich, R.C., Mueller, S.S., Strobel, E.M., and Ruiz, O.N. (2013) Transcriptional profiling suggests that multiple metabolic adaptations are required for effective proliferation of *Pseudomonas aeruginosa* in jet fuel. *Environ Sci Technol* **47**(23): 13449-13458.
Gutierrez, T., Nichols, P.D., Whitman, W.B., and Aitken, M.D. (2012) *Porticoccus hydrocarbonoclasticus* sp. nov., an aromatic hydrocarbon-degrading bacterium identified in laboratory cultures of marine phytoplankton. *Appl Environ Microbiol* **78**(3): 628-637.
Gutierrez, T., Berry, D., Yang, T., Mishamandani, S., McKay, L., Teske, A., and Aitken, M.D. (2013a) Role of bacterial exopolysaccharides (EPS) in the fate of the oil released during the Deepwater Horizon oil spill. *PloS one* **8**(6): e67717.
Gutierrez, T., Singleton, D.R., Berry, D., Yang, T., Aitken, M.D., and Teske, A. (2013b) Hydrocarbon-degrading bacteria enriched by the Deepwater Horizon oil spill identified by cultivation and DNA-SIP. *ISME J* **7**(11): 2091-2104.
Gutierrez, T., Rhodes, G., Mishamandani, S., Berry, D., Whitman, W.B., Nichols, P.D. *et al.* (2014) Polycyclic aromatic hydrocarbon degradation of phytoplankton-associated *Arenibacter* spp. and description of *Arenibacter algicola* sp. nov., an aromatic hydrocarbon-degrading bacterium. *Appl Environ Microbiol* **80**(2): 618-628.
Gutierrez, T. (2017) Dispersants: The good, the bad and the rise of a new bio-based generation. *Arch Pet Environ Biotechnol* **10**: 2574-7614.
Gutierrez, T. (2018) Preparing for the next big oil spill at sea: A microbiological perspective. *Journal of Marine Microbiology* **2**(1): 13-14.

Gutierrez, T., Morris, G., Ellis, D., Bowler, B., Jones, M., Salek, K. *et al.* (2018) Hydrocarbon-degradation and MOS-formation capabilities of the dominant bacteria enriched in sea surface oil slicks during the Deepwater Horizon oil spill. *Mar Pollut Bull* **135**: 205-215.

Gutierrez, T. (2019) Occurrence and roles of the obligate hydrocarbonoclastic bacteria in the ocean when there is no obvious hydrocarbon contamination. In *Taxonomy, genomics and ecophysiology of hydrocarbon-degrading microbes*. McGenity, T.J. (ed), pp. 337-352.

Gutierrez, T., and Kleindienst, S. (2020) Uncovering microbial hydrocarbon degradation processes: The promise of stable isotope probing. In *Marine hydrocarbon seeps*: Springer, pp. 183-199.

Haange, S.-B., Jehmlich, N., Hoffmann, M., Weber, K., Lehmann, J.r., von Bergen, M., and Slanina, U. (2019) Disease development is accompanied by changes in bacterial protein abundance and functions in a refined model of dextran sulfate sodium (DSS)-induced colitis. *J Proteome Res* **18**(4): 1774-1786.

Hackbusch, S., Noirungsee, N., Viamonte, J., Sun, X., Bubenheim, P., Kostka, J.E. *et al.* (2020) Influence of pressure and dispersant on oil biodegradation by a newly isolated *Rhodococcus* strain from deep-sea sediments of the Gulf of Mexico. *Mar Pollut Bull* **150**: 110683.

Hales, S.G. (1993) Biodegradation of the anionic surfactant dialkyl sulphosuccinate. *Environ Toxicol Chem* **12**(10): 1821-1828.

Hamdan, L.J., and Fulmer, P.A. (2011) Effects of Corexit EC9500A on bacteria from a beach oiled by the Deepwater Horizon spill. *Aquat Microb Ecol* **63**(2): 101-109.

Harriss, R. (2016) Arctic offshore oil: Great risks in an evolving ocean. *Environment: Science and Policy for Sustainable Development* **58**(3): 18-29.

Harsem, Ø., Heen, K., Rodrigues, J., and Vassdal, T. (2015) Oil exploration and sea ice projections in the Arctic. *The Polar Record* **51**(1): 91.

Harwati, T.U., Kasai, Y., Kodama, Y., Susilaningsih, D., and Watanabe, K. (2007) Characterization of diverse hydrocarbon-degrading bacteria isolated from Indonesian seawater. *Microbes and Environments* **22**(4): 412-415.

Harwati, T.U., Kasai, Y., Kodama, Y., Susilaningsih, D., and Watanabe, K. (2009) *Tropicibacter naphthalenivorans* gen. nov., sp. nov., a polycyclic aromatic hydrocarbon-degrading bacterium isolated from Semarang Port in Indonesia. *Int J Syst Evol Microbiol* **59**(2): 392-396.

Hay, I.D., Ur Rehman, Z., Moradali, M.F., Wang, Y., and Rehm, B.H. (2013) Microbial alginate production, modification and its applications. *Microb Biotechnol* **6**(6): 637-650.

Hayles, M.F., and de Winter, D.M. (2020) An introduction to cryo-FIB-SEM cross-sectioning of frozen, hydrated life science samples. *Journal of Microscopy*.

Hazen, T.C., Dubinsky, E.A., DeSantis, T.Z., Andersen, G.L., Piceno, Y.M., Singh, N. *et al.* (2010) Deep-sea oil plume enriches indigenous oil-degrading bacteria. *Science* **330**(6001): 204-208.

Hazen, T.C., Prince, R.C., and Mahmoudi, N. (2016) Marine oil biodegradation. *Environ Sci Technol* **50**(5): 2121-2129.

Head, I.M., Jones, D.M., and Röling, W.F. (2006) Marine microorganisms make a meal of oil. *Nat Rev Microbiol* **4**(3): 173-182.

Hedlund, B.P., Geiselbrecht, A.D., Bair, T.J., and Staley, J.T. (1999) Polycyclic aromatic hydrocarbon degradation by a new marine bacterium, *Neptunomonas naphthovorans* gen. nov., sp. Nov. *Appl Environ Microbiol* **65**(1): 251-259.

Hernández-López, E., Ayala, M., and Vazquez-Duhalt, R. (2015) Microbial and enzymatic biotransformations of asphaltenes. *Petroleum Science and Technology* **33**(9): 1017-1029.

Hoefs, M.J., Van Heemst, J.D., Gelin, F., Koopmans, M.P., Van Kaam-Peters, H.M., Schouten, S. *et al.* (1995) Alternative biological sources for 1,2,3,4-tetramethylbenzene in flash pyrolysates of kerogen. *Organic Geochemistry* **23**(10): 975-979.

Holder, E.L., Conmy, R.N., and Venosa, A.D. (2015) Comparative laboratory-scale testing of dispersant effectiveness of 23 crude oils using four different testing protocols. *J Environ Prot* **6**(06): 628.

Hook, S.E., and Osborn, H.L. (2012) Comparison of toxicity and transcriptomic profiles in a diatom exposed to oil, dispersants, dispersed oil. *Aquatic Toxicology* **124**: 139-151.

Hosie, A.H., Allaway, D., Jones, M., Walshaw, D., Johnston, A., and Poole, P.S. (2001) Solute-binding protein-dependent ABC transporters are responsible for solute efflux in addition to solute uptake. *Mol Microbiol* **40**(6): 1449-1459.

Hunt, A. (2016) Operational experience worldwide. In *The use of dispersants to combat oil spills in Germany at sea*. Grote, M., Nagel, A., Nies, H., Rauterberg, J., and Wahrendorf, D.-S. (eds). Berlin, Germany: Federal Institute for Risk Assessment, pp. 69-81.

Inacio, A.S., Domingues, N.S., Nunes, A., Martins, P.T., Moreno, M.J., Estronca, L.M. *et al.* (2016) Quaternary ammonium surfactant structure determines selective toxicity towards bacteria: Mechanisms of action and clinical implications in antibacterial prophylaxis. *J Antimicrob Chemother* **71**(3): 641-654.

ITOPF (2020). Oil tanker spill statistics 2019. London, UK: International Tanker Owners Pollution Federation. Available from: http://www.itopf.org/fileadmin/data/Documents/Company_Lit/Oil_Spill_Stats_brochure_2020_for_web.pdf [Accessed May 27, 2020].
Jernelöv, A., and Lindén, O. (1981) Ixtoc I: A case study of the world's largest oil spill. *Ambio*: 299-306.
John, V., Arnosti, C., Field, J., Kujawinski, E., and McCormick, A. (2016) The role of dispersants in oil spill remediation: Fundamental concepts, rationale for use, fate, and transport issues. *Oceanography* **29**(3): 108-117.
Johnson, K., Baker, P., Kan, H., Maurissen, J., Spencer, P., and Marty, M. (2005) Diethylene glycol monobutyl ether (DGBE): Two-and thirteen-week oral toxicity studies in Fischer 344 rats. *Food and chemical toxicology* **43**(3): 467-481.
Jones, P.M., and George, A.M. (2013) Mechanism of the ABC transporter ATPase domains: Catalytic models and the biochemical and biophysical record. *Crit Rev Biochem Mol Biol* **48**(1): 39-50.
Joye, S., Kleindienst, S., and Pena-Montenegro, T.D. (2018) Snapshot: Microbial hydrocarbon bioremediation. *Cell* **172**(6): 1336-1336 e1331.
Joye, S.B. (2015) Deepwater Horizon, 5 years on. *Science* **349**(6248): 592-593.
Joye, S.B., Bracco, A., Özgökmen, T.M., Chanton, J.P., Grosell, M., MacDonald, I.R. *et al.* (2016a) The Gulf of Mexico ecosystem, six years after the Macondo oil well blowout. *Deep Sea Res Part II Top Stud Oceanogr* **129**: 4-19.
Joye, S.B., Kleindienst, S., Gilbert, J.A., Handley, K.M., Weisenhorn, P., Overholt, W.A., and Kostka, J.E. (2016b) Responses of microbial communities to hydrocarbon exposures. *Oceanography* **29**(3): 136-149.
Joye, S.B., and Kleindienst, S. (2017) Hydrocarbon seep ecosystems. In *Life at vents and seeps*. Kallmeyer, J. (ed), pp. 33-52.
Julsing, M.K., Schrewe, M., Cornelissen, S., Hermann, I., Schmid, A., and Bühler, B. (2012) Outer membrane protein AlkL boosts biocatalytic oxyfunctionalization of hydrophobic substrates in *Escherichia coli*. *Appl Environ Microbiol* **78**(16): 5724-5733.
Jung, J., Noh, J., and Park, W. (2011) Physiological and metabolic responses for hexadecane degradation in *Acinetobacter oleivorans* DR1. *The Journal of Microbiology* **49**(2): 208-215.
Kaberdin, V.R., Montanchez, I., Parada, C., Orruno, M., Arana, I., and Barcina, I. (2015) Unveiling the metabolic pathways associated with the adaptive reduction of cell size during *Vibrio harveyi* persistence in seawater microcosms. *Microb Ecol* **70**(3): 689-700.
Kanehisa, M., Sato, Y., and Morishima, K. (2016) BlastKOALA and GhostKOALA: KEGG tools for functional characterization of genome and metagenome sequences. *J Mol Biol* **428**(4): 726-731.
Kanehisa, M., and Sato, Y. (2020) KEGG mapper for inferring cellular functions from protein sequences. *Protein Sci* **29**(1): 28-35.
Kasai, Y., Kishira, H., and Harayama, S. (2002) Bacteria belonging to the genus *Cycloclasticus* play a primary role in the degradation of aromatic hydrocarbons released in a marine environment. *Appl Environ Microbiol* **68**(11): 5625-5633.
Kaster, A.-K., and Sobol, M.S. (2020) Microbial single-cell omics: The crux of the matter. *Appl Microbiol Biotechnol*: 1-12.
Kato, T., Miyanaga, A., Kanaya, S., and Morikawa, M. (2009) Alkane inducible proteins in *Geobacillus thermoleovorans* B23. *BMC Microbiology* **9**(1): 60.
Khadka, N.S. (2020) Why the Mauritius oil spill is so serious. In *BBC News*. Published on: August 12, 2020. Available from: https://www.bbc.com/news/world-africa-53754751 [Accessed August 28, 2020].
Khleifat, K.M. (2007) Effect of substrate adaptation, carbon starvation and cell density on the biodegradation of phenol by *Actinobacillus* sp. *Fresenius Environ Bull* **16**(7): 726-730.
Kirby, M.F., and Law, R.J. (2008) Oil spill treatment products approval: The UK approach and potential application to the Gulf region. *Mar Pollut Bull* **56**(7): 1243-1247.
Kirby, M.F., and Law, R.J. (2010) Accidental spills at sea: Risk, impact, mitigation and the need for co-ordinated post-incident monitoring. *Mar Pollut Bull* **60**(6): 797-803.
Kirchman, D. (2001) Measuring bacterial biomass production and growth rates from leucine incorporation in natural aquatic environments. *Methods Microbiol* **30**: 227–237.
Kjelleberg, S., and Hermansson, M. (1984) Starvation-induced effects on bacterial surface characteristics. *Appl Environ Microbiol* **48**(3): 497-503.
Klein, B., Grossi, V., Bouriat, P., Goulas, P., and Grimaud, R. (2008) Cytoplasmic wax ester accumulation during biofilm-driven substrate assimilation at the alkane–water interface by *Marinobacter hydrocarbonoclasticus* SP17. *Res Microbiol* **159**(2): 137-144.
Kleindienst, S., Paul, J.H., and Joye, S.B. (2015a) Using dispersants after oil spills: Impacts on the composition and activity of microbial communities. *Nat Rev Microbiol* **13**(6): 388-396.

Kleindienst, S., Seidel, M., Ziervogel, K., Grim, S., Loftis, K., Harrison, S. *et al.* (2015b) Chemical dispersants can suppress the activity of natural oil-degrading microorganisms. *Proc Natl Acad Sci USA* **112**(48): 14900-14905.
Kleindienst, S., Grim, S., Sogin, M., Bracco, A., Crespo-Medina, M., and Joye, S.B. (2016a) Diverse, rare microbial taxa responded to the Deepwater Horizon deep-sea hydrocarbon plume. *ISME J* **10**(2): 400-415.
Kleindienst, S., Grim, S., Sogin, M., Bracco, A., Crespo-Medina, M., and Joye, S.B. (2016b) Diverse, rare microbial taxa responded to the Deepwater Horizon deep-sea hydrocarbon plume. *ISME J* **10**(2): 400-415.
Kleindienst, S., and Joye, S.B. (2017) Global aerobic degradation of hydrocarbons in aquatic systems. *Aerobic Utilization of Hydrocarbons, Oils and Lipids*: 1-18.
Knapik, K., Bagi, A., Krolicka, A., and Baussant, T. (2019) Discovery of functional gene markers of bacteria for monitoring hydrocarbon pollution in the marine environment: A metatranscriptomics approach. *bioRxiv*: 857391.
Knapik, K., Bagi, A., Krolicka, A., and Baussant, T. (2020) Metatranscriptomic analysis of oil-exposed seawater bacterial communities archived by an environmental sample processor (ESP). *Microorganisms* **8**(5): 744.
Kover, S.C., Rosario-Ortiz, F.L., and Linden, K.G. (2014) Photochemical fate of solvent constituents of Corexit oil dispersants. *Water Res* **52**: 101-111.
Krell, T., Lacal, J., Guazzaroni, M.E., Busch, A., Silva-Jimenez, H., Fillet, S. *et al.* (2012) Responses of *Pseudomonas putida* to toxic aromatic carbon sources. *J Biotechnol* **160**(1-2): 25-32.
Kujawinski, E.B., Kido Soule, M.C., Valentine, D.L., Boysen, A.K., Longnecker, K., and Redmond, M.C. (2011) Fate of dispersants associated with the Deepwater Horizon oil spill. *Environ Sci Technol* **45**(4): 1298-1306.
Kujawinski, E.B., Reddy, C.M., Rodgers, R.P., Thrash, J.C., Valentine, D.L., and White, H.K. (2020) The first decade of scientific insights from the Deepwater Horizon oil release. *Nature Reviews Earth & Environment* **1**: 237–250.
Lea-Smith, D.J., Biller, S.J., Davey, M.P., Cotton, C.A., Sepulveda, B.M.P., Turchyn, A.V. *et al.* (2015) Contribution of cyanobacterial alkane production to the ocean hydrocarbon cycle. *Proc Natl Acad Sci USA* **112**(44): 13591-13596.
Lee, K., Boufadel, M., Chen, B., Foght, J., Hodson, P., Swanson, S., and Venosa, A. (2015). Expert panel report on the behaviour and environmental impacts of crude oil released into aqueous environments. Ottawa, ON, Canada: Royal Society of Canada.
Leung, K.T., Moore, M., Lee, H., and Trevors, J.T. (2005) Effect of carbon starvation on *p*-nitrophenol degradation by a *Moraxella* strain in buffer and river water. *FEMS Microbiol Ecol* **51**(2): 237-245.
Lewis, A., Crosbie, A., Davies, L., and Lunel, T. (1998) The AEA '97 North Sea field trials on oil weathering and aerial application of dispersants. *Dispersant Use in Alaska: A Technical Update*. Trudel, B.K. (ed). Anchorage, Alaska, USA: Prince William Sound Oil Spill Recovery Insitute.
Lewis, A., and Prince, R.C. (2018) Integrating dispersants in oil spill response in Arctic and other icy environments. *Environ Sci Technol* **52**(11): 6098-6112.
Li, Y., Pan, J., and Ma, Y. (2020) Elucidation of multiple alkane hydroxylase systems in biodegradation of crude oil *n*-alkane pollution by *Pseudomonas aeruginosa* DN1. *J Appl Microbiol* **128**(1): 151-160.
Liao, Y., Geng, A., and Huang, H. (2009) The influence of biodegradation on resins and asphaltenes in the Liaohe Basin. *Organic Geochemistry* **40**(3): 312-320.
Lindstrom, J.E., and Braddock, J.F. (2002) Biodegradation of petroleum hydrocarbons at low temperature in the presence of the dispersant Corexit 9500. *Mar Pollut Bull* **44**: 739-747.
Liu, C., Wang, W., Wu, Y., Zhou, Z., Lai, Q., and Shao, Z. (2011) Multiple alkane hydroxylase systems in a marine alkane degrader *Alcanivorax dieselolei* B-5. *Environ Microbiol* **13**(5): 1168-1178.
Liu, J., Bacosa, H.P., and Liu, Z. (2017a) Potential environmental factors affecting oil-degrading bacterial populations in deep and surface waters of the northern Gulf of Mexico. *Front Microbiol* **7**: 2131.
Liu, S., Guo, C., Lin, W., Wu, F., Lu, G., Lu, J., and Dang, Z. (2017b) Comparative transcriptomic evidence for Tween80-enhanced biodegradation of phenanthrene by *Sphingomonas* sp. GY2B. *Sci Total Environ* **609**: 1161-1171.
Loeffler, J. (2019) France tries to contain oil spill as 2000 cars, freighter sink off coast. In *Interesting Engineering*. Published on: March 23, 2019. Available from: https://interestingengineering.com/france-tries-to-contain-oil-spill-as-2000-cars-freighter-sink-off-coast [Accessed August 28, 2020].
Lofthus, S., Netzer, R., Lewin, A.S., Heggeset, T.M.B., Haugen, T., and Brakstad, O.G. (2018) Biodegradation of *n*-alkanes on oil-seawater interfaces at different temperatures and microbial communities associated with the degradation. *Biodegradation* **29**(2): 141-157.

Lunel, T. (1998) *Sea Empress* spill: Dispersant operations, effectiveness and effectiveness monitoring. *Dispersant Use in Alaska: A Technical Update*. Trudel, B.K. (ed). Anchorage, Alaska, USA: Prince William Sound Oil Spill Recovery Institute.

Luter, H.M., Whalan, S., Andreakis, N., Wahab, M.A., Botté, E.S., Negri, A.P., and Webster, N.S. (2019) The effects of crude oil and dispersant on the larval sponge holobiont. *mSystems* **4**: e00743-00719.

MacDonald, I.R., Garcia-Pineda, O., Beet, A., Daneshgar Asl, S., Feng, L., Graettinger, G. *et al.* (2015) Natural and unnatural oil slicks in the Gulf of Mexico. *Journal of Geophysical Research: Oceans* **120**(12): 8364-8380.

Manilla-Pérez, E., Reers, C., Baumgart, M., Hetzler, S., Reichelt, R., Malkus, U. *et al.* (2010) Analysis of lipid export in hydrocarbonoclastic bacteria of the genus *Alcanivorax*: Identification of lipid export-negative mutants of *Alcanivorax borkumensis* SK2 and *Alcanivorax jadensis* T9. *J Bacteriol* **192**(3): 643-656.

Martin, M. (2011) Cutadapt removes adapter sequences from high-throughput sequencing reads. *EMBnet journal* **17**(1): 10-12.

Mas-Lladó, M., Piña-Villalonga, J.M., Brunet-Galmés, I., Nogales, B., and Bosch, R. (2014) Draft genome sequences of two isolates of the Roseobacter group, *Sulfitobacter* sp. strains 3SOLIMAR09 and 1FIGIMAR09, from harbors of Mallorca Island (Mediterranean sea). *Genome Announcements* **2**(3).

Mason, A.L., Taylor, J.C., and MacDonald, I.R. (2019). An integrated assessment of oil and gas release into the marine environment at the former Taylor Energy MC20 site. Silver Spring, MD, USA: NOAA National Ocean Service, N.C.f.C.O.S. Available from: https://repository.library.noaa.gov/view/noaa/20612 [Accessed August 30, 2020].

Mason, O.U., Hazen, T.C., Borglin, S., Chain, P.S., Dubinsky, E.A., Fortney, J.L. *et al.* (2012) Metagenome, metatranscriptome and single-cell sequencing reveal microbial response to Deepwater Horizon oil spill. *ISME J* **6**(9): 1715-1727.

Mason, O.U., Han, J., Woyke, T., and Jansson, J.K. (2014) Single-cell genomics reveals features of a *Colwellia* species that was dominant during the Deepwater Horizon oil spill. *Front Microbiol* **5**: 332.

Mayer-Pinto, M., Ledet, J., Crowe, T.P., and Johnston, E.L. (2020) Sublethal effects of contaminants on marine habitat-forming species: A review and meta-analysis. *Biological Reviews*(10.1111/brv.12630).

McFarlin, K.M., Prince, R.C., Perkins, R., and Leigh, M.B. (2014) Biodegradation of dispersed oil in arctic seawater at -1°C. *PloS One* **9**(1): e84297.

McFarlin, K.M. (2017) The biodegradation of oil and the dispersant Corexit 9500 in Arctic seawater. *Thesis*, PhD in Biological Sciences. University of Alaska Fairbanks, Department of Biology and Wildlife; Fairbanks, Alaska, USA.

McFarlin, K.M., Questel, J.M., Hopcroft, R.R., and Leigh, M.B. (2017) Bacterial community structure and functional potential in the northeastern Chukchi Sea. *Cont Shelf Res* **136**: 20-28.

McFarlin, K.M., Perkins, M.J., Field, J.A., and Leigh, M.B. (2018) Biodegradation of crude oil and Corexit 9500 in Arctic seawater. *Front Microbiol* **9**: 1788.

McGenity, T.J., Folwell, B.D., McKew, B.A., and Sanni, G.O. (2012) Marine crude-oil biodegradation: A central role for interspecies interactions. *Aquatic Biosystems* **8**(1): 10.

McGowan, C.J., Kwok, R.K., Engel, L.S., Stenzel, M.R., Stewart, P.A., and Sandler, D.P. (2017) Respiratory, dermal, and eye irritation symptoms associated with Corexit EC9527A/EC9500A following the Deepwater Horizon oil spill: Findings from the GuLF STUDY. *Environ Health Perspect* **125**(9): 097015.

McMurdie, P.J., and Holmes, S. (2013) Phyloseq: An R package for reproducible interactive analysis and graphics of microbiome census data. *PloS one* **8**(4): e61217.

McNutt, M.K., Camilli, R., Crone, T.J., Guthrie, G.D., Hsieh, P.A., Ryerson, T.B. *et al.* (2012) Review of flow rate estimates of the Deepwater Horizon oil spill. *Proc Natl Acad Sci USA* **109**(50): 20260-20267.

Meier, W.N., Hovelsrud, G.K., Van Oort, B.E., Key, J.R., Kovacs, K.M., Michel, C. *et al.* (2014) Arctic sea ice in transformation: A review of recent observed changes and impacts on biology and human activity. *Rev Geophys* **52**(3): 185-217.

Meng, L., Liu, H., Bao, M., and Sun, P. (2016) Microbial community structure shifts are associated with temperature, dispersants and nutrients in crude oil-contaminated seawaters. *Mar Pollut Bull* **111**(1-2): 203-212.

Methé, B.A., Nelson, K.E., Deming, J.W., Momen, B., Melamud, E., Zhang, X. *et al.* (2005) The psychrophilic lifestyle as revealed by the genome sequence of *Colwellia psychrerythraea* 34h through genomic and proteomic analyses. *Proc Natl Acad Sci USA* **102**(31): 10913-10918.

Michalska, K., Chang, C., Mack, J.C., Zerbs, S., Joachimiak, A., and Collart, F.R. (2012) Characterization of transport proteins for aromatic compounds derived from lignin: Benzoate derivative binding proteins. *J Mol Biol* **423**(4): 555-575.

Militon, C., Jezequel, R., Gilbert, F., Corsellis, Y., Sylvi, L., Cravo-Laureau, C. *et al.* (2015) Dynamics of bacterial assemblages and removal of polycyclic aromatic hydrocarbons in oil-contaminated coastal marine sediments subjected to contrasted oxygen regimes. *Environ Sci Pollut Res* **22**(20): 15260-15272.

Mojžiš, M., Bubeníková, T., Zachar, M., Kačíková, D., and Štefková, J. (2019) Comparison of natural and synthetic sorbents′ efficiency at oil spill removal. *BioResources* **14**(4): 8738-8752.

Moradali, M.F., and Rehm, B.H. (2019) The role of alginate in bacterial biofilm formation. *Extracellular Sugar-Based Biopolymers Matrices*. Cohen, E., and Merzendorfer, H. (eds): Springer, pp. 517-537.

Mounier, J., Camus, A., Mitteau, I., Vaysse, P.J., Goulas, P., Grimaud, R., and Sivadon, P. (2014) The marine bacterium *Marinobacter hydrocarbonoclasticus* SP17 degrades a wide range of lipids and hydrocarbons through the formation of oleolytic biofilms with distinct gene expression profiles. *FEMS Microbiolgy Ecology* **90**(3): 816-831.

Mounier, J., Hakil, F., Branchu, P., Naïtali, M., Goulas, P., Sivadon, P., and Grimaud, R. (2018) AupA and AupB are outer and inner membrane proteins involved in alkane uptake in *Marinobacter hydrocarbonoclasticus* SP17. *mBio* **9**(3): e00520-00518.

Mulligan, C., Fischer, M., and Thomas, G.H. (2011) Tripartite ATP-independent periplasmic (TRAP) transporters in bacteria and archaea. *FEMS Microbiol Rev* **35**(1): 68-86.

Murawski, S.A., Hollander, D.J., Gilbert, S., and Gracia, A. (2020) Deepwater oil and gas production in the Gulf of Mexico and related global trends. In *Scenarios and responses to future deep oil spills*: Springer, pp. 16-32.

Murínová, S., and Dercová, K. (2014) Response mechanisms of bacterial degraders to environmental contaminants on the level of cell walls and cytoplasmic membrane. *Int J Microbiol* **2014**: 873081.

Murphy, D., Gemmell, B., Vaccari, L., Li, C., Bacosa, H., Evans, M. *et al.* (2016) An in-depth survey of the oil spill literature since 1968: Long term trends and changes since Deepwater Horizon. *Mar Pollut Bull* **113**(1-2): 371-379.

Muyzer, G., De Waal, E.C., and Uitterlinden, A.G. (1993) Profiling of complex microbial populations by denaturing gradient gel electrophoresis analysis of polymerase chain reaction amplified genes coding for 16s rRNA. *Appl Environ Microbiol* **59**(3): 695-700.

Nadkarni, M.A., Martin, F.E., Jacques, N.A., and Hunter, N. (2002) Determination of bacterial load by real-time pcr using a broad-range (universal) probe and primers set. *Microbiology* **148**(1): 257-266.

Nagashima, H., Zulkharnain, A.B., Maeda, R., Fuse, H., Iwata, K., and Omori, T. (2010) Cloning and nucleotide sequences of carbazole degradation genes from marine bacterium *Neptuniibacter* sp. strain CAR-SF. *Curr Microbiol* **61**(1): 50-56.

Naysim, L., Kang, H.J., and Jeon, C.O. (2014) *Zhongshania aliphaticivorans* sp. nov., an aliphatic hydrocarbon-degrading bacterium isolated from marine sediment, and transfer of *Spongiibacter borealis* Jang *et al.* 2011 to the genus *Zhongshania* as *Zhongshania borealis* comb. Nov. *Int J Syst Evol Microbiol* **64**(11): 3768-3774.

Nedashkovskaya, O.I., Kukhlevskiy, A.D., Zhukova, N.V., and Kim, S.B. (2016) *Amylibacter ulvae* sp. nov., a new alphaproteobacterium isolated from the pacific green alga *Ulva fenestrata*. *Arch Microbiol* **198**(3): 251-256.

Neuparth, T., Moreira, S., Santos, M., and Reis-Henriques, M. (2012) Review of oil and HNS accidental spills in Europe: Identifying major environmental monitoring gaps and drawing priorities. *Mar Pollut Bull* **64**(6): 1085-1095.

Nevalainen, M., Helle, I., and Vanhatalo, J. (2018) Estimating the acute impacts of Arctic marine oil spills using expert elicitation. *Mar Pollut Bull* **131**: 782-792.

Ng, H.J., Lopez-Perez, M., Webb, H.K., Gomez, D., Sawabe, T., Ryan, J. *et al.* (2014) *Marinobacter salarius* sp. nov. and *Marinobacter similis* sp. nov., isolated from sea water. *PLoS One* **9**(9): e106514.

Nie, Y., Chi, C.-Q., Fang, H., Liang, J.-L., Lu, S.-L., Lai, G.-L. *et al.* (2014) Diverse alkane hydroxylase genes in microorganisms and environments. *Sci Rep* **4**: 4968.

Nikolopoulou, M., and Kalogerakis, N. (2008) Enhanced bioremediation of crude oil utilizing lipophilic fertilizers combined with biosurfactants and molasses. *Mar Pollut Bull* **56**(11): 1855-1861.

Nikolopoulou, M., and Kalogerakis, N. (2010) Biostimulation strategies for enhanced bioremediation of marine oil spills including chronic pollution. In *Handbook of hydrocarbon and lipid microbiology*, pp. 2521-2529.

Noda, K.-I., Watanabe, K., and Maruhashi, K. (2003) Isolation of the *Pseudomonas aeruginosa* gene affecting uptake of dibenzothiophene in *n*-tetradecane. *J Biosci Bioeng* **95**(5): 504-511.

Nowak, A., and Mrozik, A. (2016) Facilitation of co-metabolic transformation and degradation of monochlorophenols by *Pseudomonas* sp. CF600 and changes in its fatty acid composition. *Water Air Soil Pollut* **227**(3): 83.

O'Sullivan, A., and Richardson, A.J. (1967) The *Torrey Canyon* disaster and intertidal marine life. *Nature* **214**(5087): 448-448.

O′Toole, G.A., and Wong, G.C. (2016) Sensational biofilms: Surface sensing in bacteria. *Curr Opin Microbiol* **30**: 139-146.

Oh, J.-S., and Roh, D.-H. (2018) Draft genome sequence of *Zhongshania marina* DSW25-10 T isolated from seawater. *The Microbiological Society of Korea* **54**(4): 480-482.
Ollivier, B., and Magot, M. (2005) *Petroleum microbiology*. Washington, DC, USA: ASM Press, .
Oren, A. (2019) Aerobic hydrocarbon-degrading archaea. In *Taxonomy, genomics and ecophysiology of hydrocarbon-degrading microbes*. McGenity, T.J. (ed), pp. 41-51.
Ortmann, A.C., Anders, J., Shelton, N., Gong, L., Moss, A.G., and Condon, R.H. (2012) Dispersed oil disrupts microbial pathways in pelagic food webs. *PLoS One* **7**(7): e42548.
Ortmann, A.C., Cobanli, S.E., Wohlgeschaffen, G., Thamer, P., McIntyre, C., Mason, J., and King, T.L. (2019) Inorganic nutrients have a significant, but minimal, impact on a coastal microbial community's response to fresh diluted bitumen. *Mar Pollut Bull* **139**: 381-389.
OSAT (2010). Summary report for sub-sea and sub-surface oil and dispersant detection: Sampling and monitoring. New Orleans, USA. Available from: https://www.restorethegulf.gov/sites/default/files/documents/pdf/OSAT_Report_FINAL_17DEC.pdf [Accessed August 20, 2020].
Ostle, C., Thompson, R.C., Broughton, D., Gregory, L., Wootton, M., and Johns, D.G. (2019) The rise in ocean plastics evidenced from a 60-year time series. *Nat Comm* **10**(1): 1-6.
Otte, J.M., Blackwell, N., Soos, V., Rughöft, S., Maisch, M., Kappler, A. *et al.* (2018) Sterilization impacts on marine sediment - are we able to inactivate microorganisms in environmental samples? *FEMS Microbiol Ecol* **94**(12).
Overholt, W.A., Marks, K.P., Romero, I.C., Hollander, D.J., Snell, T.W., and Kostka, J.E. (2016) Hydrocarbon-degrading bacteria exhibit a species-specific response to dispersed oil while moderating ecotoxicity. *Appl Environ Microbiol* **82**(2): 518-527.
Ozhan, K., and Bargu, S. (2014) Distinct responses of Gulf of Mexico phytoplankton communities to crude oil and the dispersant Corexit EC9500A under different nutrient regimes. *Ecotoxicology* **23**(3): 370-384.
Ozhan, K., Parsons, M.L., and Bargu, S. (2014) How were phytoplankton affected by the Deepwater Horizon oil spill? *BioScience* **64**(9): 829-836.
P.O.S.T., U. (1996). The *Sea Empress* oil spill (p.O.S.T. Note 75). Parliamentary office of Science and Technology (UK). Available from: http://www.parliament.uk/documents/post/pn075.pdf [Accessed August 29, 2020].
Parales, R.E., and Ditty, J.L. (2017) Chemotaxis to hydrocarbons. *Cellular Ecophysiology of Microbe. Handbook of Hydrocarbon and Lipid Microbiology*. Krell, T. (ed): Springer International Publishing, pp. 1-20. 10.1007/978-3-319-20796-4_43-1.
Park, C., Shin, B., Jung, J., Lee, Y., and Park, W. (2017) Metabolic and stress responses of *Acinetobacter oleivorans* DR1 during long-chain alkane degradation. *Microb Biotechnol* **10**(6): 1809-1823.
Parker, A.M., Ferrer, I., Thurman, E.M., Rosario-Ortiz, F.L., and Linden, K.G. (2014) Determination of corexit components used in the Deepwater Horizon cleanup by liquid chromatography-ion trap mass spectrometry. *Anal Methods* **6**(15): 5498-5502.
Partearroyo, M.A., Ostolaza, H., Goñi, F.M., and Barberá-Guillem, E. (1990) Surfactant-induced cell toxicity and cell lysis: A study using B16 melanoma cells. *Biochem Pharmacol* **40**(6): 1323-1328.
Passow, U. (2016) Formation of rapidly-sinking, oil-associated marine snow. *Deep Sea Res Part II Top Stud Oceanogr* **129**: 232-240.
Passow, U., and Ziervogel, K. (2016) Marine snow sedimented oil released during the Deepwater Horizon spill. *Oceanography* **29**(3): 118-125.
Peña-Montenegro, T.D., Kleindienst, S., Allen, A.E., Eren, M.A., Sánchez, J.A., Arnold, J., and Joye, S.B. Metatranscriptomic analysis reveals responses of deepsea microbial communities to oil and dispersant exposure.
Pérez-Pantoja, D., González, B., and Pieper, D. (2010) Aerobic degradation of aromatic hydrocarbons. In *Handbook of hydrocarbon and lipid microbiology*. K.N., T. (ed). Berlin, Heidelberg, Germany: Springer.
Perez-Riverol, Y., Csordas, A., Bai, J., Bernal-Llinares, M., Hewapathirana, S., Kundu, D.J. *et al.* (2019) The PRIDE database and related tools and resources in 2019: Improving support for quantification data. *Nucleic Acids Res* **47**(D1): D442-D450.
Perfumo, A., Banat, I.M., and Marchant, R. (2018) Going green and cold: Biosurfactants from low-temperature environments to biotechnology applications. *Trends Biotech* **36**(3): 277-289.
Perkins, M.J. (2017) Assessing chemical dispersants used during the Deepwater Horizon oil spill: Method innovation and application. *Thesis*, PhD in Toxicology. Department of Environmental and Molecular Toxicology, Oregon State University; Corvallis, Oregon, USA.
Personna, Y.R., King, T., Boufadel, M.C., Zhang, S., and Axe, L. (2016) Dual effects of a dispersant and nutrient supplementation on weathered Endicott oil biodegradation in seawater. *AIMS Environmental Science* **3**(4): 739.

Peterson, C.H., Rice, S.D., Short, J.W., Esler, D., Bodkin, J.L., Ballachey, B.E., and Irons, D.B. (2003) Long-term ecosystem response to the *Exxon Valdez* oil spill. *Science* **302**(5653): 2082-2086.
Place, B.J., Perkins, M.J., Sinclair, E., Barsamian, A.L., Blakemore, P.R., and Field, J.A. (2016) Trace analysis of surfactants in Corexit oil dispersant formulations and seawater. *Deep Sea Res Part II Top Stud Oceanogr* **129**: 273-281.
Pluskal, T., Castillo, S., Villar-Briones, A., and Orešič, M. (2010) MZmine 2: Modular framework for processing, visualizing, and analyzing mass spectrometry-based molecular profile data. *BMC Bioinformatics* **11**(1): 395.
Polovina, J.J., Howell, E.A., and Abecassis, M. (2008) Ocean's least productive waters are expanding. *Geophys Res Lett* **35**(3): L03618.
Pomeroy, L.R., leB. WILLIAMS, P.J., Azam, F., and Hobbie, J.E. (2007) The microbial loop. *Oceanography* **20**(2): 28-33.
Prince, R., Kelley, B., and Butler, J. (2016) Three widely-available dispersants substantially increase the biodegradation of otherwise undispersed oil. *J Marine Sci Res Dev* **6**: 183.
Prince, R.C. (2015) Oil spill dispersants: Boon or bane? *Environ Sci Technol* **49**(11): 6376-6384.
Prince, R.C. (2019) Eukaryotic hydrocarbon degraders. In *Taxonomy, genomics and ecophysiology of hydrocarbon-degrading microbes*. McGenity, T.J. (ed), pp. 1-20.
Prince, R.C., Amande, T.J., and McGenity, T.J. (2019) Prokaryotic hydrocarbon degraders. In *Taxonomy, genomics and ecophysiology of hydrocarbon-degrading microbes*. McGenity, T.J. (ed), pp. 1-39.
Pruesse, E., Quast, C., Knittel, K., Fuchs, B.M., Ludwig, W., Peplies, J., and Glöckner, F.O. (2007) SILVA: A comprehensive online resource for quality checked and aligned ribosomal rna sequence data compatible with ARB. *Nucleic Acids Res* **35**(21): 7188-7196.
Putthividhya, A., Kukor, J.J., and Abriola, L.M. (2016) The effects of substrate exposure history and carbon starvation-induced stress on the EPS synthesis of TCE degrading toluene oxidizing soil bacteria. *Environ Earth Sci* **75**(9).
R Core Team (2019). R: A language and environment for statistical computing. Vienna, Austria.
Radniecki, T.S., Schneider, M.C., and Semprini, L. (2013) The influence of Corexit 9500A and weathering on Alaska North Slope crude oil toxicity to the ammonia oxidizing bacterium *Nitrosomonas europaea*. *Mar Pollut Bull* **68**(1-2): 64-70.
Rahlff, J., Herlemann, D., Giebel, H.-A., Mustaffa, N.I.H., Wurl, O., and Stolle, C. (2019) Marine foams represent compressed sea-surface microlayer with distinctive bacterial communities. *bioRxiv*: 820696.
Rahsepar, S., Smit, M.P., Murk, A.J., Rijnaarts, H.H., and Langenhoff, A.A. (2016) Chemical dispersants: Oil biodegradation friend or foe? *Mar Pollut Bull* **108**(1): 113-119.
Rambeloarisoa, E., Rontani, J., Giusti, G., Duvnjak, Z., and Bertrand, J. (1984) Degradation of crude oil by a mixed population of bacteria isolated from sea-surface foams. *Marine Biology* **83**(1): 69-81.
Ramos, J.L., Duque, E., Gallegos, M.T., Godoy, P., Ramos-Gonzalez, M.I., Rojas, A. *et al.* (2002) Mechanisms of solvent tolerance in gram-negative bacteria. *Annu Rev Microbiol* **56**: 743-768.
Reddy, C.M., Arey, J.S., Seewald, J.S., Sylva, S.P., Lemkau, K.L., Nelson, R.K. *et al.* (2012) Composition and fate of gas and oil released to the water column during the Deepwater Horizon oil spill. *Proc Natl Acad Sci USA* **109**(50): 20229-20234.
Redmond, M.C., and Valentine, D.L. (2012) Natural gas and temperature structured a microbial community response to the Deepwater Horizon oil spill. *Proc Natl Acad Sci USA* **109**(50): 20292-20297.
Ribicic, D., Netzer, R., Hazen, T.C., Techtmann, S.M., Drabløs, F., and Brakstad, O.G. (2018) Microbial community and metagenome dynamics during biodegradation of dispersed oil reveals potential key-players in cold Norwegian seawater. *Mar Pollut Bull* **129**(1): 370-378.
Rico-Martínez, R., Snell, T.W., and Shearer, T.L. (2013) Synergistic toxicity of Macondo crude oil and dispersant Corexit 9500A® to the *Brachionus plicatilis* species complex (Rotifera). *Environ Pollut* **173**: 5-10.
Rivers, A.R., Sharma, S., Tringe, S.G., Martin, J., Joye, S.B., and Moran, M.A. (2013) Transcriptional response of bathypelagic marine bacterioplankton to the Deepwater Horizon oil spill. *ISME J* **7**(12): 2315-2329.
Rodrigues, E.M., Morais, D.K., Pylro, V.S., Redmile-Gordon, M., de Oliveira, J.A., Roesch, L.F.W. *et al.* (2018) Aliphatic hydrocarbon enhances phenanthrene degradation by autochthonous prokaryotic communities from a pristine seawater. *Microb Ecol* **75**(3): 688-700.
Rodriguez-R, L.M., Overholt, W.A., Hagan, C., Huettel, M., Kostka, J.E., and Konstantinidis, K.T. (2015) Microbial community successional patterns in beach sands impacted by the Deepwater Horizon oil spill. *ISME J* **9**(9): 1928-1940.
Rojo, F. (2009) Degradation of alkanes by bacteria. *Environ Microbiol* **11**(10): 2477-2490.
Rosa, L.T., Bianconi, M.E., Thomas, G.H., and Kelly, D.J. (2018) Tripartite ATP-independent periplasmic (TRAP) transporters and tripartite tricarboxylate transporters (TTT): From uptake to pathogenicity. *Front Cell Infect Microbiol* **8**: 33.

Rubin-Blum, M., Antony, C.P., Borowski, C., Sayavedra, L., Pape, T., Sahling, H. *et al.* (2017) Short-chain alkanes fuel mussel and sponge *Cycloclasticus* symbionts from deep-sea gas and oil seeps. *Nat Microbiol* **2**(8): 17093.

Sabirova, J.S., Becker, A., Lünsdorf, H., Nicaud, J.-M., Timmis, K.N., and Golyshin, P.N. (2011) Transcriptional profiling of the marine oil-degrading bacterium *Alcanivorax borkumensis* during growth on *n*-alkanes. *FEMS Microbiol Lett* **319**(2): 160-168.

Salerno, J.L., Little, B., Lee, J., and Hamdan, L.J. (2018) Exposure to crude oil and chemical dispersant may impact marine microbial biofilm composition and steel corrosion. *Front Mar Sci* **5**: 196.

Salmon, R.C., Cliff, M.J., Rafferty, J.B., and Kelly, D.J. (2013) The CouPSTU and TarPQM transporters in *Rhodopseudomonas palustris*: Redundant, promiscuous uptake systems for lignin-derived aromatic substrates. *PloS One* **8**(3): e59844.

Sánchez, S.A., Tricerri, M., Gunther, G., and Gratton, E. (2007) Laurdan generalized polarization: From cuvette to microscope. *Modern Research and Educational Topics in Microscopy* **2**: 1007-1014.

Sanni, G.O., Coulon, F., and McGenity, T.J. (2015) Dynamics and distribution of bacterial and archaeal communities in oil-contaminated temperate coastal mudflat mesocosms. *Environ Sci Pollut Res* **22**(20): 15230-15247.

Santisi, S., Genovese, M., Crisafi, F., Gentile, G., Volta, A., Bonsignore, M., and Cappello, S. (2015) Effects of growth conditions on hydrophobicity in marine obligate hydrocarbonoclastic bacteria. *Intern J Microbiol Appl* **2**(2): 50-55.

Sauer, K., Camper, A.K., Ehrlich, G.D., Costerton, J.W., and Davies, D.G. (2002) *Pseudomonas aeruginosa* displays multiple phenotypes during development as a biofilm. *J Bacteriol* **184**(4): 1140-1154.

Schindelin, J., Arganda-Carreras, I., Frise, E., Kaynig, V., Longair, M., Pietzsch, T. *et al.* (2012) Fiji: An open-source platform for biological image analysis. *Nat Methods* **9**(7): 676–682.

Schneiker, S., Martins dos Santos, V.A., Bartels, D., Bekel, T., Brecht, M., Buhrmester, J. *et al.* (2006) Genome sequence of the ubiquitous hydrocarbon-degrading marine bacterium *Alcanivorax borkumensis*. *Nat Biotechnol* **24**(8): 997-1004.

Schobert, H. (2013) *Chemistry of fossil fuels and biofuels*. New York, USA: Cambridge University Press.

Sebastian, M., Estrany, M., Ruiz-Gonzalez, C., Forn, I., Sala, M.M., Gasol, J.M., and Marrase, C. (2019) High growth potential of long-term starved deep ocean opportunistic heterotrophic bacteria. *Front Microbiol* **10**: 760.

Seidel, M., Kleindienst, S., Dittmar, T., Joye, S.B., and Medeiros, P.M. (2016) Biodegradation of crude oil and dispersants in deep seawater from the Gulf of Mexico: Insights from ultra-high resolution mass spectrometry. *Deep Sea Res Part II Top Stud Oceanogr* **129**: 108-118.

Severin, T., Bacosa, H., Sato, A., and Erdner, D. (2016) Dynamics of *Heterocapsa* sp. and the associated attached and free-living bacteria under the influence of dispersed and undispersed crude oil. *Letters in applied microbiology* **63**(6): 419-425.

Shin, B., Bociu, I., Kolton, M., Huettel, M., and Kostka, J.E. (2019) Succession of microbial populations and nitrogen-fixation associated with the biodegradation of sediment-oil-agglomerates buried in a Florida sandy beach. *Sci Rep* **9**(1): 1-11.

Shitashiro, M., Tanaka, H., soo Hong, C., Kuroda, A., Takiguchi, N., Ohtake, H., and Kato, J. (2005) Identification of chemosensory proteins for trichloroethylene in *Pseudomonas aeruginosa*. *J Biosci Bioeng* **99**(4): 396-402.

Short, J.W. (2017) Advances in understanding the fate and effects of oil from accidental spills in the United States beginning with the *Exxon Valdez*. *Arch Environ Contam Toxicol* **73**(1): 5-11.

Sieradzki, E.T., Morando, M., and Fuhrman, J.A. (2019) Metagenomics and stable isotope probing offer insights into metabolism of polycyclic aromatic hydrocarbons degraders in chronically polluted seawater. *bioRxiv*: 777730.

Signorini, S.R., Franz, B.A., and McClain, C.R. (2015) Chlorophyll variability in the oligotrophic gyres: Mechanisms, seasonality and trends. *Front Mar Sci* **2**: 1-11.

Sikkema, J., de Bont, J.A., and Poolman, B. (1995) Mechanisms of membrane toxicity of hydrocarbons. *Microbiol Rev* **59**(2): 201-222.

Simanzhenkov, V., and Idem, R. (2003) *Crude oil chemistry*. New York, USA: Marcel Dekker, Inc.

Singer, E., Webb, E.A., Nelson, W.C., Heidelberg, J.F., Ivanova, N., Pati, A., and Edwards, K.J. (2011) Genomic potential of *Marinobacter aquaeolei*, a biogeochemical "opportunitroph". *Appl Environ Microbiol* **77**(8): 2763-2771.

Sitarek, K., Gromadzińska, J., Lutz, P., Stetkiewicz, J., Świercz, R., and Wąsowicz, W. (2012) Fertility and developmental toxicity studies of diethylene glycol monobutyl ether (DGBE) in rats. *International Journal of Occupational Medicine and Environmental Health* **25**(4): 404-417.

Skarbo, S. (2020) Poisonous fuel from major Norilsk diesel leak may already be in the Arctic ocean. In *The Siberian Times*. Published on: June 24, 2020. Available from:

http://siberiantimes.com/other/others/news/poisonous-fuel-from-major-norilsk-diesel-leak-may-already-be-in-the-arctic-ocean/ [Accessed August 28, 2020].
Sørheim, K.R., Daling, P.S., Cooper, D., Buist, I., Faksness, L.-G., Altin, D. *et al.* (2020). Characterization of low sulfur fuel oils (LSFO): A new generation of marine fuel oils. Trondheim, Norway: SINTEF Ocean AS. Report No.: OC2020 A-050. Available from: http://www.itopf.org/fileadmin/data/Documents/RDaward/Final_report_LSFO_Multipartner__3.1_.pdf [Accessed July 16, 2020].
Spang, A., Caceres, E.F., and Ettema, T.J. (2017) Genomic exploration of the diversity, ecology, and evolution of the archaeal domain of life. *Science* **357**(6351).
Steen, A., and Findlay, A. (2008) Frequency of dispersant use worldwide. *International Oil Spill Conference*: American Petroleum Institute, pp. 645-649.
Steinle, L., Schmidt, M., Bryant, L., Haeckel, M., Linke, P., Sommer, S. *et al.* (2016) Linked sediment and water-column methanotrophy at a man-made gas blowout in the North Sea: Implications for methane budgeting in seasonally stratified shallow seas. *Limnol Oceanogr* **61**(S1): S367-S386.
Straškrabová, V. (1983) The effect of substrate shock on populations of starving aquatic bacteria. *J Appl Bacteriol* **54**: 217-224.
Straub, D., Blackwell, N., Langarica-Fuentes, A., Peltzer, A., Nahnsen, S., and Kleindienst, S. (2020) Interpretations of environmental microbial community studies are biased by the selected 16s rRNA (gene) amplicon sequencing pipeline. *Front Microbiol* **11**: 2652.
Strom, S.L. (2008) Microbial ecology of ocean biogeochemistry: A community perspective. *science* **320**(5879): 1043-1045.
Suja, L.D., Summers, S., and Gutierrez, T. (2017) Role of EPS, dispersant and nutrients on the microbial response and MOS formation in the subarctic northeast atlantic. *Front Microbiol* **8**: 676.
Sun, H., Gao, W., Fan, H., Wang, H., and Wei, D. (2015) Cloning, purification and evaluation of the enzymatic properties of a novel arylacetonitrilase from *Luminiphilus syltensis* NOR5-1B: A potential biocatalyst for the synthesis of mandelic acid and its derivatives. *Biotechnology Letters* **37**(8): 1655-1661.
Sun, X., and Kostka, J.E. (2019) Hydrocarbon-degrading microbial communities are site specific, and their activity is limited by synergies in temperature and nutrient availability in surface ocean waters. *Appl Environ Microbiol* **85**(15): e00443-00419.
Suzuki, T., Yazawa, T., Morishita, N., Maruyama, A., and Fuse, H. (2019) Genetic and physiological characteristics of a novel marine propylene-assimilating *Halieaceae* bacterium isolated from seawater and the diversity of its alkene and epoxide metabolism genes. *Microbes and Environments*: ME18053.
Swannell, R.P., Lee, K., and McDonagh, M. (1996) Field evaluations of marine oil spill bioremediation. *Microbiol Rev* **60**(2): 342-365.
Tavassoli, T., Mousavi, S., Shojaosadati, S., and Salehizadeh, H. (2012) Asphaltene biodegradation using microorganisms isolated from oil samples. *Fuel* **93**: 142-148.
Techtmann, S.M., Zhuang, M., Campo, P., Holder, E., Elk, M., Hazen, T.C. *et al.* (2017) Corexit 9500 enhances oil biodegradation and changes active bacterial community structure of oil-enriched microcosms. *Appl Environ Microbiol* **83**(10): e03462-03416.
Teeling, H., Fuchs, B.M., Becher, D., Klockow, C., Gardebrecht, A., Bennke, C.M. *et al.* (2012) Substrate-controlled succession of marine bacterioplankton populations induced by a phytoplankton bloom. *Science* **336**(6081): 608-611.
Tissot, B.P., and Welte, D.H. (1978) *Petroleum formation and occurrence: A new approach to oil and gas exploration*. Berlin, Germany: Springer-Verlag.
Tremblay, J., Yergeau, E., Fortin, N., Cobanli, S., Elias, M., King, T.L. *et al.* (2017) Chemical dispersants enhance the activity of oil- and gas condensate-degrading marine bacteria. *ISME J* **11**(12): 2793-2808.
Tremblay, J., Fortin, N., Elias, M., Wasserscheid, J., King, T.L., Lee, K., and Greer, C.W. (2019) Metagenomic and metatranscriptomic responses of natural oil degrading bacteria in the presence of dispersants. *Environ Microbiol* **21**(7): 2307-2319.
Trudel, B.K. (1998) Dispersant application in Alaska: A technical update. *Dispersant Use in Alaska: A Technical Update*. Trudel, B.K. (ed). Anchorage, Alaska, USA: Prince William Sound Oil Spill Recovery Institute.
Tyanova, S., Temu, T., Sinitcyn, P., Carlson, A., Hein, M.Y., Geiger, T. *et al.* (2016) The Perseus computational platform for comprehensive analysis of (prote)omics data. *Nat Methods* **13**(9): 731-740.
Ugbomeh, A., Bob-manuel, K., Green, A., and Taylorharry, O. (2019) Biochemical toxicity of Corexit 9500 dispersant on the gills, liver and kidney of juvenile *Clarias gariepinus*. *Fisheries and Aquatic Sciences* **22**(1): 15.
UniProt Consortium (2019) Uniprot: A worldwide hub of protein knowledge. *Nucleic Acids Res* **47**(D1): D506-D515.

Urtuvia, V., Maturana, N., Acevedo, F., Pena, C., and Diaz-Barrera, A. (2017) Bacterial alginate production: An overview of its biosynthesis and potential industrial production. *World J Microbiol Biotechnol* **33**(11): 198.
US NASEM (2020). The use of dispersants in marine oil spill response. Washington, DC: The National Academies Press (US).
US Nat. Comm. DWH (2011). The use of surface and subsea dispersants during the BP Deepwater Horizon oil spill. Working Paper. Washington, DC, USA: National Commission on the BP Deepwater Horizon Oil Spill and Offshore Drilling. Available from: http://purl.fdlp.gov/GPO/gpo184 [Accessed April 20, 2019].
US NPC (2015). Arctic potential: Realizing the promise of U.S. Arctic oil and gas resources. Washington, DC, USA: National Petroleum Council. Available from: https://www.npcarcticreport.org/ [Accessed July 19, 2020].
US NRC (2003). Oil in the sea III: Inputs, fates, and effects. Washington, DC, USA: The National Academies Press (US). Report No.: 0309084385. Available from: https://www.nap.edu/catalog/10388/oil-in-the-sea-iii-inputs-fates-and-effects
US NRC (2014). Responding to oil spills in the U.S. Arctic marine environment. Washington, DC, USA: The National Academies Press. Report No.: 978-0-309-29886-5
Valencia-Agami, S.S., Cerqueda-García, D., Putzeys, S., Uribe-Flores, M.M., García-Cruz, N.U., Pech, D. *et al.* (2019) Changes in the bacterioplankton community structure from southern Gulf of Mexico during a simulated crude oil spill at mesocosm scale. *Microorganisms* **7**(10): 441.
Van Beilen, J.B., Marín, M.M., Smits, T.H., Röthlisberger, M., Franchini, A.G., Witholt, B., and Rojo, F. (2004) Characterization of two alkane hydroxylase genes from the marine hydrocarbonoclastic bacterium *Alcanivorax borkumensis*. *Environ Microbiol* **6**(3): 264-273.
Van der Werf, M., Hartmans, S., and Van den Tweel, W. (1995) Permeabilization and lysis of *Pseudomonas pseudoalcaligenes* cells by Triton X-100 for efficient production of D-malate. *Appl Microbiol Biotechnol* **43**(4): 590-594.
Vaysse, P.J., Sivadon, P., Goulas, P., and Grimaud, R. (2011) Cells dispersed from *Marinobacter hydrocarbonoclasticus* SP17 biofilm exhibit a specific protein profile associated with a higher ability to reinitiate biofilm development at the hexadecane–water interface. *Environ Microbiol* **13**(3): 737-746.
Venosa, A.D., and Holder, E.L. (2007) Biodegradability of dispersed crude oil at two different temperatures. *Mar Pollut Bull* **54**(5): 545-553.
Vergeynst, L., Kjeldsen, K.U., Lassen, P., and Rysgaard, S. (2018a) Bacterial community succession and degradation patterns of hydrocarbons in seawater at low temperature. *J Hazard Mat* **353**: 127-134.
Vergeynst, L., Wegeberg, S., Aamand, J., Lassen, P., Gosewinkel, U., Fritt-Rasmussen, J. *et al.* (2018b) Biodegradation of marine oil spills in the Arctic with a Greenland perspective. *Sci Total Environ* **626**: 1243-1258.
Wang, C., Huang, Y., Zhang, Z., Hao, H., and Wang, H. (2020) Absence of the nahG-like gene caused the syntrophic interaction between *Marinobacter* and other microbes in PAH-degrading process. *J Hazard Mat* **384**: 121387.
Wang, S., Parsek, M.R., Wozniak, D.J., and Ma, L.Z. (2013) A spider web strategy of type IV pili-mediated migration to build a fibre-like Psl polysaccharide matrix in *Pseudomonas aeruginosa* biofilms. *Environ Microbiol* **15**(8): 2238-2253.
Wang, W., and Shao, Z. (2013) Enzymes and genes involved in aerobic alkane degradation. *Front Microbiol* **4**: 116.
Wang, W., Zhong, R., Shan, D., and Shao, Z. (2014) Indigenous oil-degrading bacteria in crude oil-contaminated seawater of the yellow sea, China. *Appl Microbiol Biotechnol* **98**(16): 7253-7269.
Wang, Z., Fingas, M., Blenkinsopp, S., Sergy, G., Landriault, M., Sigouin, L. *et al.* (1998) Comparison of oil composition changes due to biodegradation and physical weathering in different oils. *Journal of Chromatography A* **809**(1-2): 89-107.
Wentzel, A., Ellingsen, T.E., Kotlar, H.-K., Zotchev, S.B., and Throne-Holst, M. (2007) Bacterial metabolism of long-chain *n*-alkanes. *Appl Microbiol Biotechnol* **76**(6): 1209-1221.
White, H.K., Lyons, S.L., Harrison, S.J., Findley, D.M., Liu, Y., and Kujawinski, E.B. (2014) Long-term persistence of dispersants following the Deepwater Horizon oil spill. *Environmental Science & Technology Letters* **1**(7): 295-299.
Wickham, H. (2016) Ggplot2: Elegant graphics for data analysis. New York, USA: Springer.
Widdel, F., and Rabus, R. (2001) Anaerobic biodegradation of saturated and aromatic hydrocarbons. *Curr Opin Biotechnol* **12**(3): 259-276.
Widdel, F., and Musat, F. (2019) Energetic and other quantitative aspects of microbial hydrocarbon utilization: An introduction. In *Aerobic utilization of hydrocarbons, oils and lipids*, pp. 1-41.

Wilkinson, J., Beegle-Krause, C.J., Evers, K.-U., Hughes, N., Lewis, A., Reed, M., and Wadhams, P. (2017) Oil spill response capabilities and technologies for ice-covered Arctic marine waters: A review of recent developments and established practices. *Ambio* **46**(3): 423-441.

Wiltshire, K.H., Kraberg, A., Bartsch, I., Boersma, M., Franke, H.-D., Freund, J. *et al.* (2010) Helgoland Roads, North Sea: 45 years of change. *Estuaries and Coasts* **33**(2): 295-310.

Wise, J., and Wise, J.P. (2011) A review of the toxicity of chemical dispersants. *Rev Environ Health* **26**(4): 281-300.

Word, J.Q., Clark, J.R., and Word, L.S. (2014) Comparison of the acute toxicity of Corexit 9500 and household cleaning products. *Hum Ecol Risk Assess* **21**(3): 707-725.

Wurl, O., Ekau, W., Landing, W.M., and Zappa, C.J. (2017) Sea surface microlayer in a changing ocean – a perspective. *Elem Sci Anth* **5**: 31.

Xu, W., You, Y., Wang, Z., Chen, W., Zeng, J., Zhao, X., and Su, Y. (2018) Dibutyl phthalate alters the metabolic pathways of microbes in black soils. *Sci Rep* **8**(1): 2605.

Yakimov, M.M., Giuliano, L., Gentile, G., Crisafi, E., Chernikova, T.N., Abraham, W.-R. *et al.* (2003) *Oleispira antarctica* gen. nov., sp. nov., a novel hydrocarbonoclastic marine bacterium isolated from Antarctic coastal sea water. *Int J Syst Evol Microbiol* **53**(3): 779-785.

Yakimov, M.M., Timmis, K.N., and Golyshin, P.N. (2007) Obligate oil-degrading marine bacteria. *Curr Opin Biotechnol* **18**(3): 257-266.

Yam, E.M., and Tang, K.W. (2007) Effects of starvation on aggregate colonization and motility of marine bacteria. *Aquat Microb Ecol* **48**(3): 207-215.

Yang, T., Nigro, L.M., Gutierrez, T., Joye, S.B., Highsmith, R., and Teske, A. (2016) Pulsed blooms and persistent oil-degrading bacterial populations in the water column during and after the Deepwater Horizon blowout. *Deep Sea Res Part II Top Stud Oceanogr* **129**: 282-291.

Young, L., and Mitchell, R. (1973) Negative chemotaxis of marine bacteria to toxic chemicals. *Appl Microbiol* **25**(6): 972-975.

Zadjelovic, V., Gibson, M., Dorador, C., and Christie-Oleza, J. (2020) Genome of *Alcanivorax* sp. 24: A hydrocarbon degrading bacterium isolated from marine plastic debris. *Marine Genomics* **49**: 100686.

Zakharenko, A.S., Galachyants, Y.P., Morozov, I.V., Shubenkova, O.V., Morozov, A.A., Ivanov, V.G. *et al.* (2019) Bacterial communities in areas of oil and methane seeps in pelagic of Lake Baikal. *Microb Ecol* **78**(2): 269-285.

Zhou, L., Yu, Y., Chen, X., Diab, A.A., Ruan, L., He, J. *et al.* (2015) The multiple DSF-family QS signals are synthesized from carbohydrate and branched-chain amino acids via the FAS elongation cycle. *Sci Rep* **5**: 13294.

Zhou, L., Zhang, L.H., Camara, M., and He, Y.W. (2017) The DSF family of quorum sensing signals: Diversity, biosynthesis, and turnover. *Trends Microbiol* **25**(4): 293-303.

7 Statement of personal contribution

The work described in this PhD Thesis was funded by grants from the Baden-Württemberg Foundation's Elite Program for Postdocs and from the Deutsche Forschungsgemeinschaft (DFG, German Research Foundation - fellowship grant #326028733) to Jun.-Prof. Sara Kleindienst. The conceptual background to this project was designed by Jun.-Prof. Sara Kleindienst, who was also the main supervisor. Prof. Andreas Kappler was the second supervisor. Unless otherwise stated, experiments were conceptualized by myself and Jun.-Prof. Sara Kleindienst and carried out by me. The discussion and analysis of the obtained results, as well as writing of all manuscripts were completed in cooperation with Jun.-Prof. Sara Kleindienst; for chapter 2 also in cooperation with Prof. A. Kappler. In detail, the contributions of all co-authors including myself and additionally involved people, are as stated below:

Chapter 2: The microcosm experiment was designed by myself and Jun.-Prof. Sara Kleindienst. Preparation of water-accommodated fractions, establishment of microcosms, daily rotations of microcosms, sampling of microcosms, radiotracer assays, DNA extraction and amplification for amplicon sequencing or qPCR, hydrocarbon extraction, data visualization and statistical data analysis were performed by myself. Bioinformatic analysis of sequencing data was performed by Dr. Daniel Straub and results were interpreted by myself together with Dr. Daniel Straub and Jun.-Prof. Sara Kleindienst. GC-MS measurements of hydrocarbon extracts were performed by Dr. Rafael Tarozo and Dr. Christian Hallmann, the resulting chromatograms were analysed by myself with their input and the results were interpreted by myself together with Dr. Rafael Tarozo, Dr. Christian Hallmann and Jun.-Prof. Sara Kleindienst. The results from all other analyses were interpreted by myself together with Jun.-Prof. Sara Kleindienst and input from Prof. Andreas Kappler. The manuscript was written by myself and revised by all co-authors. Dr. Daniel Straub, Dr. Rafael Tarozo and Dr. Christian Hallmann wrote the method descriptions for bioinformatics analyses and GC-MS measurements, respectively.
Additionally, the following people were involved in helping me with this experiment: Dr. Gunter Wegener provided seawater samples, Dr. Stephane Le Floch provided Corexit EC9500A, BP provided the Macondo crude oil, Ellen Röhm performed CFA measurements, Bernice Nisch performed DOC measurements, Dr. Thomas Haug provided facilities to perform radiotracer assays, Wolfgang Gerber helped to take macroscopic aggregate photographs, Juliane Riedel helped with cell counting, and sampling assistance was provided by Dr. Lu Lu and Anjela Vogel.

Chapter 3: The microcosm experiment was designed by myself and Jun.-Prof. Sara Kleindienst. Preparation of water-accommodated fractions, establishment of microcosms, daily rotations of microcosms, sampling of microcosms, radiotracer assays, DNA extraction and amplification for amplicon sequencing, hydrocarbon extraction, data visualization, data interpretation and statistical data analysis were performed by myself. Bioinformatic analysis of sequencing data was performed by Dr. Daniel Straub. GC-MS measurements of hydrocarbon extracts were performed by Dr. Rafael Tarozo and Dr. Christian Hallmann and the resulting chromatograms were analysed by myself with their input. The manuscript was written by myself.

Additionally, the following people were involved in helping me with this experiment: Ute Kieb provided seawater samples, Maximilian Schmidt provided seawater transport assistance, Dr. Stephane Le Floch provided the Grane crude oil and Corexit EC9500A, Franziska Schädler performed qPCR assays, Ellen Röhm performed CFA measurements, Bernice Nisch performed DOC measurements, Dr. Thomas Haug provided facilities to perform radiotracer assays, and Juliane Riedel helped with cell counting.

Chapter 4: The experiments were conceptualised by myself and Jun.-Prof. Sara Kleindienst. The strain *Marinobacter* sp. TT1 was isolated and provided by Prof. Tony Gutierrez. Starved-culture experiments including cell counts and *n*-hexadecane quantifications were performed by myself and Anjela Vogel. Well-fed culture experiments including cell counts and *n*-hexadecane quantifications were performed by myself. Data visualization and statistical analysis were performed by myself. Data were interpreted and discussed by myself together with Jun.-Prof. Sara Kleindienst, Prof. Tony Gutierrez, and Prof. Samantha B. Joye. The manuscript was written by myself under the supervision of Jun.-Prof. Sara Kleindienst and revised by all co-authors.
Besides the co-authors, Prof. Peter Grathwohl provided the necessary facilities and equipment for GC-MS measurements, Renate Seelig performed GC-MS measurements, and Anja Pohl helped with culture maintenance.

Chapter 5: The microcosm experiment was designed by myself and Jun.-Prof. Sara Kleindienst with input from Dr. Nico Jehmlich. The strain *Marinobacter* sp. TT1 was isolated and provided by Prof. Tony Gutierrez. I performed the experiment and subsequent cell counts and *n*-hexadecane quantifications. Protein extraction, LC-MS/MS analysis and mass spectra analysis were performed by Dr. Nico Jehmlich. Subsequent analysis of quantification data including data visualization and statistical analysis was performed by myself with input from Dr. Nico Jehmlich. Results were interpreted and discussed by myself together with Jun.-Prof. Sara Kleindienst and Dr. Nico Jehmlich. The manuscript was written by myself under the supervision of Jun.-Prof. Sara Kleindienst and revised by all co-authors.
Additionally, the following people were involved in helping me with this experiment: Prof. Grunde Jomaas and Dr. Kim Gustavson provided the DUC crude oil, the U.S. National Oceanic and Atmospheric Administration provided Corexit EC9500A, Ellen Röhm performed HPLC measurements, Prof. Peter Grathwohl provided the necessary facilities and equipment for GC-MS measurements, Renate Seelig performed GC-MS measurements, Constantin App prepared (CE)WAF solutions and Anja Pohl helped with culture maintenance and sampling.

I hereby declare that I have independently written this thesis, that I have used only the indicated references, and that I have not plagiarized any of the text. Chapters 4 and 5 have been published in scientific journals. Chapters 2 and 3 will be submitted to different scientific journals and thus, they may be published in a slightly modified version elsewhere in the future.

8 Acknowledgements

This thesis would not exist without the support that I received from a lot of different people in many different ways during the last years and I want to express my deep gratitude for this support.

First of all, I would like to thank my main supervisor Sara Kleindienst for offering me this interesting and highly relevant research project and supporting me during the challenging process of establishing the various required laboratory protocols. Thank you for sharing your enthusiasm about the project and any new data points that I got with me, for connecting me with fantastic collaborators around the world and guiding me through this project.

I am also very grateful to my second supervisor Andreas Kappler for welcoming me into his research group, into his labs and his fun group events. It was a privilege to be able to benefit from the diverse expertise that you and your group members can offer and to be able to discuss challenging project parts and data sets with you when I needed a different knowledgeable perspective.

I would also like to thank my other thesis committee members Christiane Zarfl and Tony Gutierrez for supporting me in finishing this PhD by generously offering their valuable time.

Additionally, I was very lucky to work with several fantastic collaboration partners who supported me during different parts of my PhD project and in different ways. I would like to thank all of them for offering their expertise, always taking time to meet/talk/email with me whenever I needed help or feedback to improve my manuscripts. I really appreciate all your support!
Tony Gutierrez: Thank you for providing me with your interesting isolates, welcoming me into your lab for a few days and always being interested in discussing my project.
Nico Jehmlich: Thank you for always patiently answering my phone calls with questions about the proteomic study and sharing your calm optimism with me.
Christian Hallmann and Rafael Tarozo: Thank you for patiently figuring out how to extract and measure my hydrocarbon samples together with me, and for warmly welcoming me into your group and your lab a few times. I always had a great and successful time in Bremen.
Mandy Joye: Thank you for providing your input on the many questions I've sent you and for spontaneously meeting with me in Bremen. Our discussion in that meeting really helped me understand my data better and pointed me in new, interesting directions.

All of my lab work would not have been possible without the patience and support of the lab technicians at the institute, specifically Ellen Röhm, Bernice Nisch, Renate Seelig, Franziska Schädler and Lars Grimm. I also want to thank Wolfgang Kürner (institute workshop) and Gerhard Schönle (isotope lab workshop) for their support in finding innovative and practical solutions for equipment issues and for many friendly conversations that brightened long days in the lab. Finally, I want to thank Ute Kieb (BAH, Helgoland) for repeatedly providing me with seawater samples and her friendly help during hectic trips to Helgoland.

I also want to thank all past and present members of the Geomicrobiology and Microbial Ecology groups for helpful discussions, friendly conversations, and fun group events. I really enjoyed watching the Microbial Ecology grow and am grateful that I got to meet, work and laugh with all of you.
In particular, I would like to thank all the office mates I had during the last years for celebrating and/or commiserating in the ups and downs of life and research with me, for sharing laughs, our plant children, office supplies, food and drinks and for decorating the office walls together: Casey Bryce, Nia Blackwell, Chao Peng, Yu-Ming Huang, Constantin App, Adrian Langarica-Fuentes – Thank you!
Nia: Thank you so much for always listening and encouraging me when I needed it. Your friendship and mentorship was and is very much appreciated!
Constantin and Adrian: Thank you for becoming my lunch buddies and joining the exclusive Mensa lifestyle. It was always so nice to take a break with you (during lunch or after work) and be able to discuss whatever was on my mind! Constantin, thank you for becoming my close team mate, always helping me out in the lab, brainstorming with me, co-parenting my plants with me, sharing recipes, driving me and my samples through Germany and being a good friend.
Constantin and Anjela: Thank you for becoming my 'Oil team' teammates and the many helpful discussions we've had together, either in person or online during the last months.

There were also a number of students that helped me in the lab, either as student lab assistants or as a part of B.Sc./M.Sc. thesis projects that I supervised: Juliane Riedel, Nelly Wang, Anjela Thon, Katrin Wunsch and Anja Pohl. Thank you for your help and always bringing fresh perspectives and enthusiasm to the project!

Finally, I would like to thank my friends and family for supporting me and cheering me on during these last years. I may not always have had as much time for you as I would have liked but I appreciated every meeting, phone call, text message or vacation that we shared. All of you helped me reach the finish line. Nora: *Merci* for joining me when I needed to escape to the mountains or another country for a bit, for always waiting for me and for just getting me. Julia: Thank you for becoming my mentor and close friend. I could not imagine my time in Tübingen without you. Max: Thank you for your never-ending patience, love and support.
And last but not least, I would like to acknowledge the vital support that this PhD project received from the Mensa Tübingen, Fritz Kola, as well as the Stadtwerke Tübingen/Heidelberg that provided me with Freibad access to clear my mind during countless swimming sessions after work.

9 Curriculm vitae (incl. publication list)

PERSONAL INFORMATION

Name	Saskia Rughöft
Current address	Sandwingert 89, 69123 Heidelberg, Germany
Email	saskia@rughoeft.de
Date of birth	May 4, 1989 in Berlin (Germany)

EDUCATION

2016 – 2021 **PhD in Environmental Sciences**
Eberhard Karls University Tübingen, Germany
- Supervisors: Jun.-Prof. S. Kleindienst (Microbial Ecology), Prof. A. Kappler (Geomicrobiology)
- Thesis: Impacts of chemical dispersants on oil-degrading microorganisms

07/2019 Course AB-827 **Arctic Microbiology** (10 ECTS credits, Grade B) with Prof. Øvreås (Bergen University, Norway) at UNIS, Svalbard

02/2018 Course **Arctic Science** (4.5 credits, Pass with distinction, Grade A) with Prof. Norberg (Umeå University, Sweden) in Kiruna, Sweden

2012 – 2015 **M.Sc., Biogeosciences (Grade 1.1 – A)**
Friedrich Schiller University Jena, Germany
- Supervisor: Prof. K. Küsel (Aquatic Geomicrobiology)
- Thesis: Soil microbial communities involved in nitrogen cycling along two geologically different catenas in Kruger National Park (South Africa)

2008 – 2012 **B.Sc., Biology (Grade 1.1 – A)**
Free University Berlin, Germany
- Supervisor: Prof. T. Romeis (Plant Biochemistry)
- Thesis: The role of CDPK isoforms in cold priming processes in *Arabidopsis thaliana*

8/2010 – 12/2010 **Erasmus** semester at the University of Bergen (Norway)

2001 – 2008 **Abitur** at Herder-Gymnasium (Berlin, Germany), Grade 1.0 (A)

RESEARCH & PROFESSIONAL EXPERIENCE

10/2015 – 03/2016 **Student assistant job** at Chair of Aquatic Geomicrobiology (Prof. K. Küsel), University Jena, Germany

04/2014 – 06/2014 **Research project** under Prof. G. Gleixner (Molecular Biogeo-chemistry) at the MPI for Biogeochemistry, Jena, Germany

- Characterization of microbial communities in forest soil from rhizospheres of two distinct tree species (*Fagus sylvatica, Fraxinus excelsior*)

06/2012 – 07/2012 **Paid internship** at the Office of Technology Assessment at the German Bundestag (Berlin, Germany)

- Research on 'Valorization of Biodiversity'

01/2011 – 03/2011 **Research internship** with Prof. L. Øvreås (Marine Microbiology) at the University of Bergen (Norway)

- Molecular work on microbial communities from hydrothermal vent sites in the Lau basin and mine drainage on Svalbard

04/2009 – 08/2010 **Student research assistant** with Dr. B. Brembs at the Free University Berlin (Germany)

- (Heritability of) Mating preferences in *Dr. melanogaster*

TEACHING AND SUPERVISION EXPERIENCE

03/2018 – 11/2018 **Master thesis supervision**, M.Sc. Appl. and Environm. Geoscience

- Effects of crude oil versus water-accommodated fraction (WAF) addition on marine microbial communities and hydrocarbon degrading bacteria

10/2016 – 10/2017 **Master thesis supervision**, M.Sc. Geoecology

- Effects of surfactants on marine hydrocarbon degrading microorganisms

05/2017 – 09/2017 **Bachelor thesis supervision**, B.Sc. Environmental Sciences

- Identification of potential crude oil or chemical dispersant degrading marine bacteria

2017 – 2019 **Training and supervision** of four student lab assistants

2016/2017 **Geomicrobiology lab courses**, teaching and supervision (M.Sc. students, 1-3 weeks per year)

SCIENTIFIC CONTRIBUTIONS

Peer-reviewed publications

- **Rughöft S**, Jehmlich N, Gutierrez T, Kleindienst S (2021). Comparative proteomics of Marinobacter sp. TT1 reveals Corexit impacts on hydrocarbon metabolism, chemotactic motility and biofilm formation. *Microorganisms,* 9:1, 3. doi: *10.3390/microorganisms9010003*
- **Rughöft S**, Vogel AL, Joye SB, Gutierrez T, Kleindienst S (2020). Starvation-dependent inhibition of the hydrocarbon degrader Marinobacter sp. TT1 by a chemical dispersant. *Journal of Marine Science and Engineering*, 8:11, 925. doi: *10.3390/jmse8110925*
- Otte JM, Blackwell N, Soos V, **Rughöft S**, Maisch M, Kappler A, Kleindienst S, Schmidt C (2018). Sterilization impacts on marine sediment---Are we able to inactivate microorganisms in environmental samples? *FEMS Microbiology Ecology*, 94:12, fiy189. doi: *10.1093/femsec/fiy189*
- **Rughöft S,** Herrmann M, Lazar C, Levick S, Trumbore S, Cesarz S, Küsel K (2016). Distinct soil microbial communities with high nitrification potentials along South African savanna catenas. *Frontiers in Microbiology,* 7:1638*.* doi: *10.3389/fmicb.2016.01638*

Publications in preparation

- **Rughöft S**, Hallmann C, Straub D, Kappler A, Kleindienst S. The effects of nutrient or dispersant application on potentially oil-degrading microbial communities in Arctic Ocean oil spill scenarios.
- **Rughöft S**, Straub D, Tarozo R, Hallmann C, Kappler A, Kleindienst. Chemical dispersant addition affects the composition and growth of North Sea microbial communities under simulated oil spill conditions..

Selected poster presentations (* = presenting author)

- **Rughöft S*,** Straub D, Hallmann C, Thon A, Grathwohl P, Gutierrez T, Kappler A, Kleindienst S (2019). Impacts of chemical dispersants – From arctic microbial community dynamics to taxon-specific responses. Poster P75, 16th Symposium of Aquatic Microbial Ecology (SAME), September 2019, Potsdam, Germany
- **Rughöft S*,** Straub D, Hallmann C, Kappler A, Kleindienst S (2018). Dispersant impacts on Arctic microbial community dynamics and oil biodegradation potential. Poster 090B, 17th International Symposium on Microbial Ecology, August 2018, Leipzig, Germany
- **Rughöft S*,** Straub D, Hallmann C, Kappler A, Kleindienst S (2018). Dispersant impacts on Arctic microbial community dynamics and oil biodegradation potential. Poster Tue_125_BE-3_1019, POLAR2018 – SCAR/IASC Open Science Conference, June 2018, Davos, CH

- **Rughöft S*,** Kappler A, Kleindienst S (2017). Dispersant impacts on microbial activities and oil biodegradation potential in the Arctic Ocean. P 248, Annual Conference 2017 of the UK Microbiology Society, Edinburgh, UK
- Herrmann M*, **Rughöft S**, Trumbore S, Küsel K (2015). Archaea dominate the ammonia oxidizing communities in Savanna soils along a granitic and basaltic toposequence in Kruger National Park (South Africa). MEcV01, Annual Conference of the Association for General and Applied Microbiology (VAAM), May 2015, Marburg, Germany
- Brembs B*, **Rughöft S,** Leinhoß K (2010). Unattractive males can sire attractive sons in *Drosophila melanogaster*. P 92, 9th International Congress of Neuroethology, Salamanca, Spain

Invited talks

- **Rughöft S** and App C (2019) Microbial degradation of petroleum hydrocarbons in the marine environment. Invited by Dr. Christian Hallmann at MARUM, University of Bremen, Bremen, Germany
- **Rughöft S** and Kleindienst S (2017) Molecular biological methods to identify and quantify microbial pollutant degraders. Training seminar 'Future topics in soil, groundwater and brownfield site remediation', Ulm, Germany
- **Rughöft S** (2017) Dispersant impacts on oil degrading microorganisms. Invited by Ass. Prof. of Microbiology Tony Gutierrez at Heriot-Watt University, Edinburgh, UK

Peer review activity

- Koedoe (2020): 1 manuscript
- Water, Air & Soil Pollution (2018): 1 manuscript
- Applied and Environmental Microbiology (2017): 2 manuscripts

GRANTS, PRIZES AND SCHOLARSHIPS

09/2019 **Travel grant** from SAME16 (Symposium of Aquatic Microbial Ecology) for conference participation in Potsdam, Germany

06/2018 **Conference travel scholarship** from DAAD (German Academic Exchange Service) for conference participation at POLAR2018 in Davos, CH

07/2018 **PhD poster prize** (3rd place) at the Quenstedt symposium, Tübingen, Germany

07/2017 **PhD poster prize** (2nd place) at the Quenstedt symposium, Tübingen, Germany

12/2008 – 06/2015 Scholarship from the **German National Academic Foundation** (Studienstiftung des Deutschen Volkes)

OUTREACH ACTIVITY

- Participation in **children's university day** (Kinder-Uni) at Tübingen University, supervision of basic microbiology and microscopy projects (2017, 2018)

- **Podcast interview** about my PhD project for 'Microbe Talk', the podcast of the UK Microbiology Society (April 2016)

ADDITIONAL INFORMATION

Language skills

Fluent	German, English
C1 level	French, Norwegian
B1 level	Spanish, Latin
A1 level	Turkish

Current scientific memberships

International society for microbial ecology (ISME)

10 Appendix

10.1 Supplementary tables for Chapter 5

Table S 1: Proteins with significantly different detected abundances in *Marinobacter* sp. TT1 growing on pyruvate versus *n*-hexadecane according to a Student's T-test (permutation-based FDR: $q < 0.05$).

UniProt ID	Pyruvate	Hexadecane	Description	-Log *p*-value	*q*-value	Student's T-test Diff. (log2 FC)	Student's T-test statistic	Gene names
A0A1I4JZU0	-Infinity	Infinity	Isocitrate lyase	4.30	0.0102	-2.66	-35.38	SAMN04487868_1082
A0A1I4KEY9	-Infinity	Infinity	Putative Cytochrome P450	4.58	0.0181	-4.57	-43.90	SAMN04487868_109135
A0A1I4MCC3	-Infinity	Infinity	UDP-N-acetylmuramoylalanine--D-glutamate ligase	4.15	0.0074	-1.80	-31.51	murD SAMN04487868_12114
A0A1I4J3K6	-Infinity	Infinity	Uncharacterized protein	4.69	0.0204	-5.09	-47.63	SAMN04487868_10556
A0A1I4LME1	-Infinity	Infinity	Sporulation related domain-containing protein	5.36	0.0000	-0.59	-79.73	SAMN04487868_11567
A0A1I4LQZ7	-Infinity	Infinity	Phenylacetaldehyde dehydrogenase	4.80	0.0000	-3.04	-51.88	SAMN04487868_11616
A0A1I4KCV9	-Infinity	Infinity	Regulator of protease activity HflC. stomatin/ prohibitin superfamily	4.15	0.0071	-2.85	-31.40	SAMN04487868_10970
A0A1I4L9J0	-Infinity	Infinity	Heat shock protein Hsp20	4.35	0.0116	-4.72	-36.71	SAMN04487868_11369
A0A1I4KET0	-Infinity	Infinity	3-phenylpropionate/trans-cinnamate dioxygenase ferredoxin reductase subunit	5.09	0.0000	-5.53	-64.70	SAMN04487868_109137
A0A1I4L7K6	-Infinity	Infinity	Putative acyl-CoA dehydrogenase	4.23	0.0086	-6.40	-33.54	SAMN04487868_11332
A0A1I4LG98	-Infinity	Infinity	Phosphomannomutase	4.29	0.0096	-6.49	-35.12	SAMN04487868_11456
A0A1I4LDR7	-Infinity	Infinity	Uncharacterized conserved protein	4.54	0.0148	-4.57	-42.51	SAMN04487868_11416
A0A1I4K9L1	-Infinity	Infinity	AraC-type DNA-binding protein	5.86	0.0000	-6.91	-117.06	SAMN04487868_10916
A0A1I4K9D1	-4.8884	4.8884	Fe-ADH domain-containing protein	4.08	0.0060	-1.97	-29.83	SAMN04487868_10910
A0A1I4HFZ4	-4.8437	4.8437	Putative peptide ABC transporter substrate-binding protein	4.08	0.0058	-1.92	-29.71	SAMN04487868_101333
A0A1I4LF78	-4.5513	4.5513	Alginate export porin	4.03	0.0056	-5.85	-28.60	SAMN04487868_11448
A0A1I4HSM5	-4.3335	4.3335	1-acyl-sn-glycerol-3-phosphate acyltransferase	3.97	0.0053	-1.54	-27.37	SAMN04487868_10226
A0A1I4LMS6	-4.3007	4.3007	Predicted acylesterase/phospholipase RssA. contains patatin domain	3.96	0.0051	-2.13	-27.15	SAMN04487868_11570
A0A1I4J3P7	-4.2721	4.2721	Alcohol dehydrogenase	3.95	0.0049	-3.26	-26.95	SAMN04487868_10555
A0A1I4L895	-4.2501	4.2501	Predicted unusual protein kinase regulating ubiquinone biosynthesis. AarF/ABC1/UbiB family	3.94	0.0048	-2.06	-26.79	SAMN04487868_11343
A0A1I4L4Z4	-4.2322	4.2322	RNA polymerase sigma factor RpoH	3.94	0.0047	-4.29	-26.66	rpoH SAMN04487868_112117
A0A1I4K6E3	-4.2044	4.2044	RNA polymerase-associated protein RapA	3.93	0.0045	-3.54	-26.45	rapA SAMN04487868_108156
A0A1I4JJW2	-4.1199	4.1199	Uncharacterized protein	3.89	0.0041	-5.10	-25.76	SAMN04487868_106116
A0A1I4HYY3	-4.0797	4.0797	Exodeoxyribonuclease 7 large subunit	3.87	0.0039	-1.03	-25.41	xseA SAMN04487868_102129
A0A1I4IET9	-4.0718	4.0718	Nucleotide-binding universal stress protein. UspA family	3.87	0.0038	-4.99	-25.34	SAMN04487868_103212
A0A1I4MGW8	-4.0396	4.0396	2.4-dienoyl-CoA reductase (NADPH2)	3.86	0.0037	-1.86	-25.04	SAMN04487868_12212
A0A1I4MKE3	-4.0157	4.0157	Aconitate hydratase	3.84	0.0035	-3.26	-24.82	SAMN04487868_12330
A0A1I4LC62	-4.0060	4.0060	Mercuric reductase	3.84	0.0035	-1.73	-24.73	SAMN04487868_113112
A0A1I4M4T7	-3.9715	3.9715	Aspartokinase	3.82	0.0033	-3.15	-24.39	SAMN04487868_11911
A0A1I4I1J3	-3.9424	3.9424	Nitroreductase	3.81	0.0032	-2.13	-24.10	SAMN04487868_102251
A0A1I4L0W0	-3.9101	3.9101	Polyhydroxyalkanoate synthase	3.79	0.0031	-2.56	-23.76	SAMN04487868_11232
A0A1I4LWZ1	-3.8647	3.86 47	Uncharacterized protein	3.76	0.0030	-2.35	-23.28	SAMN04487868_11742

A0A1I4MNC9	-3.7236	3.7236	Glycolate oxidase	3.67	0.0054	-1.76	-21.66	SAMN04487868_1249
A0A1I4MRV4	-3.6991	3.6991	Patatin-like phospholipase	3.65	0.0052	-1.31	-21.36	SAMN04487868_12519
A0A1I4HJP7	-3.6967	3.6967	3-oxoacyl-[acyl-carrier protein] reductase	3.65	0.0050	-2.31	-21.33	SAMN04487868_101414
A0A1I4HA08	-3.6948	3.6948	Citronellyl-CoA synthetase	3.65	0.0050	-5.79	-21.31	SAMN04487868_101218
A0A1I4MH59	-3.6814	3.6814	Uncharacterized protein	3.64	0.0049	-3.91	-21.14	SAMN04487868_12228
A0A1I4KZP2	-3.6736	3.6736	Uncharacterized protein	3.63	0.0048	-1.41	-21.04	SAMN04487868_1127
A0A1I4L200	-3.6580	3.6580	PAS domain-containing protein	3.62	0.0047	-1.01	-20.85	SAMN04487868_11257
A0A1I4HCC1	-3.6553	3.6553	Putative acyl-CoA dehydrogenase	3.62	0.0046	-2.15	-20.82	SAMN04487868_101277
A0A1I4I9A3	-3.6514	3.6514	HAMP domain-containing protein	3.61	0.0045	-4.04	-20.77	SAMN04487868_10375
A0A1I4H4U0	-3.6456	3.6456	PA domain-containing protein	3.61	0.0045	-4.29	-20.70	SAMN04487868_10190
A0A1I4LG50	-3.6251	3.6251	Acetyl-CoA C-acetyltransferase	3.59	0.0044	-1.53	-20.44	SAMN04487868_11459
A0A1I4JKB4	-3.6152	3.6152	Ig-like domain-containing protein	3.58	0.0043	-4.60	-20.31	SAMN04487868_106132
A0A1I4J422	-3.6147	3.6147	Catalase-peroxidase	3.58	0.0042	-1.97	-20.31	katG SAMN04487868_10566
A0A1I4KU53	-3.6111	3.6111	Putative serine protein kinase. PrkA	3.58	0.0041	-2.57	-20.26	SAMN04487868_11167
A0A1I4MSP4	-3.6076	3.6076	Uncharacterized protein	3.58	0.0040	-1.79	-20.22	SAMN04487868_12537
A0A1I4HV96	-3.5808	3.5808	Glycosyltransferase involved in cell wall bisynthesis	3.56	0.0059	-1.39	-19.88	SAMN04487868_10287
A0A1I4KCQ3	-3.5538	3.5538	CubicO group peptidase. beta-lactamase class C family	3.53	0.0058	-5.08	-19.53	SAMN04487868_10993
A0A1I4K5K4	-3.4841	3.4841	Aldehyde dehydrogenase	3.47	0.0055	-4.96	-18.63	SAMN04487868_108111
A0A1I4HJQ8	-3.4647	3.4647	Acetyl-CoA C-acetyltransferase	3.45	0.0053	-2.84	-18.38	SAMN04487868_101415
A0A1I4JHN2	-3.4606	3.4606	Molybdopterin molybdenumtransferase	3.45	0.0052	-0.57	-18.32	SAMN04487868_10653
A0A1I4K1M6	-3.4575	3.4575	Aminotransferase	3.45	0.0051	-3.71	-18.28	SAMN04487868_10835
A0A1I4LGW8	-3.4235	3.4235	Mannose-6-phosphate isomerase. type 2	3.42	0.0049	-3.82	-17.84	SAMN04487868_11455
A0A1I4HAB2	-3.4124	3.4124	Uncharacterized protein	3.41	0.0049	-4.63	-17.70	SAMN04487868_101188
A0A1I4L479	-3.4119	3.4119	Uncharacterized protein	3.41	0.0048	-6.28	-17.69	SAMN04487868_112121
A0A1I4HMI1	-3.4021	3.4021	DUF58 domain-containing protein	3.40	0.0047	-2.28	-17.57	SAMN04487868_101490
A0A1I4K5U9	-3.3816	3.3816	Acyl-CoA thioesterase-2	3.38	0.0046	-2.54	-17.31	SAMN04487868_108129
A0A1I4LX43	-3.3603	3.3603	General secretion pathway protein E	3.36	0.0054	-2.65	-17.04	SAMN04487868_11761
A0A1I4MNB3	-3.3550	3.3550	RND family efflux transporter. MFP subunit	3.35	0.0053	-3.23	-16.97	SAMN04487868_12421
A0A1I4ND73	-3.3495	3.3495	Serine phosphatase RsbU. regulator of sigma subunit	3.35	0.0053	-1.83	-16.90	SAMN04487868_13415
A0A1I4HJH4	-3.3143	3.3143	General secretion pathway protein N	3.31	0.0050	-1.62	-16.46	SAMN04487868_101399
A0A1I4MCR2	-3.2924	3.2924	UDP-N-acetylmuramate--L-alanine ligase	3.29	0.0049	-1.15	-16.19	murC SAMN04487868_12117
A0A1I4MEZ8	-3.2862	3.2862	ABC1 family protein	3.28	0.0049	-2.50	-16.12	SAMN04487868_12163
A0A1I4KLH1	-3.2855	3.2855	Uncharacterized protein	3.28	0.0049	-0.62	-16.11	SAMN04487868_110103
A0A1I4JFL9	-3.2675	3.2675	Bacterioferritin	3.27	0.0061	-1.07	-15.89	SAMN04487868_10630
A0A1I4MAT6	-3.2508	3.2508	3-hydroxyacyl-CoA dehydrogenase	3.25	0.0060	-1.82	-15.69	SAMN04487868_12059
A0A1I4HIF2	-3.2491	3.2491	Sugar transferase involved in LPS biosynthesis (Colanic. teichoic acid)	3.25	0.0059	-1.80	-15.67	SAMN04487868_101371
A0A1I4KV85	-3.2364	3.2364	Curved DNA-binding protein	3.24	0.0058	-4.34	-15.52	SAMN04487868_11193
A0A1I4HTH8	-3.2327	3.2327	PA14 domain-containing protein	3.23	0.0058	-4.01	-15.47	SAMN04487868_10238
A0A1I4JRX0	-3.2239	3.2239	3-hydroxyacyl-CoA dehydrogenase / enoyl-CoA hydratase / 3-hydroxybutyryl-CoA epimerase	3.22	0.0057	-3.24	-15.37	SAMN04487868_10730

A0A1I4K0T4	-3.2200	3.2200	Geranylgeranyl reductase family	3.22	0.0057	-2.69	-15.32	SAMN04487868_10818
A0A1I4HA60	-3.2168	3.2168	NADPH:quinone reductase	3.22	0.0057	-2.61	-15.28	SAMN04487868_101217
A0A1I4KC65	-3.2105	3.2105	AraC-type DNA-binding protein	3.21	0.0056	-4.73	-15.21	SAMN04487868_10980
A0A1I4L2L6	-3.2032	3.2032	Uncharacterized protein	3.20	0.0055	-3.26	-15.13	SAMN04487868_11276
A0A1I4LGJ8	-3.1773	3.1773	2-(1.2-epoxy-1.2-dihydrophenyl)acetyl-CoA isomerase	3.18	0.0054	-2.60	-14.83	SAMN04487868_11466
A0A1I4HB22	-3.1398	3.1398	Uncharacterized protein	3.14	0.0076	-4.49	-14.40	SAMN04487868_101207
A0A1I4JVX5	-3.1284	3.1284	Lipid-A-disaccharide synthase	3.13	0.0074	-3.53	-14.28	lpxB SAMN04487868_107147
A0A1I4KP39	-3.1272	3.1272	Lon protease	3.13	0.0074	-2.23	-14.26	SAMN04487868_110154
A0A1I4LJZ2	-3.1159	3.1159	Glutamine-dependent NAD(+) synthetase	3.12	0.0072	-0.90	-14.14	nadE SAMN04487868_11511
A0A1I4KL02	-3.1074	3.1074	Fumarate hydratase class II	3.11	0.0071	-1.45	-14.05	fumC SAMN04487868_11092
A0A1I4K1F6	-3.0992	3.0992	Inositol-1-monophosphatase	3.10	0.0071	-2.35	-13.96	SAMN04487868_10836
A0A1I4N719	-3.0981	3.0981	Fumarate hydratase class I	3.10	0.0070	-0.71	-13.95	SAMN04487868_13029
A0A1I4LAT1	-3.0921	3.0921	DNA-binding beta-propeller fold protein YncE	3.09	0.0079	-4.57	-13.88	SAMN04487868_113104
A0A1I4L4M5	-3.0827	3.0827	Acyl-coenzyme A thioesterase PaaI. contains HGG motif	3.08	0.0078	-4.23	-13.78	SAMN04487868_112126
A0A1I4KUW8	-3.0785	3.0785	Chaperone modulatory protein CbpM	3.08	0.0078	-2.24	-13.74	SAMN04487868_11194
A0A1I4MZM2	-3.0621	3.0621	Uncharacterized protein	3.06	0.0077	-5.37	-13.56	SAMN04487868_12752
A0A1I4MMR8	-3.0531	3.0531	Multidrug efflux pump subunit AcrB	3.05	0.0077	-3.21	-13.47	SAMN04487868_12420
A0A1I4HHX4	-3.0490	3.0490	Pyruvate carboxylase subunit A	3.05	0.0077	-3.33	-13.43	SAMN04487868_101418
A0A1I4HVQ3	-3.0408	3.0408	Sugar transferase. PEP-CTERM system associated/exopolysaccharide biosynthesis polyprenyl glycosylphosphotransferase	3.04	0.0076	-4.72	-13.34	SAMN04487868_10267
A0A1I4HIU5	-3.0384	3.0384	Superoxide dismutase	3.04	0.0075	-1.91	-13.32	SAMN04487868_101405
A0A1I4NFZ1	-3.0333	3.0333	Ubiquinol-cytochrome c reductase cytochrome c1 subunit	3.03	0.0075	-0.54	-13.26	SAMN04487868_13713
A0A1I4J898	-3.0251	3.0251	Succinate dehydrogenase flavoprotein subunit	3.03	0.0074	-2.78	-13.18	SAMN04487868_105169
A0A1I4J838	-3.0235	3.0235	3-ketoacyl-CoA thiolase	3.02	0.0073	-1.84	-13.16	fadA SAMN04487868_105163
A0A1I4MR32	-3.0230	3.0230	Cytochrome bd-I ubiquinol oxidase subunit 1 apoprotein	3.02	0.0073	-5.05	-13.16	SAMN04487868_12511
A0A1I4L9P4	-3.0200	3.0200	Oligopeptidase A	3.02	0.0072	-1.47	-13.13	SAMN04487868_11372
A0A1I4H4P3	-3.0149	3.0149	DUF2063 domain-containing protein	3.01	0.0072	-3.75	-13.07	SAMN04487868_10133
A0A1I4ILL9	-3.0087	3.0087	Amidase	3.01	0.0071	-2.25	-13.01	SAMN04487868_10415
A0A1I4HW41	-3.0022	3.0022	Glucans biosynthesis protein	3.00	0.0070	-3.40	-12.95	SAMN04487868_10278
A0A1I4MR63	-2.9988	2.9988	Electron-transferring-flavoprotein dehydrogenase	3.00	0.0070	-1.77	-12.91	SAMN04487868_1251
A0A1I4MJN7	-2.9953	2.9953	Glycerophosphoryl diester phosphodiesterase	3.00	0.0069	-2.11	-12.88	SAMN04487868_1239
A0A1I4JR92	-2.9922	2.9922	Vitamin B12 transporter	2.99	0.0068	-3.04	-12.85	SAMN04487868_10712
A0A1I4J926	-2.9811	2.9811	Fatty acid oxidation complex subunit alpha	2.98	0.0068	-2.72	-12.73	SAMN04487868_105162
A0A1I4HCT6	-2.9808	2.9808	Uncharacterized protein	2.98	0.0067	-4.76	-12.73	SAMN04487868_101227
A0A1I4HFQ5	-2.9666	2.9666	Lipopolysaccharide export system ATP-binding protein	2.97	0.0075	-1.79	-12.59	SAMN04487868_101314
A0A1I4HK54	-2.9623	2.9623	Uncharacterized protein	2.96	0.0075	-3.56	-12.55	SAMN04487868_101435
A0A1I4J7P3	-2.9570	2.9570	Uncharacterized protein	2.96	0.0074	-1.37	-12.50	SAMN04487868_105152
A0A1I4I8Z6	-2.9421	2.9421	CBS domain-containing protein	2.94	0.0072	-1.90	-12.35	SAMN04487868_10332
A0A1I4ICL7	-2.9394	2.9394	Putative intracellular protease/amidase	2.94	0.0072	-2.67	-12.33	SAMN04487868_103177

A0A1I4MRG2	-2.9357	2.9357	ATP-binding cassette. subfamily C. CydC	2.94	0.0071	-4.18	-12.29	SAMN04487868_1258
A0A1I4J413	-2.9323	2.9323	Uncharacterized protein	2.93	0.0070	-1.34	-12.26	SAMN04487868_10567
A0A1I4MLI4	-2.9174	2.9174	Enoyl-CoA hydratase/carnithine racemase	2.92	0.0069	-1.51	-12.12	SAMN04487868_12350
A0A1I4N7Z6	-2.9146	2.9146	Glucosyl-3-phosphoglycerate synthase	2.91	0.0068	-1.34	-12.09	SAMN04487868_13033
A0A1I4LN31	-2.8997	2.8997	5-methyltetrahydropteroyltriglutamate--homocysteine methyltransferase	2.90	0.0068	-5.41	-11.95	metE SAMN04487868_11577
A0A1I4K9I6	-2.8773	2.8773	Glutamine synthetase	2.88	0.0079	-2.19	-11.74	SAMN04487868_10912
A0A1I4ILN8	-2.8671	2.8671	Proline racemase	2.87	0.0078	-0.88	-11.65	SAMN04487868_10422
A0A1I4HU28	-2.8632	2.8632	Long-chain acyl-CoA synthetase	2.86	0.0077	-3.90	-11.62	SAMN04487868_1022
A0A1I4IT61	-2.8628	2.8628	Aminotransferase	2.86	0.0077	-1.28	-11.61	SAMN04487868_104165
A0A1I4J513	-2.8598	2.8598	Chaperone protein HtpG	2.86	0.0077	-0.28	-11.59	htpG SAMN04487868_10561
A0A1I4J8Q0	-2.8577	2.8577	PAS domain S-box-containing protein/diguanylate cyclase (GGDEF) domain-containing protein	2.86	0.0076	-1.97	-11.57	SAMN04487868_105149
A0A1I4K168	-2.8525	2.8525	Cyclopropane-fatty-acyl-phospholipid synthase	2.85	0.0075	-2.87	-11.52	SAMN04487868_10817
A0A1I4HLM5	-2.8516	2.8516	Chromosome partitioning protein	2.85	0.0074	-1.96	-11.51	SAMN04487868_101471
A0A1I4J8S8	-2.8401	2.8401	Diguanylate cyclase (GGDEF) domain-containing protein	2.84	0.0073	-1.77	-11.41	SAMN04487868_105180
A0A1I4N7P5	-2.8383	2.8383	Virulence factor lipase N-terminal	2.84	0.0073	-2.36	-11.39	SAMN04487868_13027
A0A1I4JI76	-2.8353	2.8353	Transcriptional regulator. AraC family	2.84	0.0072	-2.26	-11.37	SAMN04487868_10689
A0A1I4LW57	-2.8216	2.8216	Nicotinamidase-related amidase	2.82	0.0078	-3.14	-11.24	SAMN04487868_11718
A0A1I4MLB5	-2.8205	2.8205	OmpA-OmpF porin. OOP family	2.82	0.0078	-2.13	-11.23	SAMN04487868_12345
A0A1I4LF83	-2.8162	2.8162	Alginate biosynthesis protein Alg44	2.82	0.0077	-4.13	-11.20	SAMN04487868_11446
A0A1I4J372	-2.8159	2.8159	Ribosome modulation factor	2.82	0.0077	-4.53	-11.20	rmf SAMN04487868_10544
A0A1I4NHV7	-2.8149	2.8149	Putative pterin-4-alpha-carbinolamine dehydratase	2.81	0.0077	-3.12	-11.19	SAMN04487868_1396
A0A1I4I713	-2.8090	2.8090	1-Cys peroxiredoxin	2.81	0.0076	-1.83	-11.13	SAMN04487868_10329
A0A1I4MP15	-2.8014	2.8014	Arginine N-succinyltransferase	2.80	0.0083	-2.07	-11.07	SAMN04487868_12425
A0A1I4K0T2	-2.7963	2.7963	Dihydrolipoamide dehydrogenase	2.80	0.0082	-1.81	-11.02	SAMN04487868_10822
A0A1I4LAM4	-2.7884	2.7884	Sulfoxide reductase catalytic subunit YedY	2.79	0.0082	-3.58	-10.96	SAMN04487868_113101
A0A1I4I8Q7	-2.7840	2.7840	Multifunctional fusion protein	2.78	0.0081	-2.63	-10.92	msrB msrA SAMN04487868_10376
A0A1I4MQQ2	-2.7813	2.7813	Electron transfer flavoprotein beta subunit	2.78	0.0080	-1.52	-10.90	SAMN04487868_1252
A0A1I4MM83	-2.7738	2.7738	Glycolate oxidase iron-sulfur subunit	2.77	0.0086	-2.34	-10.83	SAMN04487868_1247
A0A1I4MEM9	-2.7719	2.7719	Pyrophosphate--fructose 6-phosphate 1-phosphotransferase	2.77	0.0086	-2.08	-10.82	pfp SAMN04487868_12167
A0A1I4K119	-2.7703	2.7703	Multidrug efflux pump	2.77	0.0085	-3.01	-10.80	SAMN04487868_10828
A0A1I4HLA6	-2.7600	2.7600	Ribosomal RNA small subunit methyltransferase C	2.76	0.0088	-2.46	-10.72	rsmC SAMN04487868_101495
A0A1I4HVB5	-2.7503	2.7503	FemAB-related protein. PEP-CTERM system-associated	2.75	0.0091	-2.77	-10.63	SAMN04487868_10261
A0A1I4HXZ9	-2.7428	2.7428	Thioredoxin reductase	2.74	0.0091	-1.54	-10.57	SAMN04487868_102154
A0A1I4M5M9	-2.7411	2.7411	Valine-pyruvate aminotransferase apoenzyme	2.74	0.0090	-1.09	-10.56	SAMN04487868_11933
A0A1I4JKC5	-2.7362	2.7362	Long-chain fatty acid transport protein	2.74	0.0090	-4.86	-10.52	SAMN04487868_106133
A0A1I4L1V4	-2.7359	2.7359	Pimeloyl-ACP methyl ester carboxylesterase	2.74	0.0089	-1.64	-10.51	SAMN04487868_11253
A0A1I4LFP8	-2.7343	2.7343	Acyl-CoA dehydrogenase	2.73	0.0089	-1.12	-10.50	SAMN04487868_11458
A0A1I4IF66	-2.7285	2.7285	Uncharacterized protein	2.73	0.0089	-3.20	-10.45	SAMN04487868_103223

A0A1I4KEI4	-2.7226	2.7226	Choline dehydrogenase	2.72	0.0088	-3.65	-10.41	SAMN04487868_109136
A0A1I4K4V6	-2.7187	2.7187	Polyphosphate kinase	2.72	0.0088	-3.08	-10.37	ppk SAMN04487868_108116
A0A1I4JSV9	-2.7057	2.7057	Uncharacterized protein	2.71	0.0086	-3.47	-10.27	SAMN04487868_10759
A0A1I4HY69	-2.7041	2.7041	ATP-dependent Clp protease ATP-binding subunit ClpA	2.70	0.0086	-1.06	-10.26	SAMN04487868_102159
A0A1I4HV56	-2.7027	2.7027	Acetyltransferase (GNAT) domain-containing protein	2.70	0.0085	-5.06	-10.24	SAMN04487868_10260
A0A1I4LL12	-2.7004	2.7004	Acyltransferase. WS/DGAT/MGAT	2.70	0.0085	-5.41	-10.23	SAMN04487868_11536
A0A1I4MAB6	-2.6964	2.6964	Uncharacterized protein	2.70	0.0084	-2.76	-10.19	SAMN04487868_12048
A0A1I4JH16	-2.6942	2.6942	Diguanylate cyclase (GGDEF) domain-containing protein	2.69	0.0083	-1.94	-10.18	SAMN04487868_10638
A0A1I4MYG0	-2.6933	2.6933	Oligopeptide transport system ATP-binding protein	2.69	0.0083	-1.98	-10.17	SAMN04487868_12739
A0A1I4H8Z4	-2.6860	2.6860	Enoyl-CoA hydratase/carnithine racemase	2.69	0.0088	-3.83	-10.11	SAMN04487868_101181
A0A1I4ISQ2	-2.6852	2.6852	Predicted dithiol-disulfide oxidoreductase. DUF899 family	2.69	0.0088	-1.21	-10.11	SAMN04487868_104125
A0A1I4IG23	-2.6824	2.6824	Malonate-semialdehyde dehydrogenase (Acetylating) / methylmalonate-semialdehyde dehydrogenase	2.68	0.0093	-2.06	-10.08	SAMN04487868_103232
A0A1I4KCF9	-2.6776	2.6776	Predicted DNA-binding transcriptional regulator YafY. contains an HTH and WYL domains	2.68	0.0091	-2.50	-10.04	SAMN04487868_10977
A0A1I4M0T4	-2.6657	2.6657	3-isopropylmalate dehydratase large subunit	2.67	0.0089	-1.68	-9.95	leuC SAMN04487868_11830
A0A1I4JV83	-2.6632	2.6632	Multicopper oxidase with three cupredoxin domains (Includes cell division protein FtsP and spore coat protein CotA)	2.66	0.0088	-0.89	-9.93	SAMN04487868_107103
A0A1I4IUP3	-2.6627	2.6627	Periplasmic serine endoprotease DegP-like	2.66	0.0088	-1.67	-9.93	SAMN04487868_104200
A0A1I4J450	-2.6602	2.6602	Fructose-bisphosphate aldolase	2.66	0.0088	-1.62	-9.91	SAMN04487868_10565
A0A1I4LFF1	-2.6595	2.6595	Alginate O-acetyltransferase complex protein AlgF	2.66	0.0088	-3.72	-9.90	SAMN04487868_11452
A0A1I4KTB2	-2.6591	2.6591	Fatty acid desaturase	2.66	0.0087	-6.83	-9.90	SAMN04487868_11155
A0A1I4LKX0	-2.6524	2.6524	Pseudouridine synthase	2.65	0.0087	-0.53	-9.85	SAMN04487868_1159
A0A1I4ITF9	-2.6447	2.6447	Outer membrane protein OmpA	2.64	0.0086	-2.26	-9.79	SAMN04487868_104152
A0A1I4K4U0	-2.6372	2.6372	Choline dehydrogenase	2.64	0.0085	-4.42	-9.73	SAMN04487868_108113
A0A1I4JRY3	-2.6369	2.6369	Acetyl-CoA C-acetyltransferase	2.64	0.0085	-2.45	-9.73	SAMN04487868_10729
A0A1I4KUJ8	-2.6317	2.6317	Uncharacterized protein	2.63	0.0085	-4.39	-9.69	SAMN04487868_11178
A0A1I4MKZ2	-2.6316	2.6316	Response regulator of citrate/malate metabolism	2.63	0.0084	-0.86	-9.69	SAMN04487868_12335
A0A1I4K9Q6	-2.6288	2.6288	Acyl-CoA reductase	2.63	0.0089	-1.02	-9.67	SAMN04487868_10911
A0A1I4KKG5	-2.6285	2.6285	Uncharacterized protein	2.63	0.0088	-1.77	-9.66	SAMN04487868_11065
A0A1I4IEU2	-2.6160	2.6160	Enoyl-CoA hydratase/carnithine racemase	2.62	0.0087	-2.19	-9.57	SAMN04487868_103234
A0A1I4IVM8	-2.6157	2.6157	L-aspartate oxidase	2.62	0.0087	-1.24	-9.57	SAMN04487868_104205
A0A1I4HD98	-2.6130	2.6130	Nitrilase	2.61	0.0086	-0.86	-9.55	SAMN04487868_101306
A0A1I4K9Q2	-2.6118	2.6118	Short-chain dehydrogenase	2.61	0.0086	-4.40	-9.54	SAMN04487868_10919
A0A1I4LK07	-2.6055	2.6055	Chaperone protein ClpB	2.61	0.0085	-1.49	-9.49	clpB SAMN04487868_1157
A0A1I4HI22	-2.5968	2.5968	Acyl-CoA dehydrogenase	2.60	0.0085	-7.22	-9.43	SAMN04487868_101424
A0A1I4MPI2	-2.5963	2.5963	2.4-dienoyl-CoA reductase	2.60	0.0084	-3.52	-9.42	SAMN04487868_12454
A0A1I4JSI6	-2.5945	2.5945	Acetyltransferase	2.59	0.0084	-2.40	-9.41	SAMN04487868_10742
A0A1I4KTY5	-2.5913	2.5913	Transcriptional regulator. TetR family	2.59	0.0087	-1.31	-9.38	SAMN04487868_11157
A0A1I4KB32	-2.5852	2.5852	Aspartate kinase	2.59	0.0086	-0.62	-9.34	SAMN04487868_10929
A0A1I4H2T3	-2.5850	2.5850	Peptidyl-prolyl cis-trans isomerase	2.59	0.0089	-0.77	-9.34	SAMN04487868_10122

A0A1I4ML73	-2.5838	2.5838	D-amino-acid dehydrogenase	2.58	0.0091	-2.66	-9.33	SAMN04487868_12342
A0A1I4J7G7	-2.5806	2.5806	GTPase Der	2.58	0.0090	-1.94	-9.31	der SAMN04487868_105148
A0A1I4KU15	-2.5790	2.5790	UPF0229 protein SAMN04487868_11166	2.58	0.0092	-1.96	-9.29	SAMN04487868_11166
A0A1I4HLM4	-2.5620	2.5620	Flagellar motor switch protein FliM	2.56	0.0097	-2.11	-9.17	SAMN04487868_101451
A0A1I4L6L4	-2.5619	2.5619	AAA domain-containing protein	2.56	0.0096	-1.33	-9.17	SAMN04487868_11310
A0A1I4JJB8	-2.5526	2.5526	Twitching motility protein PilU	2.55	0.0096	-1.65	-9.10	SAMN04487868_106110
A0A1I4LXS4	-2.5500	2.5500	Glutathione reductase (NADPH)	2.55	0.0098	-5.31	-9.08	SAMN04487868_11751
A0A1I4J654	-2.5492	2.5492	ABC-2 type transport system ATP-binding protein	2.55	0.0097	-1.70	-9.08	SAMN04487868_105112
A0A1I4L3J5	-2.5486	2.5486	Phosphoenolpyruvate carboxykinase (ATP)	2.55	0.0097	-0.53	-9.07	pckA SAMN04487868_112106
A0A1I4MD12	-2.5468	2.5468	Cell division protein FtsA	2.55	0.0097	-3.04	-9.06	ftsA SAMN04487868_12120
A0A1I4HDA1	-2.5423	2.5423	Magnesium transporter MgtE	2.54	0.0101	-4.09	-9.03	SAMN04487868_101308
A0A1I4KA18	-2.5401	2.5401	TRAP-type mannitol/chloroaromatic compound transport system. substrate-binding protein	2.54	0.0101	-1.73	-9.01	SAMN04487868_10913
A0A1I4N7Q2	-2.5316	2.5316	Putative NAD(P)H quinone oxidoreductase. PIG3 family	2.53	0.0102	-0.97	-8.95	SAMN04487868_13036
A0A1I4HMG9	-2.5313	2.5313	Glutamate dehydrogenase	2.53	0.0101	-3.23	-8.95	SAMN04487868_101492
A0A1I4M0H2	-2.5250	2.5250	General secretion pathway protein A	2.52	0.0103	-1.04	-8.91	SAMN04487868_1188
A0A1I4LW20	-2.5246	2.5246	ATP-grasp domain-containing protein	2.52	0.0103	-2.37	-8.90	SAMN04487868_11731
A0A1I4KIB4	-2.5224	2.5224	Bifunctional purine biosynthesis protein PurH	2.52	0.0103	-1.78	-8.89	purH SAMN04487868_11012
A0A1I4HYS0	-2.5110	2.5110	Protease HtpX	2.51	0.0106	-2.50	-8.81	htpX SAMN04487868_102176
A0A1I4HI90	-2.5088	2.5088	UDP-N-acetyl-D-galactosamine dehydrogenase	2.51	0.0105	-0.88	-8.79	SAMN04487868_101377
A0A1I4HAC6	-2.5028	2.5028	Multisubunit potassium/proton antiporter. PhaG subunit	2.50	0.0105	-2.64	-8.75	SAMN04487868_101175
A0A1I4HID5	-2.4977	2.4977	Acyl-CoA dehydrogenase	2.50	0.0104	-1.89	-8.72	SAMN04487868_101423
A0A1I4KM89	-2.4952	2.4952	4-hydroxy-tetrahydrodipicolinate reductase	2.50	0.0106	-1.28	-8.70	dapB SAMN04487868_110122
A0A1I4MDH0	-2.4944	2.4944	UDP-N-acetylglucosamine--N-acetylmuramyl-(pentapeptide) pyrophosphoryl-undecaprenol N-acetylglucosamine transferase	2.49	0.0106	-2.22	-8.69	murG SAMN04487868_12116
A0A1I4LLS5	-2.4866	2.4866	Serine hydroxymethyltransferase	2.49	0.0107	-1.34	-8.64	glyA SAMN04487868_11546
A0A1I4I0E5	-2.4822	2.4822	Uncharacterized protein	2.48	0.0107	-0.69	-8.61	SAMN04487868_102201
A0A1I4I866	-2.4803	2.4803	S-formylglutathione hydrolase	2.48	0.0111	-2.89	-8.60	SAMN04487868_10333
A0A1I4INM0	-2.4794	2.4794	L-serine dehydratase	2.48	0.0110	-2.36	-8.59	SAMN04487868_10462
A0A1I4LLP6	-2.4737	2.4737	Isoleucine--tRNA ligase	2.47	0.0114	-1.85	-8.55	ileS SAMN04487868_11525
A0A1I4HAL1	-2.4703	2.4703	2.4-dienoyl-CoA reductase (NADPH2)	2.47	0.0114	-2.96	-8.53	SAMN04487868_101182
A0A1I4INT7	-2.4663	2.4663	Phosphatidylserine/phosphatidylglycerophosphate/cardiolipin synthase	2.47	0.0117	-2.06	-8.50	SAMN04487868_10431
A0A1I4I9I3	-2.4650	2.4650	Uncharacterized conserved protein. Alpha-E superfamily	2.46	0.0117	-2.61	-8.49	SAMN04487868_103107
A0A1I4JH64	-2.4631	2.4631	Adenylate cyclase	2.46	0.0117	-2.86	-8.48	SAMN04487868_10666
A0A1I4MEC5	-2.4606	2.4606	Acyl-CoA thioesterase	2.46	0.0116	-0.69	-8.46	SAMN04487868_12139
A0A1I4M6W6	-2.4580	2.4580	CTP synthase	2.46	0.0116	-1.70	-8.45	pyrG SAMN04487868_11957
A0A1I4KDM3	-2.4522	2.4522	Ornithine decarboxylase	2.45	0.0115	-1.25	-8.41	SAMN04487868_109110
A0A1I4N535	-2.4406	2.4406	MSHA biogenesis protein MshQ	2.44	0.0119	-1.98	-8.33	SAMN04487868_12948
A0A1I4LFN3	-2.4386	2.4386	GDP-mannose 6-dehydrogenase	2.44	0.0118	-3.37	-8.32	SAMN04487868_11444

A0A1I4MC29	-2.4129	2.4129	Ribosomal RNA small subunit methyltransferase H	2.41	0.0125	-1.01	-8.15	rsmH SAMN04487868_1218
A0A1I4IVV3	-2.4085	2.4085	Uncharacterized protein	2.41	0.0124	-1.23	-8.12	SAMN04487868_104208
A0A1I4H7V1	-2.4039	2.4039	Uncharacterized protein	2.40	0.0124	-3.54	-8.09	SAMN04487868_101161
A0A1I4N287	-2.4024	2.4024	Acetoin utilization deacetylase AcuC	2.40	0.0123	-3.14	-8.08	SAMN04487868_12839
A0A1I4KPK4	-2.4006	2.4006	Glucose/arabinose dehydrogenase. beta-propeller fold	2.40	0.0123	-1.22	-8.07	SAMN04487868_110153
A0A1I4IML6	-2.3997	2.3997	Uncharacterized conserved protein YbaA. DUF1428 family	2.40	0.0123	-2.19	-8.06	SAMN04487868_10442
A0A1I4MTD7	-2.3980	2.3980	RES domain-containing protein	2.40	0.0122	-1.56	-8.05	SAMN04487868_12546
A0A1I4MVL8	-2.3915	2.3915	Soluble pyridine nucleotide transhydrogenase	2.39	0.0124	-1.40	-8.01	sthA SAMN04487868_12620
A0A1I4H2L7	-2.3913	2.3913	Uncharacterized protein	2.39	0.0124	-3.01	-8.01	SAMN04487868_10128
A0A1I4N6I5	-2.3787	2.3787	TRAP transporter. 4TM/12TM fusion protein	2.38	0.0125	-2.66	-7.93	SAMN04487868_1303
A0A1I4J708	-2.3680	2.3680	Protein-export membrane protein SecF	2.37	0.0132	-1.76	-7.86	secF SAMN04487868_105134
A0A1I4H8J3	-2.3658	2.3658	Maleate cis-trans isomerase	2.37	0.0132	-2.94	-7.85	SAMN04487868_101119
A0A1I4M0W2	-2.3563	2.3563	Phospholipid-binding lipoprotein MlaA	2.36	0.0133	-1.39	-7.79	SAMN04487868_1186
A0A1I4ISC0	-2.3559	2.3559	DUF4398 domain-containing protein	2.36	0.0133	-1.85	-7.79	SAMN04487868_104151
A0A1I4MVC6	-2.3376	2.3376	Glycerophosphoryl diester phosphodiesterase	2.34	0.0135	-2.39	-7.67	SAMN04487868_12621
A0A1I4H8K6	-2.3368	2.3368	Animal haem peroxidase	2.34	0.0134	-0.95	-7.67	SAMN04487868_101136
A0A1I4MWL7	-2.3288	2.3288	SH3 domain protein	2.33	0.0134	-0.53	-7.62	SAMN04487868_12644
A0A1I4MHM9	-2.3237	2.3237	Acetyl esterase/lipase	2.32	0.0136	-2.92	-7.59	SAMN04487868_12257
A0A1I4HV10	-2.3192	2.3192	Predicted ATP-dependent carboligase. ATP-grasp superfamily	2.32	0.0135	-1.22	-7.56	SAMN04487868_10256
A0A1I4NF09	-2.3177	2.3177	Elongation factor G	2.32	0.0134	-1.95	-7.55	fusA SAMN04487868_1362
A0A1I4LWY6	-2.3163	2.3163	Isoquinoline 1-oxidoreductase. beta subunit	2.32	0.0134	-1.62	-7.55	SAMN04487868_11726
A0A1I4IVT0	-2.3151	2.3151	Uncharacterized protein	2.32	0.0134	-1.62	-7.54	SAMN04487868_104225
A0A1I4MJP4	-2.3112	2.3112	Cysteine synthase	2.31	0.0133	-1.34	-7.51	SAMN04487868_12313
A0A1I4I077	-2.3087	2.3087	Alanine-synthesizing transaminase	2.31	0.0133	-0.95	-7.50	SAMN04487868_102174
A0A1I4MVI1	-2.3080	2.3080	MscS family membrane protein	2.31	0.0132	-2.77	-7.49	SAMN04487868_1267
A0A1I4MDA1	-2.3075	2.3075	D-alanine--D-alanine ligase	2.31	0.0132	-0.93	-7.49	ddl SAMN04487868_12118
A0A1I4JL59	-2.3047	2.3047	ATP-dependent DNA helicase RecG	2.30	0.0132	-3.02	-7.48	recG SAMN04487868_106128
A0A1I4JFL3	-2.3019	2.3019	Phospholipase A1	2.30	0.0134	-3.74	-7.46	SAMN04487868_10632
A0A1I4KLE3	-2.3019	2.3019	Biotin carboxylase	2.30	0.0134	-1.08	-7.46	SAMN04487868_110100
A0A1I4M6Y3	-2.2985	2.2985	DNA polymerase III subunit alpha	2.30	0.0133	-2.53	-7.44	SAMN04487868_11960
A0A1I4KXJ6	-2.2832	2.2832	Uncharacterized protein	2.28	0.0152	-1.18	-7.35	SAMN04487868_111138
A0A1I4HEI9	-2.2725	2.2725	Uncharacterized protein	2.27	0.0155	-1.89	-7.28	SAMN04487868_101334
A0A1I4KDA2	-2.2717	2.2717	Hydroxybutyrate-dimer hydrolase	2.27	0.0155	-1.42	-7.28	SAMN04487868_109103
A0A1I4J7S7	-2.2702	2.2702	Flagellar hook-associated protein 3 FlgL	2.27	0.0154	-2.63	-7.27	SAMN04487868_105128
A0A1I4L6P6	-2.2669	2.2669	Taurine dioxygenase	2.27	0.0153	-2.67	-7.25	SAMN04487868_1133
A0A1I4IWP8	-2.2631	2.2631	Mg2+ and Co2+ transporter CorB. contains DUF21. CBS pair. and CorC-HlyC domains	2.26	0.0152	-2.44	-7.23	SAMN04487868_104224
A0A1I4M7J0	-2.2613	2.2613	CBS domain-containing protein	2.26	0.0152	-1.56	-7.22	SAMN04487868_11974
A0A1I4IQ39	-2.2557	2.2557	NADH-quinone oxidoreductase	2.26	0.0151	-4.06	-7.19	SAMN04487868_10496
A0A1I4LMK3	-2.2514	2.2514	Type IV pilus assembly protein PilM	2.25	0.0150	-1.11	-7.16	SAMN04487868_11560

A0A1I4KLH5	-2.2435	2.2435	Acetolactate synthase-1/2/3 large subunit	2.24	0.0157	-2.57	-7.12	SAMN04487868_110102
A0A1I4LSW4	-2.2389	2.2389	Uncharacterized protein	2.24	0.0158	-1.44	-7.09	SAMN04487868_11652
A0A1I4JAI9	-2.2382	2.2382	Nuclease-related domain-containing protein	2.24	0.0158	-3.47	-7.09	SAMN04487868_105218
A0A1I4MMY3	-2.2378	2.2378	N-succinylglutamate 5-semialdehyde dehydrogenase	2.24	0.0157	-1.28	-7.08	astD SAMN04487868_12424
A0A1I4MNQ1	-2.2360	2.2360	Cobalt-zinc-cadmium resistance protein CzcA	2.24	0.0157	-2.58	-7.07	SAMN04487868_12433
A0A1I4KD18	-2.2355	2.2355	Acetoacetyl-CoA synthetase	2.24	0.0157	-3.77	-7.07	SAMN04487868_10997
A0A1I4LXA2	-2.2343	2.2343	Sugar (Pentulose or hexulose) kinase	2.23	0.0156	-1.45	-7.06	SAMN04487868_11766
A0A1I4KBY1	-2.2335	2.2335	NADH dehydrogenase	2.23	0.0156	-0.95	-7.06	SAMN04487868_10966
A0A1I4KRK3	-2.2271	2.2271	Protein-export protein SecB	2.23	0.0155	-0.64	-7.02	secB SAMN04487868_11112
A0A1I4IUK7	-2.2259	2.2259	Elongation factor 4	2.23	0.0154	-2.26	-7.02	lepA SAMN04487868_104198
A0A1I4MDC6	-2.2218	2.2218	Phosphatidylglycerol--prolipoprotein diacylglyceryl transferase	2.22	0.0153	-4.17	-6.99	lgt SAMN04487868_12135
A0A1I4MK57	-2.2209	2.2209	1-acyl-sn-glycerol-3-phosphate acyltransferase	2.22	0.0153	-3.10	-6.99	SAMN04487868_12323
A0A1I4M565	-2.2205	2.2205	Oxaloacetate decarboxylase beta chain	2.22	0.0153	-3.65	-6.99	SAMN04487868_1192
A0A1I4KMS0	-2.2168	2.2168	Chaperone protein DnaK	2.22	0.0154	-0.92	-6.97	dnaK SAMN04487868_110120
A0A1I4IFE9	-2.2093	2.2093	Acyl-CoA dehydrogenase	2.21	0.0158	-1.88	-6.92	SAMN04487868_103233
A0A1I4MJF2	-2.2079	2.2079	Membrane-anchored ribosome-binding protein. inhibits growth in stationary phase. ElaB/YqjD/DUF883 family	2.21	0.0157	-3.39	-6.92	SAMN04487868_1237
A0A1I4KAE5	-2.2075	2.2075	Pyruvate/2-oxoglutarate dehydrogenase complex. dihydrolipoamide dehydrogenase (E3) component	2.21	0.0159	-2.54	-6.91	SAMN04487868_10935
A0A1I4K3Z9	-2.1960	2.1960	Heat shock protein HslJ	2.20	0.0160	-0.88	-6.85	SAMN04487868_10873
A0A1I4H898	-2.1833	2.1833	AbiTii domain-containing protein	2.18	0.0165	-1.81	-6.78	SAMN04487868_101129
A0A1I4ILS6	-2.1749	2.1749	NADPH:quinone reductase	2.17	0.0168	-1.60	-6.73	SAMN04487868_10423
A0A1I4MK80	-2.1725	2.1725	Opacity protein	2.17	0.0167	-5.36	-6.72	SAMN04487868_12312
A0A1I4JTP5	-2.1711	2.1711	Phosphatidylglycerol--prolipoprotein diacylglyceryl transferase	2.17	0.0167	-3.84	-6.71	lgt SAMN04487868_10784
A0A1I4KUL6	-2.1707	2.1707	S-adenosylmethionine synthase	2.17	0.0166	-0.80	-6.71	metK SAMN04487868_11187
A0A1I4HTY9	-2.1615	2.1615	Uncharacterized protein	2.16	0.0170	-2.57	-6.66	SAMN04487868_10213
A0A1I4HXV7	-2.1612	2.1612	Lipoprotein-releasing system permease protein	2.16	0.0169	-4.15	-6.66	SAMN04487868_102148
A0A1I4NA25	-2.1599	2.1599	Response regulator receiver modulated diguanylate cyclase	2.16	0.0169	-0.62	-6.65	SAMN04487868_1324
A0A1I4MSF3	-2.1583	2.1583	Outer membrane protein beta-barrel domain-containing protein	2.16	0.0168	-5.22	-6.64	SAMN04487868_12542
A0A1I4KLY5	-2.1565	2.1565	SsrA-binding protein	2.16	0.0170	-0.97	-6.64	smpB SAMN04487868_110112
A0A1I4MH62	-2.1527	2.1527	Uncharacterized protein	2.15	0.0169	-2.92	-6.61	SAMN04487868_12242
A0A1I4HCI0	-2.1459	2.1459	Citronellol/citronellal dehydrogenase	2.15	0.0170	-0.88	-6.58	SAMN04487868_101219
A0A1I4NEW1	-2.1457	2.1457	Phosphate transport system permease protein PstA	2.15	0.0170	-1.18	-6.58	SAMN04487868_13510
A0A1I4JMC5	-2.1433	2.1433	Anhydro-N-acetylmuramic acid kinase	2.14	0.0172	-1.58	-6.56	anmK SAMN04487868_106184
A0A1I4HV19	-2.1370	2.1370	Predicted ATP-dependent carboligase. ATP-grasp superfamily	2.14	0.0172	-1.89	-6.53	SAMN04487868_10257
A0A1I4HX57	-2.1302	2.1302	GMP synthase [glutamine-hydrolyzing]	2.13	0.0173	-2.37	-6.50	guaA SAMN04487868_102127
A0A1I4HBX0	-2.1302	2.1302	Uncharacterized protein	2.13	0.0172	-3.30	-6.50	SAMN04487868_101228
A0A1I4LHA6	-2.1285	2.1285	Methyl-accepting chemotaxis sensory transducer with Cache sensor	2.13	0.0171	-1.26	-6.49	SAMN04487868_11478

A0A1I4K695	-2.1248	2.1248	Acyl-CoA dehydrogenase	2.12	0.0171	-3.54	-6.47	SAMN04487868_108155
A0A1I4NE73	-2.1245	2.1245	Acyl-CoA thioesterase YciA	2.12	0.0171	-0.77	-6.47	SAMN04487868_1357
A0A1I4LG24	-2.1229	2.1229	Small-conductance mechanosensitive channel	2.12	0.0170	-3.12	-6.46	SAMN04487868_11463
A0A1I4M122	-2.1160	2.1160	LuxR family transcriptional regulator. maltose regulon positive regulatory protein	2.12	0.0172	-2.87	-6.42	SAMN04487868_11811
A0A1I4I9T9	-2.1115	2.1115	Transglutaminase-like enzyme. putative cysteine protease	2.11	0.0178	-2.23	-6.40	SAMN04487868_103106
A0A1I4MH48	-2.1105	2.1105	DNA mismatch repair protein MutS	2.11	0.0177	-1.25	-6.39	mutS SAMN04487868_12225
A0A1I4N9N4	-2.1077	2.1077	PAS domain S-box-containing protein	2.11	0.0176	-2.51	-6.38	SAMN04487868_1323
A0A1I4MFG3	-2.1057	2.1057	Acyl-CoA dehydrogenase	2.11	0.0176	-3.01	-6.37	SAMN04487868_12170
A0A1I4HX76	-2.1055	2.1055	Inosine-5'-monophosphate dehydrogenase	2.11	0.0176	-0.65	-6.37	guaB SAMN04487868_102128
A0A1I4K4P8	-2.1046	2.1046	Uncharacterized protein	2.10	0.0175	-2.77	-6.36	SAMN04487868_108112
A0A1I4HD24	-2.1028	2.1028	Sulfate adenylyltransferase subunit 1	2.10	0.0174	-2.49	-6.35	cysN SAMN04487868_101293
A0A1I4HU98	-2.1022	2.1022	Glycosyltransferase involved in cell wall bisynthesis	2.10	0.0174	-4.77	-6.35	SAMN04487868_10253
A0A1I4IA78	-2.0997	2.0997	DNA-binding response regulator. OmpR family. contains REC and winged-helix (WHTH) domain	2.10	0.0173	-2.26	-6.34	SAMN04487868_10374
A0A1I4HUA9	-2.0970	2.0970	Polysaccharide deacetylase family protein. PEP-CTERM locus subfamily	2.10	0.0173	-0.92	-6.32	SAMN04487868_10262
A0A1I4L302	-2.0943	2.0943	Uncharacterized protein	2.09	0.0171	-4.96	-6.31	SAMN04487868_11278
A0A1I4I6L1	-2.0862	2.0862	Amidase	2.09	0.0171	-0.43	-6.27	SAMN04487868_10316
A0A1I4M2I2	-2.0842	2.0842	Uncharacterized protein	2.08	0.0170	-0.93	-6.26	SAMN04487868_11851
A0A1I4MRH0	-2.0799	2.0799	ATP-binding cassette. subfamily C. CydD	2.08	0.0171	-4.06	-6.24	SAMN04487868_1259
A0A1I4MSG1	-2.0763	2.0763	Predicted amidohydrolase	2.08	0.0170	-1.78	-6.22	SAMN04487868_12534
A0A1I4HFZ3	-2.0717	2.0717	Uncharacterized protein	2.07	0.0172	-2.36	-6.19	SAMN04487868_101366
A0A1I4HUS0	-2.0711	2.0711	Glycosyltransferase involved in cell wall bisynthesis	2.07	0.0171	-1.78	-6.19	SAMN04487868_10244
A0A1I4IBR5	-2.0691	2.0691	S-(hydroxymethyl)glutathione dehydrogenase	2.07	0.0171	-2.66	-6.18	SAMN04487868_103118
A0A1I4JJI9	-2.0681	2.0681	Long-chain fatty acid transport protein	2.07	0.0173	-2.27	-6.18	SAMN04487868_106111
A0A1I4LG07	-2.0610	2.0610	Poly(Beta-D-mannuronate) lyase	2.06	0.0172	-3.11	-6.14	SAMN04487868_11454
A0A1I4MDQ6	-2.0606	2.0606	HD-like signal output (HDOD) domain. no enzymatic activity	2.06	0.0172	-0.59	-6.14	SAMN04487868_12146
A0A1I4J332	-2.0594	2.0594	Glutathione synthase/RimK-type ligase. ATP-grasp superfamily	2.06	0.0172	-1.40	-6.13	SAMN04487868_10541
A0A1I4JTH8	-2.0575	2.0575	Transferase 2. rSAM/selenodomain-associated	2.06	0.0177	-0.75	-6.12	SAMN04487868_10751
A0A1I4JZW2	-2.0512	2.0512	Trk K+ transport system. NAD-binding component	2.05	0.0175	-5.00	-6.09	SAMN04487868_1083
A0A1I4HYU6	-2.0440	2.0440	Lrp/AsnC family transcriptional regulator. leucine-responsive regulatory protein	2.04	0.0181	-1.60	-6.06	SAMN04487868_102133
A0A1I4NBN2	-2.0379	2.0379	Branched-chain-amino-acid aminotransferase	2.04	0.0185	-2.96	-6.03	ilvE SAMN04487868_1336
A0A1I4MDY4	-2.0372	2.0372	Octanoyltransferase	2.04	0.0185	-1.02	-6.02	lipB SAMN04487868_12161
A0A1I4HKW3	-2.0352	2.0352	Flagellar protein	2.04	0.0184	-0.73	-6.01	SAMN04487868_101453
A0A1I4KER7	-2.0330	2.0330	Multidrug efflux pump subunit AcrB	2.03	0.0185	-2.05	-6.00	SAMN04487868_109127
A0A1I4JML5	-2.0327	2.0327	Penicillin-binding protein 1B	2.03	0.0184	-1.24	-6.00	SAMN04487868_106167
A0A1I4K659	-2.0309	2.0309	Alanine dehydrogenase	2.03	0.0185	-2.68	-5.99	SAMN04487868_108150
A0A1I4HB97	-2.0284	2.0284	Multifunctional fusion protein	2.03	0.0184	-0.97	-5.98	nnrE nnrD SAMN04487868_101252
A0A1I4JJL7	-2.0261	2.0261	Polyamine aminopropyltransferase	2.03	0.0184	-0.30	-5.97	speE SAMN04487868_10691

A0A1I4N682	-2.0237	2.0237	50S ribosomal protein L35	2.02	0.0183	-5.20	-5.96	rpmI SAMN04487868_1307
A0A1I4HU23	-2.0215	2.0215	Glycosyltransferase involved in cell wall bisynthesis	2.02	0.0185	-1.67	-5.94	SAMN04487868_10259
A0A1I4HV88	-2.0188	2.0188	6-pyruvoyl-tetrahydropterin synthase	2.02	0.0188	-0.59	-5.93	SAMN04487868_10288
A0A1I4KUC8	-2.0184	2.0184	Ribulose-5-phosphate 4-epimerase/Fuculose-1-phosphate aldolase	2.02	0.0187	-1.08	-5.93	SAMN04487868_11159
A0A1I4HBM6	-2.0165	2.0165	Citronellyl-CoA dehydrogenase	2.02	0.0187	-0.74	-5.92	SAMN04487868_101222
A0A1I4M4Z4	-2.0164	2.0164	Probable cytosol aminopeptidase	2.02	0.0187	-0.63	-5.92	pepA SAMN04487868_11916
A0A1I4L3G4	-2.0159	2.0159	Restriction endonuclease	2.02	0.0186	-1.80	-5.92	SAMN04487868_112103
A0A1I4HTF0	-2.0140	2.0140	Glycosyltransferase. catalytic subunit of cellulose synthase and poly-beta-1.6-N-acetylglucosamine synthase	2.01	0.0190	-4.11	-5.91	SAMN04487868_10241
A0A1I4ISL3	-2.0069	2.0069	NAD(P)-dependent dehydrogenase. short-chain alcohol dehydrogenase family	2.01	0.0195	-3.47	-5.87	SAMN04487868_104154
A0A1I4JL89	-2.0026	2.0026	Anaerobic selenocysteine-containing dehydrogenase	2.00	0.0194	-3.27	-5.85	SAMN04487868_106131
A0A1I4K202	-2.0020	2.0020	Amino acid ABC transporter substrate-binding protein. PAAT family	2.00	0.0197	-0.43	-5.85	SAMN04487868_10834
A0A1I4HH93	-1.9989	1.9989	UDP-4-amino-4.6-dideoxy-N-acetyl-beta-L-altrosamine N-acetyltransferase	2.00	0.0196	-2.04	-5.84	SAMN04487868_101364
A0A1I4MJN9	-1.9978	1.9978	Periplasmic/7TM domain sensor diguanylate cyclase	2.00	0.0195	-1.39	-5.83	SAMN04487868_12314
A0A1I4JSM9	-1.9953	1.9953	Carboxyl-terminal processing protease	2.00	0.0195	-0.67	-5.82	SAMN04487868_10732
A0A1I4KU28	-1.9910	1.9910	Stage V sporulation protein R	1.99	0.0199	-2.70	-5.80	SAMN04487868_11165
A0A1I4MP11	-1.9833	1.9833	Uncharacterized protein	1.98	0.0206	-1.05	-5.76	SAMN04487868_12443
A0A1I4NGG6	-1.9820	1.9820	Type III pantothenate kinase	1.98	0.0205	-1.69	-5.76	coaX SAMN04487868_1387
A0A1I4JTH2	-1.9809	1.9809	Thioester reductase domain-containing protein	1.98	0.0205	-1.75	-5.75	SAMN04487868_10747
A0A1I4N2X0	-1.9716	1.9716	50S ribosomal protein L2	1.97	0.0207	-2.15	-5.71	rplB SAMN04487868_1296
A0A1I4MGX2	-1.9695	1.9695	Two component transcriptional regulator. LuxR family	1.97	0.0207	-1.97	-5.70	SAMN04487868_12218
A0A1I4K6R2	-1.9588	1.9588	1-acyl-sn-glycerol-3-phosphate acyltransferase	1.96	0.0211	-2.81	-5.65	SAMN04487868_108152
A0A1I4HUG1	-1.9576	1.9576	UDP-glucose 4-epimerase	1.96	0.0210	-1.56	-5.64	SAMN04487868_10227
A0A1I4HZ52	-1.9455	1.9455	Cbb3-type cytochrome c oxidase subunit	1.95	0.0208	-1.09	-5.58	SAMN04487868_102189
A0A1I4L8Z5	-1.9432	1.9432	Peptide deformylase	1.94	0.0207	-1.05	-5.57	def SAMN04487868_11360
A0A1I4H8Z3	-1.9392	1.9392	Glutathione S-transferase	1.94	0.0210	-1.94	-5.56	SAMN04487868_101142
A0A1I4HT95	-1.9369	1.9369	Acetyltransferase involved in cellulose biosynthesis. CelD/BcsL family	1.94	0.0212	-1.63	-5.55	SAMN04487868_10236
A0A1I4H9M8	-1.9362	1.9362	Lysophospholipase. alpha-beta hydrolase superfamily	1.94	0.0211	-1.68	-5.54	SAMN04487868_101204
A0A1I4KIB0	-1.9349	1.9349	Acyl-CoA dehydrogenase	1.93	0.0211	-1.94	-5.54	SAMN04487868_11024
A0A1I4HD60	-1.9321	1.9321	Aspartyl/glutamyl-tRNA(Asn/Gln) amidotransferase subunit B	1.93	0.0210	-1.75	-5.52	gatB SAMN04487868_101297
A0A1I4MP26	-1.9309	1.9309	Arginine N-succinyltransferase	1.93	0.0210	-1.00	-5.52	SAMN04487868_12426
A0A1I4HDH6	-1.9292	1.9292	Nucleotide-binding protein SAMN04487868_101310	1.93	0.0209	-0.33	-5.51	SAMN04487868_101310
A0A1I4K3J9	-1.9267	1.9267	CRP/FNR family transcriptional regulator. cyclic AMP receptor protein	1.93	0.0208	-0.78	-5.50	SAMN04487868_10883
A0A1I4MV02	-1.9235	1.9235	Glyceraldehyde-3-phosphate dehydrogenase	1.92	0.0210	-0.95	-5.48	SAMN04487868_12611
A0A1I4NBQ1	-1.9206	1.9206	Glycosyl transferase. family 25	1.92	0.0211	-2.23	-5.47	SAMN04487868_13312
A0A1I4HXF7	-1.9172	1.9172	UPF0434 protein SAMN04487868_102140	1.92	0.0213	-1.09	-5.46	SAMN04487868_102140
A0A1I4MB50	-1.9143	1.9143	Acyl-CoA dehydrogenase	1.91	0.0213	-1.78	-5.44	SAMN04487868_12056
A0A1I4MDW7	-1.9104	1.9104	D-alanyl-D-alanine carboxypeptidase (Penicillin-binding protein 5/6)	1.91	0.0216	-0.80	-5.42	SAMN04487868_12159
A0A1I4MCN4	-1.9059	1.9059	Transcriptional regulator MraZ	1.91	0.0219	-0.82	-5.40	mraZ SAMN04487868_1217

A0A1I4NF77	-1.9051	1.9051	DNA-directed RNA polymerase subunit beta'	1.91	0.0219	-2.20	-5.40	rpoC SAMN04487868_1365
A0A1I4MDE3	-1.8988	1.8988	Predicted PurR-regulated permease PerM	1.90	0.0221	-2.47	-5.37	SAMN04487868_12143
A0A1I4HFP7	-1.8963	1.8963	RNAse G	1.90	0.0220	-0.59	-5.36	SAMN04487868_101304
A0A1I4JWH1	-1.8870	1.8870	Bifunctional uridylyltransferase/uridylyl-removing enzyme	1.89	0.0220	-1.96	-5.32	glnD SAMN04487868_107163
A0A1I4NEW3	-1.8869	1.8869	Phosphate import ATP-binding protein PstB	1.89	0.0220	-1.01	-5.32	pstB SAMN04487868_13511
A0A1I4HJ48	-1.8859	1.8859	Histidine kinase-like ATPase domain-containing protein	1.89	0.0219	-2.69	-5.32	SAMN04487868_101447
A0A1I4J6W2	-1.8855	1.8855	Protein translocase subunit SecD	1.89	0.0219	-2.52	-5.31	secD SAMN04487868_105133
A0A1I4HCI8	-1.8826	1.8826	Chemotaxis protein MotA	1.88	0.0219	-3.34	-5.30	SAMN04487868_101247
A0A1I4ITJ7	-1.8789	1.8789	Glycerol-3-phosphate acyltransferase	1.88	0.0221	-2.98	-5.28	plsB SAMN04487868_104177
A0A1I4L8E0	-1.8786	1.8786	ATP-binding cassette. subfamily B	1.88	0.0221	-1.23	-5.28	SAMN04487868_11351
A0A1I4JK20	-1.8780	1.8780	Homoserine O-succinyltransferase	1.88	0.0220	-2.49	-5.28	metXS SAMN04487868_106104
A0A1I4NCS6	-1.8777	1.8777	Uncharacterized protein	1.88	0.0220	-1.12	-5.28	SAMN04487868_13327
A0A1I4HBX1	-1.8766	1.8766	Outer membrane protein OmpA	1.88	0.0220	-0.26	-5.27	SAMN04487868_101205
A0A1I4KU96	-1.8753	1.8753	Amino acid ABC transporter membrane protein. PAAT family	1.88	0.0219	-1.67	-5.27	SAMN04487868_11183
A0A1I4LQV7	-1.8673	1.8673	Predicted helicase	1.87	0.0218	-2.20	-5.23	SAMN04487868_11613
A0A1I4LRB9	-1.8655	1.8655	Quinohemoprotein ethanol dehydrogenase	1.87	0.0218	-1.86	-5.23	SAMN04487868_11617
A0A1I4H7D9	-1.8617	1.8617	ATPase components of ABC transporters with duplicated ATPase domains	1.86	0.0219	-0.53	-5.21	SAMN04487868_101152
A0A1I4MV92	-1.8573	1.8573	Transcription-repair-coupling factor	1.86	0.0218	-2.55	-5.19	mfd SAMN04487868_12610
A0A1I4L8G6	-1.8528	1.8528	Membrane protein insertase YidC	1.85	0.0219	-1.89	-5.17	yidC SAMN04487868_11337
A0A1I4I841	-1.8506	1.8506	3-hydroxyacyl-CoA dehydrogenase	1.85	0.0219	-1.03	-5.16	SAMN04487868_10368
A0A1I4MKS4	-1.8409	1.8409	Uncharacterized protein	1.84	0.0217	-1.90	-5.12	SAMN04487868_12357
A0A1I4HT91	-1.8355	1.8355	Putative glucose-6-phosphate 1-epimerase	1.84	0.0219	-1.60	-5.10	SAMN04487868_10225
A0A1I4M153	-1.8300	1.8300	NTE family protein	1.83	0.0221	-0.63	-5.07	SAMN04487868_11825
A0A1I4I6I5	-1.8286	1.8286	PAS domain S-box-containing protein/diguanylate cyclase (GGDEF) domain-containing protein	1.83	0.0225	-1.63	-5.07	SAMN04487868_10313
A0A1I4M0F6	-1.8267	1.8267	NTE family protein	1.83	0.0227	-0.35	-5.06	SAMN04487868_1187
A0A1I4HFQ6	-1.8243	1.8243	Uncharacterized protein	1.82	0.0230	-1.09	-5.05	SAMN04487868_101305
A0A1I4IY46	-1.8238	1.8238	Site-determining protein	1.82	0.0231	-2.14	-5.05	SAMN04487868_104245
A0A1I4MAL5	-1.8234	1.8234	Acetyl-CoA C-acetyltransferase	1.82	0.0231	-3.19	-5.05	SAMN04487868_12058
A0A1I4IFA7	-1.8216	1.8216	Glutamate--putrescine ligase	1.82	0.0231	-1.12	-5.04	SAMN04487868_103247
A0A1I4L866	-1.8196	1.8196	ATP synthase subunit a	1.82	0.0233	-2.85	-5.03	atpB SAMN04487868_11323
A0A1I4IVI2	-1.8180	1.8180	23S rRNA (uracil(1939)-C(5))-methyltransferase RlmD	1.82	0.0233	-0.66	-5.02	rlmD SAMN04487868_104189
A0A1I4KD46	-1.8168	1.8168	TRAP-type mannitol/chloroaromatic compound transport system. small permease component	1.82	0.0233	-1.01	-5.02	SAMN04487868_109100
A0A1I4MZD4	-1.8088	1.8088	Uncharacterized protein	1.81	0.0233	-3.16	-4.98	SAMN04487868_12745
A0A1I4HM20	-1.8077	1.8077	Flagellar biosynthesis protein FlhA	1.81	0.0233	-1.72	-4.98	flhA SAMN04487868_101461
A0A1I4JI22	-1.8066	1.8066	Sodium/proton antiporter. CPA1 family	1.81	0.0233	-4.79	-4.97	SAMN04487868_10685
A0A1I4I1B2	-1.8053	1.8053	Carbohydrate ABC transporter substrate-binding protein. CUT1 family	1.81	0.0233	-0.71	-4.97	SAMN04487868_102238

A0A1I4MTJ3	-1.8046	1.8046	Iron complex outermembrane recepter protein	1.80	0.0233	-3.06	-4.97	SAMN04487868_12557
A0A1I4JME3	-1.8039	1.8039	Uncharacterized protein	1.80	0.0232	-0.64	-4.96	SAMN04487868_106181
A0A1I4M6V0	-1.8023	1.8023	General secretion pathway protein E	1.80	0.0236	-1.46	-4.96	SAMN04487868_11965
A0A1I4HXX4	-1.8012	1.8012	UDP-glucose 4-epimerase	1.80	0.0235	-0.84	-4.95	SAMN04487868_102124
A0A1I4HDY8	-1.7961	1.7961	Uncharacterized protein	1.80	0.0235	-0.46	-4.93	SAMN04487868_101278
A0A1I4MYY2	-1.7953	1.7953	Ribosome-binding ATPase YchF	1.80	0.0238	-0.83	-4.93	ychF SAMN04487868_12731
A0A1I4MT08	-1.7903	1.7903	Acyl carrier protein phosphodiesterase	1.79	0.0241	-0.93	-4.91	SAMN04487868_12543
A0A1I4MPU8	-1.7903	1.7903	Putative hydro-lyase SAMN04487868_12447	1.79	0.0241	-1.67	-4.91	SAMN04487868_12447
A0A1I4K5K0	-1.7897	1.7897	Transcriptional regulator. TetR family	1.79	0.0240	-0.96	-4.90	SAMN04487868_108110
A0A1I4L6W0	-1.7889	1.7889	Glutamine--fructose-6-phosphate aminotransferase [isomerizing]	1.79	0.0240	-0.64	-4.90	glmS SAMN04487868_11314
A0A1I4L1D6	-1.7875	1.7875	1-acyl-sn-glycerol-3-phosphate acyltransferase	1.79	0.0239	-2.25	-4.90	SAMN04487868_11233
A0A1I4KJF1	-1.7873	1.7873	L-threonine dehydratase	1.79	0.0239	-1.44	-4.89	ilvA SAMN04487868_11026
A0A1I4K4C5	-1.7854	1.7854	Pimeloyl-ACP methyl ester carboxylesterase	1.79	0.0238	-2.69	-4.89	SAMN04487868_10882
A0A1I4KK08	-1.7848	1.7848	Uncharacterized protein	1.78	0.0239	-2.67	-4.88	SAMN04487868_11042
A0A1I4JXV5	-1.7830	1.7830	Mannose-6-phosphate isomerase. type 2	1.78	0.0241	-2.09	-4.88	SAMN04487868_107172
A0A1I4N6S4	-1.7799	1.7799	Inactive transglutaminase fused to 7 transmembrane helices	1.78	0.0243	-2.10	-4.86	SAMN04487868_13018
A0A1I4ISW8	-1.7775	1.7775	ATP-binding cassette. subfamily B	1.78	0.0244	-1.87	-4.85	SAMN04487868_104140
A0A1I4MA46	-1.7767	1.7767	NTE family protein	1.78	0.0243	-2.72	-4.85	SAMN04487868_12049
A0A1I4L190	-1.7765	1.7765	Acyl-CoA dehydrogenase	1.78	0.0243	-1.99	-4.85	SAMN04487868_11217
A0A1I4HYT4	-1.7648	1.7648	N-carbamoylputrescine amidase	1.76	0.0246	-1.27	-4.80	SAMN04487868_102152
A0A1I4L063	-1.7630	1.7630	HEXXH motif-containing protein	1.76	0.0250	-1.80	-4.79	SAMN04487868_1126
A0A1I4I8G3	-1.7602	1.7602	Acetyl-CoA C-acetyltransferase	1.76	0.0253	-1.48	-4.78	SAMN04487868_10364
A0A1I4KC90	-1.7504	1.7504	Membrane-bound serine protease (ClpP class)	1.75	0.0254	-2.21	-4.74	SAMN04487868_10971
A0A1I4KA74	-1.7503	1.7503	Uncharacterized protein	1.75	0.0254	-1.90	-4.74	SAMN04487868_10932
A0A1I4I1L6	-1.7470	1.7470	Biopolymer transport protein ExbD	1.75	0.0254	-0.41	-4.73	SAMN04487868_102209
A0A1I4L8Z2	-1.7384	1.7384	Trk system potassium uptake protein TrkA	1.74	0.0257	-0.83	-4.70	SAMN04487868_11357
A0A1I4MVP9	-1.7313	1.7313	Na(+)-translocating NADH-quinone reductase subunit B	1.73	0.0259	-3.03	-4.67	nqrB SAMN04487868_12613
A0A1I4MI03	-1.7295	1.7295	Alcohol dehydrogenase. propanol-preferring	1.73	0.0259	-4.19	-4.66	SAMN04487868_12256
A0A1I4MDU9	-1.7291	1.7291	Cell division protein FtsZ	1.73	0.0262	-0.77	-4.66	ftsZ SAMN04487868_12121
A0A1I4MJP7	-1.7268	1.7268	Uncharacterized protein	1.73	0.0262	-0.72	-4.65	SAMN04487868_12315
A0A1I4K5F9	-1.7229	1.7229	Rubredoxin-NAD+ reductase	1.72	0.0268	-1.23	-4.63	SAMN04487868_108130
A0A1I4KV29	-1.7187	1.7187	Protein-disulfide isomerase	1.72	0.0270	-1.03	-4.62	SAMN04487868_11198
A0A1I4JHA8	-1.7187	1.7187	Diaminopimelate epimerase	1.72	0.0269	-1.24	-4.62	dapF SAMN04487868_10669
A0A1I4MAK6	-1.7144	1.7144	Acyl-CoA dehydrogenase	1.71	0.0274	-1.81	-4.60	SAMN04487868_12057
A0A1I4HW21	-1.7117	1.7117	2-methylcitrate dehydratase	1.71	0.0275	-0.90	-4.59	SAMN04487868_10270
A0A1I4H572	-1.7108	1.7108	DUF4399 domain-containing protein	1.71	0.0275	-1.41	-4.59	SAMN04487868_10157
A0A1I4HW52	-1.7026	1.7026	Tol-Pal system protein TolB	1.70	0.0273	-1.15	-4.55	tolB SAMN04487868_102111
A0A1I4HIE1	-1.7003	1.7003	60 kDa chaperonin	1.70	0.0273	-0.52	-4.55	groL groEL SAMN04487868_101398
A0A1I4I9T4	-1.6919	1.6919	Uncharacterized conserved protein. circularly permuted ATPgrasp superfamily	1.69	0.0282	-0.79	-4.51	SAMN04487868_103108

A0A1I4L023	-1.6885	1.6885	Subtilase family protein	1.69	0.0285	-1.06	-4.50	SAMN04487868_1123
A0A1I4H513	-1.6869	1.6869	Alkyl hydroperoxide reductase AhpD	1.69	0.0285	-1.85	-4.49	SAMN04487868_10185
A0A1I4JW48	-1.6840	1.6840	Zinc metalloprotease	1.68	0.0285	-1.26	-4.48	SAMN04487868_107153
A0A1I4LJV0	-1.6781	1.6781	Two-component system. NtrC family. sensor histidine kinase PilS	1.68	0.0291	-3.46	-4.46	SAMN04487868_11512
A0A1I4J302	-1.6712	1.6712	UvrABC system protein B	1.67	0.0294	-0.89	-4.43	uvrB SAMN04487868_10539
A0A1I4LGZ9	-1.6698	1.6698	Fatty-acyl-CoA synthase	1.67	0.0294	-0.96	-4.43	SAMN04487868_11457
A0A1I4K5L8	-1.6664	1.6664	Glutamate decarboxylase	1.67	0.0295	-0.28	-4.42	SAMN04487868_108123
A0A1I4MAA3	-1.6659	1.6659	Gluconate 5-dehydrogenase	1.67	0.0294	-0.86	-4.41	SAMN04487868_12055
A0A1I4HUP5	-1.6655	1.6655	2-methylaconitate cis-trans isomerase	1.67	0.0294	-1.97	-4.41	SAMN04487868_10273
A0A1I4MSF5	-1.6640	1.6640	Selenophosphate synthase	1.66	0.0299	-1.00	-4.41	SAMN04487868_12531
A0A1I4N747	-1.6608	1.6608	Acyl-homoserine-lactone acylase	1.66	0.0300	-0.63	-4.39	SAMN04487868_13026
A0A1I4HVV0	-1.6606	1.6606	Putative permease	1.66	0.0300	-3.89	-4.39	SAMN04487868_102103
A0A1I4JTN6	-1.6606	1.6606	OmpA family protein	1.66	0.0300	-1.69	-4.39	SAMN04487868_10744
A0A1I4J3C8	-1.6568	1.6568	Hydrolase_4 domain-containing protein	1.66	0.0300	-3.35	-4.38	SAMN04487868_10550
A0A1I4K564	-1.6562	1.6562	Metal-dependent hydrolase. endonuclease/exonuclease/phosphatase family	1.66	0.0300	-4.70	-4.38	SAMN04487868_108101
A0A1I4J955	-1.6439	1.6439	DNA ligase	1.64	0.0308	-0.76	-4.33	ligA SAMN04487868_105184
A0A1I4KUP4	-1.6426	1.6426	Transketolase	1.64	0.0307	-1.83	-4.33	SAMN04487868_11189
A0A1I4HIB0	-1.6411	1.6411	Amidase	1.64	0.0307	-0.52	-4.32	SAMN04487868_101421
A0A1I4JHN5	-1.6399	1.6399	NTE family protein	1.64	0.0308	-2.45	-4.32	SAMN04487868_10677
A0A1I4JBR5	-1.6379	1.6379	PglZ domain-containing protein	1.64	0.0309	-2.39	-4.31	SAMN04487868_105227
A0A1I4MFT2	-1.6266	1.6266	MaoC like domain-containing protein	1.63	0.0316	-2.67	-4.27	SAMN04487868_12216
A0A1I4HW60	-1.6239	1.6239	Quinolinate synthase A	1.62	0.0316	-1.35	-4.26	nadA SAMN04487868_102106
A0A1I4MGI2	-1.6235	1.6235	PSII_BNR domain-containing protein	1.62	0.0316	-1.40	-4.26	SAMN04487868_1223
A0A1I4H6A9	-1.6184	1.6184	Uncharacterized protein	1.62	0.0319	-0.54	-4.24	SAMN04487868_101117
A0A1I4KSF3	-1.6128	1.6128	Phosphoglycolate phosphatase	1.61	0.0321	-1.18	-4.22	SAMN04487868_11142
A0A1I4JQL9	-1.6122	1.6122	Formate-dependent phosphoribosylglycinamide formyltransferase	1.61	0.0321	-1.86	-4.21	purT SAMN04487868_1072
A0A1I4MPD7	-1.6113	1.6113	Uncharacterized protein	1.61	0.0323	-1.33	-4.21	SAMN04487868_12441
A0A1I4NGH3	-1.6090	1.6090	Bifunctional ligase/repressor BirA	1.61	0.0325	-0.74	-4.20	birA SAMN04487868_1388
A0A1I4HMV9	-1.6078	1.6078	Ca-activated chloride channel family protein	1.61	0.0325	-1.33	-4.20	SAMN04487868_101487
A0A1I4HF75	-1.6068	1.6068	Protein involved in polysaccharide export. contains SLBB domain of the beta-grasp fold	1.61	0.0324	-1.23	-4.19	SAMN04487868_101355
A0A1I4N791	-1.6054	1.6054	Betaine/carnitine transporter. BCCT family	1.61	0.0326	-3.03	-4.19	SAMN04487868_13016
A0A1I4H696	-1.6043	1.6043	Uncharacterized protein	1.60	0.0326	-0.72	-4.18	SAMN04487868_101127
A0A1I4NAA3	-1.5964	1.5964	Formate dehydrogenase subunit gamma	1.60	0.0333	-1.25	-4.16	SAMN04487868_13210
A0A1I4JJ49	-1.5951	1.5951	Biosynthetic arginine decarboxylase	1.60	0.0332	-1.46	-4.15	speA SAMN04487868_10690
A0A1I4L9R4	-1.5946	1.5946	Uncharacterized protein	1.59	0.0332	-3.24	-4.15	SAMN04487868_11379
A0A1I4LL56	-1.5922	1.5922	50S ribosomal protein L21	1.59	0.0333	-2.02	-4.14	rplU SAMN04487868_11532
A0A1I4L6Z3	-1.5909	1.5909	ChrR Cupin-like domain-containing protein	1.59	0.0333	-1.27	-4.14	SAMN04487868_1131
A0A1I4HVE4	-1.5900	1.5900	Glycosyl transferases group 1	1.59	0.0334	-0.46	-4.13	SAMN04487868_10251
A0A1I4MLF9	-1.5895	1.5895	tRNA(Met) cytidine acetyltransferase TmcA	1.59	0.0335	-0.90	-4.13	tmcA SAMN04487868_12348

A0A1I4HJ67	-1.5886	1.5886	Anti-anti-sigma factor	1.59	0.0336	-0.84	-4.13	SAMN04487868_101446
A0A1I4KMV7	-1.5855	1.5855	Phosphoglucosamine mutase	1.59	0.0338	-0.90	-4.12	glmM SAMN04487868_110130
A0A1I4LKB1	-1.5847	1.5847	Polyphenol oxidase	1.58	0.0339	-1.80	-4.11	SAMN04487868_1158
A0A1I4I892	-1.5829	1.5829	Acyl-CoA dehydrogenase	1.58	0.0340	-1.66	-4.11	SAMN04487868_10361
A0A1I4HER3	-1.5821	1.5821	Cell shape-determining protein MreB	1.58	0.0339	-0.57	-4.10	SAMN04487868_101300
A0A1I4MAK0	-1.5783	1.5783	NAD(P) transhydrogenase subunit beta	1.58	0.0344	-1.81	-4.09	SAMN04487868_12050
A0A1I4HJG7	-1.5740	1.5740	Sodium/proton antiporter. NhaD family	1.57	0.0349	-3.24	-4.08	SAMN04487868_101420
A0A1I4JLN8	-1.5738	1.5738	Sugar fermentation stimulation protein homolog	1.57	0.0350	-0.69	-4.07	sfsA SAMN04487868_106164
A0A1I4L3I1	-1.5737	1.5737	Uncharacterized protein	1.57	0.0350	-1.05	-4.07	SAMN04487868_11290
A0A1I4N3W7	-1.5662	1.5662	30S ribosomal protein S3	1.57	0.0353	-1.61	-4.05	rpsC SAMN04487868_1299
A0A1I4N103	-1.5662	1.5662	D-amino-acid dehydrogenase	1.57	0.0352	-1.61	-4.05	SAMN04487868_12818
A0A1I4K3D0	-1.5630	1.5630	Lysophospholipase. alpha-beta hydrolase superfamily	1.56	0.0354	-0.45	-4.04	SAMN04487868_10877
A0A1I4L9E8	-1.5621	1.5621	Cellulose biosynthesis protein BcsQ	1.56	0.0356	-2.28	-4.03	SAMN04487868_11348
A0A1I4JKW2	-1.5581	1.5581	tRNA N6-adenosine threonylcarbamoyltransferase	1.56	0.0356	-1.83	-4.02	tsaD SAMN04487868_106150
A0A1I4KJI5	-1.5581	1.5581	Acyltransferase. WS/DGAT/MGAT	1.56	0.0356	-2.21	-4.02	SAMN04487868_11056
A0A1I4I9J8	-1.5569	1.5569	Two-component system. sensor histidine kinase RegB	1.56	0.0355	-6.30	-4.01	SAMN04487868_103100
A0A1I4HLH0	-1.5516	1.5516	Protein-glutamate methylesterase/protein-glutamine glutaminase	1.55	0.0358	-0.84	-4.00	cheB SAMN04487868_101468
A0A1I4LXT9	-1.5488	1.5488	Iron complex outermembrane recepter protein	1.55	0.0360	-1.64	-3.99	SAMN04487868_11748
A0A1I4H7I4	-1.5455	1.5455	Bifunctional protein PutA	1.55	0.0363	-1.09	-3.97	SAMN04487868_101108
A0A1I4MPE6	-1.5413	1.5413	Phosphate-selective porin OprO and OprP	1.54	0.0366	-2.29	-3.96	SAMN04487868_12442
A0A1I4L7E2	-1.5412	1.5412	ATP synthase subunit alpha	1.54	0.0366	-0.64	-3.96	atpA SAMN04487868_11319
A0A1I4HJY4	-1.5405	1.5405	Site-determining protein	1.54	0.0366	-0.60	-3.96	SAMN04487868_101463
A0A1I4MYS3	-1.5341	1.5341	Outer-membrane lipoprotein LolB	1.53	0.0372	-1.59	-3.93	lolB SAMN04487868_12726
A0A1I4H7H6	-1.5325	1.5325	Haloalkane dehalogenase	1.53	0.0372	-1.42	-3.93	dhmA SAMN04487868_101153
A0A1I4IF42	-1.5264	1.5264	Gamma-glutamyl-gamma-aminobutyraldehyde dehydrogenase	1.53	0.0373	-0.77	-3.91	SAMN04487868_103248
A0A1I4KM07	-1.5219	1.5219	Outer membrane protein assembly factor BamE	1.52	0.0376	-1.48	-3.89	bamE SAMN04487868_110116
A0A1I4JIH9	-1.5194	1.5194	Diguanylate cyclase	1.52	0.0376	-0.41	-3.88	SAMN04487868_10672
A0A1I4JWE0	-1.5155	1.5155	Outer membrane protein assembly factor BamA	1.52	0.0378	-0.53	-3.87	bamA SAMN04487868_107152
A0A1I4KTE7	-1.5122	1.5122	Predicted HD phosphohydrolase	1.51	0.0382	-0.31	-3.86	SAMN04487868_11158
A0A1I4MFU3	-1.5119	1.5119	Histidine kinase	1.51	0.0382	-0.95	-3.86	SAMN04487868_12217
A0A1I4K4D3	-1.5110	1.5110	Cytochrome c553	1.51	0.0383	-1.03	-3.86	SAMN04487868_108103
A0A1I4LNK0	-1.5102	1.5102	Rhs element Vgr protein (Fragment)	1.51	0.0383	-2.33	-3.85	SAMN04487868_11583
A0A1I4MP03	-1.5089	1.5089	Copper-resistance protein. CopA family	1.51	0.0382	-3.89	-3.85	SAMN04487868_12428
A0A1I4MKB4	-1.5077	1.5077	PAS domain S-box-containing protein	1.51	0.0382	-0.56	-3.84	SAMN04487868_12332
A0A1I4ILJ5	-1.5021	1.5021	Multidrug efflux pump	1.50	0.0387	-1.49	-3.82	SAMN04487868_10418
A0A1I4MQ10	-1.4969	1.4969	Biotin-dependent carboxylase uncharacterized domain-containing protein	1.50	0.0394	-1.55	-3.81	SAMN04487868_12453

A0A1I4J769	-1.4914	1.4914	Serine O-acetyltransferase	1.49	0.0394	-0.70	-3.79	SAMN04487868_105137
A0A1I4H8J9	-1.4854	1.4854	DUF1338 domain-containing protein	1.49	0.0398	-0.84	-3.77	SAMN04487868_101133
A0A1I4HHJ3	-1.4849	1.4849	dTDP-4-amino-4.6-dideoxygalactose transaminase	1.48	0.0398	-2.27	-3.77	SAMN04487868_101372
A0A1I4M8X9	-1.4799	1.4799	Acetoin utilization deacetylase AcuC	1.48	0.0404	-1.47	-3.75	SAMN04487868_12013
A0A1I4LEV0	-1.4753	1.4753	Methylglutaconyl-CoA hydratase	1.48	0.0406	-0.57	-3.73	SAMN04487868_11438
A0A1I4KNI9	-1.4748	1.4748	L-leucine ABC transporter membrane protein /L-isoleucine ABC transporter membrane protein /L-valine ABC transporter membrane protein	1.47	0.0407	-2.01	-3.73	SAMN04487868_110148
A0A1I4HU51	-1.4701	1.4701	Glycosyltransferase involved in cell wall bisynthesis	1.47	0.0411	-1.35	-3.72	SAMN04487868_10248
A0A1I4MYZ7	-1.4695	1.4695	Alanine racemase	1.47	0.0411	-0.83	-3.71	SAMN04487868_12753
A0A1I4MQU2	-1.4663	1.4663	Uncharacterized conserved protein	1.47	0.0412	-0.85	-3.70	SAMN04487868_1257
A0A1I4MCP0	-1.4622	1.4622	UDP-N-acetylmuramoyl-tripeptide--D-alanyl-D-alanine ligase	1.46	0.0414	-0.84	-3.69	murF SAMN04487868_12112
A0A1I4MEM8	-1.4570	1.4570	Diguanylate cyclase (GGDEF) domain-containing protein	1.46	0.0421	-4.40	-3.67	SAMN04487868_12149
A0A1I4MJN1	-1.4555	1.4555	Rhomboid family protein	1.46	0.0420	-2.32	-3.67	SAMN04487868_12327
A0A1I4I0H3	-1.4531	1.4531	Signal transduction histidine kinase	1.45	0.0419	-1.26	-3.66	SAMN04487868_102171
A0A1I4J5S2	-1.4487	1.4487	Long-chain acyl-CoA synthetase (AMP-forming)	1.45	0.0424	-0.43	-3.65	SAMN04487868_105104
A0A1I4HYY0	-1.4450	1.4450	Pseudouridine synthase	1.45	0.0432	-2.74	-3.63	SAMN04487868_102162
A0A1I4KRV5	-1.4409	1.4409	Flagellar assembly protein T. N-terminal domain	1.44	0.0433	-1.20	-3.62	SAMN04487868_11120
A0A1I4I018	-1.4389	1.4389	Maltose operon substrate-binding protein (MalM)	1.44	0.0437	-2.45	-3.61	SAMN04487868_102199
A0A1I4LW51	-1.4373	1.4373	Probable malate:quinone oxidoreductase	1.44	0.0437	-1.07	-3.61	mqo SAMN04487868_11732
A0A1I4LFE9	-1.4341	1.4341	3-methylcrotonyl-CoA carboxylase alpha subunit	1.43	0.0440	-3.04	-3.60	SAMN04487868_11437
A0A1I4KP75	-1.4332	1.4332	Thioredoxin	1.43	0.0442	-0.61	-3.60	SAMN04487868_110155
A0A1I4J485	-1.4327	1.4327	Aspartate racemase	1.43	0.0443	-0.89	-3.59	SAMN04487868_10572
A0A1I4M785	-1.4325	1.4325	Isoquinoline 1-oxidoreductase. beta subunit	1.43	0.0442	-1.27	-3.59	SAMN04487868_11970
A0A1I4HAK5	-1.4325	1.4325	Citronellol/citronellal dehydrogenase	1.43	0.0442	-1.95	-3.59	SAMN04487868_101224
A0A1I4HIB9	-1.4294	1.4294	Translocation and assembly module TamB	1.43	0.0444	-3.26	-3.58	SAMN04487868_101426
A0A1I4M0U9	-1.4262	1.4262	Uncharacterized protein	1.43	0.0445	-1.00	-3.57	SAMN04487868_11817
A0A1I4IU14	-1.4215	1.4215	GTP pyrophosphokinase	1.42	0.0448	-1.26	-3.56	SAMN04487868_104188
A0A1I4MZU6	-1.4178	1.4178	Ribonuclease R	1.42	0.0454	-1.04	-3.55	rnr SAMN04487868_12760
A0A1I4M7F4	-1.4170	1.4170	Isoquinoline 1-oxidoreductase. alpha subunit	1.42	0.0455	-1.09	-3.54	SAMN04487868_11971
A0A1I4KNW9	-1.4159	1.4159	DUF4105 domain-containing protein	1.42	0.0453	-1.44	-3.54	SAMN04487868_110142
A0A1I4IMI1	-1.4151	1.4151	Uncharacterized protein	1.42	0.0453	-0.73	-3.54	SAMN04487868_1046
A0A1I4HSB6	-1.4118	1.4118	MoxR-like ATPase	1.41	0.0453	-0.37	-3.53	SAMN04487868_10214
A0A1I4HGK6	-1.4099	1.4099	LuxR family transcriptional regulator. maltose regulon positive regulatory protein	1.41	0.0452	-2.02	-3.52	SAMN04487868_101335
A0A1I4J871	-1.4060	1.4060	DNA topoisomerase 1	1.41	0.0457	-1.10	-3.51	topA SAMN04487868_105164
A0A1I4JND1	-1.4037	1.4037	N-acetyl-gamma-glutamyl-phosphate reductase	1.40	0.0458	-0.34	-3.50	argC SAMN04487868_106180
A0A1I4MH37	-1.4014	1.4014	Ferredoxin	1.40	0.0465	-1.22	-3.49	SAMN04487868_12226
A0A1I4MI95	-1.3965	1.3965	Predicted flavoprotein CzcO associated with the cation diffusion facilitator CzcD	1.40	0.0466	-2.09	-3.48	SAMN04487868_12258
A0A1I4MNW8	-1.3925	1.3925	Acetylornithine aminotransferase	1.39	0.0471	-0.31	-3.46	argD SAMN04487868_12427
A0A1I4MYM3	-1.3900	1.3900	Release factor glutamine methyltransferase	1.39	0.0476	-1.68	-3.46	prmC SAMN04487868_12722

A0A1I4HT60	-1.3885	1.3885	Cupin-like domain-containing protein	1.39	0.0477	-0.75	-3.45	SAMN04487868_10237
A0A1I4H4G9	-1.3839	1.3839	Phenylpyruvate tautomerase PptA. 4-oxalocrotonate tautomerase family	1.38	0.0479	-0.71	-3.44	SAMN04487868_1017
A0A1I4KD04	-1.3835	1.3835	TRAP-type mannitol/chloroaromatic compound transport system. substrate-binding protein	1.38	0.0480	-0.34	-3.44	SAMN04487868_109101
A0A1I4MTC4	-1.3832	1.3832	Signal transduction histidine kinase	1.38	0.0482	-3.33	-3.44	SAMN04487868_12551
A0A1I4MFB0	-1.3828	1.3828	Methyl-accepting chemotaxis sensory transducer with Cache sensor	1.38	0.0484	-0.50	-3.43	SAMN04487868_12165
A0A1I4H5P2	-1.3817	1.3817	Alcohol dehydrogenase	1.38	0.0483	-1.42	-3.43	SAMN04487868_10160
A0A1I4JJQ7	-1.3812	1.3812	Exodeoxyribonuclease-3	1.38	0.0483	-0.43	-3.43	SAMN04487868_106119
A0A1I4N170	-1.3794	1.3794	Crotonobetaine/carnitine-CoA ligase	1.38	0.0482	-0.92	-3.42	SAMN04487868_12810
A0A1I4IG64	-1.3788	1.3788	Enoyl-CoA hydratase/carnithine racemase	1.38	0.0481	-0.77	-3.42	SAMN04487868_103235
A0A1I4J7K6	-1.3699	1.3699	NADPH-dependent 7-cyano-7-deazaguanine reductase	1.37	0.0490	-0.44	-3.39	queF SAMN04487868_105114
A0A1I4K5C7	-1.3679	1.3679	Phosphate transporter	1.37	0.0490	-2.61	-3.39	SAMN04487868_108125
A0A1I4J6X8	-1.3666	1.3666	Sec translocon accessory complex subunit YajC	1.37	0.0492	-0.46	-3.38	yajC SAMN04487868_105132
A0A1I4MVD7	-1.3662	1.3662	Uncharacterized protein	1.37	0.0495	-3.58	-4.66	SAMN04487868_1264
A0A1I4HGV5	-1.3640	1.3640	Flagellin	1.36	0.0496	-0.66	-3.38	SAMN04487868_101384
A0A1I4L334	-1.3628	1.3628	Uncharacterized protein	1.36	0.0498	-1.11	-3.37	SAMN04487868_11291
A0A1I4HLK7	-1.3624	1.3624	Purine-binding chemotaxis protein CheW	1.36	0.0499	-1.50	-3.37	SAMN04487868_101473
A0A1I4IWD7	1.3633	-1.3633	Ribosome maturation factor RimM	1.36	0.0496	0.35	3.37	rimM SAMN04487868_104220
A0A1I4M9S0	1.3660	-1.3660	RNA polymerase sigma-70 factor. ECF subfamily	1.37	0.0494	0.80	3.38	SAMN04487868_12039
A0A1I4KS80	1.3664	-1.3664	3-hydroxydecanoyl-[acyl-carrier-protein] dehydratase	1.37	0.0492	1.05	3.38	SAMN04487868_11130
A0A1I4M9X1	1.3689	-1.3689	Transcriptional regulator. HxlR family	1.37	0.0489	1.27	3.39	SAMN04487868_12044
A0A1I4K1P2	1.3703	-1.3703	Bis(5'-nucleosyl)-tetraphosphatase. symmetrical	1.37	0.0490	0.47	3.39	SAMN04487868_10841
A0A1I4HN11	1.3721	-1.3721	MoxR-like ATPase	1.37	0.0488	0.24	3.40	SAMN04487868_101491
A0A1I4HKR8	1.3755	-1.3755	Cytochrome c-type biogenesis protein	1.38	0.0484	0.35	3.41	SAMN04487868_101484
A0A1I4MX27	1.3782	-1.3782	Pseudouridine synthase	1.38	0.0482	0.82	3.42	SAMN04487868_12649
A0A1I4M257	1.3791	-1.3791	Acetyl-coenzyme A carboxylase carboxyl transferase subunit beta	1.38	0.0482	0.69	3.42	accD SAMN04487868_11839
A0A1I4JH42	1.3826	-1.3826	Porphobilinogen deaminase	1.38	0.0483	0.42	3.43	hemC SAMN04487868_10661
A0A1I4N5C6	1.3880	-1.3880	DNA-binding transcriptional regulator NtrC	1.39	0.0476	0.63	3.45	ntrC SAMN04487868_12949
A0A1I4MWT1	1.3883	-1.3883	Putative phosphoenolpyruvate synthase regulatory protein	1.39	0.0477	0.37	3.45	SAMN04487868_12640
A0A1I4MWG3	1.3926	-1.3926	Acyl carrier protein	1.39	0.0471	1.26	3.47	acpP SAMN04487868_12658
A0A1I4MY13	1.3952	-1.3952	Tetratricopeptide repeat-containing protein	1.40	0.0468	0.66	3.47	SAMN04487868_12725
A0A1I4N141	1.3978	-1.3978	Alcohol dehydrogenase. class IV	1.40	0.0466	0.30	3.48	SAMN04487868_1283
A0A1I4J5B3	1.3985	-1.3985	Uncharacterized protein	1.40	0.0467	1.27	3.48	SAMN04487868_10597
A0A1I4ND11	1.3990	-1.3990	3'.5'-cyclic adenosine monophosphate phosphodiesterase CpdA	1.40	0.0466	1.65	3.49	cpdA SAMN04487868_13335
A0A1I4M109	1.3999	-1.3999	DNA polymerase-3 subunit delta	1.40	0.0467	0.98	3.49	SAMN04487868_11821
A0A1I4N753	1.4016	-1.4016	Uncharacterized protein	1.40	0.0465	0.80	3.49	SAMN04487868_13020
A0A1I4MNH9	1.4039	-1.4039	TRAP-type mannitol/chloroaromatic compound transport system. substrate-binding protein	1.40	0.0459	1.47	3.50	SAMN04487868_12413

A0A1I4MYQ2	1.4050	-1.4050	Glutamyl-tRNA reductase	1.41	0.0458	3.28	3.50	hemA SAMN04487868_12724
A0A1I4LJZ0	1.4065	-1.4065	Type IV pilus assembly protein PilV	1.41	0.0456	1.10	3.51	SAMN04487868_11516
A0A1I4N413	1.4107	-1.4107	50S ribosomal protein L17	1.41	0.0452	0.91	3.52	rplQ SAMN04487868_12928
A0A1I4MY49	1.4114	-1.4114	50S ribosomal protein L25	1.41	0.0452	0.47	3.53	rplY ctc SAMN04487868_12729
A0A1I4IMP5	1.4125	-1.4125	MerR family transcriptional regulator. redox-sensitive transcriptional activator SoxR	1.41	0.0453	1.68	3.53	SAMN04487868_10444
A0A1I4LLE3	1.4126	-1.4126	ATP-binding cassette protein. ChvD family	1.41	0.0454	0.51	3.53	SAMN04487868_11547
A0A1I4JJM8	1.4153	-1.4153	tRNA (guanine-N(7)-)-methyltransferase	1.42	0.0453	0.21	3.54	trmB SAMN04487868_10698
A0A1I4IXB4	1.4161	-1.4161	Iron(III) transport system ATP-binding protein	1.42	0.0454	0.89	3.54	SAMN04487868_104229
A0A1I4MND4	1.4168	-1.4168	GntR family transcriptional regulator. glc operon transcriptional activator	1.42	0.0454	0.67	3.54	SAMN04487868_12414
A0A1I4K1X1	1.4183	-1.4183	Chaperone SurA	1.42	0.0455	0.71	3.55	surA SAMN04487868_10844
A0A1I4IE19	1.4235	-1.4235	Alpha/beta hydrolase family protein	1.42	0.0446	1.23	3.56	SAMN04487868_103220
A0A1I4MW32	1.4246	-1.4246	tRNA-dihydrouridine(20/20a) synthase	1.42	0.0445	0.71	3.57	dusA SAMN04487868_12625
A0A1I4M6A5	1.4261	-1.4261	Phosphoribosylglycinamide formyltransferase	1.43	0.0445	0.78	3.57	purN SAMN04487868_11931
A0A1I4LSK4	1.4264	-1.4264	Uncharacterized protein	1.43	0.0446	0.86	3.57	SAMN04487868_11648
A0A1I4LX52	1.4264	-1.4264	Uncharacterized protein	1.43	0.0446	1.13	3.57	SAMN04487868_11747
A0A1I4KLQ5	1.4270	-1.4270	Predicted ATP-dependent endonuclease of the OLD family. contains P-loop ATPase and TOPRIM domains	1.43	0.0446	0.75	3.58	SAMN04487868_110108
A0A1I4K4F0	1.4279	-1.4279	Acetylornithine deacetylase	1.43	0.0446	0.45	3.58	SAMN04487868_10892
A0A1I4LJC0	1.4280	-1.4280	Ketol-acid reductoisomerase (NADP(+))	1.43	0.0446	0.22	3.58	ilvC SAMN04487868_1153
A0A1I4KEY6	1.4347	-1.4347	Uncharacterized domain 1-containing protein	1.43	0.0441	1.60	5.06	SAMN04487868_109131
A0A1I4JW98	1.4409	-1.4409	Ribosome-recycling factor	1.44	0.0433	0.43	3.62	frr SAMN04487868_107157
A0A1I4KJ53	1.4416	-1.4416	Cell division protein ZapB	1.44	0.0434	1.97	3.62	SAMN04487868_11033
A0A1I4IV58	1.4430	-1.4430	HD-like signal output (HDOD) domain. no enzymatic activity	1.44	0.0433	0.87	3.63	SAMN04487868_104209
A0A1I4KKP1	1.4433	-1.4433	Amino acid ABC transporter substrate-binding protein. PAAT family	1.44	0.0432	2.60	3.63	SAMN04487868_11071
A0A1I4IW42	1.4447	-1.4447	Two-component system. OmpR family. response regulator RstA	1.44	0.0431	0.47	3.63	SAMN04487868_104232
A0A1I4H9Z9	1.4455	-1.4455	D-3-phosphoglycerate dehydrogenase	1.45	0.0429	0.30	3.64	SAMN04487868_101208
A0A1I4HGF6	1.4503	-1.4503	Dephospho-CoA kinase	1.45	0.0424	0.90	3.65	coaE SAMN04487868_101343
A0A1I4M7L1	1.4568	-1.4568	Histidine kinase-. DNA gyrase B-. and HSP90-like ATPase	1.46	0.0420	1.26	3.67	SAMN04487868_11981
A0A1I4HWX4	1.4568	-1.4568	Phosphoribosylaminoimidazole-succinocarboxamide synthase	1.46	0.0420	0.59	3.67	purC SAMN04487868_10299
A0A1I4L725	1.4609	-1.4609	ATP synthase subunit delta	1.46	0.0415	0.74	3.69	atpH SAMN04487868_11320
A0A1I4L5H5	1.4629	-1.4629	FHA domain protein	1.46	0.0414	1.22	3.69	SAMN04487868_112132
A0A1I4KI15	1.4634	-1.4634	Ribosomal protein L11 methyltransferase	1.46	0.0414	1.13	3.69	prmA SAMN04487868_11016
A0A1I4HGT2	1.4686	-1.4686	AraC-type DNA-binding protein	1.47	0.0411	0.83	3.71	SAMN04487868_101390
A0A1I4KUT7	1.4688	-1.4688	Methyl-accepting chemotaxis protein	1.47	0.0411	4.65	3.71	SAMN04487868_11196
A0A1I4N3V9	1.4689	-1.4689	50S ribosomal protein L22	1.47	0.0412	0.52	3.71	rplV SAMN04487868_1298
A0A1I4J621	1.4709	-1.4709	Uncharacterized protein	1.47	0.0408	1.03	3.72	SAMN04487868_10586
A0A1I4LKX5	1.4864	-1.4864	Octaprenyl-diphosphate synthase	1.49	0.0398	0.82	3.77	SAMN04487868_11533
A0A1I4J333	1.4875	-1.4875	Uncharacterized protein	1.49	0.0398	1.60	3.78	SAMN04487868_10510

A0A1I4JAI8	1.4889	-1.4889	Uncharacterized protein	1.49	0.0396	0.51	3.78	SAMN04487868_105220
A0A1I4IGW2	1.4893	-1.4893	Nucleotidyl transferase AbiEii toxin. Type IV TA system	1.49	0.0396	0.76	3.78	SAMN04487868_103251
A0A1I4HW09	1.4894	-1.4894	2-methylisocitrate lyase	1.49	0.0396	0.75	3.78	prpB SAMN04487868_10276
A0A1I4MCV8	1.4904	-1.4904	GTP cyclohydrolase-2	1.49	0.0396	0.57	3.79	ribA SAMN04487868_12129
A0A1I4HGN2	1.4950	-1.4950	Type IV pilus assembly protein PilA	1.49	0.0392	0.93	3.80	SAMN04487868_101348
A0A1I4N428	1.4953	-1.4953	MSHA biogenesis protein MshK	1.50	0.0393	0.86	3.80	SAMN04487868_12935
A0A1I4LLA8	1.4965	-1.4965	GTPase Obg	1.50	0.0393	0.71	3.81	obg SAMN04487868_11530
A0A1I4LY39	1.5000	-1.5000	General secretion pathway protein F	1.50	0.0389	0.49	3.82	SAMN04487868_11760
A0A1I4I1H0	1.5011	-1.5011	Trigger factor	1.50	0.0388	0.57	3.82	tig SAMN04487868_102269
A0A1I4J7F3	1.5067	-1.5067	4-hydroxy-3-methylbut-2-en-1-yl diphosphate synthase (flavodoxin)	1.51	0.0384	0.88	3.84	ispG SAMN04487868_105144
A0A1I4IBH7	1.5081	-1.5081	Chemotaxis protein MotA	1.51	0.0382	1.45	3.85	SAMN04487868_103111
A0A1I4JWC4	1.5108	-1.5108	Elongation factor Ts	1.51	0.0382	0.66	3.85	tsf SAMN04487868_107159
A0A1I4MD85	1.5123	-1.5123	Cyclic pyranopterin monophosphate synthase	1.51	0.0382	0.80	3.86	moaC SAMN04487868_12128
A0A1I4M4W8	1.5222	-1.5222	ATP-independent RNA helicase DbpA	1.52	0.0376	0.20	3.89	SAMN04487868_1195
A0A1I4L9V3	1.5228	-1.5228	Carbonic anhydrase or acetyltransferase. isoleucine patch superfamily	1.52	0.0377	0.95	3.90	SAMN04487868_11371
A0A1I4JIL1	1.5249	-1.5249	Nitrogen regulatory protein P-II family	1.52	0.0374	1.21	3.90	SAMN04487868_10695
A0A1I4L2W0	1.5254	-1.5254	RND family efflux transporter. MFP subunit	1.53	0.0374	3.01	3.90	SAMN04487868_11281
A0A1I4NF43	1.5282	-1.5282	30S ribosomal protein S7	1.53	0.0371	0.56	3.91	rpsG SAMN04487868_1363
A0A1I4JT04	1.5294	-1.5294	Diaminopimelate decarboxylase	1.53	0.0371	2.74	3.92	SAMN04487868_10766
A0A1I4KF83	1.5303	-1.5303	Outer membrane protein	1.53	0.0372	1.89	3.92	SAMN04487868_109138
A0A1I4HVJ7	1.5304	-1.5304	Polysaccharide chain length determinant protein. PEP-CTERM locus subfamily	1.53	0.0372	1.00	3.92	SAMN04487868_10265
A0A1I4I0V6	1.5323	-1.5323	Transcriptional regulator. DeoR family	1.53	0.0372	0.42	3.93	SAMN04487868_102246
A0A1I4J894	1.5336	-1.5336	Nucleoside diphosphate kinase	1.53	0.0372	1.14	3.93	ndk SAMN04487868_105140
A0A1I4N6Y6	1.5343	-1.5343	Uncharacterized protein	1.53	0.0372	0.97	3.94	SAMN04487868_13022
A0A1I4J712	1.5346	-1.5346	tRNA (cytidine/uridine-2'-O-)-methyltransferase TrmJ	1.53	0.0373	0.43	3.94	trmJ SAMN04487868_105136
A0A1I4IUR5	1.5363	-1.5363	tRNA threonylcarbamoyladenosine biosynthesis protein TsaB	1.54	0.0371	1.12	3.94	SAMN04487868_104181
A0A1I4JKF6	1.5373	-1.5373	tRNA-binding protein	1.54	0.0372	1.01	3.95	SAMN04487868_106137
A0A1I4IN19	1.5451	-1.5451	Spermidine synthase	1.55	0.0363	0.84	3.97	SAMN04487868_10452
A0A1I4L9N8	1.5469	-1.5469	Chemotaxis protein MotB	1.55	0.0361	0.57	3.98	SAMN04487868_11367
A0A1I4K4E9	1.5482	-1.5482	S-adenosylmethionine decarboxylase proenzyme	1.55	0.0360	0.63	3.98	speD SAMN04487868_10885
A0A1I4JMF5	1.5496	-1.5496	Tyrosine--tRNA ligase	1.55	0.0361	0.74	3.99	tyrS SAMN04487868_106186
A0A1I4L8I1	1.5521	-1.5521	Beta sliding clamp	1.55	0.0357	0.47	4.00	SAMN04487868_11342
A0A1I4N695	1.5549	-1.5549	Bacterial translation initiation factor 3 (BIF-3)	1.55	0.0355	1.27	4.01	SAMN04487868_1305
A0A1I4JSP1	1.5595	-1.5595	Ribonuclease T	1.56	0.0356	1.01	4.02	rnt SAMN04487868_10746
A0A1I4KE56	1.5681	-1.5681	Uncharacterized protein	1.57	0.0351	1.74	4.05	SAMN04487868_109114
A0A1I4J8I2	1.5684	-1.5684	Dihydrolipoyl dehydrogenase	1.57	0.0352	0.47	4.06	SAMN04487868_105173
A0A1I4LA48	1.5701	-1.5701	Diguanylate cyclase (GGDEF) domain-containing protein	1.57	0.0352	1.46	4.06	SAMN04487868_11380
A0A1I4N542	1.5708	-1.5708	MSHA pilin protein MshA	1.57	0.0351	1.96	4.06	SAMN04487868_12943
A0A1I4HAB9	1.5711	-1.5711	Transcriptional regulator. TetR family	1.57	0.0351	0.72	4.07	SAMN04487868_101226

A0A1I4JV26	1.5723	-1.5723	Uncharacterized protein	1.57	0.0350	1.45	4.07	SAMN04487868_107122
A0A1I4ICV2	1.5726	-1.5726	Amino acid ABC transporter substrate-binding protein. PAAT family (TC 3.A.1.3.-)	1.57	0.0350	1.09	4.07	SAMN04487868_103178
A0A1I4ISI5	1.5761	-1.5761	Predicted kinase. aminoglycoside phosphotransferase (APT) family	1.58	0.0347	1.14	4.08	SAMN04487868_104156
A0A1I4LX81	1.5789	-1.5789	3-oxoacyl-[acyl-carrier-protein] synthase 3	1.58	0.0345	1.44	4.09	fabH SAMN04487868_11743
A0A1I4K6V2	1.5794	-1.5794	Dihydroxy-acid dehydratase	1.58	0.0345	0.31	4.09	ilvD SAMN04487868_108144
A0A1I4NGC4	1.5838	-1.5838	2-isopropylmalate synthase	1.58	0.0338	0.19	4.11	leuA SAMN04487868_1374
A0A1I4N4R4	1.5845	-1.5845	MSHA biogenesis protein MshI	1.58	0.0339	1.16	4.11	SAMN04487868_12933
A0A1I4KFC9	1.5894	-1.5894	Transcriptional regulator. TetR family	1.59	0.0334	1.19	4.13	SAMN04487868_109132
A0A1I4IM19	1.5926	-1.5926	FHA domain-containing protein	1.59	0.0334	3.13	4.14	SAMN04487868_10428
A0A1I4JUU2	1.5938	-1.5938	Methyltransferase domain-containing protein	1.59	0.0333	1.37	4.15	SAMN04487868_10782
A0A1I4LMA8	1.5964	-1.5964	3-dehydroquinate synthase	1.60	0.0332	0.39	4.16	aroB SAMN04487868_11554
A0A1I4K486	1.5964	-1.5964	Phosphoribulokinase	1.60	0.0333	1.15	4.16	SAMN04487868_10888
A0A1I4KD92	1.5987	-1.5987	Transcriptional regulator containing PAS. AAA-type ATPase. and DNA-binding Fis domains	1.60	0.0331	0.77	4.16	SAMN04487868_109102
A0A1I4MWP3	1.6055	-1.6055	Uncharacterized conserved protein	1.60	0.0327	2.78	6.22	SAMN04487868_12637
A0A1I4MWV5	1.6104	-1.6104	Protease-4	1.61	0.0323	1.31	4.21	SAMN04487868_12651
A0A1I4KMT7	1.6113	-1.6113	UPF0125 protein SAMN04487868_110115	1.61	0.0323	0.91	4.21	SAMN04487868_110115
A0A1I4KTW8	1.6128	-1.6128	Glycerate dehydrogenase	1.61	0.0322	0.82	4.22	SAMN04487868_11169
A0A1I4H9N3	1.6145	-1.6145	Transcriptional regulator. LysR family	1.61	0.0320	0.98	4.22	SAMN04487868_101145
A0A1I4I8L7	1.6171	-1.6171	2-nitropropane dioxygenase	1.62	0.0321	1.35	4.23	SAMN04487868_10373
A0A1I4KIA5	1.6174	-1.6174	Biotin carboxyl carrier protein of acetyl-CoA carboxylase	1.62	0.0321	1.51	4.23	SAMN04487868_11018
A0A1I4NF34	1.6198	-1.6198	tRNA 2-selenouridine synthase	1.62	0.0318	0.85	4.24	selU SAMN04487868_13517
A0A1I4IMS4	1.6222	-1.6222	GTPase. G3E family	1.62	0.0316	1.12	4.25	SAMN04487868_10446
A0A1I4KU55	1.6244	-1.6244	Thiopurine S-methyltransferase	1.62	0.0317	0.53	4.26	tpm SAMN04487868_11168
A0A1I4M8X2	1.6290	-1.6290	Uncharacterized protein	1.63	0.0316	2.58	4.28	SAMN04487868_1206
A0A1I4LTD6	1.6353	-1.6353	Uncharacterized protein	1.64	0.0311	1.43	4.30	SAMN04487868_11662
A0A1I4KN12	1.6386	-1.6386	Ribosome maturation factor RimP	1.64	0.0307	0.73	4.31	rimP SAMN04487868_110134
A0A1I4L7H9	1.6387	-1.6387	TRAP-type mannitol/chloroaromatic compound transport system. substrate-binding protein	1.64	0.0308	0.88	4.31	SAMN04487868_1136
A0A1I4KJC2	1.6413	-1.6413	Uncharacterized protein	1.64	0.0307	1.36	4.32	SAMN04487868_11038
A0A1I4JUA7	1.6435	-1.6435	Disulphide bond corrector protein DsbC	1.64	0.0308	1.52	4.33	SAMN04487868_10795
A0A1I4K122	1.6458	-1.6458	Uncharacterized protein	1.65	0.0307	0.81	4.34	SAMN04487868_10810
A0A1I4LXI7	1.6487	-1.6487	ABC-type uncharacterized transport system. substrate-binding protein	1.65	0.0304	1.55	4.35	SAMN04487868_11749
A0A1I4M613	1.6492	-1.6492	Uncharacterized protein	1.65	0.0304	0.66	4.35	SAMN04487868_11934
A0A1I4K5I8	1.6503	-1.6503	Hypoxanthine phosphoribosyltransferase	1.65	0.0305	0.64	4.35	SAMN04487868_108132
A0A1I4MN11	1.6527	-1.6527	Amino acid ABC transporter substrate-binding protein. PAAT family	1.65	0.0302	0.83	4.36	SAMN04487868_12416
A0A1I4MEF8	1.6578	-1.6578	Lon N-terminal domain-containing protein	1.66	0.0299	1.22	4.38	SAMN04487868_12147
A0A1I4L3W6	1.6582	-1.6582	2-hydroxy-3-oxopropionate reductase	1.66	0.0299	0.54	4.38	SAMN04487868_112118
A0A1I4N556	1.6604	-1.6604	D-aminoacyl-tRNA deacylase	1.66	0.0299	1.91	4.39	dtd SAMN04487868_12955

A0A1I4HCX3	1.6610	-1.6610	Ribosomal protein S12 methylthiotransferase RimO	1.66	0.0301	0.49	4.40	rimO SAMN04487868_101296
A0A1I4JRM6	1.6670	-1.6670	Membrane-bound lytic murein transglycosylase F	1.66	0.0296	2.90	6.68	mltF SAMN04487868_10725
A0A1I4J3L5	1.6680	-1.6680	Putative Zn-dependent protease. contains TPR repeats	1.67	0.0293	0.36	4.42	SAMN04487868_10557
A0A1I4HGY0	1.6688	-1.6688	UPF0234 protein SAMN04487868_101392	1.67	0.0294	0.93	4.42	SAMN04487868_101392
A0A1I4I6U4	1.6713	-1.6713	Outer membrane transport energization protein ExbB	1.67	0.0295	6.94	4.43	SAMN04487868_10312
A0A1I4KAY1	1.6768	-1.6768	Amino acid ABC transporter substrate-binding protein. PAAT family	1.68	0.0293	1.23	4.46	SAMN04487868_10942
A0A1I4JWI0	1.6768	-1.6768	Succinyldiaminopimelate aminotransferase apoenzyme	1.68	0.0294	0.27	4.46	SAMN04487868_107164
A0A1I4HB66	1.6776	-1.6776	Oligoribonuclease	1.68	0.0291	0.85	4.46	orn SAMN04487868_101250
A0A1I4HGN3	1.6786	-1.6786	3'(2').5'-bisphosphate nucleotidase CysQ	1.68	0.0292	0.86	4.46	cysQ SAMN04487868_101351
A0A1I4KRI3	1.6788	-1.6788	Acetyl-CoA C-acetyltransferase	1.68	0.0291	0.31	4.46	SAMN04487868_11115
A0A1I4K652	1.6791	-1.6791	Dienelactone hydrolase	1.68	0.0291	1.72	4.46	SAMN04487868_108151
A0A1I4JLB7	1.6891	-1.6891	Reactive intermediate/imine deaminase	1.69	0.0285	1.53	4.50	SAMN04487868_106125
A0A1I4MGJ3	1.6896	-1.6896	Protein RecA	1.69	0.0284	0.94	4.50	recA SAMN04487868_12223
A0A1I4JVG1	1.6958	-1.6958	Uncharacterized copper-binding protein. cupredoxin-like subfamily	1.69	0.0279	2.48	6.92	SAMN04487868_107126
A0A1I4HZY7	1.6996	-1.6996	Peroxiredoxin	1.70	0.0272	1.30	4.54	SAMN04487868_102219
A0A1I4I9T3	1.7029	-1.7029	Putative proteasome-type protease	1.70	0.0273	0.66	4.56	SAMN04487868_103105
A0A1I4J2N7	1.7033	-1.7033	30S ribosomal protein S1	1.70	0.0274	0.41	4.56	SAMN04487868_10532
A0A1I4LGW3	1.7078	-1.7078	DNA-binding transcriptional regulator. LysR family	1.71	0.0274	1.55	4.58	SAMN04487868_11474
A0A1I4I251	1.7097	-1.7097	Peptidylprolyl isomerase	1.71	0.0274	0.90	4.58	SAMN04487868_102264
A0A1I4N6M9	1.7124	-1.7124	Predicted lactoylglutathione lyase	1.71	0.0273	0.57	4.59	SAMN04487868_13013
A0A1I4LL34	1.7150	-1.7150	Uncharacterized protein	1.71	0.0274	0.99	4.60	SAMN04487868_11537
A0A1I4IKS8	1.7161	-1.7161	Predicted ATP-dependent endonuclease of the OLD family. contains P-loop ATPase and TOPRIM domains	1.72	0.0273	1.02	4.61	SAMN04487868_1044
A0A1I4K4W7	1.7174	-1.7174	Acetylglutamate kinase	1.72	0.0269	1.07	4.61	argB SAMN04487868_10894
A0A1I4M5L9	1.7183	-1.7183	Phosphoribosylformylglycinamidine cyclo-ligase	1.72	0.0269	0.52	4.62	purM SAMN04487868_11930
A0A1I4L7V3	1.7209	-1.7209	tRNA uridine 5-carboxymethylaminomethyl modification enzyme MnmG	1.72	0.0270	2.59	4.63	mnmG gidA SAMN04487868_11328
A0A1I4LLK4	1.7304	-1.7304	Shikimate kinase	1.73	0.0259	1.18	4.66	aroK SAMN04487868_11555
A0A1I4LSD5	1.7338	-1.7338	Uncharacterized protein	1.73	0.0259	0.72	4.68	SAMN04487868_11636
A0A1I4JGB6	1.7376	-1.7376	Peptidyl-prolyl cis-trans isomerase	1.74	0.0258	0.64	4.69	SAMN04487868_10645
A0A1I4LLQ9	1.7381	-1.7381	Transcription antitermination protein NusB	1.74	0.0257	1.01	4.69	nusB SAMN04487868_11541
A0A1I4MSM7	1.7393	-1.7393	DNA-binding transcriptional regulator. LysR family	1.74	0.0258	4.01	4.70	SAMN04487868_12547
A0A1I4KRD5	1.7400	-1.7400	Imidazole glycerol phosphate synthase subunit HisF	1.74	0.0256	1.06	4.70	hisF SAMN04487868_1116
A0A1I4ID71	1.7412	-1.7412	Catechol 1.2-dioxygenase	1.74	0.0256	3.51	4.71	SAMN04487868_103169
A0A1I4H4A3	1.7439	-1.7439	Uncharacterized protein	1.74	0.0255	1.48	4.72	SAMN04487868_10173
A0A1I4K2A8	1.7448	-1.7448	Ribosomal RNA small subunit methyltransferase A	1.74	0.0256	0.77	4.72	rsmA ksgA SAMN04487868_10842
A0A1I4KV37	1.7452	-1.7452	Phosphoglycerate kinase	1.75	0.0254	0.75	4.72	pgk SAMN04487868_11191
A0A1I4HXE4	1.7461	-1.7461	Peroxiredoxin Q/BCP	1.75	0.0254	1.11	4.73	SAMN04487868_102102
A0A1I4KJ92	1.7528	-1.7528	Diguanylate cyclase/phosphodiesterase	1.75	0.0252	1.11	4.75	SAMN04487868_11021

A0A1I4IS01	1.7540	-1.7540	UPF0178 protein SAMN04487868_104139	1.75	0.0252	0.86	4.76	SAMN04487868_104139
A0A1I4HH40	1.7553	-1.7553	Diguanylate cyclase/phosphodiesterase	1.76	0.0252	1.40	4.76	SAMN04487868_101404
A0A1I4HT89	1.7554	-1.7554	Formyl transferase	1.76	0.0253	0.20	4.76	SAMN04487868_10235
A0A1I4KRW8	1.7558	-1.7558	2.3-bisphosphoglycerate-independent phosphoglycerate mutase	1.76	0.0253	1.25	4.77	gpmI SAMN04487868_11110
A0A1I4L4T6	1.7633	-1.7633	Type VI secretion system protein VasD	1.76	0.0248	1.13	4.80	SAMN04487868_112133
A0A1I4KV06	1.7720	-1.7720	Nitronate monooxygenase	1.77	0.0243	1.33	4.83	SAMN04487868_11197
A0A1I4KRY0	1.7748	-1.7748	1-(5-phosphoribosyl)-5-[(5-phosphoribosylamino)methylideneamino] imidazole-4-carboxamide isomerase	1.77	0.0243	0.83	4.84	hisA SAMN04487868_1115
A0A1I4I8T4	1.7781	-1.7781	Bifunctional adenosylcobalamin biosynthesis protein	1.78	0.0244	0.84	4.86	SAMN04487868_10379
A0A1I4L2L8	1.7783	-1.7783	MCP methyltransferase. CheR-type	1.78	0.0244	2.73	4.86	SAMN04487868_11264
A0A1I4JN46	1.7787	-1.7787	Opacity-associated protein A LysM-like domain-containing protein	1.78	0.0245	3.57	4.86	SAMN04487868_106185
A0A1I4HF25	1.7880	-1.7880	Transcriptional antiterminator RfaH	1.79	0.0239	1.04	4.90	SAMN04487868_101352
A0A1I4JJL6	1.7883	-1.7883	DUF4124 domain-containing protein	1.79	0.0240	1.03	4.90	SAMN04487868_106117
A0A1I4KI98	1.7986	-1.7986	Inorganic pyrophosphatase	1.80	0.0235	1.17	4.94	ppa SAMN04487868_11023
A0A1I4N1V0	1.8037	-1.8037	Alkyl hydroperoxide reductase C	1.80	0.0232	1.92	4.96	SAMN04487868_12840
A0A1I4HEA8	1.8075	-1.8075	Histidinol-phosphate aminotransferase	1.81	0.0232	0.41	4.98	hisC SAMN04487868_101328
A0A1I4HF54	1.8098	-1.8098	Signal transduction histidine kinase	1.81	0.0233	1.78	4.99	SAMN04487868_101341
A0A1I4J881	1.8123	-1.8123	Cysteine desulfurase IscS	1.81	0.0232	1.19	5.00	SAMN04487868_105139
A0A1I4HVJ1	1.8127	-1.8127	Polysaccharide export outer membrane protein	1.81	0.0233	0.73	5.00	SAMN04487868_10266
A0A1I4KJP9	1.8142	-1.8142	Two component transcriptional regulator. LuxR family	1.81	0.0232	0.57	5.01	SAMN04487868_11060
A0A1I4HKV5	1.8159	-1.8159	Cytochrome c-type biogenesis protein CcmE	1.82	0.0232	1.30	5.01	ccmE cycJ SAMN04487868_101481
A0A1I4KUB7	1.8173	-1.8173	Adenosylmethionine-8-amino-7-oxononanoate aminotransferase	1.82	0.0233	1.39	5.02	bioA SAMN04487868_11180
A0A1I4J6P3	1.8190	-1.8190	Uncharacterized conserved protein. DUF1330 family	1.82	0.0232	2.36	5.03	SAMN04487868_10594
A0A1I4HZG9	1.8265	-1.8265	Agmatine deiminase	1.83	0.0227	1.10	5.06	SAMN04487868_102151
A0A1I4K2B6	1.8286	-1.8286	Phosphoglycolate phosphatase	1.83	0.0223	3.64	5.07	SAMN04487868_10852
A0A1I4M0I0	1.8338	-1.8338	General secretion pathway protein B	1.83	0.0218	0.67	5.09	SAMN04487868_1189
A0A1I4H3Z8	1.8345	-1.8345	Uncharacterized protein	1.83	0.0219	3.55	5.09	SAMN04487868_10164
A0A1I4M5K7	1.8384	-1.8384	Regulatory inactivation of DnaA Hda protein	1.84	0.0218	1.09	5.11	SAMN04487868_11927
A0A1I4J3K8	1.8399	-1.8399	Putative ABC transport system ATP-binding protein	1.84	0.0216	0.93	5.12	SAMN04487868_10552
A0A1I4NAN1	1.8418	-1.8418	Molybdopterin guanine dinucleotide biosynthesis accessory protein MobB	1.84	0.0217	1.03	5.12	SAMN04487868_13222
A0A1I4NHD3	1.8419	-1.8419	Sulfide:quinone oxidoreductase	1.84	0.0217	1.08	5.12	SAMN04487868_1402
A0A1I4H8U7	1.8461	-1.8461	Amino acid ABC transporter substrate-binding protein. PAAT family	1.85	0.0217	4.53	5.14	SAMN04487868_101126
A0A1I4KN10	1.8469	-1.8469	Transcription termination/antitermination protein NusA	1.85	0.0218	0.59	5.15	nusA SAMN04487868_110135
A0A1I4I0J1	1.8474	-1.8474	Glutathione peroxidase	1.85	0.0218	1.19	5.15	SAMN04487868_102173
A0A1I4M1I6	1.8487	-1.8487	Alpha/beta hydrolase fold	1.85	0.0218	1.57	5.15	SAMN04487868_11823
A0A1I4J3P5	1.8503	-1.8503	GST-like protein	1.85	0.0219	0.37	5.16	SAMN04487868_10521
A0A1I4LKP5	1.8529	-1.8529	Type IV pilus assembly protein PilX	1.85	0.0219	1.59	5.17	SAMN04487868_11518
A0A1I4LJU1	1.8549	-1.8549	Outer membrane protein assembly factor BamD	1.85	0.0218	0.37	5.18	bamD SAMN04487868_11510

A0A1I4MDZ2	1.8576	-1.8576	Uncharacterized conserved protein. contains NRDE domain	1.86	0.0218	1.25	5.19	SAMN04487868_12133
A0A1I4J6T4	1.8603	-1.8603	Putative ABC transport system substrate-binding protein	1.86	0.0218	1.44	5.20	SAMN04487868_105103
A0A1I4JV61	1.8606	-1.8606	Copper-resistance protein. CopA family	1.86	0.0219	1.26	5.20	SAMN04487868_107125
A0A1I4MYE2	1.8611	-1.8611	Uncharacterized protein	1.86	0.0219	2.52	5.21	SAMN04487868_12712
A0A1I4KRF8	1.8645	-1.8645	Rhodanese-related sulfurtransferase	1.86	0.0220	0.86	5.22	SAMN04487868_11111
A0A1I4I000	1.8655	-1.8655	HZS_alpha domain-containing protein	1.87	0.0218	2.15	5.23	SAMN04487868_102222
A0A1I4JTB9	1.8687	-1.8687	Outer membrane protein TolC	1.87	0.0219	0.71	5.24	SAMN04487868_10778
A0A1I4IE42	1.8727	-1.8727	Luciferase family oxidoreductase. group 1	1.87	0.0219	0.65	5.26	SAMN04487868_103221
A0A1I4JGH4	1.8733	-1.8733	Molybdopterin synthase subunit MoaE	1.87	0.0219	0.90	5.26	SAMN04487868_10651
A0A1I4LLD0	1.8791	-1.8791	3.4-dihydroxy-2-butanone 4-phosphate synthase	1.88	0.0221	0.43	5.29	ribB SAMN04487868_11543
A0A1I4MZE2	1.8793	-1.8793	Uncharacterized protein	1.88	0.0222	1.23	5.29	SAMN04487868_12746
A0A1I4IP03	1.8837	-1.8837	Cold-shock DNA-binding protein family	1.88	0.0219	1.37	5.31	SAMN04487868_10475
A0A1I4JK41	1.8911	-1.8911	Replication fork clamp-binding protein CrfC (Dynamin-like GTPase family)	1.89	0.0219	1.74	5.34	SAMN04487868_106105
A0A1I4M3N5	1.8938	-1.8938	Sulfite reductase (NADPH) hemoprotein beta-component	1.89	0.0219	0.69	5.35	SAMN04487868_11868
A0A1I4LM37	1.8940	-1.8940	Type IV pilus assembly protein PilN	1.89	0.0220	0.54	5.35	SAMN04487868_11559
A0A1I4KC48	1.8963	-1.8963	L.D-transpeptidase ErfK/SrfK	1.90	0.0220	2.00	5.36	SAMN04487868_10972
A0A1I4N1H7	1.8982	-1.8982	Uncharacterized protein	1.90	0.0221	2.56	5.37	SAMN04487868_12831
A0A1I4KUU1	1.8992	-1.8992	Amino acid ABC transporter substrate-binding protein. PAAT family	1.90	0.0221	0.92	5.37	SAMN04487868_11184
A0A1I4JWG7	1.9001	-1.9001	1-deoxy-D-xylulose 5-phosphate reductoisomerase	1.90	0.0220	1.30	5.38	dxr SAMN04487868_107154
A0A1I4IW95	1.9005	-1.9005	Predicted oxidoreductase	1.90	0.0218	0.86	5.38	SAMN04487868_104238
A0A1I4HI66	1.9086	-1.9086	Putative amidoligase enzyme	1.91	0.0219	1.30	5.42	SAMN04487868_101430
A0A1I4HZS9	1.9113	-1.9113	Tetratricopeptide repeat-containing protein	1.91	0.0216	2.24	5.43	SAMN04487868_102213
A0A1I4KZP6	1.9138	-1.9138	Uncharacterized protein	1.91	0.0213	1.94	5.44	SAMN04487868_1125
A0A1I4HGS6	1.9148	-1.9148	Exodeoxyribonuclease I	1.91	0.0214	0.42	5.44	SAMN04487868_101382
A0A1I4KWH5	1.9155	-1.9155	Uncharacterized protein	1.92	0.0213	0.50	5.45	SAMN04487868_111131
A0A1I4J6F1	1.9197	-1.9197	Nitroreductase	1.92	0.0211	0.71	5.47	SAMN04487868_105117
A0A1I4K0X0	1.9232	-1.9232	Phospho-2-dehydro-3-deoxyheptonate aldolase	1.92	0.0210	2.32	5.48	SAMN04487868_10824
A0A1I4LKE6	1.9281	-1.9281	4-hydroxy-3-methylbut-2-enyl diphosphate reductase	1.93	0.0208	1.25	5.50	ispH SAMN04487868_11522
A0A1I4H903	1.9286	-1.9286	Uncharacterized protein	1.92	0.0212	3.70	9.06	SAMN04487868_101192
A0A1I4L6Y6	1.9289	-1.9289	ATP synthase subunit beta	1.93	0.0209	0.52	5.51	atpD SAMN04487868_11317
A0A1I4K4T4	1.9297	-1.9297	Uncharacterized conserved protein YdgA. DUF945 family	1.93	0.0209	1.28	5.51	SAMN04487868_108115
A0A1I4IVV5	1.9336	-1.9336	Pyridoxine 5'-phosphate synthase	1.93	0.0210	0.71	5.53	pdxJ SAMN04487868_104192
A0A1I4I7I8	1.9340	-1.9340	Uncharacterized protein	1.93	0.0211	1.50	5.53	SAMN04487868_10315
A0A1I4M212	1.9351	-1.9351	Phospho-2-dehydro-3-deoxyheptonate aldolase	1.94	0.0211	1.16	5.54	SAMN04487868_11850
A0A1I4HU57	1.9366	-1.9366	Putative PEP-CTERM system TPR-repeat lipoprotein	1.94	0.0212	0.71	5.54	SAMN04487868_10230
A0A1I4M294	1.9406	-1.9406	Outer-membrane lipoprotein carrier protein	1.94	0.0210	1.70	5.56	lolA SAMN04487868_11846
A0A1I4L2E3	1.9418	-1.9418	Twitching motility two-component system response regulator PilH	1.94	0.0209	1.26	5.57	SAMN04487868_11267
A0A1I4MEC9	1.9469	-1.9469	Putative peptidoglycan binding domain-containing protein	1.95	0.0208	2.51	5.59	SAMN04487868_12144
A0A1I4J6Y7	1.9519	-1.9519	HD domain-containing protein	1.95	0.0208	1.95	5.61	SAMN04487868_105110

A0A1I4M1P7	1.9527	-1.9527	DNA-binding transcriptional regulator. LysR family	1.95	0.0209	0.82	5.62	SAMN04487868_11829
A0A1I4L0F8	1.9544	-1.9544	Succinylglutamate desuccinylase / Aspartoacylase family protein	1.95	0.0209	1.37	5.63	SAMN04487868_11223
A0A1I4HTJ9	1.9551	-1.9551	Glucose/arabinose dehydrogenase. beta-propeller fold	1.96	0.0209	4.08	5.63	SAMN04487868_10233
A0A1I4LXJ6	1.9552	-1.9552	Type II secretion system protein M	1.96	0.0210	1.16	5.63	SAMN04487868_11753
A0A1I4J7Y2	1.9579	-1.9579	ATP-binding cassette. subfamily F. uup	1.96	0.0210	0.51	5.64	SAMN04487868_105158
A0A1I4N3I4	1.9592	-1.9592	30S ribosomal protein S5	1.96	0.0211	0.58	5.65	rpsE SAMN04487868_12920
A0A1I4KSI9	1.9616	-1.9616	Signal transduction histidine kinase	1.96	0.0211	0.97	5.66	SAMN04487868_11145
A0A1I4IP83	1.9626	-1.9626	Short-chain dehydrogenase	1.96	0.0210	1.44	5.66	SAMN04487868_10481
A0A1I4M4M4	1.9660	-1.9660	Uncharacterized protein	1.97	0.0206	0.60	5.68	SAMN04487868_1196
A0A1I4HEB8	1.9660	-1.9660	PilZ domain-containing protein	1.97	0.0206	2.59	5.68	SAMN04487868_101295
A0A1I4HZ71	1.9687	-1.9687	Uncharacterized protein	1.97	0.0206	2.27	5.69	SAMN04487868_102191
A0A1I4H5C9	1.9714	-1.9714	Anti-sigma-K factor RskA	1.97	0.0207	1.14	5.71	SAMN04487868_101101
A0A1I4J8G8	1.9766	-1.9766	Putative negative regulator of RcsB-dependent stress response	1.98	0.0206	1.48	5.73	SAMN04487868_105146
A0A1I4L2Y2	1.9878	-1.9878	Beta-lactamase	1.99	0.0204	0.90	5.78	SAMN04487868_11286
A0A1I4K326	1.9907	-1.9907	Glycine betaine/proline transport system substrate-binding protein	1.99	0.0199	4.03	5.80	SAMN04487868_10869
A0A1I4HH13	1.9915	-1.9915	Zn-dependent protease with chaperone function	1.99	0.0199	0.71	5.80	SAMN04487868_101402
A0A1I4KER1	1.9967	-1.9967	Fatty-acyl-CoA synthase	2.00	0.0195	1.46	5.83	SAMN04487868_109139
A0A1I4JT47	1.9985	-1.9985	UPF0246 protein SAMN04487868_10739	2.00	0.0196	0.87	5.83	SAMN04487868_10739
A0A1I4KEP5	2.0020	-2.0020	Uncharacterized domain 1-containing protein	2.00	0.0196	1.69	5.85	SAMN04487868_109130
A0A1I4HBP2	2.0074	-2.0074	Uncharacterized protein	2.01	0.0195	1.31	5.88	SAMN04487868_101265
A0A1I4H7A3	2.0087	-2.0087	RNA polymerase sigma-70 factor. ECF subfamily	2.01	0.0195	1.84	5.88	SAMN04487868_101102
A0A1I4HGT8	2.0097	-2.0097	3-oxoacyl-[acyl-carrier protein] reductase	2.01	0.0194	0.86	5.89	SAMN04487868_101395
A0A1I4JR64	2.0108	-2.0108	Iron complex transport system substrate-binding protein	2.01	0.0190	0.38	5.89	SAMN04487868_10710
A0A1I4H921	2.0143	-2.0143	Methyl-accepting chemotaxis protein	2.01	0.0190	1.54	5.91	SAMN04487868_101189
A0A1I4HIJ7	2.0223	-2.0223	Uncharacterized protein	2.02	0.0183	0.82	5.95	SAMN04487868_101427
A0A1I4JK68	2.0271	-2.0271	DUF2489 domain-containing protein	2.03	0.0184	1.68	5.97	SAMN04487868_106130
A0A1I4JX88	2.0288	-2.0288	2.3.4.5-tetrahydropyridine-2.6-dicarboxylate N-succinyltransferase	2.03	0.0185	0.45	5.98	dapD SAMN04487868_107166
A0A1I4LF53	2.0316	-2.0316	Antitoxin	2.03	0.0184	1.15	5.99	SAMN04487868_11433
A0A1I4MDW3	2.0323	-2.0323	1-deoxy-D-xylulose-5-phosphate synthase	2.03	0.0184	0.98	6.00	dxs SAMN04487868_12130
A0A1I4IMF9	2.0327	-2.0327	Uncharacterized protein	2.03	0.0185	1.50	6.00	SAMN04487868_1043
A0A1I4K4U1	2.0346	-2.0346	Phosphopantetheine adenylyltransferase	2.03	0.0184	0.80	6.01	coaD SAMN04487868_108114
A0A1I4JFJ7	2.0353	-2.0353	Phosphomannomutase	2.04	0.0184	0.16	6.01	SAMN04487868_10631
A0A1I4H9H2	2.0397	-2.0397	Sigma54 specific transcriptional regulator. Fis family	2.04	0.0184	0.38	6.03	SAMN04487868_101200
A0A1I4LLK0	2.0461	-2.0461	DNA repair protein RadA	2.05	0.0182	0.39	6.07	radA SAMN04487868_11548
A0A1I4MYU6	2.0466	-2.0466	4-diphosphocytidyl-2-C-methyl-D-erythritol kinase	2.05	0.0182	0.64	6.07	ispE SAMN04487868_12727
A0A1I4LRQ2	2.0467	-2.0467	Uncharacterized protein	2.05	0.0181	1.53	6.07	SAMN04487868_11627
A0A1I4JR08	2.0468	-2.0468	Cobaltochelatase CobN	2.05	0.0181	1.15	6.07	SAMN04487868_10711
A0A1I4M1E2	2.0505	-2.0505	3-isopropylmalate dehydrogenase	2.05	0.0179	0.95	6.09	leuB SAMN04487868_11832

A0A1I4M7D8	2.0514	-2.0514	Acetyl-coenzyme A carboxylase carboxyl transferase subunit alpha	2.05	0.0175	0.92	6.09	accA SAMN04487868_11959
A0A1I4I1W7	2.0538	-2.0538	Peptidyl-prolyl cis-trans isomerase	2.05	0.0176	0.78	6.10	SAMN04487868_102278
A0A1I4MU46	2.0545	-2.0545	Rhodanese-related sulfurtransferase	2.05	0.0176	1.73	6.11	SAMN04487868_12569
A0A1I4IS09	2.0568	-2.0568	Glucose/arabinose dehydrogenase. beta-propeller fold	2.06	0.0176	2.94	6.12	SAMN04487868_104144
A0A1I4K4A1	2.0622	-2.0622	Thiol:disulfide interchange protein	2.06	0.0172	2.13	6.15	SAMN04487868_108102
A0A1I4KN33	2.0687	-2.0687	Ribosome-binding factor A	2.07	0.0173	1.34	6.18	rbfA SAMN04487868_110137
A0A1I4J8K1	2.0706	-2.0706	Dihydrolipoyllysine-residue succinyltransferase component of 2-oxoglutarate dehydrogenase complex	2.07	0.0171	1.28	6.19	SAMN04487868_105172
A0A1I4KIX2	2.0710	-2.0710	3-dehydroquinate dehydratase	2.07	0.0171	2.51	6.19	aroQ SAMN04487868_11019
A0A1I4LKX7	2.0716	-2.0716	30S ribosomal protein S20	2.07	0.0172	0.79	6.19	rpsT SAMN04487868_11528
A0A1I4IFL2	2.0718	-2.0718	Uncharacterized protein	2.07	0.0172	1.40	6.19	SAMN04487868_103261
A0A1I4LH94	2.0724	-2.0724	Hydroxypyruvate isomerase	2.07	0.0173	1.12	6.20	SAMN04487868_11495
A0A1I4M5F6	2.0778	-2.0778	Uncharacterized protein	2.08	0.0170	1.47	6.22	SAMN04487868_11923
A0A1I4HCM8	2.0794	-2.0794	Elongation factor P	2.08	0.0171	2.09	6.23	efp SAMN04487868_101244
A0A1I4NC48	2.0851	-2.0851	Uncharacterized protein	2.09	0.0170	1.47	6.26	SAMN04487868_1337
A0A1I4N4A2	2.0888	-2.0888	DNA-directed RNA polymerase subunit alpha	2.09	0.0171	0.63	6.28	rpoA SAMN04487868_12927
A0A1I4IT64	2.0901	-2.0901	Male sterility protein	2.09	0.0171	2.03	6.29	SAMN04487868_104169
A0A1I4I0X1	2.0947	-2.0947	Amino acid/amide ABC transporter substrate-binding protein. HAAT family	2.09	0.0172	1.72	6.31	SAMN04487868_102234
A0A1I4L6Z7	2.0959	-2.0959	Alpha-ketoglutarate-dependent 2.4-dichlorophenoxyacetate dioxygenase	2.10	0.0172	0.34	6.32	SAMN04487868_1138
A0A1I4ML72	2.0960	-2.0960	Uncharacterized protein	2.10	0.0172	0.75	6.32	SAMN04487868_12352
A0A1I4KVW9	2.1014	-2.1014	L-lactate dehydrogenase complex protein LldE	2.10	0.0173	2.11	6.35	SAMN04487868_111115
A0A1I4HE71	2.1026	-2.1026	Nucleoid-associated protein	2.10	0.0174	1.42	6.35	SAMN04487868_101292
A0A1I4JKK0	2.1027	-2.1027	Pilus retraction ATPase PilT	2.10	0.0174	1.07	6.35	SAMN04487868_106109
A0A1I4JSB8	2.1034	-2.1034	Methylmalonyl-CoA mutase	2.10	0.0175	1.62	6.36	SAMN04487868_10716
A0A1I4KE09	2.1038	-2.1038	Uncharacterized protein	2.10	0.0175	2.25	6.36	SAMN04487868_109115
A0A1I4LDQ4	2.1092	-2.1092	Uncharacterized protein	2.11	0.0177	1.09	6.39	SAMN04487868_1143
A0A1I4KNC6	2.1106	-2.1106	Uncharacterized protein	2.11	0.0177	2.12	6.39	SAMN04487868_110143
A0A1I4L9M5	2.1141	-2.1141	Hemoglobin	2.11	0.0172	1.82	6.41	SAMN04487868_11378
A0A1I4L4X9	2.1175	-2.1175	Type VI secretion system protein ImpJ	2.12	0.0170	2.60	6.43	SAMN04487868_112134
A0A1I4KW48	2.1218	-2.1218	L-lactate dehydrogenase complex protein LldG	2.12	0.0170	2.81	6.45	SAMN04487868_111113
A0A1I4K4V3	2.1263	-2.1263	Uncharacterized protein	2.13	0.0171	0.42	6.47	SAMN04487868_10893
A0A1I4K353	2.1288	-2.1288	Glycine betaine/proline transport system ATP-binding protein	2.13	0.0172	1.88	6.49	SAMN04487868_10871
A0A1I4L305	2.1295	-2.1295	Outer membrane protein. multidrug efflux system	2.13	0.0172	1.36	6.49	SAMN04487868_11283
A0A1I4H4A7	2.1311	-2.1311	Predicted ATPase	2.13	0.0173	0.46	6.50	SAMN04487868_10171
A0A1I4L2M5	2.1312	-2.1312	DNA-binding protein HU-alpha	2.13	0.0173	1.91	6.50	SAMN04487868_11277
A0A1I4L4R3	2.1333	-2.1333	Putative hydrolase of the HAD superfamily	2.13	0.0172	2.11	6.51	SAMN04487868_112109
A0A1I4K653	2.1377	-2.1377	Membrane-bound lytic murein transglycosylase B	2.14	0.0173	0.74	6.54	SAMN04487868_108138
A0A1I4M3G8	2.1381	-2.1381	Fe/S biogenesis protein NfuA	2.14	0.0173	3.28	6.54	nfuA SAMN04487868_11871
A0A1I4MWM6	2.1446	-2.1446	PilZ domain-containing protein	2.14	0.0169	2.03	6.57	SAMN04487868_12643
A0A1I4HWA0	2.1479	-2.1479	Putative beta-barrel assembly-enhancing protease	2.15	0.0170	2.20	6.59	SAMN04487868_102105

A0A1I4HBL1	2.1480	-2.1480	Adenylosuccinate synthetase	2.15	0.0170	0.39	6.59	purA SAMN04487868_101262
A0A1I4HLK8	2.1504	-2.1504	Flagellar protein FliL	2.15	0.0169	1.89	6.60	SAMN04487868_101450
A0A1I4LLP5	2.1608	-2.1608	Riboflavin biosynthesis protein RibD	2.16	0.0169	0.42	6.66	SAMN04487868_11544
A0A1I4I9T6	2.1612	-2.1612	NADP-dependent 3-hydroxy acid dehydrogenase YdfG	2.16	0.0170	1.25	6.66	SAMN04487868_103115
A0A1I4M6Z7	2.1658	-2.1658	Arsenate reductase	2.17	0.0167	2.10	6.69	SAMN04487868_11962
A0A1I4HBV7	2.1662	-2.1662	Biotin synthase	2.17	0.0166	2.88	6.69	bioB SAMN04487868_101270
A0A1I4KRM8	2.1711	-2.1711	Uncharacterized protein	2.17	0.0166	1.15	6.71	SAMN04487868_1112
A0A1I4N4W6	2.1717	-2.1717	Single-stranded DNA-binding protein	2.17	0.0167	1.01	6.72	SAMN04487868_12931
A0A1I4JS83	2.1800	-2.1800	Phosphoglycolate phosphatase	2.18	0.0165	0.83	6.76	SAMN04487868_10736
A0A1I4KK47	2.1839	-2.1839	Cytochrome c-550 PedF	2.18	0.0165	1.61	6.78	SAMN04487868_11070
A0A1I4LYJ8	2.1883	-2.1883	Amino acid/amide ABC transporter ATP-binding protein 2. HAAT family	2.19	0.0166	1.64	6.81	SAMN04487868_11772
A0A1I4M2D6	2.1913	-2.1913	Microcin C transport system substrate-binding protein	2.19	0.0163	0.93	6.82	SAMN04487868_11857
A0A1I4I225	2.1955	-2.1955	Concanavalin A-like lectin/glucanases superfamily protein	2.20	0.0160	1.27	6.85	SAMN04487868_102224
A0A1I4L1I2	2.1998	-2.1998	Diguanylate cyclase (GGDEF) domain-containing protein	2.20	0.0161	1.14	6.87	SAMN04487868_11242
A0A1I4HE21	2.2058	-2.2058	ATP phosphoribosyltransferase	2.21	0.0158	0.74	6.90	hisG SAMN04487868_101326
A0A1I4KUY6	2.2066	-2.2066	Uncharacterized protein	2.21	0.0158	3.05	6.91	SAMN04487868_11173
A0A1I4M292	2.2088	-2.2088	Enoyl-[acyl-carrier-protein] reductase [NADH]	2.21	0.0157	1.17	6.92	SAMN04487868_11853
A0A1I4MS36	2.2223	-2.2223	ATP-dependent DNA helicase RecQ	2.22	0.0154	1.87	7.00	SAMN04487868_12538
A0A1I4L135	2.2241	-2.2241	Uncharacterized protein	2.22	0.0154	3.87	7.01	SAMN04487868_11238
A0A1I4NIT6	2.2317	-2.2317	Uncharacterized protein	2.23	0.0155	2.05	7.05	SAMN04487868_1424
A0A1I4L9Z5	2.2328	-2.2328	Uncharacterized protein	2.23	0.0155	6.71	7.06	SAMN04487868_11381
A0A1I4H9T9	2.2331	-2.2331	Amino acid ABC transporter substrate-binding protein. PAAT family (TC 3.A.1.3.-)	2.23	0.0156	0.86	7.06	SAMN04487868_101149
A0A1I4IS31	2.2388	-2.2388	Iron complex transport system substrate-binding protein	2.24	0.0158	3.28	7.09	SAMN04487868_104142
A0A1I4I0W0	2.2481	-2.2481	Predicted oxidoreductase	2.25	0.0152	1.06	7.14	SAMN04487868_102233
A0A1I4KP17	2.2552	-2.2552	High-affinity branched-chain amino acid transport ATP-binding protein	2.26	0.0151	1.42	7.18	SAMN04487868_110145
A0A1I4HT14	2.2578	-2.2578	Acyl dehydratase	2.26	0.0151	1.78	7.20	SAMN04487868_1023
A0A1I4K3R5	2.2592	-2.2592	Uncharacterized protein	2.26	0.0152	1.25	7.21	SAMN04487868_10865
A0A1I4HYA0	2.2661	-2.2661	Cell division and transport-associated protein TolA	2.27	0.0153	1.14	7.25	SAMN04487868_102112
A0A1I4L4Q9	2.2679	-2.2679	Type VI secretion system protein ImpL	2.27	0.0153	1.70	7.26	SAMN04487868_112140
A0A1I4M6R2	2.2692	-2.2692	RNA polymerase sigma factor RpoS	2.27	0.0154	0.54	7.27	rpoS SAMN04487868_11946
A0A1I4I217	2.2706	-2.2706	Uncharacterized protein	2.27	0.0154	2.66	7.27	SAMN04487868_102223
A0A1I4JEZ1	2.2902	-2.2902	2-hydroxychromene-2-carboxylate isomerase	2.29	0.0147	2.21	7.39	SAMN04487868_10613
A0A1I4JLA1	2.2905	-2.2905	Pantothenate synthetase	2.29	0.0147	0.86	7.39	panC SAMN04487868_106155
A0A1I4JK26	2.2989	-2.2989	Transcriptional regulator. LysR family	2.30	0.0133	1.09	7.44	SAMN04487868_106127
A0A1I4J726	2.3009	-2.3009	Uncharacterized protein	2.30	0.0134	1.23	7.45	SAMN04487868_105109
A0A1I4IU16	2.3010	-2.3010	HD-like signal output (HDOD) domain. no enzymatic activity	2.30	0.0134	0.60	7.45	SAMN04487868_104171
A0A1I4MNN6	2.3038	-2.3038	DNA-binding response regulator. OmpR family. contains REC and winged-helix (WHTH) domain	2.30	0.0131	1.19	7.47	SAMN04487868_12431

A0A1I4HYM0	2.3085	-2.3085	DNA-binding transcriptional regulator. MarR family	2.31	0.0132	0.78	7.50	SAMN04487868_102172
A0A1I4KRQ7	2.3099	-2.3099	Imidazole glycerol phosphate synthase subunit HisH	2.31	0.0133	1.08	7.51	hisH SAMN04487868_1114
A0A1I4LA44	2.3170	-2.3170	Protein SCO1/2	2.29	0.0143	5.37	13.94	SAMN04487868_11392
A0A1I4LHL4	2.3182	-2.3182	DNA-binding transcriptional regulator. GntR family	2.32	0.0135	0.93	7.56	SAMN04487868_11498
A0A1I4NE01	2.3186	-2.3186	Anti-anti-sigma factor	2.32	0.0135	2.41	7.56	SAMN04487868_13416
A0A1I4J8L9	2.3200	-2.3200	Type IV pilus assembly protein PilF	2.32	0.0135	1.42	7.57	SAMN04487868_105142
A0A1I4KS39	2.3241	-2.3241	Fe-S cluster assembly ATP-binding protein	2.32	0.0136	1.39	7.59	SAMN04487868_11126
A0A1I4NED8	2.3276	-2.3276	Arsenical resistance protein ArsH	2.33	0.0133	0.98	7.61	SAMN04487868_1353
A0A1I4H705	2.3285	-2.3285	Putative membrane protein	2.33	0.0133	0.95	7.62	SAMN04487868_101140
A0A1I4I173	2.3317	-2.3317	Transcriptional regulator. TetR family	2.33	0.0134	1.79	7.64	SAMN04487868_102196
A0A1I4N0Y0	2.3375	-2.3375	Iron complex outermembrane recepter protein	2.34	0.0135	1.18	7.67	SAMN04487868_12820
A0A1I4MW68	2.3381	-2.3381	Zinc transport system substrate-binding protein	2.34	0.0135	1.87	7.68	SAMN04487868_12629
A0A1I4NF26	2.3421	-2.3421	50S ribosomal protein L1	2.34	0.0136	0.85	7.70	rplA SAMN04487868_1369
A0A1I4HFB7	2.3421	-2.3421	Type IV pilus assembly protein PilC	2.34	0.0136	1.32	7.70	SAMN04487868_101345
A0A1I4J8K7	2.3506	-2.3506	Succinate--CoA ligase [ADP-forming] subunit alpha	2.35	0.0132	0.94	7.75	sucD SAMN04487868_105175
A0A1I4L4V5	2.3566	-2.3566	Type VI secretion system protein ImpK	2.33	0.0134	5.32	14.53	SAMN04487868_112135
A0A1I4I1U9	2.3577	-2.3577	Uncharacterized protein	2.36	0.0133	1.86	7.80	SAMN04487868_102225
A0A1I4HCH0	2.3626	-2.3626	DNA polymerase III. delta subunit	2.36	0.0134	0.80	7.83	SAMN04487868_101281
A0A1I4M733	2.3667	-2.3667	Thiol-disulfide isomerase or thioredoxin	2.37	0.0132	1.00	7.85	SAMN04487868_11961
A0A1I4MJW2	2.3749	-2.3749	Methylglyoxal synthase	2.37	0.0127	1.54	7.91	mgsA SAMN04487868_12316
A0A1I4JH14	2.3822	-2.3822	Uroporphyrin-3 C-methyltransferase	2.38	0.0124	0.64	7.95	SAMN04487868_10659
A0A1I4N3N0	2.3987	-2.3987	30S ribosomal protein S19	2.40	0.0123	0.73	8.06	rpsS SAMN04487868_1297
A0A1I4J3R2	2.4032	-2.4032	Gamma-glutamyltranspeptidase / glutathione hydrolase	2.40	0.0124	2.19	8.09	SAMN04487868_10524
A0A1I4MPW6	2.4088	-2.4088	TRAP-type C4-dicarboxylate transport system. substrate-binding protein	2.41	0.0125	2.68	8.12	SAMN04487868_12448
A0A1I4HF76	2.4106	-2.4106	LPS O-antigen chain length determinant protein. WzzB/FepE family	2.41	0.0125	1.66	8.13	SAMN04487868_101356
A0A1I4IW44	2.4144	-2.4144	Peptidyl-prolyl cis-trans isomerase	2.41	0.0126	0.72	8.16	SAMN04487868_104235
A0A1I4M151	2.4167	-2.4167	Phosphoserine phosphatase	2.42	0.0126	1.07	8.17	SAMN04487868_11814
A0A1I4JT02	2.4170	-2.4170	Siderophore synthetase component	2.42	0.0126	4.19	8.18	SAMN04487868_10769
A0A1I4M3E0	2.4270	-2.4270	DNA polymerase III subunit epsilon	2.43	0.0120	2.52	8.24	dnaQ SAMN04487868_11862
A0A1I4HJN6	2.4287	-2.4287	LemA protein	2.43	0.0121	0.91	8.25	SAMN04487868_101403
A0A1I4JLY8	2.4326	-2.4326	Hydroxymethylpyrimidine/phosphomethylpyrimidine kinase	2.43	0.0121	1.15	8.28	SAMN04487868_106177
A0A1I4MYL7	2.4346	-2.4346	O-acetylhomoserine sulfhydrylase	2.43	0.0117	0.67	8.29	SAMN04487868_12743
A0A1I4I2H7	2.4372	-2.4372	Glucokinase	2.44	0.0118	3.14	8.31	glk SAMN04487868_102252
A0A1I4H7P7	2.4398	-2.4398	Uncharacterized protein	2.44	0.0118	1.93	8.32	SAMN04487868_101123
A0A1I4J9Q5	2.4465	-2.4465	Leucine dehydrogenase	2.45	0.0119	2.53	8.37	SAMN04487868_105197
A0A1I4I189	2.4486	-2.4486	Transcriptional regulator. RpiR family	2.45	0.0119	1.75	8.38	SAMN04487868_102260
A0A1I4L4N0	2.4560	-2.4560	Uncharacterized protein	2.46	0.0116	0.93	8.43	SAMN04487868_112105
A0A1I4LFA8	2.4620	-2.4620	Isovaleryl-CoA dehydrogenase	2.46	0.0117	0.41	8.47	SAMN04487868_11440
A0A1I4HI95	2.4756	-2.4756	Response regulator receiver modulated diguanylate cyclase	2.48	0.0114	0.38	8.57	SAMN04487868_101391

A0A1I4I7X9	2.4774	-2.4774	D-methionine transport system substrate-binding protein	2.48	0.0114	2.24	8.58	SAMN04487868_10328
A0A1I4HBC0	2.4866	-2.4866	N-acetylmuramoyl-L-alanine amidase	2.49	0.0107	2.61	8.64	SAMN04487868_101254
A0A1I4LME5	2.4899	-2.4899	Type IV pilus assembly protein PilP	2.49	0.0108	0.89	8.66	SAMN04487868_11557
A0A1I4HZS1	2.4960	-2.4960	TolA-binding protein	2.50	0.0104	1.15	8.70	SAMN04487868_102214
A0A1I4J2U2	2.4993	-2.4993	Aminotransferase	2.50	0.0105	1.03	8.73	SAMN04487868_10538
A0A1I4HBS1	2.5085	-2.5085	Uncharacterized protein	2.51	0.0105	2.59	8.79	SAMN04487868_101267
A0A1I4ILV6	2.5161	-2.5161	Protein phosphatase	2.52	0.0101	1.09	8.84	SAMN04487868_10429
A0A1I4L4P8	2.5169	-2.5169	Type VI secretion system protein VasG	2.52	0.0102	1.06	8.85	SAMN04487868_112136
A0A1I4N3H1	2.5204	-2.5204	30S ribosomal protein S8	2.52	0.0102	1.01	8.87	rpsH SAMN04487868_12917
A0A1I4J8U8	2.5211	-2.5211	DNA-binding transcriptional regulator. GntR family	2.52	0.0102	1.00	8.88	SAMN04487868_105181
A0A1I4M177	2.5329	-2.5329	50S ribosomal protein L3 glutamine methyltransferase	2.53	0.0100	0.84	8.96	prmB SAMN04487868_11826
A0A1I4LRK9	2.5382	-2.5382	Chromosome partitioning protein. ParB family	2.54	0.0100	0.86	9.00	SAMN04487868_11626
A0A1I4H4E3	2.5392	-2.5392	SWIM/SEC-C metal-binding motif-containing protein. PBPRA1643 family	2.54	0.0100	3.10	9.01	SAMN04487868_10168
A0A1I4L0Z5	2.5477	-2.5477	Uncharacterized protein	2.55	0.0097	3.20	9.07	SAMN04487868_11235
A0A1I4L110	2.5516	-2.5516	Uncharacterized protein	2.55	0.0098	3.88	9.10	SAMN04487868_11236
A0A1I4HC89	2.5539	-2.5539	ATP-dependent dethiobiotin synthetase BioD	2.55	0.0096	1.86	9.11	bioD SAMN04487868_101274
A0A1I4H9E2	2.5799	-2.5799	Peptidase_M75 domain-containing protein	2.58	0.0092	3.09	9.30	SAMN04487868_101193
A0A1I4JHV1	2.5828	-2.5828	Esterase	2.58	0.0090	0.75	9.32	SAMN04487868_10681
A0A1I4MSQ8	2.6008	-2.6008	Acyltransferase	2.60	0.0085	0.56	9.46	SAMN04487868_12539
A0A1I4K2R4	2.6040	-2.6040	Hemoglobin/transferrin/lactoferrin receptor protein	2.60	0.0085	3.95	9.48	SAMN04487868_10862
A0A1I4MW08	2.6073	-2.6073	Na(+)-translocating NADH-quinone reductase subunit C	2.61	0.0086	1.37	9.50	nqrC SAMN04487868_12614
A0A1I4N6X6	2.6154	-2.6154	DNA recombination protein RmuC	2.62	0.0087	0.72	9.56	SAMN04487868_13021
A0A1I4H963	2.6167	-2.6167	TRAP-type C4-dicarboxylate transport system. substrate-binding protein	2.62	0.0087	1.09	9.57	SAMN04487868_101197
A0A1I4L7Y5	2.6170	-2.6170	Chromosomal replication initiator protein DnaA	2.62	0.0088	0.86	9.58	dnaA SAMN04487868_11341
A0A1I4N1U3	2.6205	-2.6205	DNA-binding transcriptional regulator. LysR family	2.62	0.0088	2.10	9.60	SAMN04487868_12828
A0A1I4H5D6	2.6215	-2.6215	Uncharacterized protein	2.62	0.0088	3.86	9.61	SAMN04487868_101100
A0A1I4JTB8	2.6287	-2.6287	Siderophore synthetase component	2.63	0.0089	4.72	9.67	SAMN04487868_10767
A0A1I4JHZ0	2.6316	-2.6316	Transcription termination factor Rho	2.63	0.0084	0.63	9.69	rho SAMN04487868_10655
A0A1I4M6I2	2.6434	-2.6434	Enolase	2.64	0.0086	0.57	9.78	eno SAMN04487868_11955
A0A1I4N6E2	2.6445	-2.6445	DNA-binding transcriptional regulator. MerR family	2.64	0.0086	0.85	9.79	SAMN04487868_13012
A0A1I4LRJ6	2.6519	-2.6519	CobQ/CobB/MinD/ParA nucleotide binding domain-containing protein	2.65	0.0086	0.86	9.84	SAMN04487868_11625
A0A1I4LLA1	2.6538	-2.6538	Type IV pilus assembly protein PilW	2.65	0.0087	0.52	9.86	SAMN04487868_11517
A0A1I4H4K1	2.6676	-2.6676	Two component transcriptional regulator. LuxR family	2.67	0.0089	3.42	9.97	SAMN04487868_10183
A0A1I4M219	2.6692	-2.6692	N-(5'-phosphoribosyl)anthranilate isomerase	2.67	0.0089	0.80	9.98	trpF SAMN04487868_11836
A0A1I4KRA5	2.6699	-2.6699	Imidazoleglycerol-phosphate dehydratase	2.67	0.0090	0.80	9.98	hisB SAMN04487868_1113
A0A1I4N550	2.6710	-2.6710	MSHA biogenesis protein MshN	2.67	0.0090	2.33	9.99	SAMN04487868_12938
A0A1I4M2K3	2.6724	-2.6724	Membrane-bound lytic murein transglycosylase D	2.67	0.0090	2.47	10.00	SAMN04487868_11858
A0A1I4KIR5	2.6768	-2.6768	Uncharacterized protein	2.68	0.0091	1.16	10.04	SAMN04487868_11022
A0A1I4KSE0	2.6770	-2.6770	Cysteine desulfurase	2.68	0.0091	1.76	10.04	SAMN04487868_11124

A0A1I4JAQ5	2.6797	-2.6797	Uncharacterized protein	2.68	0.0092	1.04	10.06	SAMN04487868_105222
A0A1I4ISP1	2.6805	-2.6805	Tripartite ATP-independent transporter solute receptor. DctP family	2.68	0.0092	1.76	10.07	SAMN04487868_104121
A0A1I4K2Y0	2.6823	-2.6823	Glutathione S-transferase	2.68	0.0092	0.81	10.08	SAMN04487868_10866
A0A1I4L3L5	2.6829	-2.6829	Pyrimidine operon attenuation protein / uracil phosphoribosyltransferase	2.68	0.0093	1.16	10.09	SAMN04487868_11273
A0A1I4L264	2.6838	-2.6838	Chemosensory pili system protein ChpC	2.68	0.0093	1.67	10.09	SAMN04487868_11261
A0A1I4KSC8	2.6840	-2.6840	cAMP-binding domain of CRP or a regulatory subunit of cAMP-dependent protein kinases	2.68	0.0094	1.28	10.10	SAMN04487868_11134
A0A1I4L154	2.6904	-2.6904	Uncharacterized protein	2.69	0.0089	4.91	10.15	SAMN04487868_11239
A0A1I4J7Y0	2.6957	-2.6957	MOSC domain-containing protein	2.70	0.0084	0.53	10.19	SAMN04487868_105157
A0A1I4L4D9	2.6998	-2.6998	Type VI secretion system protein ImpB	2.70	0.0084	5.35	10.22	SAMN04487868_112127
A0A1I4N0Y1	2.7004	-2.7004	Ribonucleoside-diphosphate reductase subunit beta	2.70	0.0085	1.81	10.23	SAMN04487868_12825
A0A1I4LN66	2.7029	-2.7029	HAD-superfamily subfamily IB hydrolase. TIGR01490	2.70	0.0086	1.10	10.25	SAMN04487868_11573
A0A1I4I2R1	2.7062	-2.7062	Ferredoxin--NADP+ reductase	2.71	0.0087	1.88	10.27	SAMN04487868_102292
A0A1I4HDI1	2.7083	-2.7083	Lipopolysaccharide export system protein LptC	2.71	0.0087	1.73	10.29	lptC SAMN04487868_101316
A0A1I4JTI7	2.7097	-2.7097	Iron complex transport system ATP-binding protein	2.71	0.0087	2.73	10.30	SAMN04487868_10761
A0A1I4LGD8	2.7268	-2.7268	Two-component system. chemotaxis family. response regulator CheV	2.73	0.0088	1.92	10.44	SAMN04487868_11462
A0A1I4KW64	2.7399	-2.7399	Uncharacterized protein	2.74	0.0090	1.91	10.55	SAMN04487868_111107
A0A1I4N1N6	2.7690	-2.7690	Ribonucleoside-diphosphate reductase	2.77	0.0085	1.54	10.79	SAMN04487868_12824
A0A1I4KK30	2.7758	-2.7758	ABC-2 type transport system ATP-binding protein	2.78	0.0086	1.40	10.85	SAMN04487868_11067
A0A1I4I3C1	2.7805	-2.7805	Amino acid ABC transporter substrate-binding protein. PAAT family	2.78	0.0080	0.54	10.89	SAMN04487868_102283
A0A1I4L2E6	2.7864	-2.7864	Twitching motility protein PilI	2.79	0.0081	2.56	10.94	SAMN04487868_11266
A0A1I4HEE9	2.7962	-2.7962	Bax protein	2.80	0.0082	1.39	11.02	SAMN04487868_101337
A0A1I4KA27	2.8088	-2.8088	Uncharacterized protein involved in outer membrane biogenesis	2.81	0.0076	0.91	11.13	SAMN04487868_10924
A0A1I4MYQ6	2.8240	-2.8240	Ribosome biogenesis GTPase A	2.82	0.0078	0.43	11.27	SAMN04487868_12747
A0A1I4N3Q2	2.8264	-2.8264	50S ribosomal protein L4	2.83	0.0079	0.57	11.29	rplD SAMN04487868_1294
A0A1I4JSB7	2.8351	-2.8351	Acetoin utilization deacetylase AcuC	2.84	0.0072	0.96	11.36	SAMN04487868_10743
A0A1I4KV49	2.8374	-2.8374	UPF0176 protein SAMN04487868_111100	2.84	0.0073	3.47	11.38	SAMN04487868_111100
A0A1I4J5D5	2.8457	-2.8457	Uncharacterized protein	2.85	0.0074	3.31	11.46	SAMN04487868_10598
A0A1I4JT98	2.8462	-2.8462	Fe(3+) dicitrate transport protein	2.85	0.0074	3.57	11.46	SAMN04487868_10765
A0A1I4KE68	2.8544	-2.8544	Type I restriction enzyme. S subunit	2.85	0.0075	0.77	11.54	SAMN04487868_109119
A0A1I4J8R1	2.8549	-2.8549	Segregation and condensation protein B	2.85	0.0075	1.41	11.54	SAMN04487868_105178
A0A1I4MX91	2.8555	-2.8555	Malonyl CoA-acyl carrier protein transacylase	2.86	0.0076	1.77	11.55	SAMN04487868_12656
A0A1I4IT43	2.8563	-2.8563	Two component transcriptional regulator. LuxR family	2.86	0.0076	1.60	11.55	SAMN04487868_104167
A0A1I4K1Q0	2.8659	-2.8659	Uncharacterized protein	2.87	0.0078	1.26	11.64	SAMN04487868_10825
A0A1I4LK02	2.8721	-2.8721	Type IV fimbrial biogenesis protein FimT	2.87	0.0079	2.18	11.70	SAMN04487868_11515
A0A1I4KTW4	2.8828	-2.8828	Sulfotransferase	2.88	0.0075	3.52	11.80	SAMN04487868_11170
A0A1I4M605	2.8958	-2.8958	Protein-L-isoaspartate O-methyltransferase	2.90	0.0067	1.25	11.92	pcm SAMN04487868_11949
A0A1I4N067	2.8977	-2.8977	30S ribosomal protein S6	2.90	0.0068	0.91	11.93	rpsF SAMN04487868_12758
A0A1I4MP75	2.9190	-2.9190	Acetyltransferase component of pyruvate dehydrogenase complex	2.92	0.0069	3.28	12.13	SAMN04487868_12455
A0A1I4N191	2.9206	-2.9206	Transcriptional regulator. LysR family	2.92	0.0069	1.17	12.15	SAMN04487868_12829

A0A1I4N342	2.9306	-2.9306	50S ribosomal protein L29	2.93	0.0070	1.75	12.24	rpmC SAMN04487868_12911
A0A1I4ITR2	2.9350	-2.9350	Adenylate kinase	2.93	0.0071	1.33	12.29	adk SAMN04487868_104182
A0A1I4KCY2	2.9383	-2.9383	Isocitrate dehydrogenase [NADP]	2.94	0.0071	1.81	12.32	SAMN04487868_10995
A0A1I4KTZ9	2.9401	-2.9401	Uncharacterized protein	2.94	0.0072	4.26	12.33	SAMN04487868_11172
A0A1I4IRH3	2.9455	-2.9455	Uncharacterized protein	2.95	0.0073	0.89	12.39	SAMN04487868_104107
A0A1I4JVR3	2.9547	-2.9547	DNA-binding response regulator. OmpR family. contains REC and winged-helix (WHTH) domain	2.95	0.0073	4.18	12.48	SAMN04487868_107141
A0A1I4JIT3	2.9564	-2.9564	DNA-binding transcriptional regulator. GntR family	2.96	0.0074	1.82	12.49	SAMN04487868_10678
A0A1I4M9W3	2.9611	-2.9611	ATP-dependent RNA helicase RhlE	2.96	0.0074	4.40	12.54	rhlE SAMN04487868_12043
A0A1I4KIH7	2.9785	-2.9785	MJ0042 family finger-like domain-containing protein	2.98	0.0067	0.44	12.71	SAMN04487868_11015
A0A1I4L2M7	2.9930	-2.9930	Twitching motility protein PilJ	2.99	0.0068	1.72	12.85	SAMN04487868_11265
A0A1I4H6S1	2.9963	-2.9963	LemA protein	3.00	0.0069	0.74	12.89	SAMN04487868_101138
A0A1I4LA25	2.9979	-2.9979	Uncharacterized protein	3.00	0.0070	1.66	12.90	SAMN04487868_11389
A0A1I4HX61	3.0076	-3.0076	2-isopropylmalate synthase	3.01	0.0071	2.68	13.00	leuA SAMN04487868_102132
A0A1I4I8D2	3.0210	-3.0210	TRAP-type mannitol/chloroaromatic compound transport system. substrate-binding protein	3.02	0.0072	2.59	13.14	SAMN04487868_10343
A0A1I4H915	3.0262	-3.0262	CxxC motif-containing protein. DUF1111 family	3.03	0.0074	2.05	13.19	SAMN04487868_101194
A0A1I4LYD4	3.0449	-3.0449	Protein SCO1/2	3.04	0.0076	2.74	13.38	SAMN04487868_11768
A0A1I4L781	3.0954	-3.0954	Chromosome partitioning protein. ParB family	3.10	0.0069	0.61	13.92	SAMN04487868_11325
A0A1I4I2I7	3.0979	-3.0979	Phosphogluconate dehydratase	3.10	0.0070	3.97	13.94	edd SAMN04487868_102253
A0A1I4M2T2	3.0985	-3.0985	Microcin C transport system ATP-binding protein	3.10	0.0070	0.91	13.95	SAMN04487868_11854
A0A1I4KBX0	3.1211	-3.1211	Iron complex outermembrane recepter protein	3.12	0.0072	3.16	14.20	SAMN04487868_10946
A0A1I4J779	3.1217	-3.1217	Dual-specificity RNA methyltransferase RlmN	3.12	0.0073	4.09	14.20	rlmN SAMN04487868_105141
A0A1I4L0U2	3.1219	-3.1219	Uncharacterized protein	3.12	0.0073	3.53	14.21	SAMN04487868_11220
A0A1I4I239	3.1304	-3.1304	Bifunctional protein FolD	3.13	0.0075	0.54	14.30	folD SAMN04487868_102274
A0A1I4IVE4	3.1339	-3.1339	Thiol:disulfide interchange protein	3.13	0.0075	3.56	14.34	SAMN04487868_104216
A0A1I4L0Y9	3.1698	-3.1698	PDZ domain (Also known as DHR or GLGF)	3.17	0.0054	5.09	14.74	SAMN04487868_11234
A0A1I4KRS4	3.1772	-3.1772	Cysteine desulfuration protein SufE	3.18	0.0054	2.35	14.83	SAMN04487868_11121
A0A1I4KRC1	3.1894	-3.1894	Septal ring factor EnvC. activator of murein hydrolases AmiA and AmiB	3.19	0.0055	4.13	14.97	SAMN04487868_1119
A0A1I4L2Z4	3.2161	-3.2161	Nitroreductase	3.22	0.0056	3.25	15.28	SAMN04487868_11284
A0A1I4J6L0	3.2437	-3.2437	Vitamin B12-dependent ribonucleotide reductase	3.24	0.0059	6.00	15.60	SAMN04487868_10599
A0A1I4KL11	3.2594	-3.2594	PQQ-dependent catabolism-associated beta-propeller protein	3.26	0.0060	2.72	15.79	SAMN04487868_11068
A0A1I4KID5	3.2623	-3.2623	DNA-binding protein Fis	3.26	0.0061	4.83	15.83	SAMN04487868_11013
A0A1I4KME1	3.2834	-3.2834	Carbamoyl-phosphate synthase small chain	3.28	0.0048	0.61	16.08	carA SAMN04487868_110123
A0A1I4I692	3.3051	-3.3051	Uncharacterized protein	3.30	0.0050	1.19	16.35	SAMN04487868_1036
A0A1I4K2S4	3.3148	-3.3148	Iron complex transport system substrate-binding protein	3.31	0.0051	3.83	16.47	SAMN04487868_10861
A0A1I4JU49	3.3327	-3.3327	4-hydroxy-2-oxoheptanedioate aldolase	3.33	0.0051	5.37	16.69	SAMN04487868_10771
A0A1I4IF13	3.3350	-3.3350	TRAP-type mannitol/chloroaromatic compound transport system. substrate-binding protein	3.33	0.0052	2.53	16.72	SAMN04487868_103200

A0A1I4J9P7	3.3485	-3.3485	Succinate--CoA ligase [ADP-forming] subunit beta	3.34	0.0052	0.95	16.89	sucC SAMN04487868_105174
A0A1I4MYU8	3.3713	-3.3713	3-oxoacyl-[acyl-carrier-protein] synthase-1	3.37	0.0045	1.63	17.18	SAMN04487868_12750
A0A1I4HA38	3.3857	-3.3857	Peroxiredoxin. Ohr subfamily	3.38	0.0046	4.86	17.36	SAMN04487868_101156
A0A1I4HHL7	3.3969	-3.3969	CBS domain-containing protein	3.39	0.0047	2.35	17.50	SAMN04487868_101417
A0A1I4N796	3.4046	-3.4046	Mannosyl-3-phosphoglycerate phosphatase	3.40	0.0048	2.43	17.60	SAMN04487868_13032
A0A1I4L7X8	3.4326	-3.4326	Amino acid ABC transporter substrate-binding protein. PAAT family	3.42	0.0050	4.52	17.96	SAMN04487868_11333
A0A1I4I143	3.4383	-3.4383	Pyruvate kinase	3.43	0.0050	4.33	18.03	SAMN04487868_102255
A0A1I4HUB9	3.4584	-3.4584	Exopolysaccharide/PEP-CTERM locus tyrosine autokinase	3.45	0.0051	1.53	18.29	SAMN04487868_10264
A0A1I4HZ74	3.4607	-3.4607	tRNA-cytidine(32) 2-sulfurtransferase	3.45	0.0052	2.59	18.32	ttcA SAMN04487868_102195
A0A1I4I2L2	3.4813	-3.4813	2-dehydro-3-deoxyphosphogluconate aldolase / (4S)-4-hydroxy-2-oxoglutarate aldolase	3.47	0.0053	4.01	18.59	SAMN04487868_102257
A0A1I4MPD9	3.4821	-3.4821	Pyruvate dehydrogenase E1 component	3.47	0.0054	3.31	18.60	SAMN04487868_12456
A0A1I4KA41	3.4882	-3.4882	Diaminobutyrate--2-oxoglutarate transaminase	3.48	0.0055	2.50	18.68	SAMN04487868_10930
A0A1I4I168	3.4992	-3.4992	Glucose-6-phosphate 1-dehydrogenase	3.48	0.0056	3.86	18.82	zwf SAMN04487868_102259
A0A1I4JWN5	3.5267	-3.5267	Succinyl-diaminopimelate desuccinylase	3.51	0.0057	1.05	19.18	dapE SAMN04487868_107167
A0A1I4HE57	3.5424	-3.5424	8-amino-7-oxononanoate synthase	3.52	0.0057	3.35	19.38	bioF SAMN04487868_101271
A0A1I4N658	3.5784	-3.5784	Uncharacterized protein	3.55	0.0059	1.54	19.84	SAMN04487868_1302
A0A1I4M8N0	3.6037	-3.6037	Alkyl hydroperoxide reductase subunit F	3.57	0.0040	2.07	20.17	SAMN04487868_1203
A0A1I4KBB5	3.6133	-3.6133	Iron complex outermembrane recepter protein	3.58	0.0041	4.99	20.29	SAMN04487868_10952
A0A1I4I2L9	3.6240	-3.6240	6-phosphogluconolactonase	3.59	0.0043	5.72	20.42	pgl SAMN04487868_102258
A0A1I4KRN4	3.6435	-3.6435	Plasmid transfer operon. TraF. protein	3.61	0.0044	3.82	20.67	SAMN04487868_11118
A0A1I4HEE3	3.6635	-3.6635	Uncharacterized protein	3.62	0.0048	1.80	20.92	SAMN04487868_101330
A0A1I4K120	3.6982	-3.6982	TRAP-type mannitol/chloroaromatic compound transport system. substrate-binding protein	3.65	0.0051	4.28	21.35	SAMN04487868_10814
A0A1I4N3Y7	3.7162	-3.7162	50S ribosomal protein L5	3.66	0.0053	0.62	21.57	rplE SAMN04487868_12915
A0A1I4KT69	3.7366	-3.7366	3-oxoacyl-[acyl-carrier-protein] synthase-1	3.68	0.0028	1.02	21.81	SAMN04487868_11129
A0A1I4IEE4	3.7831	-3.7831	Putrescine-binding periplasmic protein	3.71	0.0028	2.63	22.36	SAMN04487868_103204
A0A1I4JHD2	3.8129	-3.8129	Uncharacterized protein	3.73	0.0029	4.18	22.70	SAMN04487868_10670
A0A1I4MXA1	3.8193	-3.8193	3-oxoacyl-[acyl-carrier-protein] reductase	3.73	0.0029	2.31	22.77	SAMN04487868_12657
A0A1I4IDM7	3.8324	-3.8324	Transcriptional regulator. IclR family	3.74	0.0030	0.91	22.92	SAMN04487868_103165
A0A1I4JSV3	3.8716	-3.8716	Iron complex transport system substrate-binding protein	3.76	0.0031	4.26	23.35	SAMN04487868_10764
A0A1I4L2X3	3.9565	-3.9565	AraC-type DNA-binding protein	3.81	0.0033	4.57	24.24	SAMN04487868_11280
A0A1I4ITR4	3.9762	-3.9762	HD-like signal output (HDOD) domain. no enzymatic activity	3.82	0.0034	0.79	24.44	SAMN04487868_104183
A0A1I4KHU1	4.0172	-4.0172	Pimeloyl-ACP methyl ester carboxylesterase	3.84	0.0036	3.23	24.83	SAMN04487868_11010
A0A1I4H608	4.0610	-4.0610	Phosphonate transport system substrate-binding protein	3.15	0.0055	5.74	37.43	SAMN04487868_10150
A0A1I4IDB3	4.0883	-4.0883	Methyl-accepting chemotaxis sensory transducer with Cache sensor	3.88	0.0040	2.85	25.48	SAMN04487868_103199
A0A1I4IQS8	4.1606	-4.1606	Osmoprotectant transport system substrate-binding protein	3.91	0.0042	2.81	26.10	SAMN04487868_104112
A0A1I4H6H5	4.1655	-4.1655	Signal transduction histidine kinase	3.91	0.0043	3.63	26.14	SAMN04487868_10182
A0A1I4KTX9	4.1946	-4.1946	Ig-like domain-containing protein	3.92	0.0044	2.77	26.37	SAMN04487868_11171
A0A1I4MRT4	4.5202	-4.5202	Phosphonate transport system substrate-binding protein	4.02	0.0054	2.58	28.45	SAMN04487868_12529

A0A1I4H600	5.1247	-5.1247	TRAP-type mannitol/chloroaromatic compound transport system. substrate-binding protein	4.10	0.0063	6.41	30.34	SAMN04487868_10179
A0A1I4JSF8	5.2112	-5.2112	Dihydroorotase	4.11	0.0065	0.89	30.47	pyrC SAMN04487868_10745
A0A1I4HAK3	5.9494	-5.9494	Putative iron-regulated protein	4.13	0.0068	4.30	30.99	SAMN04487868_101195
A0A1I4MP49	Infinity	-Infinity	Fe(3+) dicitrate transport protein	4.34	0.0109	4.50	36.36	SAMN04487868_12430
A0A1I4J5U0	Infinity	-Infinity	Iron(III) transport system substrate-binding protein	4.56	0.0163	2.98	43.03	SAMN04487868_105107
A0A1I4JU40	Infinity	-Infinity	ATP-grasp domain-containing protein	5.10	0.0000	7.53	65.36	SAMN04487868_10770
A0A1I4I1M1	Infinity	-Infinity	Glyceraldehyde-3-phosphate dehydrogenase	5.05	0.0000	5.53	62.90	SAMN04487868_102254
A0A1I4NCV6	Infinity	-Infinity	Phosphomethylpyrimidine synthase	4.93	0.0000	5.43	57.30	thiC SAMN04487868_13332
A0A1I4I396	Infinity	-Infinity	ATP-dependent Clp protease ATP-binding subunit ClpX	4.21	0.0078	0.88	32.95	clpX SAMN04487868_102267
A0A1I4L4C8	Infinity	-Infinity	Type VI secretion system protein ImpC	4.38	0.0125	3.10	37.57	SAMN04487868_112128
A0A1I4L217	Infinity	-Infinity	Uncharacterized protein	4.23	0.0082	4.71	33.38	SAMN04487868_11237
A0A1I4MQ55	Infinity	-Infinity	L-lysine 2.3-aminomutase	4.44	0.0136	3.12	39.30	SAMN04487868_12457
A0A1I4IC04	Infinity	-Infinity	Muconate cycloisomerase	4.24	0.0091	3.99	33.70	SAMN04487868_103167

Table S 2: Proteins with significantly different detected abundances in *Marinobacter* sp. TT1 growing on *n*-hexadecane versus *n*-hexadecane and Corexit according to a Student's T-test (permutation-based FDR: $q < 0.05$).

UniProt ID	Hexadecane	Hxdc+Corexit	Description	-Log *p*-value	*q*-value	Student's T-test Diff. (log2 FC)	Student's T-test Test statistic	Gene names
A0A1I4MNH9	-4.0202	4.0202	TRAP-type mannitol/chloroaromatic compound transport system. substrate-binding protein	4.05	0.1070	-2.61	-15.99	SAMN04487868_12413
A0A1I4H696	-3.8126	3.8126	Uncharacterized protein	3.83	0.0428	-0.75	-14.04	SAMN04487868_101127
A0A1I4KRN4	-3.6668	3.6668	Plasmid transfer operon. TraF. protein	3.67	0.0411	-2.14	-12.85	SAMN04487868_11118
A0A1I4I3J1	-3.5274	3.5274	Amino acid ABC transporter ATP-binding protein. PAAT family	3.53	0.0492	-0.58	-11.82	SAMN04487868_102280
A0A1I4N9T3	-3.5065	3.5065	Formate dehydrogenase beta subunit	3.51	0.0403	-2.61	-11.67	SAMN04487868_13211
A0A1I4KD04	-3.4426	3.4426	TRAP-type mannitol/chloroaromatic compound transport system. substrate-binding protein	3.45	0.0369	-1.03	-11.23	SAMN04487868_109101
A0A1I4L217	-3.3683	3.3683	Uncharacterized protein	3.37	0.0367	-1.94	-10.74	SAMN04487868_11237
A0A1I4K653	-3.3163	3.3163	Membrane-bound lytic murein transglycosylase B	3.32	0.0306	-1.04	-10.41	SAMN04487868_108138
A0A1I4IF13	-3.2769	3.2769	TRAP-type mannitol/chloroaromatic compound transport system. substrate-binding protein	3.28	0.0355	-1.42	-10.17	SAMN04487868_103200
A0A1I4KHU1	-3.2690	3.2690	Pimeloyl-ACP methyl ester carboxylesterase	3.27	0.0338	-1.15	-10.12	SAMN04487868_11010
A0A1I4LRX3	-3.2367	3.2367	Uncharacterized protein	3.24	0.0321	-0.56	-9.93	SAMN04487868_11628
A0A1I4H9T9	-3.2135	3.2135	Amino acid ABC transporter substrate-binding protein. PAAT family (TC 3.A.1.3.-)	3.22	0.0307	-1.15	-9.79	SAMN04487868_101149
A0A1I4IEE4	-3.1886	3.1886	Putrescine-binding periplasmic protein	3.19	0.0372	-1.28	-9.65	SAMN04487868_103204
A0A1I4L2Z4	-3.1864	3.1864	Nitroreductase	3.19	0.0357	-1.02	-9.64	SAMN04487868_11284
A0A1I4LFA8	-3.1332	3.1332	Isovaleryl-CoA dehydrogenase	3.13	0.0385	-0.81	-9.33	SAMN04487868_11440
A0A1I4IU16	-3.0906	3.0906	HD-like signal output (HDOD) domain. no enzymatic activity	3.09	0.0386	-0.60	-9.10	SAMN04487868_104171
A0A1I4MSJ0	-3.0846	3.0846	Methyl-accepting chemotaxis sensory transducer with Cache sensor	3.09	0.0373	-0.48	-9.07	SAMN04487868_12535
A0A1I4NAC5	-3.0485	3.0485	Chaperone TorD involved in molybdoenzyme TorA maturation	3.05	0.0381	-1.81	-8.87	SAMN04487868_13214
A0A1I4M6R2	-2.9968	2.9968	RNA polymerase sigma factor RpoS	3.00	0.0403	-1.05	-8.60	rpoS SAMN04487868_11946

A0A1I4KRC1	-2.9513	2.9513	Septal ring factor EnvC. activator of murein hydrolases AmiA and AmiB	2.95	0.0431	-1.89	-8.37	SAMN04487868_1119
A0A1I4LG07	2.9585	-2.9585	Poly(Beta-D-mannuronate) lyase	2.96	0.0443	1.17	8.40	SAMN04487868_11454
A0A1I4MCV8	2.9795	-2.9795	GTP cyclohydrolase-2	2.98	0.0391	0.39	8.51	ribA SAMN04487868_12129
A0A1I4H2W3	3.0733	-3.0733	UPF0276 protein SAMN04487868_10132	3.07	0.0361	1.63	9.00	SAMN04487868_10132
A0A1I4H4S2	3.0978	-3.0978	Putative DNA-binding domain-containing protein	3.10	0.0399	1.45	9.14	SAMN04487868_10136
A0A1I4JB86	3.1016	-3.1016	Uncharacterized protein	3.10	0.0414	1.86	9.16	SAMN04487868_105204
A0A1I4KEY9	3.2029	-3.2029	Putative Cytochrome P450	3.20	0.0293	0.71	9.73	SAMN04487868_109135
A0A1I4K1M6	3.3296	-3.3296	Aminotransferase	3.33	0.0324	0.86	10.50	SAMN04487868_10835
A0A1I4L9J0	3.3438	-3.3438	Heat shock protein Hsp20	3.35	0.0344	1.46	10.59	SAMN04487868_11369
A0A1I4L2L6	3.3754	-3.3754	Uncharacterized protein	3.38	0.0393	2.34	10.79	SAMN04487868_11276
A0A1I4LG50	3.4309	-3.4309	Acetyl-CoA C-acetyltransferase	3.43	0.0341	1.17	11.15	SAMN04487868_11459
A0A1I4K9D1	3.5252	-3.5252	Fe-ADH domain-containing protein	3.53	0.0443	0.98	11.80	SAMN04487868_10910
A0A1I4HID5	3.7332	-3.7332	Acyl-CoA dehydrogenase	3.74	0.0306	0.55	13.37	SAMN04487868_101423
A0A1I4LMS6	3.7946	-3.7946	Predicted acylesterase/phospholipase RssA. contains patatin domain	3.81	0.0357	1.48	13.88	SAMN04487868_11570
A0A1I4J513	3.8541	-3.8541	Chaperone protein HtpG	3.87	0.0535	0.89	14.40	htpG SAMN04487868_10561
A0A1I4K5Z0	3.9326	-3.9326	Putative acyl-CoA dehydrogenase	3.95	0.0713	1.43	15.12	SAMN04487868_108121
A0A1I4KTN3	4.4066	-4.4066	Ferredoxin-NADP reductase	4.49	0.0000	2.43	20.73	SAMN04487868_11156

Table S 3: Proteins with significantly different detected abundances in *Marinobacter* sp. TT1 growing on *n*-hexadecane versus Corexit according to a Student's T-test (permutation-based FDR: $q < 0.05$).

UniProt ID	Hexadecane	Corexit	Description	-Log *p*-value	*q*-value	Student's T-test Diff. (log2 FC)	Student's T-test statistic	Gene names
A0A1I4KFD0	-Infinity	Infinity	Alkane 1-monooxygenase	4.58	0.0020	-7.98	-43.84	SAMN04487868_109143
A0A1I4I0J4	-Infinity	Infinity	Maltodextrin-binding protein	4.30	0.0013	-1.65	-35.14	SAMN04487868_102231
A0A1I4LA44	-Infinity	Infinity	Protein SCO1/2	4.46	0.0017	-4.37	-39.75	SAMN04487868_11392
A0A1I4M7N9	-12.1505	12.1505	Putative solute:sodium symporter small subunit	6.88	0.0000	-2.78	-82.22	SAMN04487868_11976
A0A1I4MSJ0	-10.8920	10.8920	Methyl-accepting chemotaxis sensory transducer with Cache sensor	6.73	0.0000	-2.39	-75.16	SAMN04487868_12535
A0A1I4L217	-7.6136	7.6136	Uncharacterized protein	6.15	0.0000	-5.10	-53.96	SAMN04487868_11237
A0A1I4MNH9	-7.4033	7.4033	TRAP-type mannitol/chloroaromatic compound transport system. substrate-binding protein	6.10	0.0000	-5.93	-52.34	SAMN04487868_12413
A0A1I4I3C1	-6.8033	6.8033	Amino acid ABC transporter substrate-binding protein. PAAT family	5.93	0.0000	-1.95	-47.45	SAMN04487868_102283
A0A1I4I3J1	-6.6658	6.6658	Amino acid ABC transporter ATP-binding protein. PAAT family	5.88	0.0000	-2.21	-46.26	SAMN04487868_102280
A0A1I4LE66	-6.5707	6.5707	Phytoene dehydrogenase-related protein	5.85	0.0000	-5.44	-45.42	SAMN04487868_11410
A0A1I4IEP8	-6.5546	6.5546	Acetyl-CoA synthetase	5.85	0.0000	-1.70	-45.28	SAMN04487868_103237
A0A1I4MGW8	-6.4819	6.4819	2.4-dienoyl-CoA reductase (NADPH2)	5.82	0.0000	-2.94	-44.63	SAMN04487868_12212
A0A1I4MFG3	-6.1657	6.1657	Acyl-CoA dehydrogenase	5.70	0.0000	-3.14	-41.70	SAMN04487868_12170
A0A1I4IDB3	-5.9339	5.9339	Methyl-accepting chemotaxis sensory transducer with Cache sensor	5.61	0.0000	-2.48	-39.44	SAMN04487868_103199
A0A1I4I0X1	-5.8572	5.8572	Amino acid/amide ABC transporter substrate-binding protein. HAAT family	5.57	0.0000	-3.16	-38.67	SAMN04487868_102234
A0A1I4N747	-5.6946	5.6946	Acyl-homoserine-lactone acylase	5.50	0.0000	-3.73	-36.98	SAMN04487868_13026
A0A1I4NA52	-5.5440	5.5440	4Fe-4S binding domain-containing protein	5.42	0.0000	-3.15	-35.37	SAMN04487868_13217
A0A1I4KJP9	-5.4119	5.4119	Two component transcriptional regulator. LuxR family	5.35	0.0000	-1.95	-33.90	SAMN04487868_11060
A0A1I4HFZ4	-5.3739	5.3739	Putative peptide ABC transporter substrate-binding protein	5.32	0.0000	-1.41	-33.46	SAMN04487868_101333
A0A1I4KKP8	-5.3017	5.3017	Alcohol dehydrogenase (Cytochrome c)	5.28	0.0000	-4.11	-32.63	SAMN04487868_11072
A0A1I4H9T9	-4.9606	4.9606	Amino acid ABC transporter substrate-binding protein. PAAT family (TC 3.A.1.3.-)	5.04	0.0000	-2.60	-28.44	SAMN04487868_101149
A0A1I4MPP2	-4.9481	4.9481	Uncharacterized protein	5.03	0.0000	-1.81	-28.28	SAMN04487868_12444
A0A1I4K120	-4.9443	4.9443	TRAP-type mannitol/chloroaromatic compound transport system. substrate-binding protein	5.03	0.0000	-3.01	-28.23	SAMN04487868_10814
A0A1I4IU16	-4.9336	4.9336	HD-like signal output (HDOD) domain. no enzymatic activity	5.02	0.0000	-2.69	-28.09	SAMN04487868_104171
A0A1I4KL11	-4.8534	4.8534	PQQ-dependent catabolism-associated beta-propeller protein	4.95	0.0027	-4.31	-27.02	SAMN04487868_11068
A0A1I4J3J4	-4.7974	4.7974	Putative ABC transport system permease protein	4.90	0.0027	-1.99	-26.27	SAMN04487868_10553
A0A1I4IN19	-4.7742	4.7742	Spermidine synthase	4.88	0.0025	-1.44	-25.95	SAMN04487868_10452
A0A1I4KK30	-4.7407	4.7407	ABC-2 type transport system ATP-binding protein	4.85	0.0025	-2.72	-25.49	SAMN04487868_11067
A0A1I4MLH2	-4.7264	4.7264	Ankyrin repeat	4.84	0.0024	-4.05	-25.29	SAMN04487868_12349
A0A1I4N0J7	-4.7157	4.7157	TRAP-type mannitol/chloroaromatic compound transport system. substrate-binding protein	4.83	0.0023	-1.78	-25.14	SAMN04487868_1285
A0A1I4IEE4	-4.6878	4.6878	Putrescine-binding periplasmic protein	4.80	0.0023	-2.05	-24.75	SAMN04487868_103204
A0A1I4MEH2	-4.6497	4.6497	Diguanylate cyclase (GGDEF) domain-containing protein	4.76	0.0022	-4.14	-24.21	SAMN04487868_12162
A0A1I4KAH7	-4.6321	4.6321	Uncharacterized protein	4.74	0.0022	-1.12	-23.96	SAMN04487868_10917
A0A1I4LXM2	-4.5731	4.5731	Methyl-accepting chemotaxis protein	4.68	0.0021	-3.46	-23.11	SAMN04487868_11735

A0A1I4KPK4	-4.4530	4.4530	Glucose/arabinose dehydrogenase. beta-propeller fold	4.55	0.0019	-2.44	-21.39	SAMN04487868_110153
A0A1I4HTJ9	-4.4387	4.4387	Glucose/arabinose dehydrogenase. beta-propeller fold	4.53	0.0018	-3.35	-21.18	SAMN04487868_10233
A0A1I4MP11	-4.4035	4.4035	Uncharacterized protein	4.49	0.0017	-2.13	-20.69	SAMN04487868_12443
A0A1I4IF13	-4.3757	4.3757	TRAP-type mannitol/chloroaromatic compound transport system. substrate-binding protein	4.46	0.0017	-2.80	-20.30	SAMN04487868_103200
A0A1I4KUY6	-4.3562	4.3562	Uncharacterized protein	4.44	0.0016	-2.56	-20.03	SAMN04487868_11173
A0A1I4H608	-4.3443	4.3443	Phosphonate transport system substrate-binding protein	3.97	0.0016	-6.38	-27.44	SAMN04487868_10150
A0A1I4KD04	-4.3280	4.3280	TRAP-type mannitol/chloroaromatic compound transport system. substrate-binding protein	4.40	0.0016	-2.52	-19.64	SAMN04487868_109101
A0A1I4KRN4	-4.3242	4.3242	Plasmid transfer operon. TraF. protein	4.40	0.0015	-4.53	-19.59	SAMN04487868_11118
A0A1I4IQS8	-4.3242	4.3242	Osmoprotectant transport system substrate-binding protein	4.40	0.0015	-2.21	-19.59	SAMN04487868_104112
A0A1I4N9T3	-4.3034	4.3034	Formate dehydrogenase beta subunit	4.37	0.0015	-4.70	-19.32	SAMN04487868_13211
A0A1I4LMF4	-4.2480	4.2480	Ig-like domain (Group 1)	4.31	0.0014	-0.81	-18.60	SAMN04487868_11565
A0A1I4LX91	-4.2474	4.2474	Putative peptidoglycan binding domain-containing protein	4.31	0.0014	-6.27	-18.59	SAMN04487868_11736
A0A1I4M035	-4.2307	4.2307	LysR family transcriptional regulator. cys regulon transcriptional activator	4.29	0.0013	-1.13	-18.38	SAMN04487868_11812
A0A1I4HGN2	-4.2266	4.2266	Type IV pilus assembly protein PilA	4.28	0.0013	-1.87	-18.33	SAMN04487868_101348
A0A1I4HGW5	-4.2228	4.2228	Flagellin	4.28	0.0013	-2.01	-18.28	SAMN04487868_101385
A0A1I4ISK2	-4.2214	4.2214	Short-chain dehydrogenase	4.28	0.0012	-1.23	-18.26	SAMN04487868_104157
A0A1I4L7X8	-4.2150	4.2150	Amino acid ABC transporter substrate-binding protein. PAAT family	4.27	0.0012	-3.17	-18.18	SAMN04487868_11333
A0A1I4JQL9	-4.2121	4.2121	Formate-dependent phosphoribosylglycinamide formyltransferase	4.27	0.0012	-0.60	-18.15	purT SAMN04487868_1072
A0A1I4I6L1	-4.1982	4.1982	Amidase	4.25	0.0012	-1.42	-17.98	SAMN04487868_10316
A0A1I4I0E5	-4.1958	4.1958	Putative flagellar protein	4.25	0.0012	-1.90	-17.95	SAMN04487868_102201
A0A1I4LK02	-4.1957	4.1957	Type IV fimbrial biogenesis protein FimT	4.25	0.0012	-1.45	-17.95	SAMN04487868_11515
A0A1I4HH13	-4.1938	4.1938	Zn-dependent protease with chaperone function	4.24	0.0012	-1.74	-17.92	SAMN04487868_101402
A0A1I4MP49	-4.1767	4.1767	Fe(3+) dicitrate transport protein	4.22	0.0011	-1.48	-17.72	SAMN04487868_12430
A0A1I4L8E1	-4.1611	4.1611	tRNA modification GTPase MnmE	4.21	0.0011	-1.90	-17.53	mnmE trmE SAMN04487868_11336
A0A1I4KTW4	-4.1595	4.1595	Sulfotransferase	4.20	0.0011	-2.83	-17.51	SAMN04487868_11170
A0A1I4KW64	-4.1414	4.1414	Uncharacterized protein	4.18	0.0011	-2.67	-17.30	SAMN04487868_111107
A0A1I4MNB7	-4.1242	4.1242	TRAP-type mannitol/chloroaromatic compound transport system. small permease component	4.16	0.0010	-2.72	-17.11	SAMN04487868_12412
A0A1I4IBF4	-4.1200	4.1200	Uncharacterized protein	4.16	0.0010	-4.17	-17.06	SAMN04487868_103146
A0A1I4KRC1	-4.1181	4.1181	Septal ring factor EnvC. activator of murein hydrolases AmiA and AmiB	4.16	0.0010	-3.87	-17.04	SAMN04487868_1119
A0A1I4I1J3	-4.1177	4.1177	Nitroreductase	4.16	0.0010	-1.15	-17.03	SAMN04487868_102251
A0A1I4HFB7	-4.1075	4.1075	Type IV pilus assembly protein PilC	4.15	0.0010	-1.23	-16.92	SAMN04487868_101345
A0A1I4L110	-4.0903	4.0903	Uncharacterized protein	4.13	0.0010	-3.83	-16.73	SAMN04487868_11236
A0A1I4IF29	-4.0676	4.0676	Amino acid/amide ABC transporter substrate-binding protein. HAAT family	4.10	0.0009	-3.97	-16.48	SAMN04487868_103242
A0A1I4J808	-4.0535	4.0535	Uncharacterized protein	4.08	0.0009	-2.00	-16.33	SAMN04487868_105161
A0A1I4NA64	-4.0335	4.0335	Iron-sulfur cluster carrier protein	4.06	0.0009	-3.82	-16.12	SAMN04487868_13218
A0A1I4MJN9	-4.0247	4.0247	Periplasmic/7TM domain sensor diguanylate cyclase	4.05	0.0018	-2.23	-16.03	SAMN04487868_12314
A0A1I4KZV5	-4.0100	4.0100	Amino acid/amide ABC transporter substrate-binding protein. HAAT family	4.04	0.0018	-2.26	-15.88	SAMN04487868_11214

A0A1I4LM79	-3.9983	3.9983	Penicillin-binding protein 1A	4.02	0.0017	-1.67	-15.76	SAMN04487868_11561
A0A1I4LYJ8	-3.9864	3.9864	Amino acid/amide ABC transporter ATP-binding protein 2. HAAT family	4.01	0.0017	-3.03	-15.64	SAMN04487868_11772
A0A1I4KV15	-3.9803	3.9803	Methyl-accepting chemotaxis protein	4.00	0.0017	-1.68	-15.58	SAMN04487868_11175
A0A1I4MAS4	-3.9668	3.9668	Transcriptional regulator. TetR family	3.99	0.0016	-1.05	-15.45	SAMN04487868_12060
A0A1I4I8D2	-3.9662	3.9662	TRAP-type mannitol/chloroaromatic compound transport system. substrate-binding protein	3.99	0.0016	-3.52	-15.44	SAMN04487868_10343
A0A1I4MEF9	-3.9633	3.9633	Flavin prenyltransferase UbiX	3.99	0.0016	-1.80	-15.42	ubiX SAMN04487868_12169
A0A1I4JKK0	-3.9630	3.9630	Pilus retraction ATPase PilT	3.99	0.0016	-0.88	-15.41	SAMN04487868_106109
A0A1I4N6E2	-3.9398	3.9398	DNA-binding transcriptional regulator. MerR family	3.96	0.0015	-1.08	-15.19	SAMN04487868_13012
A0A1I4KHU1	-3.9392	3.9392	Pimeloyl-ACP methyl ester carboxylesterase	3.96	0.0015	-1.62	-15.18	SAMN04487868_11010
A0A1I4JIT3	-3.8887	3.8887	DNA-binding transcriptional regulator. GntR family	3.91	0.0022	-0.70	-14.71	SAMN04487868_10678
A0A1I4JRY3	-3.8869	3.8869	Acetyl-CoA C-acetyltransferase	3.90	0.0022	-2.45	-14.70	SAMN04487868_10729
A0A1I4I9U1	-3.8745	3.8745	Amino acid/amide ABC transporter substrate-binding protein. HAAT family	3.89	0.0021	-1.80	-14.58	SAMN04487868_10357
A0A1I4LGD8	-3.8612	3.8612	Two-component system. chemotaxis family. response regulator CheV	3.88	0.0029	-1.73	-14.46	SAMN04487868_11462
A0A1I4HCQ1	-3.8559	3.8559	Uncharacterized protein	3.87	0.0028	-3.73	-14.42	SAMN04487868_101225
A0A1I4LMK3	-3.8536	3.8536	Type IV pilus assembly protein PilM	3.87	0.0028	-1.24	-14.40	SAMN04487868_11560
A0A1I4IDA3	-3.8519	3.8519	Choline dehydrogenase	3.87	0.0028	-2.32	-14.38	SAMN04487868_103156
A0A1I4MVF2	-3.8519	3.8519	Uncharacterized conserved protein. tellurite resistance protein B (TerB) family	3.87	0.0028	-1.07	-14.38	SAMN04487868_12623
A0A1I4JRX0	-3.8508	3.8508	3-hydroxyacyl-CoA dehydrogenase / enoyl-CoA hydratase / 3-hydroxybutyryl-CoA epimerase	3.87	0.0027	-2.50	-14.37	SAMN04487868_10730
A0A1I4LEV0	-3.8412	3.8412	Methylglutaconyl-CoA hydratase	3.86	0.0027	-1.52	-14.29	SAMN04487868_11438
A0A1I4KF71	-3.8405	3.8405	Choline dehydrogenase	3.85	0.0027	-4.63	-14.28	SAMN04487868_109140
A0A1I4MFZ2	-3.8375	3.8375	Uncharacterized protein	3.85	0.0027	-4.83	-14.25	SAMN04487868_1224
A0A1I4MRT4	-3.8156	3.8156	Phosphonate transport system substrate-binding protein	3.83	0.0026	-1.43	-14.06	SAMN04487868_12529
A0A1I4L2M5	-3.8109	3.8109	DNA-binding protein HU-alpha	3.82	0.0026	-2.50	-14.02	SAMN04487868_11277
A0A1I4LYW9	-3.8097	3.8097	Amino acid/amide ABC transporter substrate-binding protein. HAAT family	3.82	0.0026	-2.96	-14.01	SAMN04487868_11776
A0A1I4HC58	-3.8080	3.8080	Geranyl-CoA carboxylase beta subunit	3.82	0.0026	-2.30	-14.00	SAMN04487868_101223
A0A1I4L0Z5	-3.7782	3.7782	Uncharacterized protein	3.79	0.0026	-2.59	-13.75	SAMN04487868_11235
A0A1I4MEC9	-3.7778	3.7778	Putative peptidoglycan binding domain-containing protein	3.79	0.0025	-2.16	-13.74	SAMN04487868_12144
A0A1I4K2Y0	-3.7658	3.7658	Glutathione S-transferase	3.78	0.0025	-0.87	-13.64	SAMN04487868_10866
A0A1I4MM83	-3.7536	3.7536	Glycolate oxidase iron-sulfur subunit	3.76	0.0038	-1.42	-13.54	SAMN04487868_1247
A0A1I4N7P5	-3.7322	3.7322	Virulence factor lipase N-terminal	3.74	0.0038	-1.25	-13.37	SAMN04487868_13027
A0A1I4KTZ9	-3.7225	3.7225	Uncharacterized protein	3.73	0.0037	-3.66	-13.29	SAMN04487868_11172
A0A1I4LA02	-3.7221	3.7221	Cytochrome c oxidase subunit 2	3.73	0.0037	-2.16	-13.28	SAMN04487868_11384
A0A1I4HK54	-3.6977	3.6977	Uncharacterized protein	3.71	0.0036	-2.78	-13.09	SAMN04487868_101435
A0A1I4L2E6	-3.6747	3.6747	Twitching motility protein PilI	3.68	0.0036	-1.48	-12.91	SAMN04487868_11266
A0A1I4KF83	-3.6712	3.6712	Outer membrane protein	3.68	0.0036	-4.53	-12.88	SAMN04487868_109138
A0A1I4HZS1	-3.6682	3.6682	TolA-binding protein	3.68	0.0035	-1.33	-12.86	SAMN04487868_102214
A0A1I4J5U0	-3.6666	3.6666	Iron(III) transport system substrate-binding protein	3.67	0.0035	-0.63	-12.85	SAMN04487868_105107
A0A1I4KL18	-3.6631	3.6631	Amino acid/amide ABC transporter substrate-binding protein. HAAT family	3.67	0.0035	-3.12	-12.82	SAMN04487868_11069

A0A1I4NAA3	-3.6432	3.6432	Formate dehydrogenase subunit gamma	3.65	0.0034	-2.97	-12.67	SAMN04487868_13210
A0A1I4L135	-3.6389	3.6389	Uncharacterized protein	3.65	0.0034	-2.93	-12.63	SAMN04487868_11238
A0A1I4I1B2	-3.6068	3.6068	Carbohydrate ABC transporter substrate-binding protein. CUT1 family	3.61	0.0038	-1.67	-12.39	SAMN04487868_102238
A0A1I4LME5	-3.6066	3.6066	Type IV pilus assembly protein PilP	3.61	0.0038	-0.92	-12.39	SAMN04487868_11557
A0A1I4JF87	-3.5933	3.5933	Peptide/nickel transport system substrate-binding protein	3.60	0.0038	-1.66	-12.29	SAMN04487868_10622
A0A1I4MAB0	-3.5921	3.5921	Uncharacterized protein	3.60	0.0038	-4.21	-12.28	SAMN04487868_12042
A0A1I4KKB9	-3.5898	3.5898	Aldehyde dehydrogenase	3.60	0.0038	-1.83	-12.27	SAMN04487868_11076
A0A1I4KSI9	-3.5793	3.5793	Signal transduction histidine kinase	3.58	0.0037	-1.99	-12.19	SAMN04487868_11145
A0A1I4LGY6	-3.5729	3.5729	Amino acid/amide ABC transporter substrate-binding protein. HAAT family	3.58	0.0037	-4.67	-12.14	SAMN04487868_11470
A0A1I4KBX0	-3.5710	3.5710	Iron complex outermembrane recepter protein	3.58	0.0037	-1.93	-12.13	SAMN04487868_10946
A0A1I4MYT3	-3.5656	3.5656	Uncharacterized protein	3.57	0.0036	-1.89	-12.09	SAMN04487868_12719
A0A1I4M2D6	-3.5434	3.5434	Microcin C transport system substrate-binding protein	3.55	0.0036	-1.35	-11.93	SAMN04487868_11857
A0A1I4NAM0	-3.5424	3.5424	Uncharacterized protein	3.55	0.0036	-2.34	-11.92	SAMN04487868_13216
A0A1I4HTA6	-3.5285	3.5285	Outer membrane transport energization protein ExbB	3.53	0.0035	-1.75	-11.82	SAMN04487868_1027
A0A1I4KD46	-3.5236	3.5236	TRAP-type mannitol/chloroaromatic compound transport system. small permease component	3.53	0.0035	-1.71	-11.79	SAMN04487868_109100
A0A1I4M538	-3.5068	3.5068	Methyl-accepting chemotaxis protein	3.51	0.0034	-1.13	-11.67	SAMN04487868_11920
A0A1I4KER1	-3.4943	3.4943	Fatty-acyl-CoA synthase	3.50	0.0034	-2.17	-11.58	SAMN04487868_109139
A0A1I4HT89	-3.4758	3.4758	Formyl transferase	3.48	0.0033	-0.44	-11.46	SAMN04487868_10235
A0A1I4H904	-3.4753	3.4753	Long-chain acyl-CoA synthetase (AMP-forming)	3.48	0.0033	-2.26	-11.45	SAMN04487868_101143
A0A1I4MA89	-3.4679	3.4679	Uncharacterized protein	3.47	0.0033	-2.62	-11.40	SAMN04487868_12041
A0A1I4MW08	-3.4473	3.4473	Na(+)-translocating NADH-quinone reductase subunit C	3.45	0.0032	-1.77	-11.26	nqrC SAMN04487868_12614
A0A1I4ISQ6	-3.4439	3.4439	Uncharacterized protein	3.45	0.0032	-2.34	-11.24	SAMN04487868_104159
A0A1I4MPW6	-3.4402	3.4402	TRAP-type C4-dicarboxylate transport system. substrate-binding protein	3.44	0.0032	-2.49	-11.22	SAMN04487868_12448
A0A1I4N4C1	-3.4366	3.4366	MSHA biogenesis protein MshE	3.44	0.0032	-0.98	-11.19	SAMN04487868_12939
A0A1I4JK41	-3.4316	3.4316	Replication fork clamp-binding protein CrfC (Dynamin-like GTPase family)	3.44	0.0032	-1.70	-11.16	SAMN04487868_106105
A0A1I4MEH6	-3.4186	3.4186	Uncharacterized protein	3.42	0.0031	-3.16	-11.07	SAMN04487868_12171
A0A1I4JVR3	-3.4124	3.4124	DNA-binding response regulator. OmpR family. contains REC and winged-helix (WHTH) domain	3.42	0.0031	-3.08	-11.03	SAMN04487868_107141
A0A1I4HBM6	-3.4029	3.4029	Citronellyl-CoA dehydrogenase	3.41	0.0031	-1.69	-10.97	SAMN04487868_101222
A0A1I4KE09	-3.3833	3.3833	Uncharacterized protein	3.39	0.0031	-2.30	-10.84	SAMN04487868_109115
A0A1I4K353	-3.3784	3.3784	Glycine betaine/proline transport system ATP-binding protein	3.38	0.0030	-2.14	-10.81	SAMN04487868_10871
A0A1I4HCT6	-3.3734	3.3734	Uncharacterized protein	3.38	0.0030	-0.24	-10.78	SAMN04487868_101227
A0A1I4KA27	-3.3580	3.3580	Uncharacterized protein involved in outer membrane biogenesis	3.36	0.0030	-1.15	-10.68	SAMN04487868_10924
A0A1I4HEI9	-3.3503	3.3503	Uncharacterized protein	3.35	0.0029	-0.90	-10.63	SAMN04487868_101334
A0A1I4HH20	-3.3427	3.3427	Uncharacterized protein	3.35	0.0029	-0.76	-10.58	SAMN04487868_101358
A0A1I4LLY9	-3.3415	3.3415	Type IV pilus assembly protein PilO	3.34	0.0029	-1.05	-10.57	SAMN04487868_11558
A0A1I4KTV8	-3.3397	3.3397	Bile acid:Na+ symporter. BASS family	3.34	0.0029	-2.34	-10.56	SAMN04487868_11161
A0A1I4I0V6	-3.3232	3.3232	Transcriptional regulator. DeoR family	3.33	0.0029	-0.77	-10.46	SAMN04487868_102246
A0A1I4MA24	-3.3221	3.3221	Uncharacterized protein. PEP-CTERM system associated	3.32	0.0028	-2.25	-10.45	SAMN04487868_12036

A0A1I4JTB9	-3.3187	3.3187	Outer membrane protein TolC	3.32	0.0028	-0.96	-10.43	SAMN04487868_10778
A0A1I4H9T4	-3.3159	3.3159	Fatty-acyl-CoA synthase	3.32	0.0028	-1.15	-10.41	SAMN04487868_101173
A0A1I4NAC3	-3.3134	3.3134	Formate dehydrogenase major subunit	3.32	0.0028	-3.77	-10.40	SAMN04487868_13212
A0A1I4K328	-3.3074	3.3074	Glycine betaine/proline transport system permease protein	3.31	0.0028	-3.28	-10.36	SAMN04487868_10870
A0A1I4I9T9	-3.3064	3.3064	Transglutaminase-like enzyme. putative cysteine protease	3.31	0.0028	-1.32	-10.35	SAMN04487868_103106
A0A1I4L008	-3.2925	3.2925	Amino acid/amide ABC transporter ATP-binding protein 1. HAAT family	3.29	0.0028	-1.77	-10.27	SAMN04487868_11216
A0A1I4KT65	-3.2876	3.2876	Sucrose porin	3.29	0.0027	-3.18	-16.13	SAMN04487868_11146
A0A1I4ILV6	-3.2839	3.2839	Protein phosphatase	3.29	0.0028	-1.38	-10.22	SAMN04487868_10429
A0A1I4NAC5	-3.2722	3.2722	Chaperone TorD involved in molybdoenzyme TorA maturation	3.27	0.0027	-2.17	-10.14	SAMN04487868_13214
A0A1I4JRD4	-3.2337	3.2337	Methylmalonyl-CoA mutase. C-terminal domain	3.24	0.0027	-1.92	-9.91	SAMN04487868_10719
A0A1I4MAT6	-3.2309	3.2309	3-hydroxyacyl-CoA dehydrogenase	3.23	0.0026	-0.80	-9.90	SAMN04487868_12059
A0A1I4I1U9	-3.2266	3.2266	Uncharacterized protein	3.23	0.0026	-1.75	-9.87	SAMN04487868_102225
A0A1I4KBZ4	-3.2263	3.2263	Transcriptional regulator. MarR family	3.23	0.0026	-0.85	-9.87	SAMN04487868_10975
A0A1I4LH16	-3.2162	3.2162	Long-chain acyl-CoA synthetase	3.22	0.0026	-4.23	-9.81	SAMN04487868_11472
A0A1I4MXK6	-3.2091	3.2091	Transcriptional regulatory protein	3.21	0.0026	-0.99	-9.77	SAMN04487868_1278
A0A1I4M9Z3	-3.2051	3.2051	Diguanylate cyclase	3.21	0.0026	-1.86	-9.74	SAMN04487868_12014
A0A1I4M8X2	-3.1988	3.1988	Uncharacterized protein	3.20	0.0026	-1.75	-9.71	SAMN04487868_1206
A0A1I4N786	-3.1968	3.1968	D-glycerate 3-kinase	3.20	0.0025	-0.86	-9.70	SAMN04487868_13031
A0A1I4H5C2	-3.1913	3.1913	Iron complex outermembrane recepter protein	3.19	0.0025	-1.60	-9.66	SAMN04487868_101103
A0A1I4HUB9	-3.1883	3.1883	Exopolysaccharide/PEP-CTERM locus tyrosine autokinase	3.19	0.0025	-0.96	-9.65	SAMN04487868_10264
A0A1I4HEE9	-3.1786	3.1786	Bax protein	3.18	0.0025	-0.90	-9.59	SAMN04487868_101337
A0A1I4LYD4	-3.1737	3.1737	Protein SCO1/2	3.18	0.0025	-1.78	-9.56	SAMN04487868_11768
A0A1I4LFA8	-3.1669	3.1669	Isovaleryl-CoA dehydrogenase	3.17	0.0025	-0.99	-9.52	SAMN04487868_11440
A0A1I4HAX6	-3.1633	3.1633	Methyl-accepting chemotaxis protein	3.16	0.0024	-1.27	-9.50	SAMN04487868_101237
A0A1I4I9T4	-3.1452	3.1452	Uncharacterized conserved protein. circularly permuted ATPgrasp superfamily	3.15	0.0024	-1.06	-9.40	SAMN04487868_103108
A0A1I4K1Q0	-3.1390	3.1390	Uncharacterized protein	3.14	0.0024	-1.39	-9.37	SAMN04487868_10825
A0A1I4HXW9	-3.1369	3.1369	Propionyl-CoA synthetase	3.14	0.0024	-1.05	-9.35	SAMN04487868_102130
A0A1I4LEZ5	-3.1321	3.1321	Fatty-acyl-CoA synthase	3.13	0.0024	-2.38	-9.33	SAMN04487868_11434
A0A1I4KKP1	-3.1273	3.1273	Amino acid ABC transporter substrate-binding protein. PAAT family	3.13	0.0023	-5.14	-9.30	SAMN04487868_11071
A0A1I4IDM7	-3.1271	3.1271	Transcriptional regulator. IclR family	3.13	0.0023	-1.12	-9.30	SAMN04487868_103165
A0A1I4IMF2	-3.1216	3.1216	Putative signal transducing protein	3.12	0.0023	-3.59	-9.27	SAMN04487868_10438
A0A1I4KCV9	-3.1086	3.1086	Regulator of protease activity HflC. stomatin/prohibitin superfamily	3.11	0.0023	-0.73	-9.20	SAMN04487868_10970
A0A1I4J5S2	-3.1037	3.1037	Long-chain acyl-CoA synthetase (AMP-forming)	3.10	0.0023	-0.89	-9.17	SAMN04487868_105104
A0A1I4N522	-3.1004	3.1004	Prepilin-type N-terminal cleavage/methylation domain-containing protein	3.10	0.0023	-1.96	-9.15	SAMN04487868_12942
A0A1I4ISP1	-3.0901	3.0901	Tripartite ATP-independent transporter solute receptor. DctP family	3.09	0.0022	-1.29	-9.09	SAMN04487868_104121
A0A1I4N6Z4	-3.0878	3.0878	Crotonobetainyl-CoA:carnitine CoA-transferase CaiB	3.09	0.0022	-2.18	-9.08	SAMN04487868_13024
A0A1I4LGV8	-3.0787	3.0787	Amino acid/amide ABC transporter ATP-binding protein 1. HAAT family	3.08	0.0025	-4.58	-9.03	SAMN04487868_11467
A0A1I4MA50	-3.0770	3.0770	Virulence factor lipase N-terminal	3.08	0.0025	-2.46	-9.02	SAMN04487868_12040
A0A1I4I225	-3.0744	3.0744	Concanavalin A-like lectin/glucanases superfamily protein	3.08	0.0025	-1.81	-9.01	SAMN04487868_102224

A0A1I4JTN6	-3.0742	3.0742	OmpA family protein	3.08	0.0025	-1.98	-9.01	SAMN04487868_10744
A0A1I4MP83	-3.0648	3.0648	Uncharacterized protein	3.07	0.0025	-3.32	-8.96	SAMN04487868_12436
A0A1I4HYA0	-3.0601	3.0601	Cell division and transport-associated protein TolA	3.06	0.0025	-1.24	-8.93	SAMN04487868_102112
A0A1I4MY13	-3.0593	3.0593	Tetratricopeptide repeat-containing protein	3.06	0.0025	-0.60	-8.93	SAMN04487868_12725
A0A1I4IS09	-3.0579	3.0579	Glucose/arabinose dehydrogenase. beta-propeller fold	3.06	0.0025	-3.31	-8.92	SAMN04487868_104144
A0A1I4JR08	-3.0542	3.0542	Cobaltochelatase CobN	3.06	0.0025	-1.24	-8.90	SAMN04487868_10711
A0A1I4INM0	-3.0444	3.0444	L-serine dehydratase	3.05	0.0024	-0.62	-8.85	SAMN04487868_10462
A0A1I4KBB5	-3.0322	3.0322	Iron complex outermembrane recepter protein	3.03	0.0024	-1.76	-8.78	SAMN04487868_10952
A0A1I4H5D6	-3.0279	3.0279	Uncharacterized protein	3.03	0.0024	-2.61	-8.76	SAMN04487868_101100
A0A1I4L154	-3.0223	3.0223	Uncharacterized protein	3.02	0.0024	-3.33	-8.73	SAMN04487868_11239
A0A1I4LLA1	-3.0203	3.0203	Type IV pilus assembly protein PilW	3.02	0.0024	-1.18	-8.72	SAMN04487868_11517
A0A1I4MHD7	-3.0127	3.0127	EDD domain protein. DegV family	3.01	0.0026	-2.00	-8.68	SAMN04487868_12229
A0A1I4L1I2	-3.0062	3.0062	Diguanylate cyclase (GGDEF) domain-containing protein	3.01	0.0026	-1.07	-8.65	SAMN04487868_11242
A0A1I4M344	-3.0042	3.0042	Uncharacterized protein	3.01	0.0026	-1.61	-8.64	SAMN04487868_11863
A0A1I4MVD7	-3.0036	3.0036	Uncharacterized protein	3.00	0.0026	-2.61	-12.96	SAMN04487868_1264
A0A1I4M7L7	-2.9988	2.9988	Cation/acetate symporter	3.00	0.0029	-2.82	-8.61	SAMN04487868_11977
A0A1I4HHX4	-2.9972	2.9972	Pyruvate carboxylase subunit A	3.00	0.0029	-0.77	-8.60	SAMN04487868_101418
A0A1I4L8V6	-2.9938	2.9938	Nucleoid-associated protein YgaU. contains BON and LysM domains	2.99	0.0028	-0.90	-8.58	SAMN04487868_11361
A0A1I4K184	-2.9868	2.9868	Membrane fusion protein. multidrug efflux system	2.99	0.0028	-0.62	-8.55	SAMN04487868_10827
A0A1I4L2M7	-2.9815	2.9815	Twitching motility protein PilJ	2.98	0.0028	-0.67	-8.52	SAMN04487868_11265
A0A1I4KE56	-2.9786	2.9786	Uncharacterized protein	2.98	0.0028	-2.65	-8.50	SAMN04487868_109114
A0A1I4LRB9	-2.9680	2.9680	Quinohemoprotein ethanol dehydrogenase	2.97	0.0028	-1.67	-8.45	SAMN04487868_11617
A0A1I4KEP5	-2.9627	2.9627	Uncharacterized domain 1-containing protein	2.96	0.0030	-1.66	-8.42	SAMN04487868_109130
A0A1I4KK47	-2.9560	2.9560	Cytochrome c-550 PedF	2.96	0.0030	-1.86	-8.39	SAMN04487868_11070
A0A1I4JHD2	-2.9557	2.9557	Uncharacterized protein	2.96	0.0030	-1.13	-8.39	SAMN04487868_10670
A0A1I4I7I8	-2.9542	2.9542	Uncharacterized protein	2.95	0.0030	-1.55	-8.38	SAMN04487868_10315
A0A1I4KER7	-2.9476	2.9476	Multidrug efflux pump subunit AcrB	2.95	0.0030	-2.45	-8.35	SAMN04487868_109127
A0A1I4LHA6	-2.9374	2.9374	Methyl-accepting chemotaxis sensory transducer with Cache sensor	2.94	0.0033	-1.11	-8.30	SAMN04487868_11478
A0A1I4MNC9	-2.9358	2.9358	Glycolate oxidase	2.94	0.0033	-0.94	-8.29	SAMN04487868_1249
A0A1I4HA60	-2.9276	2.9276	NADPH:quinone reductase	2.93	0.0032	-0.76	-8.25	SAMN04487868_101217
A0A1I4IBP8	-2.9246	2.9246	Putative MetA-pathway of phenol degradation	2.92	0.0032	-4.77	-12.19	SAMN04487868_103158
A0A1I4IT54	-2.9244	2.9244	Acetyl-coenzyme A synthetase	2.93	0.0032	-0.93	-8.23	acsA SAMN04487868_104168
A0A1I4KTX9	-2.8965	2.8965	Ig-like domain-containing protein	2.90	0.0032	-2.58	-8.09	SAMN04487868_11171
A0A1I4K040	-2.8928	2.8928	Phosphocarrier protein HPr /phosphoenolpyruvate--protein phosphotransferase /PTS system D-fructose-specific IIA component (F1P-forming). Frc family	2.89	0.0032	-0.95	-8.07	SAMN04487868_1087
A0A1I4HAW7	-2.8889	2.8889	Uncharacterized protein	2.89	0.0032	-1.87	-8.06	SAMN04487868_101242
A0A1I4H921	-2.8848	2.8848	Methyl-accepting chemotaxis protein	2.89	0.0032	-1.53	-8.04	SAMN04487868_101189
A0A1I4L2J1	-2.8821	2.8821	Diguanylate cyclase (GGDEF) domain-containing protein	2.88	0.0032	-0.97	-8.02	SAMN04487868_11248
A0A1I4HGV5	-2.8803	2.8803	Flagellin	2.88	0.0031	-0.92	-8.01	SAMN04487868_101384
A0A1I4J507	-2.8742	2.8742	L-ascorbate metabolism protein UlaG. beta-lactamase superfamily	2.87	0.0034	-5.35	-7.98	SAMN04487868_10564

A0A1I4I1M1	-2.8644	2.8644	Glyceraldehyde-3-phosphate dehydrogenase	2.86	0.0034	-0.35	-7.94	SAMN04487868_102254
A0A1I4LWI5	-2.8556	2.8556	ABC-type amino acid transport substrate-binding protein	2.86	0.0036	-2.00	-7.89	SAMN04487868_11728
A0A1I4KVS9	-2.8524	2.8524	L-lactate dehydrogenase complex protein LldF	2.85	0.0036	-1.73	-7.88	SAMN04487868_111114
A0A1I4KW48	-2.8469	2.8469	L-lactate dehydrogenase complex protein LldG	2.85	0.0036	-2.64	-7.85	SAMN04487868_111113
A0A1I4K4A1	-2.8399	2.8399	Thiol:disulfide interchange protein	2.84	0.0035	-0.91	-7.82	SAMN04487868_108102
A0A1I4N4X7	-2.8208	2.8208	MSHA biogenesis protein MshI	2.82	0.0041	-1.01	-7.73	SAMN04487868_12932
A0A1I4KIR5	-2.8187	2.8187	Uncharacterized protein	2.82	0.0040	-0.45	-7.72	SAMN04487868_11022
A0A1I4K1X6	-2.8178	2.8178	LPS-assembly protein LptD	2.82	0.0040	-0.45	-7.71	lptD SAMN04487868_10845
A0A1I4HI24	-2.8151	2.8151	Pyruvate carboxylase subunit B	2.82	0.0040	-0.54	-7.70	SAMN04487868_101419
A0A1I4L0F8	-2.8072	2.8072	Succinylglutamate desuccinylase / Aspartoacylase family protein	2.81	0.0040	-1.58	-7.67	SAMN04487868_11223
A0A1I4I8W4	-2.8056	2.8056	Anti-sigma-K factor RskA	2.81	0.0040	-1.17	-7.66	SAMN04487868_10324
A0A1I4LFP8	-2.8023	2.8023	Acyl-CoA dehydrogenase	2.80	0.0040	-0.58	-7.64	SAMN04487868_11458
A0A1I4M9S0	-2.7935	2.7935	RNA polymerase sigma-70 factor. ECF subfamily	2.79	0.0042	-1.27	-7.60	SAMN04487868_12039
A0A1I4H7H6	-2.7869	2.7869	Haloalkane dehalogenase	2.79	0.0041	-1.68	-7.57	dhmA SAMN04487868_101153
A0A1I4NC60	-2.7777	2.7777	3-deoxy-D-manno-octulosonic acid kinase	2.78	0.0041	-0.74	-7.53	kdkA SAMN04487868_1339
A0A1I4KVW9	-2.7757	2.7757	L-lactate dehydrogenase complex protein LldE	2.78	0.0041	-1.95	-7.52	SAMN04487868_111115
A0A1I4L7L7	-2.7748	2.7748	Chromosome partitioning protein	2.78	0.0041	-1.29	-7.52	SAMN04487868_11326
A0A1I4IL33	-2.7486	2.7486	Nucleotide-binding universal stress protein. UspA family	2.75	0.0042	-0.61	-7.40	SAMN04487868_1048
A0A1I4LHB5	-2.7481	2.7481	Xanthine dehydrogenase small subunit	2.75	0.0042	-1.84	-7.39	SAMN04487868_11484
A0A1I4L9Z5	-2.7309	2.7309	Uncharacterized protein	2.73	0.0042	-6.02	-7.32	SAMN04487868_11381
A0A1I4KLH5	-2.7117	2.7117	Acetolactate synthase-1/2/3 large subunit	2.71	0.0044	-1.00	-7.23	SAMN04487868_110102
A0A1I4MNV3	-2.7114	2.7114	Outer membrane protein TolC	2.71	0.0044	-2.18	-7.23	SAMN04487868_12435
A0A1I4KEF4	-2.7066	2.7066	RND family efflux transporter. MFP subunit	2.71	0.0043	-1.51	-7.21	SAMN04487868_109128
A0A1I4JJI9	-2.7041	2.7041	Long-chain fatty acid transport protein	2.70	0.0043	-1.97	-7.20	SAMN04487868_106111
A0A1I4HBS1	-2.6994	2.6994	Uncharacterized protein	2.70	0.0043	-1.59	-7.18	SAMN04487868_101267
A0A1I4K9T3	-2.6915	2.6915	5'-deoxynucleotidase	2.69	0.0045	-0.61	-7.14	SAMN04487868_10922
A0A1I4L7H9	-2.6856	2.6856	TRAP-type mannitol/chloroaromatic compound transport system. substrate-binding protein	2.69	0.0045	-1.38	-7.12	SAMN04487868_1136
A0A1I4MV14	-2.6852	2.6852	Transcriptional regulator. TetR family	2.69	0.0045	-1.26	-7.11	SAMN04487868_1265
A0A1I4ID13	-2.6822	2.6822	Uncharacterized domain 1-containing protein	2.68	0.0044	-0.76	-7.10	SAMN04487868_103185
A0A1I4HF54	-2.6804	2.6804	Signal transduction histidine kinase	2.68	0.0044	-2.04	-7.09	SAMN04487868_101341
A0A1I4LJZ0	-2.6659	2.6659	Type IV pilus assembly protein PilV	2.67	0.0044	-1.71	-7.03	SAMN04487868_11516
A0A1I4HJN6	-2.6653	2.6653	LemA protein	2.67	0.0044	-0.96	-7.03	SAMN04487868_101403
A0A1I4I217	-2.6586	2.6586	Uncharacterized protein	2.66	0.0044	-1.55	-7.00	SAMN04487868_102223
A0A1I4J3R2	-2.6583	2.6583	Gamma-glutamyltranspeptidase / glutathione hydrolase	2.66	0.0044	-1.39	-7.00	SAMN04487868_10524
A0A1I4JSB8	-2.6424	2.6424	Methylmalonyl-CoA mutase	2.64	0.0045	-1.94	-6.93	SAMN04487868_10716
A0A1I4N6I7	-2.6422	2.6422	Integration host factor subunit alpha	2.64	0.0045	-0.72	-6.93	ihfA himA SAMN04487868_13011
A0A1I4JTH2	-2.6408	2.6408	Thioester reductase domain-containing protein	2.64	0.0045	-0.98	-6.92	SAMN04487868_10747
A0A1I4HAA9	-2.6184	2.6184	Isohexenylglutaconyl-CoA hydratase	2.62	0.0047	-1.53	-6.83	SAMN04487868_101221

A0A1I4KK75	-2.6032	2.6032	Outer membrane protein (Porin)	2.60	0.0051	-3.20	-6.76	SAMN04487868_11057
A0A1I4I9I3	-2.6002	2.6002	Uncharacterized conserved protein. Alpha-E superfamily	2.60	0.0050	-1.53	-6.75	SAMN04487868_103107
A0A1I4IN40	-2.5964	2.5964	YnbE-like lipoprotein	2.60	0.0050	-0.98	-6.74	SAMN04487868_10454
A0A1I4LXT9	-2.5951	2.5951	Iron complex outermembrane recepter protein	2.60	0.0050	-1.12	-6.73	SAMN04487868_11748
A0A1I4KKG3	-2.5947	2.5947	Uncharacterized protein	2.59	0.0050	-0.43	-6.73	SAMN04487868_11053
A0A1I4I7X9	-2.5930	2.5930	D-methionine transport system substrate-binding protein	2.59	0.0050	-1.60	-6.72	SAMN04487868_10328
A0A1I4NAS6	-2.5846	2.5846	Biotin-(Acetyl-CoA carboxylase) ligase	2.58	0.0052	-1.62	-9.34	SAMN04487868_13219
A0A1I4I251	-2.5803	2.5803	Peptidylprolyl isomerase	2.58	0.0052	-0.59	-6.67	SAMN04487868_102264
A0A1I4LM37	-2.5783	2.5783	Type IV pilus assembly protein PilN	2.58	0.0052	-0.92	-6.66	SAMN04487868_11559
A0A1I4MAK6	-2.5767	2.5767	Acyl-CoA dehydrogenase	2.58	0.0054	-0.53	-6.65	SAMN04487868_12057
A0A1I4IE34	-2.5743	2.5743	Heat shock protein HslJ	2.57	0.0053	-1.02	-6.64	SAMN04487868_103219
A0A1I4HAK5	-2.5738	2.5738	Citronellol/citronellal dehydrogenase	2.57	0.0053	-2.28	-6.64	SAMN04487868_101224
A0A1I4NAC8	-2.5603	2.5603	Sulfur carrier protein FdhD	2.56	0.0055	-1.50	-6.59	fdhD SAMN04487868_13224
A0A1I4MDJ5	-2.5481	2.5481	Haloalkane dehalogenase	2.55	0.0056	-1.82	-6.54	dhmA SAMN04487868_12140
A0A1I4IEU9	-2.5390	2.5390	Amino acid/amide ABC transporter ATP-binding protein 2. HAAT family	2.54	0.0056	-3.35	-6.50	SAMN04487868_103241
A0A1I4LGU0	-2.4963	2.4963	Methyl-accepting chemotaxis sensory transducer with Pas/Pac sensor	2.50	0.0066	-0.70	-6.33	SAMN04487868_11475
A0A1I4KD38	-2.4892	2.4892	Uncharacterized protein	2.49	0.0066	-2.01	-6.30	SAMN04487868_10990
A0A1I4LS44	-2.4731	2.4731	Uncharacterized protein	2.47	0.0067	-0.55	-6.24	SAMN04487868_11650
A0A1I4N542	-2.4618	2.4618	MSHA pilin protein MshA	2.46	0.0067	-2.12	-6.20	SAMN04487868_12943
A0A1I4J726	-2.4614	2.4614	Uncharacterized protein	2.46	0.0067	-1.05	-6.19	SAMN04487868_105109
A0A1I4I8V6	-2.4554	2.4554	RNA polymerase sigma-70 factor. ECF subfamily	2.46	0.0068	-0.69	-6.17	SAMN04487868_10323
A0A1I4MGB0	-2.4525	2.4525	Transcriptional regulator. AraC family	2.45	0.0068	-0.75	-6.16	SAMN04487868_12215
A0A1I4LA25	-2.4507	2.4507	Uncharacterized protein	2.45	0.0068	-1.08	-6.15	SAMN04487868_11389
A0A1I4L0U2	-2.4346	2.4346	Uncharacterized protein	2.43	0.0073	-1.48	-6.09	SAMN04487868_11220
A0A1I4MSZ0	-2.4227	2.4227	Amino acid ABC transporter substrate-binding protein. PAAT family	2.42	0.0078	-0.92	-6.05	SAMN04487868_12558
A0A1I4JJB8	-2.4200	2.4200	Twitching motility protein PilU	2.42	0.0078	-0.84	-6.04	SAMN04487868_106110
A0A1I4IUM3	-2.4109	2.4109	PAS domain S-box-containing protein/diguanylate cyclase (GGDEF) domain-containing protein	2.41	0.0079	-1.32	-6.00	SAMN04487868_104199
A0A1I4MFB0	-2.4071	2.4071	Methyl-accepting chemotaxis sensory transducer with Cache sensor	2.41	0.0079	-0.89	-5.99	SAMN04487868_12165
A0A1I4J4Y4	-2.4005	2.4005	Amino acid ABC transporter substrate-binding protein. PAAT family	2.40	0.0081	-1.02	-5.96	SAMN04487868_10554
A0A1I4MNT8	-2.3881	2.3881	Uncharacterized protein	2.39	0.0087	-0.90	-5.92	SAMN04487868_12445
A0A1I4MNR2	-2.3835	2.3835	RND family efflux transporter. MFP subunit	2.38	0.0087	-0.71	-5.90	SAMN04487868_12434
A0A1I4MXQ0	-2.3753	2.3753	Putative tricarboxylic transport membrane protein	2.38	0.0090	-1.23	-5.87	SAMN04487868_1276
A0A1I4MW68	-2.3721	2.3721	Zinc transport system substrate-binding protein	2.37	0.0090	-1.21	-5.86	SAMN04487868_12629
A0A1I4JRM3	-2.3681	2.3681	Phenylacetate-CoA ligase	2.37	0.0089	-3.44	-5.84	SAMN04487868_10718
A0A1I4HC30	-2.3621	2.3621	Geranyl-CoA carboxylase alpha subunit	2.36	0.0089	-1.95	-5.82	SAMN04487868_101220
A0A1I4KP72	-2.3593	2.3593	L-leucine-binding protein /L-isoleucine-binding protein /L-valine-binding protein	2.36	0.0089	-0.44	-5.81	SAMN04487868_110149
A0A1I4J8L9	-2.3589	2.3589	Type IV pilus assembly protein PilF	2.36	0.0089	-0.59	-5.81	SAMN04487868_105142
A0A1I4M5F6	-2.3503	2.3503	Uncharacterized protein	2.35	0.0088	-1.05	-5.78	SAMN04487868_11923

A0A1I4JL89	-2.3486	2.3486	Anaerobic selenocysteine-containing dehydrogenase	2.35	0.0088	-2.40	-5.77	SAMN04487868_106131
A0A1I4HWA0	-2.3477	2.3477	Putative beta-barrel assembly-enhancing protease	2.35	0.0088	-1.49	-5.77	SAMN04487868_102105
A0A1I4JSV9	-2.3284	2.3284	Uncharacterized protein	2.33	0.0091	-0.68	-5.70	SAMN04487868_10759
A0A1I4L9M5	-2.3206	2.3206	Hemoglobin	2.32	0.0092	-1.32	-5.67	SAMN04487868_11378
A0A1I4N191	-2.3106	2.3106	Transcriptional regulator. LysR family	2.31	0.0092	-0.56	-5.63	SAMN04487868_12829
A0A1I4M5K7	-2.3034	2.3034	Regulatory inactivation of DnaA Hda protein	2.30	0.0092	-0.86	-5.61	SAMN04487868_11927
A0A1I4JEZ0	-2.2939	2.2939	2-oxoisovalerate dehydrogenase E1 component beta subunit	2.29	0.0093	-1.03	-5.57	SAMN04487868_10617
A0A1I4MGJ3	-2.2928	2.2928	Protein RecA	2.29	0.0092	-0.82	-5.57	recA SAMN04487868_12223
A0A1I4MPI2	-2.2823	2.2823	2.4-dienoyl-CoA reductase	2.28	0.0092	-1.43	-5.53	SAMN04487868_12454
A0A1I4L0Y9	-2.2813	2.2813	PDZ domain (Also known as DHR or GLGF)	2.28	0.0091	-2.56	-5.53	SAMN04487868_11234
A0A1I4L2Z4	-2.2793	2.2793	Nitroreductase	2.28	0.0093	-1.01	-5.52	SAMN04487868_11284
A0A1I4M9R6	-2.2603	2.2603	Amino acid ABC transporter substrate-binding protein. PAAT family	2.26	0.0093	-2.09	-5.45	SAMN04487868_12033
A0A1I4K0T2	-2.2518	2.2518	Dihydrolipoamide dehydrogenase	2.25	0.0093	-0.69	-5.42	SAMN04487868_10822
A0A1I4NAN1	-2.2469	2.2469	Molybdopterin guanine dinucleotide biosynthesis accessory protein MobB	2.25	0.0093	-0.83	-5.41	SAMN04487868_13222
A0A1I4M1P7	-2.2455	2.2455	DNA-binding transcriptional regulator. LysR family	2.25	0.0093	-0.89	-5.40	SAMN04487868_11829
A0A1I4KUT7	-2.2420	2.2420	Methyl-accepting chemotaxis protein	2.24	0.0092	-5.28	-5.39	SAMN04487868_11196
A0A1I4L9F1	-2.2381	2.2381	Chemotaxis protein MotA	2.24	0.0094	-0.61	-5.38	SAMN04487868_11366
A0A1I4MG32	-2.2320	2.2320	Uncharacterized protein	2.23	0.0095	-1.01	-5.36	SAMN04487868_12211
A0A1I4KJS9	-2.2310	2.2310	Phosphoribosyl-AMP cyclohydrolase	2.23	0.0095	-0.57	-5.35	hisI SAMN04487868_11048
A0A1I4J6T4	-2.2130	2.2130	Putative ABC transport system substrate-binding protein	2.21	0.0099	-0.90	-5.29	SAMN04487868_105103
A0A1I4LFP6	-2.2031	2.2031	Alginate biosynthesis protein AlgK	2.20	0.0098	-1.79	-5.26	SAMN04487868_11447
A0A1I4L8E0	-2.2020	2.2020	ATP-binding cassette. subfamily B	2.20	0.0098	-1.10	-5.25	SAMN04487868_11351
A0A1I4HAC2	-2.1982	2.1982	Uncharacterized protein	2.20	0.0099	-0.52	-5.24	SAMN04487868_101164
A0A1I4N796	-2.1967	2.1967	Mannosyl-3-phosphoglycerate phosphatase	2.20	0.0099	-0.84	-5.24	SAMN04487868_13032
A0A1I4HD98	-2.1966	2.1966	Nitrilase	2.20	0.0098	-0.42	-5.24	SAMN04487868_101306
A0A1I4LWY6	-2.1922	2.1922	Isoquinoline 1-oxidoreductase. beta subunit	2.19	0.0098	-0.83	-5.22	SAMN04487868_11726
A0A1I4IDW1	-2.1881	2.1881	TRAP-type C4-dicarboxylate transport system. substrate-binding protein	2.19	0.0098	-0.81	-5.21	SAMN04487868_103215
A0A1I4H963	-2.1865	2.1865	TRAP-type C4-dicarboxylate transport system. substrate-binding protein	2.19	0.0097	-0.71	-5.20	SAMN04487868_101197
A0A1I4MRV4	-2.1850	2.1850	Patatin-like phospholipase	2.19	0.0097	-0.54	-5.20	SAMN04487868_12519
A0A1I4K326	-2.1666	2.1666	Glycine betaine/proline transport system substrate-binding protein	2.17	0.0103	-3.28	-5.14	SAMN04487868_10869
A0A1I4K5W3	-2.1575	2.1575	Inner membrane protein	2.16	0.0102	-1.11	-5.11	SAMN04487868_108139
A0A1I4MYS3	-2.1519	2.1519	Outer-membrane lipoprotein LolB	2.15	0.0101	-0.74	-5.09	lolB SAMN04487868_12726
A0A1I4N658	-2.1514	2.1514	Uncharacterized protein	2.15	0.0101	-0.79	-5.08	SAMN04487868_1302
A0A1I4K4V3	-2.1490	2.1490	Uncharacterized protein	2.15	0.0104	-0.28	-5.08	SAMN04487868_10893
A0A1I4JUH3	-2.1439	2.1439	Membrane fusion protein. Cu(I)/Ag(I) efflux system	2.14	0.0107	-0.93	-5.06	SAMN04487868_10781
A0A1I4MPD9	-2.1420	2.1420	Pyruvate dehydrogenase E1 component	2.14	0.0106	-0.71	-5.05	SAMN04487868_12456
A0A1I4N481	-2.1347	2.1347	MSHA biogenesis protein MshL	2.13	0.0109	-1.59	-5.03	SAMN04487868_12936
A0A1I4J621	-2.1325	2.1325	Uncharacterized protein	2.13	0.0109	-0.64	-5.02	SAMN04487868_10586
A0A1I4IAB9	-2.1320	2.1320	DNA polymerase-3 subunit epsilon	2.13	0.0108	-1.14	-5.02	SAMN04487868_10377

A0A1I4JT98	-2.1276	2.1276	Fe(3+) dicitrate transport protein	2.13	0.0111	-1.21	-5.01	SAMN04487868_10765
A0A1I4L302	-2.1218	2.1218	Uncharacterized protein	2.12	0.0114	-2.01	-4.99	SAMN04487868_11278
A0A1I4HE71	-2.1142	2.1142	Nucleoid-associated protein	2.11	0.0115	-0.69	-4.96	SAMN04487868_101292
A0A1I4MM42	-2.1112	2.1112	OST-HTH/LOTUS domain-containing protein	2.11	0.0116	-0.54	-4.95	SAMN04487868_1244
A0A1I4IDB7	-2.1096	2.1096	Benzaldehyde dehydrogenase (NAD+)	2.11	0.0116	-1.44	-4.95	SAMN04487868_103155
A0A1I4L9N8	-2.1080	2.1080	Chemotaxis protein MotB	2.11	0.0116	-0.40	-4.94	SAMN04487868_11367
A0A1I4HVJ1	-2.1049	2.1049	Polysaccharide export outer membrane protein	2.10	0.0115	-0.59	-4.93	SAMN04487868_10266
A0A1I4JV61	-2.0993	2.0993	Copper-resistance protein. CopA family	2.10	0.0116	-1.29	-4.92	SAMN04487868_107125
A0A1I4LR95	-2.0935	2.0935	Putative MetA-pathway of phenol degradation	2.09	0.0121	-1.65	-4.90	SAMN04487868_11618
A0A1I4HJZ5	-2.0900	2.0900	Two-component system. chemotaxis family. sensor kinase CheA	2.09	0.0120	-0.74	-4.89	SAMN04487868_101467
A0A1I4J6P3	-2.0830	2.0830	Uncharacterized conserved protein. DUF1330 family	2.08	0.0122	-2.29	-4.86	SAMN04487868_10594
A0A1I4J640	-2.0786	2.0786	Uncharacterized protein	2.08	0.0121	-1.28	-4.85	SAMN04487868_105111
A0A1I4NI04	-2.0709	2.0709	Uncharacterized protein	2.07	0.0122	-1.31	-4.82	SAMN04487868_1414
A0A1I4J260	-2.0660	2.0660	Glucose/arabinose dehydrogenase. beta-propeller fold	2.07	0.0123	-2.52	-4.81	SAMN04487868_10522
A0A1I4ISI5	-2.0626	2.0626	Predicted kinase. aminoglycoside phosphotransferase (APT) family	2.06	0.0126	-1.27	-4.80	SAMN04487868_104156
A0A1I4JAF8	-2.0618	2.0618	Two-component system. chemotaxis family. response regulator CheV	2.06	0.0126	-0.80	-4.80	SAMN04487868_105193
A0A1I4IGG7	-2.0421	2.0421	Amino acid/amide ABC transporter ATP-binding protein 1. HAAT family	2.04	0.0132	-1.25	-4.73	SAMN04487868_103240
A0A1I4N1Q9	-2.0366	2.0366	Kef-type potassium/proton antiporter. CPA2 family	2.04	0.0131	-1.06	-4.72	SAMN04487868_12836
A0A1I4MN58	-2.0330	2.0330	Glycolate oxidase FAD binding subunit	2.03	0.0131	-0.98	-4.71	SAMN04487868_1248
A0A1I4HGP6	-2.0231	2.0231	Uncharacterized protein	2.02	0.0133	-2.22	-4.68	SAMN04487868_101338
A0A1I4HTZ9	-2.0211	2.0211	Uncharacterized protein	2.02	0.0135	-0.62	-4.67	SAMN04487868_10252
A0A1I4J7P3	-2.0199	2.0199	Uncharacterized protein	2.02	0.0137	-0.40	-4.67	SAMN04487868_105152
A0A1I4HT95	-2.0130	2.0130	Acetyltransferase involved in cellulose biosynthesis. CelD/BcsL family	2.01	0.0138	-0.72	-4.64	SAMN04487868_10236
A0A1I4JHW6	-2.0082	2.0082	Sugar lactone lactonase YvrE	2.01	0.0139	-0.65	-4.63	SAMN04487868_10682
A0A1I4L1J7	-1.9952	1.9952	HDIG domain-containing protein	2.00	0.0142	-1.12	-4.59	SAMN04487868_11249
A0A1I4N6Y6	-1.9926	1.9926	Uncharacterized protein	1.99	0.0142	-0.90	-4.58	SAMN04487868_13022
A0A1I4LFE9	-1.9913	1.9913	3-methylcrotonyl-CoA carboxylase alpha subunit	1.99	0.0141	-1.70	-4.58	SAMN04487868_11437
A0A1I4LN08	-1.9913	1.9913	Phosphotransferase system. enzyme I. PtsP	1.99	0.0141	-0.45	-4.58	SAMN04487868_11571
A0A1I4I3B8	-1.9851	1.9851	Amino acid ABC transporter membrane protein 1. PAAT family	1.99	0.0141	-2.54	-4.56	SAMN04487868_102282
A0A1I4KNW9	-1.9843	1.9843	DUF4105 domain-containing protein	1.98	0.0141	-1.03	-4.56	SAMN04487868_110142
A0A1I4JV83	-1.9838	1.9838	Multicopper oxidase with three cupredoxin domains (Includes cell division protein FtsP and spore coat protein CotA)	1.98	0.0141	-0.35	-4.56	SAMN04487868_107103
A0A1I4H2L7	-1.9751	1.9751	Uncharacterized protein	1.98	0.0141	-1.07	-4.53	SAMN04487868_10128
A0A1I4KP17	-1.9720	1.9720	High-affinity branched-chain amino acid transport ATP-binding protein	1.97	0.0140	-0.93	-4.52	SAMN04487868_110145
A0A1I4LW40	-1.9689	1.9689	Transcriptional regulator. LysR family	1.97	0.0139	-0.75	-4.51	SAMN04487868_11717
A0A1I4HGD7	-1.9634	1.9634	Diguanylate cyclase (GGDEF) domain-containing protein	1.96	0.0140	-0.56	-4.49	SAMN04487868_101379
A0A1I4J6J2	-1.9607	1.9607	Uncharacterized damage-inducible protein DinB (Forms a four-helix bundle)	1.96	0.0140	-0.85	-4.49	SAMN04487868_10591
A0A1I4KD92	-1.9570	1.9570	Transcriptional regulator containing PAS. AAA-type ATPase. and DNA-binding Fis domains	1.96	0.0141	-0.57	-4.47	SAMN04487868_109102
A0A1I4JFL9	-1.9479	1.9479	Bacterioferritin	1.95	0.0142	-0.24	-4.45	SAMN04487868_10630

A0A1I4KA18	-1.9290	1.9290	TRAP-type mannitol/chloroaromatic compound transport system. substrate-binding protein	1.93	0.0150	-0.65	-4.39	SAMN04487868_10913
A0A1I4KZP6	-1.9238	1.9238	Uncharacterized protein	1.92	0.0150	-0.89	-4.38	SAMN04487868_1125
A0A1I4HLM5	-1.9233	1.9233	Chromosome partitioning protein	1.92	0.0151	-0.36	-4.37	SAMN04487868_101471
A0A1I4H942	-1.9232	1.9232	Butyryl-CoA dehydrogenase	1.92	0.0151	-0.56	-4.37	SAMN04487868_101185
A0A1I4LXN7	-1.9209	1.9209	Predicted flavoprotein CzcO associated with the cation diffusion facilitator CzcD	1.92	0.0152	-1.19	-4.37	SAMN04487868_11744
A0A1I4K202	-1.9200	1.9200	Amino acid ABC transporter substrate-binding protein. PAAT family	1.92	0.0152	-0.50	-4.36	SAMN04487868_10834
A0A1I4I018	-1.9132	1.9132	Maltose operon substrate-binding protein (MalM)	1.91	0.0153	-1.62	-4.34	SAMN04487868_102199
A0A1I4N0Y0	-1.9102	1.9102	Iron complex outermembrane recepter protein	1.91	0.0153	-0.42	-4.34	SAMN04487868_12820
A0A1I4KIH1	-1.9096	1.9096	5-formyltetrahydrofolate cyclo-ligase	1.91	0.0153	-0.97	-4.33	SAMN04487868_11029
A0A1I4N7Z6	-1.8872	1.8872	Glucosyl-3-phosphoglycerate synthase	1.89	0.0170	-0.48	-4.27	SAMN04487868_13033
A0A1I4I892	-1.8834	1.8834	Acyl-CoA dehydrogenase	1.88	0.0172	-1.63	-4.26	SAMN04487868_10361
A0A1I4LSJ2	-1.8761	1.8761	Uncharacterized protein	1.88	0.0174	-0.85	-4.24	SAMN04487868_11651
A0A1I4KIN4	-1.8710	1.8710	Diguanylate cyclase (GGDEF) domain-containing protein	1.87	0.0175	-1.08	-4.22	SAMN04487868_11020
A0A1I4J274	-1.8636	1.8636	Pectinacetylesterase	1.86	0.0176	-3.32	-4.20	SAMN04487868_10517
A0A1I4HCI0	-1.8534	1.8534	Citronellol/citronellal dehydrogenase	1.85	0.0179	-0.23	-4.17	SAMN04487868_101219
A0A1I4NEW1	-1.8529	1.8529	Phosphate transport system permease protein PstA	1.85	0.0179	-0.62	-4.17	SAMN04487868_13510
A0A1I4HAK3	-1.8360	1.8360	Putative iron-regulated protein	1.84	0.0184	-0.55	-4.12	SAMN04487868_101195
A0A1I4M6R2	-1.8308	1.8308	RNA polymerase sigma factor RpoS	1.83	0.0192	-0.32	-4.11	rpoS SAMN04487868_11946
A0A1I4LA48	-1.8153	1.8153	Diguanylate cyclase (GGDEF) domain-containing protein	1.82	0.0194	-1.17	-4.06	SAMN04487868_11380
A0A1I4MNQ1	-1.8148	1.8148	Cobalt-zinc-cadmium resistance protein CzcA	1.81	0.0194	-1.36	-4.06	SAMN04487868_12433
A0A1I4N416	-1.8138	1.8138	UvrABC system protein A	1.81	0.0194	-0.43	-4.06	uvrA SAMN04487868_12929
A0A1I4LK64	-1.8126	1.8126	Type IV pilus assembly protein PilE	1.81	0.0193	-1.22	-4.06	SAMN04487868_11521
A0A1I4M0U9	-1.8111	1.8111	Uncharacterized protein	1.81	0.0193	-1.48	-4.05	SAMN04487868_11817
A0A1I4NB56	-1.8080	1.8080	Simple sugar transport system substrate-binding protein	1.81	0.0193	-0.89	-4.04	SAMN04487868_13236
A0A1I4H5C9	-1.7841	1.7841	Anti-sigma-K factor RskA	1.78	0.0202	-0.68	-3.98	SAMN04487868_101101
A0A1I4JF08	-1.7815	1.7815	Dihydrolipoamide acetyltransferase component of pyruvate dehydrogenase complex	1.78	0.0203	-0.93	-3.97	SAMN04487868_10616
A0A1I4K653	-1.7790	1.7790	Membrane-bound lytic murein transglycosylase B	1.78	0.0202	-0.40	-3.96	SAMN04487868_108138
A0A1I4IEL8	-1.7677	1.7677	HDIG domain-containing protein	1.77	0.0204	-0.46	-3.93	SAMN04487868_103186
A0A1I4JHN2	-1.7619	1.7619	Molybdopterin molybdenumtransferase	1.76	0.0206	-0.29	-3.92	SAMN04487868_10653
A0A1I4KFQ9	-1.7615	1.7615	Aldehyde dehydrogenase	1.76	0.0206	-4.61	-3.92	SAMN04487868_109141
A0A1I4L4N0	-1.7615	1.7615	Uncharacterized protein	1.76	0.0206	-0.39	-3.92	SAMN04487868_112105
A0A1I4HLK8	-1.7606	1.7606	Flagellar protein FliL	1.76	0.0205	-0.83	-3.91	SAMN04487868_101450
A0A1I4LRX3	-1.7596	1.7596	Uncharacterized protein	1.76	0.0205	-0.63	-3.91	SAMN04487868_11628
A0A1I4K3R5	-1.7596	1.7596	Uncharacterized protein	1.76	0.0205	-0.41	-3.91	SAMN04487868_10865
A0A1I4NI13	-1.7595	1.7595	Uncharacterized protein	1.76	0.0205	-1.03	-3.91	SAMN04487868_1412
A0A1I4HVG9	-1.7591	1.7591	Uncharacterized protein	1.76	0.0204	-3.89	-3.91	SAMN04487868_10293
A0A1I4H531	-1.7590	1.7590	PAS domain S-box-containing protein/diguanylate cyclase (GGDEF) domain-containing protein	1.76	0.0204	-0.81	-3.91	SAMN04487868_10194
A0A1I4KEY6	-1.7572	1.7572	Uncharacterized domain 1-containing protein	1.76	0.0205	-1.24	-4.77	SAMN04487868_109131

A0A1I4LY39	-1.7494	1.7494	General secretion pathway protein F	1.75	0.0210	-0.19	-3.88	SAMN04487868_11760
A0A1I4IBH7	-1.7468	1.7468	Chemotaxis protein MotA	1.75	0.0211	-1.16	-3.88	SAMN04487868_103111
A0A1I4HZT1	-1.7467	1.7467	Uncharacterized protein	1.75	0.0210	-3.49	-3.87	SAMN04487868_102215
A0A1I4MSF5	-1.7466	1.7466	Selenophosphate synthase	1.75	0.0210	-0.53	-3.87	SAMN04487868_12531
A0A1I4L200	-1.7453	1.7453	PAS domain-containing protein	1.75	0.0211	-0.31	-3.87	SAMN04487868_11257
A0A1I4LE81	-1.7287	1.7287	DNA-binding transcriptional regulator. LysR family	1.73	0.0219	-0.54	-3.83	SAMN04487868_11414
A0A1I4IAP7	-1.7283	1.7283	2-oxopent-4-enoate/cis-2-oxohex-4-enoate hydratase	1.73	0.0218	-0.89	-3.83	SAMN04487868_103135
A0A1I4N428	-1.7273	1.7273	MSHA biogenesis protein MshK	1.73	0.0218	-0.90	-3.82	SAMN04487868_12935
A0A1I4KE81	-1.7268	1.7268	Lysophospholipase. alpha-beta hydrolase superfamily	1.73	0.0218	-1.36	-3.82	SAMN04487868_109129
A0A1I4K3J9	-1.7256	1.7256	CRP/FNR family transcriptional regulator. cyclic AMP receptor protein	1.73	0.0218	-0.32	-3.82	SAMN04487868_10883
A0A1I4KNI9	-1.7136	1.7136	L-leucine ABC transporter membrane protein /L-isoleucine ABC transporter membrane protein /L-valine ABC transporter membrane protein	1.71	0.0221	-1.54	-3.79	SAMN04487868_110148
A0A1I4HKE3	-1.7088	1.7088	Chemotaxis protein MotB	1.71	0.0224	-1.15	-3.77	SAMN04487868_101470
A0A1I4LW20	-1.7076	1.7076	ATP-grasp domain-containing protein	1.71	0.0225	-0.78	-3.77	SAMN04487868_11731
A0A1I4HZ64	-1.7020	1.7020	Transcriptional regulator. LysR family	1.70	0.0225	-0.60	-3.76	SAMN04487868_102169
A0A1I4I2I7	-1.7013	1.7013	Phosphogluconate dehydratase	1.70	0.0225	-1.08	-3.75	edd SAMN04487868_102253
A0A1I4MNV6	-1.6928	1.6928	Cobalt-zinc-cadmium resistance protein CzcA	1.69	0.0228	-0.96	-3.73	SAMN04487868_12438
A0A1I4I057	-1.6919	1.6919	HTH-type transcriptional regulator MalT	1.69	0.0228	-0.58	-3.73	malT SAMN04487868_102203
A0A1I4MV52	-1.6886	1.6886	Na(+)-translocating NADH-quinone reductase subunit A	1.69	0.0229	-0.26	-3.72	nqrA SAMN04487868_12612
A0A1I4KCV4	-1.6883	1.6883	PAS domain S-box-containing protein	1.69	0.0229	-0.98	-3.72	SAMN04487868_10989
A0A1I4KLQ5	-1.6880	1.6880	Predicted ATP-dependent endonuclease of the OLD family. contains P-loop ATPase and TOPRIM domains	1.69	0.0229	-0.58	-3.72	SAMN04487868_110108
A0A1I4MXU0	-1.6873	1.6873	Small-conductance mechanosensitive channel	1.69	0.0228	-0.68	-3.72	SAMN04487868_12718
A0A1I4MWM6	-1.6808	1.6808	PilZ domain-containing protein	1.68	0.0230	-1.10	-3.70	SAMN04487868_12643
A0A1I4NC86	-1.6748	1.6748	Lysophospholipase L1	1.67	0.0233	-0.54	-3.68	SAMN04487868_13324
A0A1I4HIU2	-1.6745	1.6745	Sigma-54 specific transcriptional regulator. flagellar regulatory protein A	1.67	0.0233	-0.43	-3.68	SAMN04487868_101437
A0A1I4IMI1	-1.6742	1.6742	Uncharacterized protein	1.67	0.0233	-0.68	-3.68	SAMN04487868_1046
A0A1I4LF31	-1.6678	1.6678	Alkyl hydroperoxide reductase AhpD	1.67	0.0240	-0.52	-3.66	SAMN04487868_11435
A0A1I4LAB0	-1.6599	1.6599	Cytochrome c oxidase subunit 1	1.66	0.0249	-2.66	-3.64	SAMN04487868_11385
A0A1I4HEE4	-1.6594	1.6594	Deoxyribonuclease-1	1.66	0.0249	-1.24	-3.64	SAMN04487868_101279
A0A1I4KV38	-1.6577	1.6577	Outer membrane autotransporter barrel domain-containing protein	1.66	0.0251	-1.93	-3.64	SAMN04487868_11199
A0A1I4HU28	-1.6534	1.6534	Long-chain acyl-CoA synthetase	1.65	0.0251	-0.58	-3.63	SAMN04487868_1022
A0A1I4K9D1	-1.6495	1.6495	Fe-ADH domain-containing protein	1.65	0.0256	-0.25	-3.62	SAMN04487868_10910
A0A1I4N4P2	-1.6493	1.6493	MSHA biogenesis protein MshO	1.65	0.0256	-1.75	-3.62	SAMN04487868_12946
A0A1I4IDP2	-1.6476	1.6476	Spermidine/putrescine import ATP-binding protein PotA	1.65	0.0258	-0.64	-3.61	potA SAMN04487868_103201
A0A1I4JHZ0	-1.6433	1.6433	Transcription termination factor Rho	1.64	0.0262	-0.21	-3.60	rho SAMN04487868_10655
A0A1I4LXI7	-1.6429	1.6429	ABC-type uncharacterized transport system. substrate-binding protein	1.64	0.0261	-1.08	-3.60	SAMN04487868_11749
A0A1I4KFC9	-1.6428	1.6428	Transcriptional regulator. TetR family	1.64	0.0261	-1.16	-3.60	SAMN04487868_109132
A0A1I4N4R4	-1.6411	1.6411	MSHA biogenesis protein MshI	1.64	0.0262	-1.07	-3.60	SAMN04487868_12933

A0A1I4HYW0	-1.6334	1.6334	Uncharacterized protein	1.63	0.0266	-0.39	-3.58	SAMN04487868_102170
A0A1I4IM19	-1.6295	1.6295	FHA domain-containing protein	1.63	0.0267	-1.76	-3.57	SAMN04487868_10428
A0A1I4NEG8	-1.6242	1.6242	Small conductance mechanosensitive channel	1.62	0.0266	-0.57	-3.55	SAMN04487868_13516
A0A1I4N4S0	-1.6129	1.6129	MSHA biogenesis protein MshG	1.61	0.0268	-1.78	-3.52	SAMN04487868_12940
A0A1I4HGN7	-1.6123	1.6123	Chain length determinant protein	1.61	0.0268	-0.91	-3.52	SAMN04487868_101353
A0A1I4M6U9	-1.6116	1.6116	Chalcone isomerase-like	1.61	0.0269	-0.84	-3.52	SAMN04487868_11945
A0A1I4HBB3	-1.6074	1.6074	Chemotaxis protein MotB	1.61	0.0274	-1.11	-3.51	SAMN04487868_101248
A0A1I4KJ92	-1.6065	1.6065	Diguanylate cyclase/phosphodiesterase	1.61	0.0273	-0.59	-3.51	SAMN04487868_11021
A0A1I4KC43	-1.5974	1.5974	Potassium/proton antiporter. CPA1 family	1.60	0.0278	-0.66	-3.48	SAMN04487868_10967
A0A1I4MKX2	-1.5954	1.5954	Signal transduction histidine kinase	1.60	0.0282	-1.01	-3.48	SAMN04487868_12333
A0A1I4H781	-1.5921	1.5921	TPM_phosphatase domain-containing protein	1.59	0.0283	-0.56	-3.47	SAMN04487868_101139
A0A1I4KC90	-1.5906	1.5906	Membrane-bound serine protease (ClpP class)	1.59	0.0285	-1.00	-3.47	SAMN04487868_10971
A0A1I4H6R8	-1.5866	1.5866	Diguanylate cyclase (GGDEF) domain-containing protein	1.59	0.0287	-0.41	-3.46	SAMN04487868_10172
A0A1I4MSX3	-1.5828	1.5828	Response regulator receiver modulated diguanylate cyclase/phosphodiesterase	1.58	0.0288	-0.47	-3.45	SAMN04487868_12553
A0A1I4H6R1	-1.5820	1.5820	DNA-binding transcriptional regulator. Lrp family	1.58	0.0288	-0.72	-3.44	SAMN04487868_101135
A0A1I4LXT7	-1.5819	1.5819	Acetyltransferase (GNAT) family protein	1.58	0.0287	-0.33	-3.44	SAMN04487868_11752
A0A1I4LEX0	-1.5785	1.5785	3-methylcrotonyl-CoA carboxylase beta subunit	1.58	0.0289	-1.20	-3.44	SAMN04487868_11439
A0A1I4MAL4	-1.5723	1.5723	NAD(P) transhydrogenase subunit alpha	1.57	0.0293	-0.72	-3.42	SAMN04487868_12051
A0A1I4MXJ4	-1.5659	1.5659	Two-component system. CitB family. sensor kinase	1.57	0.0295	-2.52	-3.40	SAMN04487868_1277
A0A1I4HXR6	-1.5563	1.5563	Outer membrane protein	1.56	0.0301	-0.76	-3.38	SAMN04487868_10298
A0A1I4MP75	-1.5541	1.5541	Acetyltransferase component of pyruvate dehydrogenase complex	1.55	0.0302	-0.70	-3.37	SAMN04487868_12455
A0A1I4JAQ5	-1.5535	1.5535	Uncharacterized protein	1.55	0.0302	-0.41	-3.37	SAMN04487868_105222
A0A1I4IE81	-1.5498	1.5498	DNA excision repair protein ERCC-2	1.55	0.0302	-0.60	-3.36	SAMN04487868_103225
A0A1I4L226	-1.5480	1.5480	Zinc import ATP-binding protein ZnuC	1.55	0.0303	-1.33	-3.98	znuC SAMN04487868_11259
A0A1I4HVJ7	-1.5445	1.5445	Polysaccharide chain length determinant protein. PEP-CTERM locus subfamily	1.54	0.0307	-0.66	-3.35	SAMN04487868_10265
A0A1I4LJ19	-1.5413	1.5413	CDP-diacylglycerol--serine O-phosphatidyltransferase	1.54	0.0312	-1.17	-3.34	SAMN04487868_1152
A0A1I4HZS9	-1.5410	1.5410	Tetratricopeptide repeat-containing protein	1.54	0.0313	-1.31	-3.34	SAMN04487868_102213
A0A1I4J658	-1.5382	1.5382	Magnesium transporter	1.54	0.0314	-1.42	-3.34	SAMN04487868_10582
A0A1I4IF50	-1.5380	1.5380	Amino acid/amide ABC transporter membrane protein 2. HAAT family	1.54	0.0314	-1.82	-3.33	SAMN04487868_103244
A0A1I4HFD7	-1.5372	1.5372	Type IV pilus assembly protein PilB	1.54	0.0313	-0.39	-3.33	SAMN04487868_101346
A0A1I4IA30	-1.5366	1.5366	Uncharacterized protein	1.54	0.0313	-0.42	-3.33	SAMN04487868_103121
A0A1I4MYE2	-1.5262	1.5262	Uncharacterized protein	1.53	0.0319	-1.35	-3.31	SAMN04487868_12712
A0A1I4K5E6	-1.5259	1.5259	Diguanylate cyclase/phosphodiesterase	1.53	0.0320	-1.15	-3.31	SAMN04487868_108128
A0A1I4N4S5	-1.5220	1.5220	MSHA biogenesis protein MshJ	1.52	0.0321	-1.64	-3.30	SAMN04487868_12934
A0A1I4MAB6	-1.5136	1.5136	Uncharacterized protein	1.51	0.0328	-0.69	-3.27	SAMN04487868_12048
A0A1I4J9P3	-1.5077	1.5077	Nicotinamidase-related amidase	1.51	0.0332	-0.47	-3.26	SAMN04487868_105199
A0A1I4N8G4	-1.5027	1.5027	NitT/TauT family transport system substrate-binding protein	1.50	0.0338	-0.49	-3.25	SAMN04487868_1311
A0A1I4KAY1	-1.5008	1.5008	Amino acid ABC transporter substrate-binding protein. PAAT family	1.50	0.0339	-0.80	-3.24	SAMN04487868_10942
A0A1I4KBK1	-1.5007	1.5007	Transcriptional regulator. TetR family	1.50	0.0339	-0.49	-3.24	SAMN04487868_10965

A0A1I4MAL5	-1.4998	1.4998	Acetyl-CoA C-acetyltransferase	1.50	0.0339	-0.70	-3.24	SAMN04487868_12058
A0A1I4L2Y2	-1.4803	1.4803	Beta-lactamase	1.48	0.0352	-0.33	-3.19	SAMN04487868_11286
A0A1I4MTJ3	-1.4725	1.4725	Iron complex outermembrane recepter protein	1.47	0.0360	-1.24	-3.18	SAMN04487868_12557
A0A1I4M1I2	-1.4690	1.4690	Pilus assembly protein FimV	1.47	0.0360	-0.89	-3.17	SAMN04487868_11834
A0A1I4IT43	-1.4669	1.4669	Two component transcriptional regulator. LuxR family	1.47	0.0362	-0.23	-3.16	SAMN04487868_104167
A0A1I4L0N3	-1.4660	1.4660	DNA-binding transcriptional regulator. LysR family	1.47	0.0363	-1.03	-3.16	SAMN04487868_11230
A0A1I4H6S1	-1.4653	1.4653	LemA protein	1.47	0.0364	-0.36	-3.16	SAMN04487868_101138
A0A1I4KNG7	-1.4643	1.4643	L-leucine ABC transporter ATP-binding protein /L-isoleucine ABC transporter ATP-binding protein /L-valine ABC transporter ATP-binding protein	1.46	0.0364	-0.84	-3.16	SAMN04487868_110146
A0A1I4LW57	-1.4549	1.4549	Nicotinamidase-related amidase	1.45	0.0370	-0.63	-3.13	SAMN04487868_11718
A0A1I4KRM8	-1.4523	1.4523	Uncharacterized protein	1.45	0.0372	-0.54	-3.13	SAMN04487868_1112
A0A1I4IMP5	-1.4495	1.4495	MerR family transcriptional regulator. redox-sensitive transcriptional activator SoxR	1.45	0.0371	-1.21	-3.12	SAMN04487868_10444
A0A1I4IT61	-1.4471	1.4471	Aminotransferase	1.45	0.0376	-0.35	-3.11	SAMN04487868_104165
A0A1I4N791	-1.4466	1.4466	Betaine/carnitine transporter. BCCT family	1.45	0.0375	-1.13	-3.11	SAMN04487868_13016
A0A1I4LY63	-1.4461	1.4461	Type II secretion system protein C (GspC)	1.45	0.0375	-0.58	-3.11	SAMN04487868_11762
A0A1I4H898	-1.4415	1.4415	AbiTii domain-containing protein	1.44	0.0378	-0.50	-3.10	SAMN04487868_101129
A0A1I4HH40	-1.4395	1.4395	Diguanylate cyclase/phosphodiesterase	1.44	0.0380	-0.95	-3.10	SAMN04487868_101404
A0A1I4KP21	-1.4293	1.4293	TPR repeat-containing protein	1.43	0.0385	-1.05	-3.07	SAMN04487868_110150
A0A1I4J2R8	-1.4270	1.4270	Integration host factor subunit beta	1.43	0.0391	-0.59	-3.07	ihfB himD SAMN04487868_10533
A0A1I4J9L6	-1.4266	1.4266	Chemotaxis protein methyltransferase	1.43	0.0390	-0.88	-3.07	SAMN04487868_105194
A0A1I4J8D4	-1.4252	1.4252	Succinate dehydrogenase subunit B	1.43	0.0390	-0.20	-3.06	SAMN04487868_105170
A0A1I4KU11	-1.4224	1.4224	HD-like signal output (HDOD) domain. no enzymatic activity	1.42	0.0389	-0.20	-3.06	SAMN04487868_11177
A0A1I4IDR8	-1.4203	1.4203	Alanine or glycine:cation symporter. AGCS family	1.42	0.0389	-1.46	-3.05	SAMN04487868_103211
A0A1I4I8X7	-1.4199	1.4199	HDOD domain-containing protein	1.42	0.0389	-0.80	-3.05	SAMN04487868_10325
A0A1I4JKB7	-1.4160	1.4160	Methionine biosynthesis protein MetW	1.42	0.0391	-0.45	-3.04	SAMN04487868_106103
A0A1I4MN11	-1.4145	1.4145	Amino acid ABC transporter substrate-binding protein. PAAT family	1.41	0.0393	-0.46	-3.04	SAMN04487868_12416
A0A1I4K9I6	-1.4027	1.4027	Glutamine synthetase	1.40	0.0395	-0.37	-3.01	SAMN04487868_10912
A0A1I4IA63	-1.4016	1.4016	Two-component system. response regulator RegA	1.40	0.0394	-0.28	-4.86	SAMN04487868_10399
A0A1I4IWR2	-1.3834	1.3834	Uncharacterized protein	1.38	0.0412	-0.57	-2.96	SAMN04487868_104247
A0A1I4JK68	-1.3792	1.3792	DUF2489 domain-containing protein	1.38	0.0415	-0.64	-2.95	SAMN04487868_106130
A0A1I4K964	-1.3761	1.3761	Nitrate/nitrite transport system substrate-binding protein	1.38	0.0418	-0.59	-2.95	SAMN04487868_1092
A0A1I4MGI2	-1.3734	1.3734	PSII_BNR domain-containing protein	1.37	0.0419	-0.71	-2.94	SAMN04487868_1223
A0A1I4N864	-1.3729	1.3729	PKS_ER domain-containing protein	1.37	0.0420	-0.49	-2.94	SAMN04487868_13037
A0A1I4NCC4	-1.3684	1.3684	Outer membrane protein	1.37	0.0427	-0.38	-2.93	SAMN04487868_13330
A0A1I4K3X4	-1.3669	1.3669	FMN-dependent NADH-azoreductase	1.37	0.0428	-0.84	-2.93	azoR SAMN04487868_10886
A0A1I4L7I8	-1.3643	1.3643	ATP synthase gamma chain	1.36	0.0430	-0.20	-2.92	atpG SAMN04487868_11318
A0A1I4KV06	-1.3596	1.3596	Nitronate monooxygenase	1.36	0.0430	-0.76	-2.91	SAMN04487868_11197
A0A1I4M785	-1.3573	1.3573	Isoquinoline 1-oxidoreductase. beta subunit	1.36	0.0432	-0.65	-2.90	SAMN04487868_11970
A0A1I4KZP2	-1.3512	1.3512	Uncharacterized protein	1.35	0.0446	-0.14	-2.89	SAMN04487868_1127

A0A1I4JWS4	-1.3488	1.3488	Cold-shock DNA-binding protein family	1.35	0.0446	-0.73	-2.88	SAMN04487868_107169
A0A1I4MAA3	-1.3476	1.3476	Gluconate 5-dehydrogenase	1.35	0.0450	-0.75	-2.88	SAMN04487868_12055
A0A1I4LRK9	-1.3447	1.3447	Chromosome partitioning protein. ParB family	1.34	0.0453	-0.33	-2.88	SAMN04487868_11626
A0A1I4JML5	-1.3434	1.3434	Penicillin-binding protein 1B	1.34	0.0453	-0.34	-2.87	SAMN04487868_106167
A0A1I4JYD1	-1.3401	1.3401	Diguanylate cyclase (GGDEF) domain-containing protein	1.34	0.0455	-1.88	-2.87	SAMN04487868_107175
A0A1I4I060	-1.3401	1.3401	FAD:protein FMN transferase	1.34	0.0455	-1.19	-3.30	SAMN04487868_102226
A0A1I4L6W4	-1.3368	1.3368	TRAP transporter. DctM subunit	1.34	0.0454	-1.13	-2.86	SAMN04487868_1134
A0A1I4MA46	-1.3365	1.3365	NTE family protein	1.34	0.0453	-0.47	-2.86	SAMN04487868_12049
A0A1I4LDQ4	-1.3276	1.3276	Uncharacterized protein	1.33	0.0462	-0.31	-2.84	SAMN04487868_1143
A0A1I4LIK8	-1.3274	1.3274	(S)-ureidoglycine aminohydrolase	1.33	0.0461	-0.50	-2.84	SAMN04487868_11492
A0A1I4JJ39	-1.3255	1.3255	NADPH2:quinone reductase	1.33	0.0462	-0.52	-2.83	SAMN04487868_10684
A0A1I4KDF2	-1.3251	1.3251	3-hydroxybutyrate dehydrogenase	1.33	0.0462	-0.42	-2.83	SAMN04487868_10998
A0A1I4HZ71	-1.3240	1.3240	Uncharacterized protein	1.32	0.0463	-0.80	-2.83	SAMN04487868_102191
A0A1I4H5Q2	-1.3236	1.3236	Esterase. PHB depolymerase family	1.32	0.0463	-1.16	-3.25	SAMN04487868_101110
A0A1I4IWV9	-1.3236	1.3236	PhoH-like ATPase	1.32	0.0463	-0.09	-2.83	SAMN04487868_104250
A0A1I4KRV5	-1.3229	1.3229	Flagellar assembly protein T. N-terminal domain	1.32	0.0464	-0.37	-2.83	SAMN04487868_11120
A0A1I4HDY8	-1.3211	1.3211	Uncharacterized protein	1.32	0.0466	-0.24	-2.82	SAMN04487868_101278
A0A1I4H9M8	-1.3177	1.3177	Lysophospholipase. alpha-beta hydrolase superfamily	1.32	0.0467	-0.63	-2.81	SAMN04487868_101204
A0A1I4LG74	-1.3172	1.3172	DNA-binding transcriptional regulator. MerR family	1.32	0.0466	-0.47	-2.81	SAMN04487868_11441
A0A1I4H5P2	-1.3037	1.3037	Alcohol dehydrogenase	1.30	0.0477	-0.48	-2.78	SAMN04487868_10160
A0A1I4H5H9	-1.3020	1.3020	Glutamate dehydrogenase	1.30	0.0478	-0.90	-2.78	SAMN04487868_101107
A0A1I4M0A5	0.0000	0.0000	Acyl-CoA thioester hydrolase	1.30	0.0482	0.74	2.77	SAMN04487868_1185
A0A1I4IE19	0.0000	0.0000	Alpha/beta hydrolase family protein	1.28	0.0494	0.77	2.74	SAMN04487868_103220
A0A1I4LY48	0.0000	0.0000	Crotonobetainyl-CoA:carnitine CoA-transferase CaiB	1.28	0.0494	0.51	2.74	SAMN04487868_11769
A0A1I4I3F5	0.0000	0.0000	Cysteine--tRNA ligase	1.30	0.0483	0.45	2.77	cysS SAMN04487868_102276
A0A1I4K422	0.0000	0.0000	Deoxyuridine 5'-triphosphate nucleotidohydrolase	1.28	0.0495	0.42	2.73	dut SAMN04487868_10896
A0A1I4J779	0.0000	0.0000	Dual-specificity RNA methyltransferase RlmN	1.28	0.0495	0.95	3.12	rlmN SAMN04487868_105141
A0A1I4HEJ2	0.0000	0.0000	Leucine--tRNA ligase	1.29	0.0492	0.58	2.75	leuS SAMN04487868_101283
A0A1I4IE42	0.0000	0.0000	Luciferase family oxidoreductase. group 1	1.28	0.0494	0.48	2.74	SAMN04487868_103221
A0A1I4HHH1	0.0000	0.0000	N5-carboxyaminoimidazole ribonucleotide mutase	1.30	0.0481	0.75	2.77	purE SAMN04487868_101407
A0A1I4K3Y5	0.0000	0.0000	Phosphomannomutase / phosphoglucomutase	1.29	0.0487	-0.56	-2.76	SAMN04487868_10895
A0A1I4HAR2	0.0000	0.0000	Polyisoprenoid-binding protein YceI	1.30	0.0482	0.43	2.77	SAMN04487868_101236
A0A1I4LLK4	0.0000	0.0000	Shikimate kinase	1.29	0.0494	0.65	2.74	aroK SAMN04487868_11555
A0A1I4KE75	0.0000	0.0000	Small GTP-binding protein domain-containing protein	1.28	0.0499	0.20	2.73	SAMN04487868_109107
A0A1I4HW16	0.0000	0.0000	Sulfurtransferase TusA	1.28	0.0494	0.73	2.74	SAMN04487868_102104
A0A1I4MPV9	0.0000	0.0000	TRAP-type C4-dicarboxylate transport system. small permease component	1.28	0.0500	1.56	2.72	SAMN04487868_12449
A0A1I4MK06	0.0000	0.0000	Uncharacterized protein	1.29	0.0491	0.79	2.75	SAMN04487868_12337
A0A1I4HZ28	1.3015	-1.3015	Cytochrome c oxidase accessory protein FixG	1.30	0.0478	0.75	2.78	SAMN04487868_102190

A0A1I4MZ76	1.3066	-1.3066	50S ribosomal protein L9	1.31	0.0476	0.34	2.79	rplI SAMN04487868_12755
A0A1I4N4K1	1.3071	-1.3071	50S ribosomal protein L15	1.31	0.0477	0.38	2.79	rplO SAMN04487868_12922
A0A1I4H6A9	1.3082	-1.3082	Uncharacterized protein	1.31	0.0475	0.44	2.79	SAMN04487868_101117
A0A1I4K6U9	1.3132	-1.3132	Alkaline phosphatase D	1.31	0.0470	2.14	2.80	SAMN04487868_108147
A0A1I4HY17	1.3169	-1.3169	Lipoprotein-releasing system ATP-binding protein LolD	1.32	0.0465	0.56	2.81	lolD SAMN04487868_102147
A0A1I4IVC2	1.3173	-1.3173	GTPase Era	1.32	0.0466	0.39	2.81	era SAMN04487868_104194
A0A1I4HCK4	1.3177	-1.3177	Uncharacterized protein	1.32	0.0467	1.48	2.81	SAMN04487868_101280
A0A1I4LMC3	1.3185	-1.3185	50S ribosomal protein L31	1.32	0.0467	0.62	2.82	rpmE SAMN04487868_11563
A0A1I4KUU1	1.3187	-1.3187	Amino acid ABC transporter substrate-binding protein. PAAT family	1.32	0.0467	0.39	2.82	SAMN04487868_11184
A0A1I4K485	1.3209	-1.3209	50S ribosomal protein L33	1.32	0.0465	1.13	2.82	rpmG SAMN04487868_108100
A0A1I4NFL6	1.3283	-1.3283	30S ribosomal protein S12	1.33	0.0462	0.65	2.84	rpsL SAMN04487868_1364
A0A1I4IUZ0	1.3291	-1.3291	Antitoxin CptB	1.33	0.0461	0.74	2.84	SAMN04487868_104206
A0A1I4LL56	1.3298	-1.3298	50S ribosomal protein L21	1.33	0.0461	0.52	2.84	rplU SAMN04487868_11532
A0A1I4HT60	1.3338	-1.3338	Cupin-like domain-containing protein	1.33	0.0456	0.36	2.85	SAMN04487868_10237
A0A1I4KK12	1.3374	-1.3374	Ubiquinone/menaquinone biosynthesis C-methyltransferase UbiE	1.34	0.0454	0.56	2.86	ubiE SAMN04487868_11051
A0A1I4K9Q2	1.3378	-1.3378	Short-chain dehydrogenase	1.34	0.0454	0.30	2.86	SAMN04487868_10919
A0A1I4LKX0	1.3379	-1.3379	Pseudouridine synthase	1.34	0.0454	0.80	2.86	SAMN04487868_1159
A0A1I4J8U0	1.3383	-1.3383	Sirohydrochlorin cobaltochelatase	1.34	0.0454	0.67	2.86	SAMN04487868_105153
A0A1I4KJC2	1.3397	-1.3397	Uncharacterized protein	1.34	0.0455	0.90	2.86	SAMN04487868_11038
A0A1I4HII9	1.3428	-1.3428	Uncharacterized protein	1.34	0.0454	1.51	2.87	SAMN04487868_101434
A0A1I4JWC4	1.3443	-1.3443	Elongation factor Ts	1.34	0.0453	0.38	2.87	tsf SAMN04487868_107159
A0A1I4H3Z8	1.3482	-1.3482	Uncharacterized protein	1.35	0.0448	3.03	2.88	SAMN04487868_10164
A0A1I4N287	1.3494	-1.3494	Acetoin utilization deacetylase AcuC	1.35	0.0446	0.49	2.89	SAMN04487868_12839
A0A1I4HI10	1.3505	-1.3505	UDP-4-amino-4.6-dideoxy-N-acetyl-beta-L-altrosamine transaminase	1.35	0.0446	0.62	2.89	SAMN04487868_101361
A0A1I4ND96	1.3535	-1.3535	Poly(Hydroxyalkanoate) granule-associated protein	1.35	0.0439	0.50	2.90	SAMN04487868_1342
A0A1I4N3N1	1.3556	-1.3556	30S ribosomal protein S13	1.36	0.0435	0.71	2.90	rpsM SAMN04487868_12924
A0A1I4HDH4	1.3596	-1.3596	PTS IIA-like nitrogen-regulatory protein PtsN	1.36	0.0430	0.84	2.91	SAMN04487868_101311
A0A1I4ITS3	1.3597	-1.3597	Phosphoenolpyruvate carboxylase	1.36	0.0430	0.49	2.91	ppc SAMN04487868_104184
A0A1I4L2E9	1.3600	-1.3600	UPF0301 protein SAMN04487868_11271	1.36	0.0431	0.47	2.91	SAMN04487868_11271
A0A1I4HSB6	1.3601	-1.3601	MoxR-like ATPase	1.36	0.0431	0.20	2.91	SAMN04487868_10214
A0A1I4I7N3	1.3631	-1.3631	Acyl-CoA dehydrogenase	1.36	0.0429	0.83	2.92	SAMN04487868_10348
A0A1I4J2N7	1.3638	-1.3638	30S ribosomal protein S1	1.36	0.0429	0.23	2.92	SAMN04487868_10532
A0A1I4K5F9	1.3663	-1.3663	Rubredoxin-NAD+ reductase	1.37	0.0429	0.61	2.93	SAMN04487868_108130
A0A1I4MSF3	1.3685	-1.3685	Outer membrane protein beta-barrel domain-containing protein	1.37	0.0427	2.07	2.93	SAMN04487868_12542
A0A1I4M3E0	1.3725	-1.3725	DNA polymerase III subunit epsilon	1.37	0.0420	1.20	2.94	dnaQ SAMN04487868_11862
A0A1I4JXP9	1.3734	-1.3734	Uncharacterized protein	1.37	0.0420	1.58	2.94	SAMN04487868_107170
A0A1I4M1T7	1.3745	-1.3745	DNA segregation ATPase FtsK/SpoIIIE. S-DNA-T family	1.37	0.0419	0.86	2.94	SAMN04487868_11845
A0A1I4M2T2	1.3761	-1.3761	Microcin C transport system ATP-binding protein	1.38	0.0418	0.76	2.95	SAMN04487868_11854
A0A1I4LS30	1.3783	-1.3783	Uncharacterized conserved protein. DUF1778 family	1.38	0.0416	1.09	2.95	SAMN04487868_11632

A0A1I4HHJ3	1.3824	-1.3824	dTDP-4-amino-4.6-dideoxygalactose transaminase	1.38	0.0412	1.16	2.96	SAMN04487868_101372
A0A1I4IVM8	1.3827	-1.3827	L-aspartate oxidase	1.38	0.0412	0.40	2.96	SAMN04487868_104205
A0A1I4KN10	1.3849	-1.3849	Transcription termination/antitermination protein NusA	1.38	0.0410	0.22	2.97	nusA SAMN04487868_110135
A0A1I4M1M5	1.3857	-1.3857	Chorismate synthase	1.39	0.0411	0.39	2.97	aroC SAMN04487868_11827
A0A1I4LYK1	1.3870	-1.3870	Uncharacterized protein	1.39	0.0410	0.47	2.97	SAMN04487868_11783
A0A1I4M5P0	1.3887	-1.3887	Valine--tRNA ligase	1.39	0.0408	0.53	2.98	valS SAMN04487868_11918
A0A1I4M5Y8	1.3928	-1.3928	dCTP deaminase	1.39	0.0403	1.20	2.99	dcd SAMN04487868_11935
A0A1I4K2X7	1.3929	-1.3929	Anthranilate synthase. component II	1.39	0.0403	0.55	2.99	SAMN04487868_10854
A0A1I4JSF8	1.3947	-1.3947	Dihydroorotase	1.39	0.0402	0.43	2.99	pyrC SAMN04487868_10745
A0A1I4HFQ5	1.3965	-1.3965	Lipopolysaccharide export system ATP-binding protein	1.40	0.0401	0.37	3.00	SAMN04487868_101314
A0A1I4KI15	1.3986	-1.3986	Ribosomal protein L11 methyltransferase	1.40	0.0397	0.56	3.00	prmA SAMN04487868_11016
A0A1I4KN14	1.4013	-1.4013	RNA-binding protein	1.40	0.0394	0.91	3.01	SAMN04487868_110126
A0A1I4IWL8	1.4018	-1.4018	DUF1244 domain-containing protein	1.40	0.0395	0.61	3.01	SAMN04487868_104242
A0A1I4JJ69	1.4031	-1.4031	Anti-ECFsigma factor. ChrR	1.40	0.0395	0.40	3.01	SAMN04487868_10687
A0A1I4MJC2	1.4038	-1.4038	DUF4124 domain-containing protein	1.40	0.0394	2.85	3.01	SAMN04487868_1235
A0A1I4L1V4	1.4053	-1.4053	Pimeloyl-ACP methyl ester carboxylesterase	1.41	0.0394	0.54	3.02	SAMN04487868_11253
A0A1I4J8W0	1.4074	-1.4074	Chromosome partition protein Smc	1.41	0.0393	0.60	3.02	smc SAMN04487868_105182
A0A1I4KSF3	1.4082	-1.4082	Phosphoglycolate phosphatase	1.41	0.0393	1.02	3.02	SAMN04487868_11142
A0A1I4M212	1.4120	-1.4120	Phospho-2-dehydro-3-deoxyheptonate aldolase	1.41	0.0393	0.68	3.03	SAMN04487868_11850
A0A1I4L0M2	1.4161	-1.4161	Thiol peroxidase	1.42	0.0392	0.88	3.04	tpx SAMN04487868_11228
A0A1I4KKJ1	1.4177	-1.4177	PqqA peptide cyclase	1.42	0.0391	0.59	3.04	pqqE SAMN04487868_11080
A0A1I4MHU4	1.4189	-1.4189	Cyclopentanol dehydrogenase	1.42	0.0389	2.87	3.55	SAMN04487868_12259
A0A1I4JKH7	1.4218	-1.4218	Uncharacterized protein	1.42	0.0388	1.65	3.05	SAMN04487868_106138
A0A1I4KMI1	1.4247	-1.4247	Ribosomal RNA large subunit methyltransferase E	1.42	0.0389	0.65	3.06	rlmE ftsJ rrmJ SAMN04487868_110127
A0A1I4MYZ7	1.4248	-1.4248	Alanine racemase	1.42	0.0389	0.58	3.06	SAMN04487868_12753
A0A1I4H9B8	1.4260	-1.4260	Peptidylprolyl isomerase	1.43	0.0390	1.03	3.06	SAMN04487868_101151
A0A1I4HHF8	1.4279	-1.4279	Sulfotransferase family protein	1.43	0.0388	0.89	3.07	SAMN04487868_101370
A0A1I4HM77	1.4337	-1.4337	Cytochrome c-type biogenesis protein CcmH	1.43	0.0383	0.75	3.08	SAMN04487868_101485
A0A1I4KK71	1.4339	-1.4339	Phosphoribosyl-ATP pyrophosphatase	1.43	0.0384	0.62	3.08	hisE SAMN04487868_11047
A0A1I4LMG6	1.4355	-1.4355	Malate dehydrogenase (Oxaloacetate-decarboxylating)(NADP+)	1.44	0.0383	0.30	3.09	SAMN04487868_11562
A0A1I4KP08	1.4401	-1.4401	Uncharacterized protein	1.44	0.0379	0.92	3.10	SAMN04487868_110144
A0A1I4M613	1.4440	-1.4440	Uncharacterized protein	1.44	0.0379	0.34	3.11	SAMN04487868_11934
A0A1I4HD24	1.4468	-1.4468	Sulfate adenylyltransferase subunit 1	1.45	0.0375	0.31	3.11	cysN SAMN04487868_101293
A0A1I4JFV6	1.4470	-1.4470	ATP-dependent DNA helicase Rep	1.45	0.0375	0.98	3.11	rep SAMN04487868_10637
A0A1I4KC79	1.4477	-1.4477	Pimeloyl-ACP methyl ester carboxylesterase	1.45	0.0375	2.20	3.12	SAMN04487868_10979
A0A1I4JF60	1.4500	-1.4500	Uncharacterized conserved protein YaeQ. suppresses RfaH defect	1.45	0.0372	0.51	3.12	SAMN04487868_10619
A0A1I4NE01	1.4500	-1.4500	Anti-anti-sigma factor	1.45	0.0372	0.76	3.12	SAMN04487868_13416
A0A1I4KUB7	1.4533	-1.4533	Adenosylmethionine-8-amino-7-oxononanoate aminotransferase	1.45	0.0371	0.54	3.13	bioA SAMN04487868_11180

A0A1I4J3G3	1.4536	-1.4536	tRNA(Arg) A34 adenosine deaminase TadA	1.45	0.0371	1.16	3.13	SAMN04487868_10515
A0A1I4KCY2	1.4583	-1.4583	Isocitrate dehydrogenase [NADP]	1.46	0.0366	0.33	3.14	SAMN04487868_10995
A0A1I4MND4	1.4612	-1.4612	GntR family transcriptional regulator. glc operon transcriptional activator	1.46	0.0363	0.48	3.15	SAMN04487868_12414
A0A1I4J7G7	1.4629	-1.4629	GTPase Der	1.46	0.0364	0.47	3.15	der SAMN04487868_105148
A0A1I4HJQ2	1.4632	-1.4632	O-Methyltransferase involved in polyketide biosynthesis	1.46	0.0364	2.09	3.15	SAMN04487868_101458
A0A1I4K4U0	1.4678	-1.4678	Choline dehydrogenase	1.47	0.0361	0.63	3.16	SAMN04487868_108113
A0A1I4JKZ0	1.4684	-1.4684	7.8-dihydroneopterin aldolase	1.47	0.0361	1.28	3.17	SAMN04487868_106152
A0A1I4N0H7	1.4693	-1.4693	Unsaturated chondroitin disaccharide hydrolase	1.47	0.0361	0.97	3.17	SAMN04487868_12812
A0A1I4J8S8	1.4723	-1.4723	Diguanylate cyclase (GGDEF) domain-containing protein	1.47	0.0360	4.36	3.17	SAMN04487868_105180
A0A1I4JM67	1.4784	-1.4784	Thiamine-phosphate synthase	1.48	0.0354	0.61	3.19	thiE SAMN04487868_106176
A0A1I4JM62	1.4809	-1.4809	2-amino-4-hydroxy-6-hydroxymethyldihydropteridine diphosphokinase	1.48	0.0353	2.07	3.20	SAMN04487868_106157
A0A1I4HD09	1.4815	-1.4815	Glutamyl-tRNA(Gln) amidotransferase subunit A	1.48	0.0352	0.62	3.20	gatA SAMN04487868_101298
A0A1I4ILX7	1.4871	-1.4871	Probable transcriptional regulatory protein SAMN04487868_10426	1.49	0.0346	0.91	3.21	SAMN04487868_10426
A0A1I4MJE1	1.4885	-1.4885	Two-component system. OmpR family. response regulator	1.49	0.0346	0.22	3.21	SAMN04487868_12320
A0A1I4HZS3	1.4978	-1.4978	Cold shock protein (Beta-ribbon. CspA family)	1.50	0.0340	2.37	3.24	SAMN04487868_102161
A0A1I4N3H1	1.5020	-1.5020	30S ribosomal protein S8	1.50	0.0338	0.67	3.25	rpsH SAMN04487868_12917
A0A1I4HW09	1.5023	-1.5023	2-methylisocitrate lyase	1.50	0.0339	0.46	3.25	prpB SAMN04487868_10276
A0A1I4HVC2	1.5035	-1.5035	Riboflavin-specific deaminase C-terminal domain-containing protein	1.50	0.0338	1.15	3.25	SAMN04487868_10285
A0A1I4JHF5	1.5070	-1.5070	ATP-binding cassette. subfamily F. member 3	1.51	0.0334	0.51	3.26	SAMN04487868_10648
A0A1I4JG83	1.5097	-1.5097	Regulator of sigma D	1.51	0.0329	1.34	3.27	SAMN04487868_10644
A0A1I4K697	1.5107	-1.5107	Glutathione S-transferase	1.51	0.0330	0.46	3.27	SAMN04487868_108149
A0A1I4MVJ4	1.5128	-1.5128	L.D-transpeptidase catalytic domain	1.51	0.0328	0.80	3.27	SAMN04487868_1266
A0A1I4HTH1	1.5139	-1.5139	Glycosyltransferase involved in cell wall bisynthesis	1.51	0.0328	0.26	3.28	SAMN04487868_10243
A0A1I4HSG6	1.5165	-1.5165	Nucleoid-associated protein SAMN04487868_10221	1.52	0.0328	1.96	3.28	SAMN04487868_10221
A0A1I4LYL3	1.5169	-1.5169	Uncharacterized protein	1.52	0.0327	0.79	3.28	SAMN04487868_11782
A0A1I4I896	1.5183	-1.5183	Alcohol dehydrogenase GroES-like domain-containing protein	1.52	0.0324	1.17	3.29	SAMN04487868_10370
A0A1I4I9T6	1.5254	-1.5254	NADP-dependent 3-hydroxy acid dehydrogenase YdfG	1.53	0.0320	0.98	3.30	SAMN04487868_103115
A0A1I4N3N3	1.5286	-1.5286	30S ribosomal protein S17	1.53	0.0318	0.31	3.31	rpsQ SAMN04487868_12912
A0A1I4N4A2	1.5308	-1.5308	DNA-directed RNA polymerase subunit alpha	1.53	0.0317	0.13	3.32	rpoA SAMN04487868_12927
A0A1I4JZU0	1.5329	-1.5329	Isocitrate lyase	1.53	0.0316	0.25	3.32	SAMN04487868_1082
A0A1I4MYG0	1.5373	-1.5373	Oligopeptide transport system ATP-binding protein	1.54	0.0313	0.53	3.33	SAMN04487868_12739
A0A1I4L4T6	1.5393	-1.5393	Type VI secretion system protein VasD	1.54	0.0313	1.17	3.34	SAMN04487868_112133
A0A1I4KIQ6	1.5398	-1.5398	Uncharacterized protein	1.54	0.0313	0.60	3.34	SAMN04487868_11030
A0A1I4MJP4	1.5451	-1.5451	Cysteine synthase	1.55	0.0307	0.18	3.35	SAMN04487868_12313
A0A1I4K092	1.5466	-1.5466	Beta-N-acetylglucosaminidase	1.55	0.0303	0.30	3.36	SAMN04487868_10811
A0A1I4J3C8	1.5466	-1.5466	Hydrolase_4 domain-containing protein	1.55	0.0304	1.96	3.36	SAMN04487868_10550
A0A1I4LLM0	1.5476	-1.5476	Uroporphyrinogen decarboxylase	1.55	0.0303	0.74	3.36	hemE SAMN04487868_11550
A0A1I4MZM2	1.5490	-1.5490	Uncharacterized protein	1.55	0.0301	1.00	3.36	SAMN04487868_12752
A0A1I4HJ48	1.5570	-1.5570	Histidine kinase-like ATPase domain-containing protein	1.56	0.0302	0.39	3.38	SAMN04487868_101447

A0A1I4JJ49	1.5614	-1.5614	Biosynthetic arginine decarboxylase	1.56	0.0299	0.53	3.39	speA SAMN04487868_10690
A0A1I4HWZ6	1.5616	-1.5616	4-hydroxy-tetrahydrodipicolinate synthase	1.56	0.0299	0.56	3.39	dapA SAMN04487868_102101
A0A1I4KS39	1.5617	-1.5617	Fe-S cluster assembly ATP-binding protein	1.56	0.0300	0.63	3.39	SAMN04487868_11126
A0A1I4MVC5	1.5620	-1.5620	Riboflavin synthase alpha chain	1.56	0.0299	0.94	3.39	SAMN04487868_1263
A0A1I4MVL2	1.5644	-1.5644	Probable S-methyl-5'-thioinosine phosphorylase	1.56	0.0296	0.55	3.40	SAMN04487868_1268
A0A1I4K564	1.5656	-1.5656	Metal-dependent hydrolase. endonuclease/exonuclease/phosphatase family	1.57	0.0295	0.75	3.40	SAMN04487868_108101
A0A1I4LYN0	1.5723	-1.5723	Acyl-CoA dehydrogenase	1.57	0.0294	0.14	3.42	SAMN04487868_11780
A0A1I4ML53	1.5767	-1.5767	HD domain-containing protein	1.58	0.0289	0.75	3.43	SAMN04487868_12340
A0A1I4HGS6	1.5785	-1.5785	Exodeoxyribonuclease I	1.58	0.0289	0.45	3.44	SAMN04487868_101382
A0A1I4MW65	1.5862	-1.5862	FAD:protein FMN transferase	1.59	0.0288	1.21	3.46	SAMN04487868_12618
A0A1I4HE21	1.5894	-1.5894	ATP phosphoribosyltransferase	1.59	0.0284	0.46	3.46	hisG SAMN04487868_101326
A0A1I4MKZ2	1.5958	-1.5958	Response regulator of citrate/malate metabolism	1.60	0.0282	0.44	3.48	SAMN04487868_12335
A0A1I4ICX9	1.5968	-1.5968	Glycosyltransferase involved in cell wall bisynthesis	1.60	0.0279	0.51	3.48	SAMN04487868_103188
A0A1I4MI95	1.5992	-1.5992	Predicted flavoprotein CzcO associated with the cation diffusion facilitator CzcD	1.60	0.0278	3.22	3.49	SAMN04487868_12258
A0A1I4MXA1	1.6026	-1.6026	3-oxoacyl-[acyl-carrier-protein] reductase	1.60	0.0274	0.53	3.50	SAMN04487868_12657
A0A1I4KJJ9	1.6029	-1.6029	Putative polyhydroxyalkanoic acid system protein	1.60	0.0274	0.46	3.50	SAMN04487868_11052
A0A1I4JSB2	1.6046	-1.6046	Phosphoribosylformylglycinamidine synthase	1.60	0.0274	0.60	3.50	purL SAMN04487868_10724
A0A1I4IW42	1.6083	-1.6083	Two-component system. OmpR family. response regulator RstA	1.61	0.0273	0.46	3.51	SAMN04487868_104232
A0A1I4NFS7	1.6087	-1.6087	30S ribosomal protein S9	1.61	0.0271	0.73	3.51	rpsI SAMN04487868_13710
A0A1I4L6Z0	1.6095	-1.6095	Glycerol dehydrogenase	1.61	0.0270	0.71	3.51	SAMN04487868_1137
A0A1I4HYG2	1.6101	-1.6101	50S ribosomal protein L16 3-hydroxylase	1.61	0.0270	0.45	3.52	SAMN04487868_102167
A0A1I4IU03	1.6103	-1.6103	ATP diphosphatase	1.61	0.0271	1.55	3.52	SAMN04487868_104187
A0A1I4I866	1.6111	-1.6111	S-formylglutathione hydrolase	1.61	0.0269	1.04	3.52	SAMN04487868_10333
A0A1I4JS93	1.6115	-1.6115	NAD(P)-dependent dehydrogenase. short-chain alcohol dehydrogenase family	1.61	0.0269	0.82	3.52	SAMN04487868_10737
A0A1I4IA51	1.6124	-1.6124	Aldehyde dehydrogenase (NAD+)	1.61	0.0269	0.65	3.52	SAMN04487868_10371
A0A1I4J2E8	1.6150	-1.6150	Chorismate mutase	1.61	0.0268	0.42	3.53	SAMN04487868_10528
A0A1I4K661	1.6175	-1.6175	Uncharacterized protein	1.62	0.0266	1.36	3.53	SAMN04487868_108124
A0A1I4HCA8	1.6179	-1.6179	EAL domain. c-di-GMP-specific phosphodiesterase class I (Or its enzymatically inactive variant)	1.62	0.0267	0.58	3.54	SAMN04487868_101234
A0A1I4HFZ3	1.6215	-1.6215	Uncharacterized protein	1.62	0.0266	0.37	3.54	SAMN04487868_101366
A0A1I4K1P2	1.6291	-1.6291	Bis(5'-nucleosyl)-tetraphosphatase. symmetrical	1.63	0.0266	0.55	3.56	SAMN04487868_10841
A0A1I4M2K0	1.6327	-1.6327	Methionine synthase	1.63	0.0267	0.46	3.57	SAMN04487868_11870
A0A1I4I932	1.6331	-1.6331	Uncharacterized protein	1.63	0.0267	0.63	3.57	SAMN04487868_10397
A0A1I4H8Z3	1.6339	-1.6339	Glutathione S-transferase	1.63	0.0265	0.70	3.58	SAMN04487868_101142
A0A1I4LJZ2	1.6374	-1.6374	Glutamine-dependent NAD(+) synthetase	1.64	0.0262	0.45	3.59	nadE SAMN04487868_11511
A0A1I4MEF0	1.6390	-1.6390	UPF0250 protein SAMN04487868_12160	1.64	0.0262	0.86	3.59	SAMN04487868_12160
A0A1I4MSN4	1.6458	-1.6458	Response regulator receiver domain-containing protein	1.65	0.0261	0.37	3.61	SAMN04487868_12552
A0A1I4N829	1.6500	-1.6500	Transcriptional regulator. TetR family	1.65	0.0255	0.53	3.62	SAMN04487868_13110
A0A1I4HD71	1.6510	-1.6510	tRNA threonylcarbamoyladenosine biosynthesis protein TsaE	1.65	0.0253	0.93	3.62	SAMN04487868_101253

A0A1I4HU57	1.6547	-1.6547	Putative PEP-CTERM system TPR-repeat lipoprotein	1.65	0.0251	0.37	3.63	SAMN04487868_10230
A0A1I4H9R3	1.6565	-1.6565	NAD-dependent protein deacylase	1.66	0.0252	0.86	3.64	cobB SAMN04487868_101211
A0A1I4LLQ9	1.6591	-1.6591	Transcription antitermination protein NusB	1.66	0.0249	0.62	3.64	nusB SAMN04487868_11541
A0A1I4MDW7	1.6670	-1.6670	D-alanyl-D-alanine carboxypeptidase (Penicillin-binding protein 5/6)	1.67	0.0243	0.44	3.66	SAMN04487868_12159
A0A1I4M1M4	1.6674	-1.6674	DedD protein	1.67	0.0243	0.63	3.66	SAMN04487868_11841
A0A1I4K2F6	1.6727	-1.6727	Anthranilate phosphoribosyltransferase	1.67	0.0233	0.23	3.68	trpD SAMN04487868_10855
A0A1I4JAZ7	1.6730	-1.6730	Two component transcriptional regulator. LuxR family	1.67	0.0234	0.51	3.68	SAMN04487868_105207
A0A1I4HFP1	1.6861	-1.6861	UDP-N-acetylglucosamine 1-carboxyvinyltransferase	1.69	0.0229	0.69	3.71	murA SAMN04487868_101325
A0A1I4HDA6	1.6861	-1.6861	GTPase HflX	1.69	0.0228	0.38	3.71	hflX SAMN04487868_101258
A0A1I4ME63	1.6890	-1.6890	Geranylgeranyl diphosphate synthase. type II	1.69	0.0228	1.53	3.72	SAMN04487868_12131
A0A1I4NCS6	1.6895	-1.6895	Uncharacterized protein	1.69	0.0228	0.48	3.72	SAMN04487868_13327
A0A1I4MCN4	1.6917	-1.6917	Transcriptional regulator MraZ	1.69	0.0227	0.72	3.73	mraZ SAMN04487868_1217
A0A1I4KSG1	1.6922	-1.6922	Fe-S cluster assembly protein SufD	1.69	0.0228	0.41	3.73	SAMN04487868_11125
A0A1I4HKK1	1.6931	-1.6931	Autotransporter secretion outer membrane protein TamA	1.69	0.0228	0.30	3.73	SAMN04487868_101425
A0A1I4L2B7	1.6946	-1.6946	Patatin-like phospholipase	1.69	0.0229	0.24	3.74	SAMN04487868_11255
A0A1I4I9S4	1.6982	-1.6982	Uncharacterized protein	1.70	0.0225	2.37	3.74	SAMN04487868_10389
A0A1I4N6P1	1.7024	-1.7024	Uncharacterized conserved protein	1.70	0.0225	0.35	3.76	SAMN04487868_13019
A0A1I4N3L6	1.7032	-1.7032	50S ribosomal protein L6	1.70	0.0225	0.75	3.76	rplF SAMN04487868_12918
A0A1I4LMV3	1.7039	-1.7039	ATP-dependent protease subunit HslV	1.70	0.0225	0.91	3.76	hslV SAMN04487868_11568
A0A1I4M8X9	1.7063	-1.7063	Acetoin utilization deacetylase AcuC	1.71	0.0224	1.02	3.77	SAMN04487868_12013
A0A1I4LQZ7	1.7077	-1.7077	Phenylacetaldehyde dehydrogenase	1.71	0.0225	0.62	3.77	SAMN04487868_11616
A0A1I4IR68	1.7113	-1.7113	Glyoxalase superfamily enzyme. possibly 3-demethylubiquinone-9 3-methyltransferase	1.71	0.0223	1.22	3.78	SAMN04487868_104126
A0A1I4JKF6	1.7167	-1.7167	tRNA-binding protein	1.72	0.0220	0.67	3.79	SAMN04487868_106137
A0A1I4LXS4	1.7170	-1.7170	Glutathione reductase (NADPH)	1.72	0.0220	1.25	3.79	SAMN04487868_11751
A0A1I4MB51	1.7176	-1.7176	AraC family transcriptional regulator. regulatory protein of adaptative response / methylated-DNA-[protein]-cysteine methyltransferase	1.72	0.0221	0.46	3.80	SAMN04487868_12069
A0A1I4LL12	1.7202	-1.7202	Acyltransferase. WS/DGAT/MGAT	1.72	0.0221	0.87	3.80	SAMN04487868_11536
A0A1I4K168	1.7231	-1.7231	Cyclopropane-fatty-acyl-phospholipid synthase	1.72	0.0219	0.57	3.81	SAMN04487868_10817
A0A1I4M535	1.7292	-1.7292	DNA polymerase III. chi subunit	1.73	0.0218	1.79	3.83	SAMN04487868_11917
A0A1I4MAB5	1.7322	-1.7322	SmpA / OmlA family protein	1.73	0.0216	0.62	3.84	SAMN04487868_12046
A0A1I4HZN7	1.7369	-1.7369	AB hydrolase-1 domain-containing protein	1.74	0.0214	0.94	3.85	SAMN04487868_102185
A0A1I4N6T3	1.7392	-1.7392	Phenylalanine--tRNA ligase alpha subunit	1.74	0.0214	0.52	3.85	pheS SAMN04487868_1309
A0A1I4KX42	1.7411	-1.7411	N-6 DNA Methylase	1.74	0.0214	2.05	4.71	SAMN04487868_111133
A0A1I4KK14	1.7419	-1.7419	Pimeloyl-ACP methyl ester carboxylesterase	1.74	0.0213	1.25	4.71	SAMN04487868_11054
A0A1I4HCC4	1.7449	-1.7449	LPS-assembly lipoprotein LptE	1.74	0.0211	0.32	3.87	lptE SAMN04487868_101282
A0A1I4HA03	1.7472	-1.7472	Glycolate oxidase. subunit GlcD	1.75	0.0211	0.46	3.88	SAMN04487868_101209
A0A1I4K486	1.7529	-1.7529	Phosphoribulokinase	1.75	0.0209	0.89	3.89	SAMN04487868_10888
A0A1I4MH59	1.7538	-1.7538	Uncharacterized protein	1.75	0.0208	0.43	3.89	SAMN04487868_12228

A0A1I4MCV8	1.7571	-1.7571	GTP cyclohydrolase-2	1.76	0.0204	0.72	3.90	ribA SAMN04487868_12129
A0A1I4MY18	1.7575	-1.7575	Adenylyltransferase and sulfurtransferase	1.76	0.0205	0.83	3.90	SAMN04487868_12721
A0A1I4I692	1.7581	-1.7581	Uncharacterized protein	1.76	0.0205	0.35	3.91	SAMN04487868_1036
A0A1I4IV93	1.7583	-1.7583	Peptide chain release factor 2	1.76	0.0205	0.31	3.91	prfB SAMN04487868_104212
A0A1I4LX28	1.7642	-1.7642	Uncharacterized protein	1.76	0.0206	1.26	3.92	SAMN04487868_11741
A0A1I4HYF9	1.7656	-1.7656	Adenylosuccinate lyase	1.77	0.0205	0.41	3.93	SAMN04487868_102166
A0A1I4ILZ9	1.7684	-1.7684	GMP synthase (Glutamine-hydrolysing)	1.77	0.0204	0.65	3.93	SAMN04487868_10427
A0A1I4JSI8	1.7701	-1.7701	Uncharacterized protein	1.77	0.0205	1.30	3.94	SAMN04487868_10723
A0A1I4I1W7	1.7703	-1.7703	Peptidyl-prolyl cis-trans isomerase	1.77	0.0205	0.50	3.94	SAMN04487868_102278
A0A1I4N753	1.7759	-1.7759	Uncharacterized protein	1.78	0.0203	1.56	3.95	SAMN04487868_13020
A0A1I4MRF5	1.7797	-1.7797	Uncharacterized protein	1.78	0.0202	0.89	3.97	SAMN04487868_1255
A0A1I4MYQ6	1.7799	-1.7799	Ribosome biogenesis GTPase A	1.78	0.0202	0.18	3.97	SAMN04487868_12747
A0A1I4JS43	1.7812	-1.7812	Cobyric acid synthase	1.78	0.0202	0.92	3.97	cobQ SAMN04487868_1075
A0A1I4KDQ4	1.7815	-1.7815	Type I restriction enzyme R Protein	1.78	0.0203	0.67	3.97	SAMN04487868_109118
A0A1I4JKE6	1.7831	-1.7831	Glutathione S-transferase	1.78	0.0202	0.34	3.97	SAMN04487868_106136
A0A1I4MJF2	1.7870	-1.7870	Membrane-anchored ribosome-binding protein. inhibits growth in stationary phase. ElaB/YqjD/DUF883 family	1.79	0.0201	2.34	3.99	SAMN04487868_1237
A0A1I4J7C0	1.7950	-1.7950	Cytoskeleton protein RodZ	1.80	0.0195	0.62	4.01	SAMN04487868_105143
A0A1I4ML72	1.7964	-1.7964	Uncharacterized protein	1.80	0.0194	0.46	4.01	SAMN04487868_12352
A0A1I4MX91	1.8006	-1.8006	Malonyl CoA-acyl carrier protein transacylase	1.80	0.0192	0.44	4.02	SAMN04487868_12656
A0A1I4HX50	1.8044	-1.8044	Acyl-CoA thioester hydrolase	1.80	0.0192	0.41	4.03	SAMN04487868_102115
A0A1I4I9A3	1.8049	-1.8049	HAMP domain-containing protein	1.80	0.0192	1.04	4.03	SAMN04487868_10375
A0A1I4N535	1.8097	-1.8097	MSHA biogenesis protein MshQ	1.81	0.0193	1.84	4.05	SAMN04487868_12948
A0A1I4JWG5	1.8116	-1.8116	30S ribosomal protein S2	1.81	0.0193	0.70	4.05	rpsB SAMN04487868_107160
A0A1I4N5Q2	1.8128	-1.8128	GTP-binding protein	1.81	0.0194	0.27	4.06	SAMN04487868_12953
A0A1I4HBI3	1.8207	-1.8207	Predicted unusual protein kinase regulating ubiquinone biosynthesis. AarF/ABC1/UbiB family	1.82	0.0192	0.97	4.08	SAMN04487868_101212
A0A1I4J4G4	1.8226	-1.8226	Uncharacterized protein	1.82	0.0191	1.79	4.08	SAMN04487868_10573
A0A1I4HYU6	1.8227	-1.8227	Lrp/AsnC family transcriptional regulator. leucine-responsive regulatory protein	1.82	0.0191	0.58	4.08	SAMN04487868_102133
A0A1I4LR04	1.8227	-1.8227	Uncharacterized protein	1.82	0.0191	0.96	4.08	SAMN04487868_1166
A0A1I4HGT8	1.8244	-1.8244	3-oxoacyl-[acyl-carrier protein] reductase	1.82	0.0192	0.30	4.09	SAMN04487868_101395
A0A1I4HH41	1.8255	-1.8255	UPF0716 protein FxsA	1.83	0.0192	1.21	4.09	SAMN04487868_101396
A0A1I4JWN5	1.8269	-1.8269	Succinyl-diaminopimelate desuccinylase	1.83	0.0192	0.41	4.10	dapE SAMN04487868_107167
A0A1I4M3K5	1.8313	-1.8313	Putative quinone oxidoreductase. YhdH/YhfP family	1.83	0.0193	0.61	4.11	SAMN04487868_11866
A0A1I4HER3	1.8337	-1.8337	Cell shape-determining protein MreB	1.83	0.0187	0.33	4.12	SAMN04487868_101300
A0A1I4ISQ2	1.8382	-1.8382	Predicted dithiol-disulfide oxidoreductase. DUF899 family	1.84	0.0181	1.99	4.13	SAMN04487868_104125
A0A1I4K540	1.8437	-1.8437	50S ribosomal protein L28	1.84	0.0180	0.55	4.14	rpmB SAMN04487868_10899
A0A1I4KRI3	1.8479	-1.8479	Acetyl-CoA C-acetyltransferase	1.85	0.0178	0.40	4.16	SAMN04487868_11115
A0A1I4IWD7	1.8491	-1.8491	Ribosome maturation factor RimM	1.85	0.0179	0.46	4.16	rimM SAMN04487868_104220

A0A1I4M642	1.8507	-1.8507	Methionine--tRNA ligase	1.85	0.0179	0.45	4.16	metG SAMN04487868_11937
A0A1I4MRV2	1.8551	-1.8551	Ribosomal protein S12 methylthiotransferase accessory factor	1.86	0.0179	0.61	4.18	SAMN04487868_12517
A0A1I4M1Z5	1.8648	-1.8648	Tryptophan synthase alpha chain	1.86	0.0176	0.33	4.20	trpA SAMN04487868_11838
A0A1I4KDT3	1.8721	-1.8721	Phage integrase family protein	1.87	0.0175	0.92	4.22	SAMN04487868_109116
A0A1I4IA11	1.8725	-1.8725	Acetyl-CoA C-acetyltransferase	1.87	0.0176	0.75	4.23	SAMN04487868_10369
A0A1I4L4P3	1.8758	-1.8758	33 kDa chaperonin	1.88	0.0173	0.71	4.24	hslO SAMN04487868_112107
A0A1I4HFH9	1.8766	-1.8766	UDP-2.4-diacetamido-2.4.6-trideoxy-beta-L-altropyranose hydrolase	1.88	0.0174	1.65	4.24	SAMN04487868_101363
A0A1I4JTK9	1.8769	-1.8769	Mercuric reductase	1.88	0.0174	1.02	5.28	SAMN04487868_10755
A0A1I4K6C6	1.8797	-1.8797	L-asparaginase	1.88	0.0174	0.74	4.25	SAMN04487868_108141
A0A1I4KIX2	1.8804	-1.8804	3-dehydroquinate dehydratase	1.88	0.0172	0.81	4.25	aroQ SAMN04487868_11019
A0A1I4ITT8	1.8837	-1.8837	Phosphoglycerate dehydrogenase	1.88	0.0172	0.94	4.26	SAMN04487868_104166
A0A1I4M5T7	1.9004	-1.9004	Iron-sulfur cluster carrier protein	1.90	0.0157	0.72	4.31	SAMN04487868_11936
A0A1I4HBM5	1.9068	-1.9068	ATP phosphoribosyltransferase regulatory subunit	1.91	0.0154	0.52	4.33	hisZ SAMN04487868_101261
A0A1I4HH98	1.9097	-1.9097	N5-carboxyaminoimidazole ribonucleotide synthase	1.91	0.0153	0.52	4.33	purK SAMN04487868_101406
A0A1I4L150	1.9108	-1.9108	Uncharacterized protein	1.91	0.0153	3.43	5.43	SAMN04487868_11240
A0A1I4MPD4	1.9112	-1.9112	Nitrogen regulatory protein P-II family	1.91	0.0154	0.38	4.34	SAMN04487868_12437
A0A1I4MHL3	1.9120	-1.9120	Thiolase. C-terminal domain	1.91	0.0154	1.82	4.34	SAMN04487868_12252
A0A1I4KNA2	1.9128	-1.9128	Dihydropteroate synthase	1.91	0.0154	0.56	4.34	SAMN04487868_110129
A0A1I4KHT6	1.9179	-1.9179	Phosphoribosylamine--glycine ligase	1.92	0.0152	0.69	4.36	purD SAMN04487868_11011
A0A1I4HAG9	1.9188	-1.9188	Serine protease	1.92	0.0152	2.40	5.46	SAMN04487868_101230
A0A1I4I2R1	1.9207	-1.9207	Ferredoxin--NADP+ reductase	1.92	0.0152	0.72	4.37	SAMN04487868_102292
A0A1I4HW48	1.9255	-1.9255	Peptidoglycan-associated protein	1.93	0.0151	0.77	4.38	pal SAMN04487868_102110
A0A1I4LRP3	1.9261	-1.9261	Uncharacterized protein	1.93	0.0151	0.80	4.38	SAMN04487868_11633
A0A1I4J2M5	1.9271	-1.9271	3-phosphoshikimate 1-carboxyvinyltransferase	1.93	0.0149	0.49	4.39	aroA SAMN04487868_10530
A0A1I4MDV8	1.9292	-1.9292	UDP-3-O-acyl-N-acetylglucosamine deacetylase	1.93	0.0150	0.62	4.39	lpxC SAMN04487868_12122
A0A1I4I1I3	1.9391	-1.9391	ATP-dependent Clp protease proteolytic subunit	1.94	0.0143	0.39	4.42	clpP SAMN04487868_102268
A0A1I4IFL3	1.9401	-1.9401	Uncharacterized protein	1.94	0.0144	0.32	4.42	SAMN04487868_103255
A0A1I4MVC6	1.9422	-1.9422	Glycerophosphoryl diester phosphodiesterase	1.94	0.0142	1.83	4.43	SAMN04487868_12621
A0A1I4NA25	1.9432	-1.9432	Response regulator receiver modulated diguanylate cyclase	1.94	0.0142	0.37	4.43	SAMN04487868_1324
A0A1I4JLY8	1.9442	-1.9442	Hydroxymethylpyrimidine/phosphomethylpyrimidine kinase	1.94	0.0143	0.81	4.44	SAMN04487868_106177
A0A1I4KJK9	1.9449	-1.9449	Aminopeptidase P. Metallo peptidase. MEROPS family M24B	1.94	0.0143	0.45	4.44	SAMN04487868_11039
A0A1I4HD67	1.9552	-1.9552	Phosphoserine phosphatase	1.96	0.0140	0.31	4.47	SAMN04487868_101240
A0A1I4HU23	1.9586	-1.9586	Glycosyltransferase involved in cell wall bisynthesis	1.96	0.0139	0.45	4.48	SAMN04487868_10259
A0A1I4MRC1	1.9647	-1.9647	Uncharacterized protein	1.96	0.0140	0.41	4.50	SAMN04487868_1254
A0A1I4HFL8	1.9660	-1.9660	N-acetylneuraminate synthase	1.97	0.0140	0.73	4.50	SAMN04487868_101365
A0A1I4L6Z3	1.9673	-1.9673	ChrR Cupin-like domain-containing protein	1.97	0.0140	1.04	4.50	SAMN04487868_1131
A0A1I4J8K7	1.9673	-1.9673	Succinate--CoA ligase [ADP-forming] subunit alpha	1.97	0.0140	0.65	4.50	sucD SAMN04487868_105175
A0A1I4H7D9	1.9689	-1.9689	ATPase components of ABC transporters with duplicated ATPase domains	1.97	0.0140	0.51	4.51	SAMN04487868_101152

A0A1I4MWK2	1.9690	-1.9690	4-hydroxy-4-methyl-2-oxoglutarate aldolase	1.97	0.0140	0.68	4.51	SAMN04487868_12642
A0A1I4HUP5	1.9723	-1.9723	2-methylaconitate cis-trans isomerase	1.97	0.0140	0.30	4.52	SAMN04487868_10273
A0A1I4MA08	1.9724	-1.9724	Uncharacterized conserved protein	1.97	0.0140	1.87	4.52	SAMN04487868_12047
A0A1I4ILL9	1.9728	-1.9728	Amidase	1.97	0.0140	0.74	4.52	SAMN04487868_10415
A0A1I4L8K5	1.9752	-1.9752	Glycine--tRNA ligase alpha subunit	1.98	0.0141	0.25	4.53	glyQ SAMN04487868_11356
A0A1I4IRH8	1.9795	-1.9795	Branched-chain-amino-acid aminotransferase	1.98	0.0141	2.02	4.54	SAMN04487868_104128
A0A1I4LLE3	1.9856	-1.9856	ATP-binding cassette protein. ChvD family	1.99	0.0142	0.30	4.56	SAMN04487868_11547
A0A1I4HZ40	1.9869	-1.9869	3-deoxy-manno-octulosonate cytidylyltransferase	1.99	0.0142	0.37	4.56	kdsB SAMN04487868_102139
A0A1I4L2R1	1.9872	-1.9872	Dihydroorotase	1.99	0.0141	0.24	4.57	SAMN04487868_11275
A0A1I4NF36	1.9875	-1.9875	50S ribosomal protein L11	1.99	0.0141	0.89	4.57	rplK SAMN04487868_13610
A0A1I4JW98	1.9917	-1.9917	Ribosome-recycling factor	1.99	0.0141	0.47	4.58	frr SAMN04487868_107157
A0A1I4HN11	1.9926	-1.9926	MoxR-like ATPase	1.99	0.0141	0.27	4.58	SAMN04487868_101491
A0A1I4JX81	1.9966	-1.9966	Uridylate kinase	2.00	0.0142	0.69	4.59	pyrH SAMN04487868_107158
A0A1I4KSC8	2.0002	-2.0002	cAMP-binding domain of CRP or a regulatory subunit of cAMP-dependent protein kinases	2.00	0.0141	0.52	4.60	SAMN04487868_11134
A0A1I4KA74	2.0040	-2.0040	Uncharacterized protein	2.00	0.0138	1.50	4.62	SAMN04487868_10932
A0A1I4N413	2.0063	-2.0063	50S ribosomal protein L17	2.01	0.0138	0.83	4.62	rplQ SAMN04487868_12928
A0A1I4HL94	2.0091	-2.0091	Flagellar motor switch protein FliG	2.01	0.0139	0.75	4.63	SAMN04487868_101442
A0A1I4MID8	2.0143	-2.0143	Succinate-semialdehyde dehydrogenase / glutarate-semialdehyde dehydrogenase	2.01	0.0138	2.13	4.65	SAMN04487868_12264
A0A1I4L3B3	2.0234	-2.0234	VOC domain-containing protein	2.02	0.0133	1.32	4.68	SAMN04487868_11292
A0A1I4KLV9	2.0273	-2.0273	Peptide methionine sulfoxide reductase MsrB	2.03	0.0133	1.08	4.69	msrB SAMN04487868_11097
A0A1I4LNK0	2.0286	-2.0286	Rhs element Vgr protein (Fragment)	2.03	0.0133	3.62	4.69	SAMN04487868_11583
A0A1I4L280	2.0329	-2.0329	RNAse R	2.03	0.0130	0.46	4.71	SAMN04487868_11241
A0A1I4HI66	2.0330	-2.0330	Putative amidoligase enzyme	2.03	0.0131	0.69	4.71	SAMN04487868_101430
A0A1I4KLH8	2.0374	-2.0374	Peptide methionine sulfoxide reductase MsrA	2.04	0.0131	1.23	4.72	msrA SAMN04487868_11096
A0A1I4L0C6	2.0385	-2.0385	PEP-CTERM protein-sorting domain-containing protein	2.04	0.0131	2.87	4.72	SAMN04487868_11222
A0A1I4LVP8	2.0403	-2.0403	Zinc-type alcohol dehydrogenase-like protein	2.04	0.0131	1.11	4.73	SAMN04487868_1174
A0A1I4JJM8	2.0461	-2.0461	tRNA (guanine-N(7)-)-methyltransferase	2.05	0.0132	0.23	4.75	trmB SAMN04487868_10698
A0A1I4IV85	2.0491	-2.0491	Homoserine dehydrogenase	2.05	0.0132	0.10	4.76	SAMN04487868_104215
A0A1I4IRD5	2.0596	-2.0596	Succinylglutamate desuccinylase / Aspartoacylase family protein	2.06	0.0128	1.60	4.79	SAMN04487868_104124
A0A1I4I105	2.0604	-2.0604	Transcriptional regulator of acetoin/glycerol metabolism	2.06	0.0127	1.03	6.14	SAMN04487868_102244
A0A1I4MMG2	2.0612	-2.0612	Uncharacterized protein	2.06	0.0127	1.06	4.79	SAMN04487868_1242
A0A1I4MVN6	2.0625	-2.0625	Molybdenum cofactor cytidylyltransferase	2.06	0.0126	2.40	4.80	SAMN04487868_12634
A0A1I4MWS3	2.0663	-2.0663	M16C_associated domain-containing protein	2.07	0.0122	0.52	4.81	SAMN04487868_12639
A0A1I4M4M4	2.0692	-2.0692	Uncharacterized protein	2.07	0.0122	0.58	4.82	SAMN04487868_1196
A0A1I4I841	2.0773	-2.0773	3-hydroxyacyl-CoA dehydrogenase	2.08	0.0121	0.59	4.85	SAMN04487868_10368
A0A1I4KM07	2.0796	-2.0796	Outer membrane protein assembly factor BamE	2.08	0.0121	1.76	4.85	bamE SAMN04487868_110116
A0A1I4LKX5	2.0799	-2.0799	Octaprenyl-diphosphate synthase	2.08	0.0121	0.63	4.85	SAMN04487868_11533

A0A1I4MDY4	2.0811	-2.0811	Octanoyltransferase	2.08	0.0122	1.04	4.86	lipB SAMN04487868_12161
A0A1I4HGG0	2.0827	-2.0827	Acetyl-CoA C-acetyltransferase	2.08	0.0122	0.72	4.86	SAMN04487868_101332
A0A1I4MC29	2.0843	-2.0843	Ribosomal RNA small subunit methyltransferase H	2.08	0.0122	0.85	4.87	rsmH SAMN04487868_1218
A0A1I4LF83	2.0847	-2.0847	Alginate biosynthesis protein Alg44	2.08	0.0122	1.87	4.87	SAMN04487868_11446
A0A1I4HWX4	2.0862	-2.0862	Phosphoribosylaminoimidazole-succinocarboxamide synthase	2.09	0.0122	0.63	4.87	purC SAMN04487868_10299
A0A1I4HYS0	2.0865	-2.0865	Protease HtpX	2.09	0.0121	1.06	4.87	htpX SAMN04487868_102176
A0A1I4HZ52	2.0908	-2.0908	Cbb3-type cytochrome c oxidase subunit	2.09	0.0120	0.92	4.89	SAMN04487868_102189
A0A1I4HT37	2.0933	-2.0933	Two-component system. NtrC family. response regulator	2.09	0.0120	1.10	4.90	SAMN04487868_10229
A0A1I4JH42	2.0933	-2.0933	Porphobilinogen deaminase	2.09	0.0120	0.57	4.90	hemC SAMN04487868_10661
A0A1I4M4U8	2.1005	-2.1005	Translational regulator CsrA	2.10	0.0116	1.63	4.92	csrA SAMN04487868_11910
A0A1I4MT53	2.1015	-2.1015	Uncharacterized protein	2.10	0.0117	1.78	4.92	SAMN04487868_12562
A0A1I4KRX9	2.1018	-2.1018	Iron-regulated ABC transporter membrane component SufB	2.10	0.0117	0.85	4.92	SAMN04487868_11127
A0A1I4JI76	2.1085	-2.1085	Transcriptional regulator. AraC family	2.11	0.0116	1.45	4.95	SAMN04487868_10689
A0A1I4J769	2.1091	-2.1091	Serine O-acetyltransferase	2.11	0.0116	1.24	4.95	SAMN04487868_105137
A0A1I4IWN8	2.1147	-2.1147	HopJ type III effector protein	2.11	0.0115	2.05	4.97	SAMN04487868_104243
A0A1I4I1T5	2.1252	-2.1252	Malate synthase G	2.13	0.0114	0.38	5.00	glcB SAMN04487868_102275
A0A1I4LLK0	2.1271	-2.1271	DNA repair protein RadA	2.13	0.0111	0.33	5.01	radA SAMN04487868_11548
A0A1I4MH73	2.1312	-2.1312	Fatty-acyl-CoA synthase	2.13	0.0108	1.62	5.02	SAMN04487868_12232
A0A1I4K6Q6	2.1315	-2.1315	Cold-shock DNA-binding protein family	2.13	0.0108	1.93	5.02	SAMN04487868_108153
A0A1I4M0Q1	2.1343	-2.1343	Phosphoadenosine phosphosulfate reductase	2.13	0.0109	0.48	5.03	SAMN04487868_11813
A0A1I4JRY7	2.1369	-2.1369	Ubiquinone biosynthesis O-methyltransferase	2.14	0.0107	1.09	5.04	ubiG SAMN04487868_10735
A0A1I4HGG9	2.1369	-2.1369	Argininosuccinate synthase	2.14	0.0108	0.42	5.04	argG SAMN04487868_101389
A0A1I4MFU3	2.1389	-2.1389	Histidine kinase	2.14	0.0108	0.75	5.04	SAMN04487868_12217
A0A1I4ITB5	2.1402	-2.1402	Uncharacterized protein	2.14	0.0108	1.36	5.05	SAMN04487868_104135
A0A1I4I0W0	2.1460	-2.1460	Predicted oxidoreductase	2.15	0.0104	1.13	5.07	SAMN04487868_102233
A0A1I4HDH6	2.1487	-2.1487	Nucleotide-binding protein SAMN04487868_101310	2.15	0.0104	0.38	5.08	SAMN04487868_101310
A0A1I4L063	2.1500	-2.1500	HEXXH motif-containing protein	2.15	0.0102	2.48	5.08	SAMN04487868_1126
A0A1I4J654	2.1539	-2.1539	ABC-2 type transport system ATP-binding protein	2.15	0.0101	0.37	5.09	SAMN04487868_105112
A0A1I4JT02	2.1560	-2.1560	Siderophore synthetase component	2.16	0.0101	2.01	5.10	SAMN04487868_10769
A0A1I4KRW8	2.1564	-2.1564	2.3-bisphosphoglycerate-independent phosphoglycerate mutase	2.16	0.0102	1.00	5.10	gpmI SAMN04487868_11110
A0A1I4J712	2.1573	-2.1573	tRNA (cytidine/uridine-2'-O-)-methyltransferase TrmJ	2.16	0.0102	0.53	5.10	trmJ SAMN04487868_105136
A0A1I4KN54	2.1581	-2.1581	tRNA pseudouridine synthase B	2.16	0.0102	0.87	5.11	truB SAMN04487868_110138
A0A1I4JWI0	2.1595	-2.1595	Succinyldiaminopimelate aminotransferase apoenzyme	2.16	0.0102	0.72	5.11	SAMN04487868_107164
A0A1I4MCH9	2.1597	-2.1597	UDP-N-acetylmuramoyl-L-alanyl-D-glutamate--2.6-diaminopimelate ligase	2.16	0.0102	0.34	5.11	murE SAMN04487868_12111
A0A1I4J7Y0	2.1600	-2.1600	MOSC domain-containing protein	2.16	0.0102	0.27	5.11	SAMN04487868_105157
A0A1I4NF43	2.1658	-2.1658	30S ribosomal protein S7	2.17	0.0103	0.63	5.13	rpsG SAMN04487868_1363
A0A1I4HX66	2.1663	-2.1663	UDP-glucuronate 4-epimerase	2.17	0.0103	1.07	5.13	SAMN04487868_10297
A0A1I4M672	2.1829	-2.1829	2-C-methyl-D-erythritol 4-phosphate cytidylyltransferase	2.18	0.0097	0.62	5.19	ispD SAMN04487868_11953

A0A1I4HZS8	2.1836	-2.1836	Outer membrane transport energization protein ExbB	2.18	0.0097	1.36	5.19	SAMN04487868_102211
A0A1I4MS36	2.1854	-2.1854	ATP-dependent DNA helicase RecQ	2.19	0.0097	2.52	6.79	SAMN04487868_12538
A0A1I4JUU2	2.1854	-2.1854	Methyltransferase domain-containing protein	2.19	0.0097	1.75	5.20	SAMN04487868_10782
A0A1I4IWW2	2.1864	-2.1864	Ornithine carbamoyltransferase	2.19	0.0097	0.35	5.20	SAMN04487868_104228
A0A1I4KN69	2.1888	-2.1888	30S ribosomal protein S15	2.19	0.0098	0.20	5.21	rpsO SAMN04487868_110139
A0A1I4IKS8	2.1900	-2.1900	Predicted ATP-dependent endonuclease of the OLD family. contains P-loop ATPase and TOPRIM domains	2.19	0.0098	1.05	5.21	SAMN04487868_1044
A0A1I4HHD4	2.1907	-2.1907	10 kDa chaperonin	2.19	0.0098	1.14	5.22	groS groES SAMN04487868_101397
A0A1I4INC2	2.1957	-2.1957	Uncharacterized conserved protein	2.20	0.0098	1.33	5.23	SAMN04487868_10441
A0A1I4IFA7	2.1980	-2.1980	Glutamate--putrescine ligase	2.20	0.0099	2.26	5.24	SAMN04487868_103247
A0A1I4J332	2.2010	-2.2010	Glutathione synthase/RimK-type ligase. ATP-grasp superfamily	2.20	0.0097	0.83	5.25	SAMN04487868_10541
A0A1I4I396	2.2017	-2.2017	ATP-dependent Clp protease ATP-binding subunit ClpX	2.20	0.0097	0.42	5.25	clpX SAMN04487868_102267
A0A1I4N3R3	2.2024	-2.2024	50S ribosomal protein L24	2.20	0.0098	0.68	5.26	rplX SAMN04487868_12914
A0A1I4N141	2.2054	-2.2054	Alcohol dehydrogenase. class IV	2.21	0.0098	0.59	5.27	SAMN04487868_1283
A0A1I4HAB2	2.2068	-2.2068	Uncharacterized protein	2.21	0.0098	1.32	5.27	SAMN04487868_101188
A0A1I4JLN8	2.2110	-2.2110	Sugar fermentation stimulation protein homolog	2.21	0.0098	0.83	5.28	sfsA SAMN04487868_106164
A0A1I4HYF5	2.2113	-2.2113	ATP-dependent Clp protease adapter protein ClpS	2.21	0.0098	2.74	5.29	clpS SAMN04487868_102160
A0A1I4HWA6	2.2114	-2.2114	Tol-Pal system protein TolQ	2.21	0.0099	0.53	5.29	tolQ SAMN04487868_102114
A0A1I4LLP6	2.2124	-2.2124	Isoleucine--tRNA ligase	2.21	0.0099	0.76	5.29	ileS SAMN04487868_11525
A0A1I4MX27	2.2160	-2.2160	Pseudouridine synthase	2.22	0.0096	0.94	5.30	SAMN04487868_12649
A0A1I4M2I2	2.2208	-2.2208	Uncharacterized protein	2.22	0.0096	0.40	5.32	SAMN04487868_11851
A0A1I4J7H1	2.2257	-2.2257	Histidine--tRNA ligase	2.23	0.0096	0.88	5.33	hisS SAMN04487868_105145
A0A1I4HYZ5	2.2259	-2.2259	Ribosomal RNA large subunit methyltransferase M	2.23	0.0096	0.94	5.34	rlmM SAMN04487868_102183
A0A1I4M2K3	2.2266	-2.2266	Membrane-bound lytic murein transglycosylase D	2.23	0.0096	1.09	5.34	SAMN04487868_11858
A0A1I4M6B5	2.2307	-2.2307	Uncharacterized protein	2.23	0.0095	1.48	5.35	SAMN04487868_11932
A0A1I4M0W2	2.2413	-2.2413	Phospholipid-binding lipoprotein MlaA	2.24	0.0092	0.93	5.39	SAMN04487868_1186
A0A1I4HLD5	2.2486	-2.2486	Two-component system. chemotaxis family. response regulator CheY	2.25	0.0093	0.38	5.41	SAMN04487868_101465
A0A1I4H7Z5	2.2532	-2.2532	L-threonine aldolase	2.25	0.0093	0.95	5.43	SAMN04487868_101104
A0A1I4HA08	2.2532	-2.2532	Citronellyl-CoA synthetase	2.25	0.0093	1.22	5.43	SAMN04487868_101218
A0A1I4M6I5	2.2629	-2.2629	5'-nucleotidase SurE	2.26	0.0093	0.43	5.46	surE SAMN04487868_11950
A0A1I4INU2	2.2662	-2.2662	PAS domain S-box-containing protein/diguanylate cyclase (GGDEF) domain-containing protein	2.27	0.0094	0.67	5.48	SAMN04487868_10468
A0A1I4MLN4	2.2682	-2.2682	Succinate-semialdehyde dehydrogenase / glutarate-semialdehyde dehydrogenase	2.27	0.0092	0.50	5.48	SAMN04487868_12355
A0A1I4H3K7	2.2707	-2.2707	Phosphonates import ATP-binding protein PhnC	2.27	0.0092	0.57	5.49	phnC SAMN04487868_10149
A0A1I4KF26	2.2737	-2.2737	Uncharacterized protein	2.27	0.0092	1.62	5.50	SAMN04487868_109125
A0A1I4LGW8	2.2779	-2.2779	Mannose-6-phosphate isomerase. type 2	2.28	0.0093	5.08	7.32	SAMN04487868_11455
A0A1I4M5J7	2.2790	-2.2790	Chromosome partitioning protein	2.28	0.0093	0.88	5.52	SAMN04487868_11926
A0A1I4JAY1	2.2806	-2.2806	Acylphosphatase	2.28	0.0091	1.42	5.53	SAMN04487868_105203

A0A1I4M177	2.2859	-2.2859	50S ribosomal protein L3 glutamine methyltransferase	2.29	0.0092	0.69	5.54	prmB SAMN04487868_11826
A0A1I4IVI2	2.2866	-2.2866	23S rRNA (uracil(1939)-C(5))-methyltransferase RlmD	2.29	0.0092	0.68	5.55	rlmD SAMN04487868_104189
A0A1I4M6I2	2.2869	-2.2869	Enolase	2.29	0.0092	0.44	5.55	eno SAMN04487868_11955
A0A1I4HFX2	2.2933	-2.2933	Phospholipid/cholesterol/gamma-HCH transport system ATP-binding protein	2.29	0.0092	0.87	5.57	SAMN04487868_101319
A0A1I4J979	2.2939	-2.2939	Uncharacterized protein	2.29	0.0092	1.49	7.41	SAMN04487868_105189
A0A1I4MD12	2.2971	-2.2971	Cell division protein FtsA	2.30	0.0093	0.96	5.58	ftsA SAMN04487868_12120
A0A1I4JLA1	2.2987	-2.2987	Pantothenate synthetase	2.30	0.0093	0.52	5.59	panC SAMN04487868_106155
A0A1I4HED9	2.2988	-2.2988	tRNA-2-methylthio-N(6)-dimethylallyladenosine synthase	2.30	0.0093	0.97	5.59	miaB SAMN04487868_101290
A0A1I4H9Z9	2.3013	-2.3013	D-3-phosphoglycerate dehydrogenase	2.30	0.0093	0.36	5.60	SAMN04487868_101208
A0A1I4HFP7	2.3209	-2.3209	RNAse G	2.32	0.0092	0.52	5.67	SAMN04487868_101304
A0A1I4JWG7	2.3211	-2.3211	1-deoxy-D-xylulose 5-phosphate reductoisomerase	2.32	0.0092	0.58	5.67	dxr SAMN04487868_107154
A0A1I4NH57	2.3213	-2.3213	UPF0271 protein	2.32	0.0092	1.08	5.67	SAMN04487868_1404
A0A1I4J485	2.3274	-2.3274	Aspartate racemase	2.33	0.0092	1.16	5.69	SAMN04487868_10572
A0A1I4HEN1	2.3305	-2.3305	Aspartyl/glutamyl-tRNA(Asn/Gln) amidotransferase subunit C	2.33	0.0091	1.31	5.70	gatC SAMN04487868_101299
A0A1I4N9M6	2.3351	-2.3351	PAS domain S-box-containing protein/diguanylate cyclase (GGDEF) domain-containing protein	2.34	0.0091	0.60	5.72	SAMN04487868_1325
A0A1I4HXZ9	2.3380	-2.3380	Thioredoxin reductase	2.34	0.0089	0.91	5.73	SAMN04487868_102154
A0A1I4HL67	2.3404	-2.3404	Carbonic anhydrase	2.34	0.0088	0.72	5.74	SAMN04487868_101493
A0A1I4I1M3	2.3443	-2.3443	Glutamine--tRNA ligase	2.34	0.0088	0.58	5.75	glnS SAMN04487868_102277
A0A1I4M3N5	2.3563	-2.3563	Sulfite reductase (NADPH) hemoprotein beta-component	2.36	0.0088	0.41	5.80	SAMN04487868_11868
A0A1I4JS87	2.3622	-2.3622	ADP-ribose pyrophosphatase YjhB. NUDIX family	2.36	0.0089	1.24	5.82	SAMN04487868_10722
A0A1I4I8Q7	2.3624	-2.3624	Multifunctional fusion protein	2.36	0.0089	2.85	5.82	msrB msrA SAMN04487868_10376
A0A1I4MNP7	2.3656	-2.3656	Signal transduction histidine kinase	2.37	0.0089	2.27	5.83	SAMN04487868_12432
A0A1I4JX88	2.3699	-2.3699	2.3.4.5-tetrahydropyridine-2.6-dicarboxylate N-succinyltransferase	2.37	0.0090	0.45	5.85	dapD SAMN04487868_107166
A0A1I4JRX8	2.3746	-2.3746	5-methylthioadenosine/S-adenosylhomocysteine deaminase	2.37	0.0090	1.00	5.87	mtaD SAMN04487868_10734
A0A1I4MEP1	2.3760	-2.3760	UDP-N-acetylmuramate--L-alanyl-gamma-D-glutamyl-meso-2.6-diaminoheptandioate ligase	2.38	0.0090	0.44	5.87	mpl SAMN04487868_12168
A0A1I4L4P8	2.3781	-2.3781	Type VI secretion system protein VasG	2.38	0.0090	0.47	5.88	SAMN04487868_112136
A0A1I4L6Z7	2.3857	-2.3857	Alpha-ketoglutarate-dependent 2.4-dichlorophenoxyacetate dioxygenase	2.39	0.0087	1.44	5.91	SAMN04487868_1138
A0A1I4JGB6	2.3864	-2.3864	Peptidyl-prolyl cis-trans isomerase	2.39	0.0087	0.54	5.91	SAMN04487868_10645
A0A1I4HX32	2.3919	-2.3919	UDP-glucose 6-dehydrogenase	2.39	0.0082	0.90	5.93	SAMN04487868_102123
A0A1I4IEB8	2.3925	-2.3925	5'-nucleotidase	2.39	0.0082	2.59	5.93	SAMN04487868_103222
A0A1I4HXX4	2.3995	-2.3995	UDP-glucose 4-epimerase	2.40	0.0080	0.91	5.96	SAMN04487868_102124
A0A1I4JH20	2.3999	-2.3999	S1 motif domain-containing protein	2.40	0.0080	0.44	5.96	SAMN04487868_10639
A0A1I4HBH2	2.4025	-2.4025	Protein HflK	2.40	0.0079	0.13	5.97	SAMN04487868_101259
A0A1I4KVH1	2.4047	-2.4047	Alkane 1-monooxygenase	2.40	0.0079	4.37	5.98	SAMN04487868_111110
A0A1I4K1B3	2.4138	-2.4138	Starvation-inducible DNA-binding protein	2.41	0.0078	1.16	6.01	SAMN04487868_10820
A0A1I4M2K1	2.4181	-2.4181	O-succinylhomoserine sulfhydrylase	2.42	0.0078	0.53	6.03	metZ SAMN04487868_11844

A0A1I4K4U1	2.4303	-2.4303	Phosphopantetheine adenylyltransferase	2.43	0.0073	0.57	6.07	coaD SAMN04487868_108114
A0A1I4MYG1	2.4336	-2.4336	Secondary thiamine-phosphate synthase enzyme	2.43	0.0073	0.80	6.09	SAMN04487868_12714
A0A1I4NIL6	2.4371	-2.4371	Adenine DNA glycosylase	2.44	0.0071	1.19	6.10	SAMN04487868_1417
A0A1I4I8N8	2.4441	-2.4441	Uncharacterized protein	2.44	0.0069	0.63	6.13	SAMN04487868_10388
A0A1I4MFH0	2.4455	-2.4455	Aminopeptidase N	2.45	0.0070	0.67	6.13	SAMN04487868_1225
A0A1I4N7G7	2.4531	-2.4531	Alpha-L-glutamate ligase-related protein	2.45	0.0068	0.61	6.16	SAMN04487868_13017
A0A1I4M7I9	2.4583	-2.4583	Acireductone dioxygenase	2.46	0.0068	1.39	6.18	mtnD SAMN04487868_11968
A0A1I4J955	2.4607	-2.4607	DNA ligase	2.46	0.0066	0.74	6.19	ligA SAMN04487868_105184
A0A1I4I6I5	2.4618	-2.4618	PAS domain S-box-containing protein/diguanylate cyclase (GGDEF) domain-containing protein	2.46	0.0067	0.75	6.20	SAMN04487868_10313
A0A1I4N3Y1	2.4671	-2.4671	30S ribosomal protein S4	2.47	0.0067	0.59	6.22	rpsD SAMN04487868_12926
A0A1I4JS61	2.4676	-2.4676	Corrinoid adenosyltransferase	2.47	0.0067	0.63	6.22	SAMN04487868_1076
A0A1I4I8W0	2.4704	-2.4704	Nicotinate-nucleotide--dimethylbenzimidazole phosphoribosyltransferase	2.47	0.0067	0.86	6.23	cobT SAMN04487868_10381
A0A1I4JLM8	2.4805	-2.4805	DUF4382 domain-containing protein	2.48	0.0067	2.36	6.27	SAMN04487868_106169
A0A1I4H452	2.4817	-2.4817	Aminopyrimidine aminohydrolase	2.48	0.0067	0.54	6.27	SAMN04487868_10169
A0A1I4H4K1	2.4825	-2.4825	Two component transcriptional regulator. LuxR family	2.48	0.0066	1.32	6.28	SAMN04487868_10183
A0A1I4NCV6	2.4887	-2.4887	Phosphomethylpyrimidine synthase	2.49	0.0066	0.55	6.30	thiC SAMN04487868_13332
A0A1I4HV16	2.4920	-2.4920	UTP--glucose-1-phosphate uridylyltransferase	2.49	0.0066	0.94	6.31	SAMN04487868_10283
A0A1I4IRH3	2.4957	-2.4957	Uncharacterized protein	2.50	0.0066	0.32	6.33	SAMN04487868_104107
A0A1I4L2X3	2.4986	-2.4986	AraC-type DNA-binding protein	2.50	0.0064	2.24	8.72	SAMN04487868_11280
A0A1I4I1L6	2.5058	-2.5058	Biopolymer transport protein ExbD	2.51	0.0060	0.95	6.37	SAMN04487868_102209
A0A1I4MW15	2.5103	-2.5103	POLIIIAc domain-containing protein	2.51	0.0061	1.41	6.39	SAMN04487868_12646
A0A1I4JTA4	2.5120	-2.5120	Recombination-associated protein RdgC	2.51	0.0061	0.55	6.39	rdgC SAMN04487868_10741
A0A1I4K4C5	2.5143	-2.5143	Pimeloyl-ACP methyl ester carboxylesterase	2.51	0.0061	2.12	6.40	SAMN04487868_10882
A0A1I4JLG6	2.5154	-2.5154	APH domain-containing protein	2.52	0.0061	0.29	6.41	SAMN04487868_106166
A0A1I4HF75	2.5171	-2.5171	Protein involved in polysaccharide export. contains SLBB domain of the beta-grasp fold	2.52	0.0061	1.16	6.41	SAMN04487868_101355
A0A1I4LC62	2.5219	-2.5219	Mercuric reductase	2.52	0.0061	0.62	6.43	SAMN04487868_113112
A0A1I4HW05	2.5239	-2.5239	Helix-turn-helix domain-containing protein	2.52	0.0059	0.67	6.44	SAMN04487868_10284
A0A1I4MAM1	2.5301	-2.5301	Predicted flavoprotein CzcO associated with the cation diffusion facilitator CzcD	2.53	0.0058	1.48	6.46	SAMN04487868_12031
A0A1I4IW95	2.5314	-2.5314	Predicted oxidoreductase	2.53	0.0058	0.25	6.47	SAMN04487868_104238
A0A1I4LMK5	2.5332	-2.5332	ATP-dependent protease ATPase subunit HslU	2.53	0.0056	0.97	6.48	hslU SAMN04487868_11569
A0A1I4IW44	2.5350	-2.5350	Peptidyl-prolyl cis-trans isomerase	2.54	0.0056	0.75	6.48	SAMN04487868_104235
A0A1I4HJQ8	2.5384	-2.5384	Acetyl-CoA C-acetyltransferase	2.54	0.0056	0.97	6.50	SAMN04487868_101415
A0A1I4LG07	2.5466	-2.5466	Poly(Beta-D-mannuronate) lyase	2.55	0.0056	4.81	6.53	SAMN04487868_11454
A0A1I4IF66	2.5474	-2.5474	Uncharacterized protein	2.55	0.0056	2.38	6.53	SAMN04487868_103223
A0A1I4HKR8	2.5503	-2.5503	Cytochrome c-type biogenesis protein	2.55	0.0057	0.86	6.55	SAMN04487868_101484
A0A1I4HBD1	2.5505	-2.5505	DNA mismatch repair protein MutL	2.55	0.0057	1.00	6.55	mutL SAMN04487868_101255
A0A1I4N3I4	2.5613	-2.5613	30S ribosomal protein S5	2.56	0.0055	0.57	6.59	rpsE SAMN04487868_12920

A0A1I4J3S1	2.5617	-2.5617	Formyltetrahydrofolate deformylase	2.56	0.0055	0.54	6.59	purU SAMN04487868_10525
A0A1I4HH93	2.5635	-2.5635	UDP-4-amino-4.6-dideoxy-N-acetyl-beta-L-altrosamine N-acetyltransferase	2.56	0.0055	1.10	6.60	SAMN04487868_101364
A0A1I4HYD0	2.5659	-2.5659	tRNA-specific 2-thiouridylase MnmA	2.57	0.0055	0.60	6.61	mnmA SAMN04487868_102164
A0A1I4HTS9	2.5709	-2.5709	YcgL domain-containing protein SAMN04487868_10218	2.57	0.0053	2.48	6.63	SAMN04487868_10218
A0A1I4LKE6	2.5746	-2.5746	4-hydroxy-3-methylbut-2-enyl diphosphate reductase	2.57	0.0053	1.56	6.65	ispH SAMN04487868_11522
A0A1I4KUF0	2.5749	-2.5749	Adenosylhomocysteinase	2.58	0.0054	0.55	6.65	ahcY SAMN04487868_11186
A0A1I4KEI4	2.5751	-2.5751	Choline dehydrogenase	2.58	0.0054	1.32	6.65	SAMN04487868_109136
A0A1I4KM83	2.5832	-2.5832	Chaperone protein DnaJ	2.58	0.0052	1.04	6.68	dnaJ SAMN04487868_110121
A0A1I4IWP2	2.6028	-2.6028	Cell division topological specificity factor	2.60	0.0051	1.04	6.76	minE SAMN04487868_104246
A0A1I4MI03	2.6050	-2.6050	Alcohol dehydrogenase. propanol-preferring	2.61	0.0051	1.80	6.77	SAMN04487868_12256
A0A1I4JR18	2.6060	-2.6060	Cobyrinic acid a.c-diamide synthase	2.61	0.0051	0.75	6.78	SAMN04487868_1077
A0A1I4M4Z4	2.6106	-2.6106	Probable cytosol aminopeptidase	2.61	0.0049	0.68	6.80	pepA SAMN04487868_11916
A0A1I4MZE1	2.6122	-2.6122	Lipoyl synthase	2.61	0.0049	1.98	6.80	lipA SAMN04487868_12744
A0A1I4KC65	2.6210	-2.6210	AraC-type DNA-binding protein	2.62	0.0047	0.96	6.84	SAMN04487868_10980
A0A1I4HX57	2.6222	-2.6222	GMP synthase [glutamine-hydrolyzing]	2.62	0.0047	0.47	6.84	guaA SAMN04487868_102127
A0A1I4KL19	2.6236	-2.6236	Metallophos_2 domain-containing protein	2.62	0.0047	1.18	6.85	SAMN04487868_11094
A0A1I4I173	2.6257	-2.6257	Transcriptional regulator. TetR family	2.63	0.0047	1.52	6.86	SAMN04487868_102196
A0A1I4ILD3	2.6412	-2.6412	Co-chaperone protein DjlA	2.64	0.0045	0.36	6.92	djlA SAMN04487868_10414
A0A1I4JH41	2.6414	-2.6414	Glutamate--cysteine ligase	2.64	0.0045	0.59	6.93	gshA SAMN04487868_10640
A0A1I4HTQ1	2.6439	-2.6439	Ribonuclease D	2.64	0.0045	0.44	6.94	SAMN04487868_10219
A0A1I4HB66	2.6473	-2.6473	Oligoribonuclease	2.65	0.0046	0.63	6.95	orn SAMN04487868_101250
A0A1I4LM95	2.6500	-2.6500	Arginine--tRNA ligase	2.65	0.0046	0.73	6.96	argS SAMN04487868_11566
A0A1I4MLB5	2.6529	-2.6529	OmpA-OmpF porin. OOP family	2.65	0.0046	1.34	6.97	SAMN04487868_12345
A0A1I4HU51	2.6642	-2.6642	Glycosyltransferase involved in cell wall bisynthesis	2.66	0.0044	0.80	7.02	SAMN04487868_10248
A0A1I4KTE7	2.6650	-2.6650	Predicted HD phosphohydrolase	2.67	0.0044	0.68	7.03	SAMN04487868_11158
A0A1I4IP03	2.6667	-2.6667	Cold-shock DNA-binding protein family	2.67	0.0044	1.90	7.03	SAMN04487868_10475
A0A1I4HGQ0	2.6724	-2.6724	Flagellar secretion chaperone FliS	2.67	0.0044	2.03	7.06	SAMN04487868_101388
A0A1I4ME43	2.6777	-2.6777	Gamma-glutamyl phosphate reductase	2.68	0.0044	0.75	7.08	proA SAMN04487868_12151
A0A1I4J8A7	2.6837	-2.6837	Citrate synthase	2.68	0.0045	0.43	7.11	SAMN04487868_105166
A0A1I4HXF7	2.6891	-2.6891	UPF0434 protein SAMN04487868_102140	2.69	0.0045	1.97	10.14	SAMN04487868_102140
A0A1I4I2E8	2.6958	-2.6958	Lon protease	2.70	0.0043	0.96	7.16	lon SAMN04487868_102266
A0A1I4MRM2	2.6971	-2.6971	Uncharacterized protein	2.70	0.0043	1.57	7.17	SAMN04487868_12525
A0A1I4MYA2	2.7015	-2.7015	Peptide chain release factor 1	2.70	0.0043	0.55	7.19	prfA SAMN04487868_12723
A0A1I4HG20	2.7069	-2.7069	Metallo-beta-lactamase family protein	2.71	0.0043	2.69	7.21	SAMN04487868_101376
A0A1I4H9H2	2.7094	-2.7094	Sigma54 specific transcriptional regulator. Fis family	2.71	0.0043	0.66	7.22	SAMN04487868_101200
A0A1I4HHL7	2.7096	-2.7096	CBS domain-containing protein	2.71	0.0043	1.00	7.22	SAMN04487868_101417
A0A1I4IU14	2.7161	-2.7161	GTP pyrophosphokinase	2.72	0.0044	1.09	7.25	SAMN04487868_104188
A0A1I4HV19	2.7192	-2.7192	Predicted ATP-dependent carboligase. ATP-grasp superfamily	2.72	0.0044	1.40	7.26	SAMN04487868_10257

A0A1I4HEQ9	2.7199	-2.7199	Endoribonuclease YbeY	2.72	0.0044	2.01	7.27	ybeY SAMN04487868_101288
A0A1I4N067	2.7264	-2.7264	30S ribosomal protein S6	2.73	0.0042	0.80	7.30	rpsF SAMN04487868_12758
A0A1I4I1F2	2.7339	-2.7339	Glycerol-3-phosphate dehydrogenase	2.73	0.0042	1.14	7.33	SAMN04487868_102247
A0A1I4N3Y7	2.7463	-2.7463	50S ribosomal protein L5	2.75	0.0042	0.46	7.39	rplE SAMN04487868_12915
A0A1I4NE44	2.7464	-2.7464	Peptidyl-prolyl cis-trans isomerase	2.75	0.0042	2.35	7.39	SAMN04487868_13420
A0A1I4HIE1	2.7515	-2.7515	60 kDa chaperonin	2.75	0.0042	0.92	7.41	groL groEL SAMN04487868_101398
A0A1I4JGY3	2.7521	-2.7521	CDP-4-dehydro-6-deoxyglucose reductase	2.75	0.0042	1.08	7.41	SAMN04487868_10657
A0A1I4MYY2	2.7523	-2.7523	Ribosome-binding ATPase YchF	2.75	0.0043	0.33	7.41	ychF SAMN04487868_12731
A0A1I4MDQ6	2.7555	-2.7555	HD-like signal output (HDOD) domain. no enzymatic activity	2.76	0.0043	0.74	7.43	SAMN04487868_12146
A0A1I4HTH8	2.7573	-2.7573	PA14 domain-containing protein	2.76	0.0043	1.32	7.44	SAMN04487868_10238
A0A1I4H683	2.7588	-2.7588	RNA polymerase. sigma subunit. ECF family	2.76	0.0043	3.30	7.44	SAMN04487868_10186
A0A1I4IG64	2.7631	-2.7631	Enoyl-CoA hydratase/carnithine racemase	2.76	0.0043	0.85	7.46	SAMN04487868_103235
A0A1I4N3N0	2.7660	-2.7660	30S ribosomal protein S19	2.77	0.0043	0.50	7.48	rpsS SAMN04487868_1297
A0A1I4M151	2.7678	-2.7678	Phosphoserine phosphatase	2.77	0.0043	0.85	7.48	SAMN04487868_11814
A0A1I4N0B6	2.7719	-2.7719	NADP-dependent aldehyde dehydrogenase	2.77	0.0041	0.72	7.50	SAMN04487868_1288
A0A1I4L3J5	2.7785	-2.7785	Phosphoenolpyruvate carboxykinase (ATP)	2.78	0.0041	0.64	7.53	pckA SAMN04487868_112106
A0A1I4L6V6	2.7796	-2.7796	Bifunctional protein GlmU	2.78	0.0041	0.50	7.54	glmU SAMN04487868_11315
A0A1I4J3P5	2.7796	-2.7796	GST-like protein	2.78	0.0041	0.30	7.54	SAMN04487868_10521
A0A1I4M238	2.7849	-2.7849	Uroporphyrin-III C-methyltransferase	2.79	0.0041	0.59	7.56	SAMN04487868_11849
A0A1I4HV88	2.7890	-2.7890	6-pyruvoyl-tetrahydropterin synthase	2.79	0.0042	0.69	7.58	SAMN04487868_10288
A0A1I4JFL3	2.7953	-2.7953	Phospholipase A1	2.80	0.0039	0.56	7.61	SAMN04487868_10632
A0A1I4K5Z0	2.7990	-2.7990	Putative acyl-CoA dehydrogenase	2.80	0.0039	1.25	7.63	SAMN04487868_108121
A0A1I4JI32	2.8011	-2.8011	Diaminopimelate decarboxylase	2.80	0.0040	0.71	7.64	lysA SAMN04487868_10668
A0A1I4NHE7	2.8057	-2.8057	YrhK-like protein	2.81	0.0040	1.66	7.66	SAMN04487868_1397
A0A1I4KU53	2.8060	-2.8060	Putative serine protein kinase. PrkA	2.81	0.0040	0.92	7.66	SAMN04487868_11167
A0A1I4HEC8	2.8095	-2.8095	Dinuclear metal center protein. YbgI/SA1388 family	2.81	0.0040	0.85	7.68	SAMN04487868_101329
A0A1I4IML6	2.8173	-2.8173	Uncharacterized conserved protein YbaA. DUF1428 family	2.82	0.0040	2.18	7.71	SAMN04487868_10442
A0A1I4L431	2.8302	-2.8302	Transcription elongation factor GreB	2.83	0.0035	2.70	7.77	greB SAMN04487868_112122
A0A1I4J2X8	2.8304	-2.8304	Ribosomal-protein-alanine acetyltransferase	2.83	0.0035	1.16	7.77	SAMN04487868_10540
A0A1I4K1F6	2.8421	-2.8421	Inositol-1-monophosphatase	2.84	0.0035	0.50	7.83	SAMN04487868_10836
A0A1I4HVE4	2.8562	-2.8562	Glycosyl transferases group 1	2.86	0.0036	0.69	7.90	SAMN04487868_10251
A0A1I4IA78	2.8574	-2.8574	DNA-binding response regulator. OmpR family. contains REC and winged-helix (WHTH) domain	2.86	0.0033	1.75	7.90	SAMN04487868_10374
A0A1I4MNN6	2.8617	-2.8617	DNA-binding response regulator. OmpR family. contains REC and winged-helix (WHTH) domain	2.86	0.0033	0.56	7.92	SAMN04487868_12431
A0A1I4NF26	2.8628	-2.8628	50S ribosomal protein L1	2.86	0.0034	0.42	7.93	rplA SAMN04487868_1369
A0A1I4KMT7	2.8668	-2.8668	UPF0125 protein SAMN04487868_110115	2.87	0.0034	1.42	7.95	SAMN04487868_110115
A0A1I4HCU7	2.8760	-2.8760	Phosphate starvation-inducible protein PhoH	2.88	0.0034	0.69	7.99	SAMN04487868_101289
A0A1I4H5B4	2.8785	-2.8785	Alcohol dehydrogenase. class IV	2.88	0.0034	0.99	8.00	SAMN04487868_10151

A0A1I4L031	2.8811	-2.8811	ATPase family associated with various cellular activities (AAA)	2.88	0.0032	2.21	8.02	SAMN04487868_1124
A0A1I4MEN0	2.8861	-2.8861	Dihydroxy-acid dehydratase	2.89	0.0032	0.99	8.04	ilvD SAMN04487868_12145
A0A1I4K4E9	2.9089	-2.9089	S-adenosylmethionine decarboxylase proenzyme	2.91	0.0032	1.06	8.15	speD SAMN04487868_10885
A0A1I4HV96	2.9125	-2.9125	Glycosyltransferase involved in cell wall bisynthesis	2.91	0.0032	1.22	8.17	SAMN04487868_10287
A0A1I4IML8	2.9147	-2.9147	Protease I	2.92	0.0032	2.19	8.18	SAMN04487868_10447
A0A1I4N4F4	2.9304	-2.9304	30S ribosomal protein S11	2.93	0.0033	0.61	8.26	rpsK SAMN04487868_12925
A0A1I4LJZ7	2.9326	-2.9326	Two-component system. NtrC family. response regulator PilR	2.93	0.0033	0.52	8.27	SAMN04487868_11513
A0A1I4HDK1	2.9343	-2.9343	Arabinose 5-phosphate isomerase	2.94	0.0033	0.82	8.28	SAMN04487868_101318
A0A1I4KUT6	2.9585	-2.9585	Fructose-1.6-bisphosphate aldolase	2.96	0.0030	0.97	8.40	SAMN04487868_11192
A0A1I4I2G5	2.9683	-2.9683	Uncharacterized protein	2.97	0.0028	2.90	8.45	SAMN04487868_102288
A0A1I4HEA8	2.9699	-2.9699	Histidinol-phosphate aminotransferase	2.97	0.0028	0.64	8.46	hisC SAMN04487868_101328
A0A1I4HX70	2.9768	-2.9768	Holliday junction ATP-dependent DNA helicase RuvB	2.98	0.0028	1.08	8.50	ruvB SAMN04487868_102116
A0A1I4KA41	2.9769	-2.9769	Diaminobutyrate--2-oxoglutarate transaminase	2.98	0.0028	1.05	8.50	SAMN04487868_10930
A0A1I4H4P3	2.9807	-2.9807	DUF2063 domain-containing protein	2.98	0.0028	5.38	8.52	SAMN04487868_10133
A0A1I4HFC2	2.9909	-2.9909	Sulfate adenylyltransferase subunit 2	2.99	0.0028	0.71	8.57	cysD SAMN04487868_101294
A0A1I4KT69	2.9998	-2.9998	3-oxoacyl-[acyl-carrier-protein] synthase-1	3.00	0.0029	0.34	8.61	SAMN04487868_11129
A0A1I4LDR7	3.0075	-3.0075	Uncharacterized conserved protein	3.01	0.0026	3.74	8.65	SAMN04487868_11416
A0A1I4IF35	3.0179	-3.0179	Gamma-glutamylputrescine oxidase	3.02	0.0024	1.69	8.71	SAMN04487868_103249
A0A1I4N4W2	3.0226	-3.0226	MSHA biogenesis protein MshM	3.02	0.0024	2.36	8.73	SAMN04487868_12937
A0A1I4KVQ3	3.0278	-3.0278	Lactoylglutathione lyase	3.03	0.0024	1.81	8.76	SAMN04487868_111111
A0A1I4KV37	3.0406	-3.0406	Phosphoglycerate kinase	3.04	0.0024	0.59	8.83	pgk SAMN04487868_11191
A0A1I4J7K6	3.0419	-3.0419	NADPH-dependent 7-cyano-7-deazaguanine reductase	3.04	0.0024	1.06	8.84	queF SAMN04487868_105114
A0A1I4INT7	3.0478	-3.0478	Phosphatidylserine/phosphatidylglycerophosphate/cardiolipin synthase	3.05	0.0024	0.97	8.87	SAMN04487868_10431
A0A1I4HJP7	3.0489	-3.0489	3-oxoacyl-[acyl-carrier protein] reductase	3.05	0.0024	0.64	8.87	SAMN04487868_101414
A0A1I4MTP6	3.0515	-3.0515	Uncharacterized protein	3.05	0.0024	2.29	8.89	SAMN04487868_12559
A0A1I4ITZ5	3.0529	-3.0529	Uncharacterized protein	3.05	0.0025	0.87	8.89	SAMN04487868_104163
A0A1I4LLS5	3.0541	-3.0541	Serine hydroxymethyltransferase	3.06	0.0025	0.80	8.90	glyA SAMN04487868_11546
A0A1I4M257	3.0620	-3.0620	Acetyl-coenzyme A carboxylase carboxyl transferase subunit beta	3.06	0.0025	0.39	8.94	accD SAMN04487868_11839
A0A1I4JGH6	3.0902	-3.0902	Thioredoxin	3.09	0.0022	1.77	9.10	SAMN04487868_10650
A0A1I4KU28	3.0959	-3.0959	Stage V sporulation protein R	3.10	0.0023	1.26	9.13	SAMN04487868_11165
A0A1I4IX40	3.1003	-3.1003	CBS domain-containing protein	3.10	0.0023	1.61	9.15	SAMN04487868_104249
A0A1I4N1N6	3.1060	-3.1060	Ribonucleoside-diphosphate reductase	3.11	0.0023	1.26	9.18	SAMN04487868_12824
A0A1I4M4T6	3.1121	-3.1121	Alanine--tRNA ligase	3.11	0.0023	0.33	9.22	alaS SAMN04487868_11912
A0A1I4LAT1	3.1181	-3.1181	DNA-binding beta-propeller fold protein YncE	3.12	0.0023	1.37	9.25	SAMN04487868_113104
A0A1I4KUL6	3.1187	-3.1187	S-adenosylmethionine synthase	3.12	0.0023	0.69	9.25	metK SAMN04487868_11187
A0A1I4HGN3	3.1198	-3.1198	3'(2').5'-bisphosphate nucleotidase CysQ	3.12	0.0023	0.95	9.26	cysQ SAMN04487868_101351
A0A1I4HEZ0	3.1265	-3.1265	Ribosome-associated protein	3.13	0.0023	0.78	9.30	SAMN04487868_101307
A0A1I4IY46	3.1320	-3.1320	Site-determining protein	3.13	0.0023	1.69	9.33	SAMN04487868_104245

A0A1I4N0Y1	3.1396	-3.1396	Ribonucleoside-diphosphate reductase subunit beta	3.14	0.0024	1.76	9.37	SAMN04487868_12825
A0A1I4HT45	3.1462	-3.1462	Recombination protein RecR	3.15	0.0024	0.78	9.41	recR SAMN04487868_10220
A0A1I4KBY0	3.1553	-3.1553	Uncharacterized protein	3.16	0.0024	2.43	9.46	SAMN04487868_10969
A0A1I4NDC1	3.1588	-3.1588	Uncharacterized protein	3.16	0.0024	2.92	9.48	SAMN04487868_13419
A0A1I4HE95	3.1619	-3.1619	Histidinol dehydrogenase	3.16	0.0024	0.54	9.50	hisD SAMN04487868_101327
A0A1I4MT08	3.1628	-3.1628	Acyl carrier protein phosphodiesterase	3.16	0.0024	2.05	9.50	SAMN04487868_12543
A0A1I4IXN4	3.1643	-3.1643	Probable septum site-determining protein MinC	3.17	0.0024	1.21	9.51	minC SAMN04487868_104244
A0A1I4N1V0	3.1648	-3.1648	Alkyl hydroperoxide reductase C	3.17	0.0024	3.68	9.51	SAMN04487868_12840
A0A1I4KL02	3.1675	-3.1675	Fumarate hydratase class II	3.17	0.0025	0.77	9.53	fumC SAMN04487868_11092
A0A1I4KED8	3.1680	-3.1680	AraC-type DNA-binding protein	3.17	0.0025	1.64	9.53	SAMN04487868_109133
A0A1I4MV02	3.1688	-3.1688	Glyceraldehyde-3-phosphate dehydrogenase	3.17	0.0025	0.59	9.54	SAMN04487868_12611
A0A1I4M8N0	3.1785	-3.1785	Alkyl hydroperoxide reductase subunit F	3.18	0.0025	3.41	9.59	SAMN04487868_1203
A0A1I4N3Q2	3.1811	-3.1811	50S ribosomal protein L4	3.18	0.0025	0.44	9.61	rplD SAMN04487868_1294
A0A1I4MK80	3.1813	-3.1813	Opacity protein	3.18	0.0025	5.43	9.61	SAMN04487868_12312
A0A1I4L6W0	3.1909	-3.1909	Glutamine--fructose-6-phosphate aminotransferase [isomerizing]	3.19	0.0025	0.89	9.66	glmS SAMN04487868_11314
A0A1I4MW32	3.1998	-3.1998	tRNA-dihydrouridine(20/20a) synthase	3.20	0.0026	2.52	15.09	dusA SAMN04487868_12625
A0A1I4KB32	3.2086	-3.2086	Aspartate kinase	3.21	0.0026	0.53	9.77	SAMN04487868_10929
A0A1I4MQ10	3.2289	-3.2289	Biotin-dependent carboxylase uncharacterized domain-containing protein	3.23	0.0026	2.66	9.88	SAMN04487868_12453
A0A1I4KMV7	3.2289	-3.2289	Phosphoglucosamine mutase	3.23	0.0026	1.15	9.88	glmM SAMN04487868_110130
A0A1I4KDM3	3.2436	-3.2436	Ornithine decarboxylase	3.25	0.0027	1.35	9.97	SAMN04487868_109110
A0A1I4H8J3	3.2464	-3.2464	Maleate cis-trans isomerase	3.25	0.0027	0.78	9.99	SAMN04487868_101119
A0A1I4HHM2	3.2470	-3.2470	Adenylyl-sulfate kinase	3.25	0.0027	1.41	9.99	cysC SAMN04487868_101374
A0A1I4ITE0	3.2502	-3.2502	PAS domain S-box-containing protein/diguanylate cyclase (GGDEF) domain-containing protein	3.25	0.0027	3.51	10.01	SAMN04487868_104172
A0A1I4J7F3	3.2505	-3.2505	4-hydroxy-3-methylbut-2-en-1-yl diphosphate synthase (flavodoxin)	3.25	0.0027	0.88	10.01	ispG SAMN04487868_105144
A0A1I4LKS1	3.2628	-3.2628	Peptidyl-prolyl cis-trans isomerase	3.26	0.0027	1.24	10.09	SAMN04487868_11523
A0A1I4KTB2	3.2696	-3.2696	Fatty acid desaturase	3.27	0.0027	2.37	10.13	SAMN04487868_11155
A0A1I4ML59	3.2766	-3.2766	TatD DNase family protein	3.28	0.0027	1.27	10.17	SAMN04487868_12341
A0A1I4HC89	3.3019	-3.3019	ATP-dependent dethiobiotin synthetase BioD	3.30	0.0028	0.39	10.33	bioD SAMN04487868_101274
A0A1I4M285	3.3024	-3.3024	Amidophosphoribosyltransferase	3.30	0.0028	0.62	10.33	purF SAMN04487868_11843
A0A1I4MWL7	3.3233	-3.3233	SH3 domain protein	3.33	0.0029	1.56	10.46	SAMN04487868_12644
A0A1I4J450	3.3237	-3.3237	Fructose-bisphosphate aldolase	3.33	0.0029	1.57	10.46	SAMN04487868_10565
A0A1I4MCP0	3.3322	-3.3322	UDP-N-acetylmuramoyl-tripeptide--D-alanyl-D-alanine ligase	3.33	0.0029	1.16	10.51	murF SAMN04487868_12112
A0A1I4KP75	3.3399	-3.3399	Thioredoxin	3.34	0.0029	0.99	10.56	SAMN04487868_110155
A0A1I4L944	3.3507	-3.3507	Oxygen-dependent coproporphyrinogen-III oxidase	3.35	0.0030	0.60	10.63	hemF SAMN04487868_11364
A0A1I4MHM9	3.3518	-3.3518	Acetyl esterase/lipase	3.35	0.0030	3.99	10.64	SAMN04487868_12257
A0A1I4KTY5	3.3543	-3.3543	Transcriptional regulator. TetR family	3.36	0.0030	1.25	10.65	SAMN04487868_11157
A0A1I4LF78	3.3587	-3.3587	Alginate export porin	3.36	0.0030	6.27	10.68	SAMN04487868_11448

A0A1I4K5K0	3.3618	-3.3618	Transcriptional regulator. TetR family	3.36	0.0030	1.66	10.70	SAMN04487868_108110
A0A1I4MVE3	3.3638	-3.3638	3-deoxy-D-arabinoheptulosonate-7-phosphate synthase	3.37	0.0030	1.21	10.71	SAMN04487868_12622
A0A1I4KMH8	3.3840	-3.3840	Protein GrpE	3.39	0.0031	2.04	10.85	grpE SAMN04487868_110119
A0A1I4HW41	3.3870	-3.3870	Glucans biosynthesis protein	3.39	0.0031	1.13	10.86	SAMN04487868_10278
A0A1I4L8Z5	3.3900	-3.3900	Peptide deformylase	3.39	0.0031	1.29	10.88	def SAMN04487868_11360
A0A1I4ITT6	3.3947	-3.3947	2.5-diketo-D-gluconate reductase B	3.40	0.0031	2.68	10.92	SAMN04487868_104146
A0A1I4HBX1	3.4355	-3.4355	Outer membrane protein OmpA	3.44	0.0032	0.91	11.18	SAMN04487868_101205
A0A1I4JKX8	3.4514	-3.4514	Glucose-6-phosphate isomerase	3.46	0.0032	0.58	11.29	pgi SAMN04487868_106154
A0A1I4MMY3	3.4519	-3.4519	N-succinylglutamate 5-semialdehyde dehydrogenase	3.46	0.0033	0.95	11.29	astD SAMN04487868_12424
A0A1I4MDA1	3.4595	-3.4595	D-alanine--D-alanine ligase	3.46	0.0033	1.10	11.35	ddl SAMN04487868_12118
A0A1I4LLP5	3.4646	-3.4646	Riboflavin biosynthesis protein RibD	3.47	0.0033	1.21	11.38	SAMN04487868_11544
A0A1I4L7K6	3.4713	-3.4713	Uncharacterized protein	3.48	0.0033	1.69	11.43	SAMN04487868_11332
A0A1I4H8K6	3.4766	-3.4766	Animal haem peroxidase	3.48	0.0033	2.25	11.46	SAMN04487868_101136
A0A1I4HJ99	3.4846	-3.4846	HPt (Histidine-containing phosphotransfer) domain-containing protein	3.49	0.0034	2.05	11.52	SAMN04487868_101448
A0A1I4M294	3.4903	-3.4903	Outer-membrane lipoprotein carrier protein	3.49	0.0034	1.74	11.56	lolA SAMN04487868_11846
A0A1I4KP39	3.4987	-3.4987	Lon protease	3.50	0.0034	1.40	11.62	SAMN04487868_110154
A0A1I4J9P7	3.4993	-3.4993	Succinate--CoA ligase [ADP-forming] subunit beta	3.50	0.0034	0.40	11.62	sucC SAMN04487868_105174
A0A1I4J8R1	3.5087	-3.5087	Segregation and condensation protein B	3.51	0.0035	0.73	11.68	SAMN04487868_105178
A0A1I4HW60	3.5105	-3.5105	Quinolinate synthase A	3.52	0.0035	2.98	11.70	nadA SAMN04487868_102106
A0A1I4M0F6	3.5273	-3.5273	NTE family protein	3.53	0.0035	1.25	11.82	SAMN04487868_1187
A0A1I4J302	3.5324	-3.5324	UvrABC system protein B	3.54	0.0035	1.86	11.85	uvrB SAMN04487868_10539
A0A1I4KUW8	3.5389	-3.5389	Chaperone modulatory protein CbpM	3.54	0.0035	2.28	11.90	SAMN04487868_11194
A0A1I4HX76	3.5463	-3.5463	Inosine-5'-monophosphate dehydrogenase	3.55	0.0036	1.18	11.95	guaB SAMN04487868_102128
A0A1I4L9J0	3.5501	-3.5501	Heat shock protein Hsp20	3.56	0.0036	5.76	11.98	SAMN04487868_11369
A0A1I4M1X5	3.5638	-3.5638	Putative ATPase	3.57	0.0036	1.15	12.08	SAMN04487868_11847
A0A1I4HI95	3.5671	-3.5671	Response regulator receiver modulated diguanylate cyclase	3.57	0.0037	2.86	12.10	SAMN04487868_101391
A0A1I4KUI8	3.5683	-3.5683	Methylenetetrahydrofolate reductase	3.57	0.0037	1.25	12.11	SAMN04487868_11185
A0A1I4NHV7	3.5893	-3.5893	Putative pterin-4-alpha-carbinolamine dehydratase	3.60	0.0038	2.99	12.26	SAMN04487868_1396
A0A1I4KRK3	3.6198	-3.6198	Protein-export protein SecB	3.63	0.0033	0.86	12.49	secB SAMN04487868_11112
A0A1I4HIU5	3.6244	-3.6244	Superoxide dismutase	3.63	0.0033	1.44	12.52	SAMN04487868_101405
A0A1I4HID5	3.6366	-3.6366	Acyl-CoA dehydrogenase	3.64	0.0034	1.77	12.62	SAMN04487868_101423
A0A1I4K3Z9	3.6391	-3.6391	Heat shock protein HslJ	3.65	0.0034	1.61	12.64	SAMN04487868_10873
A0A1I4JFJ7	3.6442	-3.6442	Phosphomannomutase	3.65	0.0034	0.90	12.67	SAMN04487868_10631
A0A1I4KSE0	3.6446	-3.6446	Cysteine desulfurase	3.65	0.0034	1.68	12.68	SAMN04487868_11124
A0A1I4IVB9	3.6667	-3.6667	Threonine synthase	3.67	0.0035	0.48	12.85	SAMN04487868_104214
A0A1I4HW52	3.6699	-3.6699	Tol-Pal system protein TolB	3.68	0.0035	0.58	12.87	tolB SAMN04487868_102111
A0A1I4IF42	3.6946	-3.6946	Gamma-glutamyl-gamma-aminobutyraldehyde dehydrogenase	3.70	0.0036	1.33	13.07	SAMN04487868_103248
A0A1I4L4C8	3.6982	-3.6982	Type VI secretion system protein ImpC	3.71	0.0036	0.97	13.09	SAMN04487868_112128

A0A1I4LG98	3.7219	-3.7219	Phosphomannomutase	3.73	0.0037	6.18	13.28	SAMN04487868_11456
A0A1I4HB22	3.7234	-3.7234	Uncharacterized protein	3.73	0.0037	2.93	13.30	SAMN04487868_101207
A0A1I4N7Q2	3.7262	-3.7262	Putative NAD(P)H quinone oxidoreductase. PIG3 family	3.74	0.0037	1.23	13.32	SAMN04487868_13036
A0A1I4KM89	3.7293	-3.7293	4-hydroxy-tetrahydrodipicolinate reductase	3.74	0.0038	1.40	13.34	dapB SAMN04487868_110122
A0A1I4MCR2	3.7485	-3.7485	UDP-N-acetylmuramate--L-alanine ligase	3.76	0.0038	0.99	13.50	murC SAMN04487868_12117
A0A1I4N8X2	3.7644	-3.7644	Isopenicillin N synthase	3.78	0.0025	3.11	13.63	SAMN04487868_13119
A0A1I4ICL7	3.7841	-3.7841	Putative intracellular protease/amidase	3.80	0.0026	3.46	13.79	SAMN04487868_103177
A0A1I4MPU8	3.8021	-3.8021	Putative hydro-lyase SAMN04487868_12447	3.81	0.0026	4.48	13.95	SAMN04487868_12447
A0A1I4KMS0	3.8238	-3.8238	Chaperone protein DnaK	3.84	0.0027	1.49	14.13	dnaK SAMN04487868_110120
A0A1I4KV85	3.8473	-3.8473	Curved DNA-binding protein	3.86	0.0027	2.34	14.34	SAMN04487868_11193
A0A1I4HI90	3.8539	-3.8539	UDP-N-acetyl-D-galactosamine dehydrogenase	3.87	0.0028	1.36	14.40	SAMN04487868_101377
A0A1I4KXJ6	3.8573	-3.8573	Uncharacterized protein	3.87	0.0029	2.20	14.43	SAMN04487868_111138
A0A1I4MKE3	3.8729	-3.8729	Aconitate hydratase	3.89	0.0021	1.71	14.57	SAMN04487868_12330
A0A1I4M698	3.8806	-3.8806	tRNA pseudouridine synthase D	3.90	0.0022	0.99	14.64	truD SAMN04487868_11951
A0A1I4JW48	3.8814	-3.8814	Zinc metalloprotease	3.90	0.0022	1.71	14.65	SAMN04487868_107153
A0A1I4JND1	3.9044	-3.9044	N-acetyl-gamma-glutamyl-phosphate reductase	3.92	0.0015	0.56	14.86	argC SAMN04487868_106180
A0A1I4KET0	3.9049	-3.9049	3-phenylpropionate/trans-cinnamate dioxygenase ferredoxin reductase subunit	3.92	0.0015	1.30	14.86	SAMN04487868_109137
A0A1I4MJN7	3.9054	-3.9054	Glycerophosphoryl diester phosphodiesterase	3.92	0.0015	1.73	14.87	SAMN04487868_1239
A0A1I4I777	3.9112	-3.9112	Type VI secretion system secreted protein Hcp	3.93	0.0015	2.84	14.92	SAMN04487868_1038
A0A1I4L479	3.9209	-3.9209	Uncharacterized protein	3.94	0.0015	3.40	15.01	SAMN04487868_112121
A0A1I4HIF2	3.9422	-3.9422	Sugar transferase involved in LPS biosynthesis (Colanic. teichoic acid)	3.96	0.0016	2.23	15.21	SAMN04487868_101371
A0A1I4MNU1	3.9533	-3.9533	N-succinylarginine dihydrolase	3.98	0.0016	1.01	15.32	astB SAMN04487868_12423
A0A1I4LAM4	3.9606	-3.9606	Sulfoxide reductase catalytic subunit YedY	3.98	0.0016	1.15	15.39	SAMN04487868_113101
A0A1I4L0W0	3.9690	-3.9690	Polyhydroxyalkanoate synthase	3.99	0.0017	2.48	15.47	SAMN04487868_11232
A0A1I4K2K4	3.9731	-3.9731	Thiazole synthase	4.00	0.0017	1.23	15.51	thiG SAMN04487868_10838
A0A1I4LFF1	4.0060	-4.0060	Alginate O-acetyltransferase complex protein AlgF	4.03	0.0017	4.10	15.84	SAMN04487868_11452
A0A1I4MEM9	4.0076	-4.0076	Pyrophosphate--fructose 6-phosphate 1-phosphotransferase	4.03	0.0017	0.71	15.86	pfp SAMN04487868_12167
A0A1I4KEJ5	4.0086	-4.0086	Uncharacterized protein	4.04	0.0017	1.19	15.87	SAMN04487868_109124
A0A1I4MLI4	4.0201	-4.0201	Enoyl-CoA hydratase/carnithine racemase	4.05	0.0018	1.08	15.98	SAMN04487868_12350
A0A1I4KN45	4.0249	-4.0249	ATP-dependent zinc metalloprotease FtsH	4.05	0.0018	0.91	16.03	ftsH SAMN04487868_110128
A0A1I4L9P4	4.0309	-4.0309	Oligopeptidase A	4.06	0.0018	1.30	16.10	SAMN04487868_11372
A0A1I4K5K4	4.0470	-4.0470	Aldehyde dehydrogenase	4.08	0.0009	4.15	16.26	SAMN04487868_108111
A0A1I4LDJ0	4.0580	-4.0580	Glutathione S-transferase	4.09	0.0009	4.35	16.38	SAMN04487868_1148
A0A1I4HGX9	4.0900	-4.0900	UDP-N-acetylglucosamine 4.6-dehydratase (Inverting)	4.13	0.0010	1.14	16.73	SAMN04487868_101360
A0A1I4MSP4	4.1112	-4.1112	Uncharacterized protein	4.15	0.0010	1.63	16.96	SAMN04487868_12537
A0A1I4LN31	4.1146	-4.1146	5-methyltetrahydropteroyltriglutamate--homocysteine methyltransferase	4.15	0.0010	3.47	17.00	metE SAMN04487868_11577
A0A1I4N719	4.1170	-4.1170	Fumarate hydratase class I	4.16	0.0010	0.35	17.03	SAMN04487868_13029
A0A1I4MNW8	4.1323	-4.1323	Acetylornithine aminotransferase	4.17	0.0010	0.57	17.20	argD SAMN04487868_12427

A0A1I4IVV3	4.1555	-4.1555	Uncharacterized protein	4.20	0.0011	1.47	17.47	SAMN04487868_104208
A0A1I4IUP3	4.1582	-4.1582	Periplasmic serine endoprotease DegP-like	4.20	0.0011	1.18	17.50	SAMN04487868_104200
A0A1I4L4Z4	4.1722	-4.1722	RNA polymerase sigma factor RpoH	4.22	0.0011	3.34	17.66	rpoH SAMN04487868_112117
A0A1I4I713	4.1798	-4.1798	1-Cys peroxiredoxin	4.23	0.0011	2.89	17.75	SAMN04487868_10329
A0A1I4L8U1	4.1801	-4.1801	4-aminobutyrate aminotransferase / (S)-3-amino-2-methylpropionate transaminase	4.23	0.0012	0.63	17.76	SAMN04487868_11349
A0A1I4J513	4.2324	-4.2324	Chaperone protein HtpG	4.29	0.0013	2.15	18.40	htpG SAMN04487868_10561
A0A1I4HFG8	4.2396	-4.2396	N-acylneuraminate cytidylyltransferase	4.30	0.0013	1.49	18.49	SAMN04487868_101362
A0A1I4N103	4.2409	-4.2409	D-amino-acid dehydrogenase	4.30	0.0014	1.10	18.51	SAMN04487868_12818
A0A1I4HY69	4.2520	-4.2520	ATP-dependent Clp protease ATP-binding subunit ClpA	4.31	0.0014	1.43	18.65	SAMN04487868_102159
A0A1I4KEY9	4.2670	-4.2670	Putative Cytochrome P450	4.33	0.0014	1.24	18.84	SAMN04487868_109135
A0A1I4MPB6	4.2752	-4.2752	UPF0271 protein	4.34	0.0014	5.08	18.94	SAMN04487868_12451
A0A1I4H2W3	4.2992	-4.2992	UPF0276 protein SAMN04487868_10132	4.37	0.0015	6.03	19.26	SAMN04487868_10132
A0A1I4J7V6	4.3540	-4.3540	Queuine tRNA-ribosyltransferase	4.43	0.0016	0.91	20.00	tgt SAMN04487868_105131
A0A1I4KTN3	4.3618	-4.3618	Ferredoxin-NADP reductase	4.44	0.0016	4.96	20.11	SAMN04487868_11156
A0A1I4IVT0	4.3657	-4.3657	Uncharacterized protein	4.45	0.0016	2.30	20.16	SAMN04487868_104225
A0A1I4JT47	4.4152	-4.4152	UPF0246 protein SAMN04487868_10739	4.50	0.0018	2.17	20.85	SAMN04487868_10739
A0A1I4NGC4	4.4153	-4.4153	2-isopropylmalate synthase	4.51	0.0018	0.15	20.85	leuA SAMN04487868_1374
A0A1I4HCC1	4.4440	-4.4440	Uncharacterized protein	4.54	0.0018	1.79	21.26	SAMN04487868_101277
A0A1I4L3I1	4.4449	-4.4449	Uncharacterized protein	4.54	0.0019	5.00	21.27	SAMN04487868_11290
A0A1I4H4U0	4.4567	-4.4567	PA domain-containing protein	4.55	0.0019	4.33	21.44	SAMN04487868_10190
A0A1I4HI22	4.4696	-4.4696	Acyl-CoA dehydrogenase	4.57	0.0020	2.99	21.62	SAMN04487868_101424
A0A1I4HBL1	4.5584	-4.5584	Adenylosuccinate synthetase	4.67	0.0021	0.49	22.90	purA SAMN04487868_101262
A0A1I4L895	4.5788	-4.5788	Predicted unusual protein kinase regulating ubiquinone biosynthesis. AarF/ABC1/UbiB family	4.69	0.0021	1.99	23.19	SAMN04487868_11343
A0A1I4H4S2	4.7373	-4.7373	Putative DNA-binding domain-containing protein	4.85	0.0024	4.25	25.44	SAMN04487868_10136
A0A1I4LK07	4.7912	-4.7912	Chaperone protein ClpB	4.90	0.0026	2.47	26.18	clpB SAMN04487868_1157
A0A1I4KCQ3	4.8628	-4.8628	CubicO group peptidase. beta-lactamase class C family	4.96	0.0028	3.53	27.15	SAMN04487868_10993
A0A1I4KLH1	4.8970	-4.8970	Uncharacterized protein	4.99	0.0029	2.78	27.61	SAMN04487868_110103
A0A1I4LMS6	4.9110	-4.9110	Predicted acylesterase/phospholipase RssA. contains patatin domain	5.00	0.0030	2.97	27.79	SAMN04487868_11570
A0A1I4JJW2	4.9683	-4.9683	Uncharacterized protein	5.05	0.0000	4.17	28.54	SAMN04487868_106116
A0A1I4K1M6	4.9766	-4.9766	Aminotransferase	5.05	0.0000	2.60	28.64	SAMN04487868_10835
A0A1I4I1H0	4.9786	-4.9786	Trigger factor	5.06	0.0000	0.57	28.67	tig SAMN04487868_102269
A0A1I4KCF9	5.0736	-5.0736	Predicted DNA-binding transcriptional regulator YafY. contains an HTH and WYL domains	5.13	0.0000	3.22	29.88	SAMN04487868_10977
A0A1I4MCC3	5.0977	-5.0977	UDP-N-acetylmuramoylalanine--D-glutamate ligase	5.14	0.0000	1.17	30.18	murD SAMN04487868_12114
A0A1I4L7Y5	5.1214	-5.1214	Chromosomal replication initiator protein DnaA	5.16	0.0000	2.42	30.47	dnaA SAMN04487868_11341
A0A1I4H863	5.4271	-5.4271	Translation initiation factor 1	5.35	0.0000	1.13	34.07	SAMN04487868_101171
A0A1I4LFN3	5.4874	-5.4874	GDP-mannose 6-dehydrogenase	5.39	0.0000	4.61	34.74	SAMN04487868_11444
A0A1I4JL69	5.5144	-5.5144	HD-like signal output (HDOD) domain. no enzymatic activity	5.40	0.0000	1.84	35.04	SAMN04487868_106129

A0A1I4J3P7	5.5249	-5.5249	Alcohol dehydrogenase	5.41	0.0000	3.05	35.16	SAMN04487868_10555
A0A1I4LG50	6.3633	-6.3633	Acetyl-CoA C-acetyltransferase	5.78	0.0000	1.73	43.55	SAMN04487868_11459
A0A1I4MDU9	6.9878	-6.9878	Cell division protein FtsZ	5.98	0.0000	5.13	49.00	ftsZ SAMN04487868_12121
A0A1I4J3K6	10.0122	-10.0122	Uncharacterized protein	6.60	0.0000	5.09	70.05	SAMN04487868_10556
A0A1I4JWB2	13.0298	-13.0298	Ditrans.polycis-undecaprenyl-diphosphate synthase ((2E.6E)-farnesyl-diphosphate specific)	7.33	0.0000	2.48	106.49	uppS SAMN04487868_107156

Table S 4: Proteins with significantly different detected abundances in *Marinobacter* sp. TT1 growing on WAF versus CEWAF according to a Student's T-test (permutation-based FDR: $q < 0.05$).

UniProt ID	WAF	CEWAF	Description	-Log *p*-value	*q*-value	Student's T-test Diff. (log2 FC value)	Student's T-test Test statistic	Gene names
A0A1I4KDA2	-5.1171	5.1171	Hydroxybutyrate-dimer hydrolase	5.16	0.0000	-4.24	-30.42	SAMN04487868_109103
A0A1I4ICK9	4.0364	-4.0364	4-oxalocrotonate decarboxylase	4.07	0.0000	6.49	16.15	SAMN04487868_103138

Table S 5: Proteins assigned to non-alkane hydrocarbon metabolism with significantly higher detected abundances in *Marinobacter* sp. TT1 growing on Corexit versus *n*-hexadecane according to a Student's T-test (permutation-based FDR: $q < 0.05$).

UniProt ID	Hexadecane	Corexit	Assigned pathway	Description	-Log *p*-value	*q*-value	Student's T-test Diff. (log2 FC)	Student's T-test statistic	Gene names
A0A1I4MEF9	-3.9633	3.9633	Aminobenzoate metabolism	Flavin prenyltransferase UbiX	3.99	0.0016	-1.80	-15.42	ubiX SAMN04487868_12169
A0A1I4IDB7	-2.1096	2.1096	Aminobenzoate metabolism	Benzaldehyde dehydrogenase (NAD+)	2.11	0.0116	-1.44	-4.95	SAMN04487868_103155
A0A1I4I6L1	-4.1982	4.1982	Aminobenzoate metabolism	Amidase	4.25	0.0012	-1.42	-17.98	SAMN04487868_10316
A0A1I4JRX0	-3.8508	3.8508	Benzoate metabolism	3-hydroxyacyl-CoA dehydrogenase / enoyl-CoA hydratase / 3-hydroxybutyryl-CoA epimerase	3.87	0.0027	-2.50	-14.37	SAMN04487868_10730
A0A1I4MAT6	-3.2309	3.2309	Benzoate metabolism	3-hydroxyacyl-CoA dehydrogenase	3.23	0.0026	-0.80	-9.90	SAMN04487868_12059
A0A1I4JRY3	-3.8869	3.8869	Benzoate metabolism	Acetyl-CoA C-acetyltransferase	3.90	0.0022	-2.45	-14.70	SAMN04487868_10729
A0A1I4LXN7	-1.9209	1.9209	Cycloaliphatics metabolism	Putative cyclohexanone monooxygenase. Predicted flavoprotein CzcO associated with the cation diffusion facilitator CzcD	1.92	0.0152	-1.19	-4.37	SAMN04487868_11744
A0A1I4H7H6	-2.7869	2.7869	Haloalkane metabolism	Haloalkane dehalogenase	2.79	0.0041	-1.68	-7.57	dhmA SAMN04487868_101153
A0A1I4MDJ5	-2.5481	2.5481	Haloalkane metabolism	Haloalkane dehalogenase	2.55	0.0056	-1.82	-6.54	dhmA SAMN04487868_12140
A0A1I4I1J3	-4.1177	4.1177	Nitrotoluene metabolism	Nitroreductase	4.16	0.0010	-1.15	-17.03	SAMN04487868_102251
A0A1I4IBP8	-2.9246	2.9246	Phenol metabolism	Putative MetA-pathway of phenol degradation	2.92	0.0032	-4.77	-12.19	SAMN04487868_103158
A0A1I4LR95	-2.0935	2.0935	Phenol metabolism	Putative MetA-pathway of phenol degradation	2.09	0.0121	-1.65	-4.90	SAMN04487868_11618

Table S 6: Proteins with significantly different detected abundances in *Marinobacter* sp. TT1 growing on WAF versus CEWAF according to a Student's T-test without multiple testing correction ($p < 0.05$).

UniProt ID	WAF	CEWAF	Description	-Log *p*-value	Student's T-test Diff. (log2 FC)	Student's T-test Test statistic	Gene names
A0A1I4KDA2	-5.1171	5.1171	Hydroxybutyrate-dimer hydrolase	5.16	-4.24	-30.42	SAMN04487868_109103
A0A1I4MY13	-3.2456	3.2456	Tetratricopeptide repeat-containing protein	3.25	-1.04	-9.98	SAMN04487868_12725
A0A1I4J3G1	-2.4778	2.4778	M18 family aminopeptidase	2.48	-0.85	-6.26	SAMN04487868_10548
A0A1I4JMC5	-2.4062	2.4062	Anhydro-N-acetylmuramic acid kinase	2.41	-0.91	-5.98	anmK SAMN04487868_106184
A0A1I4KM03	-2.3689	2.3689	Uncharacterized protein	2.37	-1.24	-5.84	SAMN04487868_110101
A0A1I4ILS6	-2.3525	2.3525	NADPH:quinone reductase	2.35	-1.16	-5.78	SAMN04487868_10423
A0A1I4M1I2	-2.3246	2.3246	Pilus assembly protein FimV	2.32	-0.83	-5.68	SAMN04487868_11834
A0A1I4JAI9	-2.2709	2.2709	Nuclease-related domain-containing protein	2.27	-1.20	-5.49	SAMN04487868_105218
A0A1I4MWL1	-2.2175	2.2175	Sodium/proline symporter	2.22	-1.07	-5.31	SAMN04487868_12665
A0A1I4LS21	-2.2129	2.2129	Replication region DNA-binding N-term	2.21	-0.77	-5.29	SAMN04487868_11631
A0A1I4K987	-2.1970	2.1970	Acyltransferase. WS/DGAT/MGAT	2.20	-1.68	-5.24	SAMN04487868_1098
A0A1I4JS87	-2.1803	2.1803	ADP-ribose pyrophosphatase YjhB. NUDIX family	2.18	-1.96	-6.76	SAMN04487868_10722
A0A1I4JLR2	-2.1054	2.1054	Putative zinc-finger	2.11	-1.36	-4.94	SAMN04487868_106171
A0A1I4HHH1	-2.0831	2.0831	N5-carboxyaminoimidazole ribonucleotide mutase	2.08	-0.98	-4.86	purE SAMN04487868_101407
A0A1I4MJW2	-1.9938	1.9938	Methylglyoxal synthase	1.99	-0.57	-4.59	mgsA SAMN04487868_12316
A0A1I4IE06	-1.9867	1.9867	TRAP transporter. DctM subunit	1.99	-1.35	-4.56	SAMN04487868_103213
A0A1I4MTJ3	-1.9627	1.9627	Iron complex outermembrane recepter protein	1.96	-0.91	-4.49	SAMN04487868_12557
A0A1I4MX91	-1.9354	1.9354	Malonyl CoA-acyl carrier protein transacylase	1.94	-1.62	-4.41	SAMN04487868_12656
A0A1I4LXM2	-1.8927	1.8927	Methyl-accepting chemotaxis protein	1.89	-2.11	-4.28	SAMN04487868_11735
A0A1I4L200	-1.8922	1.8922	PAS domain-containing protein	1.89	-1.84	-4.28	SAMN04487868_11257
A0A1I4MB07	-1.8762	1.8762	Pseudouridine synthase	1.88	-2.62	-4.24	SAMN04487868_12065
A0A1I4HSU0	-1.8759	1.8759	DNA polymerase III subunit gamma/tau	1.88	-0.74	-4.24	dnaX SAMN04487868_10222
A0A1I4J7M9	-1.8442	1.8442	Flagellar P-ring protein	1.84	-1.40	-5.13	flgI SAMN04487868_105125
A0A1I4KJ92	-1.8226	1.8226	Diguanylate cyclase/phosphodiesterase	1.82	-1.61	-4.08	SAMN04487868_11021
A0A1I4H1U9	-1.7535	1.7535	Transcription termination factor Rho	1.75	-1.49	-4.76	rho SAMN04487868_1012
A0A1I4MLH2	-1.7392	1.7392	Ankyrin repeat	1.74	-1.22	-3.85	SAMN04487868_12349
A0A1I4KD04	-1.7359	1.7359	TRAP-type mannitol/chloroaromatic compound transport system. substrate-binding protein	1.74	-2.17	-3.85	SAMN04487868_109101
A0A1I4LXJ6	-1.6951	1.6951	Type II secretion system protein M	1.70	-1.53	-3.74	SAMN04487868_11753
A0A1I4KD92	-1.6950	1.6950	Transcriptional regulator containing PAS. AAA-type ATPase. and DNA-binding Fis domains	1.70	-0.83	-4.53	SAMN04487868_109102
A0A1I4L410	-1.6845	1.6845	Signal transduction histidine kinase	1.68	-1.81	-3.71	SAMN04487868_112120

A0A1I4JSH8	-1.6830	1.6830	Uncharacterized protein	1.68	-1.37	-4.48	SAMN04487868_10750
A0A1I4N6X6	-1.6621	1.6621	DNA recombination protein RmuC	1.66	-0.83	-3.65	SAMN04487868_13021
A0A1I4K4D3	-1.6617	1.6617	Cytochrome c553	1.66	-0.69	-3.65	SAMN04487868_108103
A0A1I4MNV6	-1.6600	1.6600	Cobalt-zinc-cadmium resistance protein CzcA	1.66	-0.75	-3.64	SAMN04487868_12438
A0A1I4K9I6	-1.6590	1.6590	Glutamine synthetase	1.66	-1.18	-3.64	SAMN04487868_10912
A0A1I4HL94	-1.6156	1.6156	Flagellar motor switch protein FliG	1.62	-1.19	-3.53	SAMN04487868_101442
A0A1I4KKB9	-1.5989	1.5989	Aldehyde dehydrogenase	1.60	-1.62	-3.49	SAMN04487868_11076
A0A1I4HH41	-1.5931	1.5931	UPF0716 protein FxsA	1.59	-0.60	-3.47	SAMN04487868_101396
A0A1I4HDC9	-1.5915	1.5915	Protein HflC	1.59	-0.60	-3.47	SAMN04487868_101260
A0A1I4HUM8	-1.5882	1.5882	dTDP-4-amino-4.6-dideoxygalactose transaminase	1.59	-1.73	-3.46	SAMN04487868_10240
A0A1I4JTI2	-1.5723	1.5723	Uncharacterized protein	1.57	-0.64	-3.42	SAMN04487868_10748
A0A1I4HYS0	-1.5710	1.5710	Protease HtpX	1.57	-1.50	-3.42	htpX SAMN04487868_102176
A0A1I4MYI0	-1.5537	1.5537	Probable alpha-L-glutamate ligase	1.55	-0.35	-3.37	rimK SAMN04487868_12716
A0A1I4HWA6	-1.5482	1.5482	Tol-Pal system protein TolQ	1.55	-0.82	-3.36	tolQ SAMN04487868_102114
A0A1I4HD32	-1.5425	1.5425	tRNA U34 carboxymethyltransferase	1.54	-0.81	-3.35	cmoB SAMN04487868_101263
A0A1I4IUP3	-1.5372	1.5372	Periplasmic serine endoprotease DegP-like	1.54	-0.65	-3.33	SAMN04487868_104200
A0A1I4LW57	-1.5088	1.5088	Nicotinamidase-related amidase	1.51	-1.73	-3.26	SAMN04487868_11718
A0A1I4L3L5	-1.5051	1.5051	Pyrimidine operon attenuation protein / uracil phosphoribosyltransferase	1.51	-0.63	-3.25	SAMN04487868_11273
A0A1I4KDF2	-1.4989	1.4989	3-hydroxybutyrate dehydrogenase	1.50	-1.19	-3.24	SAMN04487868_10998
A0A1I4L735	-1.4979	1.4979	ATP synthase subunit b	1.50	-1.11	-3.24	atpF SAMN04487868_11321
A0A1I4MKL8	-1.4940	1.4940	Uncharacterized protein	1.49	-1.33	-3.23	SAMN04487868_12325
A0A1I4MSA8	-1.4927	1.4927	Phosphonate transport system ATP-binding protein	1.49	-1.06	-3.22	SAMN04487868_12528
A0A1I4KRV7	-1.4850	1.4850	Carboxyl-terminal processing protease	1.49	-0.43	-3.21	SAMN04487868_1118
A0A1I4KJE2	-1.4822	1.4822	Ribose-5-phosphate isomerase A	1.48	-0.76	-3.20	rpiA SAMN04487868_11025
A0A1I4HT95	-1.4684	1.4684	Acetyltransferase involved in cellulose biosynthesis. CelD/BcsL family	1.47	-0.92	-3.17	SAMN04487868_10236
A0A1I4N287	-1.4542	1.4542	Acetoin utilization deacetylase AcuC	1.45	-0.73	-3.13	SAMN04487868_12839
A0A1I4K4T4	-1.4534	1.4534	Uncharacterized conserved protein YdgA. DUF945 family	1.45	-0.48	-3.13	SAMN04487868_108115
A0A1I4JJX9	-1.4207	1.4207	dITP/XTP pyrophosphatase	1.42	-0.76	-3.05	SAMN04487868_106101
A0A1I4HYA9	-1.4164	1.4164	Tol-Pal system protein TolR	1.42	-1.56	-3.04	tolR SAMN04487868_102113
A0A1I4LDP0	-1.4146	1.4146	Transcriptional regulator. TetR family	1.41	-1.54	-3.04	SAMN04487868_11411
A0A1I4N753	-1.4121	1.4121	Uncharacterized protein	1.41	-1.00	-3.03	SAMN04487868_13020
A0A1I4JHP2	-1.4024	1.4024	HemY protein	1.40	-0.74	-3.01	SAMN04487868_10658
A0A1I4HI10	-1.4001	1.4001	UDP-4-amino-4.6-dideoxy-N-acetyl-beta-L-altrosamine transaminase	1.40	-0.59	-3.00	SAMN04487868_101361
A0A1I4L1S7	-1.3920	1.3920	Uncharacterized protein	1.39	-1.16	-2.98	SAMN04487868_11247

A0A1I4HW21	-1.3906	1.3906	2-methylcitrate dehydratase	1.39	-1.20	-2.98	SAMN04487868_10270
A0A1I4HME7	-1.3866	1.3866	Hook-length control protein FliK	1.39	-0.81	-2.97	SAMN04487868_101476
A0A1I4HAX6	-1.3863	1.3863	Methyl-accepting chemotaxis protein	1.39	-1.50	-2.97	SAMN04487868_101237
A0A1I4L866	-1.3862	1.3862	ATP synthase subunit a	1.39	-1.01	-2.97	atpB SAMN04487868_11323
A0A1I4I2G5	-1.3696	1.3696	Uncharacterized protein	1.37	-1.30	-2.93	SAMN04487868_102288
A0A1I4JIK9	-1.3691	1.3691	Amino acid-binding domain sensor histidine kinase	1.37	-0.73	-2.93	SAMN04487868_10674
A0A1I4HYW0	-1.3562	1.3562	Uncharacterized protein	1.36	-0.82	-2.90	SAMN04487868_102170
A0A1I4KU52	-1.3522	1.3522	Ribosomal RNA small subunit methyltransferase E	1.35	-1.25	-2.89	SAMN04487868_11179
A0A1I4KA68	-1.3444	1.3444	Membrane protein implicated in regulation of membrane protease activity	1.34	-0.76	-2.87	SAMN04487868_10920
A0A1I4N535	-1.3415	1.3415	MSHA biogenesis protein MshQ	1.34	-0.95	-2.87	SAMN04487868_12948
A0A1I4MFB0	-1.3362	1.3362	Methyl-accepting chemotaxis sensory transducer with Cache sensor	1.34	-0.51	-2.86	SAMN04487868_12165
A0A1I4I1W7	-1.3354	1.3354	Peptidyl-prolyl cis-trans isomerase	1.34	-0.34	-2.85	SAMN04487868_102278
A0A1I4MA50	-1.3322	1.3322	Virulence factor lipase N-terminal	1.33	-1.66	-2.85	SAMN04487868_12040
A0A1I4NIR1	-1.3226	1.3226	AsmA protein	1.32	-0.30	-2.83	SAMN04487868_1418
A0A1I4K4E9	-1.3220	1.3220	S-adenosylmethionine decarboxylase proenzyme	1.32	-0.93	-2.82	speD SAMN04487868_10885
A0A1I4HXQ3	-1.3209	1.3209	Lipid A export ATP-binding/permease protein MsbA	1.32	-0.92	-2.82	msbA SAMN04487868_102142
A0A1I4IXE3	-1.3207	1.3207	Two-component system. OmpR family. sensor histidine kinase RstB	1.32	-0.36	-2.82	SAMN04487868_104231
A0A1I4NED8	-1.3150	1.3150	Arsenical resistance protein ArsH	1.31	-1.42	-4.37	SAMN04487868_1353
A0A1I4K122	-1.3098	1.3098	Uncharacterized protein	1.31	-1.12	-2.80	SAMN04487868_10810
A0A1I4KTY4	-1.3084	1.3084	tRNA-processing RNAse BN	1.31	-1.40	-2.79	SAMN04487868_11176
A0A1I4IW42	-1.3071	1.3071	Two-component system. OmpR family. response regulator RstA	1.31	-0.61	-2.79	SAMN04487868_104232
A0A1I4M153	1.3057	-1.3057	NTE family protein	1.31	0.68	2.79	SAMN04487868_11825
A0A1I4ICV2	1.3135	-1.3135	Amino acid ABC transporter substrate-binding protein. PAAT family (TC 3.A.1.3.-)	1.31	1.65	2.80	SAMN04487868_103178
A0A1I4IUM3	1.3408	-1.3408	PAS domain S-box-containing protein/diguanylate cyclase (GGDEF) domain-containing protein	1.34	1.00	2.87	SAMN04487868_104199
A0A1I4L2K5	1.3491	-1.3491	Aspartate carbamoyltransferase	1.35	0.78	2.89	pyrB SAMN04487868_11274
A0A1I4KIA2	1.3592	-1.3592	Acyl-CoA hydrolase	1.36	0.45	2.91	SAMN04487868_1102
A0A1I4MI03	1.3725	-1.3725	Alcohol dehydrogenase. propanol-preferring	1.37	3.18	2.94	SAMN04487868_12256
A0A1I4IBP8	1.3737	-1.3737	Putative MetA-pathway of phenol degradation	1.37	2.88	2.94	SAMN04487868_103158
A0A1I4MX30	1.3857	-1.3857	3-oxoacyl-[acyl-carrier-protein] synthase 2	1.39	0.57	2.97	SAMN04487868_12659
A0A1I4MKS4	1.4062	-1.4062	Uncharacterized protein	1.41	2.03	3.02	SAMN04487868_12357
A0A1I4JRM3	1.4063	-1.4063	Phenylacetate-CoA ligase	1.41	2.09	3.51	SAMN04487868_10718
A0A1I4IBL2	1.4146	-1.4146	Acetaldehyde dehydrogenase	1.41	3.89	3.04	SAMN04487868_103136
A0A1I4IT61	1.4186	-1.4186	Aminotransferase	1.42	1.46	3.05	SAMN04487868_104165

A0A1I4K3X4	1.4191	-1.4191	FMN-dependent NADH-azoreductase	1.42	2.60	3.05	azoR SAMN04487868_10886
A0A1I4M0U9	1.4249	-1.4249	Uncharacterized protein	1.42	1.58	3.57	SAMN04487868_11817
A0A1I4J979	1.4264	-1.4264	Uncharacterized protein	1.43	1.34	3.57	SAMN04487868_105189
A0A1I4MNT8	1.4352	-1.4352	Uncharacterized protein	1.44	0.72	3.09	SAMN04487868_12445
A0A1I4MHU4	1.4399	-1.4399	Cyclopentanol dehydrogenase	1.44	4.14	3.62	SAMN04487868_12259
A0A1I4KUB7	1.4505	-1.4505	Adenosylmethionine-8-amino-7-oxononanoate aminotransferase	1.45	1.19	3.12	bioA SAMN04487868_11180
A0A1I4H9Z9	1.4721	-1.4721	D-3-phosphoglycerate dehydrogenase	1.47	0.71	3.17	SAMN04487868_101208
A0A1I4K2B6	1.4749	-1.4749	Phosphoglycolate phosphatase	1.47	0.89	3.73	SAMN04487868_10852
A0A1I4J6P3	1.4912	-1.4912	Uncharacterized conserved protein. DUF1330 family	1.49	2.22	5.42	SAMN04487868_10594
A0A1I4MTP4	1.5008	-1.5008	Acetolactate synthase-1/2/3 large subunit	1.50	2.18	3.24	SAMN04487868_12554
A0A1I4HXZ9	1.5099	-1.5099	Thioredoxin reductase	1.51	1.67	3.27	SAMN04487868_102154
A0A1I4N938	1.5159	-1.5159	Transcriptional regulator. TetR family	1.52	0.85	3.87	SAMN04487868_13127
A0A1I4MGI2	1.5170	-1.5170	PSII_BNR domain-containing protein	1.52	0.40	3.28	SAMN04487868_1223
A0A1I4MID8	1.5252	-1.5252	Succinate-semialdehyde dehydrogenase / glutarate-semialdehyde dehydrogenase	1.53	2.63	3.30	SAMN04487868_12264
A0A1I4L334	1.5427	-1.5427	Uncharacterized protein	1.54	0.69	3.35	SAMN04487868_11291
A0A1I4NCC4	1.5490	-1.5490	Outer membrane protein	1.55	0.66	3.36	SAMN04487868_13330
A0A1I4JRY3	1.5518	-1.5518	Acetyl-CoA C-acetyltransferase	1.55	1.32	3.37	SAMN04487868_10729
A0A1I4L3W6	1.5904	-1.5904	2-hydroxy-3-oxopropionate reductase	1.59	2.73	3.47	SAMN04487868_112118
A0A1I4IC98	1.6044	-1.6044	Catechol 2.3-dioxygenase	1.60	6.39	3.50	SAMN04487868_103132
A0A1I4H5C2	1.6143	-1.6143	Iron complex outermembrane recepter protein	1.61	1.50	3.53	SAMN04487868_101103
A0A1I4K5L8	1.6182	-1.6182	Glutamate decarboxylase	1.62	0.96	3.54	SAMN04487868_108123
A0A1I4MDC6	1.6227	-1.6227	Phosphatidylglycerol--prolipoprotein diacylglyceryl transferase	1.62	3.83	6.34	lgt SAMN04487868_12135
A0A1I4LRB9	1.6604	-1.6604	Quinohemoprotein ethanol dehydrogenase	1.66	2.40	3.65	SAMN04487868_11617
A0A1I4IBU4	1.6875	-1.6875	2-hydroxychromene-2-carboxylate isomerase	1.69	6.52	3.72	SAMN04487868_103139
A0A1I4I057	1.6886	-1.6886	HTH-type transcriptional regulator MalT	1.69	0.97	3.72	malT SAMN04487868_102203
A0A1I4K168	1.7070	-1.7070	Cyclopropane-fatty-acyl-phospholipid synthase	1.71	2.53	3.77	SAMN04487868_10817
A0A1I4I9J8	1.7126	-1.7126	Two-component system. sensor histidine kinase RegB	1.71	1.98	4.59	SAMN04487868_103100
A0A1I4MI95	1.7412	-1.7412	Predicted flavoprotein CzcO associated with the cation diffusion facilitator CzcD	1.74	1.51	3.86	SAMN04487868_12258
A0A1I4KTX9	1.7628	-1.7628	Ig-like domain-containing protein	1.76	0.87	3.92	SAMN04487868_11171
A0A1I4L2B7	1.7733	-1.7733	Patatin-like phospholipase	1.77	1.17	3.95	SAMN04487868_11255
A0A1I4K4A1	1.8232	-1.8232	Thiol:disulfide interchange protein	1.82	0.59	4.09	SAMN04487868_108102
A0A1I4K6Q6	1.8656	-1.8656	Cold-shock DNA-binding protein family	1.87	1.02	4.21	SAMN04487868_108153
A0A1I4M1P7	1.8747	-1.8747	DNA-binding transcriptional regulator. LysR family	1.87	0.62	4.23	SAMN04487868_11829
A0A1I4JH17	1.9075	-1.9075	Argininosuccinate lyase	1.91	0.41	4.33	argH SAMN04487868_10664

A0A1I4IDA3	1.9145	-1.9145	Choline dehydrogenase	1.91	4.02	4.35	SAMN04487868_103156
A0A1I4IA16	1.9748	-1.9748	Uncharacterized protein	1.97	5.64	4.53	SAMN04487868_103120
A0A1I4KED8	1.9824	-1.9824	AraC-type DNA-binding protein	1.97	1.24	9.64	SAMN04487868_109133
A0A1I4ICG1	2.0206	-2.0206	2-hydroxymuconate semialdehyde hydrolase	2.02	5.02	4.67	SAMN04487868_103134
A0A1I4MHM9	2.1509	-2.1509	Acetyl esterase/lipase	2.15	3.50	5.08	SAMN04487868_12257
A0A1I4IAB4	2.1540	-2.1540	Phenol 2-monooxygenase P1 subunit	2.15	4.82	5.09	SAMN04487868_103126
A0A1I4MGX2	2.1677	-2.1677	Two component transcriptional regulator. LuxR family	2.17	0.73	5.14	SAMN04487868_12218
A0A1I4IAN3	2.2641	-2.2641	2-hydroxymuconate semialdehyde dehydrogenase	2.26	4.20	5.47	SAMN04487868_103133
A0A1I4IAR0	2.3497	-2.3497	4-hydroxy-2-oxovalerate aldolase	2.35	5.55	5.77	SAMN04487868_103137
A0A1I4IAA5	2.4093	-2.4093	PSII_BNR domain-containing protein	2.41	6.27	8.13	SAMN04487868_103123
A0A1I4IAG2	2.7722	-2.7722	Phenol 2-monooxygenase P5 subunit	2.77	5.58	7.50	SAMN04487868_103130
A0A1I4MHW6	2.7829	-2.7829	Uncharacterized protein	2.78	6.57	7.55	SAMN04487868_12262
A0A1I4IP03	2.9382	-2.9382	Cold-shock DNA-binding protein family	2.94	1.18	8.30	SAMN04487868_10475
A0A1I4IA30	3.0773	-3.0773	Uncharacterized protein	3.08	4.51	9.03	SAMN04487868_103121
A0A1I4IAP7	3.2280	-3.2280	2-oxopent-4-enoate/cis-2-oxohex-4-enoate hydratase	3.23	5.45	9.88	SAMN04487868_103135
A0A1I4ICK9	4.0364	-4.0364	4-oxalocrotonate decarboxylase	4.07	6.49	16.15	SAMN04487868_103138

Table S 7: Proteins assigned to non-alkane hydrocarbon metabolism with significantly higher detected abundances in *Marinobacter* sp. TT1 growing on WAF versus CEWAF according to a Student's T-test ($p < 0.05$).

UniProt ID	WAF	CEWAF	Assigned pathway	Description	-Log *p*-value	Student's T-test Diff. (log2 FC value)	Student's T-test Test statistic	Gene names
A0A1I4IBL2	1.4146	-1.4146	Benzoate/Xylene metabolism	Acetaldehyde dehydrogenase MhpF	1.41	3.89	3.04	SAMN04487868_103136
A0A1I4JRY3	1.5518	-1.5518	Benzoate/Xylene metabolism	Acetyl-CoA C-acetyltransferase	1.55	1.32	3.37	SAMN04487868_10729
A0A1I4IC98	1.6044	-1.6044	Benzoate/Xylene metabolism	Catechol 2.3-dioxygenase	1.60	6.39	3.50	SAMN04487868_103132
A0A1I4ICG1	2.0206	-2.0206	Benzoate/Xylene metabolism	2-hydroxymuconate semialdehyde hydrolase DmpD	2.02	5.02	4.67	SAMN04487868_103134
A0A1I4IAN3	2.2641	-2.2641	Benzoate/Xylene metabolism	2-hydroxymuconate semialdehyde dehydrogenase DmpC	2.26	4.20	5.47	SAMN04487868_103133
A0A1I4IAR0	2.3497	-2.3497	Benzoate/Xylene metabolism	4-hydroxy-2-oxovalerate aldolase MhpE	2.35	5.55	5.77	SAMN04487868_103137
A0A1I4IAP7	3.2280	-3.2280	Benzoate/Xylene metabolism	2-oxopent-4-enoate/cis-2-oxohex-4-enoate hydratase	3.23	5.45	9.88	SAMN04487868_103135
A0A1I4ICK9	4.0364	-4.0364	Benzoate/Xylene metabolism	4-oxalocrotonate decarboxylase	4.07	6.49	16.15	SAMN04487868_103138
A0A1I4MHU4	1.4399	-1.4399	Cycloaliphatics metabolism	Cyclopentanol dehydrogenase	1.44	4.14	3.62	SAMN04487868_12259
A0A1I4MI95	1.7412	-1.7412	Cycloaliphatics metabolism	Cyclohexanone monooxygenase ChnB. Predicted flavoprotein CzcO associated with the cation diffusion facilitator CzcD	1.74	1.51	3.86	SAMN04487868_12258
A0A1I4MHM9	2.1509	-2.1509	Cycloaliphatics metabolism	Epsilon-lactone hydrolase MhlB. Acetyl esterase/lipase	2.15	3.50	5.08	SAMN04487868_12257
A0A1I4IBU4	1.6875	-1.6875	Naphthalene metabolism	2-hydroxychromene-2-carboxylate isomerase	1.69	6.52	3.72	SAMN04487868_103139
A0A1I4IBP8	1.3737	-1.3737	Phenol metabolism	Putative MetA-pathway of phenol degradation	1.37	2.88	2.94	SAMN04487868_103158
A0A1I4IAB4	2.1540	-2.1540	Phenol metabolism	Phenol 2-monooxygenase P1 subunit	2.15	4.82	5.09	SAMN04487868_103126
A0A1I4IAG2	2.7722	-2.7722	Phenol metabolism	Phenol 2-monooxygenase P5 subunit	2.77	5.58	7.50	SAMN04487868_103130

Table S 8: Proteins of interest detected in the comparative proteomics study with *Marinobacter* sp. TT1 and depicted in Figures 5.2, S5.4, S5.5, S5.7 and S5.8.

Depicted name	Category	UniProt ID	Description	Gene name
Put. cytochrome P450	Alkane metabolism	A0A1I4KEY9	Uncharacterized protein	SAMN04487868_109135
AlkB1 homologue	Alkane metabolism	A0A1I4KFD0	Alkane 1-monooxygenase	SAMN04487868_109143
AlkB2 homologue	Alkane metabolism	A0A1I4KVH1	Alkane 1-monooxygenase	SAMN04487868_111110
AupB homologue	Alkane metabolism	A0A1I4JKB4	Ig-like domain-containing protein	SAMN04487868_106132
AupA homologue	Alkane metabolism	A0A1I4JKC5	Long-chain fatty acid transport protein	SAMN04487868_106133
Alcohol dehydr. 4	Alkane metabolism	A0A1I4H5P2	Alcohol dehydrogenase	SAMN04487868_10160
Alcohol dehydr. 2	Alkane metabolism	A0A1I4ISL3	NAD(P)-dependent dehydrogenase, short-chain alcohol dehydrogenase family	SAMN04487868_104154
Alcohol dehydr. 1	Alkane metabolism	A0A1I4J3P7	Alcohol dehydrogenase	SAMN04487868_10555
Rubredoxin red.	Alkane metabolism	A0A1I4K5F9	Rubredoxin-NAD+ reductase	SAMN04487868_108130
Aldehyde dehydr. 1	Alkane metabolism	A0A1I4K5K4	Aldehyde dehydrogenase	SAMN04487868_108111
FA-CoA synthase	Alkane metabolism	A0A1I4KER1	Fatty-acyl-CoA synthase	SAMN04487868_109139
Choline dehydr.	Alkane metabolism	A0A1I4KF71	Choline dehydrogenase	SAMN04487868_109140
OmpW (AlkL)	Alkane metabolism	A0A1I4KF83	Outer membrane protein	SAMN04487868_109138
Aldehyde dehydr. 2	Alkane metabolism	A0A1I4KFQ9	Aldehyde dehydrogenase	SAMN04487868_109141
Aldehyde dehydr. 3	Alkane metabolism	A0A1I4KKB9	Aldehyde dehydrogenase	SAMN04487868_11076
Alcohol dehydr. 5	Alkane metabolism	A0A1I4KKP8	Alcohol dehydrogenase (Cytochrome c)	SAMN04487868_11072
Ferredoxin red.	Alkane metabolism	A0A1I4KTN3	Ferredoxin-NADP reductase	SAMN04487868_11156
Ferredoxin	Alkane metabolism	A0A1I4MH37	Ferredoxin	SAMN04487868_12226
Alcohol dehydr. 3	Alkane metabolism	A0A1I4MI03	Alcohol dehydrogenase, propanol-preferring	SAMN04487868_12256
MucB	Alginate	A0A1I4IUP7	Sigma E regulatory protein, MucB/RseB	SAMN04487868_104202
AlgR	Alginate	A0A1I4JGY9	Two component transcriptional regulator, LytTR family	SAMN04487868_10662
AlgZ	Alginate	A0A1I4JH21	Two-component system, LytT family, sensor histidine kinase AlgZ	SAMN04487868_10663
AlgA (2)	Alginate	A0A1I4JXV5	Mannose-6-phosphate isomerase, type 2	SAMN04487868_107172
AlgE	Alginate	A0A1I4LF78	Alginate export porin	SAMN04487868_11448
Alg44	Alginate	A0A1I4LF83	Alginate biosynthesis protein Alg44	SAMN04487868_11446
AlgF	Alginate	A0A1I4LFF1	Alginate O-acetyltransferase complex protein AlgF	SAMN04487868_11452
AlgD	Alginate	A0A1I4LFN3	GDP-mannose 6-dehydrogenase	SAMN04487868_11444
AlgC	Alginate	A0A1I4LG98	Phosphomannomutase	SAMN04487868_11456
AlgA	Alginate	A0A1I4LGW8	Mannose-6-phosphate isomerase, type 2	SAMN04487868_11455
LptB	Cell envelope	A0A1I4HFQ5	Lipopolysaccharide export system ATP-binding protein	SAMN04487868_101314
LPS transf.	Cell envelope	A0A1I4HIF2	Sugar transferase involved in LPS biosynthesis (Colanic, teichoic acid)	SAMN04487868_101371

MdoG	Cell envelope	A0A1I4HW41	Glucans biosynthesis protein	SAMN04487868_10278
AnmK	Cell envelope	A0A1I4JMC5	Anhydro-N-acetylmuramic acid kinase	anmK SAMN04487868_106184
MrcB	Cell envelope	A0A1I4JML5	Penicillin-binding protein 1B	SAMN04487868_106167
MurD	Cell envelope	A0A1I4MCC3	UDP-N-acetylmuramoylalanine--D-glutamate ligase	murD SAMN04487868_12114
MurE	Cell envelope	A0A1I4MCH9	UDP-N-acetylmuramoyl-L-alanyl-D-glutamate--2,6-diaminopimelate ligase	murE SAMN04487868_12111
MurF	Cell envelope	A0A1I4MCP0	UDP-N-acetylmuramoyl-tripeptide--D-alanyl-D-alanine ligase	murF SAMN04487868_12112
MurC	Cell envelope	A0A1I4MCR2	UDP-N-acetylmuramate--L-alanine ligase	murC SAMN04487868_12117
MurG	Cell envelope	A0A1I4MDH0	UDP-N-acetylglucosamine--N-acetylmuramyl-(pentapeptide) pyrophosphoryl-undecaprenol N-acetylglucosamine transferase	murG SAMN04487868_12116
Mpl	Cell envelope	A0A1I4MEP1	UDP-N-acetylmuramate--L-alanyl-gamma-D-glutamyl-meso-2,6-diaminoheptandioate ligase	mpl SAMN04487868_12168
Lysophoshpolip. 1	Phospholipases	A0A1I4H9M8	Lysophospholipase, alpha-beta hydrolase superfamily	SAMN04487868_101204
Phoshpolip. A1	Phospholipases	A0A1I4JFL3	Phospholipase A1	SAMN04487868_10632
Lysophoshpolip. 2	Phospholipases	A0A1I4K3D0	Lysophospholipase, alpha-beta hydrolase superfamily	SAMN04487868_10877
Phoshpolip. RssA	Phospholipases	A0A1I4LMS6	Predicted acylesterase/phospholipase RssA, contains patatin domain	SAMN04487868_11570
Patatin-like Phoshpolip.	Phospholipases	A0A1I4MRV4	Patatin-like phospholipase	SAMN04487868_12519
Alkyl hydroperoxide red.	Oxidative stress	A0A1I4H513	Alkyl hydroperoxide reductase AhpD	SAMN04487868_10185
AH peroxidase	Oxidative stress	A0A1I4H8K6	Animal haem peroxidase	SAMN04487868_101136
Superoxide dismutase	Oxidative stress	A0A1I4HIU5	Superoxide dismutase	SAMN04487868_101405
Thioredoxin red.	Oxidative stress	A0A1I4HXZ9	Thioredoxin reductase	SAMN04487868_102154
1-Cys peroxiredoxin	Oxidative stress	A0A1I4I713	1-Cys peroxiredoxin	SAMN04487868_10329
Catalase-peroxidase	Oxidative stress	A0A1I4J422	Catalase-peroxidase	katG SAMN04487868_10566
Thioredoxin	Oxidative stress	A0A1I4KP75	Thioredoxin	SAMN04487868_110155
MCP 3	Chemotaxis	A0A1I4HAX6	Methyl-accepting chemotaxis protein	SAMN04487868_101237
CheA	Chemotaxis	A0A1I4HJZ5	Two-component system, chemotaxis family, sensor kinase CheA	SAMN04487868_101467
CheV 1	Chemotaxis	A0A1I4JAF8	Two-component system, chemotaxis family, response regulator CheV	SAMN04487868_105193
MCP 1	Chemotaxis	A0A1I4KV15	Methyl-accepting chemotaxis protein	SAMN04487868_11175
MotA	Chemotaxis	A0A1I4L9F1	Chemotaxis protein MotA	SAMN04487868_11366
CheV 2	Chemotaxis	A0A1I4LGD8	Two-component system, chemotaxis family, response regulator CheV	SAMN04487868_11462
MCP 5	Chemotaxis	A0A1I4LGU0	Methyl-accepting chemotaxis sensory transducer with Pas/Pac sensor	SAMN04487868_11475
MCP 4	Chemotaxis	A0A1I4LHA6	Methyl-accepting chemotaxis sensory transducer with Cache sensor	SAMN04487868_11478
MCP 8	Chemotaxis	A0A1I4LXM2	Methyl-accepting chemotaxis protein	SAMN04487868_11735
MCP 2	Chemotaxis	A0A1I4M538	Methyl-accepting chemotaxis protein	SAMN04487868_11920
MCP 6	Chemotaxis	A0A1I4MFB0	Methyl-accepting chemotaxis sensory transducer with Cache sensor	SAMN04487868_12165
MCP 7	Chemotaxis	A0A1I4MSJ0	Methyl-accepting chemotaxis sensory transducer with Cache sensor	SAMN04487868_12535
PilC (T4P)	Motility	A0A1I4HFB7	Type IV pilus assembly protein PilC	SAMN04487868_101345

PilB (T4P)	Motility	A0A1I4HFD7	Type IV pilus assembly protein PilB	SAMN04487868_101346
PilA (T4P)	Motility	A0A1I4HGN2	Type IV pilus assembly protein PilA	SAMN04487868_101348
Flagellin 1	Motility	A0A1I4HGV5	Flagellin	SAMN04487868_101384
Flagellin 2	Motility	A0A1I4HGW5	Flagellin	SAMN04487868_101385
PilF (T4P)	Motility	A0A1I4J8L9	Type IV pilus assembly protein PilF	SAMN04487868_105142
PilU (Tw. mot.)	Motility	A0A1I4JJB8	Twitching motility protein PilU	SAMN04487868_106110
PilI (Tw. mot.)	Motility	A0A1I4L2E6	Twitching motility protein PilI	SAMN04487868_11266
PilJ (Tw. mot.)	Motility	A0A1I4L2M7	Twitching motility protein PilJ	SAMN04487868_11265
PilV (T4P)	Motility	A0A1I4LJZ0	Type IV pilus assembly protein PilV	SAMN04487868_11516
PilE (T4P)	Motility	A0A1I4LK64	Type IV pilus assembly protein PilE	SAMN04487868_11521
PilW (T4P)	Motility	A0A1I4LLA1	Type IV pilus assembly protein PilW	SAMN04487868_11517
PilO (T4P)	Motility	A0A1I4LLY9	Type IV pilus assembly protein PilO	SAMN04487868_11558
PilN (T4P)	Motility	A0A1I4LM37	Type IV pilus assembly protein PilN	SAMN04487868_11559
PilP (T4P)	Motility	A0A1I4LME5	Type IV pilus assembly protein PilP	SAMN04487868_11557
PilM (T4P)	Motility	A0A1I4LMK3	Type IV pilus assembly protein PilM	SAMN04487868_11560
Haloalkane dehal. 2	HC metabolism	A0A1I4H7H6	Haloalkane dehalogenase	dhmA SAMN04487868_101153
Nitroreductase	HC metabolism	A0A1I4I1J3	Nitroreductase	SAMN04487868_102251
Amidase	HC metabolism	A0A1I4I6L1	Amidase	SAMN04487868_10316
Phenol 2-monoox. P1	HC metabolism	A0A1I4IAB4	Phenol 2-monooxygenase P1 subunit	SAMN04487868_103126
Phenol 2-monoox. P5	HC metabolism	A0A1I4IAG2	Phenol 2-monooxygenase P5 subunit	SAMN04487868_103130
DmpC	HC metabolism	A0A1I4IAN3	2-hydroxymuconate semialdehyde dehydrogenase	SAMN04487868_103133
Enoate hydratase	HC metabolism	A0A1I4IAP7	2-oxopent-4-enoate/cis-2-oxohex-4-enoate hydratase	SAMN04487868_103135
Aldolase MphE	HC metabolism	A0A1I4IAR0	4-hydroxy-2-oxovalerate aldolase	SAMN04487868_103137
MhpF	HC metabolism	A0A1I4IBL2	Acetaldehyde dehydrogenase	SAMN04487868_103136
Phenol degr. 1	HC metabolism	A0A1I4IBP8	Putative MetA-pathway of phenol degradation	SAMN04487868_103158
Hydroxychromene isom.	HC metabolism	A0A1I4IBU4	2-hydroxychromene-2-carboxylate isomerase	SAMN04487868_103139
Catechol 2,3-dioxygen.	HC metabolism	A0A1I4IC98	Catechol 2,3-dioxygenase	SAMN04487868_103132
DmpD	HC metabolism	A0A1I4ICG1	2-hydroxymuconate semialdehyde hydrolase	SAMN04487868_103134
4-oxalocrotonate dec.	HC metabolism	A0A1I4ICK9	4-oxalocrotonate decarboxylase	SAMN04487868_103138
Benzaldehyde dehydr.	HC metabolism	A0A1I4IDB7	Benzaldehyde dehydrogenase (NAD+)	SAMN04487868_103155
Enoyl-CoA hydratase	HC metabolism	A0A1I4JRX0	3-hydroxyacyl-CoA dehydrogenase / enoyl-CoA hydratase / 3-hydroxybutyryl-CoA epimerase	SAMN04487868_10730
C-acetyltransf.	HC metabolism	A0A1I4JRY3	Acetyl-CoA C-acetyltransferase	SAMN04487868_10729
Phenol degr. 2	HC metabolism	A0A1I4LR95	Putative MetA-pathway of phenol degradation	SAMN04487868_11618
Put. Cyclohexanone MO	HC metabolism	A0A1I4LXN7	Predicted flavoprotein CzcO associated with the cation diffusion facilitator CzcD	SAMN04487868_11744

3-hydroxyl-CoA deh.	HC metabolism	A0A1I4MAT6	3-hydroxyacyl-CoA dehydrogenase	SAMN04487868_12059
Haloalkane dehal. 1	HC metabolism	A0A1I4MDJ5	Haloalkane dehalogenase	dhmA SAMN04487868_12140
UbiX	HC metabolism	A0A1I4MEF9	Flavin prenyltransferase UbiX	ubiX SAMN04487868_12169
MhlB	HC metabolism	A0A1I4MHM9	Acetyl esterase/lipase	SAMN04487868_12257
CpnA	HC metabolism	A0A1I4MHU4	Cyclopentanol dehydrogenase	SAMN04487868_12259
ChnB	HC metabolism	A0A1I4MI95	Predicted flavoprotein CzcO associated with the cation diffusion facilitator CzcD	SAMN04487868_12258
ABC transp. 3	Transporters	A0A1I4H9T9	Amino acid ABC transporter substrate-binding protein, PAAT family (TC 3.A.1.3.-)	SAMN04487868_101149
ABC transp. 14	Transporters	A0A1I4I3B8	Amino acid ABC transporter membrane protein 1, PAAT family	SAMN04487868_102282
ABC transp. 1	Transporters	A0A1I4I3C1	Amino acid ABC transporter substrate-binding protein, PAAT family	SAMN04487868_102283
ABC transp. 2	Transporters	A0A1I4I3J1	Amino acid ABC transporter ATP-binding protein, PAAT family	SAMN04487868_102280
ABC transp. 11	Transporters	A0A1I4IEU9	Amino acid/amide ABC transporter ATP-binding protein 2, HAAT family	SAMN04487868_103241
ABC transp. 4	Transporters	A0A1I4IF29	Amino acid/amide ABC transporter substrate-binding protein, HAAT family	SAMN04487868_103242
ABC transp. 13	Transporters	A0A1I4IF50	Amino acid/amide ABC transporter membrane protein 2, HAAT family	SAMN04487868_103244
ABC transp. 9	Transporters	A0A1I4KKP1	Amino acid ABC transporter substrate-binding protein, PAAT family	SAMN04487868_11071
ABC transp. 6	Transporters	A0A1I4KL18	Amino acid/amide ABC transporter substrate-binding protein, HAAT family	SAMN04487868_11069
ABC transp. 15	Transporters	A0A1I4KNI9	L-leucine ABC transporter membrane protein /L-isoleucine ABC transporter membrane protein/ L-valine ABC transporter membrane protein	SAMN04487868_110148
ABC transp. 5	Transporters	A0A1I4KZV5	Amino acid/amide ABC transporter substrate-binding protein, HAAT family	SAMN04487868_11214
ABC transp. 8	Transporters	A0A1I4L008	Amino acid/amide ABC transporter ATP-binding protein 1, HAAT family	SAMN04487868_11216
ABC transp. 10	Transporters	A0A1I4LGV8	Amino acid/amide ABC transporter ATP-binding protein 1, HAAT family	SAMN04487868_11467
ABC transp. 7	Transporters	A0A1I4LGY6	Amino acid/amide ABC transporter substrate-binding protein, HAAT family	SAMN04487868_11470
ABC transp. 12	Transporters	A0A1I4M9R6	Amino acid ABC transporter substrate-binding protein, PAAT family	SAMN04487868_12033
TRAP transp. 6	Transporters	A0A1I4IE06	TRAP transporter, DctM subunit	SAMN04487868_103213
TRAP transp. 3	Transporters	A0A1I4IF13	TRAP-type mannitol/chloroaromatic compound transport system, substrate-binding protein	SAMN04487868_103200
TRAP transp. 7	Transporters	A0A1I4KA18	TRAP-type mannitol/chloroaromatic compound transport system, substrate-binding protein	SAMN04487868_10913
TRAP transp. 4	Transporters	A0A1I4KD04	TRAP-type mannitol/chloroaromatic compound transport system, substrate-binding protein	SAMN04487868_109101
TRAP transp. 5	Transporters	A0A1I4MNB7	TRAP-type mannitol/chloroaromatic compound transport system, small permease component	SAMN04487868_12412
TRAP transp. 1	Transporters	A0A1I4MNH9	TRAP-type mannitol/chloroaromatic compound transport system, substrate-binding protein	SAMN04487868_12413
TRAP transp. 2	Transporters	A0A1I4N0J7	TRAP-type mannitol/chloroaromatic compound transport system, substrate-binding protein	SAMN04487868_1285
Cu/Ag efflux	Transporters	A0A1I4JUH3	Membrane fusion protein, Cu(I)/Ag(I) efflux system	SAMN04487868_10781
Multidrug efflux 1	Transporters	A0A1I4K184	Membrane fusion protein, multidrug efflux system	SAMN04487868_10827
RND efflux 1	Transporters	A0A1I4KEF4	RND family efflux transporter, MFP subunit	SAMN04487868_109128

Multidrug efflux 2	Transporters	A0A1I4KER7	Multidrug efflux pump subunit AcrB	SAMN04487868_109127
RND efflux 2	Transporters	A0A1I4MNR2	RND family efflux transporter, MFP subunit	SAMN04487868_12434
Chaperone DjlA	Chaperones	A0A1I4ILD3	Co-chaperone protein DjlA	djlA SAMN04487868_10414
Chaperone HtpG	Chaperones	A0A1I4J513	Chaperone protein HtpG	htpG SAMN04487868_10561
Chaperone SurA	Chaperones	A0A1I4K1X1	Chaperone SurA	surA SAMN04487868_10844
Chaperone DnaK	Chaperones	A0A1I4KMS0	Chaperone protein DnaK	dnaK SAMN04487868_110120
Chaperone CbpM	Chaperones	A0A1I4KUW8	Chaperone modulatory protein CbpM	SAMN04487868_11194
Chaperone ClpB	Chaperones	A0A1I4LK07	Chaperone protein ClpB	clpB SAMN04487868_1157
Chaperone TorD	Chaperones	A0A1I4NAC5	Chaperone TorD involved in molybdoenzyme TorA maturation	SAMN04487868_13214